

1974

## A direct reaction multiple scattering pion-nucleus optical potential

Charles William Lucas

*College of William & Mary - Arts & Sciences*

Follow this and additional works at: <https://scholarworks.wm.edu/etd>

---

### Recommended Citation

Lucas, Charles William, "A direct reaction multiple scattering pion-nucleus optical potential" (1974).  
*Dissertations, Theses, and Masters Projects*. Paper 1539623673.  
<https://dx.doi.org/doi:10.21220/s2-y7ab-b473>

This Dissertation is brought to you for free and open access by the Theses, Dissertations, & Master Projects at W&M ScholarWorks. It has been accepted for inclusion in Dissertations, Theses, and Masters Projects by an authorized administrator of W&M ScholarWorks. For more information, please contact [scholarworks@wm.edu](mailto:scholarworks@wm.edu).

## INFORMATION TO USERS

This material was produced from a microfilm copy of the original document. While the most advanced technological means to photograph and reproduce this document have been used, the quality is heavily dependent upon the quality of the original submitted.

The following explanation of techniques is provided to help you understand markings or patterns which may appear on this reproduction.

1. The sign or "target" for pages apparently lacking from the document photographed is "Missing Page(s)". If it was possible to obtain the missing page(s) or section, they are spliced into the film along with adjacent pages. This may have necessitated cutting thru an image and duplicating adjacent pages to insure you complete continuity.
2. When an image on the film is obliterated with a large round black mark, it is an indication that the photographer suspected that the copy may have moved during exposure and thus cause a blurred image. You will find a good image of the page in the adjacent frame.
3. When a map, drawing or chart, etc., was part of the material being photographed the photographer followed a definite method in "sectioning" the material. It is customary to begin photoing at the upper left hand corner of a large sheet and to continue photoing from left to right in equal sections with a small overlap. If necessary, sectioning is continued again — beginning below the first row and continuing on until complete.
4. The majority of users indicate that the textual content is of greatest value, however, a somewhat higher quality reproduction could be made from "photographs" if essential to the understanding of the dissertation. Silver prints of "photographs" may be ordered at additional charge by writing the Order Department, giving the catalog number, title, author and specific pages you wish reproduced.
5. PLEASE NOTE: Some pages may have indistinct print. Filmed as received.

**Xerox University Microfilms**

300 North Zeeb Road  
Ann Arbor, Michigan 48106

74-22,287

LUCAS, Charles William, Jr., 1942-  
A DIRECT REACTION MULTIPLE SCATTERING  
PION-NUCLEUS OPTICAL MODEL POTENTIAL.

The College of William and Mary in Virginia,  
Ph.D., 1974  
Physics, nuclear

University Microfilms, A XEROX Company, Ann Arbor, Michigan

**A DIRECT REACTION MULTIPLE SCATTERING PION-NUCLEUS OPTICAL MODEL POTENTIAL**

---

**A Thesis**

**Presented to**

**The Faculty of the Department of Physics  
The College of William and Mary in Virginia**

---

**In Partial Fulfillment**

**Of the Requirements for the Degree of**

**Doctor of Philosophy**

---

**by**

**Charles W. Lucas, Jr.**

**June 1974**

APPROVAL SHEET

This dissertation is submitted in partial fulfillment of  
the requirements of the degree of

Doctor of Philosophy

Charles W. Lucas, Jr.  
Author

Approved, May 1974

W. J. Kossler  
William J. Kossler

Morton Eckhause  
Morton Eckhause

Edward A. Remler  
Edward A. Remler

Hans C. von Baeyer  
Hans C. von Baeyer

Raymond W. Southworth  
Raymond W. Southworth (Mathematics)

**DEDICATED**

**To my wife, Alice**

## TABLE OF CONTENTS

	Page
ACKNOWLEDGMENTS . . . . .	vi
LIST OF TABLES . . . . .	viii
LIST OF FIGURES . . . . .	xi
ABSTRACT . . . . .	xvii
 CHAPTER	
I. INTRODUCTION . . . . .	2
II. PREVIOUS WORK ON THE PION-NUCLEUS STRONG INTERACTION POTENTIAL . . . . .	6
A. Pion-Nucleus Scattering	
B. Pion-Nucleus Absorption at Very Low Energy	
C. Pionic Atoms	
III. DEVELOPMENT OF AN OPTICAL MODEL POTENTIAL FROM A MULTIPLE SCATTERING THEORY . . . . .	24
A. Validity of the Multiple Scattering Approach	
B. Construction of the Multiple Scattering Equations	
C. Construction of the Interaction Operators	
D. Projection of the Total Pion-Nucleus Wavefunction onto the Nuclear Ground State	
E. Summation of the Series of Multiple Scattering Terms	
F. Formation of the Optical Model Potential	
IV. ANALYSIS OF PION-NUCLEUS INTERACTION DATA . . . . .	67
V. SUMMARY AND CONCLUSIONS . . . . .	72

APPENDICES	Page
A. Derivation of the Pion-Nucleon and Pion-Nucleon-Pair Interaction Operators in Terms of the Partial Wave Amplitudes . . . . .	75
B. Averages over Nucleon Scattering Operators . . . . .	94
C. Nucleon-Pair Correlation Length for an Ideal Fermi Gas of Nucleons . . . . .	96
D. Nuclear Density Parameters for Pions from Electron-Nucleus Scattering Data . . . . .	104
E. Vacuum Polarization Contributions to Pionic Atom Energy Levels . . . . .	113
F. Method of Solving the Klein-Gordon Equation for Pionic Atoms . . . . .	118
G. Fortran Computer Program for Solving the Klein-Gordon Equation for Pionic Atoms . . . . .	133
H. Method for Determining the Phase Shifts and the Differential Scattering Cross Section for Elastic Scattering . . .	173
I. A Procedure for Averaging the Theoretical Differential Scattering Cross Section over the Finite Angular Resolution of a Physical Detector . . . . .	176
J. Procedure for Fermi-Averaging the Pion-Nucleon Interaction Amplitudes . . . . .	179
K. Coordinate Transformation from the Laboratory to the Barycentric Frame of Reference . . . . .	181
L. Method of Solving the Klein-Gordon Equation for Pion-Nucleus Scattering . . . . .	184
M. Fortran Computer Program for Solving the Klein-Gordon Equation for Pion-Nucleus Scattering and Calculating the Elastic Differential Scattering Cross Section . . . . .	191
N. Evaluation of the Invariant Amplitude for Pion-Nucleon Scattering in the Pion-Nucleus CM System . . . . .	227
REFERENCES . . . . .	351

## ACKNOWLEDGMENTS

With great respect I would like to acknowledge my thesis advisor, Dr. William J. Kossler. He very graciously accepted the responsibility of advising my thesis when it was already well advanced. Wisely he expanded the scope of the thesis to include not only pionic atoms but also pion-nucleus interactions at low and intermediate energies. Without his encouragement and concern this work would never have reached its present state of completion and significance. Also, I would like to acknowledge Dr. Morton Eckhause for originally suggesting this research problem to me.

Many other people have contributed to my understanding of various aspects of the problem of pion-nucleus interactions and the way to properly analyze data. It is not possible to name everyone, but I would like to acknowledge the following: Dr. Judah M. Eisenberg and his group at the University of Virginia for help in the numerical analysis of pionic atom data; Dr. Edward A. Remler for the use of his general least square fitting program SEEK2 which turned out to be very useful in overcoming the problem of strong correlation of fitting parameters for pion-nucleus scattering; Dr. Raymond W. Southworth for suggesting the quasilinearization method to determine the parameter values in the optical potential for pionic atoms; and Dr. Hans C. von Baeyer for helpful discussions on various aspects of pion theory.

Finally, I would like to acknowledge the nuclear physics group at the Catholic University of America, consisting of Dr. Carl W. Wertz,

Dr. Hall L. Crannell, Dr. Herbert Uberall, and Dr. Francesco Cannata,  
for their expert advice on nearly every aspect of this work, and the  
privilege of continuing to work on pion-nucleus interactions with their  
group.

LIST OF TABLES

Table	Page
1. Low Energy S-Wave $\pi N$ Scattering Lengths . . . . .	238
2. Low Energy P-Wave $\pi N$ Scattering Lengths . . . . .	239
3. Low Energy S-Wave $\pi NN$ Scattering Lengths . . . . .	240
4. Low Energy P-Wave $\pi NN$ Scattering Lengths . . . . .	241
5. Summary of Data for Pionic $2p-1s$ Transitions . . . . .	242
6. Summary of Data for Pionic $3d-2p$ Transitions . . . . .	244
7. Summary of Data for Pionic $4f-3d$ Transitions . . . . .	247
8. Summary of Data for Pionic $5g-4f$ Transitions . . . . .	250
9. Elastic Differential Scattering Cross Section Data in the Pion-Nucleus CM for $\pi^+$ on ${}^4\text{He}$ at 24 MeV Pion Kinetic Energy in the Lab . . . . .	251
10. Elastic Differential Scattering Cross Section Data in the Pion-Nucleus CM for $\pi^+$ on ${}^4\text{He}$ at 51 MeV Pion Kinetic Energy in the Lab . . . . .	252
11. Elastic Differential Scattering Cross Section Data in the Pion-Nucleus CM for $\pi^+$ on ${}^4\text{He}$ at 60 MeV Pion Kinetic Energy in the Lab . . . . .	253
12. Elastic Differential Scattering Cross Section Data in the Pion-Nucleus CM for $\pi^+$ on ${}^4\text{He}$ at 68 MeV Pion Kinetic Energy in the Lab . . . . .	254
13. Elastic Differential Scattering Cross Section Data in the Pion-Nucleus CM for $\pi^+$ on ${}^4\text{He}$ at 75 MeV Pion Kinetic Energy in the Lab . . . . .	255
14. Elastic Differential Scattering Cross Section Data in the Pion-Nucleus CM for $\pi^-$ on ${}^4\text{He}$ at 110 MeV Pion Kinetic Energy in the Lab . . . . .	256
15. Elastic Differential Scattering Cross Section Data in the Pion-Nucleus CM for $\pi^-$ on ${}^4\text{He}$ at 150 MeV Pion Kinetic Energy in the Lab . . . . .	257

Table	Page
16. Elastic Differential Scattering Cross Section Data in the Pion-Nucleus CM for $\pi^-$ on ${}^4\text{He}$ at 153 MeV Pion Kinetic Energy in the Lab . . . . .	258
17. Elastic Differential Scattering Cross Section Data in the Pion-Nucleus CM for $\pi^-$ on ${}^4\text{He}$ at 180 MeV Pion Kinetic Energy in the Lab . . . . .	259
18. Elastic Differential Scattering Cross Section Data in the Pion-Nucleus CM for $\pi^-$ on ${}^4\text{He}$ at 220 MeV Pion Kinetic Energy in the Lab . . . . .	260
19. Elastic Differential Scattering Cross Section Data in the Pion-Nucleus CM for $\pi^-$ on ${}^4\text{He}$ at 260 MeV Pion Kinetic Energy in the Lab . . . . .	261
20. Elastic Differential Scattering Cross Section Data in the Pion-Nucleus CM for $\pi^-$ on ${}^{12}\text{C}$ at 27.8 MeV Pion Kinetic Energy in the Lab . . . . .	262
21. Elastic Differential Scattering Cross Section Data in the Pion-Nucleus CM for $\pi^+$ on ${}^{12}\text{C}$ at 30.2 MeV Pion Kinetic Energy in the Lab . . . . .	263
22. Elastic Differential Scattering Cross Section Data in the Pion-Nucleus CM for $\pi^+$ on ${}^{12}\text{C}$ at 31.5 MeV Pion Kinetic Energy in the Lab . . . . .	264
23. Elastic Differential Scattering Cross Section Data in the Pion-Nucleus CM for $\pi^+$ on ${}^{12}\text{C}$ at 40 MeV Pion Kinetic Energy in the Lab . . . . .	265
24. Elastic Differential Scattering Cross Section Data in the Pion-Nucleus CM for $\pi^+$ on ${}^{12}\text{C}$ at 62 MeV Pion Kinetic Energy in the Lab . . . . .	266
25. Elastic Differential Scattering Cross Section Data in the Pion-Nucleus CM for $\pi^-$ on ${}^{12}\text{C}$ at 62 MeV Pion Kinetic Energy in the Lab . . . . .	267
26. Elastic Differential Scattering Cross Section Data in the Pion-Nucleus CM for $\pi^-$ on ${}^{12}\text{C}$ at 69.5 MeV Pion Kinetic Energy in the Lab . . . . .	268
27. Elastic Differential Scattering Cross Section Data in the Pion-Nucleus CM for $\pi^-$ on ${}^{12}\text{C}$ at 80 MeV Pion Kinetic Energy in the Lab . . . . .	269
28. Elastic Differential Scattering Cross Section Data in the Pion-Nucleus CM for $\pi^-$ on ${}^{12}\text{C}$ at 87.5 MeV Pion Kinetic Energy in the Lab . . . . .	270

Table	Page
29. Elastic Differential Scattering Cross Section Data in the Pion-Nucleus CM for $\pi^-$ on $^{12}\text{C}$ at 120 MeV Pion Kinetic Energy in the Lab . . . . .	271
30. Elastic Differential Scattering Cross Section Data in the Pion-Nucleus CM for $\pi^-$ on $^{12}\text{C}$ at 150 MeV Pion Kinetic Energy in the Lab . . . . .	273
31. Elastic Differential Scattering Cross Section Data in the Pion-Nucleus CM for $\pi^-$ on $^{12}\text{C}$ at 180 MeV Pion Kinetic Energy in the Lab . . . . .	274
32. Elastic Differential Scattering Cross Section Data in the Pion-Nucleus CM for $\pi^-$ on $^{12}\text{C}$ at 200 MeV Pion Kinetic Energy in the Lab . . . . .	275
33. Elastic Differential Scattering Cross Section Data in the Pion-Nucleus CM for $\pi^-$ on $^{12}\text{C}$ at 230 MeV Pion Kinetic Energy in the Lab . . . . .	276
34. Elastic Differential Scattering Cross Section Data in the Pion-Nucleus CM for $\pi^-$ on $^{12}\text{C}$ at 260 MeV Pion Kinetic Energy in the Lab . . . . .	277
35. Elastic Differential Scattering Cross Section Data in the Pion-Nucleus CM for $\pi^-$ on $^{12}\text{C}$ at 280 MeV Pion Kinetic Energy in the Lab . . . . .	279
36. Elastic Differential Scattering Cross Section Data in the Pion-Nucleus CM for $\pi^+$ on $^{16}\text{O}$ at 30 MeV Pion Kinetic Energy in the Lab . . . . .	280
37. Elastic Differential Scattering Cross Section Data in the Pion-Nucleus CM for $\pi^-$ on $^{16}\text{O}$ at 87.5 MeV Pion Kinetic Energy in the Lab . . . . .	281
38. Elastic Differential Scattering Cross Section Data in the Pion-Nucleus CM for $\pi^-$ on $^{16}\text{O}$ at 160 MeV Pion Kinetic Energy in the Lab . . . . .	282
39. Elastic Differential Scattering Cross Section Data in the Pion-Nucleus CM for $\pi^-$ on $^{16}\text{O}$ at 170 MeV Pion Kinetic Energy in the Lab . . . . .	283
40. Elastic Differential Scattering Cross Section Data in the Pion-Nucleus CM for $\pi^-$ on $^{16}\text{O}$ at 220 MeV Pion Kinetic Energy in the Lab . . . . .	284
41. Elastic Differential Scattering Cross Section Data in the Pion-Nucleus CM for $\pi^-$ on $^{16}\text{O}$ at 230 MeV Pion Kinetic Energy in the Lab . . . . .	285

Table	Page
42. Elastic Differential Scattering Cross Section Data in the Pion-Nucleus CM for $\pi^-$ on $^{16}\text{O}$ at 240 MeV Pion Kinetic Energy in the Lab . . . . .	286
43. Elastic Differential Scattering Cross Section Data in the Pion-Nucleus CM for $\pi^+$ on $^{16}\text{O}$ at 270 MeV Pion Kinetic Energy in the Lab . . . . .	287
44. Elastic Differential Scattering Cross Section Data in the Pion-Nucleus CM for $\pi^-$ on $^{40}\text{Ca}$ at 205 MeV Pion Kinetic Energy in the Lab . . . . .	288
45. Elastic Differential Scattering Cross Section Data in the Pion-Nucleus CM for $\pi^-$ on $^{40}\text{Ca}$ at 215 MeV Pion Kinetic Energy in the Lab . . . . .	289
46. Shift in Energy Levels of Pionic Atoms Due to Vacuum Polarization . . . . .	290

## LIST OF FIGURES

Figure	Page
1. Deduced Values of " $b_0$ " from Analyzing Pionic Atom X-Ray Transition Data vs. Atomic Number . . . . .	291
2. Deduced Values of " $c_0$ " from Analyzing Pionic Atom X-Ray Transition Data vs. Atomic Number . . . . .	292
3. Deduced Values of "B" from Analyzing Pionic Atom X-Ray Transition Data vs. Atomic Number . . . . .	293
4. Deduced Values of "C" from Analyzing Pionic Atom X-Ray Transition Data vs. Atomic Number . . . . .	294
5. Plot of Distorted and Undistorted Pionic Atom 1s Bound State Wavefunctions for $^{16}\text{O}$ . . . . .	295
6. Plot of Local and Nonlocal Real Parts of the Optical Potential for $^{16}\text{O}$ . . . . .	296
7. Plot of Local and Nonlocal Imaginary Parts of Optical Potential for $^{16}\text{O}$ . . . . .	297
8. Plot of Distorted and Undistorted Pionic Atom 2p Bound State Wavefunctions for $^{40}\text{Ca}$ . . . . .	298
9. Real (" $b_0$ ") vs. $T_\pi$ for $^4\text{He}$ , $^{12}\text{C}$ , $^{16}\text{O}$ , and $^{40}\text{Ca}$ . . . . .	299
10. Imaginary (" $b_0$ ") vs. $T_\pi$ for $^4\text{He}$ , $^{12}\text{C}$ , $^{16}\text{O}$ , and $^{40}\text{Ca}$ . . . . .	300
11. Real (" $c_0$ ") vs. $T_\pi$ for $^4\text{He}$ , $^{12}\text{C}$ , $^{16}\text{O}$ , and $^{40}\text{Ca}$ . . . . .	301
12. Imaginary (" $c_0$ ") vs. $T_\pi$ for $^4\text{He}$ , $^{12}\text{C}$ , $^{16}\text{O}$ , and $^{40}\text{Ca}$ . . . . .	302
13. Fermi-averaged Value of Real ( $b_0$ ) vs. $T_\pi$ as Determined from Three Sets of $\pi N$ Phase Shifts . . . . .	303

Figure	Page
14. Fermi-averaged Value of Imaginary ( $b_0$ ) vs. $T_\pi$ as Determined from Three Sets of $\pi N$ Phase Shifts . . . . .	304
15. Fermi-averaged Value of Real ( $c_0$ ) vs. $T_\pi$ as Determined from Three Sets of $\pi N$ Phase Shifts . . . . .	305
16. Fermi-averaged Value of Imaginary ( $c_0$ ) vs. $T_\pi$ as Determined from Three Sets of $\pi N$ Phase Shifts . . . . .	306
17. Fermi-averaged Value of Real ( $d_0$ ) vs. $T_\pi$ as Determined from Three Sets of $\pi N$ Phase Shifts . . . . .	307
18. Fermi-averaged Value of Imaginary ( $d_0$ ) vs. $T_\pi$ as Determined from Three Sets of $\pi N$ Phase Shifts . . . . .	308
19. Predicted Elastic Differential Scattering Cross Section for $\pi^-$ on ${}^4\text{He}$ at 24 MeV . . . . .	309
20. Predicted Elastic Differential Scattering Cross Section for $\pi^+$ on ${}^4\text{He}$ at 24 MeV . . . . .	310
21. Predicted Elastic Differential Scattering Cross Section for $\pi^-$ on ${}^4\text{He}$ at 51 MeV . . . . .	311
22. Predicted Elastic Differential Scattering Cross Section for $\pi^+$ on ${}^4\text{He}$ at 51 MeV . . . . .	312
23. Predicted Elastic Differential Scattering Cross Section for $\pi^-$ on ${}^4\text{He}$ at 60 MeV . . . . .	313
24. Predicted Elastic Differential Scattering Cross Section for $\pi^+$ on ${}^4\text{He}$ at 60 MeV . . . . .	314
25. Predicted Elastic Differential Scattering Cross Section for $\pi^-$ on ${}^4\text{He}$ at 68 MeV . . . . .	315
26. Predicted Elastic Differential Scattering Cross Section for $\pi^+$ on ${}^4\text{He}$ at 68 MeV . . . . .	316

Figure	Page
27. Predicted Elastic Differential Scattering Cross Section for $\pi^-$ on ${}^4\text{He}$ at 75 MeV . . . . .	317
28. Predicted Elastic Differential Scattering Cross Section for $\pi^+$ on ${}^4\text{He}$ at 75 MeV . . . . .	318
29. Predicted Elastic Differential Scattering Cross Section for $\pi^-$ on ${}^4\text{He}$ at 110 MeV . . . . .	319
30. Predicted Elastic Differential Scattering Cross Section for $\pi^-$ on ${}^4\text{He}$ at 150 MeV . . . . .	320
31. Predicted Elastic Differential Scattering Cross Section for $\pi^-$ on ${}^4\text{He}$ at 153 MeV . . . . .	321
32. Predicted Elastic Differential Scattering Cross Section for $\pi^-$ on ${}^4\text{He}$ at 180 MeV . . . . .	322
33. Predicted Elastic Differential Scattering Cross Section for $\pi^-$ on ${}^4\text{He}$ at 220 MeV . . . . .	323
34. Predicted Elastic Differential Scattering Cross Section for $\pi^-$ on ${}^4\text{He}$ at 260 MeV . . . . .	324
35. Predicted Elastic Differential Scattering Cross Section for $\pi^-$ on ${}^{12}\text{C}$ at 27.8 MeV . . . . .	325
36. Predicted Elastic Differential Scattering Cross Section for $\pi^+$ on ${}^{12}\text{C}$ at 30.2 MeV . . . . .	326
37. Predicted Elastic Differential Scattering Cross Section for $\pi^+$ on ${}^{12}\text{C}$ at 31.5 MeV . . . . .	327
38. Predicted Elastic Differential Scattering Cross Section for $\pi^+$ on ${}^{12}\text{C}$ at 40 MeV . . . . .	328
39. Predicted Elastic Differential Scattering Cross Section for $\pi^+$ on ${}^{12}\text{C}$ at 62 MeV . . . . .	329

Figure	Page
40. Predicted Elastic Differential Scattering Cross Section for $\pi^-$ on $^{12}\text{C}$ at 62 MeV . . . . .	330
41. Predicted Elastic Differential Scattering Cross Section for $\pi^-$ on $^{12}\text{C}$ at 69.5 MeV . . . . .	331
42. Predicted Elastic Differential Scattering Cross Section for $\pi^-$ on $^{12}\text{C}$ at 80 MeV . . . . .	332
43. Predicted Elastic Differential Scattering Cross Section for $\pi^-$ on $^{12}\text{C}$ at 87.5 MeV . . . . .	333
44. Predicted Elastic Differential Scattering Cross Section for $\pi^-$ on $^{12}\text{C}$ at 120 MeV . . . . .	334
45. Predicted Elastic Differential Scattering Cross Section for $\pi^-$ on $^{12}\text{C}$ at 150 MeV . . . . .	335
46. Predicted Elastic Differential Scattering Cross Section for $\pi^-$ on $^{12}\text{C}$ at 180 MeV . . . . .	336
47. Predicted Elastic Differential Scattering Cross Section for $\pi^-$ on $^{12}\text{C}$ at 200 MeV . . . . .	337
48. Predicted Elastic Differential Scattering Cross Section for $\pi^-$ on $^{12}\text{C}$ at 230 MeV . . . . .	338
49. Predicted Elastic Differential Scattering Cross Section for $\pi^-$ on $^{12}\text{C}$ at 260 MeV . . . . .	339
50. Predicted Elastic Differential Scattering Cross Section for $\pi^-$ on $^{12}\text{C}$ at 280 MeV . . . . .	340
51. Predicted Elastic Differential Scattering Cross Section for $\pi^+$ on $^{16}\text{O}$ at 30 MeV . . . . .	341
52. Predicted Elastic Differential Scattering Cross Section for $\pi^-$ on $^{16}\text{O}$ at 87.5 MeV . . . . .	342

Figure	Page
53. Predicted Elastic Differential Scattering Cross Section for $\pi^-$ on $^{16}\text{O}$ at 160 MeV . . . . .	343
54. Predicted Elastic Differential Scattering Cross Section for $\pi^-$ on $^{16}\text{O}$ at 170 MeV . . . . .	344
55. Predicted Elastic Differential Scattering Cross Section for $\pi^-$ on $^{16}\text{O}$ at 220 MeV . . . . .	345
56. Predicted Elastic Differential Scattering Cross Section for $\pi^-$ on $^{16}\text{O}$ at 230 MeV . . . . .	346
57. Predicted Elastic Differential Scattering Cross Section for $\pi^-$ on $^{16}\text{O}$ at 240 MeV . . . . .	347
58. Predicted Elastic Differential Scattering Cross Section for $\pi^+$ on $^{16}\text{O}$ at 270 MeV . . . . .	348
59. Predicted Elastic Differential Scattering Cross Section for $\pi^-$ on $^{40}\text{Ca}$ at 205 MeV . . . . .	349
60. Predicted Elastic Differential Scattering Cross Section for $\pi^-$ on $^{40}\text{Ca}$ at 215 MeV . . . . .	350

## ABSTRACT

The purpose of this work is to derive an on-shell pion-nucleus optical model potential from multiple scattering theory in terms of  $\pi N$  and  $\pi NN$  interaction amplitudes and to demonstrate that this Kisslinger<sup>34</sup> type potential is adequate to satisfactorily describe pion-nucleus interaction data. The derivation of the potential leads naturally to a form of the Lorentz-Lorenz effect with contributions due to virtual charge exchange and virtual spin flip. Also the derivation properly accounts for some aspects of nucleon motion and includes relativistic kinematical factors like  $1 + E_{\pi}/m_N$ . Using the Fermi-averaged  $\pi N$  amplitudes of Donnachie and Shaw<sup>121</sup> and the calculated  $\pi NN$  amplitudes of Dover,<sup>20</sup> one finds that the potential qualitatively and quantitatively describes rather satisfactorily the pion-nucleus interaction data for  ${}^4\text{He}$ ,  ${}^{12}\text{C}$ ,  ${}^{16}\text{O}$ , and  ${}^{40}\text{Ca}$  for laboratory pion kinetic energy from 0-280 Mev.

**A DIRECT REACTION MULTIPLE SCATTERING PION-NUCLEUS OPTICAL MODEL POTENTIAL**

## CHAPTER I

### INTRODUCTION

This thesis derives an on-shell pion-nucleus strong interaction optical model potential from multiple scattering theory in the impulse approximation and demonstrates the capability of this Kisslinger<sup>34</sup>-type potential to describe pion-nucleus strong interactions over a wide energy range. By formulating the on-shell pion-nucleus optical potential in terms of the  $\pi N$  and  $\pi NN$  interaction amplitudes, one obtains an optical potential with no free parameters. The usefulness of the potential is checked by analyzing some recent experiments on pionic atoms<sup>1-7</sup> and some precise measurements of the pion-nucleus elastic differential scattering cross sections on  ${}^4\text{He}$ ,  ${}^{12}\text{C}$ ,  ${}^{16}\text{O}$ , and  ${}^{40}\text{Ca}$  at a variety of energies.<sup>8-14</sup>

The use of pions to study nuclei via the pion-nucleus interaction has developed slowly since the discovery of the pion in 1947. This has been largely due to experimental limitations. At first pion beams were low in intensity and poor in energy resolution. As a result the early experiments yielded poor statistics. Recently, however, much improved pionic atom experiments for a wide variety of nuclei have been performed at CERN<sup>7</sup> and SREL.<sup>1-4</sup> In addition to these very low energy experiments, some pion-nucleus elastic scattering experiments of good precision and angular resolution have been performed in the energy range 30-300 MeV for such nuclei as  ${}^4\text{He}$ ,  ${}^{12}\text{C}$ ,  ${}^{16}\text{O}$ , and  ${}^{40}\text{Ca}$ .<sup>8-14</sup> In the near future some of the new high intensity accelerators, the so-called "meson factories" such as LAMPF,<sup>15</sup> SIN,<sup>16</sup> Nevis,<sup>17</sup> and TRIUMF,<sup>18</sup> will

become operational with beam currents several orders of magnitude larger than those currently available. Then a large quantity of scattering data with good statistics will be taken for many nuclei, and it will be possible to study systematically the pion-nucleus differential scattering cross sections from nucleus to nucleus to see what effect the structure of the nucleus has on the scattering of pions.

In Chapter II a survey of the previous work on the pion-nucleus strong interaction optical model potential that is compatible with this work is presented. Section A covers the analysis of the early pion-nucleus scattering experiments. Section B deals with the absorption of pions by the nucleus. Section C summarizes the more recent work on pionic atoms.

A pion-nucleus optical model potential is developed in Chapter III using multiple scattering theory and the impulse approximation. This development, which is similar to that of Ericson and Ericson,<sup>19</sup> differs fundamentally from their work in that it sums the infinite series of multiple scattering equations assuming that only two nucleon correlations are important. The Ericsons truncate the series with an approximation that is strictly valid only for crystalline structures. Their quasi-crystalline approximation leads to a different form for the Lorentz-Lorenz effect than is obtained in this work. Hufner<sup>168</sup> has obtained a form for the Lorentz-Lorenz effect in agreement with this work.

Chapter IV contains an analysis of pionic atom x-ray transition data for  ${}^4\text{He}$ ,  ${}^{12}\text{C}$ ,  ${}^{16}\text{O}$ , and  ${}^{40}\text{Ca}$  using the optical model potential developed in Chapter III. The analysis indicates that inclusion of the two-nucleon correlations is sufficient to describe the experimentally observed pionic atom energy level shifts. Use of the predicted absorption

parameters for absorption on nucleon pairs by Dover<sup>20</sup> is sufficient to explain the discrepancy between the predicted and experimentally observed pionic atom energy level absorption rates as noted by many investigators.<sup>21-23</sup>

The elastic pion-nucleus differential cross sections for <sup>4</sup>He, <sup>12</sup>C, <sup>16</sup>O, and <sup>40</sup>Ca for various pion energies are also analyzed in Chapter IV. In this case the energy-dependent Fermi-averaged NN amplitudes of Donnachie and Shaw<sup>121</sup> are used in the potential and a differential cross section is predicted for each nucleus at each of the measured energies in the range 24-280 MeV. The predicted differential cross sections are in good agreement with the experimentally measured values if one normalizes the experimentally measured values to the theoretically predicted cross section.

This work is essentially an extension of the work of Auerbach, Fleming, and Sternheim<sup>24</sup> who analyzed the elastic pion-nucleus differential scattering cross sections up to 87.5 MeV. Taking into account only s- and p-wave parts of the pion-nucleon interaction, the present analysis indicates that the contributions for two-nucleon correlation effects like virtual charge exchange and virtual spin flip become less important with increasing energy. As a result the pion can only be used as a probe of the long range Pauli correlations at very low energy.

Chapter V gives a summary of the results obtained from analyzing the pionic atom data and the elastic pion-nucleus scattering data. The chapter concludes by enumerating the possible future applications of the optical potential for investigating other reaction processes.

The details of the method of analysis used in Chapter IV and a Fortran listing of the computer programs employed are given in the

appendices. In addition, appendices A and C contain explicit derivations of such important quantities as the  $TN$  and  $TNN$  scattering operators and the nucleon-pair correlation length for an ideal Fermi gas of nucleons. Appendix D gives the method of obtaining all the relevant nuclear density parameters for pions from the electron scattering nuclear charge density parameters.

## CHAPTER II

### PREVIOUS WORK ON THE PION-NUCLEUS STRONG INTERACTION POTENTIAL

#### A. Pion-Nucleus Scattering

The fundamental approach to the pion-nucleus strong interaction problem is given by the field theoretic method. Unfortunately no satisfactory Hamiltonian formalism for pion-nucleus interactions has been developed. Most of the work in the field has concentrated on the much simpler pion-nucleon interaction problem.

Despite the small progress of the purely field theoretic approaches to the pion-nucleus interaction, researchers have found it possible to describe the experimental pion-nucleus strong interaction data in terms of phenomenological pion-nucleus potentials. Recent theories leading to a phenomenological pion-nucleus potential have been predominantly direct reaction theories based on the impulse approximation, the optical model, and multiple scattering.<sup>25</sup>

A direct reaction is a reaction in which the incident particle reacts with only a part of the nucleus, while the rest remains undisturbed. In other words, a direct reaction involves only some of the degrees of freedom of the nucleus. A compound reaction, by contrast, involves many more degrees of freedom and proceeds more slowly. Direct reactions take place in times of the order of transit times of nucleons across nuclei, which are typically  $10^{-22}$  sec.

According to the impulse approximation the scattering amplitudes  $f_{2J,2T}$  for pions incident on free and bound groups of nucleons are the same except for kinematical factors due to one group being bound. From Goldberger and Watson's book <sup>26</sup> pp. 86 and 658 one sees from the Lorentz transformation of the T matrix that

$$(II-1) \quad \left(f_{2J,2T}\right)_{\text{bound}} \cong \frac{\left(1 + \frac{E_{\pi}}{M_{\text{group}}}\right)}{\left(1 + \frac{E_{\pi}}{M_{\text{Nuc}}}\right)} \left(f_{2J,2T}\right)_{\text{free}}$$

The two amplitudes are nearly the same due to the smallness of the pion mass compared to that of a nucleon or group of nucleons.

An optical model is one that is capable of describing the partial absorption and transmission of an incident wave or particle. The optical model leads to a complex potential for describing the scattering and absorption of some particle such as a pion by a nucleus. Usually the optical model potential represents the interaction in the elastic channel only, i.e. for the nucleus in its ground state with no transfer of energy from the incident particle. One of the first optical model calculations for pion-nucleus elastic scattering was performed in 1952 by Byfield et al. <sup>27</sup> in which they fitted 62 MeV  $\pi^-$  carbon elastic scattering data. The pion-nucleus interaction was represented by the complex potential

$$(II-2) \quad V(r) = \begin{cases} -V_0 - iW & r \leq R \\ 0 & r > R \end{cases}$$

where  $R = 1.37 A^{1/3} f$  is the uniform radius of the nucleus.

In multiple scattering theory the nucleus may be treated as a system containing elementary subsystems such as nucleons, nucleon pairs, alpha particles, etc. The interaction of the pion with the nucleus is

obtained by summing the interactions of the pion with the elementary subsystems being careful not to double count. This approach separates the elementary interaction problem from that of the structure of the nucleus. Using theoretical or experimental knowledge about the elementary interaction, one can gain information about the structure of the nucleus from pion-nucleus interaction data.

A multiple scattering formalism based on the Schroedinger equation has been developed by Watson and others.<sup>26</sup> In many multiple scattering theories the scattering operator  $\underline{T}$  is expressed in terms of two-body scattering operators  $\underline{t}_j$  which act only on the pion and the  $j$ -th elementary scatterer bound in the nucleus. The single scattering approximation for scattering from individual bound nucleons consists of taking

$$(II-3) \quad \underline{T} = \sum_{j=1}^A \underline{t}_j$$

where  $A$  is the number of nucleons in the nucleus. Watson et al.<sup>28,29</sup> show how to calculate the pion-nucleus potential from basic pion-nucleon scattering amplitudes in the single scattering approximation. The single scattering approximation may be considered as the lowest order contribution to a series of more complex interactions of the pion with the nucleus. It is the first term in the multiple scattering series.

The multiple scattering optical model pion-nucleus potential was first used to analyze elastic scattering data. Several attempts<sup>30,31</sup> were made in the years 1952-1956 to fit a complex square well optical model potential to the pion-nucleus scattering experiments for  $60 < T_\pi < 150$  MeV. All experienced the same difficulty, namely that while the differential cross section for small angles  $\Theta < 60^\circ$  could be fit

fairly well, the fit at larger angles was always too small.

Baker et al.<sup>32,33</sup> analyzed the data on scattering of 80 MeV pions by Li, C, and Al using a variety of local complex potentials with sharp and diffuse surface shapes. They found that even a local potential with the more realistic Woods-Saxon shape did not significantly improve the fit for the differential cross section for angles greater than  $60^\circ$ .

In order to improve the predicted differential scattering cross section at large angles Kisslinger<sup>34</sup> made a simple extension of Watson's single scattering approximation which is useful for low energy pion-nucleus scattering for which s- and p-wave pion-nucleon scattering dominate. He took into account the momentum dependence of the pion-nucleon interaction by writing the pion-nucleon scattering operator

$$(II-4) \quad \underline{t}(k', k) = \underline{t}_s + \underline{t}_p \underline{k} \cdot \underline{k}'$$

Using this one obtains an optical potential which has the configuration space form

$$(II-5) \quad V(r) \propto A_s e(r) - A_p \vec{\nabla} \cdot (e(r) \vec{\nabla})$$

where the gradient term gives rise to a nonlocal contribution.

Baker et al.<sup>32,33</sup> in analyzing their data in 1958 on scattering of 80 MeV pions did find that a nonlocal potential of the Kisslinger form with adjustable complex parameters for the strength of the volume and gradient terms predicted larger differential cross sections at large angles in substantially better agreement with the experimental data.

Three years later Edelman et al.<sup>35</sup> performed  $\pi^-$  elastic scattering experiments on carbon at 69.5 and 87.5 MeV and on oxygen at 87.5 MeV with improved energy resolution. They also found that the Kisslinger form of the potential with adjustable parameters was capable

of describing the scattering data at large angles.

Similar work by Valckx et al.<sup>36</sup> with  $\pi^+$  scattering on C and O at 87 MeV gave support to the Kisslinger form of the potential. The success of the Kisslinger form of the potential with adjustable parameters in fitting the differential cross section for large angles indicated the importance of the gradient terms derived from p-wave pion-nucleon scattering, but unfortunately these parameters could not be predicted in terms of the  $\pi N$  scattering amplitudes.

The work of Kisslinger was extended by Kerman and Logan<sup>37</sup> in 1964 to include elastic charge-exchange scattering, where the nucleus is scattered to various states of the isotopic multiplet of which the ground state of the target nucleus is a member. For the case of inelastic charge exchange the nucleus is scattered from one isotopic multiplet to another. Actually elastic charge exchange is not purely elastic, since there is a difference in energy in the various charge states of an isobar due to Coulomb effects, and the mass of the  $\pi^0$  is different from that of the charged pions.

Kerman and Logan's extension of Kisslinger's pion-nucleon scattering amplitude has the form

$$(II-6) \quad \underline{t}_i(\underline{k}, \underline{k}') = (A + B \underline{t}_\pi \cdot \underline{\tau}_i) + (C + D \underline{t}_\pi \cdot \underline{\tau}_i) \underline{k} \cdot \underline{k}'$$

where A, B, C, and D are functions of the s- and p-wave  $\pi N$  phase shifts and  $\underline{t}_\pi$  and  $\underline{\tau}_i$  are isotopic spin operators for the pion and the i-th nucleon respectively. The  $\underline{t}_\pi \cdot \underline{\tau}_i$  terms, which may be written in terms of isospin raising and lowering operators as

$$(II-7) \quad \underline{t}_\pi \cdot \underline{\tau}_i = \frac{t_+ \tau_- + t_- \tau_+}{2} + t_3 \tau_3$$

give rise to the elastic charge exchange scattering. With this extension one obtains an optical potential with the spatial form

$$(II-8) \quad V(r) \propto A' e_p(r) + B' e_n(r) + \nabla \cdot (C' e_p(r) \nabla) + \nabla \cdot (D' e_n(r) \nabla)$$

where  $e_p(r)$  is the proton density and  $e_n(r)$  is the neutron density. As a first approximation Kerman and Logan<sup>37</sup> assumed that the neutron and proton densities were the same. Then the potential may be written in the form

$$(II-9) \quad V(r) \propto \left( A + B \frac{z_n \cdot T}{N} \right) e(r) + \nabla \cdot \left\{ \left( C + D \frac{z_n \cdot T}{N} \right) e(r) \nabla \right\}$$

where  $T$  is the total isotopic spin of the nucleus,  $N$  is the number of nucleons, and  $e(r)$  is the nucleon density. This form is often used<sup>19,21-23</sup> in the analysis of pionic atom energy level shifts, and it describes the isotopic spin dependence of the data well.

In 1968 Chivers et al.<sup>38</sup> measured cross sections for single charge exchange ( $\pi^+, \pi^0$ ) at 180 MeV on several light nuclei. Because of the difficulty of detecting the  $\pi^0$  by means of its decay into two photons, they measured the cross section by an activation experiment in which the residual target nucleus state is identified by its radioactivity. From these measurements one notices that the ( $\pi^+, \pi^0$ ) cross section is largest where the final target has a bound state which is an isobaric analog of the initial state. This implies a favoring of  $\Delta T = 0$  elastic scattering.

In 1967 Auerbach et al.<sup>24</sup> made the first serious attempt to compare the parameters obtained from fitting elastic pion-nucleus differential scattering cross section data using an optical model potential of the Kisslinger form with that expected from  $\pi N$  scattering.

They obtained best fit parameters close to those predicted from  $\pi N$  phase shifts in the energy region  $24 < T_{\pi} < 87.5$  MeV.

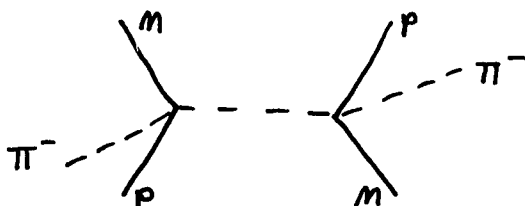
Three years later Krell and Barma<sup>39</sup> extended the analysis of Auerbach et al.<sup>24</sup> for C to the energy region  $120 < T_{\pi} < 280$  MeV. Their best fit parameters showed some deviations from those expected from  $\pi N$  phase shifts, but their fits to the differential cross sections<sup>24</sup> were poorer than those of Auerbach et al.

In 1972 Bercaw et al.<sup>14</sup> fit their differential scattering data for  $\pi^-$  on  $^{16}_0$  in the energy range  $160 < T_{\pi} < 240$  MeV. Their best fit parameters showed drastic deviations from those expected from  $\pi N$  phase shifts. They found that the parameters in the Kisslinger form of the potential are strongly correlated and not well determined by the data<sup>39</sup> contrary to the earlier work of Krell and Barma<sup>39</sup> and Auerbach et al.<sup>24</sup>

Brueckner<sup>40</sup> suggested in 1955 an effect which should also contribute to the pion-nucleus elastic scattering, particularly in the case of pionic atoms. He noted that nuclei absorb pions and that if a nucleus absorbed and subsequently emitted a slow pion, then the process would contribute to the elastic scattering amplitude. This effect had not been included in previous forms of the multiple scattering series, since the intermediate state of the system between absorption and emission contains no pion, and there was always one pion propagating through the system in previous forms of elastic multiple scattering theory.<sup>41</sup> Thouless<sup>41</sup> pointed out that it was also possible for the emission to occur before the absorption. In this case the intermediate state has two pions.<sup>40</sup> Brueckner<sup>40</sup> and Thouless<sup>41</sup> made estimates of the effect of absorption on the elastic scattering based on a simple model for absorption of the pion by two nucleons in a deuteron-like state in

the nucleus. They concluded that the absorptive process's contribution to the elastic scattering amplitude could be as large as the absorption amplitude itself.

In 1969 Kroll and Ericson,<sup>21</sup> following the suggestion of Drell,<sup>42</sup> Lipkin, and de Shalit,<sup>42</sup> introduced a type of double charge exchange called virtual charge exchange. This process may be represented by



where the pion interacts with two closely correlated nucleons. The virtual charge exchange term makes a significant contribution to the local part of the pion-nucleus potential.

In addition to the term for virtual charge exchange, Ericson and Ericson<sup>19</sup> introduced in 1966 a double scattering term to represent coherent scattering from two correlated nucleons. This double scattering term taken together with that of the virtual charge exchange gives rise to a contribution to the local part of the optical model potential proportional to

$$(II-10) \quad \xi^2 (A^2 + B^2) e^2(r)$$

where the  $B^2$  term is due to virtual charge exchange and  $\xi^2$  is the average nucleon-pair correlation length.

Following the observation of Kroll<sup>43</sup> that the derivation of the Kisslinger form of the pion-nucleus potential by Baker et al.<sup>33</sup> with arguments which were classical in nature should lead to results analogous to electric dipole scattering in a polarizable medium,

the Ericsons obtain for the nonlocal part of the optical potential a nonlinear dependence on the density of scatterers giving rise to a contribution proportional to

$$(II-11) \quad \nabla \cdot \left[ \frac{(C + D \frac{t_{n \cdot T}}{N}) e(r)}{1 + \frac{4\pi}{3} \eta (C + D \frac{t_{n \cdot T}}{N}) e(r)} \right] \nabla$$

where the correlation parameter  $\eta$  is a measure of the polarization of the medium. For a medium of uniformly smoothly distributed protons and neutrons  $\eta = 0$ , but the granular structure of nuclear matter leads to  $\eta \neq 0$  such that very short range anti-correlations between nucleons result in  $\eta = 1$ .

In order to obtain an optical model potential like those above one needs the elementary  $\pi N$  scattering amplitudes. These amplitudes may be measured experimentally or obtained from theory. There are two dynamical approaches, not based on Hamiltonians, which have been used to predict the  $\pi N$  scattering amplitudes. One is dispersion theory which has been reviewed by Hamilton.<sup>44</sup> Dispersion relation theory is important, because it provides one with methods which make it possible to treat the dynamics of strong interaction. The other dynamical approach which has been applied to low energy pion-nucleon scattering is Current Algebra theory and the "soft pion" approximations. It is important for pion-nucleon scattering, because it gives a reasonable prediction for the s-wave pion-nucleon scattering amplitudes. The Current Algebra theory has been reviewed by Adler and Dashen.<sup>45</sup>

## B. Pion-Nucleus Absorption at Very Low Energy

Most of the theoretical work on pion-nucleus absorption as a direct reaction at very low energy has been confined to a model in which two nucleons in the nucleus absorb the pion, share the rest energy between them, and leave the residual nucleus without scattering from it. This model was used by Brueckner, Serber, and Watson<sup>47</sup> in 1951 to relate the absorption probability to two-nucleon structure in the nucleus. They suggested that the two-nucleon absorption process requires such a close correlation of two nucleons in the nucleus that they must be in relative s-states.

Some direct evidence on the two-nucleon emission following pion absorption was first obtained in 1960 by Ozaki et al.<sup>48</sup> who observed the n-n and n-p pairs from stopped  $\pi^-$  absorbed in C and Al. Using counters which were sensitive to neutrons with  $E_n > 10$  MeV and protons with  $22 < E_p < 112$  MeV, they found that n-n pairs were more probable than n-p pairs by a ratio of  $3.9 \pm 1.2$  in Al and  $5.0 \pm 1.5$  in C.

In 1968 Nordberg, Kinsey, and Burman<sup>49</sup> investigated the nucleon pairs emitted when a beam of  $\pi^-$  was stopped in a variety of light nuclei using an apparatus similar to that of Ozaki et al.<sup>48</sup> but with much improved angular resolution. The relative angular distribution of the two nucleons emitted in the subsequent pion absorption was measured and found to peak at  $180^\circ$  supporting the two-nucleon model of the absorption process. However these emissions were found to account for less than half of the total absorption. Also Nordberg et al.<sup>49</sup> found that within the limit of their energy resolution the spectra of the

emitted nucleons were not sensitive to details in the nuclear structure of the target nuclei. It may be that final state interactions account for the loss of emitted pairs and the loss of information related to the nuclear structure of the target nuclei. Bertini<sup>50</sup> noted from a study of  $\pi^-$  nucleus absorption data that the ratio of emitted n-n to n-p pairs upon pion absorption is considerably different from the ratio of n-p to p-p pairs that initially absorb the  $\pi^-$ , indicating a masking of the original nuclear structure by the final state interactions. The effect of the final state interactions can be removed by performing a simultaneous total energy measurement on the two emitted nucleons in addition to demanding coincidence.

The existence of final state interactions is also supported by the work of Anderson et al.<sup>51</sup> in which they obtained neutron spectra for  $1.8 < E_n < 150$  MeV using time-of-flight counters for stopped  $\pi^-$  absorbed by C, Al, Cd, Pb, and U. The mean number of neutrons emitted per absorption in the energy range 1.8 to 150 MeV was measured to be  $2.8 \pm 0.3$ ,  $3.2 \pm 0.3$ ,  $3.6 \pm 0.4$ ,  $3.5 \pm 0.4$ , and  $5.0 \pm 0.5$  for C, Al, Cd, Pb, and U respectively. They found that the emitted neutron energy spectra are characterized by a low-energy "evaporation" part and a high energy part due to "direct" neutron emission. This description is derived from the notion<sup>52-55</sup> that the capture of stopped  $\pi^-$  mesons in complex nuclei is a two step process. First the  $\pi^-$  is captured by a pair of nucleons. Then the two nucleons share the pion's rest energy and initiate nuclear cascades in which one or more nucleons are ejected by direct emission. The energy that is not carried away by the direct emission is distributed among the remaining nucleons, raising the residual nucleus to a high temperature from which it deexcites by

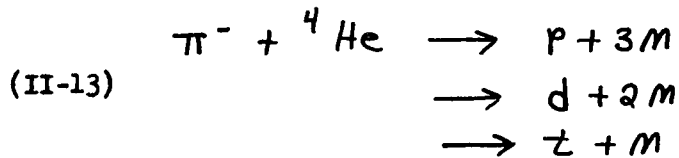
evaporating particles. Rosen<sup>56</sup> has found experimental support for the notion of a nucleon evaporation spectrum from his study of neutron emission from selected nuclei bombarded with 14 MeV neutrons. A good review of the evidence for neutron evaporation spectra from low energy neutron scattering experiments has been written by LeCouteur.<sup>57</sup>

Weisskopf<sup>58</sup> suggested that the evaporation from a nucleus in a given state of excitation should follow a Maxwellian distribution law with a temperature appropriate for the density of levels in the residual nucleus. However in an evaporation cascade in which several nucleons are emitted in series, the nucleus should cool appreciably with the emission of each particle, and consequently the energy spectrum should deviate from the Maxwellian form. LeCouteur<sup>59,60</sup> has derived a formula for the spectra at very low energies based on an improved statistical theory of emission of neutrons by evaporation from a nucleus of temperature  $\Theta$

$$(II-12) \quad N(E_N) \propto E_N^{5/11} e^{-E_N/\Theta}$$

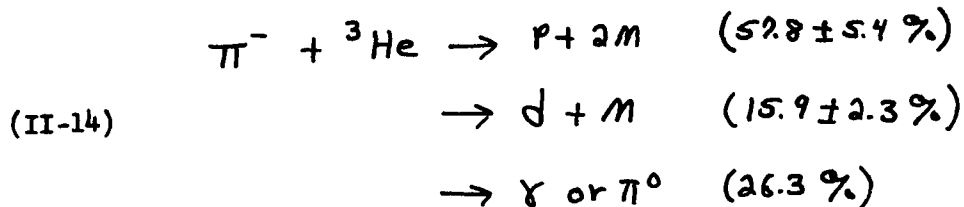
Anderson et al.<sup>51</sup> fit their data with values of  $\Theta$  ranging from 1.78 to 4.02 MeV, where  $\Theta$  represents approximately the mean excitation energy per nucleon for a nucleus in equilibrium after absorbing the pion. After Anderson et al.<sup>51</sup> subtracted this evaporation spectrum from the experimental spectrum, the mean number of neutrons emitted per pion absorption was reduced to approximately 2 for all nuclei.

Another type of experiment that has been done to see if there is some other process for pion absorption at very low energy besides absorption on pairs involves looking at the heavier particles emitted upon absorption. In particular for  $\pi^-$  absorption by  ${}^4\text{He}$  the nonradiative possibilities are



The last possibility is a two-body breakup, so the triton has a unique energy. For the p and d cases the energies of the charged particles are distributed smoothly. Thus in the charged particle energy spectrum the triton branch appears as a sharp peak on a smooth background of protons and deuterons. <sup>61</sup>Amiraju and Lederman used this idea and looked for tritons. They found few triton events and consequently assigned a branching ratio of 1/60 for this mode of absorption. Schiff <sup>62</sup>et al. performed a hydrogen bubble chamber experiment on dissolved <sup>4</sup>He and found a large triton peak with branching ratio 1/3. In order to resolve the discrepancy between these two experiments Bizzari <sup>63</sup>et al. and Bloch <sup>64</sup>et al. performed very precise <sup>4</sup>He bubble chamber experiments to obtain triton branching ratios of  $18.4 \pm 1.4 \%$  and  $19.4 \pm 1.8 \%$  respectively.

In a similar vein Zaimidoroga <sup>65</sup>et al. measured the branching ratios for <sup>3</sup>He obtaining



A  $\pi^-$  absorption experiment on nuclei in emulsion (C,N,O,Ag,Br) <sup>66</sup>has been performed by Vaisenberg et al. in which the emitted protons, deuterons, and tritons were separated and their energy spectra crudely measured. The branching ratios for p, d, and t were measured for

absorption at rest in the light nuclei (C,N,O) and in the heavy nuclei (Ag,Br). The large branching ratios obtained for emission of d and t have been interpreted by Shapiro and Kolybasov<sup>67</sup> and Kolybasov<sup>68,69</sup> as evidence for direct pion absorption on virtual alpha particles in the nucleus. Thus the process of pion absorption at low energy on pairs of nucleons is complicated by the possibility of pion absorption on virtual alpha particles and other clusters in the nucleus.

<sup>70</sup>Eckstein first suggested a model for handling pion absorption on nucleon pairs in which the unknown short range nucleon-nucleon correlation is simply replaced by some specific short-range function such as a delta function. In particular she assumed that the pion wave incident on nucleon pair ij is given by<sup>71</sup>

$$(II-15) \quad \psi^{i\dot{j}} |0\rangle = \psi(r) \delta(\vec{r} - \frac{\vec{r}_i + \vec{r}_j}{2}) \delta(\vec{r}_i - \vec{r}_j) |0\rangle$$

where  $|0\rangle$  represents the nuclear ground state and  $\vec{r}_i$  and  $\vec{r}_j$  are the positions of the i-th and j-th nucleons respectively. For s-wave absorption on nucleon pair ij, the scattering operator may be written in terms of the invariant products of the dynamical variables with the proper symmetry

$$(II-16) \quad \underline{f}_{ij}(r) = B_0 + B_1 \underline{\sigma}_i \cdot \underline{\sigma}_j + B_2 \underline{\tau}_i \cdot \underline{\tau}_j + B_3 (1 - \underline{\sigma}_i \cdot \underline{\sigma}_j) \underline{t}_\pi \cdot (\underline{\tau}_i + \underline{\tau}_j) \\ + B_4 (\underline{\sigma}_i \cdot \underline{\sigma}_j) (\underline{\tau}_i \cdot \underline{\tau}_j) + B_5 (1 - \underline{\sigma}_i \cdot \underline{\sigma}_j) [(\underline{t}_\pi \cdot \underline{\tau}_i) (\underline{t}_\pi \cdot \underline{\tau}_j) + (\underline{t}_\pi \cdot \underline{\tau}_j) (\underline{t}_\pi \cdot \underline{\tau}_i)]$$

where  $\underline{\sigma}_i$  is the Pauli spin operator for the i-th nucleon,  $\underline{\tau}_i$  is the isotopic spin operator for the i-th nucleon, and  $\underline{t}_\pi$  is the isotopic spin operator for the pion. The explicit relationship between the B's and the s-wave  $\pi$  NN amplitudes is derived in Appendix A. For a spin zero N = Z nucleus Eckstein's model for absorption gives rise to the

potential term

$$(II-17) \quad B_0 e^2(r)$$

where  $B_0$  is pure imaginary.

M. Ericson<sup>72</sup> extended Eckstein's model to include absorption of p-wave pions on correlated nucleons by adding a p-wave part to  $f_{ij}(r)$ , i. e.

$$(II-18) \quad \frac{k \cdot k'}{k^2} \left[ C_0 + C_1 \underline{v}_i \cdot \underline{v}_j + C_2 \underline{\pi}_i \cdot \underline{\pi}_j + C_3 (1 - \underline{v}_i \cdot \underline{v}_j) \underline{t}_i \cdot (\underline{\pi}_i + \underline{\pi}_j) \right. \\ \left. + C_4 (\underline{v}_i \cdot \underline{v}_j) (\underline{\pi}_i \cdot \underline{\pi}_j) + C_5 (1 - \underline{v}_i \cdot \underline{v}_j) [(\underline{t}_i \cdot \underline{\pi}_i)(\underline{t}_j \cdot \underline{\pi}_j) + (\underline{t}_i \cdot \underline{\pi}_j)(\underline{t}_j \cdot \underline{\pi}_i)] \right]$$

where the C's are explicit functions of the p-wave  $\pi$  NN amplitudes derived in Appendix A. For a spin zero  $N = Z$  nucleus, the work of Eckstein plus that of M. Ericson gives rise to the potential term in configuration space

$$(II-19) \quad B_0 e^2(r) + \nabla \cdot [C_0 e^2(r) \nabla]$$

This is essentially the form of the absorptive part of the optical potential that has been most extensively used in fitting to pionic atom data.<sup>19,21-23</sup>

### C. Pionic Atoms

Soon after the work on the pion-nucleus optical potential by Kisslinger<sup>34</sup> and others began to describe pion-nucleus elastic scattering with some success, an attempt was made to apply it to predicting the energy level shifts and widths of pionic atoms due to the strong interaction. The fact that the shifts and widths were small compared to the energy level spacing due to the electromagnetic interaction suggested that the strong interaction might be treated as a perturbation on the electromagnetic interaction. Deser et al.,<sup>73</sup> Brueckner,<sup>40</sup> and Ivanenko<sup>74</sup> and Pustovalov<sup>74</sup> tried to predict the strong interaction pionic atom energy level shifts and widths from the low energy  $\pi N$  scattering phase shifts using first order perturbation theory. In their predictions the energy level shifts and widths had a stronger atomic number dependence than the experimental shift and width data.<sup>30,31</sup> Seki and Cromer<sup>75</sup> were the first to point out that first-order perturbation theory is not valid, due to the strength of the strong interaction potential. The strong interaction potential has a small effect on the pionic atom energy levels, since only a small fraction of the pion wave function overlaps the effective interaction volume. However, the pion's wave function is significantly distorted in the vicinity of the nucleus. Since this is precisely the region where perturbation theory requires that the wave function not deviate significantly from the unperturbed value, perturbation theory is not applicable.

With the realization that perturbation theory was not valid for analyzing strong interaction shifts and widths, most investigators switched to solving the relativistic Schroedinger wave equation exactly

by numerical methods for the purpose of fitting and predicting pionic atom data. Those optical model potentials which are derived through the Schroedinger equation must be put into the relativistic Schroedinger or Klein-Gordon equation in such a way that the original Schroedinger equation is obtained in the nonrelativistic limit. Many investigators exhibit this placement by writing the relativistic wave equation in the form <sup>21,22</sup>

$$(II-20) \left[ \frac{\hbar^2}{2m_\pi} \nabla^2 + \frac{(E - V_{el}(r))^2}{2m_\pi c^2} - \frac{m_\pi c^2}{2} \right] \psi(r) = V_{st}(r) \psi(r)$$

where  $V_{el}(r)$  is the electromagnetic pion-nucleus potential,  $V_{st}(r)$  is the strong interaction pion-nucleus potential,  $m_\pi$  is the mass of the pion, and  $E$  is the total energy of the pion.

A common form of the pion-nucleus optical potential is that of the Ericsons'. <sup>19,21-23</sup> Krell and Ericson <sup>21</sup> found that their form of the potential predicted only half of the observed widths for all  $\ell = 0$  pionic atom levels.

Recently Blum <sup>76</sup> has proposed a different type of optical model based rather crudely on the microscopic picture of the scattering and absorption of pions by bound nucleons. The potential is constructed such that the real part simulates the elastic scattering of the pion by the nucleons. In analogy to the first order approximation of the multiple scattering theories, the real part of the potential is assumed to be proportional to the densities of the protons and neutrons. The imaginary part of the potential which must describe absorption of a pion by a correlated neutron-proton or proton-proton pair is taken proportional to the density of protons multiplied by the nuclear matter density. In order to allow for the possibility that the correlations

might be density dependent, a volume and a surface absorption term were introduced. Making a number of simplifying approximations for the densities and correlation properties affecting absorption, Blum obtains the potential

$$(II-21) \quad V_{ST}(r) = A s e(r) - i z A \left[ b^2 e^2(r) - a^2 \left( \frac{d e(r)}{d r} \right)^2 \right]$$

where  $A$  is the atomic number,  $Z$  is the number of protons in the nucleus,  $s$  is the strength of the elastic scattering potential,  $(de/dr)^2$  is the surface term resembling a p-wave contribution, and  $b$  and  $a$  are the strengths of the surface and volume absorption modes respectively. With this potential the pionic atom 2p-1s and 3d-2p data can be fitted as well as with the multiple scattering potentials.

Although Blum's potential gives rise to an attractively simple mathematical description of the pion-nucleus interaction, its usefulness is limited, because it is not directly related through a model to nuclear and nucleon properties.

CHAPTER III  
DEVELOPMENT OF AN OPTICAL MODEL POTENTIAL FROM A  
MULTIPLE SCATTERING THEORY

The multiple scattering method has been used extensively for a wide variety of problems. It has been applied to the scattering of molecules in gases,<sup>77</sup> neutron diffusion,<sup>78-80</sup> radiative equilibrium in stars,<sup>81,82</sup> scattering of charged particles,<sup>83</sup> scattering of gamma rays,<sup>84,85</sup> cosmic ray shower theory,<sup>86,87</sup> and the resistivity of conductors.<sup>88,89</sup>

Many of these problems have been treated using the Boltzmann integrodifferential equation for transport processes. The Boltzmann equation assumes that there are no correlations between the positions of the scatterers. In addition this approach is classical in that the wave nature of the incident particles is neglected. Such an approach is valid for wavelengths small compared to the separation between scatterers. For longer wavelengths a wave treatment is desirable, since the diffraction pattern will contain information about the correlation in scatterer positions.

The purpose of this chapter is to discuss systematically the multiple scattering of pion waves by a system of scatterers. Most of the notation comes from Iax<sup>91</sup> and Ericson and Ericson.<sup>19</sup> Similar discussions may be found in Goldberger and Watson<sup>26</sup> and in Hufner's<sup>169</sup> paper. Effects due to the correlation of nucleon pairs will be included explicitly.

### A. Validity of the Multiple Scattering Approach

The purpose of this section is to indicate qualitatively the assumptions that restrict the validity of the multiple scattering approach. Also the steps that will be taken to reduce the importance of these assumptions are indicated.

One assumption that is usually made in a multiple scattering problem is that the properties of the individual scatterers are unmodified by the fact that they are bound in a many particle system. It is possible to properly account for the main modification in scatterer properties by taking into account what is known as the chemical binding effect. Such a correction has been used in treating the scattering of neutrons by a molecule of ortho- or parahydrogen.<sup>90</sup> This same correction is applied to the interaction amplitudes in the development to follow.

Another assumption tacitly made in the multiple scattering treatment is that the scatterers move sufficiently slowly that their positions may be regarded as adiabatic parameters. With this assumption the scattered wave  $\Psi(\vec{r}; \vec{r}_1, \vec{r}_2, \dots, \vec{r}_N)$  can be computed for a fixed set of scatterer positions and then averaged over the distribution of scatterer positions in configuration space. The validity of this assumption depends on whether the velocity of the scatterer is small compared to the velocity of the wave. For nucleons the average momentum is approximately given by  $\sqrt{3/5}$  of the Fermi momentum  $P_f$  which is about 250 MeV/c for most nuclei. Thus the average nucleon velocity is

$$(III-1) \quad \overline{V_N} \cong \sqrt{3/5} P_f / M_N \cong .2 / c$$

Due to the large velocity of the nucleons this approximation that neglects the velocity of the nucleons is only weakly valid for even very high energy pion-nucleus scattering where  $v_{\pi} \approx c$ .

A further assumption implicit to the multiple scattering method is that the interaction of the projectile with the scatterers in the target is direct, i.e. there are no intermediate states in which the projectile is strongly correlated with the scatterers. In this work the contribution of such intermediate states is partially included by explicitly taking into account processes like virtual charge exchange.

One shortcoming of the multiple scattering method is that it does not conserve energy and momentum at each scattering in the same reference frame.

## B. Construction of the Multiple Scattering Equations

Let us assume that the single scattering problems for pions incident on the individual scatterers of the type found in the nucleus can be completely described in terms of experimentally measured amplitudes or phase shifts. Furthermore, let us assume that the structure of the nucleus may be expressed in terms of a many particle density function which is sensitive to correlations between the elementary scatterers.

Consider a system of scatterers whose centers are located at  $\vec{r}_1, \vec{r}_2, \dots, \vec{r}_n$ . Let the initial states of these scatterers be described by the set of parameters  $s_1, s_2, \dots, s_n$  where the parameter  $s_1$  is a shorthand notation for all the quantum numbers that describe the state of scatterer 1.

The probability that a set of  $n$  scatterers are located in a volume element  $dr_1^3 dr_2^3 \dots dr_n^3$  with states  $s_1, s_2, \dots, s_n$  is given by

$$(III-2) \quad P(\vec{r}_1, \vec{r}_2, \dots, \vec{r}_m; s_1, s_2, \dots, s_m) d^3r_1 d^3r_2 \dots d^3r_m$$

where

$$(III-3) \quad \sum_{s_1} \sum_{s_2} \dots \sum_{s_n} \int P(r_1, r_2, \dots, r_m; s_1, s_2, \dots, s_m) d^3r_1 d^3r_2 \dots d^3r_m = 1$$

The probability distribution for a single scatterer may be obtained by integrating over all other scatterers, i. e.

$$(III-4) \quad P(\vec{r}_1; s_1) = \sum_{s_2} \dots \sum_{s_m} \int P(\vec{r}_1, \vec{r}_2, \dots, \vec{r}_m; s_1, s_2, \dots, s_m) d^3r_2 \dots d^3r_m$$

and the probability for the simultaneous locations of a pair of scatterers is obtained by integrating over all but that pair of variables,

i. e.

$$(III-5) \quad P(\vec{r}_1, \vec{r}_2; s_1, s_2) = \sum_{s_3} \cdots \sum_{s_m} \int P(\vec{r}_1, \vec{r}_2, \dots, \vec{r}_m; s_1, s_2, \dots, s_m) \\ d^3r_3 \cdots d^3r_m$$

If the distribution is completely random, the particles are independent of one another. In this case the probabilities associated with a single particle are not influenced by information concerning other particles, i. e.

$$(III-6) \quad P(\vec{r}_1, \vec{r}_2, \dots, \vec{r}_m; s_1, s_2, \dots, s_m) = P(\vec{r}_1; s_1) P(\vec{r}_2; s_2) \cdots P(\vec{r}_m; s_m)$$

A measure of the correlation or nonrandomness between the pair of particles (1,2) is given by

$$(III-7) \quad P(\vec{r}_1, \vec{r}_2; s_1, s_2) - P(\vec{r}_1; s_1) P(\vec{r}_2; s_2)$$

For a nonrandom probability distribution one can factor the probability using conditional probabilities, i. e.

$$(III-8) \quad P(\vec{r}_1, \vec{r}_2, \dots, \vec{r}_m; s_1, s_2, \dots, s_m) = P(\vec{r}_1; s_1) P(\vec{r}_2, \dots, \vec{r}_m; \\ s_2, \dots, s_m)$$

where the conditional probability  $P(\vec{r}_1; s_1 \mid \vec{r}_2 \dots \vec{r}_n; s_2 \dots s_n)$  represents the distribution of particles 2, 3, ... n with the values of  $\vec{r}_1$  and  $s_1$  known or fixed. In a similar manner the pair distribution function may be factored out of the total distribution function to obtain

$$(III-9) \quad P(\vec{r}_1, \vec{r}_2, \dots, \vec{r}_m; s_1, s_2, \dots, s_m) = P(\vec{r}_1, \vec{r}_2; s_1, s_2) \cdot \\ P(\vec{r}_1, \vec{r}_2; s_1, s_2 \mid \vec{r}_3, \dots, \vec{r}_m; s_3, \dots, s_m)$$

These probability distributions may be converted to density distributions or correlations by multiplying by the appropriate power of the number of scatterers. For example

$$(III-10) \quad e(\vec{r}, s) = N_s P(r, s)$$

$$(III-11) \quad e(\vec{r}_1, \vec{r}_2; s_1, s_2) = N_{s_1} N_{s_2} P(\vec{r}_1, \vec{r}_2; s_1, s_2)$$

where  $e(r, s)$  is the density of scatterers of type  $s$  and  $e(\vec{r}_1, \vec{r}_2; s_1, s_2)$  is the density of scatterer pairs with quantum numbers  $s_1$  and  $s_2$ .

19

In the notation of Ericson and Ericson the total pion-nucleus wavefunction  $\underline{\Psi}(\hat{r}; \hat{r}_1, \hat{r}_2, \dots, \hat{r}_n; s_1, s_2, \dots, s_n)$  corresponding to both elastic and inelastic scattering of the pion can be written as

$$(III-12) \quad \underline{\Psi}(\vec{r}; \vec{r}_1, \vec{r}_2, \dots, \vec{r}_n; s_1, s_2, \dots, s_n) = \underline{\Psi}(\vec{r}; \vec{r}_1, \vec{r}_2, \dots, \vec{r}_n; s_1, s_2, \dots, s_n) |0\rangle$$

where  $|0\rangle$  refers to the nuclear ground state and  $\underline{\Psi}(\hat{r}; \hat{r}_1, \hat{r}_2, \dots, \hat{r}_n; s_1, s_2, \dots, s_n)$  is an operator which connects nuclear excited states to the ground state. This notation can be made more explicit by expanding the total pion-nucleus wavefunction in terms of a complete orthonormal set of wavefunctions  $\Psi_i(\hat{r}_1, \hat{r}_2, \dots, \hat{r}_n; s_1, s_2, \dots, s_n)$  describing the various states  $i$  of the target with energies  $\epsilon_i$ , i. e.

$$(III-13) \quad \underline{\Psi}(\vec{r}; \vec{r}_1, \vec{r}_2, \dots, \vec{r}_n; s_1, s_2, \dots, s_n) = \sum_i \Psi_i(\vec{r}; \vec{r}_1, \vec{r}_2, \dots, \vec{r}_n; s_1, s_2, \dots, s_n) \underline{\Psi}_i(\vec{r})$$

The  $i = 0$  term in this sum describes the target nucleus in its ground state with a pion of energy  $E$ . Following Ericson and Ericson this expansion may be cast into operator form, i. e.

$$(III-14) \quad \underline{\Psi}(\vec{r}; \vec{r}_1, \vec{r}_2, \dots, \vec{r}_n; s_1, s_2, \dots, s_n) = \sum_i \underline{\Psi}_i(\vec{r}) \Psi_i(\vec{r}_1, \vec{r}_2, \dots, \vec{r}_n; s_1, s_2, \dots, s_n) |0\rangle$$

where the  $\underline{\psi}_i(\vec{r}_1, \vec{r}_2, \dots, \vec{r}_n; s_1, s_2, \dots, s_n)$  are operators that connect the nuclear excited states to the ground state.

In a similar manner the incident wavefunction  $\underline{\Phi}(\vec{r}; \vec{r}_1, \vec{r}_2, \dots, \vec{r}_n; s_1, s_2, \dots, s_n)$  for the pion-nucleus system may be defined

$$(III-15) \quad \underline{\Phi}(\vec{r}; \vec{r}_1, \vec{r}_2, \dots, \vec{r}_m; s_1, s_2, \dots, s_m) = \sum_i \underline{\Phi}_i(\vec{r}) \underline{\phi}_i(\vec{r}_1, \vec{r}_2, \dots, \vec{r}_m; s_1, s_2, \dots, s_m) |0\rangle$$

where  $\underline{\phi}_i(\vec{r}_1, \vec{r}_2, \dots, \vec{r}_n; s_1, s_2, \dots, s_n)$  are operators that connect the nuclear excited states to the ground state. If initially the nucleus is in its ground state

$$(III-16) \quad \underline{\Phi}(\vec{r}; \vec{r}_1, \vec{r}_2, \dots, \vec{r}_m; s_1, s_2, \dots, s_m) = \underline{\Phi}_0(\vec{r}) \underline{\phi}_0(\vec{r}_1, \vec{r}_2, \dots, \vec{r}_m; s_1, s_2, \dots, s_m) |0\rangle \\ = \underline{\Phi}_0(\vec{r}) |0\rangle$$

91

This notation may be related to Lax's probability notation by projecting the incident pion-nucleus wavefunction onto the nuclear ground state, i. e.

$$(III-17) \quad \langle 0 | \underline{\Phi}(\vec{r}; \vec{r}_1, \vec{r}_2, \dots, \vec{r}_m; s_1, s_2, \dots, s_m) \\ = \langle 0 | \sum_i \underline{\Phi}_i(\vec{r}) \underline{\phi}_i(\vec{r}_1, \vec{r}_2, \dots, \vec{r}_m; s_1, s_2, \dots, s_m) |0\rangle \\ = \sum_{s_1} \dots \sum_{s_m} \int \underline{\Phi}_0(\vec{r}) P(\vec{r}_1 \dots \vec{r}_m; s_1 \dots s_m) d^3r_1 \dots d^3r_m \\ = \underline{\Phi}_0(\vec{r})$$

If the position and type of scatterer 1 is held fixed and all other scatterers averaged over, this is denoted by a subscript, i. e.

$$(III-18) \quad \langle 0 | \sum_i \underline{\Phi}_i(\vec{r}) \underline{\phi}_i(\vec{r}_1 \dots \vec{r}_m; s_1 \dots s_m) |0\rangle_1$$

$$\begin{aligned} &\equiv \sum_{s_2} \cdots \sum_{s_m} \int \underline{\Phi}_0(\underline{r}) P(\underline{r}_1, \dots, \underline{r}_m; s_1, \dots, s_m) d^3 r_2 \cdots d^3 r_m \\ &= \underline{\Phi}_0(\underline{r}) P(\underline{r}; s_1) \end{aligned}$$

Similarly if scatterers 1 and 2 are held fixed, then this is denoted by

$$(III-19) \quad \langle 0 | \underline{\Phi}_i(\underline{r}) \underline{\phi}_i(\underline{r}_1, \dots, \underline{r}_m; s_1, \dots, s_m) | 0 \rangle_{12}$$

$$\begin{aligned} &\equiv \sum_{s_3} \cdots \sum_{s_m} \int \underline{\Phi}_0(\underline{r}) P(\underline{r}_1, \dots, \underline{r}_m; s_1, \dots, s_m) d^3 r_3 \cdots d^3 r_m \\ &= \underline{\Phi}_0(\underline{r}) P(\underline{r}_1, \underline{r}_2; s_1, s_2) \end{aligned}$$

Now that the formalism for handling the probability density function has been defined, consider the multiple scattering equations. The total pion wave representing the incident wave plus the sum of the scattered waves from each of the scatterers is given by

$$\begin{aligned} (III-20) \quad \underline{\Psi}(\underline{r}; \underline{r}_1, \underline{r}_2, \dots, \underline{r}_m; s_1, \dots, s_m) &= \underline{\Psi}(\underline{r}; \underline{r}_1, \dots, \underline{r}_m; s_1, \dots, s_m) | 0 \rangle \\ &= \underline{\Phi}_0(\underline{r}) | 0 \rangle + \sum_{j=1}^A \int \underline{g}(\underline{r}; \underline{r}_1, \dots, \underline{r}_A; \underline{r}'; \underline{r}'_1, \dots, \underline{r}'_A; s_1, \dots, s_A) \\ &\quad \delta(\underline{r}'_j - \underline{r}') \delta s'_j s'_j \underline{f}_j(\underline{r}') \underline{\Psi}_j^{eff}(\underline{r}'; \underline{r}'_1, \dots, \underline{r}'_A; s'_1, \dots, s'_A) \\ &\quad | 0 \rangle d^3 r' \end{aligned}$$

where  $\underline{f}_j(\underline{r}')$  is the pion-nucleon interaction operator which is defined in section C of this chapter in terms of the experimentally measured pion-nucleon phase shifts. The delta functions specify the range of the interaction and insure that the scattering operator for the  $j$ -th nucleon gives no contribution unless it operates on the effective pion

wave incident on the  $j$ -th nucleon at the position of the  $j$ -th nucleon.

$\underline{g}(\vec{r}; \vec{r}_1, \vec{r}_2, \dots, \vec{r}_A; \vec{r}'_1, \vec{r}'_2, \dots, \vec{r}'_A; s_1, s_2, \dots, s_A)$  is a Green's function operator describing both the outgoing pion wave and the propagation of nuclear states. The Green's function may be defined for incident pions of energy  $E$  in terms of the nuclear states  $|m\rangle$  of energy  $\epsilon_m$  as<sup>19</sup>

$$(III-21) \quad \underline{g}(\vec{r}; \vec{r}_1, \dots, \vec{r}_A; \vec{r}'_1, \vec{r}'_2, \dots, \vec{r}'_A; s_1, \dots, s_A) = \sum_{\substack{m \\ m'}} g_m(\vec{r}, \vec{r}') |m\rangle \langle m'|$$

where  $g_n(\vec{r}, \vec{r}')$  is the pion Green's function at an energy  $E - \epsilon_n$ .

When no external potential acts on the pion, the pion's Green's function which satisfies the time independent Klein-Gordon equation has the form

$$(III-22) \quad g_m(\vec{r}, \vec{r}') = e^{ikm|\vec{r}-\vec{r}'|} / |\vec{r}-\vec{r}'|$$

where  $k_n^2 = (E - \epsilon_n)^2 - m_\pi^2$ .<sup>19,92</sup>

In a similar manner the effective wave incident on scatterer  $j$ , denoted by

$$(III-23) \quad \underline{\Psi}_j^{\text{eff}}(\vec{r}; \vec{r}_1, \dots, \vec{r}_A; s_1, \dots, s_A) = \underline{\Psi}_j^{\text{eff}}(\vec{r}; \vec{r}_1, \dots, \vec{r}_A; s_1, \dots, s_A) |0\rangle$$

is given by the sum of the incident wave plus the pion waves scattered from all the scatterers other than  $j$  under the condition that particle  $j$  with quantum numbers  $s_j$  is at  $\vec{r}_j$ , i. e.

$$(III-24) \quad \underline{\Psi}_j^{\text{eff}}(\vec{r}; \vec{r}_1, \dots, \vec{r}_A; s_1, \dots, s_A) = \underline{\Phi}_0(F^j) |0\rangle + \sum_{\substack{i=1 \\ i \neq j}}^A \int g(\vec{r}; \vec{r}_1, \dots, \vec{r}_A; \vec{r}''; \vec{r}_1'', \dots, \vec{r}_A''; s_1', \dots, s_A') \delta(\vec{r}'' - \vec{r}_i'') \delta s'' s_i'' \underline{\Psi}_{i;j}^{\text{eff}}(\vec{r}''; \vec{r}_1'', \dots, \vec{r}_A''; s_1'', \dots, s_A'') |0\rangle d^3 r''$$

Alternatively the effective wave incident on particle j may be written

$$(III-25) \quad \underline{\Psi}_j^{eff}(\vec{r}'; \vec{r}_1' \dots \vec{r}_A'; s_1' \dots s_A') |0\rangle = \underline{\Psi}(\vec{r}'; \vec{r}_1' \dots \vec{r}_A'; s_1' \dots s_A') |0\rangle$$

$$- \int \underline{g}(\vec{r}'; \vec{r}_1' \dots \vec{r}_A'; \vec{r}''; \vec{r}_1'' \dots \vec{r}_A''; s_1' \dots s_A') \delta(\vec{r}'' - \vec{r}_j'')$$

$$\delta s'' s_j'' \underline{f}_j(\vec{r}'') \underline{\Psi}_j^{eff}(\vec{r}''; \vec{r}_1'' \dots \vec{r}_A''; s_1'' \dots s_A'') d^3 r''$$

Equation (III-25) defines the effective wave incident on scatterer j to be just the total pion-nucleus wave minus the scattered wave from scatterer j.

Proceeding in this fashion one can construct a sequence of equations. The next equation would be for the scattered pion wave from particle i knowing that particle j is at  $\vec{r}_j$ , i. e.

$$(III-26) \quad \underline{\Psi}_{i;j}^{eff}(\vec{r}''; \vec{r}_1'' \dots \vec{r}_A''; s_1'' \dots s_A'') |0\rangle = \underline{\Phi}_0(\vec{r}'') |0\rangle$$

$$+ \sum_{\substack{k=1 \\ k \neq j}}^A \int \underline{g}(\vec{r}''; \vec{r}_1'' \dots \vec{r}_A''; \vec{r}'''; \vec{r}_1''' \dots \vec{r}_A'''; s_1'' \dots s_A'')$$

$$\delta(\vec{r}''' - \vec{r}_k''') \delta s''' s_k''' \underline{f}_k(\vec{r}''') \underline{\Psi}_{k;i;j}^{eff}(\vec{r}'''; \vec{r}_1''' \dots \vec{r}_A'''; s_1''' \dots s_A''')$$

$$|0\rangle d^3 r'''$$

This self-consistent method of handling wave scattering was first employed by Ewald <sup>93</sup> in order to treat the problem of the scattering of x-rays by dipole scatterers distributed on a lattice. The method of the self-consistent field assumes that a wave is emitted by each scatterer in a manner that is determined by the wave incident on

that scatterer, i. e. the effective wave. This effective wave is obtained by adding to the incident beam the waves emitted by all the other scatterers. The waves emitted by these scatterers are in turn influenced by the radiation emitted by the scatterer in question.

### C. Construction of the Interaction Operators

Before one can examine the multiple scattering equations above in detail, it is necessary to obtain an expression for the interaction operator for the pion incident on each type of scatterer in the nucleus. The interaction operator must be applicable to a bound elementary scatterer instead of a free one. In the impulse approximation these should be the same except for kinematical factors.

The effect of the nuclear binding has been investigated by <sup>94</sup>Rockmore in terms of the Born approximation. In the nonrelativistic plane wave Born approximation

$$(III-27) \quad \frac{d\sigma}{d\Omega} = |f(\theta)|^2 = \frac{\mu^2}{\hbar^4} \left| \frac{1}{2\pi} \int e^{i\mathbf{q}\cdot\mathbf{r}} V(\mathbf{r}) d^3r \right|^2$$

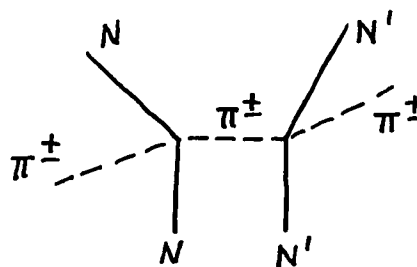
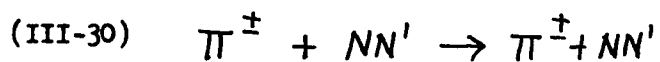
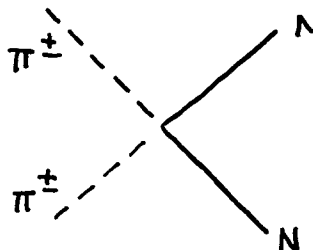
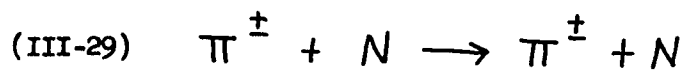
the scattering amplitude is proportional to the reduced mass of the incident particle and the target. Thus the scattering amplitude for a pion incident on a nucleon of mass  $m_N$  rigidly bound to a nucleus of mass  $m_{Nuc}$  is related to the scattering amplitude for a pion incident on a free nucleon by

$$(III-28) \quad \frac{(f_{\pi N})_{bound}}{(f_{\pi N})_{free}} = \frac{\mu_{Nuc}}{\mu_N} = \frac{1 + \frac{m_\pi}{m_N}}{1 + \frac{m_\pi}{m_{Nuc}}}$$

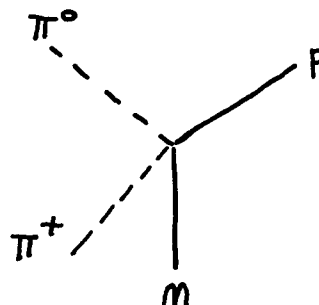
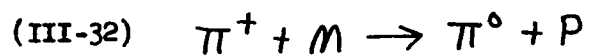
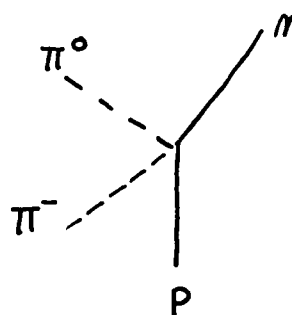
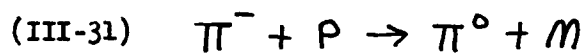
This result has been successfully used to describe the scattering of <sup>95</sup>neutrons from hydrogen molecules. The relativistic result according to Goldberger and Watson <sup>26</sup> was given in (II-1).

The basic processes or interactions involving one or two nucleons which the interaction operators should represent in order to completely describe pion-nucleon and pion-nucleon-pair interactions are as follows:

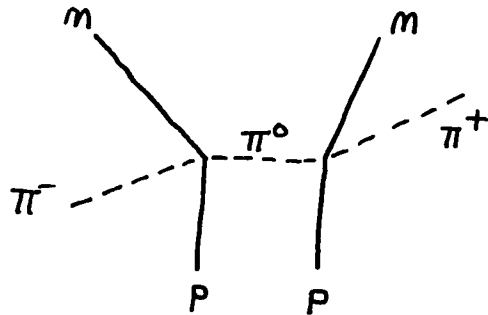
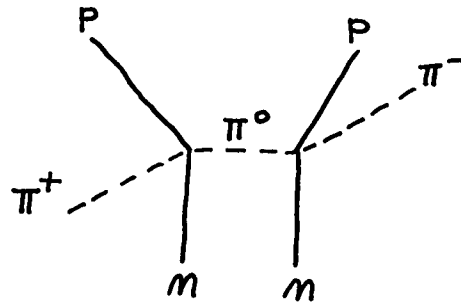
## ELASTIC SCATTERING



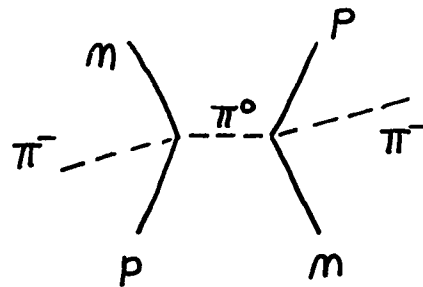
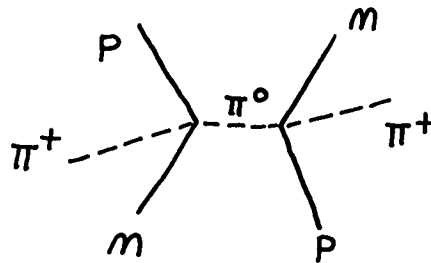
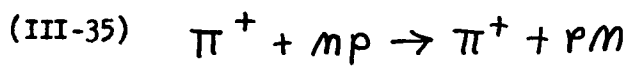
## SINGLE CHARGE EXCHANGE



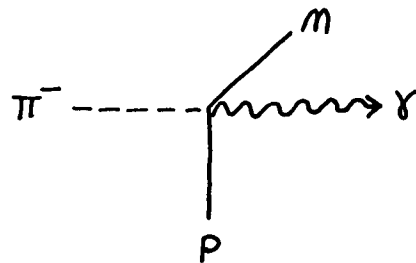
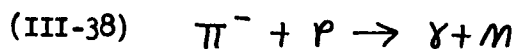
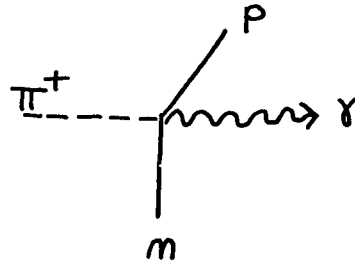
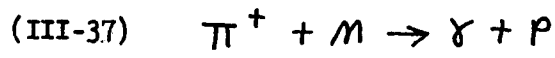
## DOUBLE CHARGE EXCHANGE



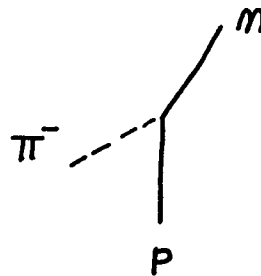
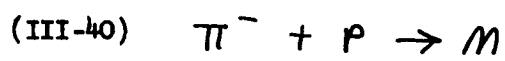
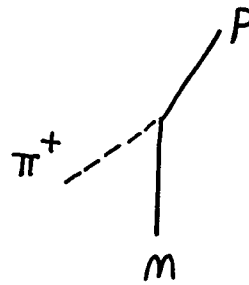
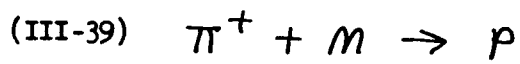
## VIRTUAL CHARGE EXCHANGE

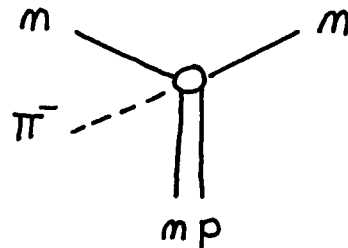
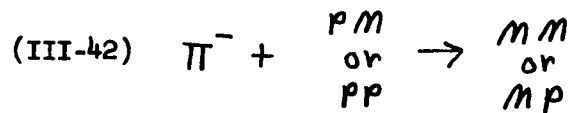
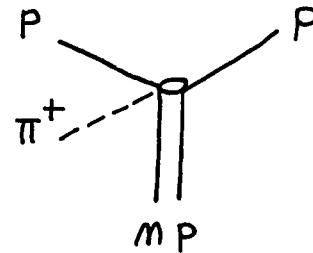
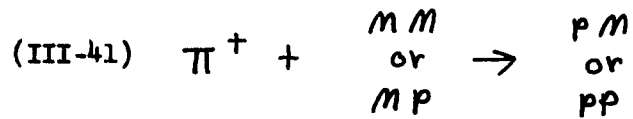


## RADIATIVE ABSORPTION



## ABSORPTION





Experimentally at very low energy ( $< 1$  MeV)<sup>96,97</sup> the contribution from single charge exchange, double charge exchange, and radiative absorption account for only a few percent of the total absorption for all but the lightest nuclei such as  $^1_1\text{H}$ <sup>98</sup> and  $^3_2\text{He}$ .<sup>65</sup> For very low energies the single and double charge exchange reactions are inhibited compared to the absorption on pairs due to the small amount of momentum phase space available for pion emission resulting from the small amount of energy released in the charge exchange reactions. The radiative pion absorption is an electromagnetic reaction which is expected to be much weaker than the strong interaction absorption processes. Panofsky, Aamodt, and Hadley<sup>97</sup> find  $\pi^-$  radiative absorption comparable in yield to the  $(\pi^-, \pi^0)$  charge exchange reaction at very low energy.

The absorption process can not occur on a free nucleon, because

energy and momentum can not be conserved in the process. It can occur, however, on a nucleon bound in a nucleus where the rest of the nucleus is available to help conserve momentum by taking up the recoil. In the impulse approximation the absorption process can be thought of as occurring on a single nucleon which has the proper Fermi momentum to conserve energy for the process. This type of process is represented by<sup>99</sup>



where the asterisk signifies that the product nucleus may be left in an excited state. The Fermi momentum required for this process is given by

$$(III-44) \quad P_f = \left[ 2 m_p (m_\pi c^2 - E_{ex} - W_p) \right]^{1/2}$$

where  $E_{ex}$  is the excitation energy of the product nucleus and  $W_p$  is the separation energy of the last proton. The momentum required is of the order 500 MeV/c, but the average Fermi momentum of a typical nucleus is 250 MeV/c.<sup>19</sup> Thus the capture of the pion on a single nucleon at very low energy should be an improbable process. One would expect the absorption of the pion on nucleon pairs to be more probable, since energy and momentum are easily conserved in this process.

In the following development the nucleon and nucleon pair will be considered as the principal elementary scatterers of the nucleus with which the pion interacts. For formulating a multiple scattering theory, it is convenient to characterize the interaction of the pion with the elementary scatterers in terms of experimentally measurable parameters such as interaction amplitudes or phase shifts.

For pion-nucleon scattering the interaction operator is conven-

iently expressed in terms of a partial wave expansion, since both the orbital angular momentum  $\ell$  and the total angular momentum  $J$  of the pion-nucleon system are conserved. In addition it is assumed that the total isotopic spin  $T$  of the pion-nucleon system is conserved. Following Ericson and Ericson<sup>19</sup> a partial wave expansion of the pion-nucleon interaction operator  $\underline{f}_i(\vec{r})$  operating on the  $i$ -th nucleon in configuration, isospin, and spin space is given by

$$(III-45) \quad \underline{f}_i(\vec{r}) = \alpha_1 \underline{\Pi}_{T=\gamma_2} + \alpha_3 \underline{\Pi}_{T=3/2} + \sum_{\ell=1}^{\infty} (2\ell+1) \\ \left[ \alpha_{1,2\ell+1} \underline{\Pi}_{T=\gamma_2} \underline{\Pi}_{J=\ell+\gamma_2} + \alpha_{3,2\ell+1} \underline{\Pi}_{T=3/2} \underline{\Pi}_{J=\ell+\gamma_2} \right. \\ \left. + \alpha_{1,2\ell-1} \underline{\Pi}_{T=\gamma_2} \underline{\Pi}_{J=\ell-\gamma_2} + \alpha_{3,2\ell-1} \underline{\Pi}_{T=3/2} \underline{\Pi}_{J=\ell-\gamma_2} \right] \\ P_\ell(\cos\theta)$$

where the partial wave amplitudes are  $\alpha_{2T}$  and  $\alpha_{2T,2J}$ , the  $\underline{\Pi}$ 's are projection operators defined in Appendix A,  $\vec{r}$  is the pion coordinate, and  $\vec{r}_i$  is the  $i$ -th nucleon coordinate.

In a similar manner a partial wave expansion of the low energy pion nucleon-pair interaction operator  $\underline{f}_{ij}(\vec{r})$  for the nucleon pair  $ij$  in configuration, isospin, and spin space is given by

$$(III-46) \quad \underline{f}_{ij}(\vec{r}) = B_{11} \underline{\Pi}_{J=1}^{sym} \underline{\Pi}_{T=1}^{Anti} + B_{00} \underline{\Pi}_{J=0}^{Anti} \underline{\Pi}_{T=0}^{sym} + B_{01} \underline{\Pi}_{J=0}^{Anti} \\ \underline{\Pi}_{T=1}^{sym} + B_{02} \underline{\Pi}_{J=0}^{Anti} \underline{\Pi}_{T=2}^{sym} + \sum_{\ell=1}^{\infty} (2\ell+1) \left[ \gamma_{\ell+1,1} \underline{\Pi}_{J=\ell+1}^{sym} \underline{\Pi}_{T=1}^{Anti} \right. \\ \left. + \gamma_{\ell-1,1} \underline{\Pi}_{J=\ell-1}^{sym} \underline{\Pi}_{T=1}^{Anti} + \gamma_{\ell,0} \underline{\Pi}_{J=\ell}^{Anti} \underline{\Pi}_{T=0}^{sym} + \gamma_{\ell,1}(0,2) \underline{\Pi}_{J=\ell}^{Anti} \right. \\ \left. \underline{\Pi}_{T=1}^{sym} + \gamma_{\ell,1}(2,0) \underline{\Pi}_{J=\ell}^{sym} \underline{\Pi}_{T=1}^{Anti} + \gamma_{\ell,2} \underline{\Pi}_{J=\ell}^{Anti} \underline{\Pi}_{T=2}^{sym} \right] P_\ell(\cos\theta)$$

where  $B_{JT}$  and  $\gamma_{JT}(S,T)$  are the pion-nucleon-pair partial wave amplitudes, the  $\underline{\pi}$ 's are projection operators defined in Appendix A in which the sym- and antisymmetric refer to the nucleon pair,  $\vec{r}$  is the pion coordinate, and  $\vec{r}_1$  and  $\vec{r}_j$  are the coordinates of the i-th and j-th nucleons.

The pion may interact significantly with other elementary scatterers besides the nucleon and the nucleon pair. For instance Kolybasov<sup>68,69</sup> finds evidence from a study of the angular correlation of protons, deuterons, and tritons emitted upon capture of  $\pi^-$  by  $^{12}\text{C}$  and  $^{16}\text{O}$  that absorption on transient alpha particles may play a dominant role in pion absorption if one neglects final state interactions. On the otherhand the inclusion of significant final state interactions may allow the pion-nucleus interaction to be described in terms of just the pion nucleon-pair interactions. In order to keep the interaction as simple as possible the latter view is adopted.

Partensky and Ericson<sup>100</sup> have estimated the effects of the d and f partial waves of the pion-nucleon interaction on the d and f angular momentum states of pionic atoms. They conclude that their contributions are negligible ( $< 10\%$  in all cases) when contrasted with the present precision of the measured pionic atom energy level shifts. Thus for the low energy pion-nucleus interaction only the s- and p-wave terms of the partial wave expansion need to be considered. For pion-nucleus scattering at energies  $T_\pi > 100$  MeV the d partial wave becomes<sup>101</sup> significant.

In order to use the interaction operators above in a multiple scattering theory to define a pion-nucleus potential for investigating nuclear structure, it is necessary to know the  $\pi N$  and  $\pi NN$  partial wave amplitudes. These are energy dependent and must be obtained by

analyzing the scattering and absorption of pions incident on the various elementary scatterers at a variety of energies. Unfortunately there are no precise  $\pi N$  scattering experiments at very low energies, so these amplitudes are obtained by extrapolating the higher energy results. Tables 1 and 2 contain a summary of the experimental extrapolations for the very low energy s- and p-wave pion-nucleon scattering amplitudes.

Some of the oldest and perhaps the best determinations of the low energy pion-nucleon s-wave amplitudes are those of Bierman<sup>102</sup> for  $\pi^- + p \rightarrow \pi^- + p$  with  $6 < E_\pi < 24$  MeV and those of Fisher and Jenkins<sup>103</sup> for  $\pi^+ + p \rightarrow \pi^+ + p$  with  $3.7 < E_\pi < 25$  MeV as obtained from liquid hydrogen bubble chamber experiments. McKinley<sup>104</sup> has analyzed a large number of pion-nucleon scattering experiments at different energies and fit the tangent of the s- and p-wave phase shifts to a power series in k. The leading terms in the series correspond to constant s- and p-wave scattering lengths. Hamilton and Woolcock<sup>105</sup> have deduced values of the pion-nucleon s- and p-wave scattering lengths using forward dispersion relations for  $\pi^\pm + p \rightarrow \pi^\pm + p$  scattering at moderate to high energy. Samaranayake and Woolcock<sup>106</sup> have made use of a sum rule by Goldberger, Miyazawa, and Oehme<sup>107</sup> to eliminate one of the scattering length combinations in the forward dispersion relations of Hamilton and Woolcock for  $\pi^\pm + p \rightarrow \pi^\pm + p$  scattering. With their improved formulation they obtain a different set of s-wave scattering lengths. More recently Hamilton<sup>108</sup> analyzed all the available  $\pi^\pm + p \rightarrow \pi^\pm + p$  scattering experiments up to 41.5 MeV and obtained another set of s-wave scattering lengths. Also Donald et al.<sup>109,110</sup> have performed  $\pi^- + p \rightarrow \pi^- + p$  and  $\pi^- + p \rightarrow \pi^0 + n$  scattering experiments at

35 and 39 MeV and analyzed their results using the method of Hamilton<sup>105</sup> and Woolcock.

Unfortunately there are no pion two-nucleon scattering or absorption data available for determining the low energy  $\pi NN$  interaction amplitudes. The best one can do is to use the principle of detailed balance to relate processes like  $N + N \rightarrow \pi + N + N$  to  $\pi + N + N \rightarrow N + N$ . Using the principle of detailed balance and the cross sections of Woodruff,<sup>115</sup> Stallwood et al.,<sup>98</sup> and Kazarinov<sup>116</sup> and Simonov,<sup>19</sup> Ericson and Ericson have been able to determine the imaginary parts of a few of the  $\pi NN$  interaction amplitudes for the absorption process. These are listed in Tables 3 and 4.

For pion-nucleus scattering in the range  $24 < T_\pi < 280$  MeV the energy dependent values of the  $\pi N$  and  $\pi NN$  partial wave interaction amplitudes are needed. The elastic parts of these amplitudes are obtained from elaborate phase shift analyses of many pion-nucleon scattering experiments in which the energy dependent phase shifts are fit to various interpolating functions of the energy and momentum. The first well known and widely used set of such functions for the experimental s- and p-wave pion-nucleon scattering phase shifts was that of Anderson.<sup>117</sup> This set was obtained by analysis of most of the scattering experiments performed before 1956. Using a three parameter relativistic Breit-Wigner formula for fitting  $\delta_{33}$  and polynomial expansions for the tangents of the other smaller phase shifts in terms of powers of  $q^2$ . Fifteen parameters were varied simultaneously to obtain the best fit to the differential cross sections for energies up to 300 MeV. An error matrix was calculated along with the optimum values of the parameters. The existence of a negative element on the

diagonal of the error matrix indicated that this fit was not entirely satisfactory.

In 1963 McKinley<sup>118</sup> fit the available data in the energy region up to 600 MeV using simple interpolating expressions for  $\tan \delta_\ell / q^{2\ell+1}$ . This form for the interpolating functions was suggested by the threshold dependence of partial wave phase shifts for a short range potential ( $\tan \delta_\ell \propto q^{2\ell+1}$ ) and by the effective range approximation for nuclear forces.<sup>119</sup> The interpolating functions that he obtained are<sup>118</sup>

$$\begin{aligned}
 \tan \delta_3/q &= -0.10 - 0.036q^2 + 0.003q^4 \\
 \tan \delta_{31}/q^3 &= (-0.13 + 0.072\omega - 0.012\omega^2)/\omega \\
 q^3 \cot \delta_{33} &= 4.108 + 0.7987q^2 - 0.8337q^4 \\
 \tan \delta_1/q &= 0.17 - 0.04q^2 + 0.01q^4 \\
 \tan \delta_{11}/q^3 &= -0.015 + 0.005q^2 \\
 \tan \delta_{13}/q^3 &= -0.0035
 \end{aligned}
 \tag{III-47}$$

McKinley noticed that the experiments at 98, 150, and 170 MeV did not follow the general trend of the other experiments for the  $j = 1/2$  phase shifts. Ignoring these three experiments he obtained an alternate set of  $j = 1/2$  phase shifts.

$$\begin{aligned}
 \tan \delta_1/q &= 0.17 + 0.02q^2 \\
 \tan \delta_{11}/q^3 &= 0.016 \\
 \tan \delta_{13}/q^3 &= \tan \delta_{31}/q^3
 \end{aligned}
 \tag{III-48}$$

Two years later Roper, Wright, and Feld<sup>120</sup> completed their exhaustive analysis of the energy dependence of pion-nucleon phase shifts. They obtained 32 different solutions. Solution no. 24 for the  $s$ ,  $p$ ,  $d$ , and  $f$  phase shifts for  $0 \leq T_\pi \leq 350$  MeV is their best one in

this energy range. For this solution Roper <sup>120</sup> et al. obtained the interpolating functions of the form  $\tan \delta/q^{2\ell+1}$ , i. e.

$$\begin{aligned} \tan \delta_1^0/q &= 0.195530 - 0.077224q + 0.016471q^2 - 0.2299 \times 10^{-4} q^3 \\ \tan \delta_3^0/q &= -0.062897 - 0.038534q - 0.008068q^2 + 0.8734 \times 10^{-4} q^3 \\ \tan \delta_{11}^1/q^3 &= -0.100852 + 0.064993q + 0.3796 \times 10^{-4} q^2 \\ \tan \delta_{31}^1/q^3 &= -0.052532 + 0.029051q - 0.006173q^2 \\ \tan \delta_{13}^1/q^3 &= -0.021752 + 0.010737q - 0.001356q^2 \\ \text{(III-49)} \quad \tan \delta_{13}^2/q^5 &= 0.001929 + 0.1559 \times 10^{-3} q \\ \tan \delta_{33}^2/q^5 &= -0.1609 \times 10^{-3} - 0.3038 \times 10^{-3} q \\ \tan \delta_{15}^2/q^5 &= 0.001745 - 0.5365 \times 10^{-3} q \\ \tan \delta_{35}^2/q^5 &= -0.001185 + 0.6529 \times 10^{-3} q \\ \tan \delta_{15}^3/q^7 &= 0.2516 \times 10^{-3} - 0.4437 \times 10^{-4} q \\ \tan \delta_{35}^3/q^7 &= -0.6241 \times 10^{-4} - 0.1785 \times 10^{-4} q \\ \tan \delta_{17}^3/q^7 &= -0.1814 \times 10^{-4} - 0.1229 \times 10^{-4} q \\ \tan \delta_{37}^3/q^7 &= 0.2684 \times 10^{-3} - 0.4306 \times 10^{-4} q \end{aligned}$$

plus the resonance amplitude

$$\text{(III-50)} \quad \alpha_{33} = - \frac{\Gamma_{el}^{(3)}}{2k} / \left[ (E - E_0^{(3)}) + i \frac{\Gamma_{el}^{(3)}}{2} \right]$$

where

$$\text{(III-51)} \quad \Gamma_{el}^{(2T)} = \frac{4 M_p}{E + E_0^{(2T)}} k r_0^{(2T)} (\gamma_\lambda^{(2T)})^2 V_\lambda(k r_0^{(2T)})$$

is the resonance<sup>n</sup> elastic width,

$$(III-52) \quad V_{\lambda} (k r_{0\lambda}^{(2\pi)}) = \frac{1}{(k r_{0\lambda}^{(2\pi)})^2} \left[ j_{\lambda}^2 (k r_{0\lambda}^{(2\pi)}) + m_{\lambda}^2 (k r_{0\lambda}^{(2\pi)}) \right]^{-1}$$

is the barrier penetration factor,

$$(III-53) \quad \Gamma_{\lambda}^{(2\pi)} = \Gamma_{e\lambda}^{(2\pi)} + \Gamma_{in\lambda}^{(2\pi)}$$

is the resonance total width,

$$(III-54) \quad \Gamma_{in\lambda}^{(3)} = \Gamma_{in\lambda}^{(2\pi)} = \overline{\Gamma}_{in\lambda} (k-k_0)^{2\lambda+1} \cong 0$$

is the resonance inelastic width,

$$(III-55) \quad k_0 = 1.479$$

is the threshold pion c. m. momentum for one-pion production,  $k$  is the pion c. m. momentum,

$$(III-56) \quad E = [M_{\pi}^2 + k^2]^{1/2}$$

is the total pion c. m. energy,

$$(III-67) \quad E_0^{(3)} = E_0^{(2\pi)} = 1.914$$

is the energy of the resonance,

$$(III-58) \quad (\gamma_1^{(3)})^2 = (\gamma_{\lambda}^{(2\pi)})^2 = 0.133$$

is the reduced elastic width, and

$$(III-59) \quad r_{0\lambda}^{(3)} = r_0^{(2\pi)} = 0.91$$

is the interaction range where  $\hat{n} = c = m_{\pi} = 1$ .

121

In 1966 Donnachie and Shaw published their best interpolating functions for the reciprocal of  $\tan \delta_{\lambda}/q^{2\lambda+1}$  for  $0 \leq T_{\pi} \leq 250$  Mev, .

i.e.

$$q \cot \delta_1 = 5.848 + 5.482q^2 - 3.830q^4 + 1.004q^6 - .1076q^8 \\ + .003977q^{10}$$

$$q \cot \delta_3 = -11.364 + 3.697q^2 - .8014q^4 + .0776q^6 - .00285q^8 \\ q^3 \cot \delta_{13} = -34.48 - 71.85q^2 + 36.70q^4 - 9.623q^6 + .968q^8 \\ - .0330q^{10}$$

$$q^3 \cot \delta_{31} = -26.30 + 8.479q^2 - 15.35q^4 + 3.834q^6 - .3560q^8 \\ + .0115q^{10}$$

$$q^3 \cot \delta_{33} = 4.6512 - .6207q^2 - .1473q^4 - .0829q^6$$

Unfortunately they did not report on a fit for  $\delta_{11}$  or include higher partial waves.

**D. Projection of the Total Pion-Nucleus Wavefunction  
onto the Nuclear Ground State**

The effect of the nucleons on the pion may be averaged by projecting the total pion-nucleus wavefunction onto the nuclear ground state.

An expression for the total pion-nucleus wavefunction may be obtained by substituting (III-24), (III-26), etc. into (III-20). The first few terms in the resulting infinite series of terms are

$$\begin{aligned}
 \text{(III-61)} \quad \underline{\Psi}(\vec{r}; \vec{r}_1, \dots, \vec{r}_A; s_1, \dots, s_A) |0\rangle &= \underbrace{\Phi_0(\vec{r}) |0\rangle}_{\text{incident WAVE}} + \sum_{j=1}^A \int \underline{g}(\vec{r}; \vec{r}_1, \dots, \vec{r}_A; \\
 &\quad \vec{r}'_j; \vec{r}_1, \dots, \vec{r}_A; s_1, \dots, s_A) \delta(\vec{r}'_j - \vec{r}) \delta s'_j s'_j \underline{f}_j(\vec{r}') \Phi_0(\vec{r}') |0'\rangle d^3 r' \\
 &\quad \underbrace{\hspace{10em}}_{\text{single scattered WAVE}} \\
 &+ \sum_{j=1}^A \sum_{\substack{i=1 \\ i \neq j}}^A \iint \underline{g}(\vec{r}; \vec{r}_1, \dots, \vec{r}_A; \vec{r}'_j; \vec{r}_1, \dots, \vec{r}_A; s_1, \dots, s_A) \delta(\vec{r}'_j - \vec{r}) \delta s'_j s'_j \underline{f}_j(\vec{r}') \\
 &\quad \underline{g}(\vec{r}'_j; \vec{r}_1, \dots, \vec{r}_A; \vec{r}''_i; \vec{r}_1, \dots, \vec{r}_A; s'_1, \dots, s'_A) \delta(\vec{r}''_i - \vec{r}'_j) \delta s''_i s''_i \underline{f}_i(\vec{r}'') \Phi_0(\vec{r}'') |0''\rangle \\
 &\quad \underbrace{\hspace{10em}}_{\text{double scattered WAVE}} \\
 &\quad d^3 r' d^3 r'' + \sum_{j=1}^A \sum_{\substack{i=1 \\ i \neq j}}^A \sum_{\substack{k=1 \\ k \neq i}}^A \iiint \underline{g}(\vec{r}; \vec{r}_1, \dots, \vec{r}_A; \vec{r}'_j; \vec{r}_1, \dots, \vec{r}_A; s_1, \dots, s_A) \\
 &\quad \delta(\vec{r}'_j - \vec{r}) \delta s'_j s'_j \underline{f}_j(\vec{r}') \underline{g}(\vec{r}'_j; \vec{r}_1, \dots, \vec{r}_A; \vec{r}''_i; \vec{r}_1, \dots, \vec{r}_A; s'_1, \dots, s'_A) \delta(\vec{r}''_i - \vec{r}'_j) \\
 &\quad \delta s''_i s''_i \underline{f}_i(\vec{r}'') \underline{g}(\vec{r}''_i; \vec{r}_1, \dots, \vec{r}_A; \vec{r}'''_k; \vec{r}_1, \dots, \vec{r}_A; s'_1, \dots, s'_A) \delta(\vec{r}'''_k - \vec{r}''_i) \\
 &\quad \delta s'''_k s'''_k \underline{f}_k(\vec{r}''') \Phi_0(\vec{r}''') |0'''\rangle d^3 r' d^3 r'' d^3 r''' + \dots \\
 &\quad \text{triple scattered WAVE} \hspace{15em} \text{higher order scattering}
 \end{aligned}$$

In order to project the total pion-nucleus wavefunction onto the nuclear ground state one needs a number of definitions and identities. From (III-6) one may write

$$(III-62) \quad P(\vec{r}'_1 \dots \vec{r}'_A; s'_1 \dots s'_A) = P_j(\vec{r}'_j; s_j) P(\vec{r}'_j; s_j | \vec{r}'_1 \dots \vec{r}'_{j-1}, \\ \vec{r}'_{j+1}, \dots, \vec{r}'_A; s'_1 \dots s'_{j-1} s'_{j+1} \dots s'_A)$$

Using the definition in (III-18) one has

$$(III-63) \quad \sum_{j=1}^A \langle 0' | \Phi_0(r') | 0' \rangle_j = \sum_{j=1}^A \sum_{s'_1} \dots \sum_{s'_{j-1}} \sum_{s'_{j+1}} \dots \sum_{s'_A} \int \dots \int \\ \Phi_0(r') P(\vec{r}'_j; s'_j | \vec{r}'_1 \dots \vec{r}'_{j-1} \vec{r}'_{j+1} \dots \vec{r}'_A; s'_1 \dots s'_{j-1} s'_{j+1} \dots s'_A) \\ d^3 r'_1 \dots d^3 r'_{j-1} d^3 r'_{j+1} \dots d^3 r'_A$$

Thus

$$(III-64) \quad \langle 0' | \delta(\vec{r}'_j - \vec{r}') \delta s'_j s' \Phi_0(r') | 0' \rangle = \sum_{s'_j} \int \delta(\vec{r}'_j - \vec{r}') \delta s'_j s' \\ P_j(\vec{r}'_j; s'_j) \Phi_0(r') d^3 r'_j = P_j(\vec{r}'; s') \Phi_0(r')$$

Using the definition in (III-10) one obtains

$$(III-65) \quad \sum_{j=1}^A \sum_{s'_j} \int \delta(\vec{r}' - \vec{r}'_j) \delta s'_j s'_j P_j(\vec{r}'_j; s'_j) d^3 r'_j = e_n(r) + e_p(r')$$

where  $e_n(r)$  and  $e_p(r)$  are the nuclear neutron and proton densities respectively.

From Appendix N the pion-nucleon scattering operator for scattering from the  $j$ -th scatterer is

$$(III-66) \quad \underline{f}_j = (1 + \frac{E\pi}{M\omega}) \underline{b}_j - \underline{c}_j (\underline{\nabla} \cdot \underline{\nabla}' + \frac{E\pi}{2M\omega} q^2) / (1 + E\pi/M\omega) \\ + \underline{d}_j \frac{2}{A} \frac{\vec{s}_j \cdot \vec{k}\pi}{r'} \frac{d}{dr'}$$

where

$$(III-67) \quad \underline{b}_j = b_0 + b_1 \underline{t}_\pi \cdot \underline{T}_j$$

$$(III-68) \quad \underline{c}_j = c_0 + c_1 \underline{t}_\pi \cdot \underline{T}_j$$

$$(III-69) \quad \underline{d}_j = d_0 + d_1 \underline{t}_\pi \cdot \underline{T}_j$$

The operator  $\underline{t}_\pi \cdot \underline{T}_j$  may be defined by

$$(III-70) \quad \underline{t}_\pi \cdot \underline{T}_j = \underline{t}_+ \underline{T}_{j-} + \underline{t}_- \underline{T}_{j+} + 2t_3 T_{j3}$$

such that for a negative pion

$$(III-71) \quad \langle 0 | \sum_{j=1}^A \underline{t}_\pi \cdot \underline{T}_j | 0 \rangle = \langle 0 | \sum_{j=1}^A 2t_3 T_{j3} | 0 \rangle = N-2$$

Thus for the proton and neutron

$$(III-72) \quad \underline{b}_p = b_0 - b_1$$

$$(III-73) \quad \underline{b}_n = b_0 + b_1$$

For arbitrary nuclei one obtains using (III-67), (III-68),

(III-69), and (III-71)

$$(III-74) \quad \begin{aligned} \langle 0' | \sum_{j=1}^A \underline{f}_j(\underline{r}') \underline{\Phi}_0(\underline{r}') | 0' \rangle &= \langle 0' | \sum_{j=1}^A \left\{ \left(1 + \frac{E_\pi}{M_N}\right) \underline{b}_j \right. \\ &\quad \left. - \underline{c}_j \left( \nabla \cdot \nabla' + \frac{E_\pi}{2M_N} q^2 \right) / \left(1 + \frac{E_\pi}{M_N}\right) + \underline{d}_j \frac{2}{A} \frac{\underline{\hat{s}}_j \cdot \underline{\hat{\lambda}}_n}{r'} \frac{d}{d r'} \right\} \underline{\Phi}_0(\underline{r}') | 0' \rangle \\ &= \langle 0' | \sum_{j=1}^A \left[ \left(1 + \frac{E_\pi}{M_N}\right) \left( b_0 + b_1 \frac{N-2}{A} \right) - \frac{(c_0 + c_1 \frac{N-2}{A}) \left( \nabla \cdot \nabla' + \frac{E_\pi}{2M_N} q^2 \right)}{\left(1 + \frac{E_\pi}{M_N}\right)} \right. \\ &\quad \left. + (d_0 + d_1 \frac{N-2}{A}) \frac{2}{A} \frac{\underline{\hat{s}}_j \cdot \underline{\hat{\lambda}}_n}{r'} \frac{d}{d r'} \right] \underline{\Phi}_0(\underline{r}') | 0' \rangle . \end{aligned}$$

From the definition of the pion-nucleus Green's function in (III-21) one obtains

$$(III-78) \quad \langle 0 | g(\vec{r}; \vec{r}_1 \dots \vec{r}_A; \vec{r}'_1 \dots \vec{r}'_A; s_1' \dots s_A) | 0' \rangle \\ = \langle 0 | \sum_{m=m'} g_m(\vec{r}_i \vec{r}'_i) | m \rangle \langle m' | 0' \rangle = g_0(\vec{r}, \vec{r}')$$

where  $g_0(\vec{r}, \vec{r}')$  is the pion Green's function at an energy  $E - \epsilon_0$ .  $\epsilon_0$  is the energy of the nuclear ground state.

Thus using (III-64), (III-65), and (III-74) one may project the second term in the series for the total pion-nucleus wavefunction given in (III-61) onto the nuclear ground state to obtain

$$(III-79) \quad \langle 0 | \underline{\Psi}(\vec{r}; \vec{r}_1 \dots \vec{r}_A; s_1 \dots s_A) | 0 \rangle = \Phi_0(r) + \int e(r') \left[ \left(1 + \frac{E_{\pi}}{M_N}\right) (b_0 + b_1 \frac{N-2}{A}) \right. \\ \left. g_0(\vec{r}, \vec{r}') - \frac{(c_0 + c_1 \frac{N-2}{A})}{1 + E_{\pi}/M_N} \left\{ \nabla g_0(\vec{r}, \vec{r}') \cdot \nabla' + g_0(\vec{r}, \vec{r}') \frac{E_{\pi}}{2M_N} \underline{\sigma}^2 \right. \right. \\ \left. \left. + (d_0 + d_1 \frac{N-2}{A}) g_0(\vec{r}, \vec{r}') \frac{1}{A} \frac{\vec{s}_i \cdot \vec{t}_i}{r'} \frac{d}{dr'} \right\} \right] \Phi_0(r') d^3 r'$$

where the shape of the neutron and proton distributions have been assumed to be the same, i.e.

$$(III-80) \quad \frac{e_n(r')}{N} = \frac{e_p(r')}{Z} = \frac{e(r')}{A}$$

In order to project the third term of the series for the total pion-nucleus wavefunction onto the nuclear ground state one needs some additional definitions and identities. From (III-9) one may write

$$(III-81) \quad P(\vec{r}_1'' \dots \vec{r}_A''; s_1'' \dots s_A'') = P(\vec{r}_1'' \vec{r}_2''; s_1'' s_2'') P(\vec{r}_1'' \vec{r}_2''; s_1'' s_2'') | \\ \vec{r}_1'' \dots \vec{r}_{i-1}'' \vec{r}_{i+1}'' \dots \vec{r}_{j-1}'' \vec{r}_{j+1}'' \dots \vec{r}_A''; s_1'' \dots s_{i-1}'' s_{i+1}'' \dots s_{j-1}'' s_{j+1}'' \\ \dots s_A'')$$

Using the definition in (III-19) one has

$$\begin{aligned}
 \text{(III-82)} \quad \sum_{j=1}^A \sum_{\substack{i=1 \\ i \neq j}}^A \langle 0'' | \Phi_0(r'') | 0'' \rangle_{ij} &= \sum_{j=1}^A \sum_{\substack{i=1 \\ i \neq j}}^A \sum_{s_1''} \dots \sum_{s_{i-1}''} \sum_{s_{i+1}''} \dots \sum_{s_{j-1}''} \sum_{s_{j+1}''} \dots \\
 &\sum_{s_A''} \int \dots \int \Phi_0(r'') P(\tilde{r}_i'' \tilde{r}_j''; s_i'' s_j'') P(\tilde{r}_1'' \tilde{r}_2''; s_1'' s_2'' | \tilde{r}_1'' \dots \\
 &\tilde{r}_{i-1}'' \dots \tilde{r}_{j-1}'' \tilde{r}_{j+1}'' \dots \tilde{r}_A''; s_1'' \dots s_{i-1}'' s_{i+1}'' \dots s_{j-1}'' s_{j+1}'' \dots s_A'') \\
 &d^3 r_1'' \dots d^3 r_{i-1}'' d^3 r_{i+1}'' \dots d^3 r_{j-1}'' d^3 r_{j+1}'' \dots d^3 r_A'' \\
 &= \Phi_0(r'') P(\tilde{r}_i'' \tilde{r}_j''; s_i'' s_j'')
 \end{aligned}$$

Thus

$$\begin{aligned}
 \text{(III-83)} \quad \sum_{j=1}^A \sum_{\substack{i=1 \\ i \neq j}}^A \langle 0' | \delta(\tilde{r}_j' - \tilde{r}') \delta s_j' s_j' | 0' \rangle \langle 0'' | \delta(\tilde{r}_i'' - \tilde{r}'') \delta s_i'' s_i'' \Phi_0(r'') | 0'' \rangle \\
 &= \sum_{j=1}^A \sum_{\substack{i=1 \\ i \neq j}}^A \sum_{s_j'} \sum_{s_i''} \iint \delta(\tilde{r}_j' - \tilde{r}') \delta s_j' s_j' \delta(\tilde{r}_i'' - \tilde{r}'') \delta s_i'' s_i'' \\
 &\quad P(\tilde{r}_j' \tilde{r}_i''; s_j' s_i'') \Phi_0(r'') d^3 r' d^3 r'' \\
 &= e(\tilde{r}', \tilde{r}''; s', s'') \Phi_0(r'')
 \end{aligned}$$

From Appendix C for a Fermi gas

$$\text{(III-84)} \quad e(\tilde{r}', \tilde{r}''; s', s'') = e(r') e(r'') \left(1 - \frac{1}{A}\right) \left(1 - \frac{A-4}{A-1} \frac{G_F(\tilde{r}', \tilde{r}'')}{4}\right)$$

is the nucleon pair density function where  $G_F(\tilde{r}', \tilde{r}'')$  is the Fermi correlation function which has the following properties

$$\text{(III-85)} \quad \lim_{|\tilde{r}' - \tilde{r}''| \rightarrow \infty} G_F(\tilde{r}', \tilde{r}'') = 0$$

$$\text{(III-86)} \quad \lim_{|\tilde{r}' - \tilde{r}''| \rightarrow 0} G_F(\tilde{r}', \tilde{r}'') = 1$$

$$\text{(III-87)} \quad \int G_F(\tilde{r}', \tilde{r}'') e(r'') d^3 r'' = 1$$

In the nucleus there are three sources of correlation, i.e. the Pauli correlations due to the Pauli Exclusion Principle, the nuclear force correlations, and the Coulomb correlations. For this work the Pauli correlations which are of longer range than the nuclear force correlations are assumed to dominate.<sup>19</sup> We assume that the nucleon pair correlation function is approximately  $G_F(\vec{r}' - \vec{r}'')$ .

Using (III-67) and Appendix C one may write

$$(III-88) \quad \sum_{j=1}^A \sum_{\substack{i=1 \\ i \neq j}}^A \langle 0' | \delta(\vec{r}_j' - \vec{r}_i') \delta s_j' s_i' | 0' \rangle \langle 0'' | \delta(\vec{r}_j'' - \vec{r}_i'') \delta s_j'' s_i'' \\ \delta_i \Phi_0(\vec{r}'') | 0'' \rangle = e(r') e(r'') (1 - \frac{1}{A}) \left[ b_0^2 + 2 b_0 b_1 \frac{N-2}{A} - \frac{b_1^2}{A-1} \right. \\ \left. - \left\{ (b_0^2 + 2 b_0 b_1 \frac{N-2}{A}) \frac{A-4}{A-1} + 2 b_1^2 \frac{A-2}{A-1} \right\} \frac{G_F(\vec{r}' - \vec{r}'')}{4} \right]$$

Finally one may project the third term in the series for the total pion-nucleus wavefunction given in (III-61) onto the nuclear ground state using (III-81), (III-82), (III-83), (III-84), and (III-88) to obtain

$$(III-89) \quad \iint e(r') e(r'') (1 - \frac{1}{A}) \left[ \left( 1 + \frac{E_N}{M_N} \right)^2 \left\{ (b_0^2 + 2 b_0 b_1 \frac{N-2}{A} - \frac{b_1^2}{A-1}) \right. \right. \\ \left. \left. - \left( \frac{A-4}{A-1} (b_0^2 + 2 b_0 b_1 \frac{N-2}{A}) + 2 b_1^2 \frac{A-2}{A-1} \right) \frac{G_F(\vec{r}' - \vec{r}'')}{4} \right\} g_0(\vec{r}_i' \vec{r}_j') g_0(\vec{r}_i'' \vec{r}_j'') \right. \\ \left. + \left\{ (c_0^2 + 2 c_0 c_1 \frac{N-2}{A} - \frac{c_1^2}{A-1}) - \left( \frac{A-4}{A-1} (c_0^2 + 2 c_0 c_1 \frac{N-2}{A}) \right. \right. \right. \\ \left. \left. + 2 c_1^2 \frac{A-2}{A-1} \right) \frac{G_F(\vec{r}' - \vec{r}'')}{4} \right\} \frac{(\nabla g_0(\vec{r}_i' \vec{r}_j') \cdot \nabla')}{1 + E_N/M_N} \right]$$

$$\begin{aligned}
& \frac{(\nabla' g_0(\vec{r}', \vec{r}'') \cdot \nabla'')}{1 + E\pi/M_N} + \left\{ (d_0^2 + 2d_0 d_1 \frac{N-2}{A} - \frac{d_1^2}{A-1}) \right. \\
& \left. - \left( \frac{A-4}{A-1} (d_0^2 + 2d_0 d_1 \frac{N-2}{A}) + 2d_1^2 \frac{A-2}{A-1} \right) \frac{G_F(\vec{r}' - \vec{r}'')}{4} \right\} \\
& \left[ (\nabla g_0(\vec{r}', \vec{r}') \times \nabla') \cdot (\nabla' g_0(\vec{r}', \vec{r}'') \times \nabla'') \right] \Phi_0(r'') d^3 r' d^3 r''
\end{aligned}$$

where the Green's function for the propagation of the neutral pion after the pion has undergone single charge exchange has been replaced by  $g_0(\vec{r}, \vec{r}')$ . Since the charge exchanged nuclear state has nearly the same energy as the ground state due to the small amount of energy released in the charge exchange process, this approximation is very reasonable.

Adding (III-89) to (III-79) one obtains for the first three terms of the total pion-nucleus wavefunction projected onto the nuclear ground state

$$\begin{aligned}
\text{(III-90)} \quad \Psi(r) &= \Phi_0(r) + \int e(r') \left[ \left(1 + \frac{E\pi}{M_N}\right) (b_0 + b_1 \frac{N-2}{A}) g_0(\vec{r}, \vec{r}') \right. \\
&\quad \left. - \frac{(c_0 + c_1 \frac{N-2}{A}) \left\{ \nabla g_0(\vec{r}, \vec{r}') \cdot \nabla' + \frac{E\pi}{2M_N} g_0(\vec{r}, \vec{r}') \nabla'^2 \right\}}{1 + E\pi/M_N} + (d_0 + d_1 \frac{N-2}{A}) \cdot \right. \\
&\quad \left. \frac{2}{A} \frac{\hat{s} \cdot \hat{r}}{r} g_0(\vec{r}, \vec{r}') \frac{d}{dr'} \right] \Phi_0(r') d^3 r' + \iint e(r') e(r'') (1 - \frac{1}{A}) \\
&\quad \left[ \left(1 + \frac{E\pi}{M_N}\right)^2 \left\{ (b_0^2 + 2b_0 b_1 \frac{N-2}{A} - \frac{b_1^2}{A-1}) - \left( \frac{A-4}{A-1} (b_0^2 + 2b_0 b_1 \frac{N-2}{A}) + \right. \right. \right.
\end{aligned}$$

$$\begin{aligned}
& \frac{A-2}{A-1} (2b_i^2) \frac{G_F(\tilde{r}^I, \tilde{r}^{II})}{4} \left\} g_0(\tilde{r}_i, \tilde{r}^I) g_0(\tilde{r}^I, \tilde{r}^{II}) + \left\{ (c_0^2 + \right. \\
& \left. 2c_0 c_i \frac{N-2}{A} - \frac{c_i^2}{A-1} \right) - \left( \frac{A-4}{A-1} (c_0^2 + 2c_0 c_i \frac{N-2}{A}) + 2c_i^2 \frac{A-2}{A-1} \right) \\
& \frac{G_F(\tilde{r}^I, \tilde{r}^{II})}{4} \left\} \frac{(\nabla g_0(\tilde{r}_i, \tilde{r}^I) \cdot \nabla^I)(\nabla^I g_0(\tilde{r}^I, \tilde{r}^{II}) \cdot \nabla^{II})}{4} - \left\{ (d_0^2 + \right. \\
& \left. 2d_0 d_i \frac{N-2}{A} - \frac{d_i^2}{A-1} \right) - \left( \frac{A-4}{A-1} (d_0^2 + 2d_0 d_i \frac{N-2}{A}) + 2d_i^2 \frac{A-2}{A-1} \right) \\
& \frac{G_F(\tilde{r}^I, \tilde{r}^{II})}{4} \left\} (\nabla g_0(\tilde{r}_i, \tilde{r}^I) \times \nabla^I) \cdot (\nabla^I g_0(\tilde{r}^I, \tilde{r}^{II}) \times \nabla^{II}) \right] \Phi_0(\tilde{r}^{II}) d^3 r^I d^3 r^{II} \\
& \frac{G_F(\tilde{r}^I, \tilde{r}^{II})}{4} \left\} (\nabla g_0(\tilde{r}_i, \tilde{r}^I) \times \nabla^I) \cdot (\nabla^I g_0(\tilde{r}^I, \tilde{r}^{II}) \times \nabla^{II}) \right] \Phi_0(\tilde{r}^{II}) d^3 r^I d^3 r^{II}
\end{aligned}$$

The higher order terms may be obtained in a similar manner; however, the first three terms are sufficient for the purpose of this work.

### E. Summation of the Series of Multiple Scattering Terms

The infinite series of terms in the expression for the total pion wave in (III-90) may be easily summed in a self consistent manner if there are no correlations, i.e. all the correlation functions  $G_P(\vec{r}', \vec{r}'')$ , etc. are zero. In this case the definition of  $\Psi(r)$  itself may be used. Thus  $\Psi(r)$  may be exactly represented in a self consistent manner by the equation

$$(III-91) \quad \Psi(r) = \Phi_0(r) + \int e(r') \left[ \left(1 + \frac{E\pi}{M_N}\right) \left(b_0 + b_1 \frac{N-2}{A}\right) g_0(\vec{r}, \vec{r}') \right. \\ \left. - \left(c_0 + c_1 \frac{N-2}{A}\right) \left\{ \nabla g_0(\vec{r}, \vec{r}') \cdot \nabla' + \frac{E\pi}{2M_N} g_0(\vec{r}, \vec{r}') \mathcal{L}^2 \right\} / \left(1 + E\pi/M_N\right) \right. \\ \left. - \left(d_0 + d_1 \frac{N-2}{A}\right) \frac{\partial}{\partial A} \frac{\vec{s} \cdot \vec{k}}{r'} g_0(\vec{r}, \vec{r}') \frac{d}{dr'} \right] \Psi(r') d^3r'$$

Substituting the definition of  $\Psi(r)$  into the right hand side of (III-91) one can see that (III-90) is reproduced provided there are no correlations.

If there are two-particle, three-particle, etc., correlations, this self consistent method of truncating the multiple scattering series will not work, because all the correlations are handled incorrectly. On the other hand, if only two particle or pair correlations are significant one may correct (III-91) in order to properly handle the pair correlations. In order to obtain the correction term one substitutes the definition of  $\Psi(r)$  given by (III-90) into (III-91) and then subtracts (III-91) from (III-90). An infinite series of correlation terms is obtained. The lowest order scattering terms involving the pair correlation function  $G_P(\vec{r}', \vec{r}'')$  are

$$(III-92) \quad - \iint e(r') e(r'') \left(1 - \frac{1}{A}\right) \frac{G_P(\vec{r}' - \vec{r}'')}{4} \left\{ \left(1 + \frac{E\pi}{M_N}\right)^2 \left[ \frac{A-4}{A-1} (b_0^2 + \right.$$

$$\begin{aligned}
& 2b_0 b_1 \frac{N-2}{A} + \frac{A-2}{A-1} 2b_1^2 \left] g_0(\tilde{r}, \tilde{r}') g_0(\tilde{r}', \tilde{r}'') - \left[ \frac{A-4}{A-1} (c_0^2 + \right. \\
& \left. 2c_0 c_1 \frac{N-2}{A} + \frac{A-2}{A-1} 2c_1^2 \right] \frac{(\nabla g_0(\tilde{r}, \tilde{r}') \cdot \nabla') (\nabla' g_0(\tilde{r}', \tilde{r}'') \cdot \nabla'')}{(1 + \epsilon\pi/MN) (1 + \epsilon\pi/MN)} \\
& - \left[ \frac{A-4}{A-1} (d_0^2 + 2d_0 d_1 \frac{N-2}{A} + \frac{A-2}{A-1} 2d_1^2 \right] (\nabla g_0(\tilde{r}, \tilde{r}') \times \nabla') \cdot \\
& (\nabla' g_0(\tilde{r}', \tilde{r}'') \times \nabla'') \left. \right\} \Phi_0(r'') d^3 r' d^3 r''
\end{aligned}$$

The contribution of all the higher order terms may be included approximately by replacing  $\Phi_0(r'')$  by  $\Psi(r'')$ . In this case all the higher order correlations are still handled incorrectly, but presumably they are not significant. Thus (III-91) may be corrected to obtain

$$\begin{aligned}
\text{(III-93)} \quad \Psi(r) &= \Phi_0(r) + \int e(r') \left[ \left(1 + \frac{\epsilon\pi}{MN}\right) (b_0 + b_1 \frac{N-2}{A}) g_0(\tilde{r}, \tilde{r}') \right. \\
& \left. - (c_0 + c_1 \frac{N-2}{A}) \left\{ \frac{\nabla g_0(\tilde{r}, \tilde{r}') \cdot \nabla' + \frac{\epsilon\pi}{2MN} g_0(\tilde{r}, \tilde{r}') Q^2}{(1 + \epsilon\pi/MN)} \right\} - (d_0 + d_1 \frac{N-2}{A}) \right. \\
& \left. \frac{\partial}{\partial r'} \frac{\tilde{r} \cdot \tilde{r}'}{r'} g_0(\tilde{r}, \tilde{r}') \frac{d}{d r'} \right] \Psi(r'') d^3 r' - \iint e(r') e(r'') (1 - \frac{1}{A}) \frac{G_E(r', r'')}{4} \\
& \left\{ \left(1 + \frac{\epsilon\pi}{MN}\right)^2 \left[ \frac{A-4}{A-1} (b_0^2 + 2b_0 b_1 \frac{N-2}{A} + 2b_1^2 \frac{A-2}{A-1}) g_0(\tilde{r}, \tilde{r}') g_0(\tilde{r}', \tilde{r}'') \right. \right. \\
& - \left[ \frac{A-4}{A-1} (c_0^2 + 2c_0 c_1 \frac{N-2}{A} + 2c_1^2 \frac{A-2}{A-1}) \right] \frac{(\nabla g_0(\tilde{r}, \tilde{r}') \cdot \nabla') (\nabla' g_0(\tilde{r}', \tilde{r}'') \cdot \nabla'')}{(1 + \frac{\epsilon\pi}{MN})^2} \\
& \left. - \left[ \frac{A-4}{A-1} (d_0^2 + 2d_0 d_1 \frac{N-2}{A} + 2d_1^2 \frac{A-2}{A-1}) \right] (\nabla g_0(\tilde{r}, \tilde{r}') \times \nabla') \cdot (\nabla' g_0(\tilde{r}', \tilde{r}'') \times \nabla'') \right\}
\end{aligned}$$

Equation (III-93) is a self-consistent equation for  $\bar{\Psi}(r)$  which correctly handles  $\bar{\Psi}(r)$  for all uncorrelated multiple scatterings and scatterings on correlated nucleon pairs. All the higher order correlated scatterings are treated in an approximate manner which is not strictly correct.

In principle one can use the method above to handle any finite number of higher order correlations. Thus a procedure has been defined that enables one to expand the self-consistent wave equation (III-91) for  $\bar{\Psi}(r)$  in terms of correlation functions to some order. The more correlations considered the more complicated (III-91) becomes due to the addition of correction terms. As a first approximation this work assumes that only pair correlations are significant and neglects all others.

### F. Formation of the Optical Model Potential

The Schrodinger equation or any wave equation of the form

$$(III-94) \quad \frac{\hbar^2}{2m_\pi} (\nabla^2 + k^2) \underline{\Psi}(r) = V(r) \underline{\Psi}(r) \quad k^2 = \frac{2m_\pi E_\pi}{\hbar^2}$$

may be used to obtain a pion-nucleus potential from  $\underline{\Psi}(r)$ . Consider the operation of

$$(III-95) \quad \frac{\hbar^2}{2m_\pi} (\nabla^2 + k^2) - V_{\text{Coul}}(r)$$

on  $\underline{\Psi}(r)$ . The pion's Green's function obeys the equation

$$(III-96) \quad \left[ \frac{\hbar^2}{2m_\pi} (\nabla^2 + k^2) - V_{\text{Coul}}(r) \right] g_0(\vec{r}, \vec{r}') = - \frac{4\pi\hbar^2}{2m_\pi} \delta(\vec{r} - \vec{r}')$$

and the incident pion field  $\underline{\Phi}_0(r)$  obeys the equation

$$(III-97) \quad \left[ \frac{\hbar^2}{2m_\pi} (\nabla^2 + k^2) - V_{\text{Coul}}(r) \right] \underline{\Phi}_0(r) = 0$$

Thus operating with (III-95) on  $\underline{\Psi}(r)$  in equation (III-93) and integrating over the delta functions obtain for negative pions

$$(III-98) \quad \left[ \frac{\hbar^2}{2m_\pi} (\nabla^2 + k^2) - V_{\text{Coul}}(r) \right] \underline{\Psi}(r) = V_{\text{ST}}(r) \underline{\Psi}(r)$$

$$= - \frac{4\pi\hbar^2}{2m_\pi} \left[ \left( 1 + \frac{E_\pi}{M_N} \right) \left( b_0 + b_1 \frac{N-2}{A} \right) e(r) - \left( c_0 + c_1 \frac{N-2}{A} \right) \left\{ \frac{\nabla \cdot \underline{e}(r) \nabla}{1 + E_\pi/M_N} \right. \right.$$

$$\left. - \frac{E_\pi}{2M_N} \nabla^2 e(r) \right] - \left( d_0 + d_1 \frac{N-2}{A} \right) \frac{2}{A} e(r) \frac{\vec{r} \cdot \nabla}{r} \frac{d}{dr} \left] \underline{\Psi}(r) + \frac{4\pi\hbar^2}{2m_\pi} \int e(r) e(r')$$

$$\left( 1 - \frac{1}{A} \right) \frac{G_F(\vec{r} - \vec{r}')}{4} \left\{ \left( 1 + \frac{E_\pi}{M_N} \right)^2 \left[ \frac{A-4}{A-1} \left( b_0^2 + 2b_0 b_1 \frac{N-2}{A} \right) + \frac{A-2}{A-1} 2b_1^2 \right] \right.$$

$$\left. g_0(\vec{r}, \vec{r}') \right\} \underline{\Psi}(r'') d^3 r'' + \frac{4\pi\hbar^2}{2m_\pi} \int e(r'') \left( 1 - \frac{1}{A} \right) \left[ \frac{A-4}{A-1} \left( c_0^2 \right. \right.$$

$$\begin{aligned}
& + 2c_0 c_1 \frac{N-2}{A} + 2c_1^2 \frac{A-2}{A-1} \left] (\nabla \cdot e(r) \frac{G_F(\vec{r}-\vec{r}')}{4} \nabla) \frac{(\nabla g_0(\vec{r}_1 \vec{r}'') \cdot \nabla'')}{(1 + \epsilon\pi/M_N)^2} \right. \\
& \underline{\Psi}(r'') d^3 r'' + \frac{4\pi\hbar^2}{2m\pi} \int e(r'') (1-\frac{1}{A}) \left[ \frac{A-4}{A-1} (d_0^2 + 2d_0 d_1 \frac{N-2}{A}) + \right. \\
& \left. \frac{A-2}{A-1} 2d_1^2 \right] (\nabla \times e(r) \frac{G_F(\vec{r}-\vec{r}'')}{4} \nabla) \cdot (\nabla g_0(\vec{r}_1 \vec{r}'') \times \nabla'') \underline{\Psi}(r'') d^3 r''
\end{aligned}$$

None of the integrals in (III-98) can be evaluated exactly except by numerical means. For the purpose of this work some simplifying approximations will be made in order to easily evaluate the integrals.

Consider the first integral in (III-98). For the Pauli pair correlation function  $G_p(\vec{r}-\vec{r}'')$  most of the contribution to the integral must come in the region  $\vec{r} \sim \vec{r}''$  for  $\vec{r}''$  inside the nucleus. Assuming  $e(r'')$  and  $\underline{\Psi}(r'')$  are smooth functions that are fairly constant over small ranges in  $\vec{r}''$ , one may remove them from the integral, i.e.

$$\begin{aligned}
\text{(III-99)} \quad & \int e(r'') \frac{G_F(\vec{r}-\vec{r}'')}{4} g_0(\vec{r}_1 \vec{r}'') \underline{\Psi}(r'') d^3 r'' \\
& \cong e(r) \underline{\Psi}(r) \int \frac{G_F(\vec{r}-\vec{r}'')}{4} g_0(\vec{r}_1 \vec{r}'') d^3 r''
\end{aligned}$$

The approximation made for  $e(r'')$  is sometimes called the local density approximation.

Also let us assume that the pion propagator may be approximated by

$$\text{(III-100)} \quad g_0(\vec{r}_1 \vec{r}'') \cong \frac{1}{|\vec{r}-\vec{r}''|}$$

due to the short range of the correlations. All these approximations are more valid the shorter the range of the pair correlation function.

Using approximations (III-99) and (III-100) one may write

$$\begin{aligned}
 \text{(III-101)} \quad \int e^{i\mathbf{r}''} \frac{G_F(\vec{r}-\vec{r}'')}{4} g_0(\vec{r}, \vec{r}'') \Psi(\mathbf{r}'') d^3r'' &\cong e^{i\mathbf{r}} \Psi(\mathbf{r}) \int \frac{1}{|\vec{r}-\vec{r}''|} \frac{G_F(\vec{r}-\vec{r}'')}{4} d^3r'' \\
 &\cong e^{i\mathbf{r}} \Psi(\mathbf{r}) \frac{9\pi}{4P_f^2}
 \end{aligned}$$

where the value of the integral was obtained by changing the variable of integration to  $\vec{x} = \vec{r}'' - \vec{r}$  and using Appendix C. Thus the contribution of the first integral in (III-98) to  $V_{st}(\mathbf{r})$  is

$$\text{(III-102)} \quad - \frac{4\pi \hbar^2}{2m\pi} \left[ - \frac{9\pi}{4P_f^2} e^{i\mathbf{r}} \left(1 - \frac{1}{A}\right) \left\{ \frac{A-4}{A-1} (b_0^2 + 2b_0 b_1 \frac{A-2}{A}) + 2b_1^2 \frac{A-2}{A-1} \right\} \right]$$

In order to evaluate the second integral in (III-98) consider the z-component of an integral of the form

$$\begin{aligned}
 \text{(III-103)} \quad \hat{k} \cdot \int_{-1}^1 \int_0^{2\pi} \hat{x} (\hat{x} \cdot \vec{A}(x)) d\cos\theta d\phi &= \int_{-1}^1 \int_0^{2\pi} \cos\theta [\sin\theta \cos\phi A_x \\
 &\quad + \sin\theta \sin\phi A_y + \cos\theta A_z] d\cos\theta d\phi
 \end{aligned}$$

where  $\vec{x} = \vec{r} - \vec{r}''$ . Integrating over  $\phi$  obtain

$$\text{(III-104)} \quad \int_0^{2\pi} \sin\phi d\phi = -\cos\phi \Big|_0^{2\pi} = 0$$

$$\text{(III-105)} \quad \int_0^{2\pi} \cos\phi d\phi = -\sin\phi \Big|_0^{2\pi} = 0$$

Thus

$$\begin{aligned}
 \text{(III-106)} \quad \hat{k} \cdot \int_{-1}^1 \int_0^{2\pi} \hat{x} (\hat{x} \cdot \vec{A}(x)) d\cos\theta d\phi &= 2\pi \int_{-1}^1 A_z(x) \cos^2\theta d\cos\theta \\
 &= 2\pi A_z(x) \frac{\cos^3\theta}{3} \Big|_{-1}^1 = \frac{4\pi}{3} A_z(x)
 \end{aligned}$$

Evaluating the other components of the integral in the same manner one obtains

$$(III-107) \int_{-1}^1 \int_0^{2\pi} \hat{x} (\hat{x} \cdot A(x)) d\cos\theta d\phi = \frac{4\pi}{3} \vec{A}(x) = \int_{-1}^1 \int_0^{2\pi} \frac{\hat{x} \cdot \hat{x}}{3} A(x) d\cos\theta d\phi$$

The third integral in (III-98) is proportional to

$$(III-108) \int e(r'') (\nabla \cdot e(r) \frac{G_F(\vec{r}-\vec{r}'')}{4} \nabla) (\nabla g_0(\vec{r}, \vec{r}'') \cdot \nabla'') \Psi(r'') d^3r''$$

Noting that  $\nabla G_F(\vec{r}-\vec{r}'') \propto \vec{r} - \vec{r}'' = \vec{x}$  and  $\nabla g_0(\vec{r}, \vec{r}'') \propto \vec{r} - \vec{r}'' = \vec{x}$  and using (III-107) with  $\vec{A}(x) = \nabla'' \Psi(r'')$  obtain

$$(III-109) \int_{-1}^1 \int_0^{2\pi} \hat{x} \frac{d}{dx} \left( \hat{x} \frac{d}{dx} g(x) \cdot \vec{A}(x) \right) d\cos\theta d\phi \\ = \frac{1}{3} \int_{-1}^1 \int_0^{2\pi} \nabla \cdot \nabla g(x) \vec{A}(x) d\cos\theta d\phi$$

Thus (III-108) may be evaluated using (III-101) and assuming

$$(III-110) \nabla^2 g_0(\vec{r}, \vec{r}'') \cong -4\pi \delta(\vec{r}-\vec{r}'')$$

to obtain

$$(III-111) \int e(r'') (\nabla \cdot e(r) \frac{G_F(\vec{r}-\vec{r}'')}{4} \nabla) (\nabla g_0(\vec{r}, \vec{r}'') \cdot \nabla'' \Psi(r'')) d^3r'' \\ \cong \frac{1}{3} \int e(r'') \nabla \cdot e(r) \frac{G_F(\vec{r}-\vec{r}'')}{4} \nabla^2 g_0(\vec{r}, \vec{r}'') \nabla'' \Psi(r'') d^3r'' \\ \cong -\frac{\pi}{3} e(r) \nabla \cdot e(r) \nabla \Psi(r)$$

From (III-111) the contribution of the second integral in (III-98) to  $V_{st}(r)$  is

$$(III-112) -\frac{4\pi\hbar^2}{3} \frac{\pi}{2m\eta} e(v) (1-\frac{1}{\lambda}) \left\{ \frac{A^4}{A-1} (c_0^2 + 2c_0 c_1 \frac{A-2}{\lambda}) + 2c_1^2 \frac{A-2}{A-1} \right\} \frac{\nabla \cdot e(v) \nabla}{(1+E_1/m\eta)^2}$$

In a very similar manner the contribution of the third integral in (III-98) to  $V_{st}(r)$  is obtained to be

$$(III-113) \quad -\frac{4\pi\hbar^2}{2M\pi} \frac{2\pi}{3} e(r) \left(1 - \frac{1}{A}\right) \left\{ \frac{A-4}{A-1} (d_0^2 + 2d_0d_1 \frac{N-2}{A}) + 2d_1^2 \frac{A-2}{A-1} \right\} \nabla \cdot e(r) \nabla$$

Substituting (III-102), (III-112) and (III-113) into (III-98)

one obtains the optical model potential  $V_{st}(r)$  to be

$$(III-114) \quad V_{ST}(r) = -\frac{4\pi\hbar^2}{2M\pi} \left[ \left(1 + \frac{E\pi}{M\pi}\right) (b_0 + b_1 \frac{N-2}{A}) e(r) - \frac{(c_0 + c_1 \frac{N-2}{A})}{(1 + E\pi/M\pi)} \left\{ \nabla \cdot e(r) \nabla - \frac{E\pi}{2M\pi} \nabla^2 e(r) \right\} - (d_0 + d_1 \frac{N-2}{A}) \frac{2}{A} e(r) \frac{5\hbar^2}{r} \frac{d}{dr} - \frac{9\pi}{4P_f^2} e^2(r) \left(1 - \frac{1}{A}\right) \right. \\ \left. \left(1 + \frac{E\pi}{M\pi}\right)^2 \left\{ \frac{A-4}{A-1} (b_0^2 + 2b_0b_1 \frac{N-2}{A}) + 2b_1^2 \frac{A-2}{A-1} \right\} + \frac{\pi}{3} e(r) \left(1 - \frac{1}{A}\right) \left\{ \frac{A-4}{A-1} (c_0^2 + 2c_0c_1 \frac{N-2}{A}) / \left(1 + \frac{E\pi}{M\pi}\right)^2 + \frac{A-4}{A-1} (2d_0^2 + 4d_0d_1 \frac{N-2}{A}) + \left( \frac{2c_1^2}{(1 + E\pi/M\pi)^2} + 4d_1^2 \right) \frac{A-2}{A-1} \right\} \nabla \cdot e(r) \nabla \right]$$

Thus we have completed the derivation of a pion-nucleus strong interaction optical model potential from the multiply scattered wave approach. The wave analysis enabled us to explicitly take into account scattering on correlated pairs.

The  $V_{st}(r)$  in (III-114) represents only the elastic pion-nucleus interaction. In addition to the elastic interaction with the nucleus the pion may be absorbed. For pionic atoms and low energy pion-nucleus scattering conservation of energy and momentum prohibits pion absorption on single nucleons. Experimentally most pion absorption at low energy occurs on nucleon pairs.<sup>48,49,51</sup>

The absorption process may be included in the multiple scattering equations in the single scattering approximation by considering the nucleon pairs for absorption as additional elementary scatterers. Thus the pion-nucleon pair absorption operators may be expressed in terms of purely imaginary pion-nucleon pair interaction amplitudes  $B_{JT}$  and

$\Upsilon_{JT}(S,T)$ . (See Appendix A for a derivation of the pion-nucleon pair interaction operator.)

If the nucleon pairs for absorption are considered as additional elementary scatterers, then in the single scattering approximation they give rise to a contribution to  $V_{st}(r)$  of

$$(III-115) \quad V_{ST}(r) = -\frac{4\pi\hbar^2}{2M\pi} \left[ \left(1 + \frac{E\pi}{2M_N}\right) B e^2(r) - C \frac{\nabla \cdot e^2(r) \nabla}{1 + E\pi/2M_N} \right]$$

where B and C are pure imaginary. Thus the pion-nucleus strong interaction optical model potential including absorption on nucleon pairs may be written

$$(III-116) \quad V_{ST}(r) = -\frac{4\pi\hbar^2}{2M\pi} \left[ \left(1 + \frac{E\pi}{M_N}\right) \left(b_0 + b_1 \frac{N-2}{A}\right) e(r) - \frac{(c_0 + c_1 \frac{N-2}{A})}{1 + E\pi/M_N} \right. \\ \left. \left\{ \nabla \cdot e(r) \nabla - \frac{E\pi}{2M_N} \nabla^2 e(r) \right\} - (d_0 + d_1 \frac{N-2}{A}) \frac{2}{A} e(r) \frac{\vec{s} \cdot \vec{\nabla}}{r} \frac{d}{dr} \right. \\ \left. - \frac{9\pi}{4\rho_F^2} e^2(r) \left(1 - \frac{1}{A}\right) \left(1 + \frac{E\pi}{M_N}\right)^2 \left\{ \frac{A-4}{A-1} (b_0^2 + 2b_0 b_1 \frac{N-2}{A}) + 2b_1^2 \frac{A-2}{A-1} \right\} + \right. \\ \left. \frac{\pi}{3} e(r) \left(1 - \frac{1}{A}\right) \left\{ \frac{A-4}{A-1} (c_0^2 + 2c_0 c_1 \frac{N-2}{A}) / \left(1 + \frac{E\pi}{M_N}\right)^2 + \frac{A-4}{A-1} (2d_0^2 + \right. \right. \\ \left. \left. 4d_0 d_1 \frac{N-2}{A}) + \left( \frac{2c_1^2}{(1 + E\pi/M_N)^2} + 4d_1^2 \right) \frac{A-2}{A-1} \right\} \nabla \cdot e(r) \nabla \right. \\ \left. + \left(1 + \frac{E\pi}{2M_N}\right) B e^2(r) - C \frac{\nabla \cdot e^2(r) \nabla}{1 + E\pi/2M_N} \right]$$

This form of the potential is significantly different from that of Ericson and Ericson<sup>19</sup> who obtained

$$\begin{aligned}
 \text{(III-117)} \quad V_{ST}(r) = & -\frac{4\pi\hbar^2}{2m\pi} \left[ \frac{\left(1 + \frac{m\pi}{mN}\right) \left(b_0 + b_1 \frac{N-2}{A}\right) e(r)}{1 + \frac{9\pi}{4r^2} \left(b_0 + b_1 \frac{N-2}{A}\right) e(r)} \right. \\
 & - \left(1 + \frac{m\pi}{mN}\right)^{-1} \frac{\nabla \cdot \left(c_0 + c_1 \frac{N-2}{A}\right) e(r)}{1 - \frac{4\pi}{3} \left(c_0 + c_1 \frac{N-2}{A}\right) e(r)} \nabla + \left(c_0 + c_1 \frac{N-2}{A}\right) \\
 & \left. \left(\frac{m\pi}{mN}\right)^2 \langle \vec{p}_N^2 \rangle e(r) - \left(d_0 + d_1 \frac{N-2}{A}\right) \frac{1}{A} e(r) \frac{\vec{s} \cdot \vec{p}_N}{r} \frac{d}{dr} + \right. \\
 & \left. \left(1 + \frac{m\pi}{2mN}\right) B e^2(r) - C \frac{\nabla \cdot e^2(r) \nabla}{1 + \frac{m\pi}{2mN}} \right]
 \end{aligned}$$

The main differences are that in this work the relativistic form involving  $E_\pi/m_N$  instead of  $m_\pi/m_N$  is obtained, the nucleon motion term is  $E_\pi/m_N$  instead of  $m_\pi/m_N$  and the form of the Lorentz-Lorenz effect must be different from the classical form due to the inclusion of effects like virtual charge exchange. Also the spin dependent d term is found to give a contribution to virtual spin exchange even for spin zero nuclei.

Krell and Ericson<sup>21</sup> in fitting their pion-nucleus optical model potential to pionic atom data for the 2p-1s transition data which is very sensitive to the form of the Lorentz-Lorenz effect, discarded the original Ericson and Ericson<sup>19</sup> form of the Lorentz-Lorenz effect in the local part of the potential and replaced it with the form derived above which includes contributions due to virtual charge exchange.

Krell and Barma<sup>21</sup> in using the optical model potential of Krell and Ericson<sup>19</sup> to fit the relativistic pion elastic scattering data on <sup>12</sup>C failed to replace the  $m_\pi/m_N$  terms with the relativistic  $E_\pi/m_N$  terms. As a result the agreement between their best fit parameters and the values deduced from  $\pi N$  experiments was not too good.

CHAPTER IV  
ANALYSIS OF PION-NUCLEUS INTERACTION DATA

The derivation of the optical model potential of Chapter III using multiple scattering theory involved a number of approximations. Although the approximations made in the derivation were reasonable, the magnitude of the terms involving correlations is only approximate due to the use of the Fermi gas model and neglecting the  $e^{ikr}$  dependence of the Green's function. As the energy of the pion increases the correlation terms must eventually disappear due to the oscillatory nature of  $e^{ikr}$  in the Green's function.

The full justification of any pion-nucleus interaction potential requires that it qualitatively and quantitatively describe the experimental data. There are many kinds of experiments in which the effect of the pion interacting strongly with the nucleus can be detected. For instance photo-pion production and electro-pion production exhibit final state pion-nucleus interactions. In some sense these kinds of experiments are two step processes. First the pion is produced electromagnetically, then it interacts strongly with the nucleus. One needs to know all the details of the production process in order to investigate the final state interactions using the experimental data.

Although experiments such as pion-production can be used to test the pion-nucleus interaction potential, it is advantageous to use the more direct processes such as elastic pion-nucleus scattering and its very low energy equivalent, pionic atoms. In these processes one need

deal with only the well known elastic electromagnetic processes in addition to the pion-nucleus strong interaction. For the purpose of testing the pion-nucleus optical model potential only these two processes are used in this work.

Tables 5-8 contain a listing of all the pionic atom x-ray transition energies and widths. Not all of the pionic atom data are equally useful for testing the pion-nucleus optical potential, because not all of the  $\pi NN$  interaction amplitudes in the optical potential are known. Also the nuclear density is only reasonably well known for  $N = Z$  spin zero nuclei. Thus the data for  ${}^4\text{He}$ ,  ${}^{12}\text{C}$ ,  ${}^{16}\text{O}$ , and  ${}^{40}\text{Ca}$  are best for testing the potential.

In testing the potential for pionic atoms one could just substitute into the potential the experimentally deduced  $\pi N$  and  $\pi NN$  interaction amplitudes, and solve the Klein-Gordon wave equation for this potential to predict the pionic atom transition data. This procedure is not fully satisfactory due to the large uncertainty in the experimentally measured  $\pi N$  and  $\pi NN$  interaction amplitudes compared to the great precision of the pionic atom transition data. A better procedure is to fit the  $\pi N$  and  $\pi NN$  interaction amplitudes to the pionic atom data via the pion-nucleus optical model potential, and then compare the resulting values with the experimentally determined ones. This procedure is outlined in great detail in Appendix F.

Following the method of analysis given in Appendix F, one obtains best fit values for the effective parameters

$$(IV-1) \quad "b_0" = b_0 - \frac{3P_F}{2\pi\hbar} \left(1 - \frac{1}{A}\right) \left(1 + \frac{E_\pi}{MN}\right) \left[ \frac{A-4}{A-1} b_0^2 + \frac{A-2}{A-1} 2b_1^2 \right]$$

$$(IV-2) \quad "c_0" = c_0 - \frac{\pi}{3} \left(\frac{A}{4\pi R^3}\right) \left(1 - \frac{1}{A}\right) \left[ \frac{\left(\frac{A-4}{A-1} c_0^2 + \frac{A-2}{A-1} 2c_1^2\right) + \left(\frac{A-4}{A-1} 2cb^2 + \frac{A-2}{A-1} 4b_1^2\right) \right] \frac{1}{1 + E_\pi/MN}$$

$$(IV-3) \quad "B" = B_0 - \frac{3}{A-1} B_1 - \frac{3}{A-1} B_2 + \frac{9}{(A-1)^2} \left(1 + \frac{3}{A-1}\right) B_4 - \frac{4}{A-1} \left(1 + \frac{3}{A-1}\right) B_5$$

$$(IV-4) \quad "C" = C_0 - \frac{3}{A-1} C_1 - \frac{3}{A-1} C_2 + \frac{9}{(A-1)^2} \left(1 + \frac{3}{A-1}\right) C_4 - \frac{4}{A-1} \left(1 + \frac{3}{A-1}\right) C_5$$

where  $R$  is the uniform radius of the density of nucleon centers and the parameters  $b_0, b_1, c_0, c_1, d_0, d_1, B_0, B_1, B_2, B_4, B_5, C_0, C_1, C_2, C_4,$  and  $C_5$  are particular combinations of  $\pi N$  and  $\pi NN$  interaction amplitudes given in Appendix A. The best fit parameter values are displayed in Figures 1-4 along with the extrapolated values from  $\pi N$  and  $\pi NN$  interaction experiments.

From Figures 1 and 2 one sees that the " $b_0$ " and " $c_0$ " predicted using the  $\pi N$  amplitudes of Hamilton and Woolcock<sup>105</sup> are not in agreement with the best fit values. On the otherhand the Fermi-averaged values of both " $b_0$ " and " $c_0$ " predicted by using the  $\pi N$  amplitudes of Donnachie and Shaw<sup>121</sup> agree satisfactorily with the best fit values.

For pion absorption on nucleon pairs, the picture is more complicated. From Figure 3 one sees that the " $B$ " predicted by Ericson<sup>19</sup> and Ericson<sup>19</sup> from pion production experiments is off by a factor of 2 from the best fit value. The only other estimate for " $B$ " is that of Dover<sup>20</sup> who explicitly calculated the contributions of the various on- and off-shell nucleon-nucleon  $T$  matrices and averaged them over the distribution of two-nucleon relative momenta in the Fermi sea. His calculations slightly overestimate the best fit values.

In the case of nonlocal absorption of pions on nucleon pairs, one sees that the " $C$ " predicted by Ericson and Ericson<sup>19</sup> from pion production experiments is in excellent agreement with the best fit value. Again Dover overestimates the value of the absorption parameter

by about 10 %.

For pedagogical reasons some figures have been included to give one a qualitative understanding of the influence of the strong interaction on pionic atoms. In Figure 5 is shown the 1s bound state wavefunctions for  $^{16}\text{O}$  with and without the effect of the strong interaction. A radial plot of the repulsive local and attractive nonlocal parts of the optical potential for  $^{16}\text{O}$  is given in Figures 6 and 7. Figure 8 displays the 2p bound state wavefunctions for  $^{40}\text{Ca}$  with and without the effect of the strong interaction.

Tables 9-45 contain a listing of the elastic pion-nucleus differential scattering cross section data for  $^4\text{He}$ ,  $^{12}\text{C}$ ,  $^{16}\text{O}$ , and  $^{40}\text{Ca}$  at a variety of pion energies. The precision of some of this data is poor, and therefore not extremely useful for testing the pion-nucleus potential. However much of the data is precise enough to make a check possible.

For testing the pion-nucleus optical potential, one finds that using the Fermi-averaged pion-nucleon amplitudes of Donnachie and Shaw<sup>121</sup> with all pair absorption amplitudes set equal to zero is satisfactory for describing the available differential cross section data. In the analysis of the elastic scattering data the pion absorption on pairs was neglected, because the effect of pair absorption on the cross section seems to be rather small and the energy dependence of the pair absorption parameters is unknown. The complicated procedure for calculating the differential cross section is described in great detail in Appendix L.

In Figures 9-12 are shown the predicted values of the complex parameters " $b_0$ " and " $c_0$ " as a function of the laboratory pion kinetic energy  $T_\pi$  for  $^{12}\text{C}$ . The Fermi-averaged values of these complex

parameters were predicted using the pion-nucleon amplitudes of Donnachie and Shaw.<sup>121</sup> Also the values of the complex parameters  $b_0$  and  $c_0$  without correlation effects are given to indicate the magnitude of the correlation effects. Figures 13-18 give a comparison of the Fermi-averaged complex parameters  $b_0$ ,  $c_0$ , and  $d_0$  as determined from the pion-nucleon amplitudes or phase shifts of McKinley,<sup>118</sup> Roper and Wright,<sup>120</sup> and Donnachie and Shaw.<sup>121</sup> Since no uncertainties are given for these sets of pion-nucleon phase shifts a comparison of the various sets gives some idea of what the uncertainties may be.

The predicted elastic differential scattering cross sections for  ${}^4\text{He}$ ,  ${}^{12}\text{C}$ ,  ${}^{16}\text{O}$ , and  ${}^{40}\text{Ca}$  are given in Figures 19-60 along with the experimental cross sections. On each figure is indicated the normalization factor by which the calculated cross section must be multiplied to obtain agreement with data. Also the average  $\chi^2$  for the predicted cross section is listed on each graph.

A cursory inspection of all the differential cross sections reveals the merit of the Kisslinger-type optical potential. The potential seems to satisfactorily predict the differential cross sections for all nuclei qualitatively and quantitatively. The quantitative fit could be improved by varying the values of the pion-nucleon amplitudes. Not all of the data is equally well predicted, because some of the data are quite old and have serious systematic errors.

CHAPTER V  
SUMMARY AND CONCLUSIONS

In this work a new pion-nucleus optical model potential has been derived from multiple scattering theory using the impulse approximation. This potential differs from previously accepted pion-nucleus optical model potentials, such as that of Ericson and Ericson,<sup>19</sup> in four important aspects.

First, the form of the Lorentz-Lorenz effect is different. The form of the Lorentz-Lorenz effect in this work is due to the fundamental approximation made to treat the series of multiple scattering equations. Ericson and Ericson<sup>19</sup> made what Iax<sup>91</sup> calls the quasi-crystalline approximation to close the series of multiple scattering equations. This approximation, as its name implies, is appropriate for crystalline structures. In this work the approximation made was to neglect all correlations of nucleons higher than pair correlations in summing exactly the entire series of multiple scatterings.

Second, the dominant contribution to the local part of the optical potential--i.e., virtual charge exchange--enters naturally from this work as one of the terms in the potential. This is not true in the case of the quasi-crystalline approximation employed by Ericson and Ericson.<sup>19</sup> As a result Krell and Ericson<sup>21</sup> were forced to add in this term ad hoc.

Third, the relativistic kinematical factors involving  $E_{\pi}/m_N$  are used. Many investigators, like Krell and Barma,<sup>39</sup> have failed to use the

proper relativistic factors in fitting to relativistic elastic pion-nucleus scattering data. Also the factor  $(1-1/A)$  multiplying the nucleon pair density and correlation terms has been included in this work. This factor has been neglected by many investigators.

Fourth, the contribution of nucleon motion is properly included resulting in a  $\frac{E_{\pi}}{2M_N} C_0 \nabla^2 e(r)$  term in the potential. Ericson and Ericson<sup>19</sup> neglected this term and instead found an  $(E_{\pi}/M_N)^2 C_0 \langle P_N^2 \rangle e(r)$  nucleon motion term. According to Krajcik and Foldy<sup>122</sup> this term should be neglected if one does not use bound nucleon spinors in calculating the potential from multiple scattering theory, because the contributions due to the nucleons being bound are of the order  $(E_{\pi}/M_N)^2$ .

In order to test the accuracy of the optical potential of Chapter III to describe pion-nucleus interactions, the effective parameters in the potential were varied in order to obtain a fit to pionic atom x-ray transition data. Then the values of the best fit effective parameters were compared to those predicted by the theory using the pion-nucleon<sup>121</sup> amplitudes of Donnachie and Shaw.

For the pionic atom data the optical potential is able to satisfactorily describe the shift of the pionic atom energy levels due to the strong interaction using the Fermi-averaged pion-nucleon amplitudes<sup>121</sup> of Donnachie and Shaw. The width of the pionic atom energy levels due to absorption on nucleon pairs is satisfactorily described for  $\ell > 0$  states using the  $\pi NN$  amplitudes obtained from pion production experiments<sup>19</sup> using the principle of detailed balance. For some reason the  $\pi NN$  amplitudes from production experiments are inadequate to describe<sup>20</sup> the  $\ell = 0$  widths. Dover has explicitly calculated the contributions of the various on- and off-shell nucleon-nucleon T matrices and averaged

them over the distribution of two-nucleon relative momenta in the Fermi sea in order to obtain effective s- and p-wave pair absorption parameters in fair agreement with the best fit values.

For the elastic pion-nucleus differential scattering cross section data the optical potential seems to be able to satisfactorily predict the more recent and more precise data. This is the first time any optical potential has been able to satisfactorily describe the elastic differential scattering cross section data for such a large energy range for even one nucleus, much less a range of nuclei!

Now that the interaction of the pion with the nucleus seems to be satisfactorily understood and described in terms of an optical potential, it is possible to seriously investigate other processes involving initial or final state pion-nucleus interactions such as photo-pion production, <sup>123</sup> electro-pion production, pion single and double charge exchange, and inelastic pion scattering.

## APPENDIX A

### Derivation of the Pion-Nucleon and Pion-Nucleon-Pair Interaction Operators in Terms of Partial Wave Amplitudes

#### 1. Pion-Nucleon Interaction Operator

Following the suggestion of Ericson and Ericson<sup>19</sup> one may expand the pion-nucleon interaction operator  $f_{\underline{1}}(\vec{r})$  in terms of the pion-nucleon partial wave amplitudes  $\alpha_{2T}$  and  $\alpha_{2T,2J}$ , since the orbital angular momentum  $\underline{l}$ , the total angular momentum  $J$ , and the total isotopic spin  $T$  of the pion-nucleon system are conserved in the interaction. In order to do this  $f_{\underline{1}}(\vec{r})$  may be written in terms of angular momentum and isospin projection operators.

$$A1 \quad \underline{f}_{\underline{1}}(\vec{r}) = \alpha_1 \underline{\pi}_{T=1/2} + \alpha_3 \underline{\pi}_{T=3/2} + \sum_{l=1}^{\infty} (2l+1) \left[ \alpha_{1,2l+1} \underline{\pi}_{T=1/2} \underline{\pi}_{J=l+1/2} \right. \\ \left. + \alpha_{3,2l+1} \underline{\pi}_{T=3/2} \underline{\pi}_{J=l+1/2} + \alpha_{1,2l-1} \underline{\pi}_{T=1/2} \underline{\pi}_{J=l-1/2} + \alpha_{3,2l-1} \right. \\ \left. \underline{\pi}_{T=3/2} \underline{\pi}_{J=l-1/2} \right] P_l(\cos \theta)$$

For s- and p-waves only  $l = 0$  or  $1$

$$A2 \quad \underline{f}_{\underline{1}}(\vec{r}) = \alpha_1 \underline{\pi}_{T=1/2} + \alpha_3 \underline{\pi}_{T=3/2} + 3 \left[ \alpha_{1,3} \underline{\pi}_{T=1/2} \underline{\pi}_{J=2+1/2} \right. \\ \left. + \alpha_{3,3} \underline{\pi}_{T=3/2} \underline{\pi}_{J=2+1/2} + \alpha_{1,1} \underline{\pi}_{T=1/2} \underline{\pi}_{J=1-1/2} + \alpha_{3,1} \underline{\pi}_{T=3/2} \underline{\pi}_{J=1-1/2} \right] P_1(\cos \theta)$$

The angular momentum projection operators may be defined using the relations

$$A3 \quad \underline{J}^2 = \underline{l}^2 + \underline{s}^2 + 2\underline{l} \cdot \underline{s}$$

$$A4 \quad J(J+1) = l(l+1) + \frac{1}{2}(1+\frac{1}{2}) + \underline{\underline{\sigma \cdot l}}$$

Note

$$A5 \quad \underline{\underline{\sigma \cdot l}} = J(J+1) - l(l+1) - \frac{3}{4} = \begin{cases} l & \text{for } J=l+\frac{1}{2} \\ -l-1 & \text{for } J=l-\frac{1}{2} \end{cases}$$

Thus the angular momentum projection operators may be defined in the spatial representation by

$$A6 \quad \underline{\underline{\Pi}}_{J=l-\frac{1}{2}} = \frac{l - \underline{\underline{\sigma \cdot l}}}{2l+1}$$

$$A7 \quad \underline{\underline{\Pi}}_{J=l+\frac{1}{2}} = \frac{l+1 + \underline{\underline{\sigma \cdot l}}}{2l+1}$$

Usually the projection operators are written in the momentum representation instead of the spatial representation. In order to perform the transformation it is necessary to group the projection operators with the angular-dependent part of the scattering operator. The required transformations are as follows

$$A8 \quad \underline{\underline{1}} P_{l=1}(\cos\theta) \Rightarrow \underline{\underline{1}} P_{l=1}\left(\frac{\underline{\underline{k \cdot k'}}}{k^2}\right) = \frac{\underline{\underline{k \cdot k'}}}{k^2}$$

$$\begin{aligned} A9 \quad \underline{\underline{\sigma \cdot l}} P_{l=1}(\cos\theta) &\Rightarrow i \underline{\underline{\sigma \cdot (\nabla_k \times k)}} \cos\theta \\ &= i \underline{\underline{\sigma \cdot \left(\frac{\hat{\theta}}{k} \frac{\partial}{\partial \theta} \cos\theta \times \underline{\underline{k}}\right)}} \\ &= i \underline{\underline{\sigma \cdot \left(-\frac{\sin\theta}{k} \hat{\theta} \times \underline{\underline{k}}\right)}} \\ &= i \underline{\underline{\sigma \cdot \frac{\underline{\underline{k'}} \times \underline{\underline{k}}}{k^2}}} \end{aligned}$$

124

Thus in the momentum representation

$$A10 \quad \prod_{J=\ell-\gamma_2} P_{\ell=1}(\cos\theta) \Rightarrow \frac{\underline{k} \cdot \underline{k}' - i \underline{\nabla} \cdot (\underline{k}' \times \underline{k})}{3k^2}$$

$$A11 \quad \prod_{J=\ell+\gamma_2} P_{\ell=1}(\cos\theta) \Rightarrow \frac{2 \underline{k} \cdot \underline{k}' + i \underline{\nabla} \cdot (\underline{k}' \times \underline{k})}{3k^2}$$

The isospin projection operators may be defined using the relations

$$A12 \quad \underline{T} = \frac{1}{2} \underline{T} + \underline{t}_n$$

$$A13 \quad \underline{T}^2 = \frac{1}{4} \underline{T}^2 + \underline{t}_n^2 + \underline{t}_n \cdot \underline{T}$$

$$A14 \quad \underline{T} \cdot \underline{t}_n = T(T+1) - 1(1+1) - \frac{1}{2}(1+\frac{1}{2}) = \begin{cases} 1 & \text{for } T = \underline{t}_n + \gamma_2 \\ -\underline{t}_n - 1 & \text{for } T = \underline{t}_n - \gamma_2 \end{cases}$$

Thus the isospin projection operators may be defined

$$A15 \quad \prod_{T = \underline{t}_n - \gamma_2} = \frac{1 - \underline{T} \cdot \underline{t}_n}{3}$$

$$A16 \quad \prod_{T = \underline{t}_n + \gamma_2} = \frac{2 + \underline{T} \cdot \underline{t}_n}{3}$$

Substituting the angular momentum and isospin projection operators into  $\underline{f}_1(\vec{r})$  obtain the interaction operator on nucleon  $\underline{i}$  to be

$$A17 \quad \underline{f}_i(\vec{r}) = \alpha_1 \left( \frac{1 - \underline{t}_n \cdot \underline{T}_i}{3} \right) + \alpha_3 \left( \frac{2 + \underline{t}_n \cdot \underline{T}_i}{3} \right) + 3\alpha_{13} \left( \frac{1 - \underline{t}_n \cdot \underline{T}_i}{3} \right) \left( \frac{2 \underline{k} \cdot \underline{k}' + i \underline{\nabla}_i \cdot (\underline{k}' \times \underline{k})}{3k^2} \right) \\ + 3\alpha_{33} \left( \frac{2 + \underline{t}_n \cdot \underline{T}_i}{3} \right) \left( \frac{2 \underline{k} \cdot \underline{k}' + i \underline{\nabla}_i \cdot (\underline{k}' \times \underline{k})}{3k^2} \right) + 3\alpha_{11} \left( \frac{1 - \underline{t}_n \cdot \underline{T}_i}{3} \right) \\ \left( \frac{\underline{k} \cdot \underline{k}' - i \underline{\nabla}_i \cdot (\underline{k}' \times \underline{k})}{3k^2} \right) + 3\alpha_{31} \left( \frac{2 + \underline{t}_n \cdot \underline{T}_i}{3} \right) \left( \frac{\underline{k} \cdot \underline{k}' - i \underline{\nabla}_i \cdot (\underline{k}' \times \underline{k})}{3k^2} \right)$$

Rewriting  $f_{\underline{1}}(\vec{r})$  and regrouping terms obtain

$$\begin{aligned}
 \text{A18} \quad \underline{f}_{\underline{1}}(\vec{r}) &= \frac{\alpha_1 + 2\alpha_3}{3} + \frac{\alpha_3 - \alpha_1}{3} (\underline{t}_{\underline{1}} \cdot \underline{\tau}_i) + \left( \frac{2\alpha_{13} + 4\alpha_{33} + \alpha_{11} + 2\alpha_{31}}{3} \right. \\
 &+ \left. \frac{2\alpha_{33} - 2\alpha_{13} - \alpha_{11} + \alpha_{31}}{3} (\underline{t}_{\underline{1}} \cdot \underline{\tau}_i) \right) \frac{\underline{k} \cdot \underline{k}'}{k^2} + \left( \frac{\alpha_{13} + 2\alpha_{33} - \alpha_{11} - 2\alpha_{31}}{3} \right. \\
 &+ \left. \frac{\alpha_{33} - \alpha_{13} + \alpha_{11} - \alpha_{31}}{3} (\underline{t}_{\underline{1}} \cdot \underline{\tau}_i) \right) i \underline{\tau}_i \cdot \frac{(\underline{k}' \times \underline{k})}{k^2} \\
 &= b_0 + b_1 (\underline{t}_{\underline{1}} \cdot \underline{\tau}_i) + (c_0 + c_1 (\underline{t}_{\underline{1}} \cdot \underline{\tau}_i)) \frac{\underline{k} \cdot \underline{k}'}{k^2} \\
 &+ (d_0 + d_1 (\underline{t}_{\underline{1}} \cdot \underline{\tau}_i)) i \underline{\tau}_i \cdot \frac{(\underline{k}' \times \underline{k})}{k^2}
 \end{aligned}$$

where

$$\begin{aligned}
 \text{A19} \quad b_0 &= \frac{\alpha_1 + 2\alpha_3}{3} & b_1 &= \frac{\alpha_3 - \alpha_1}{3} \\
 c_0 &= \frac{2\alpha_{13} + 4\alpha_{33} + \alpha_{11} + 2\alpha_{31}}{3k^2} & c_1 &= \frac{-2\alpha_{13} + 2\alpha_{33} - \alpha_{11} + \alpha_{31}}{3k^2} \\
 d_0 &= \frac{-\alpha_{13} - 2\alpha_{33} + \alpha_{11} + 2\alpha_{31}}{3k^2} & d_1 &= \frac{\alpha_{13} - \alpha_{33} - \alpha_{11} + \alpha_{31}}{3k^2}
 \end{aligned}$$

These results are in agreement with those of Ericson and Ericson.

Writing  $f_{\underline{1}}(\vec{r})$  back in the spatial representation obtain

$$\begin{aligned}
 \text{A20} \quad \underline{f}_{\underline{1}}(\vec{r}) &= b_0 + b_1 (\underline{t}_{\underline{1}} \cdot \underline{\tau}_i) - \nabla \cdot (c_0 + c_1 \underline{t}_{\underline{1}} \cdot \underline{\tau}_i) \nabla' \\
 &+ i (d_0 + d_1 \underline{t}_{\underline{1}} \cdot \underline{\tau}_i) \nabla \cdot (\underline{\nabla}(\underline{r}) \times \nabla')
 \end{aligned}$$

where

$$A21 \quad \underline{\sigma}(r) = \sum_{i=1}^A \underline{\sigma}_i \delta(\vec{r}-\vec{r}_i)$$

$$A22 \quad \underline{\vec{\sigma}}(r) = \langle 0 | \sum_{i=1}^A \underline{\sigma}_i \delta(\vec{r}-\vec{r}_i) | 0 \rangle = \frac{2 \underline{\vec{s}} e(r)}{A}$$

and  $\underline{\vec{s}}$  is the intrinsic spin of the nucleus. Thus

$$A23 \quad \underline{f}_i(r) | 0 \rangle = \left[ b_0 + b_1 \underline{t}_n \cdot \underline{\tau}_i - \nabla \cdot (c_0 + c_1 \underline{t}_n \cdot \underline{\tau}_i) \nabla' \right. \\ \left. + \frac{2i}{A} (d_0 + d_1 \underline{t}_n \cdot \underline{\tau}_i) \nabla \cdot (e(r) \underline{\vec{s}} \times \underline{\vec{\nabla}}') \right] | 0 \rangle$$

where  $| 0 \rangle$  represents the nuclear ground state.

Now for a spherical spin density distribution  $e(r)$

$$A24 \quad \nabla \cdot i \underline{\vec{s}} e(r) \times \nabla' = -\frac{1}{r} \frac{d}{dr} e(r) i \underline{\vec{s}} \cdot \vec{r} \times \nabla' \\ = \frac{\underline{\vec{s}} \cdot \underline{\vec{t}}_n}{r} \frac{d}{dr} e(r)$$

so

$$A25 \quad \underline{f}_i(r) | 0 \rangle = \left[ b_0 + b_1 \underline{t}_n \cdot \underline{\tau}_i - \nabla \cdot (c_0 + c_1 \underline{t}_n \cdot \underline{\tau}_i) \nabla' \right. \\ \left. + (d_0 + d_1 \underline{t}_n \cdot \underline{\tau}_i) \frac{2}{A} \frac{\underline{\vec{s}} \cdot \underline{\vec{t}}_n}{r} \frac{d}{dr} \right] | 0 \rangle$$

For  $l_n = 0$  or spin zero nuclei the  $d_0$  and  $d_1$  terms give no contribution.

## 2. Pion-Nucleon-Pair Interaction Operator

The pion-nucleon-pair interaction operator  $f_{ij}(\vec{r})$  may be expanded in terms of the pion-nucleon partial wave amplitudes  $B_{JT}$  and  $\gamma_{JT}(S,T)$  where  $S$  and  $T$  refer to the total spin and isospin of the nucleon pair. This expansion is valid, since the orbital angular momentum  $\ell$ , the total angular momentum  $J$ , and the total isotopic spin  $T$  of the pion-nucleon-pair system is conserved in the interaction. In order to make the expansion,  $f_{ij}(\vec{r})$  must be written in terms of angular momentum and isospin projection operators.

$$\begin{aligned}
 \text{A31} \quad \underline{f}_{ij}(\vec{r}) &= B_{11} \underline{\pi}_{J=1}^{\text{sym}} \underline{\pi}_{T=1}^{\text{Anti}} + B_{00} \underline{\pi}_{J=0}^{\text{Anti}} \underline{\pi}_{T=0}^{\text{sym}} + B_{01} \underline{\pi}_{J=0}^{\text{Anti}} \underline{\pi}_{T=1}^{\text{sym}} \\
 &+ B_{02} \underline{\pi}_{J=0}^{\text{Anti}} \underline{\pi}_{T=2}^{\text{sym}} + \sum_{\ell=1}^{\infty} (2\ell+1) \left[ \gamma_{\ell+1,1} \underline{\pi}_{J=\ell+1}^{\text{sym}} \underline{\pi}_{T=1}^{\text{Anti}} \right. \\
 &+ \gamma_{\ell-1,1} \underline{\pi}_{J=\ell-1}^{\text{sym}} \underline{\pi}_{T=1}^{\text{Anti}} + \gamma_{\ell,0} \underline{\pi}_{J=\ell}^{\text{Anti}} \underline{\pi}_{T=0}^{\text{sym}} + \gamma_{\ell,0} (0,2) \underline{\pi}_{J=\ell}^{\text{Anti}} \underline{\pi}_{T=1}^{\text{sym}} \\
 &\left. + \gamma_{\ell,1} (2,0) \underline{\pi}_{J=\ell}^{\text{sym}} \underline{\pi}_{T=1}^{\text{Anti}} + \gamma_{\ell,2} \underline{\pi}_{J=\ell}^{\text{Anti}} \underline{\pi}_{T=2}^{\text{sym}} \right] P_{\ell}(\cos\theta)
 \end{aligned}$$

where the  $\underline{\pi}$ 's are projection operators to be defined in which the sym and anti refer to the nucleon pair and  $\vec{r}$  is the pion coordinate.

For s- and p-waves only

$$\begin{aligned}
 \text{A32} \quad \underline{f}_{ij}(\vec{r}) &= B_{11} \underline{\pi}_{J=1}^{\text{sym}} \underline{\pi}_{T=1}^{\text{Anti}} + B_{00} \underline{\pi}_{J=0}^{\text{Anti}} \underline{\pi}_{T=0}^{\text{sym}} + B_{01} \underline{\pi}_{J=0}^{\text{Anti}} \underline{\pi}_{T=1}^{\text{sym}} \\
 &+ B_{02} \underline{\pi}_{J=0}^{\text{Anti}} \underline{\pi}_{T=2}^{\text{sym}} + 3 \left[ \gamma_{21} \underline{\pi}_{J=2}^{\text{sym}} \underline{\pi}_{T=1}^{\text{Anti}} + \gamma_{01} \underline{\pi}_{J=0}^{\text{sym}} \underline{\pi}_{T=1}^{\text{Anti}} \right. \\
 &\left. + \gamma_{10} \underline{\pi}_{J=1}^{\text{Anti}} \underline{\pi}_{T=0}^{\text{sym}} + \gamma_{11} (0,2) \underline{\pi}_{J=1}^{\text{Anti}} \underline{\pi}_{T=1}^{\text{sym}} + \gamma_{11} (2,0) \underline{\pi}_{J=1}^{\text{sym}} \underline{\pi}_{T=1}^{\text{Anti}} \right]
 \end{aligned}$$

$$+ \gamma_{12} \left[ \prod_{J=1}^{\text{Anti}} \prod_{T=2}^{\text{sym}} \right] \cos \theta$$

Some of the angular momentum projection operators may be defined using the relation for  $l = 0$

$$\text{A33} \quad \underline{J}^2 = \underline{S}^2 = \underline{S}_i^2 + \underline{S}_j^2 + 2 \underline{S}_i \cdot \underline{S}_j = \underline{S}_i^2 + \underline{S}_j^2 + \frac{\underline{V}_i \cdot \underline{V}_j}{2}$$

so

$$\text{A34} \quad \underline{V}_i \cdot \underline{V}_j = 2 \left[ S(S+1) - \frac{1}{2} \left(1 + \frac{1}{2}\right) - \frac{1}{2} \left(1 + \frac{1}{2}\right) \right] = \begin{cases} 1 & \text{for } S=1 \\ -3 & \text{for } S=0 \end{cases}$$

Thus the  $l = 0$  angular momentum projection operators may be written

$$\text{A35} \quad \prod_{J=0}^{\text{Anti}} = \frac{1 - \underline{V}_i \cdot \underline{V}_j}{4}$$

$$\text{A36} \quad \prod_{J=1}^{\text{sym}} = \frac{3 + \underline{V}_i \cdot \underline{V}_j}{4}$$

The isospin projection operators may be defined using the relations

$$\text{A37} \quad \underline{T} = \frac{1}{2} \underline{T}_i + \frac{1}{2} \underline{T}_j + \underline{t}_n$$

$$\text{A38} \quad \underline{T}^2 = \frac{1}{4} \underline{T}_i^2 + \frac{1}{4} \underline{T}_j^2 + \underline{t}_n^2 + \underline{t}_n \cdot (\underline{T}_i + \underline{T}_j) + \frac{1}{2} \underline{T}_i \cdot \underline{T}_j$$

so

$$\begin{aligned} \text{A39} \quad \underline{t}_n \cdot (\underline{T}_i + \underline{T}_j) + \frac{1}{2} \underline{T}_i \cdot \underline{T}_j &= T(T+1) - 1(1+1) - \frac{1}{2}(1+\frac{1}{2}) - \frac{1}{2}(1+\frac{1}{2}) \\ &= T(T+1) - \frac{3}{2} = \begin{cases} \frac{5}{2} & \text{for } T=2 \\ -\frac{3}{2} & \text{for } T=1 \\ -\frac{1}{2} & \text{for } T=0 \end{cases} \end{aligned}$$

where  $\underline{\tau}_i$  is the isospin matrix vector operating on nucleon  $i$ ,  $\underline{\tau}_\pi$  is the pion isospin vector, and  $\underline{T}$  is the total isospin vector for the pion-nucleon-pair system. Thus the isospin projection operators may be written

$$A40 \quad \underline{\Pi}_{T=0}^{\text{sym}} = - \left( \frac{\frac{3}{2} + \underline{\tau}_\pi \cdot (\underline{\tau}_i + \underline{\tau}_j) + \frac{1}{2} \underline{\tau}_i \cdot \underline{\tau}_j}{2} \right) \left( \frac{5/2 - \underline{\tau}_\pi \cdot (\underline{\tau}_i + \underline{\tau}_j) - \frac{1}{2} \underline{\tau}_i \cdot \underline{\tau}_j}{6} \right)$$

$$A41 \quad \underline{\Pi}_{T=1}^{\text{sym}} = \left( \frac{\frac{1}{2} + \underline{\tau}_\pi \cdot (\underline{\tau}_i + \underline{\tau}_j) + \frac{1}{2} \underline{\tau}_i \cdot \underline{\tau}_j}{2} \right) \left( \frac{5/2 - \underline{\tau}_\pi \cdot (\underline{\tau}_i + \underline{\tau}_j) - \frac{1}{2} \underline{\tau}_i \cdot \underline{\tau}_j}{4} \right) \left( \frac{3 + \underline{\tau}_i \cdot \underline{\tau}_j}{4} \right)$$

$$A42 \quad \underline{\Pi}_{T=2}^{\text{sym}} = \left( \frac{7/2 + \underline{\tau}_\pi \cdot (\underline{\tau}_i + \underline{\tau}_j) + \frac{1}{2} \underline{\tau}_i \cdot \underline{\tau}_j}{6} \right) \left( \frac{3/2 + \underline{\tau}_\pi \cdot (\underline{\tau}_i + \underline{\tau}_j) + \frac{1}{2} \underline{\tau}_i \cdot \underline{\tau}_j}{4} \right)$$

$$A43 \quad \underline{\Pi}_{T=1}^{\text{Anti}} = \frac{1 - \underline{\tau}_i \cdot \underline{\tau}_j}{4}$$

In order to simplify the terms in the projection operator expressions note that

$$A44 \quad [T(T+1) - 7/2]^2 = [\underline{\tau}_\pi \cdot (\underline{\tau}_i + \underline{\tau}_j) + \frac{1}{2} \underline{\tau}_i \cdot \underline{\tau}_j]^2 \\ = \underline{\tau}_\pi \cdot (\underline{\tau}_i + \underline{\tau}_j) \underline{\tau}_\pi \cdot (\underline{\tau}_i + \underline{\tau}_j) + \underline{\tau}_\pi \cdot (\underline{\tau}_i + \underline{\tau}_j) (\underline{\tau}_i \cdot \underline{\tau}_j) + \frac{1}{4} (\underline{\tau}_i \cdot \underline{\tau}_j)^2$$

In analogy to  $(\vec{\sigma} \cdot \vec{A})(\vec{\sigma} \cdot \vec{B}) = \vec{A} \cdot \vec{B} + i \vec{\sigma} \cdot \vec{A} \times \vec{B}$

$$A45 \quad (\underline{\tau}_i \cdot \underline{\tau}_\pi)(\underline{\tau}_i \cdot \underline{\tau}_\pi) = \underline{\tau}_\pi^2 + i \underline{\tau}_i \cdot (\underline{\tau}_\pi \times \underline{\tau}_\pi) = 2 - \underline{\tau}_i \cdot \underline{\tau}_\pi$$

Thus

$$A46 \quad [T(T+1) - 7/2]^2 = (\underline{\tau}_\pi \cdot \underline{\tau}_i)(\underline{\tau}_\pi \cdot \underline{\tau}_i) + (\underline{\tau}_\pi \cdot \underline{\tau}_j)(\underline{\tau}_\pi \cdot \underline{\tau}_j) + 4 \\ - \underline{\tau}_\pi \cdot (\underline{\tau}_i + \underline{\tau}_j) + \underline{\tau}_\pi \cdot (\underline{\tau}_i + \underline{\tau}_j) (\underline{\tau}_i \cdot \underline{\tau}_j) + \frac{1}{4} (\underline{\tau}_i \cdot \underline{\tau}_j)^2 + i \vec{\sigma} \cdot \vec{A} \times \vec{B}$$

Also note

$$A47 \quad -\underline{t}_n \cdot (\underline{\tau}_i + \underline{\tau}_j) + \underline{t}_n \cdot (\underline{\tau}_i + \underline{\tau}_j)(\underline{\tau}_i \cdot \underline{\tau}_j) = -4\underline{t}_n \cdot (\underline{\tau}_i + \underline{\tau}_j) \left( \frac{1 - \underline{\tau}_i \cdot \underline{\tau}_j}{4} \right) = 0$$

since  $(1 - \underline{\tau}_i \cdot \underline{\tau}_j)/4$  is nonzero only for antisymmetric  $ij$  isospin states and  $\underline{t}_n \cdot (\underline{\tau}_i + \underline{\tau}_j)$  is nonzero only for symmetric states.

In addition note that

$$A48 \quad 4 \left( \frac{3 + \underline{\tau}_i \cdot \underline{\tau}_j}{4} \right)^2 = 4 \left[ \frac{9}{16} + \frac{6}{16} \underline{\tau}_i \cdot \underline{\tau}_j + \frac{1}{16} (\underline{\tau}_i \cdot \underline{\tau}_j)^2 \right]$$

so

$$A49 \quad \frac{(\underline{\tau}_i \cdot \underline{\tau}_j)^2}{4} = -\frac{9}{4} - \frac{3}{2} \underline{\tau}_i \cdot \underline{\tau}_j + 4 \left( \frac{3 + \underline{\tau}_i \cdot \underline{\tau}_j}{4} \right)^2$$

But

$$A50 \quad \left( \frac{3 + \underline{\tau}_i \cdot \underline{\tau}_j}{4} \right)^2 = \frac{3 + \underline{\tau}_i \cdot \underline{\tau}_j}{4}$$

so

$$A51 \quad \frac{(\underline{\tau}_i \cdot \underline{\tau}_j)^2}{4} = -\frac{9}{4} - \frac{3}{2} \underline{\tau}_i \cdot \underline{\tau}_j + 3 + \underline{\tau}_i \cdot \underline{\tau}_j = \frac{3}{4} - \frac{1}{2} \underline{\tau}_i \cdot \underline{\tau}_j$$

Substituting A51 and A47 into A46 obtain

$$A52 \quad \left[ T(T+1) - \frac{3}{2} \right]^2 = (\underline{t}_n \cdot \underline{\tau}_i)(\underline{t}_n \cdot \underline{\tau}_j) + (\underline{t}_n \cdot \underline{\tau}_j)(\underline{t}_n \cdot \underline{\tau}_i) + \frac{19}{4} - \frac{1}{2} \underline{\tau}_i \cdot \underline{\tau}_j$$

Also

$$A53 \quad \left[ \underline{t}_n \cdot (\underline{\tau}_i + \underline{\tau}_j) + \frac{1}{2} \underline{\tau}_i \cdot \underline{\tau}_j \right]^2 \left( \frac{3 + \underline{\tau}_i \cdot \underline{\tau}_j}{4} \right) = \left[ \underline{t}_n \cdot (\underline{\tau}_i + \underline{\tau}_j) \underline{t}_n \cdot (\underline{\tau}_i + \underline{\tau}_j) + \underline{t}_n \cdot (\underline{\tau}_i + \underline{\tau}_j)(\underline{\tau}_i \cdot \underline{\tau}_j) + \frac{1}{4} (\underline{\tau}_i \cdot \underline{\tau}_j)^2 \right] \left( \frac{3 + \underline{\tau}_i \cdot \underline{\tau}_j}{4} \right)$$

Using

$$A54 \quad (\underline{\tau}_i \cdot \underline{\tau}_j) \left( \frac{3 + \underline{\tau}_i \cdot \underline{\tau}_j}{4} \right) = 1 \left( \frac{3 + \underline{\tau}_i \cdot \underline{\tau}_j}{4} \right)$$

$$A55 \quad \underline{t}_n \cdot (\underline{\tau}_i + \underline{\tau}_j) \left( \frac{3 + \underline{\tau}_i \cdot \underline{\tau}_j}{4} \right) = \underline{t}_n \cdot (\underline{\tau}_i + \underline{\tau}_j)$$

then

$$\begin{aligned} A56 \quad & \left[ \underline{t}_n \cdot (\underline{\tau}_i + \underline{\tau}_j) + \frac{1}{2} \underline{\tau}_i \cdot \underline{\tau}_j \right]^2 \left( \frac{3 + \underline{\tau}_i \cdot \underline{\tau}_j}{4} \right) = \underline{t}_n \cdot (\underline{\tau}_i + \underline{\tau}_j) \underline{t}_n \cdot (\underline{\tau}_i + \underline{\tau}_j) \\ & + \underline{t}_n \cdot (\underline{\tau}_i + \underline{\tau}_j) + \frac{1}{4} \left( \frac{3 + \underline{\tau}_i \cdot \underline{\tau}_j}{4} \right) \\ & = (\underline{t}_n \cdot \underline{\tau}_i)(\underline{t}_n \cdot \underline{\tau}_j) + (\underline{t}_n \cdot \underline{\tau}_j)(\underline{t}_n \cdot \underline{\tau}_i) + 4 - \underline{t}_n \cdot (\underline{\tau}_i + \underline{\tau}_j) \\ & \quad + \underline{t}_n \cdot (\underline{\tau}_i + \underline{\tau}_j) + \frac{3}{12} + \frac{\underline{\tau}_i \cdot \underline{\tau}_j}{16} \\ & = (\underline{t}_n \cdot \underline{\tau}_i)(\underline{t}_n \cdot \underline{\tau}_j) + (\underline{t}_n \cdot \underline{\tau}_j)(\underline{t}_n \cdot \underline{\tau}_i) + 4 + \frac{1}{4} \left( \frac{3 + \underline{\tau}_i \cdot \underline{\tau}_j}{4} \right) \end{aligned}$$

Substituting A52 and A56 into the expressions for the projection operators obtain

$$\begin{aligned} A57 \quad \underline{\Pi}_{T=0}^{sym} &= -\left(\frac{1}{12}\right) \left[ \frac{15}{4} + \underline{t}_n \cdot (\underline{\tau}_i + \underline{\tau}_j) + \frac{1}{2} \underline{\tau}_i \cdot \underline{\tau}_j - (\underline{t}_n \cdot \underline{\tau}_i)(\underline{t}_n \cdot \underline{\tau}_j) \right. \\ & \quad \left. - (\underline{t}_n \cdot \underline{\tau}_j)(\underline{t}_n \cdot \underline{\tau}_i) - \frac{19}{4} + \frac{1}{2} \underline{\tau}_i \cdot \underline{\tau}_j \right] \\ &= \frac{1}{12} \left[ 1 - \underline{\tau}_i \cdot \underline{\tau}_j - \underline{t}_n \cdot (\underline{\tau}_i + \underline{\tau}_j) + (\underline{t}_n \cdot \underline{\tau}_i)(\underline{t}_n \cdot \underline{\tau}_j) + (\underline{t}_n \cdot \underline{\tau}_j)(\underline{t}_n \cdot \underline{\tau}_i) \right] \end{aligned}$$

$$\begin{aligned} A58 \quad \underline{\Pi}_{T=1}^{sym} &= \frac{1}{8} \left[ \frac{35}{4} - \underline{t}_n \cdot (\underline{\tau}_i + \underline{\tau}_j) - \frac{1}{2} (\underline{\tau}_i \cdot \underline{\tau}_j) - \left\{ \underline{t}_n \cdot (\underline{\tau}_i + \underline{\tau}_j) \right. \right. \\ & \quad \left. \left. + \frac{1}{2} \underline{\tau}_i \cdot \underline{\tau}_j \right\}^2 \right] \left( \frac{3 + \underline{\tau}_i \cdot \underline{\tau}_j}{4} \right) \end{aligned}$$

But

$$\begin{aligned} \text{A59} \quad \left( \frac{35}{4} - \frac{1}{2} (\underline{\tau}_i \cdot \underline{\tau}_j) \right) \left( \frac{3 + \underline{\tau}_i \cdot \underline{\tau}_j}{4} \right) &= \left[ \frac{33}{4} + 2 \left( \frac{1 - \underline{\tau}_i \cdot \underline{\tau}_j}{4} \right) \right] \left( \frac{3 + \underline{\tau}_i \cdot \underline{\tau}_j}{4} \right) \\ &= \frac{33}{4} \left( \frac{3 + \underline{\tau}_i \cdot \underline{\tau}_j}{4} \right) \end{aligned}$$

and using previous identities for the  $\{ \}$  term obtain

$$\begin{aligned} \text{A60} \quad \prod_{T=1}^{\text{sym}} &= \frac{1}{8} \left[ \frac{33}{4} \left( \frac{3 + \underline{\tau}_i \cdot \underline{\tau}_j}{4} \right) - \underline{t}_n \cdot (\underline{\tau}_i + \underline{\tau}_j) - (\underline{t}_n \cdot \underline{\tau}_i)(\underline{t}_n \cdot \underline{\tau}_j) \right. \\ &\quad \left. - (\underline{t}_n \cdot \underline{\tau}_j)(\underline{t}_n \cdot \underline{\tau}_i) - 4 - \frac{1}{4} \left( \frac{3 + \underline{\tau}_i \cdot \underline{\tau}_j}{4} \right) \right] \\ &= \frac{1}{8} \left[ 2 + 2 \underline{\tau}_i \cdot \underline{\tau}_j - \underline{t}_n \cdot (\underline{\tau}_i + \underline{\tau}_j) - (\underline{t}_n \cdot \underline{\tau}_i)(\underline{t}_n \cdot \underline{\tau}_j) - (\underline{t}_n \cdot \underline{\tau}_j)(\underline{t}_n \cdot \underline{\tau}_i) \right] \end{aligned}$$

$$\begin{aligned} \text{A61} \quad \prod_{T=2}^{\text{sym}} &= \frac{1}{24} \left[ \frac{21}{4} + 5 \underline{t}_n \cdot (\underline{\tau}_i + \underline{\tau}_j) + \frac{5}{2} (\underline{\tau}_i \cdot \underline{\tau}_j) + (\underline{t}_n \cdot \underline{\tau}_i)(\underline{t}_n \cdot \underline{\tau}_j) \right. \\ &\quad \left. + (\underline{t}_n \cdot \underline{\tau}_j)(\underline{t}_n \cdot \underline{\tau}_i) + \frac{19}{4} - \frac{1}{2} \underline{\tau}_i \cdot \underline{\tau}_j \right] \\ &= \frac{1}{24} \left[ 10 + 5 \underline{t}_n \cdot (\underline{\tau}_i + \underline{\tau}_j) + 2 \underline{\tau}_i \cdot \underline{\tau}_j + (\underline{t}_n \cdot \underline{\tau}_i)(\underline{t}_n \cdot \underline{\tau}_j) \right. \\ &\quad \left. + (\underline{t}_n \cdot \underline{\tau}_j)(\underline{t}_n \cdot \underline{\tau}_i) \right] \end{aligned}$$

$$\text{A62} \quad \prod_{T=1}^{\text{Anti}} = \frac{1 - \underline{\tau}_i \cdot \underline{\tau}_j}{4}$$

Substituting these expressions for the projection operators into the expression for  $\underline{f}_{1j}(\vec{r})$  obtain for the  $\ell = 0$  part of the expansion

$$\begin{aligned}
 A63 \quad \underline{f}_{ij}(\underline{r}) \Big|_{x=0} &= B_{11} \left( \frac{3 + \underline{v}_i \cdot \underline{v}_j}{4} \right) \left( \frac{1 - \underline{r}_i \cdot \underline{r}_j}{4} \right) + B_{00} \left( \frac{1 - \underline{v}_i \cdot \underline{v}_j}{48} \right) \\
 &\quad \left[ 1 - \underline{r}_i \cdot \underline{r}_j - \underline{r}_i \cdot (\underline{r}_i + \underline{r}_j) + (\underline{r}_i \cdot \underline{r}_i)(\underline{r}_j \cdot \underline{r}_j) + (\underline{r}_i \cdot \underline{r}_j)(\underline{r}_j \cdot \underline{r}_i) \right] \\
 &+ B_{01} \left( \frac{1 - \underline{v}_i \cdot \underline{v}_j}{96} \right) \left[ 6 + 6 \underline{r}_i \cdot \underline{r}_j - 3 \underline{r}_i \cdot (\underline{r}_i + \underline{r}_j) - 3 (\underline{r}_i \cdot \underline{r}_i)(\underline{r}_j \cdot \underline{r}_j) \right. \\
 &\quad \left. - 3 (\underline{r}_i \cdot \underline{r}_j)(\underline{r}_j \cdot \underline{r}_i) \right] + B_{02} \left( \frac{1 - \underline{v}_i \cdot \underline{v}_j}{96} \right) \left[ 10 + 5 \underline{r}_i \cdot (\underline{r}_i + \underline{r}_j) \right. \\
 &\quad \left. + 2 \underline{r}_i \cdot \underline{r}_j + (\underline{r}_i \cdot \underline{r}_i)(\underline{r}_j \cdot \underline{r}_j) + (\underline{r}_i \cdot \underline{r}_j)(\underline{r}_j \cdot \underline{r}_i) \right] \\
 &\equiv B_0 + B_1 \underline{v}_i \cdot \underline{v}_j + B_2 \underline{r}_i \cdot \underline{r}_j + B_3 (1 - \underline{v}_i \cdot \underline{v}_j) \underline{r}_i \cdot (\underline{r}_i + \underline{r}_j) \\
 &\quad + B_4 (\underline{v}_i \cdot \underline{v}_j)(\underline{r}_i \cdot \underline{r}_j) + B_5 (1 - \underline{v}_i \cdot \underline{v}_j) \left[ (\underline{r}_i \cdot \underline{r}_i)(\underline{r}_j \cdot \underline{r}_j) + (\underline{r}_i \cdot \underline{r}_j)(\underline{r}_j \cdot \underline{r}_i) \right]
 \end{aligned}$$

where

$$A64 \quad B_0 = \frac{9B_{11} + B_{00} + 3B_{01} + 5B_{02}}{48}$$

$$B_1 = \frac{3B_{11} - B_{00} - 3B_{01} - 5B_{02}}{48}$$

$$B_2 = \frac{-9B_{11} - B_{00} + 3B_{01} + B_{02}}{48}$$

$$B_3 = \frac{-2B_{00} - 3B_{01} + 5B_{02}}{96}$$

$$B_4 = \frac{-3B_{11} + B_{00} - 3B_{01} - B_{02}}{48}$$

$$B_5 = \frac{2B_{00} - 3B_{01} + B_{02}}{96}$$

These results are not identical to those of Ericson and Ericson<sup>19</sup> who obtain a different  $B_3$ , i. e.

$$A65 \quad B_3 = \frac{-2B_{00} + 6B_{01} - 7B_{02}}{96}$$

For the  $l = 1$  case the angular momentum projection operators may be defined using the relations

$$A66 \quad \underline{J} = \underline{l} + \underline{s}_i + \underline{s}_j$$

$$A67 \quad \underline{J}^2 = \underline{l}^2 + \underline{s}_i^2 + \underline{s}_j^2 + 2\underline{l} \cdot (\underline{s}_i + \underline{s}_j) + 2\underline{s}_i \cdot \underline{s}_j$$

For the  $l = 1$  p-wave

$$A68 \quad J(J+1) = 1(1+1) + \frac{1}{2}(1+\frac{1}{2}) + \frac{1}{2}(1+\frac{1}{2}) + \underline{l} \cdot (\underline{v}_i + \underline{v}_j) + \frac{\underline{v}_i \cdot \underline{v}_j}{2}$$

or

$$A69 \quad \underline{l} \cdot (\underline{v}_i + \underline{v}_j) + \frac{\underline{v}_i \cdot \underline{v}_j}{2} = J(J+1) - \frac{3}{2} = \begin{cases} 5/2 & \text{For } J=2 \\ -3/2 & \text{For } J=1 \\ -1/2 & \text{For } J=0 \end{cases}$$

Thus the  $l = 1$  angular momentum projection operators may be defined

$$A70 \quad \underline{\pi}_{J=2}^{sym} = \left( \frac{3/2 + \underline{l} \cdot (\underline{v}_i + \underline{v}_j) + \frac{\underline{v}_i \cdot \underline{v}_j}{2}}{4} \right) \left( \frac{1/2 + \underline{l} \cdot (\underline{v}_i + \underline{v}_j) + \frac{1}{2} \underline{v}_i \cdot \underline{v}_j}{6} \right)$$

$$A71 \quad \underline{\pi}_{J=1}^{sym} = \left( \frac{5/2 - \underline{l} \cdot (\underline{v}_i + \underline{v}_j) - \frac{1}{2} \underline{v}_i \cdot \underline{v}_j}{4} \right) \left( \frac{1/2 + \underline{l} \cdot (\underline{v}_i + \underline{v}_j) + \frac{1}{2} \underline{v}_i \cdot \underline{v}_j}{2} \right) \left( \frac{3 + \underline{v}_i \cdot \underline{v}_j}{4} \right)$$

$$A72 \quad \underline{\pi}_{J=0}^{sym} = - \left( \frac{5/2 - \underline{l} \cdot (\underline{v}_i + \underline{v}_j) - \frac{1}{2} \underline{v}_i \cdot \underline{v}_j}{6} \right) \left( \frac{3/2 + \underline{l} \cdot (\underline{v}_i + \underline{v}_j) + \frac{1}{2} \underline{v}_i \cdot \underline{v}_j}{2} \right)$$

$$A73 \quad \underline{\pi}_{J=1}^{Anti} = \frac{1 - \underline{v}_i \cdot \underline{v}_j}{4}$$

In direct analogy to the simplification of the isospin projection operators for the local s-wave amplitude the angular momentum projection operators may be reduced to

$$A74 \quad \prod_{J=2}^{sym} = \frac{1}{24} \left[ 10 + 5 \underline{l} \cdot (\underline{v}_i + \underline{v}_j) + 2 \underline{v}_i \cdot \underline{v}_j + (\underline{l} \cdot \underline{v}_i)(\underline{l} \cdot \underline{v}_j) + (\underline{l} \cdot \underline{v}_j)(\underline{l} \cdot \underline{v}_i) \right]$$

$$A75 \quad \prod_{J=1}^{sym} = \frac{1}{8} \left[ 2 - \underline{l} \cdot (\underline{v}_i + \underline{v}_j) + 2 \underline{v}_i \cdot \underline{v}_j - (\underline{l} \cdot \underline{v}_i)(\underline{l} \cdot \underline{v}_j) - (\underline{l} \cdot \underline{v}_j)(\underline{l} \cdot \underline{v}_i) \right]$$

$$A76 \quad \prod_{J=0}^{sym} = \frac{1}{12} \left[ 1 - \underline{l} \cdot (\underline{v}_i + \underline{v}_j) - \underline{v}_i \cdot \underline{v}_j + (\underline{l} \cdot \underline{v}_i)(\underline{l} \cdot \underline{v}_j) + (\underline{l} \cdot \underline{v}_j)(\underline{l} \cdot \underline{v}_i) \right]$$

$$A77 \quad \prod_{J=1}^{Anti} = \frac{1 - \underline{v}_i \cdot \underline{v}_j}{4}$$

Usually the projection operators are written in the momentum representation instead of the spatial representation. In order to perform the transformation it is necessary to group the projection operators with the angular dependent part of the scattering amplitude. The required transformations are as follows:

$$A78 \quad 1 P_{l=1}(\cos \theta) \Rightarrow 1 P_{l=1}\left(\frac{\underline{k} \cdot \underline{k}'}{k^2}\right) = \frac{\underline{k} \cdot \underline{k}'}{k^2}$$

$$\begin{aligned} A79 \quad (\underline{v}_i \cdot \underline{l}) P_{l=1}(\cos \theta) &\Rightarrow i \underline{v}_i \cdot (\underline{v}_k \times \underline{k}) \cos \theta \\ &= i \underline{v}_i \cdot \left( \frac{\hat{\theta}}{k} \frac{\partial}{\partial \theta} \cos \theta \times \underline{k} \right) \\ &= i \underline{v}_i \cdot \left( -\frac{\sin \theta}{k} \hat{\theta} \times \underline{k} \right) \\ &= i \underline{v}_i \cdot \frac{\underline{k}' \times \underline{k}}{k^2} \end{aligned}$$

$$\begin{aligned} A80 \quad (\underline{v}_i \cdot \underline{l})(\underline{v}_j \cdot \underline{l}) P_{l=1}(\cos \theta) &\Rightarrow -\underline{v}_i \cdot \left( \frac{\hat{\theta}}{k} \frac{\partial}{\partial \theta} \times \underline{k} \right) \underline{v}_j \cdot \left( \frac{\hat{\theta}}{k} \frac{\partial}{\partial \theta} \times \underline{k} \right) \cos \theta \\ &= -\underline{v}_i \cdot \left( \frac{\hat{\theta}}{k} \frac{\partial}{\partial \theta} \times \underline{k} \right) \underline{v}_j \cdot \left( -\frac{\sin \theta}{k} \hat{\theta} \times \underline{k} \right) \end{aligned}$$

$$\begin{aligned}
&= \underline{v}_i \cdot \left( \frac{\cos \theta}{k} \underline{\delta} x \underline{k} \right) \underline{v}_j \cdot \left( \frac{\underline{\delta}}{k} x \underline{k} \right) \\
&= (\underline{v}_i x \underline{k}') \cdot (\underline{v}_j x \underline{k}) / k^2
\end{aligned}$$

Similarly

$$A81 \quad (\underline{v}_j \cdot \underline{l})(\underline{v}_i \cdot \underline{l}) P_{\ell=1}(\cos \theta) \Rightarrow (\underline{v}_i x \underline{k}') \cdot (\underline{v}_j x \underline{k}) / k^2$$

Thus the projection operators may be written in the momentum representation as

$$A82 \quad \underline{\Pi}_{J=2}^{sym} = \frac{1}{24k^2} \left[ 10 \underline{k} \cdot \underline{k}' + 5i(\underline{v}_i + \underline{v}_j) \cdot (\underline{k}' x \underline{k}) + 2(\underline{v}_i \cdot \underline{v}_j) \underline{k} \cdot \underline{k}' \right. \\ \left. + (\underline{v}_i x \underline{k}') \cdot (\underline{v}_j x \underline{k}) + (\underline{v}_j x \underline{k}') \cdot (\underline{v}_i x \underline{k}) \right]$$

$$A83 \quad \underline{\Pi}_{J=1}^{sym} = \frac{1}{8k^2} \left[ 2 \underline{k} \cdot \underline{k}' + 2(\underline{v}_i \cdot \underline{v}_j) \underline{k} \cdot \underline{k}' - i(\underline{v}_i + \underline{v}_j) \cdot (\underline{k}' x \underline{k}) \right. \\ \left. - (\underline{v}_i x \underline{k}') \cdot (\underline{v}_j x \underline{k}) - (\underline{v}_j x \underline{k}') \cdot (\underline{v}_i x \underline{k}) \right]$$

$$A84 \quad \underline{\Pi}_{J=0}^{sym} = \frac{1}{12k^2} \left[ \underline{k} \cdot \underline{k}' - (\underline{v}_i \cdot \underline{v}_j) \underline{k} \cdot \underline{k}' - i(\underline{v}_i + \underline{v}_j) \cdot (\underline{k}' x \underline{k}) \right. \\ \left. + (\underline{v}_i x \underline{k}') \cdot (\underline{v}_j x \underline{k}) + (\underline{v}_j x \underline{k}') \cdot (\underline{v}_i x \underline{k}) \right]$$

$$A85 \quad \underline{\Pi}_{J=1}^{Anti} = \left( \frac{1 - \underline{v}_i \cdot \underline{v}_j}{4} \right) \frac{\underline{k} \cdot \underline{k}'}{k^2}$$

The isospin projection operators are the same as for the local s-wave amplitude. Substituting in for the angular momentum and isospin projection operators obtain for the  $\ell = 1$  part of the expansion for  $\underline{f}_{1j}(\vec{r})$

$$A86 \quad \underline{f}_{1j}(\vec{r}) \Big|_{\ell=1} = \frac{\gamma_{21}}{8k^2} \left[ (10 + 2 \underline{v}_i \cdot \underline{v}_j) \underline{k} \cdot \underline{k}' + 5i(\underline{v}_i + \underline{v}_j) \cdot (\underline{k}' x \underline{k}) \right. \\ \left. + (\underline{v}_i x \underline{k}') \cdot (\underline{v}_j x \underline{k}) + (\underline{v}_j x \underline{k}') \cdot (\underline{v}_i x \underline{k}) \right] \left( \frac{1 - \underline{v}_i \cdot \underline{v}_j}{4} \right)$$

$$\begin{aligned}
& + \frac{\gamma_{01}}{4k^2} \left[ (1 - \underline{v}_i \cdot \underline{v}_j) \underline{k} \cdot \underline{k}' - i(\underline{v}_i + \underline{v}_j) \cdot (\underline{k}' \times \underline{k}) + (\underline{v}_i \times \underline{k}') \cdot (\underline{v}_j \times \underline{k}) \right. \\
& \left. + (\underline{v}_j \times \underline{k}') \cdot (\underline{v}_i \times \underline{k}) \right] \left( \frac{1 - \underline{\tau}_i \cdot \underline{\tau}_j}{4} \right) + \frac{\gamma_{10}}{k^2} \left( \frac{1 - \underline{v}_i \cdot \underline{v}_j}{4} \right) \underline{k} \cdot \underline{k}' \\
& + \frac{1}{4} \left[ 1 - \underline{\tau}_i \cdot \underline{\tau}_j - \underline{t}_i \cdot (\underline{\tau}_i + \underline{\tau}_j) + (\underline{t}_i \cdot \underline{\tau}_i)(\underline{t}_i \cdot \underline{\tau}_j) + (\underline{t}_i \cdot \underline{\tau}_j)(\underline{t}_i \cdot \underline{\tau}_i) \right] \\
& + \gamma_{11}(0,1) \left( \frac{1 - \underline{v}_i \cdot \underline{v}_j}{4} \right) \left( \frac{\underline{k} \cdot \underline{k}'}{k^2} \right) \frac{1}{8} \left[ 6 + 6 \underline{\tau}_i \cdot \underline{\tau}_j - 3 \underline{t}_i \cdot (\underline{\tau}_i + \underline{\tau}_j) \right. \\
& \left. - 3 (\underline{t}_i \cdot \underline{\tau}_i)(\underline{t}_i \cdot \underline{\tau}_j) - 3 (\underline{t}_i \cdot \underline{\tau}_j)(\underline{t}_i \cdot \underline{\tau}_i) \right] + \gamma_{11}(1,0) \frac{1}{8k^2} \left[ (6 + 6 \underline{v}_i \cdot \underline{v}_j) \underline{k} \cdot \underline{k}' \right. \\
& \left. - 3i(\underline{v}_i + \underline{v}_j) \cdot (\underline{k}' \times \underline{k}) - 3(\underline{v}_i \times \underline{k}') \cdot (\underline{v}_j \times \underline{k}) - 3(\underline{v}_j \times \underline{k}') \cdot (\underline{v}_i \times \underline{k}) \right] \\
& \left( \frac{1 - \underline{\tau}_i \cdot \underline{\tau}_j}{4} \right) + \gamma_{12} \left( \frac{1 - \underline{v}_i \cdot \underline{v}_j}{4} \right) \frac{\underline{k} \cdot \underline{k}'}{k^2} \frac{1}{8} \left[ 10 + 5 \underline{t}_i \cdot (\underline{\tau}_i + \underline{\tau}_j) \right. \\
& \left. + 2 \underline{\tau}_i \cdot \underline{\tau}_j + (\underline{t}_i \cdot \underline{\tau}_i)(\underline{t}_i \cdot \underline{\tau}_j) + (\underline{t}_i \cdot \underline{\tau}_j)(\underline{t}_i \cdot \underline{\tau}_i) \right]
\end{aligned}$$

Rewriting and regrouping terms obtain

$$\begin{aligned}
A87 \quad \underline{f}_{ij}(\vec{r}) \Big|_{r=1} &= \left( \frac{\underline{k} \cdot \underline{k}'}{k^2} \right) \left[ \left\{ \frac{10}{32} \gamma_{21} + \frac{1}{16} \gamma_{01} + \frac{1}{16} \gamma_{10} + \frac{6}{32} \gamma_{11}(0,1) \right. \right. \\
& \left. \left. + \frac{6}{32} \gamma_{11}(1,0) + \frac{10}{32} \gamma_{12} \right\} + \left\{ \frac{2}{32} \gamma_{21} - \frac{1}{16} \gamma_{01} - \frac{1}{16} \gamma_{10} \right. \right. \\
& \left. \left. - \frac{6}{32} \gamma_{11}(0,1) + \frac{6}{32} \gamma_{11}(1,0) - \frac{10}{32} \gamma_{12} \right\} \underline{v}_i \cdot \underline{v}_j + \left\{ -\frac{10}{32} \gamma_{21} \right. \right. \\
& \left. \left. - \frac{1}{16} \gamma_{01} - \frac{1}{16} \gamma_{10} + \frac{6}{32} \gamma_{11}(0,1) - \frac{6}{32} \gamma_{11}(1,0) + \frac{2}{32} \gamma_{12} \right\} \right. \\
& \left. (\underline{\tau}_i \cdot \underline{\tau}_j) + \left\{ -\frac{1}{16} \gamma_{10} - \frac{3}{32} \gamma_{11}(0,1) + \frac{5}{16} \gamma_{12} \right\} (1 - \underline{v}_i \cdot \underline{v}_j) \underline{t}_i \cdot (\underline{\tau}_i + \underline{\tau}_j) \right. \\
& \left. + \left\{ -\frac{2}{32} \gamma_{21} + \frac{1}{16} \gamma_{01} + \frac{1}{16} \gamma_{10} - \frac{6}{32} \gamma_{11}(0,1) - \frac{6}{32} \gamma_{11}(1,0) - \frac{2}{32} \gamma_{12} \right\} \right]
\end{aligned}$$

$$\begin{aligned}
& (\underline{v}_i \cdot \underline{v}_j) (\underline{\tau}_i \cdot \underline{\tau}_j) + \left\{ \frac{1}{16} \gamma_{10} - \frac{3}{32} \gamma_{11}(0,1) + \frac{1}{32} \gamma_{12} \right\} (1 - \underline{v}_i \cdot \underline{v}_j) \\
& \left\{ (\underline{t}_i \cdot \underline{\tau}_i) (\underline{t}_j \cdot \underline{\tau}_j) + (\underline{t}_i \cdot \underline{\tau}_j) (\underline{t}_j \cdot \underline{\tau}_i) \right\} + i (1 - \underline{\tau}_i \cdot \underline{\tau}_j) (\underline{v}_i + \underline{v}_j) \cdot \\
& \frac{(\underline{k}' \times \underline{k})}{k^2} \left\{ \frac{5}{32} \gamma_{21} - \frac{1}{16} \gamma_{01} - \frac{3}{32} \gamma_{11}(1,0) \right\} + \frac{(1 - \underline{\tau}_i \cdot \underline{\tau}_j)}{k^2} \\
& \left[ (\underline{v}_i \times \underline{k}') \cdot (\underline{v}_j \times \underline{k}) + (\underline{v}_j \times \underline{k}') \cdot (\underline{v}_i \times \underline{k}) \right] \left\{ \frac{1}{16} \gamma_{01} + \frac{1}{32} \gamma_{21} \right. \\
& \left. - \frac{3}{32} \gamma_{11}(1,0) \right\}
\end{aligned}$$

or

$$\begin{aligned}
\text{A88} \quad \underline{f}_{ij}(\hat{r}) \Big|_{\ell=1} &= \underline{k} \cdot \underline{k}' \left[ C_0 + C_1 \underline{v}_i \cdot \underline{v}_j + C_2 \underline{\tau}_i \cdot \underline{\tau}_j \right. \\
&+ C_3 (1 - \underline{v}_i \cdot \underline{v}_j) \underline{t}_i \cdot (\underline{\tau}_i + \underline{\tau}_j) + C_4 (\underline{v}_i \cdot \underline{v}_j) (\underline{\tau}_i \cdot \underline{\tau}_j) \\
&+ C_5 (1 - \underline{v}_i \cdot \underline{v}_j) \left[ (\underline{t}_i \cdot \underline{\tau}_i) (\underline{t}_j \cdot \underline{\tau}_j) + (\underline{t}_i \cdot \underline{\tau}_j) (\underline{t}_j \cdot \underline{\tau}_i) \right] \Big] \\
&+ i C_6 (1 - \underline{\tau}_i \cdot \underline{\tau}_j) (\underline{v}_i + \underline{v}_j) \cdot (\underline{k}' \times \underline{k}) + C_7 (1 - \underline{\tau}_i \cdot \underline{\tau}_j) \\
&\left[ (\underline{v}_i \times \underline{k}') \cdot (\underline{v}_j \times \underline{k}) + (\underline{v}_j \times \underline{k}') \cdot (\underline{v}_i \times \underline{k}) \right]
\end{aligned}$$

where

$$\begin{aligned}
\text{A89} \quad C_0 &= \frac{5\gamma_{21} + \gamma_{01} + \gamma_{10} + 3\gamma_{11}(0,1) + 3\gamma_{11}(1,0) + 5\gamma_{12}}{16k^2} \\
C_1 &= \frac{\gamma_{21} - \gamma_{01} - \gamma_{10} - 3\gamma_{11}(0,1) + 3\gamma_{11}(1,0) - 5\gamma_{12}}{16k^2} \\
C_2 &= \frac{-5\gamma_{21} - \gamma_{01} - \gamma_{10} + 3\gamma_{11}(0,1) - 3\gamma_{11}(1,0) + \gamma_{12}}{16k^2} \\
C_3 &= \frac{-2\gamma_{10} - 3\gamma_{11}(0,1) + 5\gamma_{12}}{32k^2}
\end{aligned}$$

$$C_4 = \frac{-\gamma_{21} + \gamma_{01} + \gamma_{10} - 3\gamma_{11}(0,1) - 3\gamma_{11}(1,0) - \gamma_{12}}{16k^2}$$

$$C_5 = \frac{2\gamma_{10} - 3\gamma_{11}(0,1) + \gamma_{12}}{32k^2}$$

$$C_6 = \frac{5\gamma_{21} - 2\gamma_{01} - 3\gamma_{11}(1,0)}{32k^2}$$

$$C_7 = \frac{\gamma_{21} + 2\gamma_{01} - 3\gamma_{11}(1,0)}{32k^2}$$

19

These results are not identical with those of Ericson and Ericson who obtain a different value for  $C_3$ ,  $C_5$ , and  $C_6$ , i.e.

$$A90 \quad C_3 = \frac{-2\gamma_{10} + 9\gamma_{11}(0,1) - 2\gamma_{12}}{32k^2}$$

$$C_5 = \frac{2\gamma_{10} - 3\gamma_{11}(0,1) + 2\gamma_{12}}{32k^2}$$

$$C_6 = \frac{2\gamma_{21} + 2\gamma_{01} - 9\gamma_{11}(1,0)}{32k^2}$$

Writing  $\underline{f}_{ij}(\vec{r})$  in the spatial representation and neglecting the  $C_6$  and  $C_7$  terms which are small due to the  $A^{-1}$  and  $A^{-2}$  dependence, respectively, obtain

$$A91 \quad \underline{f}_{ij}(\vec{r}) = B_0 + B_1 \underline{v}_i \cdot \underline{v}_j + B_2 \underline{\pi}_i \cdot \underline{\pi}_j + B_3 (1 - \underline{v}_i \cdot \underline{v}_j) \underline{t}_i \cdot (\underline{\pi}_i + \underline{\pi}_j) \\ + B_4 (\underline{v}_i \cdot \underline{v}_j) (\underline{\pi}_i \cdot \underline{\pi}_j) + B_5 (1 - \underline{v}_i \cdot \underline{v}_j) [(\underline{t}_i \cdot \underline{\pi}_i) (\underline{t}_i \cdot \underline{\pi}_j) \\ + (\underline{t}_i \cdot \underline{\pi}_j) (\underline{t}_i \cdot \underline{\pi}_i)] + \nabla \cdot \{ C_0 + C_1 \underline{v}_i \cdot \underline{v}_j + C_2 \underline{\pi}_i \cdot \underline{\pi}_j \\ + C_3 (1 - \underline{v}_i \cdot \underline{v}_j) \underline{t}_i \cdot (\underline{\pi}_i + \underline{\pi}_j) + C_4 (\underline{v}_i \cdot \underline{v}_j) (\underline{\pi}_i \cdot \underline{\pi}_j) \\ + C_5 (1 - \underline{v}_i \cdot \underline{v}_j) [(\underline{t}_i \cdot \underline{\pi}_i) (\underline{t}_i \cdot \underline{\pi}_j) + (\underline{t}_i \cdot \underline{\pi}_j) (\underline{t}_i \cdot \underline{\pi}_i)] \} \nabla'$$

$$\equiv \underline{B}_{ij} - \underline{C}_{ij} \nabla \cdot \nabla'$$

## APPENDIX B

### Averages over Nucleon Scattering Operators

In order to evaluate the fraction of nucleons in the nucleus that interact with the pion via any particular partial wave, it is necessary to average the projection operators for that channel over the nucleon states. For the purpose of averaging assume that the nucleon spin and isospin are statistically independent, i. e. they may be averaged separately, and the nucleus is in its ground state.

The following definitions and averages are needed for isospin

$$B1 \quad \underline{T} = \frac{1}{2} \sum_{i=1}^A \underline{\tau}_i$$

$$B2 \quad \langle 0 | \sum_{i=1}^A \underline{\tau}_i | 0 \rangle = 2 \underline{T}$$

$$B3 \quad \langle 0 | \sum_{i=1}^A \underline{\tau}_i^2 | 0 \rangle = 4A \frac{1}{2} (1 + \frac{1}{2}) = 3A$$

$$B4 \quad \langle 0 | \left( \sum_{i=1}^A \underline{\tau}_i \right)^2 | 0 \rangle = 4 \langle 0 | \underline{T}^2 | 0 \rangle = 4T(T+1)$$

$$\begin{aligned}
 B5 \quad \langle \underline{\tau}_i \cdot \underline{\tau}_j \rangle &\equiv \langle 0 | \sum_{i=1}^A \sum_{\substack{j=1 \\ j \neq i}}^A \underline{\tau}_i \cdot \underline{\tau}_j | 0 \rangle / A(A-1) \\
 &= \langle 0 | \left( \sum_{j=1}^A \underline{\tau}_j \right)^2 - \sum_{j=1}^A \underline{\tau}_j^2 | 0 \rangle / A(A-1) \\
 &= \frac{4T(T+1)}{A(A-1)} - \frac{3}{A-1}
 \end{aligned}$$

$$B6 \quad \langle \underline{t}_\pi \cdot (\underline{T}_i + \underline{T}_j) \rangle \equiv \langle 0 | \sum_{i=1}^A \sum_{\substack{j=1 \\ j \neq i}}^A \underline{t}_\pi \cdot (\underline{T}_i + \underline{T}_j) | 0 \rangle / A(A-1) = \frac{4}{A} \langle \underline{t}_\pi \cdot \underline{T}_i \rangle$$

$$\begin{aligned}
 B7 \quad & \langle (\underline{t}_\pi \cdot \underline{T}_i)(\underline{t}_\pi \cdot \underline{T}_j) + (\underline{t}_\pi \cdot \underline{T}_j)(\underline{t}_\pi \cdot \underline{T}_i) \rangle \\
 & \equiv \langle 0 | \sum_{i=1}^A \sum_{\substack{j=1 \\ j \neq i}}^A (\underline{t}_\pi \cdot \underline{T}_i)(\underline{t}_\pi \cdot \underline{T}_j) + (\underline{t}_\pi \cdot \underline{T}_j)(\underline{t}_\pi \cdot \underline{T}_i) | 0 \rangle / A(A-1) \\
 & = \langle 0 | \sum_{i=1}^A \sum_{i=1}^A (\underline{t}_\pi \cdot \underline{T}_i)(\underline{t}_\pi \cdot \underline{T}_j) + (\underline{t}_\pi \cdot \underline{T}_j)(\underline{t}_\pi \cdot \underline{T}_i) | 0 \rangle / A(A-1) \\
 & \quad - \langle 0 | \sum_{i=j=1}^A (\underline{t}_\pi \cdot \underline{T}_i)(\underline{t}_\pi \cdot \underline{T}_j) + (\underline{t}_\pi \cdot \underline{T}_j)(\underline{t}_\pi \cdot \underline{T}_i) | 0 \rangle / A(A-1) \\
 & = \langle 0 | 2 \left( \frac{\sum_{i=1}^A (\underline{t}_\pi \cdot \underline{T}_i)^2}{A(A-1)} - 2 \frac{\sum_{i=1}^A (\underline{t}_\pi \cdot \underline{T}_i)^2}{A(A-1)} \right) | 0 \rangle
 \end{aligned}$$

Using the identity

$$B8 \quad \langle (\underline{t}_\pi \cdot \underline{T}_i)(\underline{t}_\pi \cdot \underline{T}_i) \rangle = \langle \underline{t}_\pi \cdot \underline{t}_\pi + i \underline{T}_i \cdot (\underline{t}_\pi \times \underline{t}_\pi) \rangle = 2 - \langle \underline{t}_\pi \cdot \underline{T}_i \rangle$$

equation B7 is simplified to

$$\begin{aligned}
 B9 \quad & \langle (\underline{t}_\pi \cdot \underline{T}_i)(\underline{t}_\pi \cdot \underline{T}_j) + (\underline{t}_\pi \cdot \underline{T}_j)(\underline{t}_\pi \cdot \underline{T}_i) \rangle \\
 & = \frac{8 \langle \underline{t}_\pi \cdot \underline{T}_i \rangle^2}{A(A-1)} - \frac{4}{A-1} + 4 \frac{\langle \underline{t}_\pi \cdot \underline{T}_i \rangle}{A-1}
 \end{aligned}$$

In these definitions  $|0\rangle$  represents the nuclear ground state,  $T_3 = \frac{N-Z}{2}$  for  $\pi^-$  and  $\langle \underline{t}_\pi \cdot \underline{T}_i \rangle = 2(t_\pi)_3 T_3 = N - Z$ .

The spin averages are obtained in a similar manner.

## APPENDIX C

### Nucleon Pair Correlations for an Ideal Fermi Gas of Nucleons

26

According to Goldberger and Watson the pair distribution function  $P^{(2)}(\vec{x}, \vec{x}')$  for  $N$  nucleons is defined as

$$c1 \quad P^{(2)}(\vec{x}, \vec{x}') = \frac{1}{N(N-1)} \langle 0 | \sum_{\alpha \neq \beta=1}^N \delta(\vec{z}_\alpha - \vec{x}) \delta(\vec{z}_\beta - \vec{x}') | 0 \rangle$$

where  $\alpha$  and  $\beta$  refer to various nucleons. The average pair distribution function  $\overline{P^{(2)}(\vec{x}, \vec{x}')}$  is obtained by averaging over spin orientations.

The pair distribution function  $P^{(2)}(\vec{x}, \vec{x}')$  depends on the dynamical properties of the scatterer. It can be easily calculated only for such simple systems as an ideal gas.

For the ground state of atomic nuclei the pair distribution function may be calculated in terms of the degenerate Fermi gas model for nucleons. Consider such a gas of  $N$  particles confined to a box of volume  $V$ . Plane wave states for these particles are of the form

$$c2 \quad \omega_{\vec{k}}(i) = \omega_{\vec{k}}(\vec{z}_i, s_i, \tau_i) = \frac{1}{\sqrt{V}} e^{i\vec{k} \cdot \vec{z}_i} \chi_i^{\sqrt{k}} \eta_i^{\tau_i}$$

where  $\vec{k}$  is the momentum,  $\vec{z}_i$  the space coordinate,  $s_i$  the spin,  $\chi_i^{\sqrt{k}}$  the spinor,  $\tau_i$  the isospin, and  $\eta_i^{\tau_i}$  the isospinor. In the lowest state of the gas these plane wave states will all be occupied for  $k < P_f$ , the Fermi momentum, which is

$$c3 \quad P_f = \left( \frac{3\pi^2 N}{2V} \right)^{1/3}$$

The lowest state of the gas is

$$c4 \quad |0\rangle = \frac{1}{\sqrt{N!}} \sum_Q \epsilon_Q \omega_{\ell_1}(z_1, s_1, \tau_1) \cdots \omega_{\ell_N}(z_N, s_N, \tau_N)$$

where  $\ell_1 \dots \ell_N$  represent all the states having a momentum less than  $P_f$ , the  $Q$ 's represent the  $N!$  permutations of the particle coordinates, and  $\epsilon_Q = \pm 1$  depending on whether  $Q$  is an even or odd permutation.

Consider the distribution of those pairs of particles which are in space-symmetric and space-antisymmetric states. The space exchange operator for a pair of Fermi particles  $(\alpha, \beta)$  is

$$c5 \quad \underline{Q}_{\alpha\beta} = -\frac{1}{4} (1 + \underline{V}_\alpha \cdot \underline{V}_\beta) (1 + \underline{T}_\alpha \cdot \underline{T}_\beta)$$

where  $\underline{V}_\alpha$  and  $\underline{V}_\beta$  are Pauli spin matrices and  $\underline{T}_\alpha$  and  $\underline{T}_\beta$  are the isospin matrices. From the definition of the pair distribution function, the desired distributions are

$$c6 \quad \overline{P_\pm(\vec{x}, \vec{x}')} = \frac{1}{2N_\pm} \langle 0 | \sum_{\alpha \neq \beta=1}^N \delta(\vec{z}_\alpha - \vec{x}) \delta(\vec{z}_\beta - \vec{x}') \left( \frac{1 \pm \underline{Q}_{\alpha\beta}}{2} \right) | 0 \rangle_{\text{spin Averaged}}$$

where + and - refer to space-symmetric and space-antisymmetric states.

Using the definition of  $|0\rangle$  for the ground state one obtains

$$c7 \quad \overline{P_\pm(\vec{x}, \vec{x}')} = \frac{1}{4N_\pm} \sum_{\ell+m < P_f} \left[ (\omega_\ell(a) \omega_m(a), (1 \pm Q_{\ell m}) \delta(\vec{x} - \vec{z}_\ell) \delta(\vec{x}' - \vec{z}_m) \omega_\ell(a) \omega_m(a)) - (\omega_\ell(a) \omega_m(a), (1 \pm Q_{\ell m}) \delta(\vec{x} - \vec{z}_\ell) \delta(\vec{x}' - \vec{z}_m) \omega_\ell(b) \omega_m(b)) \right]$$

where

$$c8 \quad \omega_\ell(a) \omega_m(a) = \frac{e^{i\vec{\ell} \cdot \vec{z}_1}}{\sqrt{V_0}} \frac{e^{i\vec{m} \cdot \vec{z}_2}}{\sqrt{V_0}} \chi_1^{\sqrt{\ell}} \eta_1^{\tau_\ell} \chi_2^{\sqrt{m}} \eta_2^{\tau_m}$$

Using the definition of the space exchange operator

$$c9 \quad (1 \pm Q_{\ell m}) \delta(\vec{x} - \vec{z}_\ell) \delta(\vec{x}' - \vec{z}_m) e^{i\vec{\ell} \cdot \vec{z}_1} e^{i\vec{m} \cdot \vec{z}_2} = e^{i\vec{\ell} \cdot \vec{x}} e^{i\vec{m} \cdot \vec{x}'} \pm e^{i\vec{\ell} \cdot \vec{x}'} e^{i\vec{m} \cdot \vec{x}}$$

and the orthogonality of the inner product

$$C10 \quad (\chi_1^{v_2} \eta_1 \tau_2 \chi_2^{v_m} \eta_2 \tau_m, \chi_1^{v_2} \eta_1 \tau_2 \chi_2^{v_m} \eta_2 \tau_m) = 1$$

$$C11 \quad (\chi_1^{v_2} \eta_1 \tau_2 \chi_2^{v_m} \eta_2 \tau_m, \chi_2^{v_2} \eta_2 \tau_2 \chi_1^{v_m} \eta_1 \tau_m) = \delta_{v_2 v_m} \delta_{\tau_2 \tau_m}$$

equation C7 may be written

$$C12 \quad \overline{P_{\pm}(\vec{x}, \vec{x}')} = \frac{1}{4N_{\pm}} \frac{1}{V^2} \sum_{l \neq m < p_f} \left[ (1 \pm e^{i \vec{l} \cdot (\vec{x}' - \vec{x})} e^{i \vec{m} \cdot (\vec{x} - \vec{x}')} - \delta_{v_2 v_m} \delta_{\tau_2 \tau_m} (e^{i \vec{l} \cdot (\vec{x}' - \vec{x})} e^{i \vec{m} \cdot (\vec{x} - \vec{x}')} \pm 1)) \right]$$

In order to introduce the definition of the Fermi correlation function, one finds it convenient to change from a discrete to a continuous sum using the prescription

$$C13 \quad \sum_{l < p_f} e^{i \vec{l} \cdot (\vec{x}' - \vec{x})} \rightarrow \frac{4V}{(2\pi\hbar)^3} \int_{p_2 < p_f} d^3 p_2 e^{i \vec{p}_2 \cdot (\vec{x}' - \vec{x})}$$

Defining the Fermi correlation function to be

$$C14 \quad G_F(\vec{x} - \vec{x}') \equiv \left[ \frac{4V}{(2\pi\hbar)^3 A} \int_{p_2 < p_f} e^{i \vec{p}_2 \cdot (\vec{x}' - \vec{x})} d^3 p_2 \right]^2 = \frac{9\pi}{9} \frac{J_{3/2}^2(p_f |\vec{x} - \vec{x}'|)}{(p_f |\vec{x} - \vec{x}'|)^3}$$

one may write

$$C15 \quad \sum_{l \neq m < p_f} e^{i \vec{l} \cdot (\vec{x}' - \vec{x})} e^{i \vec{m} \cdot (\vec{x} - \vec{x}')} = \frac{A(A-1)}{A^2} \sum_{l < p_f} \sum_{m < p_f} e^{i(\vec{l} - \vec{m}) \cdot (\vec{x}' - \vec{x})} = A(A-1) G_F(\vec{x} - \vec{x}')$$

$$C16 \quad \sum_{l \neq m < p_f} \delta_{v_2 v_m} \delta_{\tau_2 \tau_m} e^{i \vec{l} \cdot (\vec{x}' - \vec{x})} e^{i \vec{m} \cdot (\vec{x} - \vec{x}')} = \frac{4\left(\frac{A}{9}\right)\left(\frac{A}{9}-1\right)}{A^2} \sum_{l < p_f} \sum_{m < p_f} \delta_{v_2 v_m} \delta_{\tau_2 \tau_m} e^{i(\vec{l} - \vec{m}) \cdot (\vec{x}' - \vec{x})} = A\left(\frac{A}{9}-1\right) G_F(\vec{x} - \vec{x}')$$

Thus one may rewrite C12 in terms of  $G_F(\vec{x}-\vec{x}')$  as

$$\text{C17} \quad \overline{P_{\pm}(\vec{x}, \vec{x}')} = \frac{1}{4N_{\pm}} \frac{1}{V^2} \left[ A(A-1) \pm A(A-1)G_F(\vec{x}-\vec{x}') \right. \\ \left. - A\left(\frac{A}{4}-1\right)G_F(\vec{x}-\vec{x}') \mp A\left(\frac{A}{4}-1\right) \right]$$

where

$$\text{C18} \quad \sum_{l \neq m < l \neq} 1 = A(A-1)$$

$$\text{C19} \quad \sum_{l \neq m < l \neq} \delta_{\tau_l \tau_m} \delta_{z_l z_m} = 4 \frac{A}{4} \left(\frac{A}{4}-1\right) = A\left(\frac{A}{4}-1\right)$$

26

This result does not agree with that given by Goldberger and Watson.

The average pair distribution function is given by

$$\text{C20} \quad \overline{P^{(2)}(\vec{x}, \vec{x}')} \equiv \frac{N_+ \overline{P_+(\vec{x}, \vec{x}')} + N_- \overline{P_-(\vec{x}, \vec{x}')}}{A(A-1)/2} \\ = \frac{1}{4V^2} \frac{2}{A(A-1)} \left[ 2A(A-1) - 2A\left(\frac{A}{4}-1\right)G_F(\vec{x}-\vec{x}') \right] \\ = \frac{1}{V^2} \left[ 1 - \frac{\frac{A}{4}-1}{A-1} G_F(\vec{x}-\vec{x}') \right]$$

and

$$\text{C21} \quad \sum_{i \neq j=1}^A \overline{P^{(2)}(\vec{x}_i, \vec{x}_j)} = \frac{A(A-1)}{V^2} \left[ 1 - \frac{\frac{A}{4}-1}{A-1} G_F(\vec{x}-\vec{x}') \right] \\ = e(r)e(r') \left(1 - \frac{1}{A}\right) \left[ 1 - \frac{A-4}{A-1} \frac{G_F(\vec{x}-\vec{x}')}{4} \right] \\ \equiv e(\vec{r}, \vec{r}')$$

Note that the result above for  $\overline{P^{(2)}(\vec{x}, \vec{x}')}_{26}$  does agree with that of Goldberger and Watson despite the fact that it is obtained with different expressions for  $\underline{P_+(\vec{x}, \vec{x}')}_{26}$ .

The average pair distribution function may also be defined in terms of the pair correlation function  $G(\vec{x}, \vec{x}')$ , i.e.

$$c22 \quad \overline{P^{(2)}(\vec{x}, \vec{x}')} \equiv \frac{1}{V^2} [1 + G(\vec{x} - \vec{x}')] ]$$

Comparing C22 with C20 one obtains

$$c23 \quad G(\vec{x} - \vec{x}') = - \frac{A-4}{A-1} \frac{G_F(\vec{x} - \vec{x}')}{4}$$

Substituting this function into the definition for the average pair correlation length obtain

$$c24 \quad \int_{PAULI}^2 = -2 \int_0^\infty - \left( \frac{A-4}{A-1} \right) \frac{G_F(x)}{4} x dx$$

$$= \frac{A-4}{A-1} \int_0^\infty \frac{9\pi}{4} \frac{J_{3/2}^2(P_F x)}{(P_F x)^3} x dx$$

Let  $y = P_F x$

$$c25 \quad \int_{PAULI}^2 = \frac{A-4}{A-1} \frac{9\pi}{4 P_F^2} \int_0^\infty \frac{J_{3/2}^2(y)}{y^2} dy$$

From Gradshteyn and Ryzhik <sup>125</sup> integral 6.574(2)

$$c26 \quad \int_0^\infty \frac{J_\nu^2(t)}{t^\lambda} dt = \frac{\Gamma(\lambda) \Gamma(\nu - \lambda/2 + \gamma/2)}{2^\lambda \Gamma^2(\lambda/2 + \gamma/2) \Gamma(\nu + \lambda/2 + \gamma/2)}$$

Thus

$$c27 \quad \int_0^\infty \frac{J_{3/2}^2(y)}{y^2} dy = \frac{\Gamma(2) \Gamma(1)}{2^2 \Gamma^2(3/2) \Gamma(3)} = \frac{1}{2\pi}$$

and

$$c28 \quad \int_{PAULI}^2 = \frac{9}{8P_f^2} \frac{A-4}{A-1}$$

Now that the formalism for averaging over spatially symmetric and antisymmetric pairs has been defined, we are able to calculate the very important average of  $(\underline{t}_n \cdot \underline{\tau}_1)(\underline{t}_n \cdot \underline{\tau}_2)$ . Expressing these operators in terms of unit operators and  $t_z$  values one may write

$$c29 \quad (\underline{t}_n \cdot \underline{\tau}_1)(\underline{t}_n \cdot \underline{\tau}_2) = t_z \tau_{1z} t_z \tau_{2z} + \frac{\underline{t}^+ \underline{\tau}_1^- \underline{t}^- \tau_2^+ + \underline{t}^- \tau_1^+ \underline{t}^+ \tau_2^-}{2}$$

Noting that

$$c30 \quad \eta_1^{+\tau_2} \eta_2^{+\tau_m} \left[ \tau_{1z} \tau_{2z} t_z^2 + \frac{\underline{\tau}_1^+ \underline{\tau}_2^- \underline{t}^- \underline{t}^+ + \underline{\tau}_1^- \underline{\tau}_2^+ \underline{t}^+ \underline{t}^-}{2} \right] \eta_1^{\tau_2} \eta_2^{\tau_m}$$

$$= \left[ \delta_{\tau_2, \tau_m} \delta_{\tau_2, \tau_m} + \delta_{\tau_2, -1} \delta_{\tau_m, -1} - \delta_{\tau_2, 1} \delta_{\tau_m, 1} - \delta_{\tau_2, 1} \delta_{\tau_m, 1} \right] t_z^2$$

$$c31 \quad \eta_1^{+\tau_2} \eta_2^{+\tau_m} \left[ \tau_{1z} \tau_{2z} t_z^2 + \frac{\underline{\tau}_1^+ \underline{\tau}_2^- \underline{t}^- \underline{t}^+ + \underline{\tau}_1^- \underline{\tau}_2^+ \underline{t}^+ \underline{t}^-}{2} \right] \eta_1^{\tau_m} \eta_2^{\tau_2}$$

$$= \left[ \delta_{\tau_2, \tau_m} t_z^2 + \left\{ \delta_{\tau_2, \tau_m+1} \delta_{\tau_2-1, \tau_m} \underline{t}^- \underline{t}^+ + \delta_{\tau_2, \tau_m-1} \delta_{\tau_2+1, \tau_m} \underline{t}^+ \underline{t}^- \right\} \right]$$

one may write

$$c32 \quad \overline{P_{\pm}(\bar{x}_i, \bar{x}_i) (\underline{t}_n \cdot \underline{\tau}_1)(\underline{t}_n \cdot \underline{\tau}_2)} = \frac{1}{4N_{\pm}} \frac{1}{V^2} \sum_{\ell \neq m < P_f} \left\{ \left[ 1 \pm e^{i(\bar{r}-\bar{m}) \cdot (\bar{x}'-\bar{x})} \right] \right.$$

$$\left. \left[ (\delta_{\tau_2, \tau_m} - \delta_{\tau_2, \tau_m+1} - \delta_{\tau_2+1, \tau_m}) t_z^2 \right] - \left[ e^{i(\bar{r}-\bar{m}) \cdot (\bar{x}'-\bar{x})} \pm 1 \right] \right.$$

$$\left. \left[ \delta_{\tau_2, \tau_m} \delta_{\tau_2, \tau_m} t_z^2 + \delta_{\tau_2, \tau_m} \delta_{\tau_2, \tau_m+1} \underline{t}^- \underline{t}^+ + \delta_{\tau_2, \tau_m} \delta_{\tau_2+1, \tau_m} \underline{t}^+ \underline{t}^- \right] \right\}$$

Using the identities

$$C33 \quad \sum_{l \neq m < P_f} \delta_{\tau_l, \tau_m} = 2 \frac{A}{2} \left( \frac{A}{2} - 1 \right) = \frac{A^2}{2} - A$$

$$C34 \quad \sum_{l \neq m < P_f} \delta_{\tau_l, \tau_{m+1}} = \sum_{l \neq m < P_f} \delta_{\tau_{l+1}, \tau_m} = \frac{A}{2} \left( \frac{A}{2} \right) = \frac{A^2}{4}$$

$$C35 \quad \sum_{l \neq m < P_f} e^{i(\bar{x}^l - \bar{x}^m) \cdot (\bar{x}^l - \bar{x}^m)} \delta_{\tau_l, \tau_m} = \frac{A(A-2)}{2} G_F(\bar{x} - \bar{x}^1)$$

$$C36 \quad \sum_{l \neq m < P_f} e^{i(\bar{x}^l - \bar{x}^m) \cdot (\bar{x}^l - \bar{x}^m)} \delta_{\tau_l, \tau_{m+1}} = \sum_{l \neq m < P_f} e^{i(\bar{x}^l - \bar{x}^m) \cdot (\bar{x}^l - \bar{x}^m)} \delta_{\tau_{l+1}, \tau_m}$$

$$= \sum_{l < P_f} \sum_{m < P_f} e^{i(\bar{x}^l - \bar{x}^m) \cdot (\bar{x}^l - \bar{x}^m)} \delta_{\tau_{l+1}, \tau_m} = \frac{A^2}{4} G_F(\bar{x} - \bar{x}^1)$$

$$C37 \quad \sum_{l \neq m < P_f} e^{i(\bar{x}^l - \bar{x}^m) \cdot (\bar{x}^l - \bar{x}^m)} \delta_{\nu_l, \nu_m} \delta_{\tau_l, \tau_m} = 4 \frac{A}{4} \left( \frac{A}{4} - 1 \right) G_F(\bar{x} - \bar{x}^1)$$

$$C38 \quad \sum_{l \neq m < P_f} e^{i(\bar{x}^l - \bar{x}^m) \cdot (\bar{x}^l - \bar{x}^m)} \delta_{\nu_l, \nu_m} \delta_{\tau_l, \tau_{m+1}} = \sum_{l \neq m < P_f} e^{i(\bar{x}^l - \bar{x}^m) \cdot (\bar{x}^l - \bar{x}^m)} \delta_{\nu_l, \nu_m} \delta_{\tau_{l+1}, \tau_m}$$

$$= \sum_{l < P_f} \sum_{m < P_f} e^{i(\bar{x}^l - \bar{x}^m) \cdot (\bar{x}^l - \bar{x}^m)} \delta_{\nu_l, \nu_m} \delta_{\tau_{l+1}, \tau_m} = 2 \left( \frac{A}{4} \right) \frac{A}{4} G_F(\bar{x} - \bar{x}^1)$$

$$C39 \quad \sum_{l \neq m < P_f} \delta_{\nu_l, \nu_m} \delta_{\tau_l, \tau_m} = 4 \frac{A}{4} \left( \frac{A}{4} - 1 \right) = \frac{A^2}{4} - A$$

$$C40 \quad \sum_{l \neq m < P_f} \delta_{\nu_l, \nu_m} \delta_{\tau_l, \tau_{m+1}} = \sum_{l \neq m < P_f} \delta_{\nu_l, \nu_m} \delta_{\tau_{l+1}, \tau_m} = 2 \left( \frac{A}{4} \right) \frac{A}{4} = \frac{A^2}{8}$$

C32 may be written

$$\begin{aligned}
c41 \quad \overline{P_{\pm}(\bar{x}, \bar{x}')(\underline{t}_1 \cdot \underline{T}_1)(\underline{t}_2 \cdot \underline{T}_2)} &= \frac{1}{4N_{\pm}} \frac{1}{V^2} \left\{ \left( \frac{A^2}{2} - A - \frac{A^2}{4} - \frac{A^2}{4} \right) t_2^2 \right. \\
&\pm \left( \frac{A^2}{2} - A - \frac{A^2}{4} - \frac{A^2}{4} \right) G_F(\bar{x} - \bar{x}') t_2^2 - \left( \frac{A}{4} - A \right) G_F(\bar{x} - \bar{x}') t_2^2 \\
&- \frac{A^2}{8} G_F(\bar{x} - \bar{x}') (t^- t^+ + t^+ t^-) \mp \left( \frac{A^2}{4} - A \right) t_2^2 \mp \frac{A^2}{8} (t^- t^+ + t^+ t^-) \left. \right\} \\
&= \frac{1}{4N_{\pm} V^2} \left\{ (-A \mp \frac{A^2}{4} \pm A) t_2^2 + (\mp A - \frac{A^2}{4} + A) G_F(\bar{x} - \bar{x}') t_2^2 \right. \\
&\left. \mp \frac{A^2}{8} (t^- t^+ + t^+ t^-) - \frac{A^2}{8} G_F(\bar{x} - \bar{x}') (t^- t^+ + t^+ t^-) \right\}
\end{aligned}$$

and

$$\begin{aligned}
c42 \quad \overline{P^{(2)}(\bar{x}, \bar{x}')(\underline{t}_1 \cdot \underline{T}_1)(\underline{t}_2 \cdot \underline{T}_2)} &= \frac{1}{4V^2} \frac{2}{A(A-1)} \left\{ -2A t_2^2 \right. \\
&\left. - 2\left(\frac{A^2}{4} - A\right) G_F(\bar{x} - \bar{x}') t_2^2 - 2\frac{A^2}{8} G_F(\bar{x} - \bar{x}') (t^- t^+ + t^+ t^-) \right\}
\end{aligned}$$

$$\begin{aligned}
c43 \quad \sum_{i \neq j=1}^A \overline{P^{(2)}(\bar{x}, \bar{x}')(\underline{t}_i \cdot \underline{T}_i)(\underline{t}_j \cdot \underline{T}_j)} &= e(r) e(r') \left\{ \left( -\frac{1}{A} - \left( \frac{1}{4} - \frac{1}{A} \right) G_F(\bar{x} - \bar{x}') \right) t_2^2 \right. \\
&\left. - \frac{1}{8} G_F(\bar{x} - \bar{x}') (t^- t^+ + t^+ t^-) \right\}
\end{aligned}$$

Using C21 and C43 one may evaluate terms in the optical potential involving virtual charge exchange, e.g.

$$\begin{aligned}
c44 \quad \langle 0 | \sum_{i=1}^A \sum_{\substack{j=1 \\ j \neq i}}^A (b_0 + b_i, \underline{t}_i \cdot \underline{T}_i) \delta(\bar{r} - \bar{r}_i) (b_0 + b_j, \underline{t}_j \cdot \underline{T}_j) \delta(\bar{r}' - \bar{r}_j) | 0 \rangle \\
&= e(r) e(r') (1 - \frac{1}{A}) \left\{ b_0^2 + 2b_0 b_1 \frac{N-2}{A} - \frac{b_1^2}{A-1} - \left[ (b_0^2 + 2b_0 b_1 \frac{N-2}{A}) \frac{A-4}{A-1} \right. \right. \\
&\left. \left. + 2b_1^2 \frac{A-2}{A-1} \right] \frac{G_F(\bar{x} - \bar{x}')}{4} \right\}
\end{aligned}$$

## APPENDIX D

### Nuclear Density Parameters for Pions from Electron-Nucleus Scattering Data

Two kinds of information are needed for the pion-nucleus interaction problem. For the Coulomb interaction part of the problem one needs the charge distribution of the nucleus taking into account the finite size of the proton and the pion. For the strong interaction part of the problem the distribution of nucleon centers is required. Usually one assumes that the distribution of neutron centers is the same as that for proton centers. In this work nuclear density parameters are needed for  ${}^4\text{He}$ ,  ${}^{12}\text{C}$ ,  ${}^{16}\text{O}$ , and  ${}^{40}\text{Ca}$ .

The differential scattering cross sections for the scattering of high energy electrons are the best source of information about the nuclear charge distribution for most nuclei. In order to examine the relationship between the nuclear charge density and the electron scattering differential cross section, it is useful to consider the scattering problem in the Born approximation. The differential scattering cross section for an electron in the plane wave Born approximation is

$$D1 \quad \frac{d\sigma}{d\Omega} = \frac{\mu^2}{\hbar^4} \left| \frac{1}{2\pi} \int e^{i\vec{q}\cdot\vec{r}} V(r) d^3r \right|^2 = \frac{4\mu^2}{q^2 \hbar^4} \left| \int_0^\infty \sin qr V(r) r dr \right|^2$$

where  $\hbar q = 2\hbar k \sin\theta/2$  is the momentum transfer. Integrating the integral twice by parts and using Poisson's equation

$$D2 \quad \nabla^2 V(r) = \frac{1}{r} \frac{\partial^2}{\partial r^2} (r V(r)) = 4\pi z e^2 e(r)$$

one obtains

$$D3 \quad \int_0^{\infty} \sin(qr) V(r) r dr = -\frac{4\pi z e^2}{q^2} \int_0^{\infty} \sin qr e(r) r dr.$$

Thus

$$D4 \quad \frac{d\sigma}{d\Omega} = \frac{z^2 \alpha^2 \mu^2}{\hbar^4 k^4 \sin^4 \theta/2} \left| \frac{4\pi}{q} \int_0^{\infty} \sin qr e(r) r dr \right|^2.$$

For a point nucleus the Coulomb differential scattering cross section is

$$D5 \quad \frac{d\sigma^p}{d\Omega} = \frac{z^2 \alpha^2 \mu^2}{\hbar^4 k^4 \sin^4 \theta/2}.$$

Writing the differential cross section D4 in terms of the point nucleus differential cross section

$$D6 \quad \frac{d\sigma}{d\Omega} = \frac{d\sigma^p}{d\Omega} \left| \frac{4\pi}{q} \int_0^{\infty} \sin qr e(r) r dr \right|^2 \equiv \frac{d\sigma^p}{d\Omega} |F(q^2)|^2$$

one may define a form factor  $F(q^2)$  which is a measure of the charge distribution.

The development above indicates that the form factor is what is determined from electron scattering experiments and not the charge density itself. Since  $F(q^2)$  is the Fourier transform of  $e(r)$ , it is necessary to know  $F(q^2)$  for all  $q$  in order to obtain complete information about  $e(r)$ . Experimentally  $F(q^2)$  is known only for  $1 \leq q \leq 4 \text{ fm}^{-1}$ .<sup>126</sup> As a result  $e(r)$  is known only approximately.

With the present range of momentum transfer  $q$  that can be obtained experimentally, it is possible to determine more than one parameter in the charge distribution. For spherically symmetric charge distributions

$$D7 \quad F(q^2) = \frac{4\pi}{q} \int_0^{\infty} \sin qr \bar{\rho}(r) r dr = \int e^{i\vec{q}\cdot\vec{r}} \rho(\vec{r}) d^3r.$$

If the momentum transfer  $q$  of the electron is small compared to the inverse of the nuclear radius  $R$ , i.e.  $qR \ll 1$ , then  $\sin(qr)$  may be expanded to give

$$D8 \quad F(q^2) = \frac{4\pi}{q} \int_0^{\infty} r \rho(r) \left[ qr - \frac{(qr)^3}{3!} + \frac{(qr)^5}{5!} - \dots \right] dr$$

$$= 1 - \frac{q^2}{3!} \langle r^2 \rangle + \frac{q^4}{5!} \langle r^4 \rangle - \dots$$

Thus if only one parameter of the charge distribution can be obtained for small momentum transfer  $q$ , it is the rms radius.

The form factor  $F(q^2)$  measured experimentally is the form factor of the charge distribution i.e. the density of proton centers with finite size of the proton included. In order to determine the density of proton centers for use in the pion-nucleus strong interaction potential, it is necessary to remove the effect of the finite proton size. If one assumes as a first approximation that the nucleus consists of interacting protons each with an undistorted charge density  $\rho_p(\vec{r})$ , then the charge density of the nucleus  $\rho_{ch}(\vec{r})$  is of the form

$$D9 \quad \rho_{ch}(\vec{r}) = \int \rho_p(\vec{r}-\vec{r}') f(\vec{r}') d^3r'$$

where  $f(\vec{r}')$  is the distribution function for proton centers. The form factor for the nucleus  $F(q^2)$  may be written

$$D10 \quad F(q^2) = \int e^{i\vec{q}\cdot\vec{r}} \rho_{ch}(\vec{r}) d^3r = \iint f(\vec{r}') e^{i\vec{q}\cdot\vec{r}} \rho_p(\vec{r}-\vec{r}') d^3r d^3r'$$

Transforming the  $r$  variable of integration to  $\vec{x} = \vec{r} - \vec{r}'$ , one obtains

$$D11 \quad F(q^2) = \int f(r') e^{i\vec{q} \cdot \vec{r}'} d^3r' \int e^{i\vec{q} \cdot \vec{x}} e_p(x) d^3x$$

Using the definition D7 for the form factor, one may make the following definitions:

$$D12 \quad F_p(q^2) \equiv \int e^{i\vec{q} \cdot \vec{x}} e_p(x) d^3x$$

$$D13 \quad F_{pc}(q^2) \equiv \int f(r') e^{i\vec{q} \cdot \vec{r}'} d^3r'$$

Then

$$D14 \quad F(q^2) = F_p(q^2) F_{pc}(q^2)$$

where  $F_p(q^2)$  is the form factor for the charge distribution of a proton and  $F_{pc}(q^2)$  is the form factor for the distribution of proton centers.

Expanding  $F(q^2)$ ,  $F_p(q^2)$ , and  $F_{pc}(q^2)$  as a function of  $qr$  for small  $qr$  obtain

$$D15 \quad F(q^2) = 1 - \frac{q^2}{6} \langle r^2 \rangle + \dots = (1 - \frac{q^2}{6} \langle r_{pc}^2 \rangle + \dots) (1 - \frac{q^2}{6} \langle r_p^2 \rangle + \dots) \\ = 1 - \frac{q^2}{6} (\langle r_{pc}^2 \rangle + \langle r_p^2 \rangle) + \dots$$

Equating the coefficients of the independent powers of  $q$  on each side of the equation one has

$$D16 \quad \langle r^2 \rangle = \langle r_{pc}^2 \rangle + \langle r_p^2 \rangle$$

or

$$D17 \quad \langle r_{pc}^2 \rangle = \langle r^2 \rangle - \langle r_p^2 \rangle$$

This result is in agreement with that obtained by Elton.<sup>127</sup>

Two basic approaches have been used in analyzing electron scattering data. These are based on theoretical notions concerning the form of the charge distribution.

One approach is based on the harmonic oscillator shell model. According to this shell model the distribution of proton centers  $e_{pc}(r)$  is of the modified gaussian form for p shell nuclei, i.e.

$$D18 \quad e_{pc}(r) = \frac{a}{2\pi^{3/2}a^3} \left( 1 + \frac{2-a}{3} \frac{r^2}{a^2} \right) e^{-r^2/a^2}$$

where Z is the number of protons and a is the only density parameter. The charge distribution of the nucleus including the finite size of the protons is from equation D9

$$D19 \quad e_{ch}(r) = \int e_p(\vec{r}-\vec{r}') e_{pc}(r') d^3r'$$

In the shell model the charge distribution of the proton  $e_p(r)$  is assumed to be gaussian, i.e.

$$B20 \quad e_p(r) = \frac{1}{\pi^{3/2}a_p^3} e^{-r^2/a_p^2}$$

Thus the integration may be performed to obtain

$$D21 \quad e_{ch}(r) = \frac{a}{2\pi^{3/2}b^3} \left[ 1 + \frac{2-a}{3} \left\{ \frac{3(b^2-a^2)}{2b^2} + \frac{a^2r^4}{b^4} \right\} \right] e^{-r^2/b^2}$$

where

$$D22 \quad b^2 = a^2 + a_p^2.$$

The form factor  $F(q^2)$  for the nuclear charge distribution including the finite size of the proton is given by D10 to be

$$D23 \quad F(q^2) = \left(1 - \frac{Z-2}{6} \alpha^2 q^2\right) e^{-b^2 q^2 / 4}$$

In analysis of the experimental value of  $F^2(q^2)$  to determine the charge parameters, one fits the theoretical  $F^2(q^2)$  to the experimental one. The fit is most sensitive to the first minimum in  $F^2(q^2)$  which essentially determines the parameter  $a$ . From the shell model viewpoint the first minimum originates from the interference between the  $s$ - and  $p$ -nucleons. The rms radius of the distribution of proton centers is determined from  $a$ .

Unfortunately most experimentalists <sup>128-131</sup> analyzing their electron scattering data have neglected the finite size of the proton and fit their data using a charge density of the form

$$D24 \quad \rho_{ch}(r) = \frac{2}{\pi^{3/2} B^3} \frac{1}{2+3\alpha'} \left(1 + \alpha' \frac{r^2}{B^2}\right) e^{-r^2/B^2} \quad \alpha' = \frac{Z-2}{3}$$

As a result the form factors obtained have not described the data well. In order to be able to fit the electron scattering data many experimentalists such as Crannell <sup>131</sup> have also allowed  $\alpha' = \frac{Z-2}{3}$  to be varied as a second parameter. Thus one finds that the electron scattering data have not been fitted in a proper manner for extracting directly the density of proton centers in the nucleus.

In order to obtain the density of proton centers from the electron scattering fits, one must remove the form factor for the proton from the

form factor obtained from D24, i.e.

$$D25 \quad F_{ch}(q^2) = \left(1 - \frac{B^2 \alpha' q^2}{4 + 6\alpha'}\right) e^{-q^2 B^2/4} = F_{pc}(q^2) F_p(q^2)$$

Thus one obtains

$$D26 \quad F_{pc}(q^2) = \left(1 - \frac{B^2 \alpha' q^2}{4 + 6\alpha'}\right) e^{-q^2 \bar{B}^2/4}$$

$$\bar{B} = [B^2 - a_p^2]^{1/2}$$

$$a_p = .59 \text{ fm}$$

Taking the Fourier transform of  $F_{pc}(q^2)$  one obtains the density of proton centers to be

$$D27 \quad \rho_{pc}(r) = \frac{2}{\pi^{3/2} \bar{B}^3} \frac{1}{2 + 3\alpha'} \left[ 1 + \frac{3\alpha'}{2} \left(1 - \frac{B^2}{\bar{B}^2}\right) + \alpha' \frac{B^2}{\bar{B}^2} \frac{r^2}{\bar{B}^2} \right] e^{-r^2/\bar{B}^2}$$

From Crannell<sup>131</sup> the best fit values of the parameters  $\alpha'$  and  $B$  for  $^{12}_C$  and  $^{16}_O$  are

$^{12}_C$	$\alpha' = 4/3$	$B = 1.636 \text{ fm}$
$^{16}_O$	$\alpha' = 8/5$	$B = 1.851 \text{ fm}$

For  $^4_He$  a similar procedure is followed in order to make use of the electron scattering analysis of Frosh et al.<sup>132</sup> They fit the electron-scattering data with the form factor

$$D28 \quad F_{ch}(q^2) = (1 - (a_0^2 q^2)^6) e^{-b^2 q^2/4} = F_{pc}(q^2) F_p(q^2)$$

$$a_0 = .316 \text{ fm}$$

$$b = 1.362 \text{ fm}$$

Factoring out the form factor for the proton one obtains

$$D29 \quad F_{pc}(q^2) = [1 - (a_0^2 q^2)^6] e^{-\bar{b}^2 q^2/4}$$

$$\bar{b}^2 = b^2 - a_p^2$$

Taking the Fourier transform of  $F_{pc}(q^2)$  one finds the density of proton centers to be

$$\begin{aligned}
 \text{D30} \quad \rho_{pc}(r) = & \frac{2e^{-r^2/b^2}}{\pi^{3/2} b^3} \left[ 1 - 64 \left(\frac{a_0}{b}\right)^{12} \left\{ 135135 - 540540 \frac{r^2}{b^2} \right. \right. \\
 & + 540540 \frac{r^4}{b^4} - 205920 \frac{r^6}{b^6} + 34320 \frac{r^8}{b^8} \\
 & \left. \left. - 2496 \frac{r^{10}}{b^{10}} + 64 \frac{r^{12}}{b^{12}} \right\} \right]
 \end{aligned}$$

For heavier nuclei (beyond p shell) one finds that the shell model becomes too complicated to use. In this case electron scattering experimentalists<sup>128</sup> have used a phenomenological density shape such as the Fermi density

$$\text{D31} \quad \rho_{ch}(r) = \frac{\rho_0}{1 + e^{-(r-R)/c}}$$

Uberall<sup>133</sup> has given a prescription for obtaining the density of proton centers for these heavier nuclei using the Fermi shape.

$$\text{D32} \quad \rho_{pc}(r) = \frac{\bar{\rho}_0}{1 + e^{-(r-\bar{R})/\bar{c}}}$$

where

$$\begin{aligned}
 \text{D33} \quad \bar{R} &= R + .13 A^{-1/3} \text{ fm} \\
 \bar{c} &= c/1.13
 \end{aligned}$$

This approach was used for <sup>40</sup>Ca in conjunction with the electron scattering results of Croissiaux et al.<sup>134</sup> They obtained for <sup>40</sup>Ca

$$\text{D34} \quad R = 3.602 \text{ fm} \quad c = .576 \text{ fm.}$$

For the nuclear density parameters required for the pion-nucleus Coulomb interaction one follows a similar procedure to that above.

First one needs to define

$$D35 \quad F_{\pi Nuc}(q^2) = F_{ch}(q^2) F_{\pi}(q^2)$$

Then taking the Fourier transform of  $F_{\pi Nuc}(q^2)$  one obtains the Coulomb charge distribution  $e_{\pi Nuc}(r)$ . The Coulomb potential is defined in terms of  $e_{\pi Nuc}(r)$  by

$$D36 \quad V_C(r) = -e \int \frac{e_{\pi Nuc}(r')}{|\mathbf{r}-\mathbf{r}'|} d^3r'$$

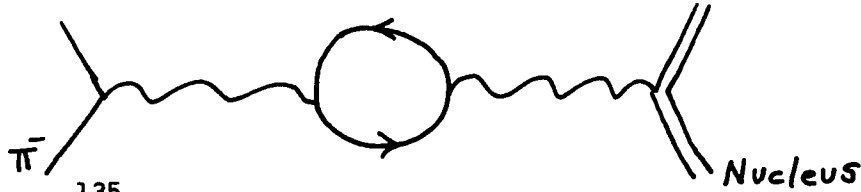
For this work the form factor of the pion is assumed to be approximately the same as that of the proton, i.e.

$$D37 \quad F_{\pi}(q^2) \cong F_p(q^2)$$

APPENDIX E

Vacuum Polarization Contributions to Pionic Atom Energy Levels

The pion-nucleus vacuum polarization potential to order  $\alpha$  due to formation of virtual electron-positron pairs represented by the Feynman graph



is given by

$$E1 \quad V_{VP}(r) = -\frac{2\alpha e}{3\pi} \int \frac{e(r')}{|\vec{r}-\vec{r}'|} \int_1^\infty e^{-\frac{2m_e c}{\hbar} |\vec{r}-\vec{r}'| S} \left(1 + \frac{1}{2S^2}\right) \frac{\sqrt{S^2-1}}{S^2} dS d^3r'$$

where  $m_e$  is the mass of the electron. Expanding  $\frac{1}{|\vec{r}-\vec{r}'|}$  in terms of spherical harmonics and integrating repeatedly by parts in order to obtain standard integrals, one obtains the vacuum polarization potential for a spherical charge distribution

$$E2 \quad V_{VP}(r) = -\frac{e}{r} \frac{\alpha \hbar}{3m_e c} \int_0^\infty e(r') r' dr' \left[ \frac{19X}{24} + \frac{X^3}{24} - \frac{3\pi X^2}{8} - \frac{\pi X^4}{48} \right. \\ \left. + \sum_{k=0}^\infty \frac{\left(\frac{X}{8}\right)^{2k+1}}{(k!)^2} \left\{ \left( \ln \frac{X}{2} - \Psi(k+1) \right) \left[ \frac{1}{k+1} \left( \frac{19X^2}{24} + \frac{X^4}{24} \right) + \frac{7}{4} \right. \right. \right. \\ \left. \left. \left. + \frac{X^2}{12} + \frac{2}{2k+1} \left( \frac{9}{8} - \frac{3X^2}{4} - \frac{X^4}{24} \right) \right] - \frac{1}{2(k+1)^2} \left( \frac{19X^2}{24} + \frac{X^4}{24} \right) \right\} \right]$$

$$-\frac{2}{(2k+1)^2} \left( \frac{9}{8} - \frac{3x^2}{4} - \frac{x^4}{24} \right) \left. \vphantom{\frac{2}{(2k+1)^2}} \right\} \left. \vphantom{\frac{9}{8}} \right] \left. \vphantom{\frac{9}{8}} \right| \begin{array}{l} x = \frac{2meC}{\hbar} |r-r'| \\ x = \frac{2meC}{\hbar} (r+r') \end{array}$$

where  $\Psi(z)$  is the digamma function<sup>136</sup> which is defined in terms of the gamma function by

$$E3 \quad \Psi(z) = \frac{d \ln \Gamma(z)}{dz} = \frac{\Gamma'(z)}{\Gamma(z)}$$

The first few terms of the expression for  $V_{vp}(r)$  above were first obtained by Barrett et al.<sup>137</sup>

According to Mickelwait and Corben<sup>138</sup> the effect of the finite size of the nucleus on the vacuum polarization potential is less than 8% for the pionic states 1S( $Z \leq 12$ ), 2P( $Z \leq 30$ ), 3D( $Z \leq 82$ ), and 4F( $Z \leq 82$ ). Since the effect of the extended nuclear charge is small, the nuclear charge distribution may be approximated by a uniform charge distribution for calculational convenience. The error made in calculating the vacuum polarization potential by this procedure is  $\leq 1\%$ .

Using the charge distribution

$$E4 \quad e(r') = \begin{cases} \frac{Ze}{\frac{4}{3}\pi R^3} & r' \leq R \\ 0 & r' > R \end{cases}$$

where the uniform radius  $R$  is defined in terms of the rms radius by

$R = \sqrt{\frac{5}{3}} r_{rms}$ , the expression for the vacuum polarization potential may be integrated to obtain

$$\begin{aligned}
 E5 \quad V_{VP}(r \leq R) = & \frac{-2\alpha e^2}{4\pi R} \left[ \left( -\frac{4}{3} - \frac{4}{3} \Psi(1) + \frac{4}{3} \ln \frac{m_e c R}{\hbar} \right) \left( \frac{r}{R} \right)^2 \right. \\
 & + \left( \frac{4}{3} + 4 \Psi(1) - 4 \ln \frac{m_e c R}{\hbar} \right) + \left( \frac{2}{3} \left( \frac{r}{R} \right)^2 - 2 + \frac{4}{3} \frac{R}{r} \right) \\
 & \ln \left( 1 - \frac{r}{R} \right) + \left( \frac{2}{3} \left( \frac{r}{R} \right)^2 - 2 - \frac{4}{3} \frac{R}{r} \right) \ln \left( 1 + \frac{r}{R} \right) + \frac{2\pi m_e c R}{\hbar} \\
 & + \left( \frac{1}{5} \left( \frac{r}{R} \right)^4 - 3 - 2 \left( \frac{r}{R} \right)^2 \right) \left( \frac{m_e c R}{\hbar} \right)^2 + \left( \frac{8\pi}{15} + \frac{8\pi}{9} \left( \frac{r}{R} \right)^2 \right) \\
 & \left. \left( \frac{m_e c R}{\hbar} \right)^3 + O \left\{ \left( \frac{m_e c R}{\hbar} \right)^4 \right\} \right]
 \end{aligned}$$

and

$$\begin{aligned}
E6 \quad V_{VP}(r \geq R) &= -\frac{2\alpha e^2}{3\pi r} \left[ 1 - \left(\frac{r}{R}\right)^2 - 2 \left( \ln \frac{m_e c r}{\hbar} - \psi(1) \right) \right. \\
&\quad - \left( 1 - \frac{3}{2} \frac{r}{R} + \frac{1}{2} \left(\frac{r}{R}\right)^3 \right) \ln \left( 1 - \frac{R}{r} \right) - \left( 1 + \frac{3}{2} \frac{r}{R} - \frac{1}{2} \left(\frac{r}{R}\right)^3 \right) \\
&\quad \ln \left( 1 + \frac{R}{r} \right) + \frac{3\pi}{2} \frac{m_e c r}{\hbar} - 3 \left( \frac{m_e c r}{\hbar} \right)^2 + \frac{2\pi}{3} \left( \frac{m_e c r}{\hbar} \right)^3 \\
&\quad \left. - \frac{3}{5} \left( \frac{m_e c R}{\hbar} \right)^2 + \frac{2\pi}{5} \frac{m_e c^3}{\hbar^3} r R^2 \right] - \frac{2\alpha e^2}{16\pi r} \left( \frac{\hbar}{m_e c R} \right)^3. \\
&\sum_{k=1}^{\infty} \frac{x^{2k+4}}{(k!)^2} \left[ \frac{4-16k}{3(2k-1)^2} \left( \frac{m_e c r / \hbar}{2k+4} - \frac{x}{2k+5} \right) \right. \\
&\quad - \frac{8k}{6k-3} \left\{ \left( \frac{x}{2k+5} - \frac{m_e c r / \hbar}{2k+4} \right) (\ln x - \psi(k)) - \frac{x}{(2k+5)^2} \right. \\
&\quad \left. \left. + \frac{m_e c r / \hbar}{(2k+4)^2} \right\} + \left( \frac{19}{3(k+1)^2} - \frac{24}{(2k+1)^2} \right) \left( \frac{m_e c r / \hbar}{2k+4} - \frac{x}{2k+5} \right) \right. \\
&\quad \left. + \frac{8k^2+16k-30}{3(k+1)(2k+1)} \left\{ \left( \frac{x}{2k+5} - \frac{m_e c r / \hbar}{2k+4} \right) (\ln x - \psi(k) - \frac{1}{k}) \right. \right. \\
&\quad \left. \left. - \frac{x}{(2k+5)^2} + \frac{m_e c r / \hbar}{(2k+4)^2} \right\} + \frac{9}{(k+1)^2 (2k+3)^2} \left( \frac{m_e c r / \hbar}{2k+4} \right. \right. \\
&\quad \left. \left. - \frac{x}{2k+5} \right) + \frac{14k+30}{(k+1)^2 (2k+3)} \left\{ \left( \frac{x}{2k+5} - \frac{m_e c r / \hbar}{2k+4} \right) (\ln x - \psi(k)) \right. \right. \\
&\quad \left. \left. - \frac{2k+1}{k^2+k} \right) - \frac{x}{(2k+5)^2} + \frac{m_e c r / \hbar}{(2k+4)^2} \right\} \Bigg] \Bigg|_{x = \frac{m_e c}{\hbar} (r-R)}^{x = \frac{m_e c}{\hbar} (r+R)}
\end{aligned}$$

From the mass dependence of the  $e \frac{-2\pi m c^2 |r-F|}{\hbar}$  factor in equation E1 for the vacuum polarization potential, the contribution of virtual muon and more massive fermion pairs is expected to be negligible. According to Fricke the formation of virtual muon pairs yields a vacuum polarization contribution of only -261 ev for the 1s state of muonic  $U^{238}$ . Due to the effect of the strong interaction, the contribution from virtual pion pairs is unknown. Fricke<sup>135</sup> has calculated the contribution for a boson with mass equal to that of the pion neglecting the effect of the strong interaction. He found the contribution to be very small (-27 ev for the 1s muonic state of  $U^{238}$ ). The fourth order contributions to the vacuum polarization potential proportional to  $\alpha^2$  give a negligible contribution of fractional value 1/500.

The vacuum polarization contribution to the energy of a particular pionic atom energy level may be obtained by numerically solving the Klein-Gordon equation. First the Klein-Gordon equation is solved for the energy of the nl state with the Coulomb, strong interaction, and vacuum polarization potentials. Then it is solved with just the Coulomb and strong interaction potentials. The difference in the two solutions for the energy of the nl state gives the contribution of vacuum polarization to the energy of that state. Table 46 gives a listing of the vacuum polarization contributions to various states of a number of nuclei as calculated by Terrill and Lucas<sup>139</sup> using the strong interaction potential of Krell and Ericson.<sup>21</sup>

## APPENDIX F

### Method of Solving the Klein-Gordon Equation for Pionic Atoms

The time-independent Klein-Gordon equation is usually written in the form resembling the time-independent Schroedinger equation in order to insert the nonrelativistic strong interaction pion-nucleus optical model potential that was derived from multiple scattering theory via the Schroedinger equation. Thus

$$F1 \left[ \frac{\hbar^2 c^2}{2M_\pi c^2} \nabla^2 + \frac{(E - V_C(r))^2 - m_\pi^2 c^4}{2M_\pi c^2} \right] \Psi(\vec{r}) = V_{ST}(r) \Psi(\vec{r})$$

$$= \frac{\hbar^2 c^2}{2M_\pi c^2} \left[ q(\vec{r}) - \nabla \cdot \alpha(\vec{r}) \nabla \right] \Psi(\vec{r})$$

where  $V_{ST}(r)$  has been separated into local and nonlocal parts  $q(\vec{r})$  and  $\alpha(\vec{r})$

$$F2 \quad q(r) = -4\pi "b_0" e(r) - 4\pi i "B" e^2(r) + 2\pi \frac{E_\pi}{M_N} c_0 \nabla^2 e(r)$$

$$\alpha(r) = -4\pi "c_0" e(r) - 4\pi i "C" e^2(r)$$

which have been written in terms of effective parameters " $b_0$ ", " $c_0$ ", " $B$ ", and " $C$ ".

For nuclei with only small deviations from spherical mass and charge distributions, assume  $q(\vec{r}) = q(r)$  and  $\alpha(\vec{r}) = \alpha(r)$  so that the orbital angular momentum  $\ell$  is a good quantum number. Using separation of variables in the wavefunction  $\Psi(\vec{r}) = R_\ell(r) Y_{\ell m}(\theta, \phi)$  obtain for the radial equation

$$\begin{aligned}
 \text{F3} \quad & (1 + \alpha(r)) \left( \frac{1}{r} \frac{\partial^2}{\partial r^2} r R_\ell(r) - \frac{\ell(\ell+1)}{r^2} R_\ell(r) \right) + \frac{(E_{m\ell} - V_c(r))^2 - m_n^2 c^4}{\hbar^2 c^2} R_\ell(r) \\
 & = g(r) R_\ell(r) - \alpha'(r) \frac{\partial R_\ell(r)}{\partial r}
 \end{aligned}$$

where  $n = n' + \ell + 1$  is the principal quantum number having only positive integer values. <sup>141</sup> ( $n' = 0, 1, 2, \dots$ )

This nonlocal wave equation can be transformed into a local one by making the substitution

$$\text{F4} \quad \phi_\ell(r) = [1 + \alpha(r)]^{1/2} r R_\ell(r)$$

to obtain

$$\begin{aligned}
 \text{F5} \quad \phi_\ell''(r) = & \left[ \frac{\ell(\ell+1)}{r^2} - \frac{1}{1+\alpha(r)} \left\{ \frac{(E_{m\ell} - V_c(r))^2 - m_n^2 c^4}{\hbar^2 c^2} - g(r) \right. \right. \\
 & \left. \left. + \frac{\alpha'(r)}{r} + \frac{\alpha'(r)^2}{4(1+\alpha(r))} + \frac{\alpha''(r)}{2} \right\} \right] \phi_\ell(r)
 \end{aligned}$$

Note that the total energy may be written

$$\text{F6} \quad E_{m\ell} = m_n c^2 + E'_{m\ell}$$

such that

$$\text{F7} \quad (E_{m\ell} - V_c(r))^2 - m_n^2 c^4 = 2 m_n c^2 (E'_{m\ell} - V_c(r)) + (E'_{m\ell} - V_c(r))^2$$

So

$$\begin{aligned}
 \text{F8} \quad \phi_\ell''(r) = & \frac{\ell(\ell+1)}{r^2} - \frac{1}{1+\alpha(r)} \left\{ \frac{2 m_n c^2 (E'_{m\ell} - V_c(r)) + (E'_{m\ell} - V_c(r))^2}{\hbar^2 c^2} \right. \\
 & \left. - g(r) + \frac{\alpha'(r)}{r} + \frac{\alpha'(r)^2}{4(1+\alpha(r))} + \frac{\alpha''(r)}{2} \right\} \phi_\ell(r)
 \end{aligned}$$

In this equation for  $\phi_2(r)$  the energy  $E_{n\ell}'$  and the strong interaction potential terms  $q(r)$  and  $\alpha(r)$  are unknown. To solve for the parameters in  $q(r)$  and  $\alpha(r)$  one needs to know  $E_{n\ell}'$ . Pionic atom experiments measure the pionic atom x-ray transition energies  $E_\gamma = E_{n+1,\ell+1} - E_{n,\ell}$  and linewidths  $\Gamma_{n\ell}$ . Since the strong interaction significantly affects only the lower energy level of a transition, the energy of the upper level  $E_{n+1,\ell+1}$  can be determined by solving the Klein-Gordon equation with the appropriate Coulomb and vacuum polarization potentials. Then the real part of the experimental energy of the lower level  $E_{n\ell}'$  can be obtained from the relation

$$F9 \quad E_{m\ell}' = E_{m+1,\ell+1}' - E_\gamma$$

Now there is a complex energy shift  $\Delta E_{n\ell}$  of the pionic atom electromagnetic energy levels due to the pion-nucleus strong interaction represented by  $V_{st}(r)$  where

$$F10 \quad E_{m\ell}' = E_{m\ell}^0 + \Delta E_{m\ell}$$

$$F11 \quad \Delta E_{m\ell} = \Delta E_{R_{m\ell}} + i \Delta E_{I_{m\ell}}$$

$$F12 \quad E_{m\ell}^0 = \text{unperturbed electromagnetic energy of } n\ell \text{ state}$$

The time dependence of the pionic atom wavefunction is given by

$$F13 \quad e^{-i E_{m\ell}' t / \hbar} = e^{-i (E_{m\ell}^0 + \Delta E_{R_{m\ell}}) t / \hbar} e^{\Delta E_{I_{m\ell}} t / \hbar}$$

Thus the probability density for finding the pion in a certain state  $n\ell$  at time  $t$ , which is given by the absolute square of the wavefunction, is

$$F14 \quad e^{2\Delta E_{I_{m\ell}} t / \hbar} = e^{-\Gamma_{m\ell} t / \hbar}$$

Therefore the imaginary part of  $V_{st}(r)$  which gives rise to  $\Delta E_{Inq}$  leads to an exponential decay of all states  $nq$  and results in a broadening of the energy levels from which pion capture occurs. The width of the observed transition x-ray gives directly the width due to the strong interaction of there is no unresolved fine or hyperfine structure present, since the electromagnetic radiation width of the levels due to the probability of making a radiative transition is negligible in the range of observation compared to the strong interaction absorption width. So the imaginary part of the energy shift is given by

$$F15 \quad \Delta E_{Imq} = - \Gamma_{mq} / 2$$

Note that the wave equation describing pion absorption must necessarily be complex, since the energy of the shifted state is complex.

In general the equation for  $\phi_q(r)$  is quite complicated and must be solved numerically. However, it is possible to separate the solution for all of space into two regions, i. e. the inner region in which the short range strong interaction potential and finite size Coulomb potential are important and the outer region in which only electromagnetic potentials for point sources are important. The wave equation for  $\phi_q(r)$  can be solved exactly in the outer region for a Coulomb potential. By using the logarithmic derivative of the outer wavefunction at the boundary of the two regions as a boundary condition on the inner wavefunction, it is possible to greatly reduce the region over which the wave equation must be numerically integrated. In practice the inner region need be only a few nuclear radii for high accuracy in the solution.

Now the vacuum polarization potential is also present in the

outer region and destroys the simple exact solution possible for the pure Coulomb point charge potential. However, the vacuum polarization may be treated separately using perturbative methods, since it gives rise to only a small shift in the energy and wavefunction of the state. To do this the wave equation is solved numerically for the energy eigenvalue using the Coulomb potential, the vacuum polarization potential, and an approximate value of the strong interaction potential. Then the same wave equation without the vacuum polarization potential is solved for the energy. The difference between the two energies obtained gives the shift in the energy of the state due to vacuum polarization. Now this energy shift may be subtracted from the experimentally determined energy of the  $n\ell$  state  $E_{n\ell}$ , and the wave equation solved with this new energy  $E_{n\ell}''$  in the absence of the vacuum polarization potential. This method of handling the vacuum polarization potential is particularly convenient, since the vacuum polarization potential is fairly long-ranged (500-2000 nuclear radii for 1 % accuracy) and rather time consuming to compute on the computer.

For the outer region the wave equation to be solved is

$$F16 \quad \phi_{\ell}''(r) + \left[ -\frac{\ell(\ell+1)}{r^2} + \frac{2m\hbar c^2 (E_{n\ell}'' - V_C(r)) + (E_{n\ell}'' - V_C(r))^2}{\hbar^2 c^2} \right] \phi_{\ell}(r) = 0 = 0$$

where  $\text{Im } E_{n\ell}'' = \Gamma_{n\ell}/2$  and

$$F17 \quad V_C(r) = -\frac{Ze^2}{r} = -\frac{Z\alpha\hbar c}{r}$$

Writing out all powers of  $r$  explicitly obtain

$$F18 \quad \phi_{\ell}''(r) + \left[ -\frac{\ell(\ell+1)}{r^2} + \frac{2m\hbar c^2 E_{n\ell}''}{\hbar^2 c^2} + \frac{E_{n\ell}''^2}{\hbar^2 c^2} + \frac{2m\hbar c^2 Z\alpha}{\hbar c r} + \frac{2E_{n\ell}'' Z\alpha}{\hbar c r} + \frac{Z^2\alpha^2}{r^2} \right] \phi_{\ell}(r) = 0$$

Let

$$F19 \quad \delta = \frac{a}{\hbar c} \left[ -2m\pi c^2 E_{n\ell}'' - E_{n\ell}''^2 \right]^{1/2}$$

$$F20 \quad \lambda = \frac{Z\alpha}{\hbar c} (E_{n\ell}'' + m\pi c^2) \frac{a}{\delta}$$

Substituting in obtain

$$F21 \quad \phi_r''(r) + \left[ -\frac{\delta^2}{4} + \frac{\lambda\delta}{r} - \frac{\ell(\ell+1) - Z^2\alpha^2}{r^2} \right] \phi_r(r) = 0$$

Dividing by  $\delta^2$ , letting  $e = \delta r$ , and replacing  $\phi_r(r)$  by  $\phi_r(e)$  obtain

$$F22 \quad \phi_r''(e) + \left[ -\frac{1}{4} + \frac{\lambda}{e} - \frac{\ell(\ell+1) - Z^2\alpha^2}{e^2} \right] \phi_r(e) = 0$$

Now Whittaker's equation is of the form 136

$$F23 \quad W''(e) + \left[ -\frac{1}{4} + \frac{k}{e} + \frac{\frac{1}{2} - \mu^2}{e^2} \right] W(e) = 0$$

with solution that is finite as  $|e| \rightarrow \infty$

$$F24 \quad W_{k\mu}(e) = N e^{-e/2} e^{\mu+1/2} \psi(\mu+1/2-k, 1+2\mu, e)$$

where N is a normalization constant,

$$F25 \quad \mu = \pm \frac{[4\ell^2 + 4\ell + 1 - 4Z^2\alpha^2]^{1/2}}{2} = \pm \frac{[(2\ell+1)^2 - 4Z^2\alpha^2]^{1/2}}{2},$$

and  $\Psi(\alpha, \gamma, z)$  is the confluent hypergeometric function of the second kind with complex arguments given by 142

$$F26 \quad \Psi(\alpha, \gamma, z) = \Gamma(1-\gamma) \Gamma(\gamma) \left[ \frac{1}{\Gamma(1+\alpha-\gamma)} \sum_{k=0}^{\infty} \frac{(\alpha)_k}{\Gamma(\gamma+k)} \frac{z^k}{k!} - \frac{1}{\Gamma(\alpha)} \sum_{k=0}^{\infty} \frac{(1+\alpha-\gamma)_k}{\Gamma(\beta-\gamma+k)} \frac{z^{k+1-\gamma}}{k!} \right]$$

where

$$F27 \quad (\alpha)_k = \alpha(\alpha+1)(\alpha+2) \cdots (\alpha+k-1)$$

$$F28 \quad (\alpha)_0 = 1$$

Let  $m = \mu + 1/2$ , then

$$F29 \quad \phi_2(e) = W_{\lambda, \mu}(e) = N e^{-e/2} e^m \Psi(m-\lambda, 2m, e)$$

Using the recursion relation for Whittaker functions from Whittaker and  
143  
Watson p. 352

$$F30 \quad e W'_{\lambda, \mu}(e) = (\lambda - e/2) W_{\lambda, \mu}(e) - [\mu^2 - (\lambda - \frac{1}{2})^2] W_{\lambda-1, \mu}(e)$$

one obtains

$$F31 \quad e \frac{W'_{\lambda, \mu}(e)}{W_{\lambda, \mu}(e)} = \lambda - e/2 - [\mu^2 - (\lambda - \frac{1}{2})^2] \frac{W_{\lambda-1, \mu}(e)}{W_{\lambda, \mu}(e)} .$$

Now

$$F32 \quad \frac{W_{\lambda-1, \mu}(e)}{W_{\lambda, \mu}(e)} = \frac{e^{\mu+\gamma_2} e^{-e/2} \Psi(\mu+\frac{1}{2} - (\lambda-1), 1+2\mu, e)}{e^{\mu+\gamma_2} e^{-e/2} \Psi(\mu+\gamma_2 - \lambda, 1+2\mu, e)} \\ = \frac{\Psi(\mu+\frac{3}{2} - \lambda, 1+2\mu, e)}{\Psi(\mu+\gamma_2 - \lambda, 1+2\mu, e)}$$

Thus the logarithmic derivative of  $\phi_2(e)$  is given by

$$F33 \quad \frac{e \phi'_2(e)}{\phi_2(e)} = \lambda - e/2 - [(m-\gamma_2)^2 - (\lambda - \gamma_2)^2] \frac{\Psi(m+1-\lambda, 2m, e)}{\Psi(m-\lambda, 2m, e)}$$

or

$$F34 \quad \phi'_2(e) = \phi_2(e) \left[ -\frac{1}{2} + \frac{\lambda}{e} - \frac{[m(m-1) - \lambda(\lambda-1)]}{e} \frac{\Psi(m+1-\lambda, 2m, e)}{\Psi(m-\lambda, 2m, e)} \right]$$

Let the boundary between the interior and exterior regions be spherical with radius  $r_0$ . The derivative of  $\phi_2(e)$  at the boundary where  $e = e_0$  is given by

$$F35 \quad \phi'_2(e)|_{e=e_0} = \phi_2(e) \left[ -\frac{1}{2} + \frac{\lambda}{e_0} - \frac{[m(m-1) - \lambda(\lambda-1)]}{e_0} \frac{\Psi(m+1-\lambda, 2m, e_0)}{\Psi(m-\lambda, 2m, e_0)} \right]$$

Now the interior equation is an eigenvalue equation for the parameters in the optical model potential. Since the eigenvalue is independent of the normalization of the wavefunction, one may for convenience use an unnormalized wavefunction at the boundary such as  $\phi_2(e_0) = 1 + i$ . In this case the boundary conditions on the interior solution are

$$F36 \quad \phi_2(e_0) = 1 + i$$

$$F37 \quad \phi_2'(e) \Big|_{e=e_0} = (1+i) \left[ -\frac{1}{2} + \frac{\lambda}{e_0} - \frac{[m(m-1) - \lambda(\lambda-1)]}{e_0} \frac{\psi(m+1-\lambda, \lambda/m, e_0)}{\psi(m-\lambda, \lambda/m, e_0)} \right]$$

In addition to these two boundary conditions on the interior solution there is a third condition resulting from the fact that  $R_2(r)$  must be finite at the origin, i.e.  $\phi_2(e) \propto rR_2(r) \xrightarrow{r \rightarrow 0} 0$ . Thus the third boundary condition is

$$F38 \quad \phi_2(e=0) = 0$$

The interior equation to be solved is

$$F39 \quad \phi_2''(e) = \left[ \frac{l(l+1)}{e^2} - \frac{1}{1+\alpha(e/\delta)} \left\{ -\frac{1}{4} - \frac{\lambda}{\delta} \frac{V_0(e/\delta)}{2\alpha\hbar c} + \frac{V_0^2(e/\delta)}{\delta^2 \hbar^2 c^2} \right. \right. \\ \left. \left. - \frac{g(e/\delta)}{\delta^2} + \frac{1}{e} \frac{d}{de} \alpha(e/\delta) + \frac{1}{4(1+\alpha(e/\delta))} \left( \frac{d}{de} \alpha(e/\delta) \right)^2 \right. \right. \\ \left. \left. + \frac{1}{2} \frac{d^2}{de^2} \alpha(e/\delta) \right] \phi_2(e)$$

In solving this complex equation it is convenient to separate  $\phi_2(e)$  into real and imaginary parts. However the use of a complex dependent variable  $e$  complicates this separation in the case of derivative terms. The most desirable procedure is to rewrite the equation in terms of the real variable  $\epsilon = e/e_0 = r/r_0$ . Thus

$$\begin{aligned}
\text{F40 } \phi_{\lambda}''(\epsilon) &= \left[ \frac{\lambda(\lambda+1)}{\epsilon^2} - \frac{1}{1+\alpha(\epsilon r_0)} \left\{ -\frac{\delta^2 r_0^2}{4} - \lambda \delta r_0^2 \frac{V_c(\epsilon r_0)}{2\alpha \hbar c} \right. \right. \\
&\quad \left. \left. + \frac{r_0^2}{\hbar^2 c^2} V_c^2(\epsilon r_0) - q(\epsilon r_0) r_0^2 + \frac{1}{\epsilon} \frac{d}{d\epsilon} \alpha(\epsilon r_0) + \frac{1}{4(1+\alpha(\epsilon r_0))} \left( \frac{d}{d\epsilon} \alpha(\epsilon r_0) \right)^2 \right. \right. \\
&\quad \left. \left. + \frac{1}{2} \frac{d^2}{d\epsilon^2} \alpha(\epsilon r_0) \right\} \right] \phi_{\lambda}(\epsilon) \\
&\equiv F_{\lambda}(\epsilon) \phi_{\lambda}(\epsilon)
\end{aligned}$$

with boundary conditions

$$\text{F41 } \phi_{\lambda}(0) = 0$$

$$\text{F42 } \phi_{\lambda}(1) = 1+i$$

$$\text{F43 } \phi_{\lambda}'(\epsilon) \Big|_{\epsilon=1} = (1+i) \left[ -\frac{\delta r_0}{2} + \lambda - [m(m-1) - \lambda(\lambda-1)] \frac{\Psi(m+\lambda-1, \lambda, \delta r_0)}{\Psi(m-\lambda, \lambda, \delta r_0)} \right]$$

Separating the real and imaginary equations obtain

$$\text{F44 } \phi_{\lambda R}''(\epsilon) = F_{\lambda R}(\epsilon) \phi_{\lambda R}(\epsilon) - F_{\lambda I}(\epsilon) \phi_{\lambda I}(\epsilon)$$

$$\text{F45 } \phi_{\lambda I}''(\epsilon) = F_{\lambda R}(\epsilon) \phi_{\lambda I}(\epsilon) + F_{\lambda I}(\epsilon) \phi_{\lambda R}(\epsilon)$$

Let us define a matrix type of notation and write the second order differential equations as two first order equations.

$$\text{F46 } \vec{X} = \begin{pmatrix} X_1(\epsilon) \equiv \phi_{\lambda R}(\epsilon) \\ X_2(\epsilon) \equiv \phi_{\lambda R}'(\epsilon) \\ X_3(\epsilon) \equiv \phi_{\lambda I}(\epsilon) \\ X_4(\epsilon) \equiv \phi_{\lambda I}'(\epsilon) \end{pmatrix}$$

In terms of this new notation the differential equations become

$$F47 \quad X_1'(\epsilon) = X_2(\epsilon) \equiv f_1(\vec{x}, \epsilon)$$

$$F48 \quad X_2'(\epsilon) = F_{2R}(\epsilon) X_1(\epsilon) - F_{2I}(\epsilon) X_3(\epsilon) \equiv f_2(\vec{x}, \epsilon)$$

$$F49 \quad X_3'(\epsilon) = X_4(\epsilon) \equiv f_3(\vec{x}, \epsilon)$$

$$F50 \quad X_4'(\epsilon) = F_{4R}(\epsilon) X_3(\epsilon) + F_{4I}(\epsilon) X_1(\epsilon) \equiv f_4(\vec{x}, \epsilon)$$

In order to solve for one real and one imaginary parameter in the optical model potential such as  $\text{Re}("b_0")$  and  $\text{Im}("B")$  the following equations must be added

$$F51 \quad \text{Re}("b_0")' = X_5'(\epsilon) = 0 \equiv f_5(\vec{x}, \epsilon)$$

$$F52 \quad \text{Im}("B")' = X_6'(\epsilon) = 0 \equiv f_6(\vec{x}, \epsilon)$$

The six boundary conditions needed to solve the six simultaneous first order differential equations are in terms of the new notation

$$F53 \quad X_1(\epsilon=0) = 0$$

$$F54 \quad X_3(\epsilon=0) = 0$$

$$F55 \quad X_1(\epsilon=1) = 1$$

$$F56 \quad X_3(\epsilon=1) = 1$$

$$F57 \quad X_2(\epsilon=1) = \text{Re} \left. \phi_{out}'(\epsilon) \right|_{\epsilon=1}$$

$$F58 \quad X_4(\epsilon=1) = \text{Im} \left. \phi_{out}'(\epsilon) \right|_{\epsilon=1}$$

Now the first order differential equations are nonlinear in the variables  $X_1, X_2, X_3, X_4, X_5, X_6$ . Their derivatives can be linearized,

however, by using a type of Newton's method called quasilinearization <sup>144,145</sup> in which the derivatives of the variables are expanded in a  $J^{\text{th}}$  order Taylor series, i.e.

$$\begin{aligned} \text{F59} \quad \dot{X}_J(\epsilon)_{k+1} &= f_J(\tilde{X}, \epsilon) \Big|_k + (X_1(\epsilon)_{k+1} - X_1(\epsilon)_k) \frac{\partial f_J(\tilde{X}, \epsilon)}{\partial X_1(\epsilon)} \Big|_k \\ &+ (X_2(\epsilon)_{k+1} - X_2(\epsilon)_k) \frac{\partial f_J(\tilde{X}, \epsilon)}{\partial X_2(\epsilon)} \Big|_k + \dots \end{aligned}$$

where  $\tilde{X}(\epsilon)_{k=0}$  represents the initial approximation for  $\tilde{X}(\epsilon)$  and  $\tilde{X}(\epsilon)_{k+1}$  represents the corrected or improved approximation to  $\tilde{X}(\epsilon)$ . Keeping only those terms through the first derivative in the Taylor series expansion, the quasilinearized equations are

$$\text{F60} \quad \dot{X}_1(\epsilon)_{k+1} = X_2(\epsilon)_k + (X_2(\epsilon)_{k+1} - X_2(\epsilon)_k) \underline{1} = X_2(\epsilon)_{k+1}$$

$$\begin{aligned} \text{F61} \quad \dot{X}_2(\epsilon)_{k+1} &= F_{2R}(\epsilon) X_1(\epsilon) \Big|_k - F_{2I}(\epsilon) X_3(\epsilon) \Big|_k + (X_1(\epsilon)_{k+1} - X_1(\epsilon)_k) \cdot \\ &F_{2R}(\epsilon) \Big|_k - (X_3(\epsilon)_{k+1} - X_3(\epsilon)_k) F_{2I}(\epsilon) \Big|_k + (X_5(\epsilon)_{k+1} \\ &- X_5(\epsilon)_k) \left( \frac{\partial F_{2R}(\epsilon)}{\partial X_5(\epsilon)} X_1(\epsilon) - \frac{\partial F_{2I}(\epsilon)}{\partial X_5(\epsilon)} X_3(\epsilon) \right) \Big|_k \\ &+ (X_6(\epsilon)_{k+1} - X_6(\epsilon)_k) \left( \frac{\partial F_{2R}(\epsilon)}{\partial X_6(\epsilon)} X_1(\epsilon) - \frac{\partial F_{2I}(\epsilon)}{\partial X_6(\epsilon)} X_3(\epsilon) \right) \Big|_k \end{aligned}$$

$$\text{F62} \quad \dot{X}_3(\epsilon)_{k+1} = X_3(\epsilon)_k + (X_3(\epsilon)_{k+1} - X_3(\epsilon)_k) \underline{1} = X_3(\epsilon)_{k+1}$$

$$\begin{aligned}
F63 \quad \dot{X}_4(\epsilon)_{k+1} &= F_{2R}(\epsilon) X_3(\epsilon) \Big|_k + F_{2I}(\epsilon) X_1(\epsilon) \Big|_k + (X_1(\epsilon)_{k+1} - X_1(\epsilon)_k) \\
&\quad F_{2I}(\epsilon) \Big|_k + (X_3(\epsilon)_{k+1} - X_3(\epsilon)_k) F_{2R}(\epsilon) \Big|_k \\
&\quad + (X_5(\epsilon)_{k+1} - X_5(\epsilon)_k) \left( \frac{\partial F_{2R}(\epsilon)}{\partial X_5(\epsilon)} X_3(\epsilon) + \frac{\partial F_{2I}(\epsilon)}{\partial X_5(\epsilon)} X_1(\epsilon) \right) \Big|_k \\
&\quad + (X_6(\epsilon)_{k+1} - X_6(\epsilon)_k) \left( \frac{\partial F_{2R}(\epsilon)}{\partial X_6(\epsilon)} X_3(\epsilon) + \frac{\partial F_{2I}(\epsilon)}{\partial X_6(\epsilon)} X_1(\epsilon) \right) \Big|_k \\
&\quad + (X_6(\epsilon)_{k+1} - X_6(\epsilon)_k) \left( \frac{\partial F_{2R}(\epsilon)}{\partial X_6(\epsilon)} X_3(\epsilon) + \frac{\partial F_{2I}(\epsilon)}{\partial X_6(\epsilon)} X_1(\epsilon) \right) \Big|_k
\end{aligned}$$

$$F64 \quad \dot{X}_5(\epsilon)_{k+1} = 0$$

$$F65 \quad \dot{X}_6(\epsilon)_{k+1} = 0$$

144

where  $k = 0, 1, 2, \dots$ . According to Bellman the solution to the quasilinearized equations will give an improved approximation for  $\vec{X}(\epsilon)$  provided the initial guess is close enough to the proper value.

In solving these quasilinearized equations, one finds it convenient to start with some arbitrary linearly independent initial conditions. When arbitrary linearly independent initial values are used, the solutions obtained must be combined with arbitrary constants to form the general solution. These constants are determined by the actual boundary conditions.

Let the homogeneous equations be solved with the initial conditions

$$F66 \quad \vec{X}(0) = \begin{pmatrix} 1 \\ 0 \\ 0 \\ 0 \\ 0 \\ 0 \end{pmatrix} \quad \text{to obtain} \quad \vec{X}(\epsilon) = \begin{pmatrix} X_1(\epsilon) \\ X_2(\epsilon) \\ X_3(\epsilon) \\ X_4(\epsilon) \\ X_5(\epsilon) \\ X_6(\epsilon) \end{pmatrix} = \begin{pmatrix} H_{11}(\epsilon) \\ H_{21}(\epsilon) \\ H_{31}(\epsilon) \\ H_{41}(\epsilon) \\ H_{51}(\epsilon) \\ H_{61}(\epsilon) \end{pmatrix}$$

$$F67 \quad \vec{X}(0) = \begin{pmatrix} 0 \\ 1 \\ 0 \\ 0 \\ 0 \\ 0 \end{pmatrix} \quad \text{to obtain} \quad \vec{X}(\epsilon) = \begin{pmatrix} H_{12}(\epsilon) \\ H_{22}(\epsilon) \\ H_{32}(\epsilon) \\ H_{42}(\epsilon) \\ H_{52}(\epsilon) \\ H_{62}(\epsilon) \end{pmatrix}$$

etc., and let the inhomogeneous equations be solved with the initial conditions

$$F68 \quad \vec{X}(0) = \begin{pmatrix} 0 \\ 0 \\ 0 \\ 0 \\ 0 \\ 0 \end{pmatrix} \quad \text{to obtain} \quad \vec{X}(\epsilon) = \begin{pmatrix} IH_1(\epsilon) \\ IH_2(\epsilon) \\ IH_3(\epsilon) \\ IH_4(\epsilon) \\ IH_5(\epsilon) \\ IH_6(\epsilon) \end{pmatrix}$$

Then the general solution obtained by adding the homogeneous and inhomogeneous solutions is given by

$$F69 \quad X_1(\epsilon) = C_1 H_{11}(\epsilon) + C_2 H_{12}(\epsilon) + C_3 H_{13}(\epsilon) + C_4 H_{14}(\epsilon) \\ + C_5 H_{15}(\epsilon) + C_6 H_{16}(\epsilon) + IH_1(\epsilon)$$

$$F70 \quad X_2(\epsilon) = C_1 H_{21}(\epsilon) + C_2 H_{22}(\epsilon) + C_3 H_{23}(\epsilon) + C_4 H_{24}(\epsilon) \\ + C_5 H_{25}(\epsilon) + C_6 H_{26}(\epsilon) + IH_2(\epsilon)$$

etc.

To evaluate the C's use the boundary conditions

$$F72 \quad X_1(0) = 0 \Rightarrow C_1 = 0$$

$$F73 \quad X_3(0) = 0 \Rightarrow C_3 = 0$$

$$F74 \quad X_5(0) = \text{Re}("b_0") \Rightarrow C_5 = \text{Re}("b_0")$$

$$F75 \quad X_6(0) = \text{Im}("B") \Rightarrow C_6 = \text{Im}("B")$$

$$F76 \quad X_1(1) = 1 \Rightarrow C_2 H_{12}(1) + C_4 H_{14}(1) + \text{Re}("b_0") H_{15}(1) \\ + \text{Im}("B") H_{16}(1) + I H_1(1) = 1$$

$$F77 \quad X_3(1) = 1 \Rightarrow C_2 H_{32}(1) + C_4 H_{34}(1) + \text{Re}("b_0") H_{35}(1) \\ + \text{Im}("B") H_{36}(1) + I H_3(1) = 1$$

$$F78 \quad X_2(1) = \text{Re} \left. \phi'_2(\epsilon) \right|_{\epsilon=1}^{\text{out}} \Rightarrow C_2 H_{22}(1) + C_4 H_{24}(1) + \text{Re}("b_0") H_{25}(1) \\ + \text{Im}("B") H_{26}(1) + I H_2(1) = \text{Re} \left. \phi'_2(\epsilon) \right|_{\epsilon=1}^{\text{out}}$$

$$F79 \quad X_4(1) = \text{Im} \left. \phi'_2(\epsilon) \right|_{\epsilon=1}^{\text{out}} \Rightarrow C_2 H_{42}(1) + C_4 H_{44}(1) + \text{Re}("b_0") H_{45}(1) \\ + \text{Im}("B") H_{46}(1) + I H_4(1) = \text{Im} \left. \phi'_2(\epsilon) \right|_{\epsilon=1}^{\text{out}}$$

Equations F76-F79 can now be solved simultaneously for  $C_2$ ,  $C_4$ ,  $\text{Re}("b_0")$ , and  $\text{Im}("B")$ .

Once the C's are known the improved approximation for  $\hat{X}(\epsilon)$  can be constructed. Using this improved approximation for  $\hat{X}(\epsilon)$  as the initial value a still better approximation may be obtained. The whole procedure is iterated until the improved approximations converge to the proper value of  $\hat{X}(\epsilon)$ . In general the approximations will converge to within

one part in  $10^{-6}$  of the correct solution of the wave equation in 3 or 4 iterations if the initial guess for  $\hat{X}(\epsilon)$  has the proper order of magnitude.

In practice the integration is not started at  $\epsilon = 0$  but at  $\epsilon = 10^{-6}$  of the integration step size due to the presence of  $1/\epsilon$  terms in the wave equation.

## APPENDIX G

### Fortran Computer Program for Solving The Klein-Gordon Equation for Pionic Atoms

In this appendix is listed the actual Fortran computer program used to analyze pionic atom data. The notation in the program conforms closely to that of Appendix F. Due to the extensive comments one can easily follow the logic of the program.



C A1,A3 - LOW ENERGY S-WAVE PION-NUCLEON SCATTERING LENGTHS A(2T)  
 C (HBARC/MP1)  
 C A11,A13,A31,A33 - LOW ENERGY P-WAVE PION-NUCLEON SCATTERING  
 C LENGTHS A(2T,2J) (HBARC/MP1)\*\*3  
 C B11,B00,B01,B02 - LOW ENERGY S-WAVE PION-TWO NUCLEON SCATTERING  
 C LENGTHS B(J,T) (HBARC/MP1)\*\*4  
 C G21,G01,G10,G12,G1101,G1110 - LOW ENERGY P-WAVE PION-TWO NUCLEON  
 C SCATTERING LENGTHS G(J,T,S,T) WHERE THE LAST  
 C S AND T REFER TO THE TOTAL SPIN AND ISOSPIN  
 C OF THE NUCLEON PAIR AND HAS BEEN OMITTED IN  
 C ALL CASES IN WHICH IT IS REDUNDANT  
 C (HBARC/MP1)\*\*6  
 C NUC - NAME OF NUCLEAR ISOTOPE FOR WHICH KLEIN-GORDON EQUATION  
 C IS BEING SOLVED.  
 C Z - NUMBER OF PROTONS IN THE NUCLEAR ISOTOPE  
 C A - ATOMIC NUMBER OF THE NUCLEAR ISOTOPE  
 C L - ANGULAR MOMENTUM FOR WHICH THE KLEIN-GORDON EQUATION IS TO  
 C BE SOLVED.  
 C MASS - MASS OF NUCLEAR ISOTOPE (C12AMU)  
 C GAM - FULL WIDTH AT HALF POWER FOR PIONS MAKING AN ELECTRO-  
 C MAGNETIC TRANSITION FROM A STATE WITH ANGULAR MOMENTUM =  
 C L+1 TO A STATE WITH ANGULAR MOMENTUM = L (MEV)  
 C ETRANS - ENERGY OF ELECTROMAGNETIC PIONIC ATOM TRANSITION FROM  
 C L+1 STATE TO L STATE (MEV)  
 C DEVP - VACUUM POLARIZATION ENERGY OF L+1 STATE - VACUUM  
 C POLARIZATION ENERGY OF L STATE (MEV)  
 C R - FERMI CHARGE DISTRIBUTION RADIUS PARAMETER  
 C RO - POINT NUCLEON FERMI DISTRIBUTION RADIUS PARAMETER  
 C CC = T/(4\*LOG(3)) - FERMI DENSITY PARAMETER FOR WHICH T IS THE  
 C SURFACE THICKNESS PARAMETER FOR THE 90%-10%  
 C CHANGE OF THE POINT NUCLEON DENSITY WITH  
 C RESPECT TO THE CENTRAL VALUE.  
 C CCC = T/(4\*LOG(3)) - FERMI DENSITY PARAMETER FOR WHICH T IS THE  
 C SURFACE THICKNESS PARAMETER FOR THE 90%-10%  
 C CHANGE OF THE NUCLEAR CHARGE DENSITY WITH  
 C RESPECT TO THE CENTRAL VALUE.



```

DIMENSION D(2),C(6),VC(61),RHO(61),UR(61),UI(61),FR(61),FRHO(61),
1FKCO(61),FRG(61),FI(61),FIBO(61),FICO(61),FIG(61),X(4,5),XO(4,2),
2X2(4,2),X1(4),U(4,7,61),H(2,2),RH(2),IH(2),CA(2),P(2),PSI2(
361),PPSI2(61),DUR(61),DUI(61),DRHO(61),DDRHO(61),FAC(31)
INTEGER I,J,K,L,N,IJ,INDEX,JJ,INTRVL,KK,KS,NK,NNK,NNNK,NNNNK
EQUIVALENCE (DU,D(1)),(RNL,RL(1)),(UC,CA(1)),(P(1),PSI)
REAL*4 W(305),SNGL
COMMON LAMBA,M,PO
COMMON FR,FRBO,FRG,FRCO,FI,FIBO,FIG,FICO,RBO,G,RCO,UR,UI,J,L
DATA FAC/1.00,1.00,2.00,6.00,2.401,1.202,7.202,5.0403,4.03204,
13.628805,3.628806,3.9916807,4.7900208,6.2270209,8.71783010,
21.30767012,2.09228013,3.55687014,6.40237015,1.21645017,
32.43290018,5.10909019,1.12400021,2.58520022,6.20448023,
41.55112025,4.03291026,1.08889028,3.04888029,8.84176030,
52.65252032/
DPSI(K) = (DCMLPX(DUR(K),DUI(K))-(1.00/((K-1.00)/INTRVL+1.0-3)*RO
1)/DAK(K)/(2.00*(II+AK(K)))*DCMLPX(UR(K),UI(K) ) ) /((K-1.00
2)/INTRVL+1.0-3)*RO*CDSORT(II+AK(K))
DPSIO(K) = (2.00*ZALPHA*MPI/((L+1)*HBARC))*#1.500/DSORT(FAC(2*L+3)
1)*#(2.00*ZALPHA*MPI*((K-1.00)/INTRVL+1.0-3)*RO/((L+1)*HHARC))*#L*DE
2XP(-ZALPHA*MPI*((K-1.00)/INTRVL+1.0-3)*RO/((L+1)*HBARC))*#L/((K-1
3.00)/INTRVL+1.0-3)*RO)-ZALPHA*MPI/((L+1)*HBARC)
10 READ(5,900) A1,A3,A11,A13,A31,A33,B11,B00,B01,B02,G21,G01,G10,G12,
1G1101,G1110,G
20 B0 = (A1+2.00*A3)/3.00
B1 = (A3-A1)/3.00
C0 = (4.00*A33+A31-2.00*A13+A11)/3.00
C1 = (2.00*A33+A31-2.00*A13-A11)/3.00
B80 = (9.00*B11+B00+3.00*B01+5.00*B02)/4.801
B81 = (3.00*B11-B00-3.00*B01-5.00*B02)/4.801
B82 = (-9.00*B11-B00+3.00*B01+B02)/4.801
B83 = (-2.00*B00-3.00*B01+5.00*B02)/9.601
B84 = (-3.00*B11+B00-3.00*B01-B02)/4.801
B85 = (2.00*B00-3.00*B01+B02)/9.601
CC0 = (5.00*G21+G01+G10+3.00*G1101+3.00*G1110+5.00*G12)/4.801
CC1 = (G21-G01-G10-3.00*G1101+3.00*G1110-5.00*G12)/4.801

```

```
CC2 = (-5.00*G21-G01-G10+3.00*G1101-3.00*G1110+G12)/4.8D1
CC3 = (-2.00*G10-3.00*G1101+5.00*G12)/9.6D1
CC4 = (-G21+G01+G10-3.00*G1101-3.00*G1110-G12)/4.8D1
CC5 = (2.00*G10-3.00*G1101+G12)/9.6D1
RR0 = .051D0
RR1 = 0.00
RR2 = 0.00
RR3 = 0.00
RR4 = 0.00
RR5 = 0.00
CC0 = .086D0
CC1 = 0.00
CC2 = 0.00
CC3 = 0.00
CC4 = 0.00
CC5 = 0.00
G = 1.00
RB0 = -.0057D0
IB0 = .0032D0
RB1 = -.084D0
IB1 = -.0014D0
RC0 = .251D0
IC0 = .0011D0
RC1 = .144D0
IC1 = .0005D0
RD0 = -.156D0
ID0 = -.0005D0
RD1 = -.099D0
ID1 = -.00026D0
RBR0 = .053D0
RCC0 = -.14D0
RBB0 = 0.00
RCC0 = 0.00
READ(5,902) NUC,Z,A,S,L,MASS,GAM,ETRAN,DEVP,R,RO,CC,CCC
IF(L.EQ.0) IH0(1) =RB0
IF(L.GT.0) IH0(1) =RC0
```

```

IHO(2) = G
WRITE(6,901) A1,A3,A11,A13,A31,A33,R11,R00,B01,B02,G21,G01,G10,G12
1,G1101,G1110,H0,H1,CO,C1,HR0,BR1,BB2,HR3,BB4,BH5,CC0,CC1,CC2,CC3,C
2C4,CC5,IHO(1),IHO(2)
IF(Z) 500,500,25
WRITE(6,903) NUC,Z,A,S,L,MASS,GAM,ETRAN,DEVP,R,RO,CC,CCC
25
C
C
C
C
CALCULATION OF REDUCED MASS = RMASS OF PIONIC ATOM WHERE MASS OF
Z-1 ELECTRONS IS INCLUDED
MPI = 139.579D0
AMASS = MASS*931.478D0-.511D0
RMASS = MPI*AMASS/(MPI+AMASS)
T = (A-2.D0*Z)/2.D0
MN = (938.256D0+939.550D0)/2.D0
N1 = (1.D0+MPI/MN)/(1.D0+MPI/AMASS)
N2 = (1.D0+MPI/(2.D0*MN))/(1.D0+MPI/AMASS)
C
C
C
C
CALCULATION OF REAL AND IMAGINARY PARTS OF ENERGY FOR KLEIN-GORDON
EQUATION ASSUMING THE PRINCIPLE QUANTUM NUMBER N = L + 1.
INTRVL = 20
N = 3*INTRVL+1
HBARC = 197.32D0
ZALPHA = Z/137.0388D0
EL1 = -RMASS*(ZALPHA**2/(2.D0*(L+2.D0)**2)+ZALPHA**4*((L+2.D0)/(L+
11.5D0)-.75D0)/(2.D0*(L+2.D0)**4))
ER = EL1+DEVP-ETRAN
EI = -GAM/2.D0
F = DCPLX(ER,EI)
DELTA = CDSORT(-2.D0*RMASS*E-E*E)*2.D0/HBARC
LAMBA = 2.D0*ZALPHA*(DCPLX(RMASS,0.D0)+E)/(HBARC*DELTA)
PO = ((N-1.D0)/INTRVL+1.D-3)*RO*DELTA
C
C
C
ASSUME A NORMALIZATION SUCH THAT AT SOME RADIUS OUTSIDE THE NUCLEUS
THE BOUNDARY CONDITIONS GIVE U(1) = (1.D0,1.D0) AND DU(1)*DELTA/U(1).

```

C THIS NORMALIZATION IS CHOSEN FOR CONVENIENCE, SINCE THE SOLUTION OF  
 C THE EIGENVALUE PROBLEM IS INDEPENDENT OF THE NORMALIZATION OF THE  
 C EIGENFUNCTION. THE ASYMPTOTIC FORM OF THE WAVEFUNCTION OUTSIDE  
 C THE NUCLEUS IS USED TO EVALUATE  $DU(1)*DELTA/U(1)$ .  
 C

```

PI = 3.1415926535900
II = (1.00,0.00)
CU = (1.00,1.00)
M = DCMPLEX(.5D0+.5D0*DSQRT((2.00*L+1.00)**2-4.00*ZALPHA**2),0.00)
DU = -(II/2.00-LAMBA/PO+((M*(M-II)-LAMBA*(LAMBA-II))*CDPSI(M-LAMBA
1+II,2.00*M,PO)/(PO*CDPSI(M-LAMBA,2.00*M,PO))))*CU*DELTA
C(1) = 1.00
C(2) = D(1)
C(3) = 1.00
C(4) = D(2)
WRITE(6,904) E,DELTA,LAMBA,PO,M,DU

```

C INITIALIZE PARAMETERS FOR QUASI-LINEARIZATION  
 C

```

INDEX = 0
SR = RO/INTRVL
IF(R.EQ.0.00) CALL POTMHO(CC,CCC,A,RO,Z,VC,RHO,DRHO,DDRHO,N,INTRVL
1,RU)
IF(R.GT.0.00) CALL POT(R0,CC,R,CCC,RU,Z,VC,RHO,DRHO,DDRHO,N,INTRVL
1,RU,A)
IF(A.EQ.4.00) CALL POTHE4(Z,RO,VC,RHO,DRHO,DDRHO,N,INTRVL,RU)

```

C STORE INITIAL APPROXIMATION FOR SOLUTION  
 C

```

CPW = HRARC/MPI
EPS = (N-1)/INTRVL
L1 = L+1
ANORM = EPS**L1*DEXP(-ZALPHA*MPI*RO*EPS/(L1*HBARC))
IF(L.EQ.0)RBO = IH0(1)
IF(L.GT.0)RCO = IH0(1)
G = IH0(2)

```

40

XBI = 4.D0\*PI\*N1\*(RB0+RB1\*(1.D0-2.D0\*Z/A))\*CPW  
XBIBO = 4.D0\*PI\*N1\*CPW  
XCI = 4.D0\*PI/N1\*(RC0+RC1\*(1.D0-2.D0\*Z/A))\*CPW\*\*3  
XCICO = 4.D0\*PI/N1\*CPW\*\*3  
XSISJ = 4.D0\*S\*(S+1.D0)/(A\*(A-1.D0))-3.D0/(A-1.D0)  
XTITJ = 4.D0\*T\*(T+1.D0)/(A\*(A-1.D0))-3.D0/(A-1.D0)  
XTT = 8.D0\*T\*(A\*(A-1.D0))+4.D0\*(T-1.D0)/(A-1.D0)  
XTT/A = 4.D0\*T/A  
XBIJ = 4.D0\*PI\*N2\*(BB0+BB1\*XSISJ+BB2\*XTITJ+BB3\*(1.D0-XSISJ))\*XTT+  
1BR4\*XSISJ\*XTITJ+BB5\*(1.D0-XSISJ)\*XTT)\*CPW\*\*4  
XBJI = 4.D0\*PI\*N2\*RRB0\*CPW\*\*4  
XCIJ = 4.D0\*PI/N2\*(CC0+CC1\*XSISJ+CC2\*XTITJ+CC3\*(1.D0-XSISJ))\*XTT+  
1CC4\*XSISJ\*XTITJ+CC5\*(1.D0-XSISJ)\*XTT)\*CPW\*\*6  
XCJI = 4.D0\*PI/N2\*RCC0\*CPW\*\*6  
PF = HBARC\*(9.D0/8.D0\*PI\*A/RU\*\*3)\*\*(1.D0/3.D0)  
XBIBI = -6.D0\*PF/MPI\*(1.D0-1.D0/A)\*((A-4.D0)/(A-1.D0))\*((RB0\*\*2+2.D0  
1\*RB0\*RB1\*(1.D0-2.D0\*Z/A))+2.D0\*RB1\*RB1\*(A-2.D0)/(A-1.D0))\*CPW  
XBIRIB = -6.D0\*PF/MPI\*(A-4.D0)/A\*(2.D0\*RB0+2.D0\*RB1\*(1.D0-2.D0\*Z/  
1A))\*CPW  
XBICI = +2.D0\*PF/MPI\*(1.D0-1.D0/A)\*((A-4.D0)/(A-1.D0))\*((RB0\*RC0+(RB  
10\*RC1+RC0\*RB1)\*(1.D0-2.D0\*Z/A))+2.D0\*RB1\*RC1\*(A-2.D0)/(A-1.D0))\*CP  
2W\*\*3  
XBICIB = +2.D0\*PF/MPI\*(A-4.D0)/A\*(RC0+RC1\*(1.D0-2.D0\*Z/A))\*CPW\*\*  
13  
XBICIC = +2.D0\*PF/MPI\*(A-4.D0)/A\*(RB0+RB1\*(1.D0-2.D0\*Z/A))\*CPW\*\*  
13  
XCICI = -4.D0\*PI\*4.D0\*PI/3.D0\*RC0\*RC0\*CPW\*\*6  
XCICIC = -4.D0\*PI\*4.D0\*PI/3.D0\*2.D0\*RC0\*CPW\*\*6  
XCICI = -4.D0\*PI\*PI/3.D0\*(1.D0-1.D0/A)\*((A-4.D0)/(A-1.D0))\*((RC0\*RC0  
1+2.D0\*RD0\*RD0+2.D0\*(RC0\*RC1+2.D0\*RD0\*RD1)\*(1.D0-2.D0\*Z/A))+2.D0\*(  
2RC1\*RC1+2.D0\*RD0\*RD0)\*(A-2.D0)/(A-1.D0))\*CPW\*\*6/A/(4.D0\*PI/3.D0\*RU  
3\*\*3)  
2RC1\*RC1+2.D0\*RD0\*RD0\*(A-2.D0)/(A-1.D0))\*CPW\*\*6  
XCICIC = -4.D0\*PI\*PI/3.D0\*(1.D0-1.D0/A)\*((A-4.D0)/(A-1.D0))\*2.D0\*RC  
10+2.D0\*RC1\*(1.D0-2.D0\*Z/A))\*CPW\*\*6/A/(4.D0\*PI/3.D0\*RU\*\*3)  
10+2.D0\*RC1\*(1.D0-2.D0\*Z/A))\*CPW\*\*6  
C  
C

```

XBC = -8.D0*PF/MPI*(1.D0-1.D0/A)*((A-4.D0)/(A-1.D0))*(RBO*RCO+(RBO*
IRCI+RBI*RCO)*(1.D0-2.D0*Z/A))+2.D0*RBI*RCI*(A-2.D0)/(A-1.D0))*CPW*
2*3
XBCB0 = -8.D0*PF/MPI*(1.D0-1.D0/A)* (A-4.D0)/(A-1.D0)*(RCO+RCI*(1.
2D0-2.D0*Z/A))*CPW**3
XBCCO = -8.D0*PF/MPI*(1.D0-1.D0/A)* (A-4.D0)/(A-1.D0)*(RBO+RBI*(1.
1D0-2.D0*Z/A))*CPW**3
XCIQ = (ER+MPI)/MN*XCI*N1*.5D0
XCIQCO = (ER+MPI)/MN*XCIQ*N1*.5D0
XBICI = 0.D0
XBICIC = 0.D0
XBICIR = 0.D0
XBC = 0.D0
XBCB0 = 0.D0
XBCCO = 0.D0
XCIQ = 0.D0
XCIQCO = 0.D0
DO 43 K = 1,N
EPS = (N-K)/(INTRVL*1.D0)+1.D-3
AKR = -XCI*RHO(K)-(XCJI+XCICI+XBC/RHO(K))*RHO(K)**2
AKR = -(XCI+XCICI)*RHO(K)
AKRG = 0.D0
AKRCO = -XCICO*RHO(K)-(XCICIC+XBCCO)*RHO(K)**2
AKRCO = -(XCICO+XCICIC)*RHO(K)
AKRBO = -XBCB0*RHO(K)
IF(L.EQ.0) AKI = -XCIJ*RHO(K)**2
IF(L.GT.0) AKI = -XCIJ*RHO(K)**2*G
AKIG = -XCIJ*RHO(K)**2
AKICO = 0.D0
AKIBO = 0.D0
AK(K) = DCPLX(AKR,AKI)
IF(INDEX.GT.0) GO TO 41
UC = CU*EPS*L1*DEXP(-ZALPHA*MPI*RO*EPS/(L1*HBARC))/(ANORM*CDSORT(
111+AK(K))/CDSORT(11+AK(1)))
UR(K) = CA(1)
UI(K) = CA(2)

```

```

41 CONTINUE
DAKR = -XCI*DRHO(K)-2.00*(XCJI+XCICI+XBC/RHO(K))*RHO(K)*DRHO(K)
DAKR = -(XCI+XCICI)*DRHO(K)
DAKRG = 0.00
DAKRCO = -XCICO*DRHO(K)-2.00*(XCICIC+XBCCO/RHO(K))*RHO(K)*DRHO(K)
DAKRCO = -(XCICO+XCICIC)*DRHO(K)
DAKRBO = -XBCHO*DRHO(K)
IF(L.EQ.0) DAKI = -XCIJ*2.00*RHO(K)*DRHO(K)
IF(L.GT.0) DAKI = -XCIJ*2.00*RHO(K)*DRHO(K)*G
DAKIG = -XCIJ*2.00*RHO(K)*DRHO(K)
DAKICO = 0.00
DAKIRO = 0.00
DAK(K) = DCMPLX(DAKR,DAKI)
DDAKR = -XCI*DDRHO(K)-2.00*(XCJI+XCICI+XBC/RHO(K))*(RHO(K)*DDRHO(K)
1)+DRHO(K)*DRHO(K)
DDAKR = -(XCI+XCICI)*DDRHO(K)
DDAKRG = 0.00
DDAKRC = -XCICO*DDRHO(K)-2.00*(XCICIC+XBCCO/RHO(K))*(RHO(K)*DDRHO(
1K)+DRHO(K)**2)
DDAKRC = -(XCICO+XCICIC)*DDRHO(K)
DDAKRB = -XBCHO*(DDRHO(K)+DRHO(K)**2/RHO(K))
IF(L.EQ.0) DDAKI = -XCIJ*2.00*(RHO(K)*DDRHO(K)+DRHO(K)**2)
IF(L.GT.0) DDAKI = -XCIJ*2.00*(RHO(K)*DDRHO(K)+DRHO(K)**2)*G
DDAKIG = -XCIJ*2.00*(RHO(K)*DDRHO(K)+DRHO(K)**2)
DDAKIC = 0.00
DDAKIB = 0.00
DEN = (1.00+AKR)**2+AKI**2
DENG = 2.00*(1.00+AKR)*AKRG+2.00*AKI*AKIG
DENCO = 2.00*(1.00+AKR)*AKRCO+2.00*AKI*AKICO
DENBO = 2.00*(1.00+AKR)*AKRBO+2.00*AKI*AKIBO
REI = (1.00+AKR)/DEN
REIG= AKRG/DEN-REI*DENG/DEN
RFICO = AKRCO/DEN-REI*DENCO/DEN
REIBO = AKRBO/DEN-REI*DENRO/DEN
IMI = -AKI/DEN
IMIG = -AKIG/DEN-IMI*DENG/DEN

```

```

IMICO = -AKICO/DEN-IM1#DENCO/DEN
IMIBO = 0.00
RE2 = ((1.00+AKR)*(DAKR**2-DAKI**2)+2.00*DAKR*DAKI#AKI)/DEN
RE2G = (AKRG *(DAKR**2-DAKI**2)+2.00*(1.00+AKR)*(DAKR*DAKRG -DAKI
1#DAKIG )+2.00*(DAKRG #DAKI#AKI+DAKR*DAKIG #AKI+DAKR*DAKI#AKIG ))/D
2EN-RE2#DENG /DEN
RE2CO = (AKRCO*(DAKR**2-DAKI**2)+2.00*(1.00+AKR)*(DAKR*DAKRCO-DAKI
1#DAKICO)+2.00*(DAKRCO#DAKI#AKI+DAKR*DAKICO#AKI+DAKR*DAKI#AKICO))/D
2EN-RE2#DENCO/DEN
RE2BO = (AKRBO*(DAKR**2-DAKI**2)+2.00*(1.00+AKR)*(DAKR*DAKRBO-DAKI
1#DAKIBO)+2.00*(DAKRBO#DAKI#AKI+DAKR*DAKIBO#AKI+DAKR*DAKI#AKIBO))/
2DEN-RE2#DENBO/DEN
IM2 = ((1.00+AKR)*2.00*DAKR*DAKI-AKI*(DAKR**2-DAKI**2))/DEN
IM2G = (AKRG #2.00*DAKR*DAKI+2.00*(1.00+AKR)*(DAKRG #DAKI+DAKR#DA
1KIG )-AKIG *(DAKR**2-DAKI**2)-AKI*2.00*(DAKR*DAKRG -DAKI#DAKIG ))/
2DEN-IM2#DENG /DEN
IM2CO = (AKRCO*2.00*DAKR*DAKI+2.00*(1.00+AKR)*(DAKRCO#DAKI+DAKR#DA
1KICO)-AKICO*(DAKR**2-DAKI**2)-AKI*2.00*(DAKR*DAKRCO-DAKI#DAKICO))/
2DEN-IM2#DENCO/DEN
IM2BO = 0.00
ANONR = -DAKR/(EPS#RO)-DDAKR/2.00+.2500*RE2
ANONRG = -DAKRG /(EPS#RO)-DDAKRG/2.00+.2500*RE2G
ANONRC = -DAKRCO/(EPS#RO)-DDAKKC/2.00+.2500*RE2CO
ANONRB = -DAKRBO/(EPS#RO)-DDAKRB/2.00+.2500*RE2BO
ANONI = -DAKI/(EPS#RO)-DDAKI/2.00+.2500*IM2
ANONIG = -DAKIG /(EPS#RO)-DDAKIG/2.00+.2500*IM2G
ANONIC = -DAKICO/(EPS#RO)-DDAKIC/2.00+.2500*IM2CO
ANONIB = 0.00
ANON(K) = -HBARC**2/(2.00*RMASS)*DCMLX(ANONR, ANONI)
OR = -XBI#RHO(K)-XBJI#RHO(K)**2
OR = -(XBI+XBJI)*RHO(K)-XBJI#RHO(K)**2-(XBICI+XCIO)*(DDRHO(K)+2.0
10/(RO#EPS)*DRHO(K))-XBICI#DRHO(K)**2/RHQ(K)
ORQ = 0.00
ORCO = 0.00
ORCO = -XBICIC*(DDRHO(K)+DRHO(K)**2/RHO(K)+2.00/(RO#EPS)*DRHO(K))
ORCO = -(XBICIC+XCIOCO)*(DDRHO(K)+2.00/(RO#EPS)*DRHO(K))-XBICIC#DR

```

```

1HD(K)**2/RHO(K)
QRBO = -XBIBO*RHOD(K)
QRBO = -XBIBO*RHOD(K)-XBIB*RHOD(K)-XBICIB*(DDRHO(K)+DRHO(K)**2/RHO
1(K)+2.0D/(RO*EPS)*DRHO(K))
IF(L.EQ.0) QI = -XBIJ*RHOD(K)**2*G
IF(L.GT.0) QI = -XBIJ*RHOD(K)**2
QIG = -XBIJ*RHOD(K)**2
IF(L.EQ.0) QIG = -XBIJ*RHOD(K)**2
IF(L.GT.0) QIG = 0.0D
Q(K) = HBARC**2/(2.0D*RMASS)*DCMPLX(QR,QI)
BRACKR = (2.0D*RMASS*(ER-VC(K))+(ER-VC(K))**2-EI**2)/HBARC**2-QR+
1ANDNR
BRACKI = (2.0D*RMASS*EI+2.0D*EI*(ER-VC(K)))/HBARC**2-QI+ANONI
FR(K) = L*(L+1.0D)/(EPS*RO)**2-REI*BRACKR+IMI*BRACKI
FRBO(K) = REI*QRBO
FRBO(K) = REI*QRBO-REI*ANONRB-REI*BO*BRACKR
IF(L.EQ.0) FRG(K) = REI*QIG-IMI*QIG
IF(L.GT.0) FRG(K) = -REI*G*BRACKR-REI*ANONRG+IMIG*BRACKI+IMI*ANONIG
FRCO(K) = -REI*CO*BRACKR-REI*ANONRC+IMICO*BRACKI+IMI*ANONRC+REI*QRC
10
FI(K) = -REI*BRACKI-IMI*BRACKR
FIBO(K) = IMI*QRBO
FIG(K) = REI*QIG+IMI*QIG
IF(L.GT.0) FIG(K) = -REI*G*BRACKI-REI*ANONIG-IMIG*BRACKR-IMI*ANONRG
FICO(K) = -REI*CO*BRACKI-REI*ANONRC-IMICO*BRACKR-IMI*ANONRC+IMI*QRC
10

```

43

C

C SOLVE QUASILINEAR APPROXIMATION TO NONLINEAR KLEIN-GORDON EQUATION.  
C FOR DIFFERENTIAL EQUATIONS THE GENERAL SOLUTION = HOMOGENEOUS  
C SOLUTION PLUS PARTICULAR OR INHOMOGENEOUS SOLUTION. ANY LINEARLY  
C INDEPENDENT INITIAL VALUES MAY BE USED FOR GETTING THE HOMOGENEOUS  
C AND PARTICULAR SOLUTIONS. WHEN ARBITRARY LINEARLY INDEPENDENT  
C INITIAL VALUES ARE USED, THE SOLUTIONS OBTAINED MUST BE COMBINED  
C WITH ARBITRARY CONSTANTS TO FORM THE GENERAL SOLUTION. THE CONSTANTS  
C ARE DETERMINED BY THE BOUNDARY CONDITIONS. THIS TECHNIQUE MAKES IT  
C POSSIBLE TO TRANSFORM A PROBLEM WITH BOUNDARY CONDITIONS AT TWO OR

```

C      MORE POINTS TO THE INITIAL VALUE PROBLEM WHICH IS EASIER TO SOLVE.
C
C      GENERATE ARBITRARY LINEARLY INDEPENDENT INITIAL VALUES FOR INTEGRATION.
C
C      JJ = 3
C      IJ = 4
C      DO 240 J = 1, JJ
C      DO 70 I = 1, IJ
C      IF (J.EQ. JJ) GO TO 50
C      X(I,1) = 0.00
C      GO TO 60
C      X(I,1) = C(I)
C      X0(I,1) = 0.00
C      X2(I,1) = 0.00
C
C      USE MODIFIED EULER'S METHOD TO START BACKWARD INTEGRATION USING
C      ADAM'S METHOD BY PROVIDING VALUES FOR THREE ADDITIONAL POINTS.
C      SEE SOUTHWORTH'S BOOK 'DIGITAL COMPUTATION AND NUMERICAL METHODS',
C      PAGE 436.
C
C      USE EULER BACKWARD INTEGRATION FORMULA
C      X(K) = X(K-1) - SR * F(X(K-1))
C      TO OBTAIN A PREDICTED VALUE OF X(K)
C
C      DO 100 K = 2, 4
C      DO 90 I = 1, IJ
C      X(I,K) = X(I,K-1) - SR * F(X(I,K-1), X(2,K-1), X(3,K-1), X(4,K-1), K-1, I)
C
C      ITERATE EULER-GAUSS BACKWARD INTEGRATION FORMULA
C      X(K) = X(K-1) - SR * (F(X(K-1)) + F(X(K))) / 2
C      TO OBTAIN BETTER VALUES FOR X(K)
C
C      DO 95 KK = 1, 3
C      DO 95 I = 1, IJ
C      X(I,K) = X(I,K-1) - SR * (F(X(I,K-1), X(2,K-1), X(3,K-1), X(4,K-1), K-1, I)
C      1 + F(X(I,K), X(2,K), X(3,K), X(4,K), K, I)) / 2.00

```

50

60

70

C

C

C

C

C

C

C

C

C

C

90

C

C

C

C

C

95

```

100 U(1,J,K) = X(1,K)
      U(2,J,K) = X(3,K)
      U(3,J,K) = X(2,K)
      U(4,J,K) = X(4,K)
C
C USE THE ADAMS-BASHFORTH PREDICTOR-CORRECTOR METHOD TO INTEGRATE
C THE REST OF THE WAY TO THE ORIGIN. SEE SOUTHWORTH'S BOOK "DIGITAL
C COMPUTATION AND NUMERICAL METHODS" PAGE 446.
C
      DO 240 K = 5,N
      DO 120 I = 1,IJ
C
C PREDICTOR EQUATION FOR BACKWARD INTEGRATION
      X0(K) = X(K-1)-SR/24*(55*F(K-1)-59*F(K-2)+37*F(K-3)-9*F(K-4))
      FOR SECOND ARGUMENT 1 = K-1,2 = K
C
      X0(I,2) = X(I,4)-SR/24.D0*(55.D0*F( X(1,4),X(2,4),X(3,4),X(4,4),K
1-1,I)-59.D0*F(X(1,3),X(2,3),X(3,3),X(4,3),K-2,I)+37.D0*F(X(1,2),X(
22,2),X(3,2),X(4,2),K-3,I)-9.D0*F(X(1,1),X(2,1),X(3,1),X(4,1),K-4,I
3))
C
C PREDICTOR EQUATION IS CORRECTED FOR ESTIMATED ERROR
      X1(K) = X0(K)-251/270*(X0(K-1)-X2(K-1))
C
120 X1(I) = X0(I,2)-251.D0/270.D0*(X0(I,1)-X2(I,1))
C
C CORRECTOR EQUATION TO IMPROVE RESULT OF PREDICTOR EQUATION
      X2(K) = X(K-1)-SR/24*(9*F(K)+19*F(K-1)-5*F(K-2)+F(K-3))
      FOR SECOND ARGUMENT 1 = K-1, 2 = K
C
      DO 130 I = 1,IJ
      X2(I,2) = X(I,4)-SR/24.D0*(9.D0*F(X1(1,1),X1(2),X1(3),X1(4),K,I)+19.
1D0*F(X(1,4),X(2,4),X(3,4),X(4,4),K-1,I)-5.D0*F(X(1,3),X(2,3),X(3,3
2),X(4,3),K-2,I)+F(X(1,2),X(2,2),X(3,2),X(4,2),K-3,I))
C
C CORRECTOR EQUATION IS CORRECTED FOR ESTIMATED ERROR

```

```

C      X(K) = X2(K)+19/720*(X0(K)-X2(K))
C      FOR SECOND ARGUMENT I = K-4, 2 = K-3, 3 = K-2, 4 = K-1, 5 = K
C
130   X(I,5) = X2(I,2)+19.D0/720.D0*(X0(I,2)-X2(I,2))
      U(1,J,K) = X(1,5)
      U(2,J,K) = X(3,5)
      U(3,J,K) = X(2,5)
      U(4,J,K) = X(4,5)
C
C      UPGRADE ALL PARAMETERS FOR NEXT STEP
C
C      DO 240 I = 1,IJ
      X0(I,1) = X0(I,2)
      X2(I,1) = X2(I,2)
      DO 240 KK = 1,4
      X(I,KK) = X(I,KK+1)
C
C      SOLVE FOR THE ARBITRARY CONSTANTS FOR FORMING THE GENERAL SOLUTION
C
      LL1 = .5D0+.5D0*DSQRT((2.D0*L+1.D0)**2-4.D0*ZALPHA**2)
      DO 250 I = 1,2
      IH(I) = -U(I,JJ,N)+1.D-3*K0/LL1      *U(I+2,JJ,N)
      DO 250 J = 1,2
      H(I,J) = U(I,J ,N)-1.D-3*K0/LL1      *U(I+2,J,N)
      CALL DSIMQ(H,IH,2,4,KS)
      WRITE(6,907) INDEX,IH(1),IH(2),KS
      C(5) = IH(1)
      C(6) = IH(2)
C
C      USE EVALUATED CONSTANTS TO FORM THE NEW GENERAL SOLUTION AND STORE
C      IN OLD ONE'S PLACE.
C
      DO 270 K = 2,N
      UR(K) = U(1,JJ,K)
      DUR(K) = U(3,JJ,K)
      UI(K) = U(2,JJ,K)

```

```

270 DUI(K) = U(4,JJ,K)
C DO 270 J = 1,2
C UR(K) = UR(K)+IH(J)*U(1,J,K)
C DUR(K) = DUR(K)+IH(J)*U(3,J,K)
C UI(K) = UI(K)+IH(J)*U(2,J,K)
C DUI(K) = DUI(K)+IH(J)*U(4,J,K)
C
C CHECK WHETHER SOLUTION HAS CONVERGED TO WITHIN PRESCRIBED RELATIVE
C TOLFRANCE = TOL.
C
C TOL = 1.0D-3
C DO 290 I = 1,2
C IF(DARS(IH(I))-IH0(I))/DARS(IH(I)).GT.TOL) GO TO 320
C CONTINUE
C WRITE(6,905)
C DO 300 K = 1,N
C EPS = (N-K)/(INTRVL*1.D0)
C EPSR = EPS*RO
C IF(K.LT.N) GO TO 295
C RNL = (0.D0,0.D0)
C IF(L.EC.0) RNL = (1.00,0.00)/CDSQRT((1.00,0.00)+AK(K))
C GO TO 300
C RNL = DCMLPX(UR(K),UI(K))/(EPS*RO*CDSQRT((1.00,0.00)+AK(K)))
C WRITE(6,906) K,UR(K),UI(K),RL(1),RL(2),Q(K),AK(K),ANDN(K),VC(K),RH
C 10(K)
C DO 301 I = 1,N
C K = N+1-I
C PSI = DCMLPX(UR(I),UI(I))/CDSQRT((I+AK(I))
C PSI2(K) = P(1)**2+P(2)**2
C EPS = (I-1.D0)/INTRVL+1.D-3
C PPSI2(I) = (2.D0*ZALPHA*MPI/((L+1)*HBARC))**3/FAC(2*L+3)*(2.D0*ZALP
C 1HA*MPI*EPS*RO/((L+1)*HBARC))**((2*L)*DEXP(-2.D0*ZALPHA*MPI*EPS*RO/(
C 2(L+1)*HBARC))*(RO*EPS))**2
C NORM = 0.00
C DO 302 K = 1,55,6
C NORM = NORM+SR/140.D0*(41.D0*PSI2(K)+216.D0*PSI2(K+1)+27.D0*PSI2(K

```

```

1+2)+272.D0*PSI2(K+3)+27.D0*PSI2(K+4)+216.D0*PSI2(K+5)+41.D0*PSI2(K
2+6))
K = 3
303 TERM = SR/140.D0*(41.D0*CPSI2(K)+216.D0*CPSI2(K+1)+27.D0*CPSI2(K+2
1)+272.D0*CPSI2(K+3)+27.D0*CPSI2(K+4)+216.D0*CPSI2(K+5)+41.D0*CPSI2
2(K+6))
NORM = NORM+TERM*INTRVL
C
C CHECK TO SEE IF THE INTEGRAL HAS CONVERGED TO WITHIN 3 SIGNIFICANT
C FIGURES.
C
C K = K+6
C IF(TERM*INTRVL/NORM.GT.1.D-3) GO TO 303
C
C COMPUTE THE PION'S NORMALIZED PROBABILITY DENSITY FOR STRONG
C INTERACTION WITH FINITE SIZE NUCLEUS AND WITHOUT STRONG
C INTERACTION FOR POINT NUCLEUS.
C
DO 304 K = 1,N
I = K-1
EPS = 1/(INTRVL*1.D0)+1.D-3
W(K) = SNGL(EPS*RO)
NK = N+K
NNK = N+N+K
NNNK = 3*N+K
NNNKK = 4*N+K
IF(K.EQ.1) GO TO 307
W(NK) = SNGL(PSI2(K)/(NORM*(EPS*RO)**2))
W(NNK) = SNGL(PPSI2(K)/(EPS*RO)**2)
W(NNKK) = SNGL(CDABS(DPSI(K))/NORM)
W(NNNKK) = SNGL(DPSIO(K))
GO TO 304
W(NK) = 0.0
W(NNK) = 0.0
W(NNKK) = 0.0
W(NNNKK) = 0.0
307

```

```

304 CONTINUE
C
C COMPUTE THE PROBABILITY OF THE PION BEING INSIDE THE NUCLEUS
C
PROR = 0.00
PRORO = 0.00
DO 305 K = 1,55,6
  PROR = PROR+SR/140.00*(41.00*PSI2(K)*RHO(N+1-K)+216.00*PSI2(K+1)*R
  IH(N-K)+27.00*PSI2(K+2)*RHO(N-K-1)+272.00*PSI2(K+3)*RHO(N-K-2)+27.
  200*PSI2(K+4)*RHO(N-K-3)+216.00*PSI2(K+5)*RHO(N-K-4)+41.00*PSI2(K+6
  3)*RHO(N-K-5))
305 PRORO = PRORO+SR/140.00*(41.00*PPSI2(K)*RHO(N+1-K)+216.00*PPSI2(K+
  11)*RHO(N-K)+27.00*PPSI2(K+2)*RHO(N-K-1)+272.00*PPSI2(K+3)*RHO(N-K-
  22)+27.00*PPSI2(K+4)*RHO(N-K-3)+216.00*PPSI2(K+5)*RHO(N-K-4)+41.00*
  3PPSI2(K+6)*RHO(N-K-5))
  PROR = PROR/NORM*(4.00*PI*RU**3/3.00)
  PRORO = PRORO*(4.00*PI*RU**3/3.00)
  WRITE(6,919) PROR,PRORO
DO 306 I = 1,N
306 WRITE(6,920) W(I),W(N+I),W(N+N+I),W(3*N+I),W(4*N+I)
DO 308 I = 1,N
  EPSR = (N-I)/(INTRVL*1.00)*RO
308 WRITE(6,925) EPSR,I,UR(I),UI(I),I,DUR(I),DUI(I)
925 FORMAT(' R = ',D14.7,' U(',I2,') = ',2D14.7,' DU(',I2,') = ',2D14.
  17)
  CALL PLOT(1,W,N,3,N,0,3*N)
  GO TO 20
320 INDEX = INDEX+1
  IF(INDEX.LE.20) GO TO 330
  WRITE(6,908) INDEX
  GO TO 20
330 DO 340 I = 1,2
340 IH(I) = IH(I)
  GO TO 40
500 STOP
900 FORMAT(8(D9.2,1X)/8(D9.2,1X)/D9.2)

```

```

901  FORMAT(5X,'A1',8X,'A3',7X,'A11',7X,'A13',7X,'A31',7X,'A33',7X,'B11
1',7X,'B00',1X,8(D9.2,1X))//4X,'B01',7X,'B02',7X,'G21',7X,'G01',7X,'
2G10',7X,'G12',6X,'G1101',6X,'G1110',1X,8(D9.2,1X))//5X,'B0',8X,'B1'
3,8X,'C0',8X,'C1',7X,'BHO',7X,'BRI',7X,'BB2',7X,'BB3',1X,8(D9.2,1X)
4//4X,'BR4',7X,'BB5',7X,'CC0',7X,'CC1',7X,'CC2',7X,'CC3',7X,'CC4',7
5X,'CC5',1X,8(D9.2,1X))//3X,'IHO(1)',4X,'IHO(2)',1X,2(D9.2,1X)//
902  FORMAT(A6,D7.1,D8.2,D7.1,I2,D13.8,D9.3,D11.5,D8.3,D9.3/D9.3,2D8.3)
903  FORMAT(' NUC.',6X,'Z',9X,'A',7X,'S',6X,'L',6X,'MASS',8X,'GAM',7X,'
IETRAN',7X,'DEVP',9X,'R',9X,'RO',8X,'CC',8X,'CCC',1X,A6,1X,D8.2,1X,
2D8.2,1X,D8.2,1X,I2,1X,D14.8,1X,D9.3,1X,D11.5,1X,D9.3,1X,D10.3,1X,
3D10.3,1X,D10.3,1X,D10.3)
904  FORMAT(' E = ',2D14.7// DELTA = ',2D14.7// LAMBA = ',2D14.7// PO =
1',2D14.7// M = ',2D14.7// DU = ',2D14.7//)
905  FORMAT(/' N',6X,'UR(K)',6X,'UI(K)',4X,'RNLR(K)',4X,'RNLI(K)',5X,'
IQR(K)',6X,'QI(K)',5X,'AKR(K)',5X,'AKI(K)',3X,'ANONR(K)',3X,'ANONI(
2K)',6X,'VC(K)',4X,'RHO(K)')//
906  FORMAT(1X,I2,4(1X,D10.3),D10.3,6(1X,D10.3),D10.3)
907  FORMAT(' AFTER ',I2,' ITERATIONS/' IH(1) = ',D10.3/' IH(2) = ',D1
10.3/' KS = ',I2//)
908  FORMAT(' SOLUTION HAS NOT CONVERGED AFTER ',I2,' ITERATIONS')
909  FORMAT(' PROB = ',D14.7// PROBO = ',D14.7//6X,'EPS',10X,'|PSI|'#2,
1,7X,'|PSIO|'#2,9X,'|DPSI|',10X,'|DPSIO|'//)
920  FORMAT(5(1X,D14.7))
      END

```

```
FUNCTION F(X1K,X2K,X3K,X4K,K,N)
```

```

C
C DOUBLE PRECISION SUBPROGRAM THAT DEFINES THE REAL AND IMAGINARY
C PARTS OF THE FIRST ORDER TAYLOR SERIES EXPANSION OF F(R).
C
C COMPLEX#16 LAMBA,M,PO
C REAL#8 UKIR,UKII,UR(61),UI(61),FR(61),FRHO(61),FRG(61),FRCO(61),FI
1(61),FIRO(61),FIG(61),FICO(61),BOKI,BOK,H0,GK1,GK,G,COKI,COK,CO,F,
2X1K,X2K,X3K,X4K

```

```

COMMON LAMBA,M,PO
COMMON FR,FRBO,FRG,FRCO,FI,FIBO,FIG,FICO,B0,G,CO,UR,UI,J,L
BOK1 = 0.DO
GK1 = 0.DO
COK1 = 0.DO
BOK = 0.DO
GK = 0.DO
COK = 0.DO
IF(J.EQ.1.AND.L.EQ.0) BOK1 = 1.DO
IF(J.EQ.1.AND.L.GT.0) COK1 = 1.DO
IF(J.EQ.2) GK1 = 1.DO
IF(J.LT.3) GO TO 10
IF(L.EQ.0) BOK = B0
IF(L.GT.0) COK = C0
GK = G
10 GO TO (15,20,25,30), N
15 F = X2K
RETURN
20 F = FR(K)*X1K -FI(K)*X3K +(BOK1-BOK)*(FRBO(K)*UR(K)-FIBO(K)*UI(K))
1+(GK1-GK)*(FRG(K)*UR(K)-FIG(K)*UI(K))+(COK1-COK)*(FRCO(K)*UR(K)-FI
2CO(K)*UI(K))
RETURN
25 F = X4K
RETURN
30 F = FR(K)*X3K +FI(K)*X1K +(BOK1-BOK)*(FRBO(K)*UI(K)+FIBO(K)*UR(K))
1+(GK1-GK)*(FRG(K)*UI(K)+FIG(K)*UR(K))+(COK1-COK)*(FRCO(K)*UI(K)+FI
3CO(K)*UR(K))
RETURN
END

```

FUNCTION CDPSI(A,B,Z)

```

C
C DOUBLE PRECISION FUNCTION SUBPROGRAM TO CALCULATE THE CONFLUENT
C HYPERGEOMETRIC FUNCTION OF THE SECOND KIND WITH COMPLEX ARGUMENTS.

```

```

C
COMPLEX*16 CDPSI,A,B,Z,CDGMMMA,TERM,SUMM,C,ZB,G1,G2,G3,PI,CDEXP,CDL
10G,DCMPLX
DOUBLE PRECISION SUM(2),TRM(2),TOL,CDABS,DABS
EQUIVALENCE (SUM(1),SUMM),(TRM(1),TERM)
C
CHECK WHETHER ASYMPTOTIC FORM OF FUNCTION FOR LARGE Z IS NEEDED
C
TOL = 1.D-8
IF(CDABS(Z).GT.22.D0) GO TO 50
PI = (3.14159265358979D0,0.D0)
K = 1
ZB = CDEXP(((1.D0,0.D0)-R)*CDLOG(Z))
C = (1.D0,0.D0)
SUMM = (0.D0,0.D0)
G1 = CDGMMMA(A)/CDGMMMA(B)
G2 = CDGMMMA(A-B+(1.D0,0.D0))/CDGMMMA((2.D0,0.D0)-B)
G3 = (1.D0,0.D0)/((1.D0,0.D0)-B)*G1*G2
GO TO 15
10
C = C*Z/DCMPLX(K*1.D0-1.D0,0.D0)
G1 = G1*(A+DCMPLX(K*1.D0-2.D0,0.D0))/(B+DCMPLX(K*1.D0-2.D0,0.D0))
G2 = G2*(A-B+DCMPLX(K*1.D0-1.D0,0.D0))/(DCMPLX(K*1.D0,0.D0)-B)
TERM = C*(G1-G2*Zb)
SUMM = SUMM+TERM
15
C
CHECK WHETHER SUM HAS CONVERGED TO WITHIN THE REQUIRED RELATIVE
TOLERANCE = TOL.
C
C
IF(DABS(TRM(1))/SUM(1)).GT.TOL) GO TO 20
IF(SUM(2).EQ.0.D0) GO TO 30
IF(DABS(TRM(2))/SUM(2)).LT.TOL) GO TO 30
K = K+1
IF(K-100) 10,40,40
CDPSI = G3*SUMM
RETURN
40
CDPSI = G3*SUMM

```

```

C      WRITE(6,900) A,B,Z,CDPSI
C      RETURN
C
C      ASYMPTOTIC FORM OF EXPANSION FOR LARGE Z
C
50     SUMM = (1.D0,0.D0)
C      TERM = (1.D0,0.D0)
C
60     K = 1
C      TERM = -(A+DCMPLX(K*1.D0-1.D0,0.D0))*(A-B+DCMPLX(K*1.D0,0.D0))/(Z*
1K)*TERM
C      SUMM = SUMM+TERM
C      IF(DABS(TRM(1)/SUM(1)).GT.TOL) GO TO 70
C      IF(SUM(2).EQ.0.D0) GO TO 80
C      IF(DABS(TRM(2)/SUM(2)).LT.TOL) GO TO 80
70     K = K + 1
C      IF(K*1.D0.GT.CDABS(Z)) GO TO 90
C      GO TO 60
80     CDPSI = SUMM*CDEXP(-A*CDLOG(Z))
C      RETURN
90     CDPSI = SUMM*CDEXP(-A*CDLOG(Z))
C      WRITE(6,910) A,B,Z,CDPSI
C      RETURN
900    FORMAT(' PSI SERIES DID NOT CONVERGE',/ ' A = ',2D15.8/ ' B = ',2D15.
18/ ' Z = ',2D15.8/ ' CDPSI = ',2D15.8)
910    FORMAT(' ASYMPTOTIC PSI SERIES DID NOT CONVERGE',/ ' A = ',2D15.8/ '
18 = ',2D15.8/ ' Z = ',2D15.8/ ' CDPSI = ',2D15.8)
C      END
C
C      SUBROUTINE POTHE4( Z,RO,VC,RHO,DRHO,DDRHO,M,INTRVL,RU)
C      IMPLICIT REAL*8(A-H,O-Z), INTEGER(I-N)
C      DIMENSION RHO(M),DRHO(M),DDRHO(M),VC(M)
C
C      INITIALIZATION OF PARAMETERS
C

```



```
30*2496.D0*R2B2**4+132.D0*64.D0*R2B2**5)*(A0/RB)**12)
```

C  
C  
C

CALCULATION OF THE COULOMB POTENTIAL

```
RB = RO*EPS/BO
R2B2 = RB**2
TERM = RB
SUM = TERM
K = 3
10 TERM = TERM*2.D0*R2B2/K
SUM = SUM+TERM
K = K+2
20 IF(DABS(TERM/SUM).GT.TOL) GO TO 10
VC(MN) = VCNORM*DEXP(-R2B2)/(RO*EPS)*((A+3.D0*B/2.D0+15.D0*C/4.D0+1
105.D0*D/8.D0+946.D0*E/16.D0+10395.D0*F/32.D0+135135.D0*G/64.D0)*SU
2M-(B/2.D0+7.D0*C/4.D0+57.D0*D/8.D0+ 561*E/16.D0+6555.D0*F/32.D0+1
312095.D0*G/64.D0)*RB-(C/2.D0+11.D0*D/4.D0+123.D0*E/8.D0+1545.D0*F/
416.D0+22005.D0*G/32.D0)*RB**3-(D/2.D0+15.D0*E/4.D0+213.D0*F/8.D0+3
5249.D0*G/16.D0)*RB**5-(E/2.D0+19.D0*F/4.D0+327.D0*G/8.D0)*RB**7-(F
6/2.D0+23.D0*G/4.D0)*RB**9-G/2.D0*RB**11)
RETURN
END
```

```
SUBROUTINE POTMHO(W,B,A,RO,Z,VC,RHO,DRHO,DDRHO,M,INTRVL,RU)
IMPLICIT REAL*8(A-H,O-S),INTEGER(I-N)
DIMENSION RHO(M),DRHO(M),DDRHO(M),VC(M)
```

C  
C  
C

INITIALIZATION OF PARAMETERS

```
AP = DSQRT(2.D0/3.D0)*.72D0
RU = DSQRT((5.D0/3.D0)*B*B*((DABS(Z)-2.D0)/DABS(Z)+1.5D0))
BB = DSQRT(B*R-AP*AP)
PI = 3.14159265359D0
HBARC = 197.32D0
```

```

C
C
C
C
ZALPHA = Z/137.0388D0
VSNORM = 2*A/(PI**1.5D0*BB**3*(2.D0+3.D0*W))
VCNORM = -2.D0*ZALPHA*HBARC/(DSORT(PI)*B)

CALCULATION OF THE STRONG INTERACTION DENSITY VST AND ITS
DERIVATIVES DVST AND DDVST.

TOL = 1.D-6
DO 20 N = 1,M
MN = M+1-N
EPS = (N-1.D0)/(INTRVL*1.D0)+1.D-3
R2BB2 = (RO*EPS/BB)**2
RHO(MN) = VSNORM*(1.D0+1.5D0*W*(1.D0-(B/BB)**2)+W*(B/BB)**2*R2BB2)
1*DEXP(-R2BB2)
DR2BB2 = 2.D0*RO*EPS/BB**2
DRHO(MN) = -VSNORM*DR2BB2*(1.D0+1.5D0*W*(B/BB)**2+W*(B/BB
1)**2*R2BB2)*DEXP(-R2BB2)
DDR2BB2 = 2.D0/BB**2
DDRHO(MN) = -VSNORM*((DDR2BB2-DR2BB2**2)*(1.D0+1.5D0*W*(B/B
1B)**2+W*(B/BB)**2*R2BB2)+DR2BB2**2*W*(B/BB)**2)*DEXP(-R2BB2)

CALCULATION OF THE COULOMB POTENTIAL

R2B2 = (RO*EPS/B)**2
TERM = 1.D0
SUM = TERM
K = 3
TERM = TERM*2.D0*R2B2/K
SUM = SUM+TERM
K = K+2
IF(DABS(TERM/SUM).GT.TOL) GO TO 10
VC(MN) = VCNORM*SUM*DEXP(-R2B2)
IF(DABS(Z).GT.2.D0) VC(MN) = VCNORM*(-W/(2.D0+3.D0*W)+SUM)*DEXP(-R
12B2)
RETURN
END

```

C  
C  
C

10

20

```

SUBROUTINE POT(RO,CO,R,C,RR,Z,VC,RHO,DRHO,DDRHO,M,INTRVL,RU,A)
REAL*8 RO,CO,R,C,Z,VC(M),RHO(M),PI,SUM,DE1,DE2,TERM,TERM1,TERM2,
1TERM3,HBARC,ZALPHA,VSNORM,VCNORM,EPS,SUMM,TERM,RR,NN, DEXP,DSORT
2,DAHS,DRHO(M),DDRHO(M),EX,RR

```

```

C
C   CALCULATION OF THE STRONG INTERACTION POTENTIAL NORMALIZATION
C   CONSTANT VSNORM
C

```

```

PI = 3.14159265359D0

```

```

SUM = 0.D0

```

```

SUMM = 0.D0

```

```

DE1 = -DEXP(-RR/CO)

```

```

TERM1 = DE1

```

```

NN = 1.D0

```

```

TERM = TERM1/NN**5

```

```

SUMM = SUMM+TERM

```

```

TERM = TERM1/NN**3

```

```

SUM = SUM+TERM

```

```

TERM1 = TERM1*DE1

```

```

NN = NN +1.D0

```

```

IF(DABS(TERM/SUMM).GT.1.D-6) GO TO 2

```

```

IF(DABS(TERM/SUM).GT.1.D-6) GO TO 6

```

```

VSNORM = A/(4.D0*PI*(PI*PI*CO*RR/3.D0+RR**3/3.D0-2.D0*CO**3*
1SUM))

```

```

RU = DSQRT(5.D0/3.D0*(RR**5/5.D0+2.D0/3.D0*CO*CO*PI*PI*RR**3+7.D0/

```

```

115.D0*(CO*PI)**4*RR-24.D0*CO**5*SUMM)*VSNORM*4.D0*PI/A)

```

```

C
C   CALCULATION OF COULOMB POTENTIAL NORMALIZATION CONSTANT VCNORM
C

```

```

HBARC = 197.32D0

```

```

ZALPHA = Z/137.0388D0

```

```

SUM = 0.D0

```

```

DE1 = -DEXP(-R/C)

```

```

20      TERM1 = DE1
      NN = 1.00
      TERM = TERM1/NN**3
      SUM = SUM+TERM
      TERM1 = TERM1*DE1
      NN = NN+1.00
      IF(DABS(TERM/SUM).GT.1.0D-15) GO TO 20
      VCNORM = -ZALPHA*HBARC/(PI*PI*C*R/3.00+R**3/3.00-2.00*C**3*SUM)
C
C      CALCULATION OF NORMALIZED POTENTIALS
C
      DO 80 N = 1,M
      MN = M+1-N
      EPS = (N-1.00)/(INTRVL*1.00)+1.0D-3
      RHO(MN) = VSNORM/(1.00+DEXP((EPS*R0-RR)/CO))
      EX = DEXP((EPS*R0-RR)/CO)
      DRHO(MN)=-RHO(MN)/CO*EX/(1.00+EX)
      IF(N.EQ.1) DRHO(MN)=0.00
      DDRHO(MN)=DRHO(MN)/CO*(1.00-2.00*EX/(1.00+EX))
      IF(N.EQ.1) DDRHO(MN)=0.00
      IF(EPS.GT.R/R0) GO TO 60
C
C      COULOMB POTENTIAL FOR EPS*R0<R
      SUM = 0.00
      NN = 1.00
      DE1 = -DEXP(-R/C)
      DE2 = -DEXP((R0*EPS-R)/C)
      TERM1 = -2.00*C**3/(R0*EPS)*DE1
      TERM2 = -C*C*DE2
      TERM3 = 2.00*C**3/(R0*EPS)*DE2
      TERM = TERM1/NN**3+TERM2/NN**2+TERM3/NN**3
      SUM = SUM+TERM
      IF(DABS(TERM1/(NN**3*SUM)).LT.1.0D-15) TERM1 = 0.00
      TERM1 = TERM1*DE1
      IF(DABS(DE2).LT.1.0D-15) DE2 = 0.00
50

```

```

TERM2 = TERM2*DE2
TERM3 = TERM3*DE2
NN = NN+1.00
IF(DABS(TERM/SUM).GT.1.0D-08) GO TO 50
VC(MN) = VCNORM*(R*R/2.00-(EPS*RO)**2/6.00+C*C*PI*PI/6.00+SUM)
GO TO 80

```

C  
C  
C  
60

```

COULOMB POTENTIAL FOR EPS*RO > R

```

```

SUM = 0.00
NN = 1.00
DE1 = -DEXP(-R/C)
DE2 = -DEXP(-(EPS*RO-R)/C)
TERM1 = -2.00*C**3*DE1
TERM2 = C*C*EPS*RO*DE2
TERM3 = 2.00*C**3*DE2
TERM = TERM1/NN**3+TERM2/NN**2+TERM3/NN**3
SUM = SUM+TERM

```

70

```

IF(DABS(TERM1/(NN**3*SUM)).LT.1.0D-15) TERM1 = 0.00
TERM1 = TERM1*DE1
IF(DABS(DE2).LT.1.0D-15) DE2 = 0.00
TERM2 = TERM2*DE2
TERM3 = TERM3*DE2
NN = NN + 1.00
IF(DABS(TERM/SUM).GT.1.0D-08) GO TO 70
VC(MN) = VCNORM*(R**3/3.00+C*C*PI*PI*R/3.00+SUM)/(EPS*RO)
CONTINUE
RETURN
END

```

80

```

FUNCTION CDGMMMA(Z)

```

C  
C  
C

```

DOUBLE PRECISION FUNCTION SUBPROGRAM TO CALCULATE THE GAMMA
FUNCTION FOR COMPLEX ARGUMENTS.

```

```

C
COMPLEX#16 CDGMMA,Z,T,TT,SUMM,TERM,DEN,ZM,ZZ,DCMPLX,CDLOG,CDEXP,CD
1SIN,PI
DOUBLE PRECISION X,Y,XDIST,A(2),C(12),SUM(2),TRM(2),CDABS,DABS,DLO
1G,TOL,DFLOAT
LOGICAL REFLEK
EQUIVALENCE (A(1),ZZ),(SUM(1),SUMM),(TRM(1),TERM)
C
SET ALL SYSTEM DEPENDENT CONSTANTS WITH DATA STATEMENT WHERE
C
IOUT = SYSTEM DEPENDENT OUTPUT CHANNEL
C
C(12) = COEFFICIENTS IN STIRLING'S APPROXIMATION FOR LN(GAMMA(T))
C
DATA TOL,IOUT,PI/1.D-15,6,(3.14159265358979D0,0.D0)/,C/.83333333333
13333D-1,-.27777777777778D-2,.793650793650794D-3,-.59523809523809
25D-3,.841750841750842D-3,-.191752691752692D-2,.641025641025641D-2
3,-.295506535947712D-1,.179644372368831D0,-.139243221690590D1,.1340
428640441684D2,-.156848284626020D3/
ZZ = Z
X = A(1)
Y = A(2)
REFLEK = .FALSE.
C
DETERMINE WHETHER Z IS TOO CLOSE TO A POLE BY FINDING NEAREST POLE
C
AND COMPUTING DISTANCE TO IT.
C
IF(X.GE.TOL) GO TO 20
XDIST = X - DFLOAT(IDINT(X-.5D0))
ZM = DCMPLX(XDIST,Y)
IF(CDABS(ZM).GE.TOL) GO TO 10
C
IF Z IS TOO CLOSE TO A POLE, PRINT ERROR MESSAGE AND RETURN WITH
C
CDGMMA = DCMPLX(1.D0/TOL,0.D0)
WRITE(IOUT,900)
CDGMMA = DCMPLX(1.D0/TOL,0.D0)
RETURN
C

```

```

C
C FOR REAL(Z) NEGATIVE EMPLOY THE REFLECTION FORMULA
C
C      GAMMA(Z) = PI/(SIN(PI*Z)*GAMMA(1-Z))
C
C AND COMPUTE GAMMA(1-Z). NOTE REFLEK IS A TAG TO INDICATE THAT
C THIS RELATION MUST BE USED LATER.
C
10 IF(X.GE.0.D0) GO TO 20
   REFLEK = .TRUE.
   ZZ = (1.D0,0.D0)-ZZ
   X = 1.D0-X
   Y = -Y
C
C IF Z IS NOT TOO CLOSE TO A POLE, MAKE REAL(Z)>10 AND ARG(Z)<PI/4
C
C      M = MAX0(IABS(IDINT(Y))-IDINT(X),10-IDINT(X),0)
20 T = DCMPLEX(X+DFLOAT(M),Y)
60 TT = T*T
   DEN = T
C
C COMPUTE STIRLING'S APPROXIMATION FOR LN(GAMMA(T))
C
SUMM = (T-(.5D0,0.D0))*CDLOG(T)-T+(.5D0,0.D0)*CDLOG((2.D0,0.D0)*PI
1)
   J = 1
   TERM = C(J)/DEN
70
C
C TEST REAL AND IMAGINARY PARTS OF LN(GAMMA(Z)) SEPARATELY FOR
C CONVERGENCE. IF Z IS REAL SKIP IMAGINARY PART OF CHECK.
C
IF(Y.EQ.0.D0) GO TO 100
IF(DABS(TRM(2)/SUM(2)).LE.TOL) GO TO 100
80 SUMM = SUMM+TERM
   J = J+1
   DEN = DEN*TT
C

```



```

C TO SOLVE A SET OF SIMULTANEOUS LINEAR EQUATIONS AX = B
C
C DESCRIPTION OF PARAMETERS
C
C A = MATRIX OF COEFFICIENTS N BY N STORED COLUMNWISE.
C
C B = VECTOR OF ORIGINAL CONSTANTS (LENGTH N). THESE ARE
C REPLACED BY FINAL SOLUTION VALUES, VECTOR X.
C
C N = NUMBER OF EQUATIONS AND VARIABLES (N>1).
C
C KS = OUTPUT DIGIT
C
C 0 FOR A NORMAL SOLUTION
C 1 FOR A SINGULAR SET OF EQUATIONS
C
C METHOD
C
C THE SIMULTANEOUS EQUATIONS ARE SOLVED BY ELIMINATION USING LARGEST
C PIVOTAL DIVISOR. EACH STAGE OF ELIMINATION CONSISTS OF INTER-
C CHANGING ROWS WHEN NECESSARY TO AVOID DIVISION BY ZERO OR SMALL
C ELEMENTS.
C THE FORWARD SOLUTION TO OBTAIN VARIABLE N IS DONE IN N STAGES.
C THE BACK SOLUTION FOR THE OTHER VARIABLES IS CALCULATED BY
C SUCCESSIVE SUBSTITUTIONS. FINAL SOLUTION VALUES ARE DEVELOPED IN
C VECTOR B, WITH VARIABLE 1 IN B(1), VARIABLE 2 IN B(2)....., VARIABLE
C N IN B(N). IF NO PIVOT CAN BE FOUND EXCEEDING A TOLERANCE OF 0.0,
C THE MATRIX IS CONSIDERED SINGULAR AND KS IS SET EQUAL TO 1.
C
C .....
C
C SUBROUTINE DSIMQ(A,B,N,NN,KS)
C DOUBLE PRECISION A(NN),B(N),TOL,BIGA,SAVE,DABS
C
C FORWARD SOLUTION
C

```

```

C
TOL = 0.00
KS=0
JJ=-N
DO 65 J=1,N
JY=J+1
JJ=JJ+N+1
BIGA = 0.00
IT=JJ-J
DO 30 I=J,N

C
C SEARCH FOR MAXIMUM COEFFICIENT IN COLUMN
C
IJ=IT+I
IF(DABS(BIGA)-DABS(A(IJ))) 20,30,30
20 BIGA=A(IJ)
IMAX=I
30 CONTINUE

C
C TEST FOR PIVOT LESS THAN TOLERANCE (SINGULAR MATRIX)
C
IF(DABS(BIGA)-TOL) 35,35,40
35 KS=1
RETURN

C
C INTERCHANGE ROWS IF NECESSARY
C
40 I1=J+N*(J-2)
IT=IMAX-J
DO 50 K=J,N
I1=I1+N
I2=I1+IT
SAVE=A(I1)
A(I1)=A(I2)
A(I2)=SAVE
C

```

C            DIVIDE EQUATION BY LEADING COEFFICIENT

C  
C

```
50 A(I1)=A(I1)/BIGA
   SAVE=B(IMAX)
   B(IMAX)=B(J)
   B(J)=SAVE/BIGA
```

C  
C  
C

          ELIMINATE NEXT VARIABLE

```
IF(J-N) 55,70,55
55 IQS=N*(J-1)
   DO 65 IX=JY,N
   IXJ=IQS+IX
   IT=J-IX
   DO 60 JX=JY,N
   IXJX=N*(JX-1)+IX
   JJX=IXJX+IT
60 A(IXJX)=A(IXJX)-(A(IXJ)*A(JJX))
65 B(IX)=B(IX)-(R(J)*A(IXJ))
```

C  
C  
C

          BACK SOLUTION

```
70 NY=N-1
   IT=N#N
   DO 80 J = 1,NY
   IA=IT-J
   IB=N-J
   IC=N
   DO 80 K=1,J
   B(IB)=B(IB)-A(IA)*B(IC)
   IA=IA-N
80 IC=IC-1
   RETURN
   END
```



```

IF(NS) 16, 16, 10
C
C      SORT BASE VARIABLE DATA IN ASCENDING ORDER
C
10 DO 15 I=1,N
DO 14 J=I,N
IF(A(I)-A(J)) 14, 14, 11
11 L=I-N
LL=J-N
DO 12 K=1,M
L=L+N
LL=LL+N
F=A(L)
A(L)=A(LL)
12 A(LL)=F
14 CONTINUE
15 CONTINUE
C
C      TEST NULL
C
16 IF(NULL) 20, 18, 20
18 NULL=50
C
C      PRINT TITLE
C
20 WRITE(6,1) NO
C
C      FIND SCALE FOR BASE VARIABLE
C
XSCAL=(A(N)-A(1))/(FLOAT(NULL-1))
C
C      FIND SCALE FOR CROSS-VARIABLES
C
M1=N+1
YMIN=A(M1)
YMAX=YMIN

```

```

M2=M*N
DO 40 J=M1,M2
IF(A(J)-YMIN) 28,26,26
26 IF(A(J)-YMAX) 40,40,30
28 YMIN=A(J)
GO TO 40
30 YMAX=A(J)
40 CONTINUE
YSCAL=(YMAX-YMIN)/100.0

C
C FIND BASE VARIABLE PRINT POSITION
C
XB=A(1)
L=1
MY=M-1
I=1
45 F=I-1
XPR=XB+F*XSCAL
IF(A(L)-XPR-.010) 50,50,70

C
C FIND CROSS-VARIABLES
C
50 DO 55 IX=1,101
55 OUT(IX)=BLANK
DO 60 J=1,MY
LL=L+J*N
JP=((A(LL)-YMIN)/YSCAL)+1.0
OUT(JP)=ANG(J)
60 CONTINUE

C
C PRINT LINE AND CLEAR, OR SKIP
WRITE(6,2)XPR,(OUT(IZ),IZ=1,101)
L=L+1
GO TO 80
70 WRITE(6,3)
80 I=I+1

```

```

IF(I-NLL) 45, 84, 86
84 XPR=A(N)
GO TO 50

```

C  
C  
C

PRINT CROSS-VARIABLES NUMBERS

```

86 WRITE(6,7)
YPR(1)=YMIN
DO 90 KN=1,9
90 YPR(KN+1)=YPR(KN)+YSCAL*10.0
YPR(11)=YMAX
WRITE(6,8)(YPR(IP),IP=1,11)
RETURN
1 FORMAT(1H1,60X,7H CHART ,I3//)
2 FORMAT(1H ,F5.1,5X,101A1)
3 FORMAT(1H )
7 FORMAT(1H ,10X,101H.
1 . . . . .
8 FORMAT(1H0,9X,11E10.3)
END

```

```

FUNCTION CPSI2(K)
REAL*8 CPSI2,PSI(2),FK(61),FRB0(61),FRG(61),FRC0(61),FI(61),FIB0(6
11),FIG(61),FICO(61),B0,G,CO,UR(61),UI(61)
COMPLEX*16 LAMBA,M,PO,CPSI,CDPSI,DCMPLX,CDEXP,CDLOG,EPS,DELTA
EQUIVALENCE (PSI(1),CPSI)
COMMON LAMBA,M,PO
COMMON FR,FRB0,FRG,FRC0,FI,FIB0,FIG,FICO,H0,G,CO,UR,UI,J,L
EPS = DCMPLX(K/3.0,0.0)
CPSI = DCMPLX(1.0,1.0)*CDEXP(-PO*(EPS-(1.0,0.0)))/(2.0)
1CDEXP(M*CDLOG(EPS))*CDPSI(M-LAMBA,2.0)*M,EPS*PO)/CDPSI(M-LAMBA,2.0
20*M,PO)
CPSI2 = PSI(1)**2+PSI(2)**2
RETURN

```

END

APPENDIX H.

Method for Determining Phase Shifts and Differential  
Scattering Cross Sections for Pion-Nucleus Elastic Scattering

26

According to Goldberger and Watson the differential cross section in the barycentric coordinate system for scattering by a Coulomb plus a short range force is given by

$$H1 \quad \frac{d\sigma(\theta)}{d\Omega} = |f(\theta)|^2$$

where  $f(\theta)$ , the total scattering amplitude, may be separated into a point Coulomb amplitude  $f_c(\theta)$  and the short range force amplitude  $f_s(\theta)$ , i.e.

$$H2 \quad f(\theta) = f_c(\theta) + f_s(\theta)$$

where

$$H3 \quad f_c(\theta) = \sum_{l=0}^{\infty} \frac{2l+1}{2ik} (e^{2i\sigma_l} - 1) P_l(\cos \theta)$$

and

$$H4 \quad f_s(\theta) = \sum_{l=0}^{\infty} \frac{2l+1}{2ik} e^{2i\sigma_l} (e^{2i\sigma_l} - 1) P_l(\cos \theta)$$

The infinite series for the Coulomb amplitude may be summed to obtain 26

$$H5 \quad f_c(\theta) = \frac{-N\hbar c}{2kc \sin^2 \frac{\theta}{2}} e^{-2iN \ln(\sin \frac{\theta}{2}) + 2i\sigma_0}$$

where

$$H6 \quad N = \frac{Z\alpha}{kC} \left( \frac{E_1 E_2}{E_1 + E_2} \right)$$

$$H7 \quad e^{2i\sigma_l} = \Gamma(l+1+iN) / \Gamma(l+1-iN)$$

and  $k$  is the momentum of the pion in the barycentric system. The number of partial waves that must be included in the sum of  $f_s(\Theta)$  depends on the energy of the pion. For  $T_\pi = 300$  MeV about 8 terms are needed for 1% accuracy. For lower energy less are needed. At higher energies more are needed.

The short range partial wave phase shifts are calculated by integrating the Klein-Gordon equation with the Coulomb potential for an extended charge distribution and the pion-nucleus strong interaction potential from the origin out to some point  $R$  beyond the range of the finite size nucleus Coulomb effects and the strong interaction potential. Outside the region where the short range potentials are important, the asymptotic form of the radial wavefunction is given by

$$H8 \quad R_l(r) \Big|_{r=R} = C \left[ F_l(N, kR) \cos \sigma_l + G_l(N, kR) \sin \sigma_l \right]$$

$$H9 \quad R'_l(r) \Big|_{r=R} = C \left[ F'_l(N, kR) \cos \sigma_l + G_l(N, kR) \sin \sigma_l \right]$$

where  $F_l(N, kR)$  and  $G_l(N, kR)$  are the regular and irregular Coulomb functions, the primes denote derivatives taken with respect to  $r$ , and  $C$  is a constant normalization factor needed to make  $R_l(r)$  match the Coulomb wavefunction.

An expression for  $\sigma_l$  may be obtained by dividing both equations by  $\cos(\sigma_l)$  and dividing the second equation by the first to eliminate the normalization constant  $C$ , i.e.

$$\text{H10} \quad \left. \frac{R_l(r)}{R_l'(r)} \right|_{r=R} = \left. \frac{F_l(N, kr) + \tan \nu_l G_l(N, kr)}{F_l'(N, kr) + \tan \nu_l G_l'(N, kr)} \right|_{r=R} \equiv \gamma_l(r) \Big|_{r=R}$$

Solving for  $\tan(\nu_l)$  gives

$$\text{H11} \quad \tan \nu_l = \left. \frac{F_l(N, kr) - \gamma_l(r) F_l'(N, kr)}{-G_l(N, kr) + \gamma_l(r) G_l'(N, kr)} \right|_{r=R}$$

Using the identity for the scattering amplitude for the  $l$ -th partial

146  
wave

$$\text{H12} \quad a_l \equiv \frac{e^{2i\nu_l} - 1}{2ik} = \frac{e^{i\nu_l} \sin \nu_l}{k} = \frac{1}{-ik + k \cot \nu_l}$$

obtain

$$\text{H13} \quad f_s(\theta) = \sum_{l=0}^{\infty} (2l+1) a_l e^{2i\nu_l} P_l(\cos \theta)$$

## APPENDIX I

### Procedure for Averaging the Theoretical Differential Scattering Cross Section over the Finite Angular Resolution of a Physical Detector

For all pion-nucleus scattering experiments there is an effective detector angular resolution due to the finite size of the detector, the finite size of the target, and the associated detector electronics. In order to predict the experimentally measured differential cross sections, it is necessary to average the theoretical differential cross section over the effective angular acceptance of the detector, i.e.

$$I1 \quad \overline{\frac{d\sigma}{d\Omega}(\Theta_0)} = \frac{1}{\Delta} \int_{\Theta_0 - \Delta/2}^{\Theta_0 + \Delta/2} \frac{d\sigma}{d\Omega}(\Theta) P(\Theta - \Theta_0) d\Theta$$

where  $P(\Theta - \Theta_0)$  is the effective angular response of the detector which is zero for  $|\Theta - \Theta_0|$  greater than some angle  $\Delta/2$ . In general  $P(\Theta - \Theta_0)$  is a function of the geometry of the detector and the target and the electronic detector circuit. Usually it is assumed to be symmetric about  $\Theta_0$ .

For any region in  $\Theta$  the differential scattering cross section may be expanded in a power series in  $\Theta$

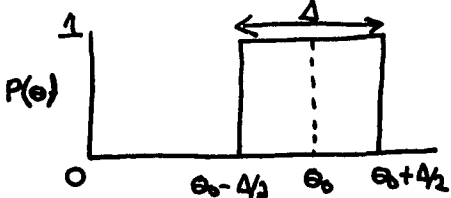
$$I2 \quad \frac{d\sigma}{d\Omega}(\Theta) = A + B\Theta + C\Theta^2 + \dots$$

Assuming  $P(\Theta - \Theta_0)$  is symmetric about  $\Theta_0$  implying

$$I3 \quad \int_{\theta_0 - \Delta/2}^{\theta_0 + \Delta/2} B \theta P(\theta - \theta_0) d\theta = 0$$

gives the result that the lowest order correction to the theoretical  $\frac{d\sigma}{d\Omega}(\theta)$  due to the finite angular resolution of a real detector depends on the quadratic or parabolic term in the expansion.

In order to estimate this correction assume as a first approximation that  $P(\theta - \theta_0)$  is purely geometrical and can be represented by

$$I4 \quad P(\theta - \theta_0) = \begin{cases} 1 & |\theta - \theta_0| \leq \Delta/2 \\ 0 & |\theta - \theta_0| > \Delta/2 \end{cases}$$


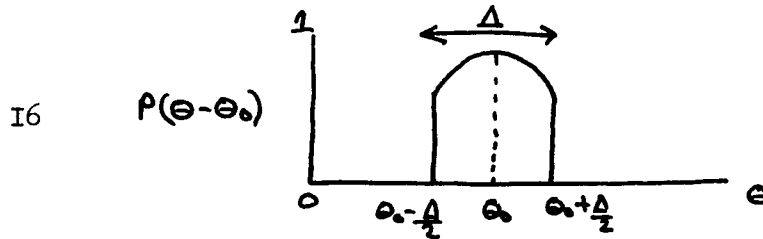
Fitting the theoretical differential scattering cross section at three points  $\theta_0$ ,  $\theta_0 + \Delta/2$ ,  $\theta_0 - \Delta/2$  with a parabola, one may use Simpson's rule to obtain an average  $\overline{\frac{d\sigma}{d\Omega}(\theta)}$  in the angular range of the detector about  $\theta_0$

$$I5 \quad \overline{\frac{d\sigma}{d\Omega}(\theta_0)} = \frac{1}{\Delta} \int_{\theta_0 - \Delta/2}^{\theta_0 + \Delta/2} \frac{d\sigma}{d\Omega}(\theta) P(\theta - \theta_0) d\theta = \frac{1}{\Delta} \int_{\theta_0 - \Delta/2}^{\theta_0 + \Delta/2} \frac{d\sigma}{d\Omega}(\theta) d\theta$$

$$\approx \frac{1}{6} \left[ \frac{d\sigma}{d\Omega}(\theta_0 + \Delta/2) + 4 \frac{d\sigma}{d\Omega}(\theta_0) + \frac{d\sigma}{d\Omega}(\theta_0 - \Delta/2) \right]$$

This result gives a first approximation to the average differential scattering cross section as measured by a detector with a purely geometrical effective angular resolution of  $\pm \Delta/2$ .

An improved estimate of  $\overline{\frac{d\sigma}{d\Omega}(\theta_0)}$  may be obtained by approximating  $P(\theta - \theta_0)$  by a parabola over the region of interest, i.e.



and using Simpson's three point integration formula to obtain

$$\overline{\frac{dV}{d\Omega}(\theta_0)} = \int_{\theta_0 - \Delta/2}^{\theta_0 + \Delta/2} \frac{dV}{d\Omega}(\theta) P(\theta - \theta_0) d\theta \bigg/ \int_{\theta_0 - \Delta/2}^{\theta_0 + \Delta/2} P(\theta - \theta_0) d\theta$$

I7

$$\begin{aligned} &= \frac{\Delta}{6} \left[ \frac{dV}{d\Omega}(\theta_0 + \Delta/2) P(\Delta/2) + 4 \frac{dV}{d\Omega}(\theta_0) P(0) \right. \\ &\quad \left. + \frac{dV}{d\Omega}(\theta_0 - \Delta/2) P(-\Delta/2) \right] \bigg/ \frac{\Delta}{6} \left[ P(\Delta/2) + 4 P(0) \right. \\ &\quad \left. + P(-\Delta/2) \right] \\ &= \frac{1}{5} \left[ \frac{1}{2} \frac{dV}{d\Omega}(\theta_0 + \Delta/2) + 4 \frac{dV}{d\Omega}(\theta_0) + \frac{1}{2} \frac{dV}{d\Omega}(\theta_0 - \Delta/2) \right] \end{aligned}$$

where

I8

$$P(\Delta/2) = P(-\Delta/2) = 1/2$$

$$P(0) = 1$$

## APPENDIX J

### Procedure for Fermi-Averaging the $\pi N$ Interaction Amplitudes

Many types of nuclear experiments indicate that the nucleons in the nucleus have a momentum distribution of some sort. Thus, in order to evaluate the  $\pi N$  interaction amplitudes which are a function of the relative momentum in the  $\pi N$  CM system in the pion-nucleus CM system, it becomes necessary to average in some way over the momentum of nucleons in the nucleus. For this work the Fermi gas model of the nucleus is used in order to obtain approximately the momentum distribution of the nucleons in the nucleus.

From the general form of the Lorentz transformation the relative momentum of a pion with laboratory momentum  $\vec{P}_\pi$  and energy  $E_\pi$  with respect to a nucleon bound in the nucleus with laboratory momentum  $\vec{P}_N$  and energy  $E_N$  is

$$J1 \quad \vec{P}_\pi^{CM} = (\vec{P}_\pi E_N - \vec{P}_N E_\pi) / [m_\pi^2 + m_N^2 + 2E_\pi E_N + 2\vec{P}_\pi \cdot \vec{P}_N]^{1/2}$$

where

$$J2 \quad |\vec{P}_\pi^{CM}| = \left[ \frac{\vec{P}_\pi^2 E_N^2 - 2\vec{P}_\pi \cdot \vec{P}_N E_\pi E_N + P_N^2 E_\pi^2}{m_\pi^2 + m_N^2 + 2E_\pi E_N + 2\vec{P}_\pi \cdot \vec{P}_N} \right]^{1/2}$$

The average value of the  $\pi N$  interaction amplitude  $\alpha_{2T,2J}(\vec{P}_\pi^{CM})$  defined in Appendix A may be defined by

$$J3 \quad \overline{\alpha_{2T,2J}(\vec{P}_\pi^{CM})} \equiv \frac{\int f(\vec{P}_N) \alpha_{2T,2J}(\vec{P}_\pi, \vec{P}_N) d^3 P_N}{\int f(\vec{P}_N) d^3 P_N}$$

where  $f(\vec{P}_N)$  is the probability of a nucleon in the nucleus having a momentum  $\vec{P}_N$ .

For the Fermi gas model of the nucleus

$$J4 \quad \overline{\alpha_{2T,2J}(\vec{P}_N^{cm})} = 2\pi \int_{-1}^1 \int_0^{P_f} \alpha_{2T,2J}(\vec{P}_N, \vec{P}_N) P_N^2 dP_N d\cos\theta_{\pi N} / \frac{4\pi}{3} P_f^3$$

where  $P_f$  is the Fermi momentum defined by

$$J5 \quad P_f = \left( \frac{3\pi}{2} \rho \right)^{1/3}$$

and  $\rho$  is the density of nucleons in the nucleus. For a first approximation  $\rho$  is taken to be the uniform density of the nucleus with the finite size of the proton removed as determined from electron scattering experiments.

The  $\overline{\alpha_{2T,2J}(\vec{P}_N^{cm})}$  are the quantities which appear in all pion-nucleus potentials derived from multiple scattering theory.

APPENDIX K

Coordinate Transformations from the Laboratory  
To the Barycentric Frame of Reference

Consider the scattering in the laboratory frame of reference of two particles having masses  $M_1$  and  $M_2$ . The incident momenta and energies of the particles are  $\vec{P}_1 \neq 0$ ,  $\vec{P}_2 = 0$ , and

$$K1 \quad \epsilon_{1,p_1} = (M_1^2 c^4 + p_1^2 c^2)^{1/2} \quad \epsilon_{2,p_2} = M_2 c^2$$

The total energy of the two particles is

$$K2 \quad E_L = \epsilon_{1,p_1} + \epsilon_{2,p_2}$$

When the scattering is completed the two particles emerge from the region of interaction with momenta  $\vec{K}_1$  and  $\vec{K}_2$  and energies  $\epsilon_{1,k_1}$  and  $\epsilon_{2,k_2}$ . An element of solid angle into which  $\vec{K}_1$  is directed may be expressed as

$$K3 \quad d\Omega_L = d\phi_L \sin\theta_L d\theta_L$$

where the polar angle  $\theta_L$  and the azimuthal angle  $\phi_L$  are measured with respect to a polar axis defined by the direction of  $\vec{P}_1$ .

In the barycentric coordinate system particles 1 and 2 have momenta  $\vec{k}$  and  $-\vec{k}$  and energies  $\epsilon_{1,k}$  and  $\epsilon_{2,k}$  prior to the scattering. The total energy of the particles is

$$K4 \quad E_B = \epsilon_{1,k} + \epsilon_{2,k}$$

After scattering the two particles will have momenta  $\vec{k}_f$  and  $-\vec{k}_f$ .

For elastic scattering conservation of energy requires that  $|\vec{k}_f| = |\vec{k}_i$  in the final asymptotic state. An element of solid angle into which  $\vec{k}_f$  is directed may be expressed as

$$K5 \quad d\Omega_B = d\phi_B \sin\theta_B d\theta_B$$

where the polar axis is defined by the direction of  $\vec{k}_i$ . Since  $\vec{P}_1$  and  $\vec{k}_i$  are parallel, this axis is the same as that about which  $(\theta_L, \phi_L)$  are measured.

26

According to Goldberger and Watson the differential cross sections in the laboratory and barycentric frames of reference are related by

$$K6 \quad \frac{d\sigma}{d\Omega_L} = J \left( \frac{\partial\Omega_B}{\partial\Omega_L} \right) \frac{d\sigma}{d\Omega_B}$$

where  $J \left( \frac{\partial\Omega_B}{\partial\Omega_L} \right)$  represents the factor for transforming the differential cross section from the barycentric to the laboratory frame of reference.

Using the Lorentz transformation equations of Chapter 6 of Goldberger and Watson, <sup>26</sup> one obtains a simplified form of their expression for

$J \left( \frac{\partial\Omega_B}{\partial\Omega_L} \right)$  which is

$$K7 \quad J \left( \frac{\partial\Omega_B}{\partial\Omega_L} \right) = \frac{k_i^2 / k^2}{\frac{k_i E_L}{k E_B} - \frac{E_i k_i}{M_2 c^2} \cos\theta_L}$$

where

$$K8 \quad E_B = (M_1^2 c^4 - M_2^2 c^4 + 2M_2 c^2 E_L)^{1/2}$$

$$k c = M_2 c^2 \left( \frac{E_L^2}{E_B^2} - 1 \right)^{1/2}$$

$$k_1 c = \frac{\frac{E_{1,k}}{\gamma} B \cos \theta_L + \sqrt{k^2 c^2 (1 - \beta^2) - M_1^2 c^4 \beta^2 (1 - \cos^2 \theta_2)}}{1 - \beta^2 \cos^2 \theta_L}$$

$$E_{1,k} = (k^2 c^2 + M_1^2 c^4) \gamma_2$$

$$E_{2,k} = (k^2 c^2 + M_2^2 c^4) \gamma_2$$

$$\beta = kc / E_{2,k}$$

$$\gamma = E_{2,k} / M_2 c^2$$

The transformation of angles from one reference frame to the other is obtained from the Lorentz transformation equations to be

$$K9 \quad \cos \theta_L = \frac{\gamma}{k_1} (k \cos \theta_B + \frac{\beta}{c} E_{1,k})$$

$$k_1 \sin \theta_L = k \sin \theta_B$$

$$\cos \theta_B = \left( \frac{E_{1,k_1}}{\gamma} - E_{1,k} \right) / \beta kc$$

## APPENDIX L

### Method of Solving the Klein-Gordon Equation

#### For Pion-Nucleus Scattering

The time-independent Klein-Gordon equation which describes pion-nucleus scattering in the barycentric coordinate system may be written in the form

$$L1 \quad \left[ \frac{\hbar^2}{2M_\pi} \nabla^2 + \frac{(E - V_C(r))^2 - M_\pi^2 c^4}{2M_\pi c^2 \left( 1 + \frac{E - V_C(r)}{M_{Nuc} c^2} - \frac{p_\pi^2 c^2}{4M_{Nuc}^2 c^4} \right)} \right] \Phi(r) = V_{ST}(r) \Phi(r)$$

where  $r$  is the pion-nucleus relative radial coordinate,  $E$  is the total pion energy,  $V_C(r)$  is the pion-nucleus Coulomb potential,  $V_{ST}(r)$  is the optical model pion-nucleus potential,  $M_\pi$  is the mass of the pion, and  $M_{Nuc}$  is the mass of the nucleus. The total pion energy  $E$  in the barycentric coordinate system is determined from the total pion energy in the lab using Appendix K. For nuclei with only small deviations from spherical mass and charge distributions, one assumes that the orbital angular momentum  $l$  is a good quantum number. Using separation of variables in the wavefunction

$$L2 \quad \Phi(r) = R_l(r) Y_{lm}(\theta, \phi)$$

one obtains the radial equation

$$L3 \quad \left[ \frac{1}{r} \frac{\partial^2 r}{\partial r^2} - \frac{l(l+1)}{r^2} + \frac{(E - V_C(r))^2 - M_\pi^2 c^4}{2M_\pi c^2 \left( 1 + \frac{E - V_C(r)}{M_{Nuc} c^2} - \frac{p_\pi^2 c^2}{4M_{Nuc}^2 c^4} \right)} \right] R_l(r) = V_{ST}(r) R_l(r)$$

Making the substitution

$$L4 \quad \phi_2(r) = r R_2(r)$$

one obtains for L3

$$L5 \quad \phi_2''(r) = \left[ \frac{l(l+1)}{r^2} - \frac{(E - V_C(r))^2 - M_\pi^2 c^4}{\hbar^2 c^2 \left( 1 + \frac{E - V_C(r)}{M_{Nuc} c^2} - \frac{\hbar^2 c^2}{4 M_{Nuc}^2 c^4} \right)} - \frac{2 M_\pi c^2 V_{ST}(r)}{\hbar^2 c^2} \right] \phi_2(r)$$

For a realistic extended nuclear charge density  $V_C(r)$  is quite complicated, and the equation for  $\phi_2(r)$  must be solved numerically. However, it is possible to separate the solution for all of space into two regions, i.e. an inner region in which the Coulomb potential due to the finite size of the nuclear charge distribution and the pion-nucleus strong interaction potential are important, and an outer region in which only the electromagnetic potential for a point source is important. The wave equation for  $\phi_2(r)$  can be solved exactly in the outer region for the Coulomb potential of a point source. By using the logarithmic derivative of the outer wave function at the boundary of the two regions as a boundary condition on the inner wavefunction, it is possible to greatly reduce the region over which the wave equation must be numerically integrated. In practice the inner region need be only a few nuclear radii for high accuracy in the solution.

For the outer region the Coulomb potential has the form

$$L6 \quad V_C(r) = -\frac{Ze^2}{r} = -\frac{Z\alpha\hbar c}{r}$$

Writing out all powers of  $r$  explicitly for equation L5 except for the  $V_C(r)$  term in the denominator obtain

$$\begin{aligned}
 \text{L7} \quad \phi_l''(r) + & \left[ \frac{-l(l+1) + z^2 \alpha^2 / \left(1 + \frac{E - V_0(r)}{M_{\text{Nuc}} c^2} - \frac{\hbar^2 c^2}{4M_{\text{Nuc}}^2 c^4}\right)}{r^2} \right. \\
 & - \frac{2Ez\alpha}{r\hbar c} \frac{1}{1 + \frac{E - V_0(r)}{M_{\text{Nuc}} c^2} - \frac{\hbar^2 c^2}{4M_{\text{Nuc}}^2 c^4}} \\
 & \left. + \frac{E^2 - M_{\text{Nuc}}^2 c^4}{\hbar^2 c^2 \left(1 + \frac{E - V_0(r)}{M_{\text{Nuc}} c^2} - \frac{\hbar^2 c^2}{4M_{\text{Nuc}}^2 c^4}\right)} \right] \phi_l(r) = 0
 \end{aligned}$$

Let

$$\text{L8} \quad \delta \equiv \frac{2i}{\hbar c} \left[ \frac{E^2 - M_{\text{Nuc}}^2 c^4}{1 + \frac{E - V_0(r)}{M_{\text{Nuc}} c^2} - \frac{\hbar^2 c^2}{4M_{\text{Nuc}}^2 c^4}} \right]^{1/2}$$

$$\text{L9} \quad i\eta \equiv \frac{2Ez\alpha}{\delta\hbar c} \frac{1}{1 + \frac{E - V_0(r)}{M_{\text{Nuc}} c^2} - \frac{\hbar^2 c^2}{4M_{\text{Nuc}}^2 c^4}}$$

Substituting these definitions into equation L7 obtain

$$\begin{aligned}
 \text{L10} \quad \phi_l''(r) + & \left[ -\frac{\delta^2}{4} + \frac{i\eta\delta}{r} - \frac{l(l+1)}{r^2} \right. \\
 & \left. + \frac{z^2 \alpha^2}{r^2} \frac{1}{1 + \frac{E - V_0(r)}{M_{\text{Nuc}} c^2} - \frac{\hbar^2 c^2}{4M_{\text{Nuc}}^2 c^4}} \right] \phi_l(r) = 0
 \end{aligned}$$

Dividing by  $\delta^2$ , letting  $\rho = \delta r$ , and replacing  $\phi_l(r)$  by  $\phi_l(\rho)$  obtain

$$\text{L11} \quad \phi_l''(\rho) + \left[ -\frac{1}{4} + \frac{i\eta}{\rho} - \frac{l(l+1) - z^2 \alpha^2 / \left(1 + \frac{E - V_0(r)}{M_{\text{Nuc}} c^2} - \frac{\hbar^2 c^2}{4M_{\text{Nuc}}^2 c^4}\right)}{\rho^2} \right] \phi_l(\rho) = 0$$

Equation L11 resembles Whittaker's equation which has the form <sup>136</sup>

$$L12 \quad W_\lambda''(e) + \left[ -\frac{1}{4} + \frac{i\eta}{e} + \frac{\frac{1}{4} - \mu^2}{e^2} \right] W_\lambda(e) = 0$$

According to Whittaker and Watson <sup>143</sup> the solution to this equation has the form

$$L13 \quad W_\lambda(e) = F_\lambda(e) \cos \nu_\lambda + G_\lambda(e) \sin \nu_\lambda$$

where  $F_\lambda(e)$  and  $G_\lambda(e)$  are the regular and irregular Coulomb wavefunctions respectively, and  $\nu_\lambda$  is the phase shift. The normalized Coulomb wavefunctions may be defined by <sup>26</sup>

$$L14 \quad F_\lambda(e) = \sqrt{\frac{2}{\pi}} \frac{Y_\lambda(e) + Y_\lambda^*(e)}{2} = \sqrt{\frac{2}{\pi}} \text{Real}(Y_\lambda(e))$$

$$L15 \quad G_\lambda(e) = \sqrt{\frac{2}{\pi}} \frac{Y_\lambda(e) - Y_\lambda^*(e)}{2i} = \sqrt{\frac{2}{\pi}} \text{Imaginary}(Y_\lambda(e))$$

where

$$L16 \quad Y_\lambda(e) \equiv i e^{-i\nu_\lambda} e^{i\pi\lambda/2} e^{\eta\pi/2} e^{-e/2} e^m \Psi(m - i\eta, 2m, e)$$

$$L17 \quad e^{2i\nu_\lambda} \equiv \Gamma(\lambda + 1 + i\eta) / \Gamma(\lambda + 1 - i\eta)$$

$$L18 \quad m = \mu + \gamma_0$$

$$L19 \quad \mu = \frac{1}{2} \left[ (2\lambda + 1)^2 - 4z^2\alpha^2 / \left( 1 + \frac{E - \mathcal{K}(V)}{M\mu c^2} - \frac{\hbar^2 c^2}{4M\mu^2 c^4} \right) \right]^{1/2}$$

$\nu_\lambda$  is the Coulomb phase factor and  $\Psi(m - i\eta, 2m, e)$  is the confluent hypergeometric function of the second kind. <sup>142</sup>

From L13 one may write an expression for  $W_\lambda'(e)$ , i.e.

$$L20 \quad W_\lambda'(e) = F_\lambda'(e) \cos \nu_\lambda + G_\lambda'(e) \sin \nu_\lambda$$

Dividing equation I20 by I13, one obtains an expression for the logarithmic derivative  $\gamma_l(e)$

$$I21 \quad \gamma_l(e) \equiv \frac{W_l'(e)}{W_l(e)} = \frac{F_l'(e) + \tan \nu_l G_l'(e)}{F_l(e) + \tan \nu_l G_l(e)}$$

Equation I21 may be solved for  $\tan \nu_l$  to obtain

$$I22 \quad \tan \nu_l = \frac{\gamma_l(e) F_l(e) - F_l'(e)}{-\gamma_l(e) G_l(e) + G_l'(e)}$$

Since the energy of the pion is known when solving equation I5, one can simply integrate numerically from the origin out to the boundary  $e = e_0$  between the interior and exterior regions. Near the origin one uses the boundary conditions

$$I23 \quad \phi_l(e) \stackrel{e \ll 1}{=} e^{l+1}$$

$$I24 \quad \phi_l'(e) \stackrel{e \ll 1}{=} \frac{l+1}{e} \phi_l(e)$$

to start the integration.

The value of  $\phi_l(e)$  is not properly normalized by this procedure, but the boundary conditions at  $e = e_0$  may be used to normalize  $\phi_l(e)$ . Using the numerical solution for  $\phi_l(e)$  and  $\phi_l'(e)$  at  $e = e_0$ , one can evaluate the logarithmic derivative  $\gamma_l(e_0)$ , i.e.

$$I25 \quad \gamma_l(e_0) = \left. \frac{\phi_l'(e)}{\phi_l(e)} \right|_{e=e_0}$$

From I22  $\tan \nu_l$  may be obtained. Once  $\tan \nu_l$  is known the normalized wavefunction may be constructed at  $e = e_0$  from

$$I26 \quad N_l \phi_l(e_0) = F_l(e_0) \cos \nu_l + G_l(e_0) \sin \nu_l$$

$$127 \quad \sin \nu_\ell = \left[ \gamma_\ell(\epsilon) F_\ell(\epsilon) - F_\ell'(\epsilon) \right] / P \Big|_{\epsilon=\epsilon_0}$$

$$128 \quad \cos \nu_\ell = \left[ -\gamma_\ell(\epsilon) G_\ell(\epsilon) + G_\ell'(\epsilon) \right] / P \Big|_{\epsilon=\epsilon_0}$$

$$129 \quad P = \left[ (-\gamma_\ell(\epsilon) F_\ell(\epsilon) + F_\ell'(\epsilon))^2 + (\gamma_\ell(\epsilon) G_\ell(\epsilon) - G_\ell'(\epsilon))^2 \right]$$

The method of Appendix H is used to calculate the pion-nucleus differential cross section from the set of phase shifts  $\nu_\ell$  obtained above. Then the cross section is averaged over the finite angular resolution of the physical detector using the method given in Appendix I. These cross sections may then be compared to the experimental data as is done in this work.

It is also possible to vary the parameters in the pion-nucleus strong interaction potential to fit the pion-nucleus differential scattering cross section data at various energies. Then these energy dependent best fit parameters may be compared to those predicted from  $\pi N$  and  $\pi NN$  interaction amplitudes.

In order to obtain a set of pion-nucleus strong interaction potential parameters that will fit the experimentally observed pion-nucleus differential scattering cross section data, it is desirable to perform some sort of weighted or constrained least squares fit to the data. Since the differential cross section is a nonlinear function of the potential parameters and the parameters are strongly correlated, most nonlinear least square fitting procedures are not suitable. The most satisfactory procedure this investigator has found is to use an ordered nonlinear least square fit in which the variables are fit two at a time. By carefully choosing the order in which the variables are

fit to be  $\text{Real}(c_0)$ ,  $\text{Imaginary}(c_0)$ ,  $\text{Real}(b_0)$ ,  $\text{Imaginary}(b_0)$ , and finally the overall normalization of the data, one can to a large extent remove the effect of correlations between the parameters and obtain fitted values in agreement with theoretical values. The program for doing this is given in Appendix M, but the results of this procedure are not presented in this work.

## APPENDIX M

### Fortran Computer Program

For Solving the Klein-Gordon Equation for Pion-Nucleus Scattering  
And Calculating the Elastic Differential Scattering Cross Section

In this appendix is listed the actual Fortran computer program used to predict the pion-nucleus elastic differential scattering cross sections for  $T_{\pi} \leq 280$  MeV. The notation in the program conforms closely to that of Appendixes F and L. Due to the extensive comments one can easily follow the logic of the program.

This program will also perform a least squares fit on the parameters in the potential if one removes the appropriate

GO TO 1

card from the main program. Due to the strong correlation of the parameters in the potential, this least square fitting program may give spurious results.

```

IMPLICIT REAL*8(A-Z)
INTEGER INTRVL,N,L,NUM,NL,LW,I,NP,J,K,IPIP,M1(4),L1(4),INDEX,IFIG
DIMENSION YK(40),UNC(40),THETA(40),DTHETA(40),X(4),VC(61),RHO(61),
1DRHO(61),DDRHO(61),FK0(40),FK1(40),DFKX(4,40),M(4,4),F(4),DX(4),UN
2CDX(4),DELTA(4)
COMMON VC,RHO,DRHO,DDRHO,YK,UNC,THETA,DTHETA,Z,A,S,MASS,EL,RO,RU,R
1BO,IBO,RB1,IB1,RCO,ICO,RC1,IC1,RDO,IDO,RD1,IDI,NORM,NUM,NL,INTRVL,
2N,LW,NP,INDEX,IFIG
IFIG = IFIG+1

C
C READ IN INFORMATION ON NUCLEUS AND DIFFERENTIAL SCATTERING CROSS
C SECTION
C
C
IFIG = 18
NP = 4
900 READ(5,900) INTRVL,N,(DELTA(I),I = 1,NP)
    FORMAT(I3,I3,5D10.3)
901 WRITE(6,901) INTRVL,N,(DELTA(I),I = 1,NP)
    FORMAT(' INTRVL = ',I3,' N = ',I3/' DELTA = ',D10.3)
    NORM = 1.00
1 READ(5,906) RBO,IBO,RB1,IB1,RCO,ICO,RC1,IC1,RDO,IDO,RD1,IDI
    IF(RHO.EQ.0.D0) GO TO 1000
    IFIG = IFIG+1
906 FORMAT(1X,4D14.7)
907 WRITE(6,907) RBO,IBO,RB1,IB1,RCO,ICO,RC1,IC1,NORM,RDO,IDO,RD1,IDI
    FORMAT(4X,'RBO',8X,'IBO',8X,'RB1',8X,'IB1',8X,'RCO',8X,'ICO',8X,'R
1C1',8X,'IC1',8X,'NORM',1X,9(D10.3,1X)/4X,'RDO',8X,'IDO',8X,'RD1',
28X,'IDI',1X,4(D10.3,1X))
902 READ(5,902) NUC,Z,A,S,L,MASS,EL,R,RO,CC,CCC
    FORMAT(A6,D7.1,D8.2,D7.1,12,D13.8,D9.3,D10.3,D9.3,D9.3/D9.3)
903 WRITE(6,903) NUC,Z,A,S,L,MASS,EL,R,RO,CC,CCC
    FORMAT(' NUC.',6X,'Z',9X,'A',7X,'S',6X,'L',6X,'MASS',9X,'EL',9X,'R
1',10X,'RO',9X,'CC',9X,'CCC',1X,A6,D9.2,1X,D8.2,1X,D8.2,1X,D8.2,1X,D1
24.8,1X,D9.3,1X,D11.5,1X,D9.3,1X,D10.3,1X,D10.3)
904 READ(5,904) NUM,NL,LW,(YK(I),UNC(I),THETA(I),DTHETA(I),I=1,NUM)
    FORMAT(3I2/(1X,4(D10.3,1X)))

```

```

905 WRITE(6,905) NUM,NL,LW,(YK(I),UNC(I),THETA(I),DTHETA(I),I=1,NUM)
    FORMAT(' NUM = ',I3,' NL = ',I3,' LW = ',I3/3X,'DSIGMA',6X,'UNC',8
    1X,'THETA',7X,'DTHETA',/(1X,4(D10.3,1X)))
    INDEX = 0
    INDEX = 5
    X(1) = 1.00
    X(2) = 1.00
    X(3) = 1.00
    X(4) = 1.00
    IF(A.EQ.4.D1) CALL POT(RO,CC,R,CCC,RO,Z,VC,RHO,DRHO,DDRHO,N,INTRVL
    1,RU,A)
    IF(R.EQ.0.D0) CALL POTMHO(CC,CCC,A,RO,Z,VC,RHO,DRHO,DDRHO,N,INTRVL
    1,RU)
    IF(A.EQ.4.D0) CALL POTHE4( Z,RO,VC,RHO,DRHO,DDRHO,N,INTRVL,RU)
    WRITE(6,6) Z,A
    6  FORMAT(' Z = ',D14.7,' A = ',D14.7)
    CALL EVAL(FKO,CH10,X)
    GO TO 1
    5  DO 10 I = 1,NP
        X(I) = X(I)*(1.D0+DELTA(I))
        NP = 0
        CALL EVAL(FK1,CHI2,X)
        NP = 4
        X(I) = X(I)/(1.D0+DELTA(I))
    10 DO 10 J = 1,NUM
        DFKX(I,J) = (FK1(J)-FK0(J))/(X(I)*DELTA(I))
    C
    C
    C
    CONSTRUCT THE SYMMETRIC MATRIX M FOR NORMAL EQUATIONS AND F
    DO 20 I = 1,NP
    F(I) = 0.D0
    DO 15 J = 1,NUM
    F(I) = F(I)+(YK(J)-FK0(J))*DFKX(I,J)/UNC(J)**2
    15 DO 20 K = 1,NP
    M(I,K) = 0.D0
    DO 16 J = 1,NUM

```

```

16 M(I,K) = M(I,K)+DFKX(I,J)*DFKX(K,J)/UNC(J)**2
20 CONTINUE
   NPNP = NP*NP
   CALL MINV(M,NP,D,M1,L1,NPNP)
C
C   CONSTRUCT VECTOR OF CORRECTIONS TO INITIAL GUESS
C
D0 21 J = 1 ,NP
UNCDX(J) = DSORT(M(J,J))
D0 25 J = 1,NP
DX(J) = 0.D0
D0 25 I = 1,NP
DX(J) = DX(J)+M(J,I)*F(I)/3.D0
D0 30 J = 1,NP
IF(-DX(J)/X(J).GT.1.D0) DX(J) = -X(J)/2.D0
X(J) = X(J)+DX(J)
WRITE(6 ,913) (X(J),UNCDX(J),J=1,NP)
913 FORMAT(' R80 = ',D14.7,' +- ',D14.7,' I80 = ',D14.7,' +- ',D14.7,'
1 RCO = ',D14.7,' +- ',D14.7,' ICO = ',D14.7,' +- ',D14.7,' NORM =
2 ',D14.7,' +- ',D14.7/')
CALL EVAL(FKO,CHI20,X)
B0 = R80*X(1)
UNB0 = R80*UNCDX(1)
B2 = I80*X(2)
UNB2 = I80*UNCDX(2)
C0 = RCO*X(3)
UNCO = RCO*UNCDX(3)
C2 = ICO*X(4)
UNC2 = ICO*UNCDX(4)
IF(DABS(CHI20-CHI0).LT..01D0.OR.INDEX.GT.4) GO TO 1
CHI0 = CHI20
INDEX = INDEX+1
GO TO 5
1000 STOP
END

```

```

SUBROUTINE POTMHO(W,B,A,RO,Z,VC,VST,DVST,DDVST,M,INTRVL,RU)
IMPLICIT REAL*8(A-H,O-S),INTEGER(I-N)
DIMENSION VST(M),DVST(M),DDVST(M),VC(M)

C
C   INITIALIZATION OF PARAMETERS
C
AP = DSORT(2.00/3.00)*.7200
RU = DSORT((5.00/3.00)*H*B*((DABS(Z)-2.00)/DABS(Z)+1.500))
BB = DSORT(B*B-AP*AP)
PI = 3.1415926535900
HBARC = 197.3200
ZALPHA = Z/137.038800
VSNORM = 2*A/(PI**1.500*BB**3*(2.00+3.00*W))
VCNORM = -2.00*ZALPHA*HBARC/(DSORT(PI)*B)

C
C   CALCULATION OF THE STRONG INTERACTION DENSITY VST AND ITS
C   DERIVATIVES DVST AND DDVST.
C
TOL = 1.0D-6
DO 20 N = 1,M
EPS = (N-1.00)/(INTRVL*1.00)+1.0D-6
R2BB2 = (RO*EPS/BB)**2
VST( N) = VSNORM*(1.00+1.500*W*(1.00-(B/BB)**2)+W*(B/BB)**2*R2BB2)
1*DEXP(-R2BB2)
DK2BB2 = 2.00*RO*EPS/BB**2
DVST( N) = -VSNORM*DK2BB2*(1.00+1.500*W-2.500*W*(B/BB)**2+W*(B/BB
1)**2*R2BB2)*DEXP(-R2BB2)
DDR2BB2 = 2.00/BB**2
DDVST( N) = -VSNORM*((DDR2BB2-DR2BB2**2)*(1.00+1.500*W-2.500*W*(B/B
1B)**2+W*(B/BB)**2*R2BB2)+DK2BB2**2*W*(B/BB)**2)*DEXP(-R2BB2)

C
C   CALCULATION OF THE COULOMB POTENTIAL
C
R2B2 = (RO*EPS/B)**2

```

```

TERM = 1.00
SUM = TERM
K = 3
10  TERM = TERM*2.00*R2R2/K
    SUM = SUM+TERM
    K = K+2
    IF(DABS(TERM/SUM).GT.TOL) GO TO 10
    VC( N) = VCNORM*(-W/(2.00+3.00*W)+SUM)*DEXP(-R2B2)
20  RETURN
    END

SUBROUTINE POTHE4( Z,RO,VC,RHO,DRHO,DDRHO,M,INTRVL,RU)
IMPLICIT REAL*8(A-H,O-Z), INTEGER(I-N)
DIMENSION RHO(M),DRHO(M),DDRHO(M),VC(M)

C
C  INITIALIZATION OF PARAMETERS
C
AP = DSQRT(2.00/3.00)*.7200
AO = .31600
BO = 1.36200
BB = DSQRT(BO*BO-AP*AP)
PI = 3.1415926535900
HBARC = 197.3200
ZALPHA = Z/137.038800
TOL = 1.0-6
A = 1.00-64.00*(AO/BO)**12*135135.00
B = 64.00*(AO/BO)**12*540540.00
C = -B
D = 64.00*(AO/BO)**12*205920.00
E = -64.00*(AO/BO)**12*34320.00
F = 64.00*(AO/BO)**12*2496.00
G = -64.00*(AO/BO)**12*64.00
RU = DSQRT((5.00/3.00)*(1.6700**2-AP**2))
C

```

```

C      CALCULATION OF THE STRONG INTERACTION DENSITY RHO AND ITS
C      DERIVATIVES DRHO AND DDRHO
C
R NORM = 2.00/(DSQRT(PI)*RB)**3
VCNORM = -2.00*ZALPHA*HBARC/DSQRT(PI)
DO 20 N = 1,M
EPS = (N-1.00)/(INTRVL*1.00)+1.0-6
R2B2 = (RO*EPS/RB)**2
RHO(N) = R NORM*DEXP(-R2B2)*(1.00-64.00*(AO/RB)**12*(135135.00-540
1540.00*R2B2+540540.00*R2B2**2-205920.00*R2B2**3+34320.00*R2B2**
2*4-2496.00*R2B2**5+64.00*R2B2**6))
DRHO(N) = -2.00*RO*EPS/RB**2*RHO(N)-128.00*DEXP(-R2B2)/((DSQRT(PI
1)*RB)**3*RO*EPS)*(-2.00*540540.00*R2B2+4.00*540540.00*R2B2**2-6.
200*205920.00*R2B2**3+8.00*34320.00*R2B2**4-10.00*2496.00*R2B2**
35+12.00*64.00*R2B2**6)*(AO/RB)**12
DDRHO(N) = -2.00/RB**2*(2.00*RO*EPS*DRHO(N)+(1.00+2.00*R2B2)*RHO(
1N)+64.00*DEXP(-R2B2)/(DSQRT(PI)*RB)**3*(-2.00*540540.00+12.00*540
2540.00*R2B2-30.00*205920.00*R2B2**2+56.00*34320.00*R2B2**3-90.00
30*2496.00*R2B2**4+132.00*64.00*R2B2**5)*(AO/RB)**12)

C      CALCULATION OF THE COULOMB POTENTIAL
C
RB = RO*EPS/BO
R2B2 = RB**2
TERM = RB
SUM = TERM
K = 3
10  TERM = TERM*2.00*R2B2/K
    SUM = SUM+TERM
    K = K+2
    IF(DABS(TERM/SUM).GT.TOL) GO TO 10
20  VC(N) = VCNORM*DEXP(-R2B2)/(RO*EPS)*((A+3.00*B/2.00+15.00*C/4.00+1
105.00*D/8.00+946.00*E/16.00+10395.00*F/32.00+135135.00*G/64.00)*SU
2M-(B/2.00+7.00*C/4.00+57.00*D/8.00+ 561*E/16.00+6555.00*F/32.00+1
312095.00*G/64.00)*KH-(C/2.00+11.00*D/4.00+123.00*E/8.00+1545.00*F/
416.00+22005.00*G/32.00)*RH**3-(D/2.00+15.00*E/4.00+213.00*F/8.00+3

```

```

5249.D0*G/16.D0)*RB**5-(E/2.D0+19.D0*F/4.D0+327.D0*G/8.D0)*RB**7-(F
6/2.D0+23.D0*G/4.D0)*RB**9-G/2.D0*RB**11)
RETURN
END

```

```

SUBROUTINE POT(R0,CO,R,C,RR,Z,VC,VST,DVST,DDVST,M,INTRVL,RU,A)
REAL*8 RO,CO,R,C,Z,VC(M),VST(M),PI,SUM,DE1,DE2,TERM,TERM1,TERM2,
1TERM3,HBARC,ZALPHA,VSNORM,VCNORM,EPS,SUMM,TERMM,RU,NN, DEXP,DSQRT
2,DABS,DVST(M),DDVST(M),EX,A,RR

```

```

C
C CALCULATION OF THE STRONG INTERACTION POTENTIAL NORMALIZATION
C CONSTANT VSNORM
C

```

```

PI = 3.14159265359D0
SUM = 0.D0
SUMM = 0.D0
DE1 = -DEXP(-RO/CO)
TERM1 = DE1
NN = 1.D0
TERMM = TERM1/NN**5
SUMM = SUMM+TERMM
TERM = TERM1/NN**3
SUM = SUM+TERM
TERM1 = TERM1*DE1
NN = NN+1.D0

```

```

IF(DABS(TERMM/SUMM).GT.1.D-6) GO TO 2
IF(DABS(TERM/SUM).GT.1.D-6) GO TO 6
VSNORM = A/(4.D0*PI*(PI*PI*CO*RO/3.D0+RO**3/3.D0-2.D0*CO**3*
1SUM))

```

```

RU = DSQRT(5.D0/3.D0*(RO**5/5.D0+2.D0/3.D0*CO*CO*PI*PI*RO**3+7.D0/
115.D0*(CO*PI)**4*RO-24.D0*CO**5*SUMM)*VSNORM**4.D0*PI/A)

```

```

C
C CALCULATION OF COULOMB POTENTIAL NORMALIZATION CONSTANT VCNORM
C

```

```

HBARC = 197.32D0
ZALPHA = Z/137.0388D0
SUM = 0.D0
DE1 = -DEXP(-R/C)
TERM1 = DE1
NN = 1.D0
TERM = TERM1/NN**3
SUM = SUM+TERM
TERM1 = TERM1*DE1
NN = NN +1.D0
IF(DABS(TERM/SUM).GT.1.D-15) GO TO 20
VCNORM = -ZALPHA*HBARC/(PI*PI*C*C*R/3.D0+R**3/3.D0-2.D0*C**3*SUM)

```

20

CALCULATION OF NORMALIZED POTENTIALS

C C C

```

DO 80 N = 1,M
EPS = (N-1.D0)/(INTRVL*1.D0)+1.D-6
VST( N) = VSNORM/(1.D0+DEXP((EPS-1.D0)*RO/CO))
EX = DEXP((EPS-1.D0)*RO/CO)
DVST( N) = -VST( N)/CO*EX/(1.D0+EX)
IF( N.EQ.1) DVST( N) = 0.D0
DDVST( N) = DVST( N)/CO*(1.D0-2.D0*EX/(1.D0+EX))
IF( N.EQ.1) DDVST( N) = 0.D0
IF(EPS.GT.R/RO) GO TO 60

```

30 40

COULOMB POTENTIAL FOR EPS\*RO<R

C C C

```

SUM = 0.D0
NN = 1.D0
DE1 = -DEXP(-R/C)
DE2 = -DEXP((RO*EPS-R)/C)
TERM1 = -2.D0*C**3/(RO*EPS)*DE1
TERM2 = -C*C*DE2
TERM3 = 2.D0*C**3/(RO*EPS)*DE2
TERM = TERM1/NN**3+TERM2/NN**2+TERM3/NN**3
SUM = SUM+TERM

```

50

```

IF(DABS(TERM1/(NN**3*SUM)).LT.1.D-15) TERM1 = 0.00
TERM1 = TERM1*DE1
IF(DABS(DE2).LT.1.D-15) DE2 = 0.00
TERM2 = TERM2*DE2
TERM3 = TERM3*DE2
NN = NN+1.00
IF(DABS(TERM/SUM).GT.1.D-08) GO TO 50
VC( N) = VCNORM*(R**R/2.00-(EPS*RO)**2/6.00+C*C*PI*PI/6.00+SUM)
GO TO 80

C
C COULOMB POTENTIAL FOR EPS*RO > R
C
60 SUM = 0.00
NN = 1.00
DE1 = -DEXP(-R/C)
DE2 = -DEXP(-(EPS*RO-R)/C)
TERM1 = -2.00*C**3*DE1
TERM2 = C*C*EPS*RO*DE2
TERM3 = 2.00*C**3*DE2
TERM = TERM1/NN**3+TERM2/NN**2+TERM3/NN**3
SUM = SUM+TERM
70 IF(DABS(TERM1/(NN**3*SUM)).LT.1.D-15) TERM1 = 0.00
TERM1 = TERM1*DE1
IF(DABS(DE2).LT.1.D-15) DE2 = 0.00
TERM2 = TERM2*DE2
TERM3 = TERM3*DE2
NN = NN + 1.00
IF(DABS(TERM/SUM).GT.1.D-08) GO TO 70
VC( N) = VCNORM*(R**3/3.00+C*C*PI*PI*R/3.00+SUM)/(EPS*RO)
CONTINUE
RETURN
END

80

```

SUBROUTINE EVAL(AIB,NCHI2,PP)

```

IMPLICIT REAL*8 (A-Z)
INTEGER I,J,K,L,N,IJ,JJ,INTRVL,KK,KS,MO,MM,LL,NUM,NV,NL,LW,NP,INDE
IX,IFIG,IA,IFIX
LOGICAL#1 SIGN1,SIGN2
REAL#4 AIM(150),SINGL
COMPLEX#16 AK(61),ANON(61),O(61),RNL,CDSQRT,DCMPLX,LNDER,ALBL,AL(1
10),CDEXP,ETA,UN,II,M,DELTA,W,YL,DYL,CDLOG,COPSI,SUMH,CDGMMA, SA
2(10),EXPSIG,TSA,CFC(40),CRHO,SINVL,COSVL,DN,L1
DIMENSION VC(61),RHO(61),FR(61),FI(61),X(4,5),XO(4,2),X1(4
1),IH(2),H(2,2),C(4),UR(61),UI(61),DUR(61),DUI(61),RL(2),AI(40),UNC
2(40),THETA(40),COSB(40),SIN2H2(40),JBL(40),AIB(40),AIL(40),Y(2),DY
3(2),SUM(2),DRHO(61),DDRHO(61),P(10),PP(4),DTHETA(40),SIN(2),COS(2)
4,RF(61),DSIGMA(40),DELSIG(40)
COMMON VC,RHO,DRHO,DDKHO,DSIGMA,DELSIG,THETA,DTHETA,Z,A,S,MASS,E,
IRO,RU,RBO,IHO,RH1,IR1,RCO,ICO,RC1,IC1,RDO,IDO,RD1,IDI,NOR,NUM,NL,
2INTRVL,N,LW,NP,INDEX,IFIG
EQUIVALENCE (RNL,RL(1)),(YL,Y(1)),(DYL,DY(1)),(SUMM,SUM(1))
EQUIVALENCE (SINVL,SIN(1)),(COSVL,COS(1))
DATA SIGN1,SIGN2/'-','+'
B0 = RBO*PP(1)
B2 = IRO*PP(2)
C0 = RCO*PP(3)
C2 = ICO*PP(4)
NORM = NOR
IF(NP.GT.0) WRITE(6,951) B0,B2,C0,C2,NORM
FORMAT(' ENTERING EVAL RBO = ',D14.7,' IBO = ',D14.7,' RCO = ',D14
1.7,' ICO = ',D14.7,' NORM = ',D14.7)
B11 = .077D0
R00 = 0.0D0
B01 = .054D0
B02 = 0.0D0
G21 = .5D0
G01 = .5D0
G10 = .5D0
G12 = .0D0
G1101 = .0D0
951

```



```

C
T = (A-2.D0*DABS(Z))/2.D0
MN = (938.256D0+939.550D0)/2.D0
HBARC = 197.32D0
ZALPHA = Z/137.0388D0

C
TRANSFORMATION OF ENERGY TO BARYCENTRIC COORDINATE SYSTEM FOR
KLEIN-GORDON EQUATION
C
C
M1 = MPI
M2 = AMASS
EL = E +M1+M2
EB = DSORT(M1**2-M2**2+2.D0*M2*EL)
KC = M2*DSORT(EL**2/EB**2-1.D0)
E1K = DSORT(KC**2+M1**2)
E2K = DSORT(KC**2+M2**2)
KVRELB = (EB-M2+((EB-M2)**2+M1**2)/(2.D0*M2))/(1.D0+(EB-M2-VC(N))/
1M2-KC**2/(4.D0*M2**2))**2
ER = EB-M1-M2
EI = 0.D0
IF(NP.GT.0) WRITE(6,904) EL,EB,KC,E1K,E2K,ER,EI

C
INITIALIZE PARAMETERS FOR DEFINING THE KLEIN-GORDON EQUATION
C
C
N1 = 1.D0+(MPI+E)/MN
N2 = 1.D0+(MPI+E)/(2.D0*MN)
PI = 3.14159265359D0
UN = (1.D0,0.D0)
II = (0.D0,1.D0)
CPW = HBARC/MPI
SR = RO/INTRVL
XSISJ = 4.D0*S*(S+1.D0)/(A*(A-1.D0))-3.D0/(A-1.D0)
XTITJ = 4.D0*T*(T+1.D0)/(A*(A-1.D0))-3.D0/(A-1.D0)
XTITT = 8.D0*T*T/(A*(A-1.D0))+4.D0*(T-1.D0)/(A-1.D0)
XTT = 4.D0*T/A
XRIJ = 4.D0*PI*N2*(RBO+RBI*XSISJ+B82*XTITJ+B83*(1.D0-XSISJ)*XTT+

```

1BB4\*XSISJ\*XTITJ+BB5\*(1.D0-XSISJ)\*XTTIT)\*CPW\*\*4  
 XBJI = 4.D0\*PI#N2#RBB0\*CPW\*\*4  
 XCIJ = 4.D0\*PI/N2\*(C0+CC1\*XSISJ+CC2\*XTITJ+CC3\*(1.D0-XSISJ)\*XTT+  
 1CC4\*XSISJ\*XTITJ+CC5\*(1.D0-XSISJ)\*XTTIT)\*CPW\*\*6  
 XCJI = 4.D0\*PI/N2#RCC0\*CPW\*\*6  
 XBI = 4.D0\*PI\*N1\*(B0+2.D0\*RB1#T/A)\*CPW  
 XB2 = 4.D0\*PI\*N1\*(B2+2.D0\*IB1#T/A)\*CPW  
 XCI = 4.D0\*PI/N1\*(C0+2.D0\*RC1#T/A)\*CPW\*\*3  
 XC2 = 4.D0\*PI/N1\*(C2+2.D0\*IC1#T/A)\*CPW\*\*3  
 PF = HBARC\*(9.D0/8.D0\*PI#A/RU\*\*3)\*\*(1.D0/3.D0)  
 XBIBIR = -6.D0\*PF/MPI\*((A-4.D0)/A\*(B0\*B0-B2\*B2+2.D0\*(B0\*RB1-B2\*IB1  
 1)\*((1.D0-2.D0\*Z/A))+2.D0\*(RB1\*RB1-IB1\*IB1)\*(A-2.D0)/A)\*CPW  
 XRBIR = -6.D0\*PF/MPI\*((A-4.D0)/A\*(2.D0\*B0\*B2+4.D0\*(B0\*IB1+B2\*RB1)  
 1\*(1.D0-2.D0\*Z/A))+4.D0\*RB1\*IB1\*(A-2.D0)/A)\*CPW  
 XBICIR = +2.D0\*PF/MPI\*((A-4.D0)/A\*(B0\*C0-B2\*C2+(B0\*RC1-B2\*IC1+C0\*R  
 1B1-C2\*IB1))\*(1.D0-2.D0\*Z/A))+2.D0\*(RB1\*RC1-IB1\*IC1)\*(A-2.D0)/A)\*CPW  
 3\*\*3  
 XBICII = +2.D0\*PF/MPI\*((A-4.D0)/A\*(B2\*C0+B0\*C2+(B0\*IC1+B2\*RC1+RB1\*  
 1C2+IB1\*C0))\*(1.D0-2.D0\*Z/A))+2.D0\*(RB1\*IC1+IB1\*RC1)\*(A-2.D0)/A)\*CPW  
 2\*\*3  
 XCICIR = -4.D0\*PI\*4.D0\*PI/3.D0\*(C0\*C0-C2\*C2)\*CPW\*\*6  
 XCICIR = -4.D0\*PI\*PI/3.D0\*((A-4.D0)/A\*(C0\*C0-C2\*C2+2.D0\*(RDO\*RDO-  
 1ID0\*ID0)+2.D0\*(C0\*RC1-C2\*IC1+2.D0\*(RDO\*RD1-ID0\*ID1))\*(1.D0-2.D0\*Z/  
 2A))+2.D0\*(RC1\*RC1-IC1\*IC1+2.D0\*(RDO\*RD0-ID0\*ID0))\*(A-2.D0)/A)\*CPW\*  
 3\*6\*A/(4.D0\*PI/3.D0\*RU\*\*3)  
 3\*6  
 XCICII = -4.D0\*PI\*4.D0\*PI/3.D0\*2.D0\*C0\*C2\*CPW\*\*6  
 XCICII = -4.D0\*PI\*PI/3.D0\*((A-4.D0)/A\*2.D0\*(C0\*C2+2.D0\*RDO\*ID0+2.D  
 10\*(C0\*IC1+C2\*RC1+2.D0\*(RDO\*ID1+ID0\*RD1))\*(1.D0-2.D0\*Z/A))+4.D0\*(RC  
 21\*IC1+2.D0\*RD1\*ID1)\*(A-2.D0)/A)\*CPW\*\*6\*A/(4.D0\*PI/3.D0\*RU\*\*3)  
 21\*IC1+2.D0\*RD1\*ID1)\*(A-2.D0)/A)\*CPW\*\*6  
 XBCR = -8.D0\*PF/MPI\*((A-4.D0)/A\*(B0\*C0-B2\*C2+(B0\*RC1+RB1\*C0-B2\*IC1  
 1-IB1\*C2))\*(1.D0-2.D0\*Z/A))+2.D0\*(RB1\*RC1-IB1\*IC1)\*(A-2.D0)/A)\*CPW\*\*  
 23  
 XBCI = -8.D0\*PF/MPI\*((A-4.D0)/A\*(B0\*C2+B2\*C0+(B0\*IC1+RB1\*C2+B2\*RC1  
 1+IB1\*C0))\*(1.D0-2.D0\*Z/A))+2.D0\*(RB1\*IC1+IB1\*RC1)\*(A-2.D0)/A)\*CPW\*\*

C

C

23

```

XCIQR = (ER+MPI)/MN*XCI*N1*.5D0
XCIQI = (ER+MPI)/MN*XC2*N1*.5D0
XBICIR = 0.D0
XBICII = 0.D0
XBCR = 0.D0
XBCI = 0.D0
L = 0
DO 43 K = 1,N
EPS = (K-1)/(INTRVL*1.D0)+1.D-6
FAC = 1.D0+(EB-M2-VC(K))/M2-KC**2/(4.D0*M2**2)
AKR = -XCI*RHO(K)-(XCJI+XCICIR+XBCR/RHO(K))*RHO(K)**2
AKR = -(XCI+XCICIR)*RHO(K)
AKI = -XC2*RHO(K)-(XCJI+XCICII+XBCI/RHO(K))*RHO(K)**2
AKI = -(XC2+XCICII)*RHO(K)
AK(K) = DCPLX(AKR,AKI)
DAKR = -XCI*DRHO(K)-(XCJI+XCICIR+XBCR/RHO(K))*2.D0*RHO(K)*DRHO(K)
DAKR = -(XCI+XCICIR)*DRHO(K)
DAKI = -XC2*DRHO(K)-(XCJI+XCICII+XBCI/RHO(K))*2.D0*RHO(K)*DRHO(K)
DAKI = -(XC2+XCICII)*DRHO(K)
DDAKR = -XCI*DDRHO(K)-(XCJI+XCICIR+XBCR/RHO(K))*2.D0*(RHO(K)*DDRHO
1(K)+DRHO(K)**2)
DDAKR = -(XCI+XCICIR)*DDRHO(K)
DDAKI = -XC2*DDRHO(K)-(XCJI+XCICII+XBCI/RHO(K))*2.D0*(RHO(K)*DDRHO
1(K)+DRHO(K)**2)
DDAKI = -(XC2+XCICII)*DDRHO(K)
DEN = (FAC +AKR)**2+AKI**2
RE1 = (FAC +AKR)/DEN
IM1 = -AKI/DEN
RE2 = ((FAC +AKR)*(DAKR**2-DAKI**2)+2.D0*DAKR*DAKI*AKI)/DEN
IM2 = ((FAC +AKR)*2.D0*DAKR*DAKI-AKI*(DAKR**2-DAKI**2))/DEN
ANONR = -DAKR/(EPS*RO)-DDAKR/2.D0+.25D0*RE2
ANONI = -DAKI/(EPS*RO)-DDAKI/2.D0+.25D0*IM2
ANON(K) = -HBARC**2/(2.D0*RMAS)*DCPLX(ANONR, ANONI)
OR = -(XBI+XBIBIR)*RHO(K)-XRJI*RHO(K)**2-(XBICIR+XCIQR)*(DDRHO(K)+
12.D0/(RO*EPS)*DRHO(K))-XBICIR*DRHO(K)**2/RHO(K)

```

```

43 QI = -(XB2+XBIBII)*RHO(K)-XBIJ*RRHO(K)**2-(XBICII+XCIQI)*(DDRHO(K)+
C 12.DO/(RO*EPS)*DRHO(K))-XBICII*DRHO(K)**2/RHO(K)
C Q(K) = HBARC**2/(2.DO*RMASS)*DCPLX(QR,QI)
C BRACKR = (2.DO*M1 *(ER-VC(K))+(ER-VC(K))**2-EI**2)/(HBARC**2
C 1)-QR+ANONR
C BRACKI = (2.DO*M1 *EI+2.DO*EI*(ER-VC(K)))/(HBARC**2 )-QI+ANON
C 1I
C RF(K) = -REI*BRACKR+IM1*BRACKI
C FR(K) = L*(L+1.DO)/(EPS*RO)**2+RF(K)
C FI(K) = -REI*BRACKI-IM1*BRACKR
C
C SOLVE THE KLEIN-GORDON EQUATION. GENERATE INITIAL VALUES FOR
C INTEGRATION.
C
C 45 IJ = 4
C DO 70 I = 1,IJ
C X0(I,1) = 0.DO
C X2(I,1) = 0.DO
C L1 = L+1.DO
C L1 = .5D0*UN+.5D0*CDSORT((2.DO*L+UN)**2-4.DO*ZALPHA**2/(UN+(EB-M2-
C 1VC(1))/M2*UN-KC**2/(4.DO*M2**2)*UN+AK(1)))
C SUMM = CDEXP(L1*DLOG(1.D-6*RO))
C UR(1) = SUM(1)
C X(1,1) = UR(1)
C UI(1) = SUM(2)
C X(3,1) = UI(1)
C SUMM = L1*CDEXP((L1-UN)*DLOG(1.D-6*RO))
C DUR(1) = SUM(1)
C X(2,1) = DUR(1)
C DUI(1) = SUM(2)
C X(4,1) = DUI(1)
C
C USE MODIFIED EULER'S METHOD TO START FORWARD INTEGRATION USING
C ADAM'S METHOD BY PROVIDING VALUES FOR THREE ADDITIONAL POINTS.
C SEE SOUTHWORTH'S BOOK 'DIGITAL COMPUTATION AND NUMERICAL METHODS'
C PAGE 436.

```

```

C C USE EULER FORWARD INTEGRATION FORMULA
C C X(K) = X(K-1)+SR*F(X(K-1))
C C TO OBTAIN A PREDICTED VALUE OF X(K)
C C
C C DO 100 K = 2,4
C C DO 90 I = 1,IJ
C C X(I,K) = X(I,K-1)+SR*F(X(1,K-1),X(2,K-1),X(3,K-1),X(4,K-1),FR(K-1)
C C 1,FI(K-1),I)
C C
C C ITERATE EULER-GAUSS FORWARD INTEGRATION FORMULA
C C X(K) = X(K-1)+SR*(F(X(K-1))+F(X(K)))/2
C C TO OBTAIN BETTER VALUES FOR X(K)
C C
C C DO 95 KK = 1,3
C C DO 95 I = 1,IJ
C C X(I,K) = X(I,K-1)+SR*(F(X(1,K-1),X(2,K-1),X(3,K-1),X(4,K-1),FR(K-1)
C C 1),FI(K-1),I)+F(X(1,K),X(2,K),X(3,K),X(4,K),FR(K),FI(K),I))/2
C C 2.DO
C C UR(K) = X(1,K)
C C DUR(K) = X(2,K)
C C UI(K) = X(3,K)
C C DUI(K) = X(4,K)
C C
C C USE THE ADAMS-BASHFORTH PREDICTOR-CORRECTOR METHOD TO INTEGRATE
C C THE REST OF THE WAY. SEE SOUTHWORTH'S BOOK "DIGITAL COMPUTATION
C C AND NUMERICAL METHODS" PAGE 446.
C C
C C DO 240 K = 5,N
C C DO 120 I = 1,IJ
C C
C C PREDICTOR EQUATION FOR FORWARD INTEGRATION
C C X0(K) = X(K-1)+SR/24*(55*F(K-1)-59*F(K-2)+37*F(K-3)-9*F(K-4))
C C FOR SECOND ARGUMENT I = K-1,2 = K
C C
C C X0(I,2) = X(I,4)+SR/24.DO*(55.DO*F(X(1,4),X(2,4),X(3,4),X(4,4),F

```

```

1R(K-1),FI(K-1)      ,I)-59.D0*F(X(1,3),X(2,3),X(3,3),X(4,3),FR(K-2),
2FI(K-2)      ,I)+37.D0*F(X(1,2),X(2,2),X(3,2),X(4,2),FR(K-3),FI(K-3)
3      ,I)-9.D0*F(X(1,1),X(2,1),X(3,1),X(4,1),FR(K-4),FI(K-4)      ,I))
C
C PREDICTOR EQUATION IS CORRECTED FOR ESTIMATED ERROR
C X1(K) = X0(K)-251/270*(X0(K-1)-X2(K-1))
C
120 X1(I) = X0(I,2)-251.D0/270.D0*(X0(I,1)-X2(I,1))
C
C CORRECTOR EQUATION TO IMPROVE RESULT OF PREDICTOR EQUATION
C X2(K) = X(K-1)+SR/24*(9*F(K)+19*F(K-1)-5*F(K-2)+F(K-3))
C FOR SECOND ARGUMENT 1 = K-1, 2 = K
C
C DO 130 I = 1,IJ
C X2(I,2) = X(I,4)+SR/24.D0*(9.D0*F(X1(1),X1(2),X1(3),X1(4),FR(K),FI
1(K) ,I)+19.D0*F(X(1,4),X(2,4),X(3,4),X(4,4),FR(K-1),FI(K-1) ,I
2)-5.D0*F(X(1,3),X(2,3),X(3,3),X(4,3),FR(K-2),FI(K-2) ,I)+F(X(1,
32),X(2,2),X(3,2),X(4,2),FR(K-3),FI(K-3) ,I))
C
C CORRECTOR EQUATION IS CORRECTED FOR ESTIMATED ERROR
C X(K) = X2(K)+19/720*(X0(K)-X2(K))
C FOR SECOND ARGUMENT 1 = K-4, 2 = K-3, 3 = K-2, 4 = K-1, 5 = K
C
130 X(I,5) = X2(I,2)+19.D0/720.D0*(X0(I,2)-X2(I,2))
UR(K) = X(1,5)
DUR(K) = X(2,5)
UI(K) = X(3,5)
DUI(K) = X(4,5)
C
C UPGRADE ALL PARAMETERS FOR NEXT STEP
C
C DO 240 I = 1,IJ
X0(I,1) = X0(I,2)
X2(I,1) = X2(I,2)
DO 240 KK = 1,4
X(I,KK) = X(I,KK+1)
240

```





```

365 FO = FO+(2*J-1)*EXPSIG*AL(J)
SA(J) = (2*J-1)*P(J)*EXPSIG*AL(J)
TSA = CFC(I)
DO 366 J = 1,LW
366 TSA = TSA+SA(J)
IF(K.EQ.1) AIB(I) = .8DO*CDABS(TSA)**2
IF(K.GT.1) AIB(I) = AIB(I)+.1DO*CDABS(TSA)**2
370 CONTINUE
K = K+1
IF(K.LT.4) GO TO 355
IF(NP.EQ.0) GO TO 374
C CALCULATE NORM FOR BEST FIT
C
C SUM1 = 0.00
SUM2 = 0.00
DO 371 I = 1,NUM
371 SUM1 = SUM1 +DSIGMA(I)*AIB(I)/DELSIG(I)**2
SUM2 = SUM2+(AIB(I)/DELSIG(I))**2
NORM = SUM1/SUM2
NOR = NORM
WRITE(6,373) NORM
373 FORMAT(' NORM = ',D14.7)
374 DO 375 I = 1,NUM
375 AIB(I) = AIB(I)*NORM
C
C PRINT AND PLOT PREDICTED DIFFERENTIAL CROSS SECTION
C
DO 380 I = 1,NUM
J = NUM+I
K = 2*NUM+I
LL = 3*NUM+I
MM = 4*NUM+I
MO = 5*NUM+I
AIM(I) = SNGL(THETA(I))
AIM(J) = SNGL(DLOG10(DSIGMA(I)))

```

```

380 AIM(K) = SNGL(DLOG10(DSIGMA(I)+DELSIG(I)))
    AIM(LL) = SNGL(DLOG10(DSIGMA(I)-DELSIG(I)))
    AIM(MM) = SNGL(DLOG10(AIB(I)))
    AIM(MO) = SNGL(DLOG10(CDABS(CFC(I))))
    CF = CDABS(CFC(I))
    IF(NP.GT.0) WRITE(6,911) I, THETA(I), DSIGMA(I), DELSIG(I), AIB(I), CF
    CONTINUE
    IF(NP.GT.0) CALL PLOT(1, AIM, NUM, 6, 49, 0, NUM*6)
    C
    C
    C
    EVALUATE CHI-SQUARED
    CH12 = 0.00
    DO 390 I = 1, NUM
    390 CH12 = CH12+(DABS(DSIGMA(I)-AIB(I))/DELSIG(I))**2
    NCH12 = CH12/NUM
    IF(NP.GT.0) WRITE(6,912) NCH12
    912 FORMAT(' NORMALIZED CHI-SQUARED = ', D14.7)
    IA = IFIX(SNGL(A))
    RETURN
    904 FORMAT(' ELAB = ', D14.7, ' ECM = ', D14.7, ' KC = ', D14.7, ' EIK = ', D
    114.7, ' E2K = ', D14.7, ' ER = ', D14.7, ' EI = ', D14.7)
    911 FORMAT(' POINT(' , I2, ') THETA = ', D14.7, ' AI(EXP) = ', D14.7, ' UNC(E
    1XP) = ', D14.7, ' AI(THE) = ', D14.7, ' CFC(I) = ', D14.7)
    END

FUNCTION F(X1K, X2K, X3K, X4K, FRK, FIK, M)
C
C
C
    DOUBLE PRECISION SUBPROGRAM THAT DEFINES THE KLEIN-GORDON EQUATION
    IMPLICIT REAL*8(A-H, O-Z), INTEGER(I-N)
    GO TO (10, 20, 30, 40), M
    10 F = X2K
    RETURN
    20 F = FRK*X1K-FIK*X3K

```

```

RETURN
F = X4K
RETURN
F = FRK*X3K+FIK*X1K
RETURN
END

```

```

30
40

```

```

FUNCTION DATANH(X)
C
C FUNCTION SUBPROGRAM TO CALCULATE THE INVERSE OF THE HYPERBOLIC
C TANGENT FUNCTION
C

```

```

C
C
C

```

```

REAL*8 DATANH,X,DEN,SUM,TERM
DEN = 1.00
TERM = X
SUM = TERM/DEN
DEN = DEN+2.00
TERM = TERM*X*X
SUM = SUM+TERM/DEN
IF(TERM/(DEN*SUM).GT.1.0D-3) GO TO 10
DATANH = SUM
RETURN
END

```

```

10

```

```

SUBROUTINE PLOT(NO,A,N,M,NL,NS,N5)

```

```

C
C
C
C
C
C
C

```

```

.....

```

```

SUBROUTINE PLOT

```

```

PURPOSE
PLOT SEVERAL CROSS-VARIABLES VERSUS A BASE VARIABLE

```



```

LL=J-N
DO 12 K=1,M
L=L+N
LL=LL+N
F=A(L)
A(L)=A(LL)
12 A(LL)=F
14 CONTINUE
15 CONTINUE
C
C      TEST NULL
C
16 IF(NLL) 20, 18, 20
18 NLL=50
C
C      PRINT TITLE
C
20 WRITE(6,1) NO
C
C      FIND SCALE FOR BASE VARIABLE
C
XSCAL=(A(N)-A(1))/(FLOAT(NLL-1))
C
C      FIND SCALE FOR CROSS-VARIABLES
C
M1=N+1
YMIN=A(M1)
YMAX=YMIN
M2=M#N
DO 40 J=M1,M2
IF(A(J)-YMIN) 28,26,26
26 IF(A(J)-YMAX) 40,40,30
28 YMIN=A(J)
GO TO 40
30 YMAX=A(J)
40 CONTINUE

```

```

C
C
C
YSCAL=(YMAX-YMIN)/100.0
    FIND BASE VARIABLE PRINT POSITION
    XB=A(1)
    L=1
    MY=M-1
    I=1
45 F=I-1
    XPR=XB+F*XSCAL
    IF(A(L)-XPR-.100) 50,50,70
C
C
C
    FIND CROSS-VARIABLES
50 DO 55 IX=1,101
55 OUT(IX)=BLANK
    DO 60 J=1,MY
    LL=L+J*N
    JP=((A(LL)-YMIN)/YSCAL)+1.0
    OUT(JP)=ANG(J)
60 CONTINUE
C
C
C
    PRINT LINE AND CLEAR, OR SKIP
WRITE(6,2)XPR,(OUT(IZ),IZ=1,101)
L=L+1
GO TO 80
70 WRITE(6,3)
80 I=I+1
    IF(I-NLL) 45, 84, 86
84 XPR=A(N)
    GO TO 50
C
C
C
    PRINT CROSS-VARIABLES NUMBERS
86 WRITE(6,7)

```

```

YPR(1)=YMIN
DO 90 KN=1,9
90 YPR(KN+1)=YPR(KN)+YSCAL*10.0
YPR(11)=YMAX
WRITE(6,8)(YPR(IP),IP=1,11)
RETURN
1 FORMAT(1H1,60X,7H CHART ,I3//)
2 FORMAT(1H ,F5.1,5X,101A1)
3 FORMAT(1H )
7 FORMAT(1H , 9X,101H.
1 . . . . .
8 FORMAT(1H0,9X,11E10.3)
END

```

```

FUNCTION CDPSI(A,B,Z)

```

```

C
C DOUBLE PRECISION FUNCTION SUBPROGRAM TO CALCULATE THE CONFLUENT
C HYPERGEOMETRIC FUNCTION OF THE SECOND KIND WITH COMPLEX ARGUMENTS.
C
C COMPLEX*16 CDPSI,A,B,Z,CDGMMMA,TERM,SUMM,C,ZB,G1,G2,G3,PI,CDEXP,CDL
C LOG,DCMPLX
C DOUBLE PRECISION SUM(2),TRM(2),TOL,CDABS,DABS
C EQUIVALENCE (SUM(1),SUMM),(TRM(1),TERM)
C
C CHECK WHETHER ASYMPTOTIC FORM OF FUNCTION FOR LARGE Z IS NEEDED
C
C
C

```

```

IOUT = 6
TOL = 1.0D-06
IF(CDABS(Z).GT.22.00) GO TO 50
PI = (3.1415926535897900,0.0D0)
K = 1
ZB = CDEXP(((1.0D,0.0D0)-B)*CDLOG(Z))
C = (1.0D,0.0D0)
SUMM = (0.0D0,0.0D0)

```

```

10 G1 = CDGMMMA(A)/CDGMMMA(B)
    G2 = CDGMMMA(A-B+(1.D0,0.D0))/CDGMMMA((2.D0,0.D0)-B)
    G3 = (1.D0,0.D0)/((1.D0,0.D0)-B)*G1*G2
    GO TO 15
15 C = C*/DCMPLX(K*1.D0-1.D0,0.D0)
    G1 = G1*(A+DCMPLX(K*1.D0-2.D0,0.D0))/(B+DCMPLX(K*1.D0-2.D0,0.D0))
    G2 = G2*(A-H+DCMPLX(K*1.D0-1.D0,0.D0))/(DCMPLX(K*1.D0,0.D0)-B)
    TFRM = C*(G1-G2*ZB)
    SUMM = SUMM+TERM
C
C CHECK WHETHER SUM HAS CONVERGED TO WITHIN THE REQUIRED RELATIVE
C TOLERANCE = TOL.
C
20 IF(DABS(TRM(1))/SUM(1)).GT.TOL) GO TO 20
    IF(SUM(2).EQ.0.D0) GO TO 30
    IF(DABS(TRM(2))/SUM(2)).LT.TOL) GO TO 30
    K = K+1
    IF(K-100) 10,40,40
30 CDPSI = G3*SUMM
    RETURN
40 CDPSI = G3*SUMM
    WRITE(IOUT,900) A,B,Z,CDPSI
    RETURN
C
C ASYMPTOTIC FORM OF EXPANSION FOR LARGE Z
C
50 SUMM = (1.D0,0.D0)
    TERM = (1.D0,0.D0)
    K = 1
60 TERM = -(A+DCMPLX(K*1.D0-1.D0,0.D0))*(A-B+DCMPLX(K*1.D0,0.D0))/(Z*
    IK)*TERM
    SUMM = SUMM+TERM
    IF(DABS(TRM(1))/SUM(1)).GT.TOL) GO TO 70
    IF(SUM(2).EQ.0.D0) GO TO 80
    IF(DABS(TRM(2))/SUM(2)).LT.TOL) GO TO 80
    K = K + 1
70

```

```

      IF(K.GT.100) GO TO 90
      GO TO 60
      CDPSI = SUMM*CDEXP(-A*CDLOG(Z))
      RETURN
90    CDPSI = SUMM*CDEXP(-A*CDLOG(Z))
      WRITE(IOUT,910) A,H,Z,CDPSI
      RETURN
900   FORMAT(' PSI SERIES DID NOT CONVERGE',' A = ',2D15.8/' B = ',2D15.
18/' Z = ',2D15.8/' CDPSI = ',2D15.8)
910   FORMAT(' ASYMPTOTIC PSI SERIES DID NOT CONVERGE',' A = ',2D15.8/'
1B = ',2D15.8/' Z = ',2D15.8/' CDPSI = ',2D15.8)
      END

```

```

FUNCTION CDGMMMA(Z)

```

```

C
C
C
C

```

```

DOUBLE PRECISION FUNCTION SUBPROGRAM TO CALCULATE THE GAMMA
FUNCTION FOR COMPLEX ARGUMENTS.

```

```

COMPLEX*16 CDGMMMA,Z,T,TT,SUMM,TERM,DEN,ZM,ZZ,DCMPLX,CDLOG,CDEXP,CD
1SIN,PI
DOUBLE PRECISION X,Y,XDIST,A(2),C(12),SUM(2),TRM(2),CDABS,DABS,DLO
1G,TOL,DFLOAT
LOGICAL REFLEK
EQUIVALENCE (A(1),ZZ),(SUM(1),SUMM),(TRM(1),TERM)

```

```

C
C
C
C
C

```

```

SET ALL SYSTEM DEPENDENT CONSTANTS WITH DATA STATEMENT WHERE
IOUT = SYSTEM DEPENDENT OUTPUT CHANNEL
C(12) = COEFFICIENTS IN STIRLING'S APPROXIMATION FOR LN(GAMMA(T))

```

```

DATA TOL,IOUT,PI/1.D-15,6,(3.14159265358979D0,0.D0)/,C/.8333333333
133333D-1,-.27777777777778D-2,.793650793650794D-3,-.59523809523809
25D-3,.841750841750842D-3,-.191752691752692D-2,.6410256410256410D-2
3,-.295506535947712D-1,.179644372368831D0,-.139243221690590D1,.1340
428640441684D2,-.156848284626020D3/

```

```

ZZ = Z
X = A(1)
Y = A(2)
REFLEK = .FALSE.
C
C DETERMINE WHETHER Z IS TOO CLOSE TO A POLE BY FINDING NEAREST POLE
C AND COMPUTING DISTANCE TO IT.
C
IF(X.GE.TOL) GO TO 20
XDIST = X - DFLOAT(IDINT(X-.5D0))
ZM = DCMLPX(XDIST,Y)
IF(CDABS(ZM).GE.TOL) GO TO 10
C
IF Z IS TOO CLOSE TO A POLE, PRINT ERROR MESSAGE AND RETURN WITH
CDGMMMA = DCMLPX(1.D0/TOL,0.D0)
C
WRITE(IOUT,900)
CDGMMMA = DCMLPX(1.D0/TOL,0.D0)
RETURN
C
FOR REAL(Z) NEGATIVE EMPLOY THE REFLECTION FORMULA
C
C GAMMA(Z) = PI/(SIN(PI*Z)*GAMMA(1-Z))
C
AND COMPUTE GAMMA(1-Z). NOTE REFLEK IS A TAG TO INDICATE THAT
THIS RELATION MUST BE USED LATER.
C
C IF(X.GE.0.D0) GO TO 20
REFLEK = .TRUE.
ZZ = (1.D0+0.D0)-ZZ
X = 1.D0-X
Y = -Y
C
IF Z IS NOT TOO CLOSE TO A POLE, MAKE REAL(Z)>10 AND ARG(Z)<PI/4
C
C M = MAX0(ABS(IDINT(Y))-IDINT(X),10-IDINT(X),0)
20

```

```

60 T = DCMPLEX(X+DFLOAT(M),Y)
   TT = T*T
   DEN = T
   C COMPUTE STIRLING'S APPROXIMATION FOR LN(GAMMA(T))
   C
   C SUMM = (T-(.5D0,0.D0))*CDLOG(T)-T+(.5D0,0.D0)*CDLOG((2.D0,0.D0)*PI
   C 1)
   J = 1
   70 TERM = C(J)/DEN
   C
   C TEST REAL AND IMAGINARY PARTS OF LN(GAMMA(Z)) SEPARATELY FOR
   C CONVERGENCE. IF Z IS REAL SKIP IMAGINARY PART OF CHECK.
   C IF(DABS(TRM(1))/SUM(1)).GT.TOL) GO TO 80
   C
   C IF(Y.EQ.0.D0) GO TO 100
   C IF(DABS(TRM(2))/SUM(2)).LE.TOL) GO TO 100
   80 SUMM = SUMM+TERM
   J = J+1
   DEN = DEN*TT
   C
   C TEST FOR NONCONVERGENCE
   C IF(J-12) 70,70,90
   C
   C STIRLING'S SERIES DID NOT CONVERGE. PRINT ERROR MESSAGE AND
   C PROCEED.
   C
   C WRITE(IOUT,910)
   C
   C RECURSION RELATION USED TO OBTAIN LN(GAMMA(Z))
   C
   C LN(GAMMA(Z)) = LN(GAMMA(Z+M))/(Z*(Z+1)*...*(Z+M-1))
   C LN(GAMMA(Z)) = LN(GAMMA(Z+M))-LN(Z)-LN(Z+1)-...-LN(Z+M-1)
   C
   100 IF(M.EQ.0) GO TO 120

```



IS ALSO CALCULATED. A DETERMINANT OF ZERO INDICATES THAT  
THE MATRIX IS SINGULAR.

.....

SUBROUTINE MINV(A,N,D,L,M,NN)  
DIMENSION A(NN),L(N),M(N)  
DOUBLE PRECISION A,D,BIGA,HOLD,DABS

SEARCH FOR LARGEST ELEMENT

D = 1.D0  
NK = -N  
DO 80 K = 1,N  
NK = NK+N  
L(K) = K  
M(K) = K  
KK = NK + K  
BIGA = A(KK)  
DO 20 J = K,N  
IZ = N\*(J-1)  
DO 20 I = K,N  
IJ = IZ+I  
IF(DABS(BIGA)-DABS(A(IJ))) 15,20,20  
BIGA = A(IJ)  
L(K) = I  
M(K) = J  
CONTINUE

INTERCHANGE ROWS

J = L(K)  
IF(J-K) 35,35,25  
KI = K-N  
DO 30 I = 1,N  
KI = KI + N

C  
C  
C  
C  
C

C  
C  
C

10  
15

20  
C  
C  
C

25

```

HOLD = -A(KI)
JI = KI-K+J
A(KI) = A(JI)
A(JI) = HOLD

```

```

30
C
C
C
C

```

```

INTERCHANGE COLUMNS

```

```

I = M(K)
IF(I-K) 45,45,38
JP = N*(I-1)
DO 40 J = 1,N
JK = NK+J
JI = JP+J
HOLD = -A(JK)
A(JK) = A(JI)
A(JI) = HOLD

```

```

40
C
C
C
C

```

```

DIVIDE COLUMN BY MINUS PIVOT (VALUE OF PIVOT ELEMENT IS STORED IN
BIGA)

```

```

IF(HIGA) 48,46,48
D = 0.DO
RETURN
DO 55 I = 1,N
IF(I-K) 50,55,50
IK = NK+I
A(IK) = A(IK)/(-BIGA)
CONTINUE

```

```

55
C
C
C

```

```

REDUCE MATRIX

```

```

DO 65 I = 1,N
IK = NK+I
HOLD = A(IK)
IJ = I-N
DO 65 J = 1,N

```

```

IJ = IJ+N
IF(I-K) 60,65,60
IF(J-K) 62,65,62
KJ = IJ-I+K
A(IJ) = HOLD*A(KJ)+A(IJ)
CONTINUE
C
C
C
DIVIDE ROW BY PIVOT
KJ = K-N
DO 75 J = 1,N
KJ = KJ+N
IF(J-K) 70,75,70
A(KJ) = A(KJ)/BIGA
CONTINUE
70
75
C
C
C
PRODUCT OF PIVOTS
D = D*BIGA
C
C
C
REPLACE PIVOT BY RECIPROCAL
A(KK) = 1.00/BIGA
CONTINUE
80
C
C
C
FINAL ROW AND COLUMN INTERCHANGE
K = N
K = (K-1)
IF(K) 150,150,105
I = L(K)
IF(I-K) 120,120,108
J0 = N*(K-1)
JR = N*(I-1)
DO 110 J = 1,N
JK = J0+J
100
105
108

```

```
110 HOLD = A(JK)
120 JI = JR+J
    A(JK) = -A(JI)
    A(JI) = HOLD
    J = M(K)
    IF(J-K) 100,100,125
125 KI = K-N
    DO 130 I = 1,N
    KI = KI+N
    HOLD = A(KI)
    JI = KI-K+J
    A(KI) = -A(JI)
130 A(JI) = HOLD
    GO TO 100
150 RETURN
    END
```

APPENDIX N

Evaluation of the Invariant Amplitude for Pion-Nucleon Scattering  
in the Pion-Nucleus CM System

26

According to Goldberger and Watson the invariant amplitude  
for pion-nucleon scattering

$$(P_N, \lambda) + (P_\pi, B) \rightarrow (P_N', \lambda') + (P_\pi', \alpha)$$

is

$$N1 \quad M_{\alpha B} = \bar{U}(\vec{P}_N') (A_{\alpha B} - i \gamma \cdot Q B_{\alpha B}) U(\vec{P}_N)$$

where

$$N2 \quad Q = \frac{P_\pi + P_\pi'}{2}$$

$$N3 \quad A_{\alpha B} = A^{(+)} \delta_{\alpha B} + A^{(-)} \frac{1}{3} [\tau_\alpha, \tau_B]$$

$$N4 \quad B_{\alpha B} = B^{(+)} \delta_{\alpha B} + B^{(-)} \frac{1}{2} [\tau_\alpha, \tau_B].$$

The scalars  $A_{\alpha B}$  and  $B_{\alpha B}$  are in general functions of the invariants  
 $s$ ,  $t$ , and  $u$  where

$$N5 \quad s = -(P_\pi + P_N)^2 = -(P_\pi' + P_N')^2$$

$$N6 \quad t = -(P_\pi - P_\pi')^2 = -(P_N - P_N')^2$$

$$N7 \quad U = -(p_{\pi} - p_{N'})^2 = -(p_{\pi'} - p_N)^2.$$

In the notation of Goldberger and Watson<sup>26</sup> the invariant amplitude is related to the S matrix by

$$N8 \quad S_{\alpha\beta} = \delta_{p_{\pi}, p_{\pi'}} \delta_{p_N, p_{N'}} \delta_{\alpha\beta} + 2\pi i \delta(p_{\pi'} + p_{N'} - p_{\pi} - p_N) \\ \delta_{p_N + p_{\pi}, p_{N'} + p_{\pi'}} \left( \frac{M_N^2}{4E_{\pi} E_{\pi'} E_N E_{N'}} \right)^{1/2} M_{\alpha\beta}$$

and to the total  $\pi N$  cross section by

$$N9 \quad \sigma_{\pi N} = \frac{(M_N)^2}{4\pi} \int \frac{d^3 p_{N'}}{E_{N'}} \int \frac{d^3 p_{\pi'}}{E_{\pi'}} \delta(E_{N'} + E_{\pi'} - E_N - E_{\pi}) |M_{\alpha\beta}|^2.$$

The differential cross section for the final pion to be in the solid angle  $d\Omega_{\pi'}$  is

$$N10 \quad \frac{d\sigma}{d\Omega_{\pi'}} = |f|^2$$

where

$$N11 \quad f = \frac{M_N}{4\pi} \sqrt{\frac{e}{V_{rel} E_{\pi} E_N}} |M_{\alpha\beta}|$$

$$N12 \quad e = \int \frac{p_{\pi'}^2 d^3 p_{\pi'}}{E_{\pi'}} \int \frac{d^3 p_{N'}}{E_{N'}} \delta(p_{N'} + p_{\pi'} - p_N - p_{\pi}).$$

In the pion-nucleon CM system

$$N13 \quad f^{\pi N} \cong \frac{|M_{\alpha\beta}|}{4\pi (1 + E_{\pi}/M_N)}$$

For a nucleon bound in the nucleus, the pion-nucleon scattering amplitude in the pion-nucleus CM system is related to the pion-nucleon scattering amplitude in the pion-nucleon CM by II-1, i.e.

$$N14 \quad f^{\pi NUC} \cong \left(1 + \frac{E_{\pi}}{M_N}\right) f^{\pi N}.$$

Thus the relationship between the pion-nucleon scattering amplitude in the pion-nucleus CM system to the invariant amplitude  $M$  is given by

$$N15 \quad f^{\pi NUC} \cong |M_{\alpha\beta}|/4\pi$$

The operator form of the invariant amplitude  $M_{\alpha\beta}$  is obtained by substituting into N1

$$N16 \quad U(P_N) = \sqrt{\frac{E_N + MN}{2MN}} \begin{pmatrix} I U_p \\ \vec{\sigma} \cdot \vec{P}_N U_p \\ E_N + MN \end{pmatrix}$$

$$N17 \quad \bar{U}(P_{N'}) = \sqrt{\frac{E_{N'} + MN}{2MN}} \left( I U_p^+ - \frac{\vec{\sigma} \cdot \vec{P}_N}{E_N + MN} U_p^+ \right)$$

$$N18 \quad \vec{\gamma} = \begin{pmatrix} 0 & -i\vec{\sigma} \\ i\vec{\sigma} & 0 \end{pmatrix} \quad \gamma_4 = \begin{pmatrix} I & 0 \\ 0 & -I \end{pmatrix}.$$

The resulting expression is

$$N19 \quad M_{\alpha\beta} = \frac{\sqrt{E_{N'} + MN} \sqrt{E_N + MN}}{2MN} U_p^+ \left[ \left\{ 1 - \frac{(\vec{\sigma} \cdot \vec{P}_{N'}) (\vec{\sigma} \cdot \vec{P}_N)}{(E_{N'} + MN)(E_N + MN)} \right\} A_{\alpha\beta} \right. \\ \left. + \left\{ \frac{E_\pi + E_{\pi'}}{2} - \frac{\vec{\sigma} \cdot (\vec{P}_\pi + \vec{P}_{\pi'})}{2} \frac{\vec{\sigma} \cdot \vec{P}_N}{E_N + MN} - \frac{(\vec{\sigma} \cdot \vec{P}_{N'}) \vec{\sigma} \cdot (\vec{P}_\pi + \vec{P}_{\pi'})}{2(E_{N'} + MN)} \right. \right. \\ \left. \left. + \left( \frac{E_\pi + E_{\pi'}}{2} \right) \frac{(\vec{\sigma} \cdot \vec{P}_{N'}) (\vec{\sigma} \cdot \vec{P}_N)}{(E_{N'} + MN)(E_N + MN)} \right\} B_{\alpha\beta} \right] U_p.$$

Note that the effect of the nuclear binding on the spinors has been neglected.

Now  $M_{\alpha\beta}$  may be written in a more symmetric way. Consider the terms in  $M_{\alpha\beta}$  of the form

$$N20 \quad \sqrt{\frac{E_N + MN}{2MN}} \sqrt{\frac{E_{N'} + MN}{2MN}} \left[ 1 \mp \frac{\vec{P}_N \cdot \vec{P}_{N'}}{4MN^2} \right] =$$

$$\begin{aligned}
&= \sqrt{\left(1 + \frac{T_N}{2MN}\right)\left(1 + \frac{T_{N'}}{2MN}\right)} \left(1 \mp \frac{\vec{P}_N \cdot \vec{P}_{N'}}{4MN^2}\right) \\
&\cong \left[1 + \frac{T_N + T_{N'}}{4MN}\right] \left[1 \mp \frac{\vec{P}_N \cdot \vec{P}_{N'}}{4MN^2}\right] \\
&= 1 + \frac{P_N^2 + P_{N'}^2}{8MN^2} \mp \frac{\vec{P}_N \cdot \vec{P}_{N'}}{4MN^2} \\
&= 1 + \frac{(\vec{P}_N \mp \vec{P}_{N'})^2}{8MN^2} .
\end{aligned}$$

Using the symmetric expression  $M_{\alpha\beta}$  may be written

$$\begin{aligned}
N21 \quad M_{\alpha\beta} &= U_P^+ \left\{ A_{\alpha\beta} \left[ 1 + \frac{(\vec{P}_N - \vec{P}_{N'})^2}{8MN^2} - i\vec{\sigma} \cdot \frac{(\vec{P}_{N'} \times \vec{P}_N)}{4MN^2} \right] \right. \\
&\quad + B_{\alpha\beta} \left[ 1 + \frac{(\vec{P}_N + \vec{P}_{N'})^2}{8MN^2} + i\vec{\sigma} \cdot \frac{(\vec{P}_{N'} \times \vec{P}_N)}{4MN^2} \right] \frac{E_N + E_{N'}}{2} \\
&\quad \left. - B_{\alpha\beta} \left[ (\vec{P}_N + \vec{P}_{N'}) - i\vec{\sigma} \times (\vec{P}_N - \vec{P}_{N'}) \right] \cdot \frac{(\vec{P}_N + \vec{P}_{N'})}{4MN} \right\} U_P .
\end{aligned}$$

In their book Goldberger and Watson<sup>26</sup> have evaluated the elastic pion-nucleon isoscalar scattering amplitude  $f^{(+)}$  in the pion-nucleon CM system and obtained

$$\begin{aligned}
N22 \quad f^{(+)} &= U_P^+ \left[ \frac{E_N + M_N}{2W} \left\{ \frac{A^{(+)} + (W - M_N)B^{(+)}}{4\pi} \right\} \right. \\
&\quad \left. + \frac{E_N - M_N}{2W} \left\{ \frac{-A^{(+)} + (W + M_N)B^{(+)}}{4\pi} \right\} (\vec{\sigma} \cdot \hat{P}_{N'}) (\vec{\sigma} \cdot \hat{P}_\pi) \right] U_P .
\end{aligned}$$

They compared this form with the phase shift form normally used in pion-nucleon scattering

$$N23 \quad f^{(+)} = U_p^+ \left[ f_1^{(+)} + f_2^{(+)} (\vec{\sigma} \cdot \hat{p}_n') (\vec{\sigma} \cdot \hat{p}_n) \right] U_p$$

and solved for  $A^{(+)}$  and  $B^{(+)}$  in terms of  $f_1^{(+)}$  and  $f_2^{(+)}$  to obtain

$$N24 \quad \frac{A^{(+)}}{4\pi} = \frac{W+M_N}{E_N+M_N} f_1^{(+)} - \frac{W-M_N}{E_N-M_N} f_2^{(+)}$$

$$N25 \quad \frac{B^{(+)}}{4\pi} = \frac{1}{E_N+M_N} f_1^{(+)} + \frac{1}{E_N-M_N} f_2^{(+)}$$

where the  $f_1^{(+)}$  and  $f_2^{(+)}$  are related to the pion-nucleon phase shifts by

$$N26 \quad f_1^{(+)} = \sum_{\ell=0}^{\infty} f_{\ell+}^{(+)} P_{\ell+1}'(\hat{p}_n \cdot \hat{p}_n') - \sum_{\ell=2}^{\infty} f_{\ell-}^{(+)} P_{\ell-1}'(\hat{p}_n \cdot \hat{p}_n')$$

$$N27 \quad f_2^{(+)} = \sum_{\ell=1}^{\infty} (f_{\ell-}^{(+)} - f_{\ell+}^{(+)}) P_{\ell}'(\hat{p}_n \cdot \hat{p}_n')$$

$$N28 \quad f_{\ell\pm}^{(+)} = e^{i\delta_{\ell\pm}^{(+)}} \frac{\sin \delta_{\ell\pm}^{(+)}}{|\hat{p}_n|} \quad \begin{array}{l} \ell+ \Rightarrow j = \ell + \gamma_a \\ \ell- \Rightarrow j = \ell - \gamma_a \end{array}$$

For s and p waves only one has

$$N29 \quad f_1^{(+)} = f_{0+}^{(+)} + 3f_{1+}^{(+)} (\hat{p}_n \cdot \hat{p}_n')$$

$$N30 \quad f_2^{(+)} = f_{1-}^{(+)} - f_{1+}^{(+)}.$$

Thus

$$N31 \quad f^{(+)} = U_p^+ \left[ f_{0+}^{(+)} + (3f_{1+}^{(+)} + f_{1-}^{(+)} - f_{1+}^{(+)}) \hat{p}_n \cdot \hat{p}_n' + (f_{1-}^{(+)} - f_{1+}^{(+)}) i \vec{\sigma} \cdot (\hat{p}_n' \times \hat{p}_n) \right] U_p.$$

19

In terms of the notation of Ericson and Ericson

$$N32 \quad b_0 = f_{0+}^{(+)}$$

$$N33 \quad c_0 = \frac{2f_{1+}^{(+)} + f_{1-}^{(+)}}{|\vec{p}_\pi|^2}$$

$$N34 \quad d_0 = \frac{f_{1-}^{(+)} - f_{1+}^{(+)}}{|\vec{p}_\pi|^2}$$

so

$$N35 \quad f^{(+)} = U_p^+ \left[ b_0 + c_0 \vec{p}_n' \cdot \vec{p}_n + i d_0 \vec{\sigma} \cdot (\vec{p}_n' \times \vec{p}_n) \right] U_p.$$

The general form of  $f$  in the pion-nucleon CM may also be written in the Ericson's notation to be

$$N36 \quad f = U_p^+ \left[ (b_0 + b_1 \underline{t}_n \cdot \underline{T}_N) + (c_0 + c_1 \underline{t}_n \cdot \underline{T}_N) \vec{p}_n' \cdot \vec{p}_n + i (d_0 + d_1 \underline{t}_n \cdot \underline{T}_N) \vec{\sigma} \cdot (\vec{p}_n' \times \vec{p}_n) \right] U_p.$$

Consider the invariant amplitude  $M_{\alpha\beta}$  in the pion-nucleus CM system. According to Krajcik and Foldy<sup>122</sup> the expression one obtains for  $M_{\alpha\beta}$  using free nucleon spinors is correct only to order  $1/M_N$ , because the effect of nuclear binding on the spinors is of order  $1/M_N^2$ . In order to obtain  $M_{\alpha\beta}$  to order  $1/M_N$  one needs to expand the coefficients of  $f_1$  and  $f_2$  in the expressions for  $A_{\alpha\beta}$  and  $B_{\alpha\beta}$  given in equations N24 and N25.

Now

$$N37 \quad \frac{1}{\widehat{E} + M_N} \cong \frac{1}{2M_N}$$

$$N38 \quad \frac{\widehat{W} + M_N}{\widehat{E} + M_N} \cong \frac{M_N \left( 1 + \frac{E_\pi + E_\pi'}{2M_N} \right) + M_N}{2M_N} = 1 + \frac{E_\pi + E_\pi'}{4M_N}$$

$$N39 \quad \frac{1}{\widehat{E} - MN} = \frac{1}{\widehat{P}_\pi \widehat{P}_{\pi'} \left(1 - \frac{\widehat{P}_\pi \cdot \widehat{P}_{\pi'}}{4MN^2}\right)} \cong \frac{1 + \frac{\vec{P}_\pi \cdot \vec{P}_{\pi'}}{4MN^2}}{\widehat{P}_\pi \cdot \widehat{P}_{\pi'}} \frac{1}{2MN}$$

$$N40 \quad - \frac{\widetilde{W} - MN}{\widehat{E} - MN} = \frac{-MN}{\widehat{P}_\pi \widehat{P}_{\pi'} \left(1 - \frac{\widehat{P}_\pi \cdot \widehat{P}_{\pi'}}{4MN^2}\right)} \left\{ \frac{E_\pi + E_{\pi'}}{2MN} - \frac{P_\pi^2 + P_{\pi'}^2}{4MN^2} \right. \\ \left. - \frac{(\vec{P}_\pi \cdot \vec{P}_N + \vec{P}_{\pi'} \cdot \vec{P}_{N'})}{2MN^2} + \frac{E_\pi}{2MN} \left( \frac{\vec{P}_N^2 + \vec{P}_{N'}^2}{2MN^2} + \frac{\vec{P}_N \cdot \vec{P}_{N'}}{MN^2} \right) \right. \\ \left. + \frac{E_{\pi'}}{2MN} \left( \frac{\vec{P}_N'^2 + \vec{P}_{N'}^2}{2MN^2} + \frac{\vec{P}_N' \cdot \vec{P}_{N'}}{MN^2} \right) \right\}$$

where the  $\sim$  signifies a pion-nucleon CM quantity. Substituting these terms into the expression for  $M_{\alpha\beta}$  given in N21 obtain after some cancellation

$$N41 \quad M_{\alpha\beta} = U_p^+ \left[ \left\{ \left(1 + \frac{E_\pi + E_{\pi'}}{4MN}\right) f_1 - \frac{2MN^2}{\widehat{P}_\pi \widehat{P}_{\pi'}} \left[ \frac{E_\pi + E_{\pi'}}{2MN} \right. \right. \right. \\ \left. \left. - \frac{\vec{P}_\pi^2 + \vec{P}_{\pi'}^2}{4MN^2} - \frac{(\vec{P}_\pi \cdot \vec{P}_N + \vec{P}_{\pi'} \cdot \vec{P}_{N'})}{2MN^2} + \frac{E_\pi}{2MN} \left( \frac{\vec{P}_N^2 + \vec{P}_{N'}^2}{2MN^2} + \right. \right. \right. \\ \left. \left. \frac{\vec{P}_N \cdot \vec{P}_{N'}}{MN^2} \right) + \frac{E_{\pi'}}{2MN} \left( \frac{\vec{P}_N'^2 + \vec{P}_{N'}^2}{2MN^2} + \frac{\vec{P}_N' \cdot \vec{P}_{N'}}{MN^2} \right) \right] f_2 \left. \right\} \left\{ 1 \right. \\ \left. + \frac{(\vec{P}_N - \vec{P}_{N'})^2}{8MN^2} - \frac{i \vec{\sigma} \cdot (\vec{P}_N' \times \vec{P}_N)}{4MN^2} \right\} + \left\{ \frac{f_1}{2MN} + \frac{2MN}{\widehat{P}_\pi \widehat{P}_{\pi'}} f_2 \right\} \\ \left\{ 1 + \frac{(\vec{P}_N + \vec{P}_{N'})^2}{8MN^2} + \frac{i \vec{\sigma} \cdot (\vec{P}_N' \times \vec{P}_N)}{4MN^2} \right\} \left( \frac{E_\pi + E_{\pi'}}{2} \right) - \left\{ \frac{f_1}{2MN} \right. \\ \left. + \frac{2MN}{\widehat{P}_\pi \widehat{P}_{\pi'}} f_2 \right\} \left\{ (\vec{P}_N + \vec{P}_{N'}) - i \vec{\sigma} \times (\vec{P}_N - \vec{P}_{N'}) \right\} \cdot \left( \frac{\vec{P}_\pi + \vec{P}_{\pi'}}{4MN} \right) \right] U_p.$$

Combining coefficients of  $f_1$  and  $f_2$  obtain

$$\begin{aligned}
 \text{N42 } M_{\alpha\beta} = & U_p^+ \left[ \left\{ 1 + \frac{E_\pi + E_{\pi'}}{2MN} \right\} f_1 + \frac{f_2}{2\hat{p}_\pi \hat{p}_{\pi'}} \left\{ \vec{p}_\pi^2 \left( 1 - \frac{E_\pi}{MN} \right) \right. \right. \\
 & + \vec{p}_\pi'^2 \left( 1 - \frac{E_{\pi'}}{MN} \right) - \frac{2E_\pi}{MN} \vec{p}_N \cdot \vec{p}_\pi - \frac{2E_{\pi'}}{MN} \vec{p}_{N'} \cdot \vec{p}_{\pi'} + (\vec{p}_\pi \cdot \vec{p}_N + \vec{p}_{\pi'} \cdot \vec{p}_{N'}) \\
 & - \vec{p}_N \cdot \vec{p}_{\pi'} - \vec{p}_{N'} \cdot \vec{p}_\pi \left. \right\} - \frac{E_\pi + E_{\pi'}}{2MN} \left[ \frac{(\vec{p}_N - \vec{p}_{N'})^2}{2} - i\vec{\sigma} \cdot (\vec{p}_N' \times \vec{p}_N) \right] - \frac{E_\pi}{MN} \vec{p}_N^2 \\
 & - \frac{E_{\pi'}}{MN} \vec{p}_{N'}^2 + \frac{E_\pi + E_{\pi'}}{2MN} \left( \frac{\vec{p}_N^2 + \vec{p}_{N'}^2 + 2\vec{p}_N \cdot \vec{p}_{N'}}{2} + i\vec{\sigma} \cdot (\vec{p}_N' \times \vec{p}_N) \right) \\
 & \left. + i\vec{\sigma} \cdot (\vec{p}_N' - \vec{p}_N) \times (\vec{p}_\pi + \vec{p}_{\pi'}) \right] U_p.
 \end{aligned}$$

For elastic pion-nucleus scattering one has  $\vec{p}_\pi^2 \approx \vec{p}_{\pi'}^2$  and

$E_\pi \approx E_{\pi'}$ . Using the identity

$$\begin{aligned}
 \text{N43 } -q^2 = & -(\vec{p}_{N'} - \vec{p}_N) \cdot (\vec{p}_\pi - \vec{p}_{\pi'}) = \vec{p}_\pi \cdot \vec{p}_N + \vec{p}_{\pi'} \cdot \vec{p}_{N'} - \vec{p}_\pi \cdot \vec{p}_{N'} - \vec{p}_{\pi'} \cdot \vec{p}_N \\
 = & -(\vec{p}_\pi - \vec{p}_{\pi'})^2 = -\vec{p}_\pi^2 - \vec{p}_{\pi'}^2 + 2\vec{p}_\pi \cdot \vec{p}_{\pi'}
 \end{aligned}$$

one obtains for elastic scattering

$$\begin{aligned}
 \text{N44 } M_{\alpha\beta} = & U_p^+ \left[ \left\{ 1 + \frac{E_\pi}{MN} \right\} f_1 + \left\{ 2\vec{p}_\pi \cdot \vec{p}_{\pi'} \left( 1 - \frac{E_\pi}{MN} \right) + \frac{E_\pi}{MN} q^2 \right. \right. \\
 & + \frac{E_\pi}{MN} \left( -2\vec{p}_N \cdot \vec{p}_\pi - 2\vec{p}_{N'} \cdot \vec{p}_{\pi'} - \vec{p}_N^2 - \vec{p}_{N'}^2 + \vec{p}_N \cdot \vec{p}_{N'} + \vec{p}_N \cdot \vec{p}_{\pi'} \right) \\
 & \left. + \frac{2E_\pi}{MN} i\vec{\sigma} \cdot (\vec{p}_N' \times \vec{p}_N) + 2i\vec{\sigma} \cdot (\vec{p}_\pi' \times \vec{p}_\pi) \right\} \frac{f_2}{2\hat{p}_\pi \hat{p}_{\pi'}} \left. \right] U_p.
 \end{aligned}$$

But

$$\text{N45 } -q^2 = -(\vec{p}_{N'} - \vec{p}_N)^2 = -\vec{p}_N^2 - \vec{p}_{N'}^2 + 2\vec{p}_N \cdot \vec{p}_{N'},$$

so

$$\begin{aligned}
 \text{N46 } M_{\alpha\beta} = & U_p^+ \left[ \left\{ 1 + \frac{E_\pi}{MN} \right\} f_1 + \left\{ \vec{p}_\pi \cdot \vec{p}_{\pi'} \left( 1 - \frac{E_\pi}{MN} \right) \right. \right. \\
 & \left. - \frac{E_\pi}{MN} (\vec{p}_N \cdot \vec{p}_\pi + \vec{p}_{N'} \cdot \vec{p}_{\pi'}) + \frac{E_\pi}{MN} i\vec{\sigma} \cdot (\vec{p}_N' \times \vec{p}_N) + i\vec{\sigma} \cdot (\vec{p}_\pi' \times \vec{p}_\pi) \right\} \frac{f_2}{\hat{p}_\pi \hat{p}_{\pi'}} \left. \right] U_p.
 \end{aligned}$$

From equations N29, N30, N32, N33, N34, and N36 one has

$$N47 \quad f_1 = b_0 + b_1 \underline{t}_\pi \cdot \underline{T}_N + (c_0 + c_1 \underline{t}_\pi \cdot \underline{T}_N - d_0 - d_1 \underline{t}_\pi \cdot \underline{T}_N) \hat{p}_\pi \cdot \hat{p}'_\pi$$

$$N48 \quad \frac{f_2}{\hat{p}_\pi \cdot \hat{p}'_\pi} = d_0 + d_1 \underline{t}_\pi \cdot \underline{T}_N.$$

Using the Lorentz transformation one finds the relationship to order  $E\pi/M_N$

$$N49 \quad \hat{p}_\pi \cdot \hat{p}'_\pi \cong \left[ \vec{p}_\pi \cdot \vec{p}'_\pi - \frac{E\pi}{M_N} (\vec{p}_N \cdot \vec{p}'_\pi + \vec{p}'_N \cdot \vec{p}_\pi) \right] / \left( 1 + \frac{E\pi}{M_N} \right)^2.$$

Thus  $M_{\alpha\beta}$  in equation N46 may be written

$$N50 \quad M_{\alpha\beta} = U_p^+ \left[ \left( 1 + \frac{E\pi}{M_N} \right) \left\{ (b_0 + b_1 \underline{t}_\pi \cdot \underline{T}_N) + (c_0 + c_1 \underline{t}_\pi \cdot \underline{T}_N - d_0 - d_1 \underline{t}_\pi \cdot \underline{T}_N) \left( \frac{\vec{p}_\pi \cdot \vec{p}'_\pi - \frac{E\pi}{M_N} (\vec{p}_N \cdot \vec{p}'_\pi + \vec{p}'_N \cdot \vec{p}_\pi)}{(1 + E\pi/M_N)^2} \right) \right\} + (d_0 + d_1 \underline{t}_\pi \cdot \underline{T}_N) \left\{ \frac{\vec{p}_\pi \cdot \vec{p}'_\pi}{1 + E\pi/M_N} - \frac{E\pi}{M_N} (\vec{p}_N \cdot \vec{p}'_\pi + \vec{p}'_N \cdot \vec{p}_\pi) + \frac{E\pi}{M_N} i \vec{\sigma} \cdot (\vec{p}'_\pi \times \vec{p}_\pi) + i \vec{\sigma} \cdot (\vec{p}'_N \times \vec{p}_N) \right\} \right] U_p$$

or cancelling out  $d_0 + d_1 \underline{t}_\pi \cdot \underline{T}_N$  terms

$$N51 \quad M_{\alpha\beta} = U_p^+ \left[ \left( 1 + \frac{E\pi}{M_N} \right) (b_0 + b_1 \underline{t}_\pi \cdot \underline{T}_N) + (c_0 + c_1 \underline{t}_\pi \cdot \underline{T}_N) \left\{ \frac{\vec{p}_\pi \cdot \vec{p}'_\pi - \frac{E\pi}{M_N} (\vec{p}_N \cdot \vec{p}'_\pi + \vec{p}'_N \cdot \vec{p}_\pi)}{1 + E\pi/M_N} \right\} + i (d_0 + d_1 \underline{t}_\pi \cdot \underline{T}_N) \left\{ \vec{\sigma} \cdot (\vec{p}'_\pi \times \vec{p}_\pi) + \frac{E\pi}{M_N} \vec{\sigma} \cdot (\vec{p}'_N \times \vec{p}_N) \right\} \right] U_p.$$

In order to evaluate the  $\vec{p}'_N \cdot \vec{p}'_\pi + \vec{p}'_N \cdot \vec{p}_\pi$  terms one needs to note that in a complex nucleus

$$\begin{aligned} \text{N52} \quad \langle 0^+ | \sum_{i=1}^A \delta(\vec{r}-\vec{r}_i) \vec{P}_{N_i} | 0^+ \rangle &= \langle 0^+ | \sum_{i=1}^A \delta(\vec{r}-\vec{r}_i) (-i \nabla_i) | 0^+ \rangle \\ &= -\frac{i}{2} \nabla e(r). \end{aligned}$$

Similarly

$$\text{N53} \quad \langle 0^+ | \sum_{i=1}^A \vec{P}_{N_i} \delta(\vec{r}-\vec{r}_i) | 0^+ \rangle = +\frac{i}{2} \nabla e(r).$$

Thus in evaluating reduced matrix integrals like

$$\text{N54} \quad \int d^3r e^{i\vec{q}\cdot\vec{r}} \vec{P}_{\pi'} \cdot \langle 0^+ | \sum_{i=1}^A \delta(\vec{r}-\vec{r}_i) \vec{P}_{N_i} | 0^+ \rangle$$

one should break  $\vec{P}_{\pi'}$  into components perpendicular and parallel to  $\vec{q}$ .

Only  $\vec{P}_{\pi}$  parallel to  $\vec{q}$  can contribute.

Let

$$\text{N55} \quad \vec{\Sigma} = \vec{P}_{\pi} + \vec{P}_{\pi'}$$

$$\text{N56} \quad \vec{q} = \vec{P}_{\pi} - \vec{P}_{\pi'}$$

Thus

$$\text{N57} \quad \vec{P}_{\pi} = \frac{\vec{\Sigma} + \vec{q}}{2}$$

$$\text{N58} \quad \vec{P}_{\pi'} = \frac{\vec{\Sigma} - \vec{q}}{2}$$

and

$$\begin{aligned} \text{N59} \quad \int d^3r e^{i\vec{q}\cdot\vec{r}} \vec{P}_{\pi'} \cdot \langle 0^+ | \sum_{i=1}^A \delta(\vec{r}-\vec{r}_i) \vec{P}_{N_i} | 0^+ \rangle \\ &= \int d^3r e^{i\vec{q}\cdot\vec{r}} \left(-\frac{\vec{q}}{2}\right) \cdot \left(-\frac{i}{2} \nabla\right) e(r) \\ &= \int d^3r e^{i\vec{q}\cdot\vec{r}} \frac{q^2}{4} e(r) \end{aligned}$$

where one integrates by parts to get the  $\nabla$  to operate on  $e^{i\vec{q}\cdot\vec{r}}$ .

Similarly

$$\begin{aligned} \text{N60} \quad \int d^3r e^{i\vec{q}\cdot\vec{r}} \vec{P}_\pi \cdot \langle 0^+ | \sum_{i=1}^A \vec{P}_{N_i} \delta(\vec{r}-\vec{r}_i) | 0^+ \rangle \\ = \int d^3r e^{i\vec{q}\cdot\vec{r}} (g/a) i \frac{\nabla}{2} e(r) \\ = \int d^3r e^{i\vec{q}\cdot\vec{r}} \frac{g^2}{4} e(r) \end{aligned}$$

Thus one obtains

$$\text{N61} \quad \vec{P}'_\pi \cdot \vec{P}_N + \vec{P}_\pi \cdot \vec{P}_{N'} = g^2/a.$$

Using N61 one obtains the final expression for  $M_{\alpha\beta}$  to be

$$\begin{aligned} \text{N62} \quad M_{\alpha\beta} = U_P^+ \left[ \left( 1 + \frac{E_\pi}{M_N} \right) (b_0 + b_1 \underline{t}_\pi \cdot \underline{T}_N) + (c_0 + c_1 \underline{t}_\pi \cdot \underline{T}_N) \right. \\ \left. \left\{ \frac{\underline{P}_\pi \cdot \underline{P}_{N'} - \frac{E_\pi}{2M_N} g^2}{1 + E_\pi/M_N} \right\} + i (d_0 + d_1 \underline{t}_\pi \cdot \underline{T}_N) \right. \\ \left. \left\{ \vec{\sigma} \cdot (\vec{P}'_\pi \times \vec{P}_\pi) + \frac{E_\pi}{M_N} \vec{\sigma} \cdot (\vec{P}'_N \times \vec{P}_N) \right\} \right] U_P \\ \equiv U_P^+ \left[ \left( 1 + \frac{E_\pi}{M_N} \right) \underline{b} + \underline{c} \left( \vec{P}_\pi \cdot \vec{P}_{N'} - \frac{E_\pi}{2M_N} g^2 \right) / \left( 1 + \frac{E_\pi}{M_N} \right) \right. \\ \left. + i \underline{d} \left\{ \vec{\sigma} \cdot (\vec{P}'_\pi \times \vec{P}_\pi) + \frac{E_\pi}{M_N} \vec{\sigma} \cdot (\vec{P}'_N \times \vec{P}_N) \right\} \right] U_P. \end{aligned}$$

This result is accurate to order  $E_\pi/M_N$ . Although this form seems unique, there are two possible ways of putting in  $\underline{q}^2$ , i.e. in nucleon operators or pion operators. Cannata, Lucas, and Werntz<sup>171</sup> used  $\underline{q}^2 = -\nabla^2 e(r)$ . A similar result was derived independently by Mach<sup>166</sup> in a different way. Kisslinger and Tabakin<sup>167</sup> attempted to derive this result but failed to obtain the coefficient of 1/2 for the nucleon motion term proportional to  $\frac{E_\pi}{M_N} \nabla^2 e(r)$ . According to Krajcik and Foldy<sup>122</sup> one must use bound state nucleon spinors if one wants to find the proper higher order terms in  $M_{\alpha\beta}$ .

TABLE 1. Low energy s-wave  $\pi N$  scattering lengths.

$\alpha_1$	$\alpha_3$	Reference
$(m_\pi^{-1})$	$(m_\pi^{-1})$	
$0.205 \pm 0.005$	$-0.115 \pm 0.003$	111, 112 <sup>a</sup>
$0.182 \pm 0.006$	$-0.103 \pm 0.006$	102, 103
0.17	-0.10	104
$0.171 \pm 0.005$	$-0.088 \pm 0.004$	105
$0.183 \pm 0.016$	$-0.109 \pm 0.016$	106
$0.179 \pm 0.019$	$-0.103 \pm 0.019$	110
$0.180 \pm 0.012$	$-0.091 \pm 0.005$	108

a. As quoted in reference 102.

TABLE 2. Low energy p-wave  $\pi N$  scattering lengths.

$\alpha_{11}$ ( $m\pi^{-3}$ )	$\alpha_{13}$ ( $m\pi^{-3}$ )	$\alpha_{31}$ ( $m\pi^{-3}$ )	$\alpha_{33}$ ( $m\pi^{-3}$ )	Reference
$-0.016 \pm 0.110$	$-0.055 \pm 0.062$	$-0.0418 \pm 0.004$	0.210	111-114 <sup>a</sup>
-0.015	-0.0035	-0.13	0.243	104 <sup>b</sup>
-0.016	-0.13	-0.13	0.201	104 <sup>b</sup>
$-0.101 \pm 0.007$	$-0.029 \pm 0.005$	$-0.038 \pm 0.005$	$0.215 \pm 0.005$	105

a. As quoted in reference 102.

b. The two entries refer to two different parameterizations.

TABLE 3. Low energy s-wave  $\pi\pi\pi$  scattering lengths.

$B_{01}$ ( $m_{\pi}^{-4}$ )	$B_{11}$ ( $m_{\pi}^{-4}$ )	$B_{00}$ ( $m_{\pi}^{-4}$ )	$B_{02}$ ( $m_{\pi}^{-4}$ )	Ref- erence
$(-0.054 \pm 0.020)(1-i)$	$(-0.044 \pm 0.004)(1-i)$	---	---	19 <sup>a</sup>
$(-0.054 \pm 0.020)(1-i)$	$(-0.077 \pm 0.007)(1-i)$	---	---	21 <sup>a</sup>

a. The real parts are crudely estimated to be of the same magnitude but opposite sign to the imaginary part.

TABLE 4. Low energy p-wave TNN scattering lengths.

$3(\chi_{01} + 5\chi_{21})$ $(m\pi)^{-6}$	$3\chi_{10}$ $(m\pi)^{-6}$	$\chi_{11}(0,1)$ $(m\pi)^{-6}$	$\chi_{12}$ $(m\pi)^{-6}$	$\chi_{11}(1,0)$ $(m\pi)^{-6}$	Ref- erence
$(-2.80 \pm 0.29)(1-i)$	$(-1.4 \pm 0.5)(1-i)$	---	---	---	19 <sup>a</sup>
$(-3.10)(1-i)$	$(-0.4)(1-i)$	---	---	---	21 <sup>a</sup>

a. The real parts are crudely estimated to be of the same magnitude but opposite sign to the imaginary part.

TABLE 5. Summary of data for pionic 2p-1s transitions.

Isotope	2p-1s Transition Energies (Kev)			
	Berkeley <sup>5,6</sup>	CERN <sup>7</sup>	W&M <sup>1-4</sup>	Average
<sup>3</sup> He	---	---	10.68 ± 0.06	10.68 ± 0.06
<sup>4</sup> He	---	---	10.70 ± 0.05	10.70 ± 0.05
<sup>6</sup> Li	23.9 ± 0.2	---	24.18 ± 0.06	24.157 ± 0.057
<sup>7</sup> Li	23.8 ± 0.2	---	24.06 ± 0.06	24.039 ± 0.057
<sup>9</sup> Be	42.1 ± 0.2	42.38 ± 0.20	42.32 ± 0.05	42.311 ± 0.047
<sup>10</sup> B	64.9 ± 0.2	65.94 ± 0.18	65.79 ± 0.11	65.663 ± 0.210
<sup>11</sup> B	64.5 ± 0.2	64.98 ± 0.18	65.00 ± 0.11	64.905 ± 0.110
<sup>12</sup> C	93.3 ± 0.5	92.94 ± 0.15	93.19 ± 0.12	93.099 ± 0.092
<sup>14</sup> N	123.9 ± 0.5	124.74 ± 0.15	---	124.671 ± 0.163
<sup>16</sup> O	160.6 ± 0.7	159.95 ± 0.25	---	160.024 ± 0.235
<sup>18</sup> O	---	155.01 ± 0.25	---	155.01 ± 0.25
<sup>19</sup> F	196.5 ± 0.5	195.9 ± 0.5	---	196.20 ± 0.35
<sup>20</sup> Ne	---	---	238.35 ± 0.50	238.35 ± 0.50
<sup>23</sup> Na	277.2 ± 1.0	276.2 ± 1.0	277.7 ± 0.5	277.37 ± 0.41
<sup>24</sup> Mg	330.3 ± 1.0	---	331.80 ± 1.65	330.70 ± 0.86

TABLE 5. Summary of data for pionic 2p-1s transitions. (Cont'd)

Isotope	Widths (Kev)			
	Berkeley <sup>5,6</sup>	CERN <sup>7</sup>	W&M <sup>1-4</sup>	Average
<sup>3</sup> He	---	---	+ 0.06	+ 0.06
<sup>4</sup> He	---	---	0.01 - 0.01	0.01 - 0.01
<sup>6</sup> Li	0.39 ± 0.36	---	0.15 ± 0.05	0.155 ± 0.050
<sup>7</sup> Li	0.57 ± 0.30	---	0.19 ± 0.05	0.200 ± 0.049
<sup>9</sup> Be	0.85 ± 0.28	1.07 ± 0.30	0.58 ± 0.05	0.601 ± 0.052
<sup>10</sup> B	1.4 ± 0.5	1.27 ± 0.25	1.68 ± 0.12	1.594 ± 0.106
<sup>11</sup> B	2.3 ± 0.5	1.87 ± 0.25	1.72 ± 0.15	1.793 ± 0.125
<sup>12</sup> C	2.6 ± 0.5	2.96 ± 0.25	3.25 ± 0.15	3.138 ± 0.125
<sup>14</sup> N	4.1 ± 0.4	4.48 ± 0.30	---	4.343 ± 0.240
<sup>16</sup> O	9.0 ± 2.0	7.56 ± 0.50	---	7.645 ± 0.485
<sup>18</sup> O	---	8.67 ± 0.70	---	8.67 ± 0.70
<sup>19</sup> F	4.6 ± 2.0	9.4 ± 1.5	---	7.67 ± 1.63
<sup>20</sup> Ne	---	---	14.2 ± 2.0	14.2 ± 2.0
<sup>23</sup> Na	4.6 ± 3.0	10.3 ± 4.0	7.2 ± 1.2	6.93 ± 1.07
<sup>24</sup> Mg	---	---	7.8 ± 5.0	7.8 ± 5.0

TABLE 6. Summary of data for pionic 3d-2p transitions.

Isotope	3d-2p Transition Energies (Kev)	2p Widths (ev) <sup>a</sup>		
	NAL <sup>147</sup>	CERN <sup>148,149</sup>	W&M <sup>150</sup>	NAL <sup>147</sup>
<sup>4</sup> He	---	---	---	0.0033 ± 0.0013
<sup>6</sup> Li	---	---	0.015 ± 0.005	---
<sup>7</sup> Li	---	---	---	0.0165 ± 0.0066
<sup>9</sup> Be	8.10 ± 0.15	0.16 ± 0.03	0.16 ± 0.03	0.0526 ± 0.0132
<sup>10</sup> B	---	0.32 ± 0.06	---	---
<sup>11</sup> B	---	0.27 ± 0.04	---	---
<sup>12</sup> C	18.40 ± 0.32	1.02 ± 0.29	2.6 ± 0.9	1.25 ± 0.20
<sup>14</sup> N	---	2.1 ± 0.3	---	---
<sup>16</sup> O	---	4.7 ± 0.8	12.0 ± 4.0	---
<sup>18</sup> O	---	3.8 ± 0.7	---	---
<sup>19</sup> F	---	11.2 ± 1.9	---	---
<sup>23</sup> Na	---	34.6 ± 7.6	---	---

TABLE 6. Summary of data for pionic 3d-2p transitions. (Cont'd)

Isotope	3d-2p Transition Energies (KeV)			
	Berkeley <sup>6,160,161</sup>	CERN <sup>162</sup>	W&M <sup>163</sup>	Average
<sup>27</sup> Al	87.53 ± 0.07	87.40 ± 0.10	---	87.48 ± 0.06
<sup>28</sup> Si	---	101.58 ± 0.15	---	101.58 ± 0.15
<sup>31</sup> P	---	116.78 ± 0.10	---	116.78 ± 0.10
<sup>32</sup> S	133.2 ± 0.3	133.06 ± 0.10	---	133.07 ± 0.09
<sup>35</sup> Cl	---	150.55 ± 0.15	---	150.55 ± 0.15
<sup>39</sup> K	188.6 ± 0.3	188.77 ± 0.18	---	188.73 ± 0.15
<sup>40</sup> Ca	209.3 ± 0.3	209.66 ± 0.18	---	209.56 ± 0.15
<sup>44</sup> Ca	208.94 ± 0.10	---	---	208.94 ± 0.10
<sup>48</sup> Ti	---	253.98 ± 0.20	---	253.98 ± 0.20
<sup>51</sup> V	278.2 ± 0.4	277.85 ± 0.20	---	277.92 ± 0.18
<sup>52</sup> Cr	302.5 ± 0.5	302.75 ± 0.25	---	302.70 ± 0.22
<sup>55</sup> Mn	328.5 ± 0.8	329.12 ± 0.25	---	329.06 ± 0.24
<sup>56</sup> Fe	356.9 ± 1.0	356.43 ± 0.30	---	356.47 ± 0.29
<sup>59</sup> Co	384.6 ± 1.0	384.74 ± 0.35	---	384.72 ± 0.33
<sup>58</sup> Ni	---	415.23 ± 0.70	414.11 ± 0.48	414.47 ± 0.40
<sup>60</sup> Ni	---	---	414.08 ± 0.51	414.08 ± 0.51
<sup>63</sup> Cu	---	446.1 ± 2.0	---	446.1 ± 2.0
<sup>64</sup> Zn	---	478.2 ± 3.0	---	478.2 ± 3.0

TABLE 6. Summary of data for pionic 3d-2p transitions. (Cont'd)

Isotope	Widths (Kev)			
	Berkeley <sup>6,161</sup>	CERN <sup>22,162</sup>	W&M <sup>163</sup>	Average
<sup>27</sup> Al	---	0.11 + 0.08 0.36 ± 0.15	---	0.11 + 0.08 0.36 ± 0.15
<sup>28</sup> Si	---	0.18 ± 0.08	---	0.18 ± 0.08
<sup>31</sup> P	---	0.20 + 0.08 0.43 ± 0.15	---	0.20 + 0.08 0.43 ± 0.15
<sup>32</sup> S	0.8 ± 0.4	0.79 ± 0.15	---	0.79 ± 0.15
<sup>35</sup> Cl	---	0.89 ± 0.25	---	0.89 ± 0.25
<sup>39</sup> K	1.90 ± 0.15	1.45 ± 0.15	---	1.68 ± 0.11
<sup>40</sup> Ca	2.29 ± 0.13	2.00 ± 0.25	---	2.23 ± 0.12
<sup>44</sup> Ca	2.07 ± 0.15	----	---	2.07 ± 0.15
<sup>48</sup> Ti	---	2.89 ± 0.25	---	2.89 ± 0.25
<sup>51</sup> V	---	3.66 ± 0.25	---	3.66 ± 0.25
<sup>52</sup> Cr	---	4.46 ± 0.35	---	4.46 ± 0.35
<sup>55</sup> Mn	---	6.38 ± 0.40	---	6.38 ± 0.40
<sup>56</sup> Fe	6.0 ± 2.5	8.65 ± 0.60	---	8.51 ± 0.58
<sup>59</sup> Co	---	7.37 ± 0.70	---	7.37 ± 0.70
<sup>58</sup> Ni	---	12.7 ± 3.0	7.6 ± 1.4	8.5 ± 1.3
<sup>60</sup> Ni	---	----	8.5 ± 1.5	8.5 ± 1.5
<sup>63</sup> Cu	---	15.9 ± 4.0	---	15.9 ± 4.0
<sup>64</sup> Zn	---	16.8 ± 6.0	---	16.8 ± 6.0

TABLE 7. Summary of data for pionic 4f-3d transitions.

Isotope	4f-3d Transition Energies (KeV)		3d Widths (ev) <sup>a</sup>
	Berkeley <sup>159</sup>		CERN <sup>22</sup>
<sup>27</sup> Al	---		0.02 ± 0.01
<sup>28</sup> Si	---		0.01 ± 0.04
<sup>31</sup> P	---		0.09 ± 0.05
<sup>32</sup> S	---		0.07 ± 0.06
Cl	---		0.30 ± 0.13
K	---		0.6 ± 0.3
<sup>40</sup> Ca	72.352 ± 0.009		0.5 ± 0.3
Ti	87.651 ± 0.009		2.5 ± 0.7
<sup>51</sup> V	---		1.7 ± 0.9
Cr	---		4.9 ± 1.1
<sup>55</sup> Mn	---		6.7 ± 1.4
Fe	---		9.2 ± 2.2
<sup>59</sup> Co	---		12.9 ± 7.0
Ni	---		12.2 ± 4.3
Cu	---		18.4 ± 6.8
Zn	---		29.5 ± 12.4

a. These widths were calculated by means of a cascade calculation that reproduced the observed yields of the 2p-1s transitions.

TABLE 7. Summary of data for pionic 4f-3d transitions. (Cont'd)

Isotope	4f-3d Transition Energies (KeV)	
	Berkeley <sup>6</sup>	CERN <sup>164</sup>
<sup>89</sup> Y	278.2 ± 0.3	---
<sup>93</sup> Nb	307.6 ± 0.3	307.7 ± 0.2
Mo	---	323.2 ± 0.2
<sup>103</sup> Rh	370.9 ± 0.4	---
In	442.1 ± 1.1	442.9 ± 0.5
<sup>116</sup> Sn	460.9 ± 0.6	---
<sup>117</sup> Sn	460.4 ± 0.6	---
<sup>118</sup> Sn	460.4 ± 0.6	---
<sup>119</sup> Sn	460.3 ± 0.6	---
<sup>120</sup> Sn	460.5 ± 0.6	---
<sup>122</sup> Sn	460.3 ± 0.6	---
<sup>124</sup> Sn	460.2 ± 0.6	---
<sup>127</sup> I	519.1 ± 1.1	520.8 ± 0.8
<sup>133</sup> Cs	560.5 ± 1.1	562.0 ± 1.5
La	603.6 ± 0.9	604.9 ± 2.0
<sup>140</sup> Ce	626.1 ± 2.0	---
<sup>141</sup> Pr	649.5 ± 2.0	648.1 ± 2.0

TABLE 7. Summary of data for pionic 4f-3d transitions. (Cont'd)

Isotope	Widths (KeV)		
	Berkeley <sup>6</sup>	CERN <sup>164</sup>	
	without hfs	without hfs	with hfs
<sup>89</sup> Y	0.8 ± 0.6	---	---
<sup>93</sup> Nb	0.6 ± 0.4	0.52 ± 0.10	---
Mo	---	0.56 ± 0.10	---
<sup>103</sup> Rh	1.2 ± 0.6	---	---
In	---	2.8 ± 0.6	2.6 ± 0.6
<sup>116</sup> Sn	1.9 ± 1.2	---	---
<sup>117</sup> Sn	2.1 ± 1.2	---	---
<sup>118</sup> Sn	2.5 ± 1.2	---	---
<sup>119</sup> Sn	1.9 ± 1.2	----	---
<sup>120</sup> Sn	2.7 ± 1.2	---	---
<sup>122</sup> Sn	2.0 ± 1.2	---	---
<sup>124</sup> Sn	2.3 ± 1.2	---	---
<sup>127</sup> I	---	4.6 ± 1.5	4.4 ± 1.5
<sup>133</sup> Cs	4.2 ± 1.8	3.3 ± 1.5	---
La	---	6.2 ± 2.0	6.2 ± 2.0
<sup>140</sup> Ce	5.8 ± 3.8	---	---
<sup>141</sup> Pr	6.7 ± 2.8	5.4 ± 2.5	---

TABLE 8. Summary of data for pionic 5g-4f transitions.

Isotope	5g-4f Transition Energies (KeV)				Widths (KeV)			
	Berkeley <sup>6</sup>		CERN <sup>164</sup>		Berkeley <sup>6</sup>		CERN <sup>164</sup>	
	W&M <sup>165</sup>		without hfs		without hfs		with hfs	
<sup>181</sup> Ta	453.1 ± 0.4	453.90 ± 0.20	453.4 ± 0.3	---	---	---	0.5 ± 0.2	
Pt	---	519.34 ± 0.24	---	---	1.8 ± 1.0	---	---	
<sup>179</sup> Au	532.5 ± 0.5	533.16 ± 0.20	---	---	1.1 ± 0.3	1.0 ± 0.3	---	
Hg	---	547.14 ± 0.25	---	---	1.4 ± 0.5	---	---	
Tl	---	561.67 ± 0.25	---	---	1.0 ± 0.2	---	---	
<sup>206</sup> Pb	---	575.62 ± 0.30	---	---	1.2 ± 0.4	---	---	
nat <sup>208</sup> Pb	---	575.56 ± 0.25	---	---	1.1 ± 0.3	---	---	
<sup>209</sup> Bi	589.8 ± 0.9	590.06 ± 0.30	---	---	1.7 ± 1.0	1.7 ± 0.5	1.7 ± 0.5	
<sup>232</sup> Th	698.0 ± 0.6	698.4 ± 0.4	---	---	6.0 ± 0.9	4.6 ± 0.8	---	
<sup>238</sup> U	731.4 ± 1.1	732.0 ± 0.4	---	---	6.1 ± 1.0	6.8 ± 0.8	---	
<sup>239</sup> Pu	766.2 ± 1.6	---	---	---	9.1 ± 2.5	---	---	

TABLE 9. Elastic differential scattering cross section data in the pion-nucleus CM for  $\pi^+$  on  ${}^4\text{He}$  at 24 MeV pion kinetic energy in the lab.<sup>151</sup>

$\Theta$ (deg)	$d\sigma/d\Omega_{\pi^+}$ (fm <sup>2</sup> /sr)	$d\sigma/d\Omega_{\pi^-}$ (fm <sup>2</sup> /sr)
51.6 $\pm$ 8.0	0.027 $\pm$ 0.005	0.079 $\pm$ 0.011
61.8 $\pm$ 8.0	0.038 $\pm$ 0.006	0.035 $\pm$ 0.008
76.9 $\pm$ 8.0	0.044 $\pm$ 0.005	0.012 $\pm$ 0.005
92.0 $\pm$ 8.0	0.073 $\pm$ 0.005	0.033 $\pm$ 0.012
107.0 $\pm$ 8.0	0.104 $\pm$ 0.008	0.075 $\pm$ 0.010
121.8 $\pm$ 8.0	0.153 $\pm$ 0.015	0.133 $\pm$ 0.013
139.3 $\pm$ 8.0	0.233 $\pm$ 0.016	0.175 $\pm$ 0.027
150.9 $\pm$ 8.0	0.248 $\pm$ 0.012	0.275 $\pm$ 0.022

TABLE 10. Elastic differential scattering cross section data in the pion-nucleus CM for  $\pi_{\pm}$  on  ${}^4\text{He}$  at 51 MeV pion kinetic energy in the lab.<sup>152</sup>

$\Theta$ (deg)	$d\sigma/d\Omega_{\pi^+}$ (fm <sup>2</sup> /sr)	$d\sigma/d\Omega_{\pi^-}$ (fm <sup>2</sup> /sr)
31.5 $\pm$ 2.5	0.1516 $\pm$ 0.0140	0.5192 $\pm$ 0.0254
36.7 $\pm$ 2.5	0.1611 $\pm$ 0.0136	0.3969 $\pm$ 0.0166
41.9 $\pm$ 2.5	0.1223 $\pm$ 0.0093	0.2978 $\pm$ 0.0145
47.1 $\pm$ 2.5	0.1131 $\pm$ 0.0093	0.2033 $\pm$ 0.0107
62.5 $\pm$ 2.5	0.0434 $\pm$ 0.0024	0.0560 $\pm$ 0.0025
67.6 $\pm$ 2.5	0.0266 $\pm$ 0.0023	0.0371 $\pm$ 0.0020
72.7 $\pm$ 2.5	0.0323 $\pm$ 0.0020	0.0269 $\pm$ 0.0019
77.8 $\pm$ 2.5	0.0375 $\pm$ 0.0023	0.0314 $\pm$ 0.0020
82.8 $\pm$ 2.5	0.0581 $\pm$ 0.0026	0.0427 $\pm$ 0.0023
92.9 $\pm$ 2.5	0.0993 $\pm$ 0.0050	0.0950 $\pm$ 0.0041
102.8 $\pm$ 2.5	0.1610 $\pm$ 0.0057	0.1638 $\pm$ 0.0053
122.5 $\pm$ 2.5	0.3433 $\pm$ 0.0144	0.3715 $\pm$ 0.0132
132.2 $\pm$ 2.5	0.4095 $\pm$ 0.0164	0.4471 $\pm$ 0.0148
141.8 $\pm$ 2.5	0.4764 $\pm$ 0.0177	0.4791 $\pm$ 0.0147
151.4 $\pm$ 2.5	0.4918 $\pm$ 0.0194	0.5034 $\pm$ 0.0156

TABLE 11. Elastic differential scattering cross section data in the pion-nucleus CM for  $\pi_{\pm}$  on  ${}^4\text{He}$  at 60 MeV pion kinetic energy in the lab.<sup>152</sup>

$\Theta$ (deg)	$d\sigma/d\Omega_{\pi^+}$ (fm <sup>2</sup> /sr)	$d\sigma/d\Omega_{\pi^-}$ (fm <sup>2</sup> /sr)
31.5 $\pm$ 2.5	0.2661 $\pm$ 0.0075	0.6712 $\pm$ 0.0146
36.7 $\pm$ 2.5	0.2634 $\pm$ 0.0071	0.5033 $\pm$ 0.0106
41.9 $\pm$ 2.5	0.2327 $\pm$ 0.0052	0.3854 $\pm$ 0.0076
47.1 $\pm$ 2.5	0.1663 $\pm$ 0.0046	0.2835 $\pm$ 0.0062
62.6 $\pm$ 2.5	0.0534 $\pm$ 0.0010	0.0747 $\pm$ 0.0013
67.7 $\pm$ 2.5	0.0366 $\pm$ 0.0009	0.0436 $\pm$ 0.0009
72.8 $\pm$ 2.5	0.0325 $\pm$ 0.0008	0.0306 $\pm$ 0.0008
77.9 $\pm$ 2.5	0.0375 $\pm$ 0.0008	0.0336 $\pm$ 0.0009
83.0 $\pm$ 2.5	0.0618 $\pm$ 0.0012	0.0521 $\pm$ 0.0011
93.0 $\pm$ 2.5	0.1128 $\pm$ 0.0021	0.1077 $\pm$ 0.0021
102.9 $\pm$ 2.5	0.1928 $\pm$ 0.0031	0.1916 $\pm$ 0.0031
122.6 $\pm$ 2.5	0.3936 $\pm$ 0.0079	0.4232 $\pm$ 0.0083
132.3 $\pm$ 2.5	0.4592 $\pm$ 0.0104	0.4875 $\pm$ 0.0109
141.9 $\pm$ 2.5	0.5422 $\pm$ 0.0150	0.5544 $\pm$ 0.0153
151.5 $\pm$ 2.5	0.5721 $\pm$ 0.0196	0.5924 $\pm$ 0.0203

TABLE 12. Elastic differential scattering cross section data in the pion-nucleus CM for  $\pi_{\pm}$  on  ${}^4\text{He}$  at 68 MeV pion kinetic energy in the lab. <sup>152</sup>

$\Theta$ (deg)	$d\sigma/d\Omega_{\pi^+}$ ( $\text{fm}^2/\text{sr}$ )	$d\sigma/d\Omega_{\pi^-}$ ( $\text{fm}^2/\text{sr}$ )
$31.6 \pm 2.5$	$0.4031 \pm 0.0190$	$0.7299 \pm 0.0273$
$36.8 \pm 2.5$	$0.3612 \pm 0.0176$	$0.5312 \pm 0.0361$
$42.0 \pm 2.5$	$0.3247 \pm 0.0135$	$0.4494 \pm 0.0164$
$47.2 \pm 2.5$	$0.2651 \pm 0.0126$	$0.3082 \pm 0.0223$
$62.7 \pm 2.5$	$0.0722 \pm 0.0025$	$0.0925 \pm 0.0034$
$67.8 \pm 2.5$	$0.0437 \pm 0.0020$	$0.0512 \pm 0.0026$
$72.9 \pm 2.5$	$0.0382 \pm 0.0018$	$0.0366 \pm 0.0022$
$78.0 \pm 2.5$	$0.0447 \pm 0.0019$	$0.0388 \pm 0.0025$
$83.1 \pm 2.5$	$0.0692 \pm 0.0025$	$0.0556 \pm 0.0030$
$93.1 \pm 2.5$	$0.1350 \pm 0.0047$	$0.1180 \pm 0.0051$
$103.0 \pm 2.5$	$0.2094 \pm 0.0063$	$0.2018 \pm 0.0069$
$122.7 \pm 2.5$	$0.4011 \pm 0.0149$	$0.4392 \pm 0.0142$
$132.4 \pm 2.5$	$0.4961 \pm 0.0176$	$0.5098 \pm 0.0163$
$142.0 \pm 2.5$	$0.5853 \pm 0.0213$	$0.5543 \pm 0.0316$
$151.5 \pm 2.5$	$0.5843 \pm 0.0267$	$0.5591 \pm 0.0333$

TABLE 13. Elastic differential scattering cross section data in the pion-nucleus CM for  $\pi_{\pm}$  on  ${}^4\text{He}$  at 75 MeV pion kinetic energy in the lab. <sup>152</sup>

$\Theta$ (deg)	$d\sigma/d\Omega \pi^+$ (fm <sup>2</sup> /sr)	$d\sigma/d\Omega \pi^-$ (fm <sup>2</sup> /sr)
31.6 $\pm$ 2.5	0.5940 $\pm$ 0.0205	0.9394 $\pm$ 0.0236
36.9 $\pm$ 2.5	0.5252 $\pm$ 0.0167	0.7080 $\pm$ 0.0215
42.1 $\pm$ 2.5	0.4268 $\pm$ 0.0141	0.5858 $\pm$ 0.0132
47.3 $\pm$ 2.5	0.3006 $\pm$ 0.0104	0.3979 $\pm$ 0.0127
62.8 $\pm$ 2.5	0.0960 $\pm$ 0.0025	0.1119 $\pm$ 0.0023
67.9 $\pm$ 2.5	0.0623 $\pm$ 0.0019	0.0667 $\pm$ 0.0017
73.0 $\pm$ 2.5	0.0458 $\pm$ 0.0017	0.0488 $\pm$ 0.0014
78.1 $\pm$ 2.5	0.0529 $\pm$ 0.0019	0.0498 $\pm$ 0.0015
83.2 $\pm$ 2.5	0.0776 $\pm$ 0.0023	0.0710 $\pm$ 0.0018
93.2 $\pm$ 2.5	0.1413 $\pm$ 0.0042	0.1325 $\pm$ 0.0035
103.1 $\pm$ 2.5	0.2203 $\pm$ 0.0057	0.2361 $\pm$ 0.0050
122.8 $\pm$ 2.5	0.4508 $\pm$ 0.0143	0.4578 $\pm$ 0.0103
132.4 $\pm$ 2.5	0.5264 $\pm$ 0.0152	0.5379 $\pm$ 0.0116
142.0 $\pm$ 2.5	0.6054 $\pm$ 0.0175	0.5646 $\pm$ 0.0169
151.6 $\pm$ 2.5	0.6114 $\pm$ 0.0200	0.6046 $\pm$ 0.0203

TABLE 14. Elastic differential scattering cross section data in the pion-nucleus CM for  $\pi^-$  on  ${}^4\text{He}$  at 110 Mev pion kinetic energy in the lab. 153

$\Theta$ (deg)	$d\sigma/d\Omega_{\pi^-}$ ( $\text{fm}^2/\text{sr}$ )	"	$\Theta$ (deg)	$d\sigma/d\Omega_{\pi^-}$ ( $\text{fm}^2/\text{sr}$ )
10.5 $\pm$ 1.0	0.900 $\pm$ 0.040	"	83.0 $\pm$ 1.0	0.013 $\pm$ 0.003
16.0 $\pm$ 1.0	0.530 $\pm$ 0.030	"	88.0 $\pm$ 1.0	0.015 $\pm$ 0.003
20.0 $\pm$ 1.0	0.400 $\pm$ 0.020	"	93.0 $\pm$ 1.0	0.023 $\pm$ 0.003
27.0 $\pm$ 1.0	0.320 $\pm$ 0.020	"	98.0 $\pm$ 1.0	0.028 $\pm$ 0.005
29.0 $\pm$ 1.0	0.280 $\pm$ 0.020	"	103.0 $\pm$ 1.0	0.024 $\pm$ 0.003
37.5 $\pm$ 1.0	0.180 $\pm$ 0.020	"	108.0 $\pm$ 1.0	0.032 $\pm$ 0.003
42.5 $\pm$ 1.0	0.120 $\pm$ 0.010	"	113.0 $\pm$ 1.0	0.038 $\pm$ 0.003
47.5 $\pm$ 1.0	0.098 $\pm$ 0.008	"	118.0 $\pm$ 1.0	0.039 $\pm$ 0.003
53.0 $\pm$ 1.0	0.065 $\pm$ 0.005	"	123.0 $\pm$ 1.0	0.051 $\pm$ 0.003
58.0 $\pm$ 1.0	0.033 $\pm$ 0.003	"	128.0 $\pm$ 1.0	0.052 $\pm$ 0.004
63.0 $\pm$ 1.0	0.020 $\pm$ 0.004	"	133.0 $\pm$ 1.0	0.047 $\pm$ 0.003
68.0 $\pm$ 1.0	0.014 $\pm$ 0.003	"	138.0 $\pm$ 1.0	0.043 $\pm$ 0.004
73.0 $\pm$ 1.0	0.0080 $\pm$ 0.0015	"	143.0 $\pm$ 1.0	0.049 $\pm$ 0.004
78.0 $\pm$ 1.0	0.0080 $\pm$ 0.0015	"	148.0 $\pm$ 1.0	0.031 $\pm$ 0.003

TABLE 15. Elastic differential scattering cross section data in the pion-nucleus CM for  $\pi^-$  on  ${}^4\text{He}$  at 150 MeV pion kinetic energy in the lab.<sup>153</sup>

$\Theta$ (deg)	$d\sigma/d\Omega_{\pi^-}$ (fm <sup>2</sup> /sr)
37.5 $\pm$ 1.0	0.17 $\pm$ 0.02
63.0 $\pm$ 1.0	0.015 $\pm$ 0.002
69.0 $\pm$ 1.0	0.0053 $\pm$ 0.0005
74.0 $\pm$ 1.0	0.0038 $\pm$ 0.0005
79.0 $\pm$ 1.0	0.0031 $\pm$ 0.0007
84.0 $\pm$ 1.0	0.0046 $\pm$ 0.0006
89.0 $\pm$ 1.0	0.0064 $\pm$ 0.0007
94.0 $\pm$ 1.0	0.0080 $\pm$ 0.0010
99.0 $\pm$ 1.0	0.010 $\pm$ 0.001
104.0 $\pm$ 1.0	0.010 $\pm$ 0.001
109.0 $\pm$ 1.0	0.010 $\pm$ 0.001
114.0 $\pm$ 1.0	0.0105 $\pm$ 0.0010
119.0 $\pm$ 1.0	0.0092 $\pm$ 0.0010
123.0 $\pm$ 1.0	0.0095 $\pm$ 0.0010
128.0 $\pm$ 1.0	0.0090 $\pm$ 0.0010
133.0 $\pm$ 1.0	0.0072 $\pm$ 0.0009
138.0 $\pm$ 1.0	0.0051 $\pm$ 0.0006
142.5 $\pm$ 1.0	0.0059 $\pm$ 0.0007
147.0 $\pm$ 1.0	0.0064 $\pm$ 0.0007

TABLE 16. Elastic differential scattering cross section data in the pion-nucleus CM for  $\pi^-$  on  ${}^4\text{He}$  at 153 MeV pion kinetic energy in the lab. <sup>154</sup>

$\Theta$ (deg)	$d\sigma/d\Omega_{\pi^-}$ (fm <sup>2</sup> /sr)
20 $\pm$ 5	4.46 $\pm$ 0.62
30 $\pm$ 5	3.88 $\pm$ 0.40
40 $\pm$ 5	2.32 $\pm$ 0.26
50 $\pm$ 5	1.37 $\pm$ 0.17
60 $\pm$ 5	0.560 $\pm$ 0.091
70 $\pm$ 5	0.098 $\pm$ 0.034
80 $\pm$ 5	0.047 $\pm$ 0.023
90 $\pm$ 5	0.185 $\pm$ 0.049
100 $\pm$ 5	0.223 $\pm$ 0.055
110 $\pm$ 5	0.184 $\pm$ 0.049
120 $\pm$ 5	0.160 $\pm$ 0.046
130 $\pm$ 5	0.121 $\pm$ 0.046
140 $\pm$ 5	0.072 $\pm$ 0.043
150 $\pm$ 5	0.069 $\pm$ 0.050
167.5 $\pm$ 12.5	0.172 $\pm$ 0.076

TABLE 17. Elastic differential scattering cross section data in the pion-nucleus CM for  $\pi^-$  on  ${}^4\text{He}$  at 180 MeV pion kinetic energy in the lab. 153

$\Theta$ (deg)	$d\sigma/d\Omega\pi^-$ ( $\text{fm}^2/\text{sr}$ )	$\Theta$ (deg)	$d\sigma/d\Omega\pi^-$ ( $\text{fm}^2/\text{sr}$ )
18 $\pm$ 1	0.60 $\pm$ 0.04	89.5 $\pm$ 1.0	0.0023 $\pm$ 0.0003
22 $\pm$ 1	0.39 $\pm$ 0.03	94.5 $\pm$ 1.0	0.0030 $\pm$ 0.0004
32.5 $\pm$ 1.0	0.21 $\pm$ 0.02	99.5 $\pm$ 1.0	0.0033 $\pm$ 0.0003
38 $\pm$ 1	0.14 $\pm$ 0.02	104.5 $\pm$ 1.0	0.0031 $\pm$ 0.0004
43 $\pm$ 1	0.085 $\pm$ 0.006	109.5 $\pm$ 1.0	0.0020 $\pm$ 0.0003
48 $\pm$ 1	0.047 $\pm$ 0.003	114.5 $\pm$ 1.0	0.0025 $\pm$ 0.0003
53 $\pm$ 1	0.030 $\pm$ 0.002	119 $\pm$ 1	0.0015 $\pm$ 0.0003
58.5 $\pm$ 1.0	0.013 $\pm$ 0.001	124 $\pm$ 1	0.0015 $\pm$ 0.0003
64 $\pm$ 1	0.0055 $\pm$ 0.0006	129 $\pm$ 1	0.0016 $\pm$ 0.0003
69 $\pm$ 1	0.0018 $\pm$ 0.0002	133.5 $\pm$ 1.0	0.0017 $\pm$ 0.0003
74.5 $\pm$ 1.0	0.0010 $\pm$ 0.0003	138 $\pm$ 1	0.0015 $\pm$ 0.0003
79 $\pm$ 1	0.0014 $\pm$ 0.0003	143 $\pm$ 1	0.0020 $\pm$ 0.0003
84.5 $\pm$ 1.0	0.0020 $\pm$ 0.0003	147.5 $\pm$ 1.0	0.0022 $\pm$ 0.0003

TABLE 18. Elastic differential scattering cross section data in the pion-nucleus CM for  $\pi^-$  on  ${}^4\text{He}$  at 220 MeV pion kinetic energy in the lab.<sup>153</sup>

$\Theta$ (deg)	$d\sigma/d\Omega_{\pi^-}$ (fm <sup>2</sup> /sr)	          	$\Theta$ (deg)	$d\sigma/d\Omega_{\pi^-}$ (fm <sup>2</sup> /sr)
38.0 ± 1.0	0.12 ± 0.01		110.0 ± 1.0	0.00053 ± 0.00015
69.5 ± 1.0	0.00067 ± 0.00017		115.0 ± 1.0	0.00044 ± 0.00010
74.5 ± 1.0	0.00028 ± 0.00010		119.5 ± 1.0	0.00031 ± 0.00007
80.0 ± 1.0	0.00075 ± 0.00017		124.5 ± 1.0	0.00035 ± 0.00009
85.0 ± 1.0	0.00045 ± 0.00010		129.0 ± 1.0	0.00052 ± 0.00010
90.0 ± 1.0	0.0009 ± 0.0002		134.0 ± 1.0	0.0011 ± 0.0002
95.0 ± 1.0	0.0008 ± 0.0002		138.5 ± 1.0	0.0010 ± 0.0002
100.0 ± 1.0	0.0011 ± 0.0002		143.0 ± 1.0	0.0010 ± 0.0002
105.0 ± 1.0	0.0007 ± 0.0002		147.0 ± 1.0	0.0011 ± 0.0002

TABLE 19. Elastic differential scattering cross section data in the pion-nucleus CM for  $\pi^-$  on  ${}^4\text{He}$  at 260 MeV pion kinetic energy in the lab.<sup>153</sup>

$\Theta$ (deg)	$d\sigma/d\Omega_{\pi^-}$ (fm <sup>2</sup> /sr)		$\Theta$ (deg)	$d\sigma/d\Omega_{\pi^-}$ (fm <sup>2</sup> /sr)
38.0 $\pm$ 1.0	0.110 $\pm$ 0.010		96.0 $\pm$ 1.0	0.00038 $\pm$ 0.00009
44.5 $\pm$ 1.0	0.073 $\pm$ 0.005		101.0 $\pm$ 1.0	0.00027 $\pm$ 0.00010
49.0 $\pm$ 1.0	0.055 $\pm$ 0.003		105.5 $\pm$ 1.0	0.00025 $\pm$ 0.00007
54.5 $\pm$ 1.0	0.017 $\pm$ 0.001		110.5 $\pm$ 1.0	0.00010 $\pm$ 0.00002
60.0 $\pm$ 1.0	0.0060 $\pm$ 0.0005		115.0 $\pm$ 1.0	0.00016 $\pm$ 0.00006
65.0 $\pm$ 1.0	0.0025 $\pm$ 0.0004		120.0 $\pm$ 1.0	0.00017 $\pm$ 0.00006
70.0 $\pm$ 1.0	0.0007 $\pm$ 0.0001		125.0 $\pm$ 1.0	0.00012 $\pm$ 0.00005
75.0 $\pm$ 1.0	0.00055 $\pm$ 0.00015		129.5 $\pm$ 1.0	0.00026 $\pm$ 0.00006
80.0 $\pm$ 1.0	0.00040 $\pm$ 0.00006		134.0 $\pm$ 1.0	0.00035 $\pm$ 0.00007
85.5 $\pm$ 1.0	0.00043 $\pm$ 0.00009		139.0 $\pm$ 1.0	0.00045 $\pm$ 0.00015
91.0 $\pm$ 1.0	0.00048 $\pm$ 0.00008		148.0 $\pm$ 1.0	0.00055 $\pm$ 0.00010

TABLE 20. Elastic differential scattering cross section data in the pion-nucleus CM for  $\pi^-$  on  $^{12}\text{C}$  at 27.8 MeV pion kinetic energy in the lab.<sup>8</sup>

$\Theta$ (deg)	$d\sigma/d\Omega_{\pi^-}$ (fm <sup>2</sup> /sr)
40.6 $\pm$ 5.0	1.564 $\pm$ 0.126
60.7 $\pm$ 5.0	0.199 $\pm$ 0.035
80.8 $\pm$ 5.0	0.163 $\pm$ 0.025
100.8 $\pm$ 5.0	0.269 $\pm$ 0.029
120.7 $\pm$ 5.0	0.801 $\pm$ 0.091

TABLE 21. Elastic differential scattering cross section data in the pion-nucleus CM for  $\pi^+$  on  $^{12}\text{C}$  at 30.2 MeV pion kinetic energy in the lab.<sup>8</sup>

$\Theta$ (deg)	$d\sigma/d\Omega_{\pi^+}$ (fm <sup>2</sup> /sr)	"	$\Theta$ (deg)	$d\sigma/d\Omega_{\pi^+}$ (fm <sup>2</sup> /sr)
$40.6 \pm 5.0$	$0.354 \pm 0.066$	"	$80.9 \pm 5.0$	$0.383 \pm 0.052$
$45.6 \pm 5.0$	$0.272 \pm 0.039$	"	$90.9 \pm 5.0$	$0.431 \pm 0.036$
$50.7 \pm 5.0$	$0.323 \pm 0.045$	"	$100.9 \pm 5.0$	$0.603 \pm 0.050$
$60.8 \pm 5.0$	$0.252 \pm 0.042$	"	$110.8 \pm 5.0$	$0.642 \pm 0.081$
$70.8 \pm 5.0$	$0.473 \pm 0.051$	"	$120.7 \pm 5.0$	$0.651 \pm 0.068$

TABLE 22. Elastic differential scattering cross section data in the pion-nucleus CM for  $\pi^+$  on  $^{12}\text{C}$  at 31.5 MeV pion kinetic energy in the lab.<sup>155</sup>

$\Theta$ (deg)	$d\sigma/d\Omega_{\pi^+}$ (fm <sup>2</sup> /sr)
$40.6 \pm 7.0$	$0.564 \pm 0.066$
$55.7 \pm 7.0$	$0.071 \pm 0.016$
$70.8 \pm 7.0$	$0.375 \pm 0.035$
$90.9 \pm 7.0$	$0.398 \pm 0.038$
$105.8 \pm 7.0$	$0.650 \pm 0.058$
$120.8 \pm 7.0$	$0.658 \pm 0.051$
$145.5 \pm 7.0$	$0.743 \pm 0.065$

TABLE 23. Elastic differential scattering cross section data in the pion-nucleus CM for  $\pi^+$  on  $^{12}\text{C}$  at 40 MeV pion kinetic energy in the lab. <sup>156</sup>

$\Theta$ (deg)	$d\sigma/d\Omega_{\pi^+}$ (fm <sup>2</sup> /sr)
$45.7 \pm 5.0$	$0.242 \pm 0.080$
$60.8 \pm 5.0$	$0.215 \pm 0.016$
$90.9 \pm 5.0$	$0.410 \pm 0.030$
$120.8 \pm 5.0$	$0.545 \pm 0.026$
$140.6 \pm 5.0$	$0.733 \pm 0.074$

TABLE 24. Elastic differential scattering cross section data in the pion-nucleus CM for  $\pi^+$  on  $^{12}\text{C}$  at 62 MeV pion kinetic energy in the lab.<sup>27</sup>

$\Theta$ (deg)	$d\sigma/d\Omega_{\pi^+}$ (fm <sup>2</sup> /sr)	" " "	$\Theta$ (deg)	$d\sigma/d\Omega_{\pi^+}$ (fm <sup>2</sup> /sr)
$10.2 \pm 3.0$	$38.62 \pm 8.69$	" " "	$55.8 \pm 5.0$	$0.686 \pm 0.392$
$15.3 \pm 2.0$	$12.08 \pm 3.38$	" " "	$71.0 \pm 10.0$	$0.692 \pm 0.494$
$20.4 \pm 5.0$	$1.45 \pm 0.58$	" " "	$91.0 \pm 10.0$	$0.200 \pm 0.199$
$30.5 \pm 6.0$	$1.94 \pm 0.78$	" " "	$111.0 \pm 10.0$	$0.304 \pm 0.152$
$38.6 \pm 2.0$	$2.92 \pm 0.97$	" " "	$133.7 \pm 8.0$	$1.127 \pm 0.410$
$45.7 \pm 5.0$	$2.34 \pm 0.59$	" " "	$162.3 \pm 20.0$	$0.414 \pm 0.413$

TABLE 25. Elastic differential scattering cross section data in the pion-nucleus CM for  $\pi^-$  on  $^{12}\text{C}$  at 62 MeV pion kinetic energy in the lab. <sup>27</sup>

$\Theta$ (deg)	$d\sigma/d\Omega \pi^-$ (fm <sup>2</sup> /sr)	''	$\Theta$ (deg)	$d\sigma/d\Omega \pi^-$ (fm <sup>2</sup> /sr)
10.2 $\pm$ 2.0	62.76 $\pm$ 9.66	''	45.7 $\pm$ 5.0	2.15 $\pm$ 0.68
15.3 $\pm$ 2.0	34.78 $\pm$ 7.73	''	55.8 $\pm$ 5.0	1.08 $\pm$ 0.29
18.3 $\pm$ 2.0	19.82 $\pm$ 4.35	''	71.0 $\pm$ 10.0	0.553 $\pm$ 0.178
22.4 $\pm$ 2.0	10.16 $\pm$ 3.39	''	91.0 $\pm$ 10.0	0.360 $\pm$ 0.170
26.5 $\pm$ 2.0	8.33 $\pm$ 2.33	''	111.0 $\pm$ 10.0	0.668 $\pm$ 0.243
30.5 $\pm$ 2.0	4.17 $\pm$ 1.75	''	130.8 $\pm$ 10.0	0.696 $\pm$ 0.246
34.6 $\pm$ 2.0	6.02 $\pm$ 2.14	''	150.5 $\pm$ 10.0	0.722 $\pm$ 0.310
38.6 $\pm$ 2.0	2.82 $\pm$ 1.46	''	170.2 $\pm$ 10.0	1.968 $\pm$ 0.932

TABLE 26. Elastic differential scattering cross section data in the pion-nucleus CM for  $\pi^-$  on  $^{12}\text{C}$  at 69.5 MeV pion kinetic energy in the lab.<sup>35</sup>

$\Theta$ (deg)	$d\sigma/d\Omega_{\pi^-}$ (fm <sup>2</sup> /sr)	"	$\Theta$ (deg)	$d\sigma/d\Omega_{\pi^-}$ (fm <sup>2</sup> /sr)
20.4 $\pm$ 3.1	14.20 $\pm$ 1.55	"	76.0 $\pm$ 4.7	0.402 $\pm$ 0.031
25.5 $\pm$ 3.1	9.00 $\pm$ 0.87	"	81.1 $\pm$ 4.7	0.445 $\pm$ 0.071
30.5 $\pm$ 3.1	7.66 $\pm$ 0.64	"	86.1 $\pm$ 4.7	0.488 $\pm$ 0.050
35.6 $\pm$ 3.1	4.90 $\pm$ 0.46	"	91.1 $\pm$ 4.7	0.507 $\pm$ 0.083
40.7 $\pm$ 3.1	4.04 $\pm$ 0.34	"	96.1 $\pm$ 4.7	0.525 $\pm$ 0.032
45.8 $\pm$ 4.0	2.62 $\pm$ 0.19	"	101.0 $\pm$ 4.7	0.538 $\pm$ 0.062
50.8 $\pm$ 4.0	1.46 $\pm$ 0.12	"	106.0 $\pm$ 4.7	0.442 $\pm$ 0.054
55.9 $\pm$ 4.0	0.872 $\pm$ 0.098	"	111.0 $\pm$ 4.7	0.497 $\pm$ 0.059
60.9 $\pm$ 4.0	0.499 $\pm$ 0.055	"	116.0 $\pm$ 4.7	0.342 $\pm$ 0.049
66.0 $\pm$ 4.0	0.409 $\pm$ 0.033	"	120.9 $\pm$ 4.7	0.322 $\pm$ 0.048
71.0 $\pm$ 4.7	0.317 $\pm$ 0.025	"	125.9 $\pm$ 4.7	0.221 $\pm$ 0.045

TABLE 27. Elastic differential scattering cross section data in the pion-nucleus CM for  $\pi^-$  on  $^{12}\text{C}$  at 80 MeV pion kinetic energy in the lab. <sup>33</sup>

$\Theta$ (deg)	$d\sigma/d\Omega \pi^-$ (fm <sup>2</sup> /sr)	"	$\Theta$ (deg)	$d\sigma/d\Omega \pi^-$ (fm <sup>2</sup> /sr)
20.4 $\pm$ 3.0	14.46 $\pm$ 1.45	"	71.1 $\pm$ 5.6	0.274 $\pm$ 0.027
25.5 $\pm$ 3.4	11.88 $\pm$ 1.06	"	76.1 $\pm$ 5.6	0.330 $\pm$ 0.064
30.6 $\pm$ 3.4	7.13 $\pm$ 0.52	"	81.1 $\pm$ 5.6	0.290 $\pm$ 0.045
35.6 $\pm$ 3.4	6.52 $\pm$ 0.58	"	86.1 $\pm$ 5.6	0.321 $\pm$ 0.060
40.7 $\pm$ 3.7	3.80 $\pm$ 0.16	"	91.1 $\pm$ 5.6	0.321 $\pm$ 0.030
45.8 $\pm$ 3.7	2.82 $\pm$ 0.23	"	96.1 $\pm$ 5.6	0.320 $\pm$ 0.060
50.9 $\pm$ 3.7	1.81 $\pm$ 0.30	"	101.1 $\pm$ 5.6	0.286 $\pm$ 0.050
55.9 $\pm$ 4.1	1.19 $\pm$ 0.18	"	106.1 $\pm$ 5.6	0.261 $\pm$ 0.056
61.0 $\pm$ 4.1	0.518 $\pm$ 0.147	"	111.0 $\pm$ 5.6	0.167 $\pm$ 0.020
66.0 $\pm$ 5.6	0.323 $\pm$ 0.059	"	118.0 $\pm$ 5.6	0.168 $\pm$ 0.061

TABLE 28. Elastic differential scattering cross section data in the pion-nucleus CM for  $\pi^-$  on  $^{12}\text{C}$  at 87.5 MeV pion kinetic energy in the lab.<sup>35</sup>

$\Theta$ (deg)	$d\sigma/d\Omega_{\pi^-}$ (fm <sup>2</sup> /sr)	" " " "	$\Theta$ (deg)	$d\sigma/d\Omega_{\pi^-}$ (fm <sup>2</sup> /sr)
25.5 $\pm$ 2.8	10.53 $\pm$ 1.02	"	81.1 $\pm$ 4.5	0.404 $\pm$ 0.044
30.6 $\pm$ 2.8	8.31 $\pm$ 0.59	"	86.2 $\pm$ 4.5	0.356 $\pm$ 0.051
35.7 $\pm$ 2.8	6.62 $\pm$ 0.47	"	91.2 $\pm$ 4.5	0.330 $\pm$ 0.030
40.7 $\pm$ 2.8	3.86 $\pm$ 0.17	"	96.1 $\pm$ 4.5	0.279 $\pm$ 0.040
45.8 $\pm$ 3.8	2.82 $\pm$ 0.25	"	101.1 $\pm$ 4.5	0.262 $\pm$ 0.031
50.9 $\pm$ 3.8	1.46 $\pm$ 0.10	"	106.1 $\pm$ 4.5	0.174 $\pm$ 0.026
56.0 $\pm$ 3.8	0.762 $\pm$ 0.050	"	111.1 $\pm$ 4.5	0.118 $\pm$ 0.023
61.0 $\pm$ 3.8	0.569 $\pm$ 0.048	"	116.0 $\pm$ 4.5	0.081 $\pm$ 0.030
66.0 $\pm$ 3.8	0.411 $\pm$ 0.033	"	121.0 $\pm$ 4.5	0.092 $\pm$ 0.029
71.1 $\pm$ 3.8	0.341 $\pm$ 0.029	"	125.9 $\pm$ 4.5	0.062 $\pm$ 0.027
76.1 $\pm$ 4.5	0.359 $\pm$ 0.026	"		

TABLE 29. Elastic differential scattering cross section data in the pion-nucleus CM for  $\pi^-$  on  $^{12}\text{C}$  at 120 Mev pion kinetic energy in the lab.<sup>10,157</sup>

$\Theta$ (deg)	$d\sigma/d\Omega\pi^-$ ( $\text{fm}^2/\text{sr}$ )	$\Theta$ (deg)	$d\sigma/d\Omega\pi^-$ ( $\text{fm}^2/\text{sr}$ )	$\Theta$ (deg)	$d\sigma/d\Omega\pi^-$ ( $\text{fm}^2/\text{sr}$ )
6.03 $\pm$ 1.00	139.36 $\pm$ 3.00	9.70 $\pm$ 1.00	46.60 $\pm$ 0.77	18.53 $\pm$ 1.60	23.79 $\pm$ 0.86
6.22 $\pm$ 1.00	121.89 $\pm$ 3.80	10.07 $\pm$ 1.00	46.33 $\pm$ 1.24	20.96 $\pm$ 1.00	19.97 $\pm$ 0.44
6.54 $\pm$ 1.00	101.69 $\pm$ 2.19	10.69 $\pm$ 1.00	41.07 $\pm$ 1.03	21.07 $\pm$ 1.60	20.08 $\pm$ 0.69
6.73 $\pm$ 1.00	90.10 $\pm$ 2.80	10.84 $\pm$ 1.60	39.81 $\pm$ 1.98	21.32 $\pm$ 1.00	20.58 $\pm$ 0.64
7.05 $\pm$ 1.00	88.25 $\pm$ 1.76	11.09 $\pm$ 1.00	40.66 $\pm$ 1.33	26.08 $\pm$ 1.00	13.32 $\pm$ 0.38
7.24 $\pm$ 1.00	79.84 $\pm$ 2.29	11.87 $\pm$ 1.60	34.86 $\pm$ 2.23	26.16 $\pm$ 1.60	13.85 $\pm$ 0.35
7.56 $\pm$ 1.00	74.23 $\pm$ 1.48	12.89 $\pm$ 1.60	32.66 $\pm$ 1.90	26.43 $\pm$ 1.00	13.25 $\pm$ 0.55
7.75 $\pm$ 1.00	67.72 $\pm$ 1.95	13.29 $\pm$ 1.00	32.71 $\pm$ 0.70	31.27 $\pm$ 1.60	8.96 $\pm$ 0.25
8.07 $\pm$ 1.00	65.67 $\pm$ 1.33	13.65 $\pm$ 1.00	31.39 $\pm$ 1.01	36.38 $\pm$ 1.60	6.00 $\pm$ 0.21
8.27 $\pm$ 1.00	60.26 $\pm$ 1.77	13.91 $\pm$ 1.60	31.43 $\pm$ 1.70	41.56 $\pm$ 1.60	2.90 $\pm$ 0.19
8.58 $\pm$ 1.00	59.24 $\pm$ 1.17	14.94 $\pm$ 1.60	29.22 $\pm$ 1.22	46.64 $\pm$ 1.60	1.24 $\pm$ 0.12
8.77 $\pm$ 1.00	55.68 $\pm$ 1.56	15.85 $\pm$ 1.00	27.75 $\pm$ 0.59	51.72 $\pm$ 1.60	0.607 $\pm$ 0.060
9.09 $\pm$ 1.00	52.45 $\pm$ 1.01	15.97 $\pm$ 1.60	25.85 $\pm$ 1.07	56.79 $\pm$ 1.60	0.326 $\pm$ 0.040
9.41 $\pm$ 1.00	48.81 $\pm$ 1.30	16.20 $\pm$ 1.00	27.35 $\pm$ 0.88	61.85 $\pm$ 1.60	0.197 $\pm$ 0.035

TABLE 29. Elastic differential scattering cross section data in the pion-nucleus CM for  $\pi^-$  on  $^{12}\text{C}$  at 120 MeV pion kinetic energy in the lab. (Cont'd)

$\theta$ (deg)	$d\sigma/d\Omega_{\pi^-}$ ( $\text{fm}^2/\text{sr}$ )
66.90 $\pm$ 1.60	0.150 $\pm$ 0.030
71.94 $\pm$ 1.60	0.175 $\pm$ 0.030
76.97 $\pm$ 1.60	0.155 $\pm$ 0.030
87.01 $\pm$ 1.60	0.075 $\pm$ 0.020
97.00 $\pm$ 1.60	0.031 $\pm$ 0.014
111.93 $\pm$ 1.60	0.0083 $\pm$ 0.0059
131.69 $\pm$ 1.60	0.060 $\pm$ 0.015
141.53 $\pm$ 1.60	0.066 $\pm$ 0.015

TABLE 30. Elastic differential scattering cross section data in the pion-nucleus CM for  $\pi^-$  on  $^{12}\text{C}$  at 150 MeV pion kinetic energy in the lab.<sup>10</sup>

$\Theta$ (deg)	$d\sigma/d\Omega_{\pi^-}$ (fm <sup>2</sup> /sr)	:	$\Theta$ (deg)	$d\sigma/d\Omega_{\pi^-}$ (fm <sup>2</sup> /sr)
10.2 $\pm$ 1.6	47.59 $\pm$ 2.86	:	61.3 $\pm$ 1.6	0.102 $\pm$ 0.009
11.2 $\pm$ 1.6	43.08 $\pm$ 1.97	:	66.3 $\pm$ 1.6	0.148 $\pm$ 0.010
12.7 $\pm$ 1.6	40.95 $\pm$ 1.62	:	71.4 $\pm$ 1.6	0.127 $\pm$ 0.010
15.3 $\pm$ 1.6	36.55 $\pm$ 1.35	:	76.4 $\pm$ 1.6	0.122 $\pm$ 0.008
20.4 $\pm$ 1.6	26.44 $\pm$ 0.62	:	81.4 $\pm$ 1.6	0.073 $\pm$ 0.006
25.6 $\pm$ 1.6	16.99 $\pm$ 0.31	:	86.5 $\pm$ 1.6	0.040 $\pm$ 0.005
30.7 $\pm$ 1.6	9.81 $\pm$ 0.21	:	91.5 $\pm$ 1.6	0.015 $\pm$ 0.004
35.8 $\pm$ 1.6	5.03 $\pm$ 0.10	:	96.5 $\pm$ 1.6	0.011 $\pm$ 0.003
40.9 $\pm$ 1.6	2.29 $\pm$ 0.07	:	101.4 $\pm$ 1.6	0.013 $\pm$ 0.003
46.0 $\pm$ 1.6	0.83 $\pm$ 0.03	:	111.4 $\pm$ 1.6	0.032 $\pm$ 0.004
51.1 $\pm$ 1.6	0.256 $\pm$ 0.014	:	121.3 $\pm$ 1.6	0.043 $\pm$ 0.006
56.2 $\pm$ 1.6	0.118 $\pm$ 0.010	:	140.9 $\pm$ 1.6	0.023 $\pm$ 0.005
58.7 $\pm$ 1.6	0.070 $\pm$ 0.017	:		

TABLE 31. Elastic differential scattering cross section data in the pion-nucleus CM for  $\pi^-$  on  $^{12}\text{C}$  at 180 MeV pion kinetic energy in the lab. <sup>10,157</sup>

$\Theta$ (deg)	$d\sigma/d\Omega_{\pi^-}$ ( $\text{fm}^2/\text{sr}$ )	$\Theta$ (deg)	$d\sigma/d\Omega_{\pi^-}$ ( $\text{fm}^2/\text{sr}$ )	$\Theta$ (deg)	$d\sigma/d\Omega_{\pi^-}$ ( $\text{fm}^2/\text{sr}$ )
5.50 ± 1.00	121.77 ± 2.19	12.75 ± 1.60	39.71 ± 1.50	45.83 ± 1.60	0.148 ± 0.019
6.01 ± 1.00	93.31 ± 1.67	13.20 ± 1.00	39.99 ± 1.07	48.38 ± 1.60	0.046 ± 0.012
6.52 ± 1.00	77.93 ± 1.38	15.32 ± 1.60	36.20 ± 1.11	50.93 ± 1.60	0.0113 ± 0.0038
7.04 ± 1.00	70.00 ± 1.25	15.77 ± 1.00	37.24 ± 1.01	53.47 ± 1.60	0.040 ± 0.009
7.55 ± 1.00	60.78 ± 0.91	17.89 ± 1.60	31.37 ± 0.70	56.01 ± 1.60	0.052 ± 0.010
8.07 ± 1.00	59.78 ± 1.09	18.35 ± 1.00	28.34 ± 0.77	61.09 ± 1.60	0.150 ± 0.018
8.58 ± 1.00	55.39 ± 1.00	20.46 ± 1.60	24.21 ± 0.37	66.15 ± 1.60	0.160 ± 0.018
9.09 ± 1.00	53.12 ± 1.17	20.91 ± 1.00	23.10 ± 0.64	71.21 ± 1.60	0.094 ± 0.014
9.61 ± 1.00	51.35 ± 1.25	25.57 ± 1.60	14.78 ± 0.29	76.25 ± 1.60	0.078 ± 0.012
10.12 ± 1.00	49.62 ± 1.20	26.05 ± 1.00	13.76 ± 0.45	86.29 ± 1.60	0.0035 ± 0.0025
10.18 ± 1.60	46.22 ± 2.94	30.71 ± 1.60	7.53 ± 0.16	101.38 ± 1.60	0.0076 ± 0.0034
10.63 ± 1.00	45.18 ± 1.25	35.81 ± 1.60	3.08 ± 0.07	140.82 ± 1.60	0.0072 ± 0.0028
11.21 ± 1.60	45.47 ± 1.90	40.73 ± 1.60	0.873 ± 0.050		

TABLE 32. Elastic differential scattering cross section data in the pion-nucleus CM for  $\pi^-$  on  $^{12}\text{C}$  at 200 MeV pion kinetic energy in the lab.<sup>10</sup>

$\Theta$ (deg)	$d\sigma/d\Omega_{\pi^-}$ (fm <sup>2</sup> /sr)		$\Theta$ (deg)	$d\sigma/d\Omega_{\pi^-}$ (fm <sup>2</sup> /sr)
11.2 $\pm$ 1.6	45.93 $\pm$ 1.64		54.0 $\pm$ 1.6	0.091 $\pm$ 0.012
12.3 $\pm$ 1.6	42.14 $\pm$ 1.31		56.5 $\pm$ 1.6	0.105 $\pm$ 0.010
15.4 $\pm$ 1.6	35.63 $\pm$ 1.08		61.5 $\pm$ 1.6	0.131 $\pm$ 0.014
20.5 $\pm$ 1.6	22.59 $\pm$ 0.36		66.6 $\pm$ 1.6	0.106 $\pm$ 0.013
25.6 $\pm$ 1.6	12.93 $\pm$ 0.27		71.6 $\pm$ 1.6	0.069 $\pm$ 0.018
30.8 $\pm$ 1.6	5.92 $\pm$ 0.18		76.7 $\pm$ 1.6	0.030 $\pm$ 0.004
35.9 $\pm$ 1.6	2.12 $\pm$ 0.07		81.7 $\pm$ 1.6	0.015 $\pm$ 0.002
41.2 $\pm$ 1.6	0.420 $\pm$ 0.031		91.7 $\pm$ 1.6	0.0013 $\pm$ 0.0006
46.3 $\pm$ 1.6	0.054 $\pm$ 0.011		101.7 $\pm$ 1.6	0.0026 $\pm$ 0.0008
48.9 $\pm$ 1.6	0.030 $\pm$ 0.008		121.5 $\pm$ 1.6	0.0021 $\pm$ 0.0006
51.4 $\pm$ 1.6	0.051 $\pm$ 0.010		141.1 $\pm$ 1.6	0.0042 $\pm$ 0.0029

TABLE 33. Elastic differential scattering cross section data in the pion-nucleus CM for  $\pi^-$  on  $^{12}\text{C}$  at 230 MeV pion kinetic energy in the lab.<sup>10</sup>

$\Theta$ (deg)	$d\sigma/d\Omega_{\pi^-}$ (fm <sup>2</sup> /sr)	"	$\Theta$ (deg)	$d\sigma/d\Omega_{\pi^-}$ (fm <sup>2</sup> /sr)
10.4 $\pm$ 1.6	45.08 $\pm$ 1.67	"	43.8 $\pm$ 1.6	0.107 $\pm$ 0.015
11.5 $\pm$ 1.6	41.44 $\pm$ 1.52	"	46.3 $\pm$ 1.6	0.077 $\pm$ 0.009
12.5 $\pm$ 1.6	39.98 $\pm$ 1.24	"	48.9 $\pm$ 1.6	0.104 $\pm$ 0.015
15.6 $\pm$ 1.6	32.29 $\pm$ 0.91	"	51.4 $\pm$ 1.6	0.108 $\pm$ 0.011
20.7 $\pm$ 1.6	18.97 $\pm$ 0.43	"	56.5 $\pm$ 1.6	0.154 $\pm$ 0.018
25.9 $\pm$ 1.6	9.39 $\pm$ 0.22	"	61.6 $\pm$ 1.6	0.145 $\pm$ 0.021
31.0 $\pm$ 1.6	3.48 $\pm$ 0.10	"	66.7 $\pm$ 1.6	0.069 $\pm$ 0.011
36.2 $\pm$ 1.6	1.17 $\pm$ 0.04	"	71.7 $\pm$ 1.6	0.060 $\pm$ 0.022
41.2 $\pm$ 1.6	0.189 $\pm$ 0.016	"		

TABLE 34. Elastic differential scattering cross section data in the pion-nucleus CM for  $\pi^-$  on  $^{12}\text{C}$  at 260 MeV pion kinetic energy in the lab. <sup>18,157</sup>

$\Theta$ (deg)	$d\sigma/d\Omega_{\pi^-}$ ( $\text{fm}^2/\text{sr}$ )	$\Theta$ (deg)	$d\sigma/d\Omega_{\pi^-}$ ( $\text{fm}^2/\text{sr}$ )	$\Theta$ (deg)	$d\sigma/d\Omega_{\pi^-}$ ( $\text{fm}^2/\text{sr}$ )
4.68 $\pm$ 1.00	119.35 $\pm$ 1.86	11.05 $\pm$ 1.00	47.56 $\pm$ 1.44	15.96 $\pm$ 1.00	31.84 $\pm$ 0.77
5.20 $\pm$ 1.00	84.31 $\pm$ 1.15	11.37 $\pm$ 1.00	44.12 $\pm$ 1.44	16.22 $\pm$ 1.00	30.38 $\pm$ 0.94
5.71 $\pm$ 1.00	68.91 $\pm$ 0.89	11.49 $\pm$ 1.60	44.54 $\pm$ 2.63	18.10 $\pm$ 1.00	26.03 $\pm$ 0.73
6.23 $\pm$ 1.00	60.92 $\pm$ 0.75	11.82 $\pm$ 1.00	45.59 $\pm$ 1.12	18.54 $\pm$ 1.00	24.25 $\pm$ 0.54
6.74 $\pm$ 1.00	55.16 $\pm$ 0.67	12.08 $\pm$ 1.00	44.66 $\pm$ 1.38	18.81 $\pm$ 1.00	24.21 $\pm$ 0.68
7.26 $\pm$ 1.00	53.41 $\pm$ 0.63	12.41 $\pm$ 1.00	43.42 $\pm$ 1.37	20.69 $\pm$ 1.00	18.17 $\pm$ 0.67
7.78 $\pm$ 1.00	52.27 $\pm$ 0.62	12.85 $\pm$ 1.00	40.56 $\pm$ 1.01	20.78 $\pm$ 1.60	18.39 $\pm$ 0.44
8.29 $\pm$ 1.00	49.78 $\pm$ 0.59	13.04 $\pm$ 1.60	45.08 $\pm$ 2.38	21.13 $\pm$ 1.00	17.17 $\pm$ 0.51
8.88 $\pm$ 1.00	49.66 $\pm$ 0.58	13.12 $\pm$ 1.00	40.56 $\pm$ 1.25	21.39 $\pm$ 1.00	15.62 $\pm$ 0.59
9.33 $\pm$ 1.00	47.86 $\pm$ 0.61	13.44 $\pm$ 1.00	39.39 $\pm$ 1.25	25.95 $\pm$ 1.60	8.35 $\pm$ 0.20
9.84 $\pm$ 1.00	47.49 $\pm$ 0.79	13.89 $\pm$ 1.00	38.67 $\pm$ 0.95	31.12 $\pm$ 1.60	3.03 $\pm$ 0.09
10.36 $\pm$ 1.00	46.53 $\pm$ 0.77	14.15 $\pm$ 1.00	37.10 $\pm$ 1.15	36.26 $\pm$ 1.60	0.82 $\pm$ 0.05
10.45 $\pm$ 1.60	52.23 $\pm$ 4.63	15.51 $\pm$ 1.00	31.09 $\pm$ 1.03	38.72 $\pm$ 1.60	0.421 $\pm$ 0.049
10.78 $\pm$ 1.00	44.85 $\pm$ 1.12	15.63 $\pm$ 1.60	30.39 $\pm$ 0.86	41.29 $\pm$ 1.60	0.172 $\pm$ 0.026



TABLE 35. Elastic differential scattering cross section data in the pion-nucleus CM for  $\pi^-$  on  $^{12}\text{C}$  at 280 MeV pion kinetic energy in the lab.<sup>10</sup>

$\Theta$ (deg)	$d\sigma/d\Omega_{\pi^-}$ (fm <sup>2</sup> /sr)	"	$\Theta$ (deg)	$d\sigma/d\Omega_{\pi^-}$ (fm <sup>2</sup> /sr)
11.0 $\pm$ 1.6	38.69 $\pm$ 1.42	"	44.0 $\pm$ 1.6	0.131 $\pm$ 0.015
12.6 $\pm$ 1.6	35.41 $\pm$ 1.27	"	46.6 $\pm$ 1.6	0.157 $\pm$ 0.017
15.1 $\pm$ 1.6	28.16 $\pm$ 0.90	"	49.2 $\pm$ 1.6	0.146 $\pm$ 0.016
17.7 $\pm$ 1.6	22.16 $\pm$ 0.68	"	51.7 $\pm$ 1.6	0.136 $\pm$ 0.016
20.3 $\pm$ 1.6	15.62 $\pm$ 0.47	"	56.8 $\pm$ 1.6	0.137 $\pm$ 0.016
25.5 $\pm$ 1.6	6.91 $\pm$ 0.24	"	61.9 $\pm$ 1.6	0.088 $\pm$ 0.012
30.6 $\pm$ 1.6	2.41 $\pm$ 0.10	"	67.0 $\pm$ 1.6	0.060 $\pm$ 0.010
35.8 $\pm$ 1.6	0.56 $\pm$ 0.04	"	72.1 $\pm$ 1.6	0.015 $\pm$ 0.005
41.5 $\pm$ 1.6	0.161 $\pm$ 0.018	"	131.1 $\pm$ 1.6	0.0025 $\pm$ 0.0020

TABLE 36. Elastic differential scattering cross section data in the pion-nucleus CM for  $\pi^+$  on  $^{16}\text{O}$  at 30 MeV pion kinetic energy in the lab.<sup>8</sup>

$\Theta$ (deg)	$d\sigma/d\Omega \pi^+$ (fm <sup>2</sup> /sr)
40.4 $\pm$ 5.0	0.586 $\pm$ 0.071
50.5 $\pm$ 5.0	0.573 $\pm$ 0.050
60.6 $\pm$ 5.0	0.556 $\pm$ 0.053
70.6 $\pm$ 5.0	0.616 $\pm$ 0.066
80.6 $\pm$ 5.0	0.718 $\pm$ 0.078
90.7 $\pm$ 5.0	0.686 $\pm$ 0.071
100.6 $\pm$ 5.0	0.827 $\pm$ 0.058
120.6 $\pm$ 5.0	0.759 $\pm$ 0.084

TABLE 37. Elastic differential scattering cross section data in the pion-nucleus CM for  $\pi^-$  on  $^{16}\text{O}$  at 87.5 MeV pion kinetic energy in the lab.<sup>9</sup>

$\Theta$ (deg)	$d\sigma/d\Omega_{\pi^-}$ (fm <sup>2</sup> /sr)	"	$\Theta$ (deg)	$d\sigma/d\Omega_{\pi^-}$ (fm <sup>2</sup> /sr)
20.3 $\pm$ 2.8	22.36 $\pm$ 1.07	"	70.8 $\pm$ 3.8	0.438 $\pm$ 0.059
25.4 $\pm$ 2.8	15.76 $\pm$ 0.88	"	75.8 $\pm$ 4.5	0.412 $\pm$ 0.062
30.4 $\pm$ 2.8	10.72 $\pm$ 0.78	"	80.9 $\pm$ 4.5	0.319 $\pm$ 0.088
35.5 $\pm$ 2.8	7.35 $\pm$ 0.42	"	85.9 $\pm$ 4.5	0.306 $\pm$ 0.055
40.6 $\pm$ 2.8	5.29 $\pm$ 0.24	"	90.9 $\pm$ 4.5	0.229 $\pm$ 0.042
45.6 $\pm$ 3.8	2.66 $\pm$ 0.22	"	95.9 $\pm$ 4.5	0.245 $\pm$ 0.046
50.7 $\pm$ 3.8	1.68 $\pm$ 0.09	"	100.9 $\pm$ 4.5	0.059 $\pm$ 0.033
55.7 $\pm$ 3.8	0.826 $\pm$ 0.069	"	110.8 $\pm$ 4.5	0.031 $\pm$ 0.031
60.8 $\pm$ 3.8	0.571 $\pm$ 0.108	"	120.7 $\pm$ 4.5	0.029 $\pm$ 0.029
65.8 $\pm$ 3.8	0.418 $\pm$ 0.070	"	130.7 $\pm$ 4.5	0.028 $\pm$ 0.028

TABLE 38. Elastic differential scattering cross section data in the pion-nucleus CM for  $\pi^-$  on  $^{16}\text{O}$  at 160 MeV pion kinetic energy in the lab.<sup>14</sup>

$\Theta$ (deg)	$d\sigma/d\Omega_{\pi^-}$ ( $\text{fm}^2/\text{sr}$ )	$\Theta$ (deg)	$d\sigma/d\Omega_{\pi^-}$ ( $\text{fm}^2/\text{sr}$ )	$\Theta$ (deg)	$d\sigma/d\Omega_{\pi^-}$ ( $\text{fm}^2/\text{sr}$ )
$15.3 \pm 2.0$	$94.15 \pm 10.77$	$41.8 \pm 2.0$	$0.790 \pm 0.090$	$68.0 \pm 2.0$	$0.160 \pm 0.021$
$17.3 \pm 2.0$	$61.96 \pm 8.26$	$43.8 \pm 2.0$	$0.211 \pm 0.035$	$70.0 \pm 2.0$	$0.201 \pm 0.021$
$19.4 \pm 2.0$	$65.12 \pm 5.16$	$45.8 \pm 2.0$	$0.166 \pm 0.023$	$72.1 \pm 2.0$	$0.120 \pm 0.015$
$21.4 \pm 2.0$	$47.33 \pm 3.65$	$47.8 \pm 2.0$	$0.193 \pm 0.025$	$74.1 \pm 2.0$	$0.029 \pm 0.004$
$23.5 \pm 2.0$	$22.23 \pm 2.00$	$49.9 \pm 2.0$	$0.080 \pm 0.018$	$76.1 \pm 2.0$	$0.015 \pm 0.002$
$25.5 \pm 2.0$	$16.25 \pm 1.26$	$51.9 \pm 2.0$	$0.116 \pm 0.021$	$78.1 \pm 2.0$	$0.016 \pm 0.002$
$27.5 \pm 2.0$	$11.58 \pm 0.96$	$53.9 \pm 2.0$	$0.150 \pm 0.029$		
$29.6 \pm 2.0$	$8.15 \pm 0.65$	$55.9 \pm 2.0$	$0.342 \pm 0.038$		
$31.6 \pm 2.0$	$6.68 \pm 0.52$	$58.0 \pm 2.0$	$0.345 \pm 0.039$		
$33.6 \pm 2.0$	$5.56 \pm 0.54$	$60.0 \pm 2.0$	$0.363 \pm 0.040$		
$35.7 \pm 2.0$	$2.64 \pm 0.25$	$62.0 \pm 2.0$	$0.232 \pm 0.028$		
$37.7 \pm 2.0$	$1.70 \pm 0.19$	$64.0 \pm 2.0$	$0.258 \pm 0.033$		
$39.7 \pm 2.0$	$1.21 \pm 0.13$	$66.0 \pm 2.0$	$0.266 \pm 0.028$		

TABLE 39. Elastic differential scattering cross section data in the pion-nucleus CM for  $\pi^-$  on  $^{16}\text{O}$  at 170 MeV pion kinetic energy in the lab.<sup>14</sup>

$\Theta$ (deg)	$d\sigma/d\Omega_{\pi^-}$ (fm <sup>2</sup> /sr)	"	$\Theta$ (deg)	$d\sigma/d\Omega_{\pi^-}$ (fm <sup>2</sup> /sr)
15.3 $\pm$ 2.0	70.52 $\pm$ 8.55	"	45.8 $\pm$ 2.0	0.127 $\pm$ 0.018
17.4 $\pm$ 2.0	60.82 $\pm$ 4.90	"	47.9 $\pm$ 2.0	0.0168 $\pm$ 0.0089
19.4 $\pm$ 2.0	40.50 $\pm$ 3.09	"	49.9 $\pm$ 2.0	0.0404 $\pm$ 0.0123
21.4 $\pm$ 2.0	32.82 $\pm$ 2.57	"	51.9 $\pm$ 2.0	0.173 $\pm$ 0.026
23.5 $\pm$ 2.0	17.30 $\pm$ 1.31	"	53.9 $\pm$ 2.0	0.242 $\pm$ 0.029
25.5 $\pm$ 2.0	13.43 $\pm$ 1.03	"	56.0 $\pm$ 2.0	0.241 $\pm$ 0.030
27.5 $\pm$ 2.0	11.27 $\pm$ 0.85	"	58.0 $\pm$ 2.0	0.439 $\pm$ 0.045
29.6 $\pm$ 2.0	8.24 $\pm$ 0.59	"	60.0 $\pm$ 2.0	0.249 $\pm$ 0.028
31.6 $\pm$ 2.0	4.81 $\pm$ 0.40	"	62.0 $\pm$ 2.0	0.243 $\pm$ 0.025
33.6 $\pm$ 2.0	4.18 $\pm$ 0.34	"	64.1 $\pm$ 2.0	0.190 $\pm$ 0.022
35.7 $\pm$ 2.0	2.33 $\pm$ 0.22	"	66.1 $\pm$ 2.0	0.101 $\pm$ 0.018
37.7 $\pm$ 2.0	1.39 $\pm$ 0.14	"	68.1 $\pm$ 2.0	0.148 $\pm$ 0.018
39.7 $\pm$ 2.0	0.749 $\pm$ 0.086	"	70.1 $\pm$ 2.0	0.140 $\pm$ 0.016
41.8 $\pm$ 2.0	0.604 $\pm$ 0.076	"	72.1 $\pm$ 2.0	0.018 $\pm$ 0.002
43.8 $\pm$ 2.0	0.159 $\pm$ 0.022	"	74.1 $\pm$ 2.0	0.009 $\pm$ 0.002

TABLE 40. Elastic differential scattering cross section data in the pion-nucleus CM for  $\pi^-$  on  $^{16}\text{O}$  at 220 MeV pion kinetic energy in the lab. <sup>14</sup>

$\Theta$ (deg)	$d\sigma/d\Omega_{\pi^-}$ (fm <sup>2</sup> /sr)	"	$\Theta$ (deg)	$d\sigma/d\Omega_{\pi^-}$ (fm <sup>2</sup> /sr)
15.4 $\pm$ 2.0	25.03 $\pm$ 2.96	"	41.9 $\pm$ 2.0	0.305 $\pm$ 0.059
17.4 $\pm$ 2.0	13.19 $\pm$ 2.01	"	43.9 $\pm$ 2.0	0.208 $\pm$ 0.038
19.5 $\pm$ 2.0	6.63 $\pm$ 0.91	"	46.0 $\pm$ 2.0	0.478 $\pm$ 0.079
21.5 $\pm$ 2.0	5.68 $\pm$ 0.79	"	48.0 $\pm$ 2.0	0.506 $\pm$ 0.080
23.5 $\pm$ 2.0	2.87 $\pm$ 0.34	"	50.0 $\pm$ 2.0	0.181 $\pm$ 0.042
25.6 $\pm$ 2.0	2.83 $\pm$ 0.37	"	52.1 $\pm$ 2.0	0.209 $\pm$ 0.041
27.6 $\pm$ 2.0	0.759 $\pm$ 0.153	"	54.1 $\pm$ 2.0	0.114 $\pm$ 0.023
29.7 $\pm$ 2.0	0.498 $\pm$ 0.096	"	56.1 $\pm$ 2.0	0.160 $\pm$ 0.029
31.7 $\pm$ 2.0	0.374 $\pm$ 0.061	"	58.1 $\pm$ 2.0	0.115 $\pm$ 0.020
33.7 $\pm$ 2.0	0.317 $\pm$ 0.052	"	60.2 $\pm$ 2.0	0.027 $\pm$ 0.010
35.8 $\pm$ 2.0	0.230 $\pm$ 0.096	"	62.2 $\pm$ 2.0	0.012 $\pm$ 0.008
37.8 $\pm$ 2.0	0.217 $\pm$ 0.039	"	64.2 $\pm$ 2.0	0.013 $\pm$ 0.009
39.9 $\pm$ 2.0	0.250 $\pm$ 0.061	"		

TABLE 41. Elastic differential scattering cross section data in the pion-nucleus CM for  $\pi^-$  on  $^{16}\text{O}$  at 230 MeV pion kinetic energy in the lab.<sup>14</sup>

$\Theta$ (deg)	$d\sigma/d\Omega_{\pi^-}$ ( $\text{fm}^2/\text{sr}$ )	"	$\Theta$ (deg)	$d\sigma/d\Omega_{\pi^-}$ ( $\text{fm}^2/\text{sr}$ )
$15.4 \pm 2.0$	$31.40 \pm 3.15$	"	$41.9 \pm 2.0$	$0.264 \pm 0.044$
$17.4 \pm 2.0$	$21.67 \pm 2.77$	"	$44.0 \pm 2.0$	$0.284 \pm 0.046$
$19.5 \pm 2.0$	$21.21 \pm 1.62$	"	$46.0 \pm 2.0$	$0.323 \pm 0.035$
$21.5 \pm 2.0$	$18.83 \pm 1.82$	"	$48.0 \pm 2.0$	$0.365 \pm 0.049$
$23.6 \pm 2.0$	$13.58 \pm 1.53$	"	$50.1 \pm 2.0$	$0.354 \pm 0.049$
$25.6 \pm 2.0$	$7.70 \pm 0.68$	"	$52.1 \pm 2.0$	$0.242 \pm 0.032$
$27.6 \pm 2.0$	$6.52 \pm 0.68$	"	$54.1 \pm 2.0$	$0.232 \pm 0.031$
$29.7 \pm 2.0$	$3.30 \pm 0.23$	"	$56.2 \pm 2.0$	$0.097 \pm 0.018$
$31.7 \pm 2.0$	$1.42 \pm 0.14$	"	$58.2 \pm 2.0$	$0.095 \pm 0.016$
$33.8 \pm 2.0$	$0.530 \pm 0.079$	"	$60.2 \pm 2.0$	$0.046 \pm 0.012$
$35.8 \pm 2.0$	$0.198 \pm 0.025$	"	$62.2 \pm 2.0$	$0.018 \pm 0.008$
$37.8 \pm 2.0$	$0.159 \pm 0.021$	"	$64.3 \pm 2.0$	$0.014 \pm 0.006$
$39.9 \pm 2.0$	$0.164 \pm 0.024$	"	$66.3 \pm 2.0$	$0.002 \pm 0.002$

TABLE 42. Elastic differential scattering cross section data in the pion-nucleus CM for  $\pi^-$  on  $^{16}\text{O}$  at 240 MeV pion kinetic energy in the lab. <sup>14</sup>

$\Theta$ (deg)	$d\sigma/d\Omega_{\pi^-}$ (fm <sup>2</sup> /sr)	"	$\Theta$ (deg)	$d\sigma/d\Omega_{\pi^-}$ (fm <sup>2</sup> /sr)
15.4 $\pm$ 2.0	20.21 $\pm$ 2.38	"	41.9 $\pm$ 2.0	0.446 $\pm$ 0.073
17.4 $\pm$ 2.0	11.25 $\pm$ 1.72	"	44.0 $\pm$ 2.0	0.445 $\pm$ 0.048
19.5 $\pm$ 2.0	7.33 $\pm$ 0.89	"	46.0 $\pm$ 2.0	0.405 $\pm$ 0.070
21.5 $\pm$ 2.0	4.96 $\pm$ 0.75	"	48.1 $\pm$ 2.0	0.243 $\pm$ 0.057
23.6 $\pm$ 2.0	2.55 $\pm$ 0.25	"	50.1 $\pm$ 2.0	0.331 $\pm$ 0.052
25.6 $\pm$ 2.0	1.06 $\pm$ 0.17	"	52.1 $\pm$ 2.0	0.270 $\pm$ 0.044
27.7 $\pm$ 2.0	0.354 $\pm$ 0.105	"	54.2 $\pm$ 2.0	0.104 $\pm$ 0.020
29.7 $\pm$ 2.0	0.358 $\pm$ 0.086	"	56.2 $\pm$ 2.0	0.0923 $\pm$ 0.0156
31.7 $\pm$ 2.0	0.315 $\pm$ 0.055	"	58.2 $\pm$ 2.0	0.0798 $\pm$ 0.0175
33.8 $\pm$ 2.0	0.173 $\pm$ 0.035	"	60.2 $\pm$ 2.0	0.0132 $\pm$ 0.0068
35.8 $\pm$ 2.0	0.254 $\pm$ 0.048	"	62.3 $\pm$ 2.0	0.0049 $\pm$ 0.0049
37.9 $\pm$ 2.0	0.201 $\pm$ 0.039	"	64.3 $\pm$ 3.0	0.0059 $\pm$ 0.0059
39.9 $\pm$ 2.0	0.577 $\pm$ 0.079	"		

TABLE 43. Elastic differential scattering cross section data in the pion-nucleus CM for  $\pi^+$  on  $^{16}\text{O}$  at 270 MeV pion kinetic energy in the lab. <sup>158</sup>

$\Theta$ (deg)	$d\sigma/d\Omega_{\pi^+}$ (fm <sup>2</sup> /sr)	"	$\Theta$ (deg)	$d\sigma/d\Omega_{\pi^+}$ (fm <sup>2</sup> /sr)
5.1 $\pm$ 1.0	293.9 $\pm$ 37.9	"	34.9 $\pm$ 1.0	0.957 $\pm$ 0.191
6.7 $\pm$ 1.0	132.7 $\pm$ 14.2	"	36.9 $\pm$ 1.0	0.670 $\pm$ 0.096
8.2 $\pm$ 1.0	102.4 $\pm$ 7.6	"	39.0 $\pm$ 1.0	0.671 $\pm$ 0.096
11.3 $\pm$ 1.0	84.44 $\pm$ 9.49	"	41.0 $\pm$ 1.0	0.672 $\pm$ 0.096
15.4 $\pm$ 1.0	56.97 $\pm$ 7.60	"	43.0 $\pm$ 1.0	0.769 $\pm$ 0.096
18.5 $\pm$ 1.0	35.16 $\pm$ 3.80	"	46.1 $\pm$ 1.0	0.722 $\pm$ 0.096
21.6 $\pm$ 1.0	12.37 $\pm$ 2.85	"	50.7 $\pm$ 1.0	0.435 $\pm$ 0.068
24.6 $\pm$ 1.0	8.57 $\pm$ 0.95	"	55.3 $\pm$ 1.0	0.252 $\pm$ 0.039
27.7 $\pm$ 1.0	6.39 $\pm$ 0.76	"	59.8 $\pm$ 1.0	0.127 $\pm$ 0.019
30.8 $\pm$ 1.0	1.91 $\pm$ 0.29	"	64.4 $\pm$ 1.0	0.059 $\pm$ 0.010

TABLE 44. Elastic differential scattering cross section data in the pion-nucleus CM for  $\pi^-$  on  $^{40}\text{Ca}$  at 205 MeV pion kinetic energy in the lab.<sup>14</sup>

$\Theta$ (deg)	$d\sigma/d\Omega_{\pi^-}$ (fm <sup>2</sup> /sr)	''	$\Theta$ (deg)	$d\sigma/d\Omega_{\pi^-}$ (fm <sup>2</sup> /sr)
15.1 $\pm$ 2.0	84.62 $\pm$ 11.63	''	45.4 $\pm$ 2.0	2.65 $\pm$ 0.28
17.2 $\pm$ 2.0	120.10 $\pm$ 15.63	''	47.4 $\pm$ 2.0	2.10 $\pm$ 0.27
19.2 $\pm$ 2.0	59.96 $\pm$ 5.63	''	49.4 $\pm$ 2.0	1.30 $\pm$ 0.15
21.2 $\pm$ 2.0	49.87 $\pm$ 6.68	''	51.4 $\pm$ 2.0	0.587 $\pm$ 0.085
23.2 $\pm$ 2.0	55.03 $\pm$ 5.44	''	53.4 $\pm$ 2.0	0.404 $\pm$ 0.091
25.2 $\pm$ 2.0	18.70 $\pm$ 5.72	''	55.4 $\pm$ 2.0	0.298 $\pm$ 0.062
27.2 $\pm$ 2.0	8.13 $\pm$ 0.94	''	57.4 $\pm$ 2.0	0.409 $\pm$ 0.090
29.3 $\pm$ 2.0	2.86 $\pm$ 0.58	''	59.5 $\pm$ 2.0	0.539 $\pm$ 0.106
31.3 $\pm$ 2.0	3.59 $\pm$ 0.41	''	61.5 $\pm$ 2.0	0.340 $\pm$ 0.051
33.3 $\pm$ 2.0	5.04 $\pm$ 0.60	''	63.5 $\pm$ 2.0	0.357 $\pm$ 0.056
35.3 $\pm$ 2.0	4.33 $\pm$ 0.40	''	65.5 $\pm$ 2.0	0.149 $\pm$ 0.077
37.3 $\pm$ 2.0	5.90 $\pm$ 0.64	''	67.5 $\pm$ 2.0	0.081 $\pm$ 0.020
39.3 $\pm$ 2.0	5.55 $\pm$ 0.65	''	69.5 $\pm$ 2.0	0.111 $\pm$ 0.024
41.4 $\pm$ 2.0	4.41 $\pm$ 0.39	''	71.5 $\pm$ 2.0	0.059 $\pm$ 0.016
43.4 $\pm$ 2.0	4.34 $\pm$ 0.56	''		

TABLE 45. Elastic differential scattering cross section data in the pion-nucleus CM for  $\pi^-$  on  $^{40}\text{Ca}$  at 215 MeV pion kinetic energy in the lab.<sup>14</sup>

$\Theta$ (deg)	$d\sigma/d\Omega_{\pi^-}$ (fm <sup>2</sup> /sr)	"	$\Theta$ (deg)	$d\sigma/d\Omega_{\pi^-}$ (fm <sup>2</sup> /sr)
15.1 $\pm$ 2.0	90.20 $\pm$ 10.10	"	43.4 $\pm$ 2.0	1.24 $\pm$ 0.39
17.2 $\pm$ 2.0	66.21 $\pm$ 7.62	"	45.4 $\pm$ 2.0	0.976 $\pm$ 0.153
19.2 $\pm$ 2.0	51.74 $\pm$ 4.96	"	47.4 $\pm$ 2.0	0.558 $\pm$ 0.153
21.2 $\pm$ 2.0	23.16 $\pm$ 2.86	"	49.4 $\pm$ 2.0	0.383 $\pm$ 0.083
23.2 $\pm$ 2.0	9.72 $\pm$ 1.10	"	51.4 $\pm$ 2.0	0.173 $\pm$ 0.057
25.2 $\pm$ 2.0	5.05 $\pm$ 0.63	"	53.4 $\pm$ 2.0	0.179 $\pm$ 0.057
27.2 $\pm$ 2.0	2.21 $\pm$ 0.43	"	55.4 $\pm$ 2.0	0.151 $\pm$ 0.049
29.3 $\pm$ 2.0	2.32 $\pm$ 0.52	"	57.5 $\pm$ 2.0	0.198 $\pm$ 0.048
31.3 $\pm$ 2.0	3.52 $\pm$ 0.50	"	59.5 $\pm$ 2.0	0.194 $\pm$ 0.036
33.3 $\pm$ 2.0	2.98 $\pm$ 0.67	"	61.5 $\pm$ 2.0	0.115 $\pm$ 0.026
35.3 $\pm$ 2.0	3.42 $\pm$ 0.40	"	63.5 $\pm$ 2.0	0.065 $\pm$ 0.014
37.3 $\pm$ 2.0	3.21 $\pm$ 0.43	"	65.5 $\pm$ 2.0	0.060 $\pm$ 0.015
39.3 $\pm$ 2.0	2.91 $\pm$ 0.40	"	67.5 $\pm$ 2.0	0.024 $\pm$ 0.010
41.4 $\pm$ 2.0	1.83 $\pm$ 0.30	"		

TABLE 46 . Shift in energy levels of pionic atoms due to vacuum polarization.

Nucleus	$\Delta E^{1s}(\text{ev})$	$\Delta E^{2p}(\text{ev})$	$\Delta E^{3d}(\text{ev})$
${}^4\text{He}$	- 29.7 $\pm$ 0.2	- 0.924	
${}^6\text{Li}$	- 94.8 $\pm$ 0.5	- 4.32	
${}^7\text{Li}$	- 92.9 $\pm$ 0.6	- 4.35	
${}^9\text{Be}$	- 199.2 $\pm$ 0.3	- 11.9	
${}^{10}\text{B}$	- 348.5 $\pm$ 2.5	- 25.0	
${}^{11}\text{B}$	- 339.0 $\pm$ 1.5	- 25.1	
${}^{12}\text{C}$	- 537.7 $\pm$ 1.4	- 44.9	
${}^{14}\text{N}$	- 777.3 $\pm$ 2.4	- 72.5	
${}^{16}\text{O}$	- 1086 $\pm$ 4	- 109	
${}^{18}\text{O}$	- 989 $\pm$ 5	- 109	
${}^{19}\text{F}$	- 1350 $\pm$ 7	- 154	
${}^{20}\text{Ne}$	- 2124	- 210	
${}^{23}\text{Na}$	- 2074 $\pm$ 6	- 276	
${}^{24}\text{Mg}$	- 2610 $\pm$ 14	- 354	
${}^{40}\text{Ca}$		- 1430	- 220

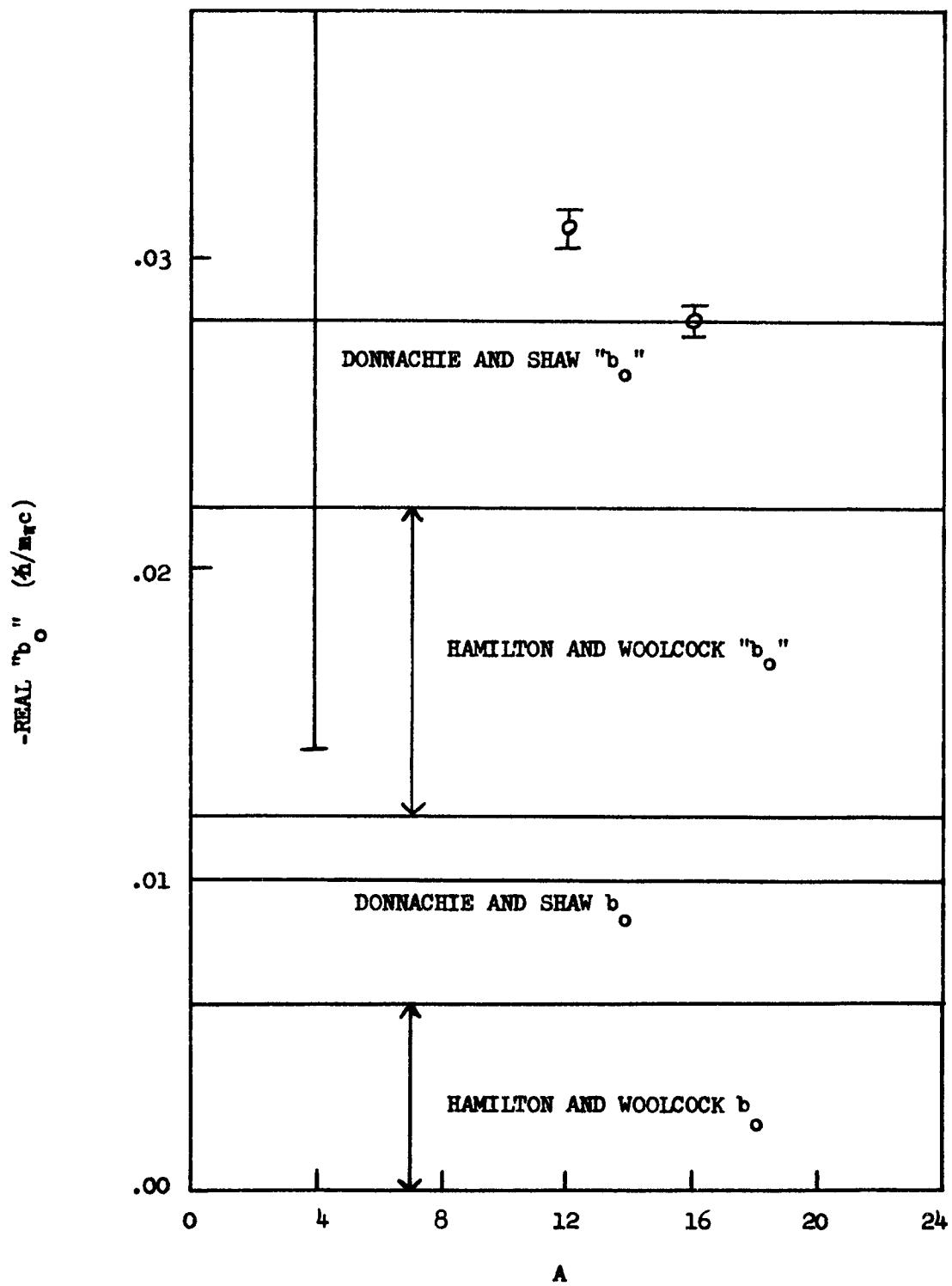


FIGURE 1.

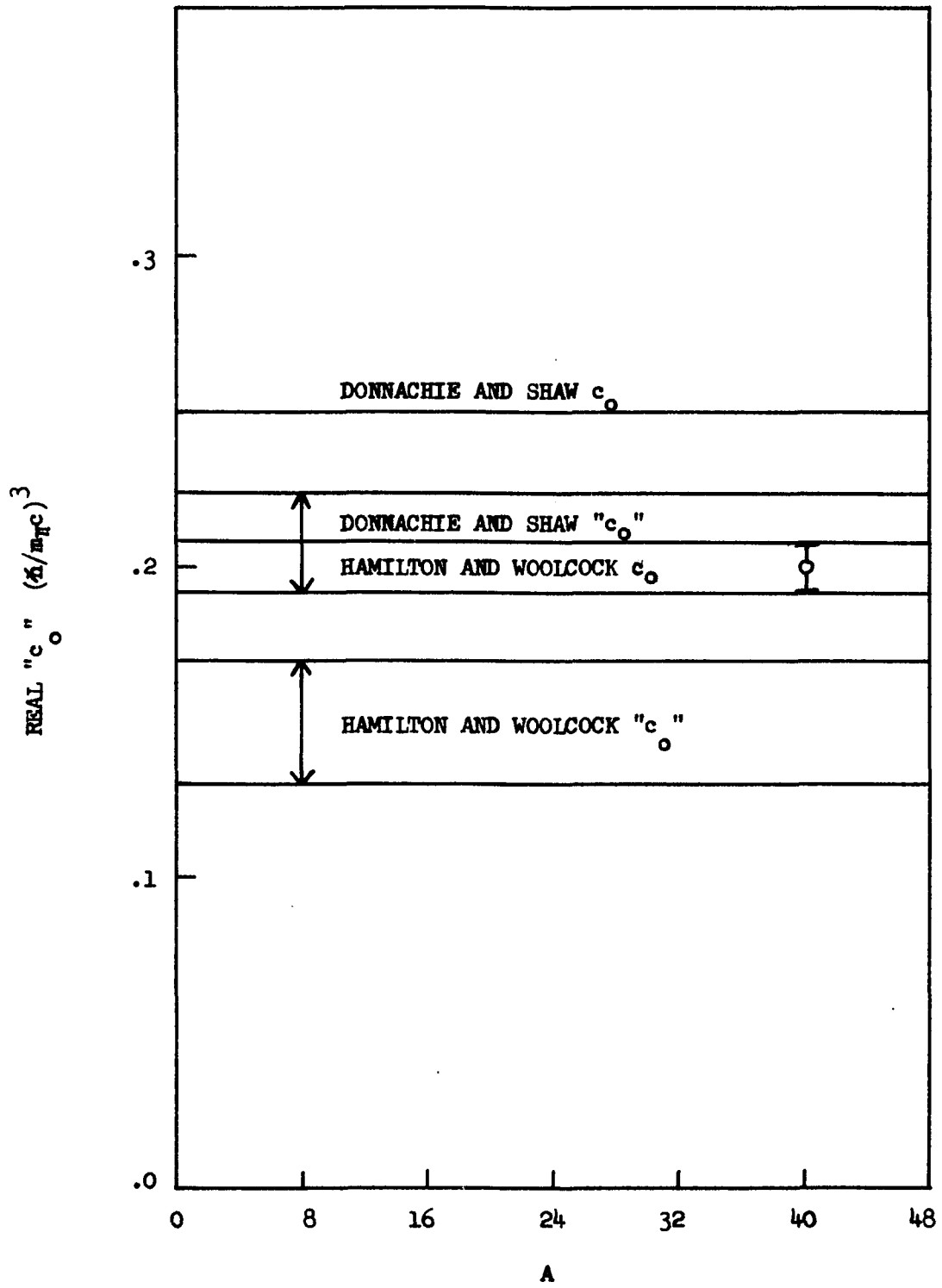


FIGURE 2.

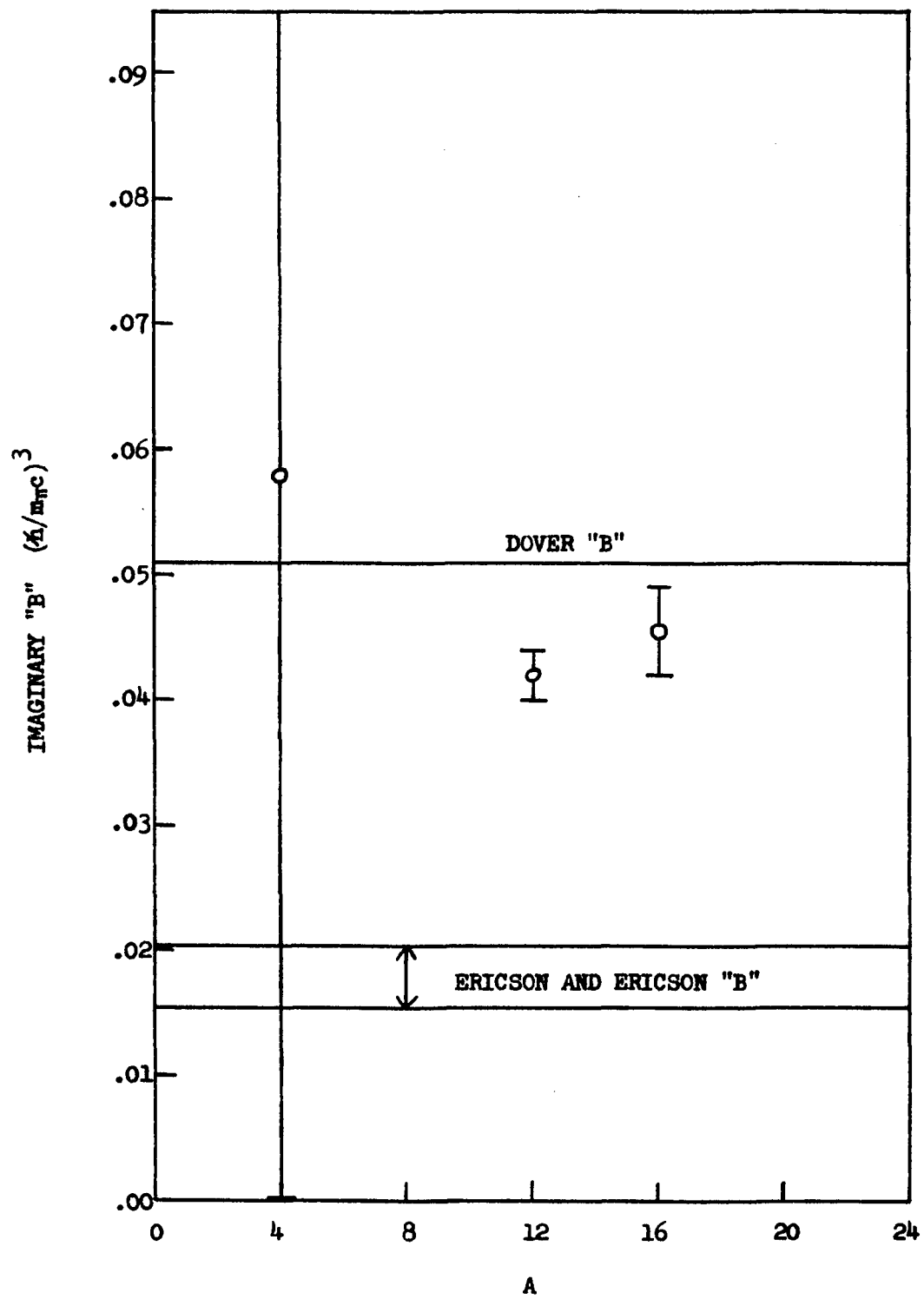


FIGURE 3.

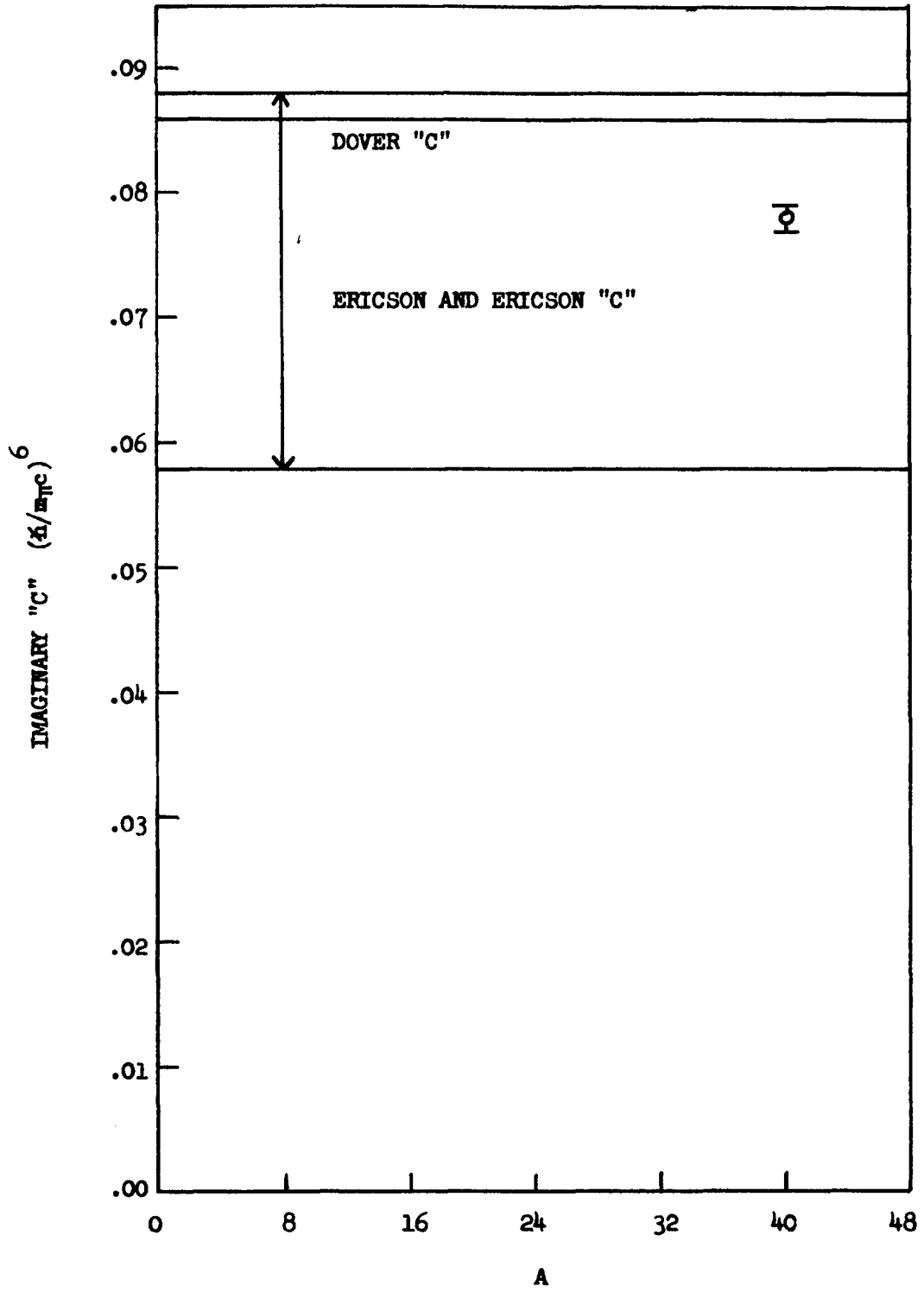


FIGURE 4.

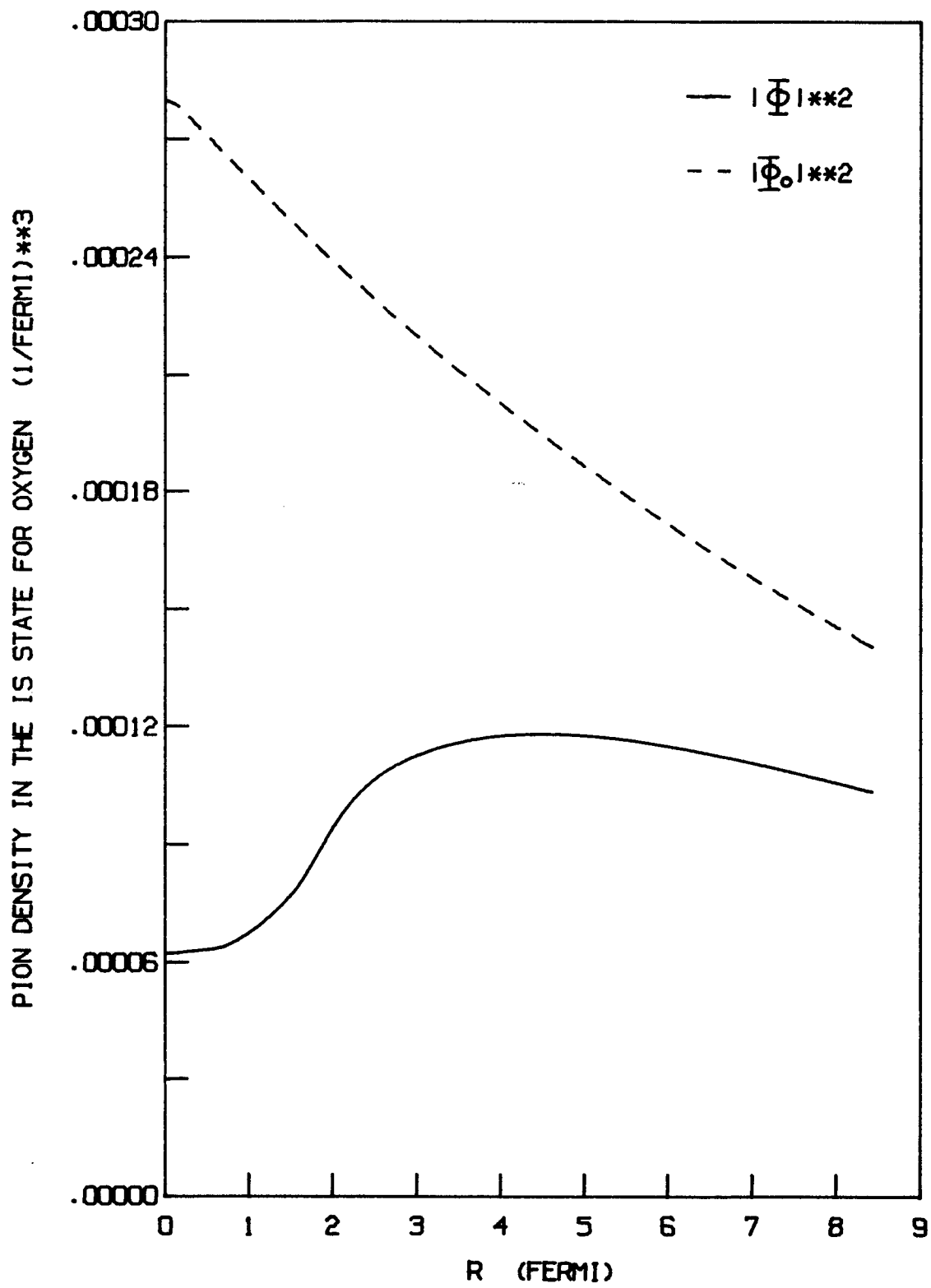


FIGURE 5.

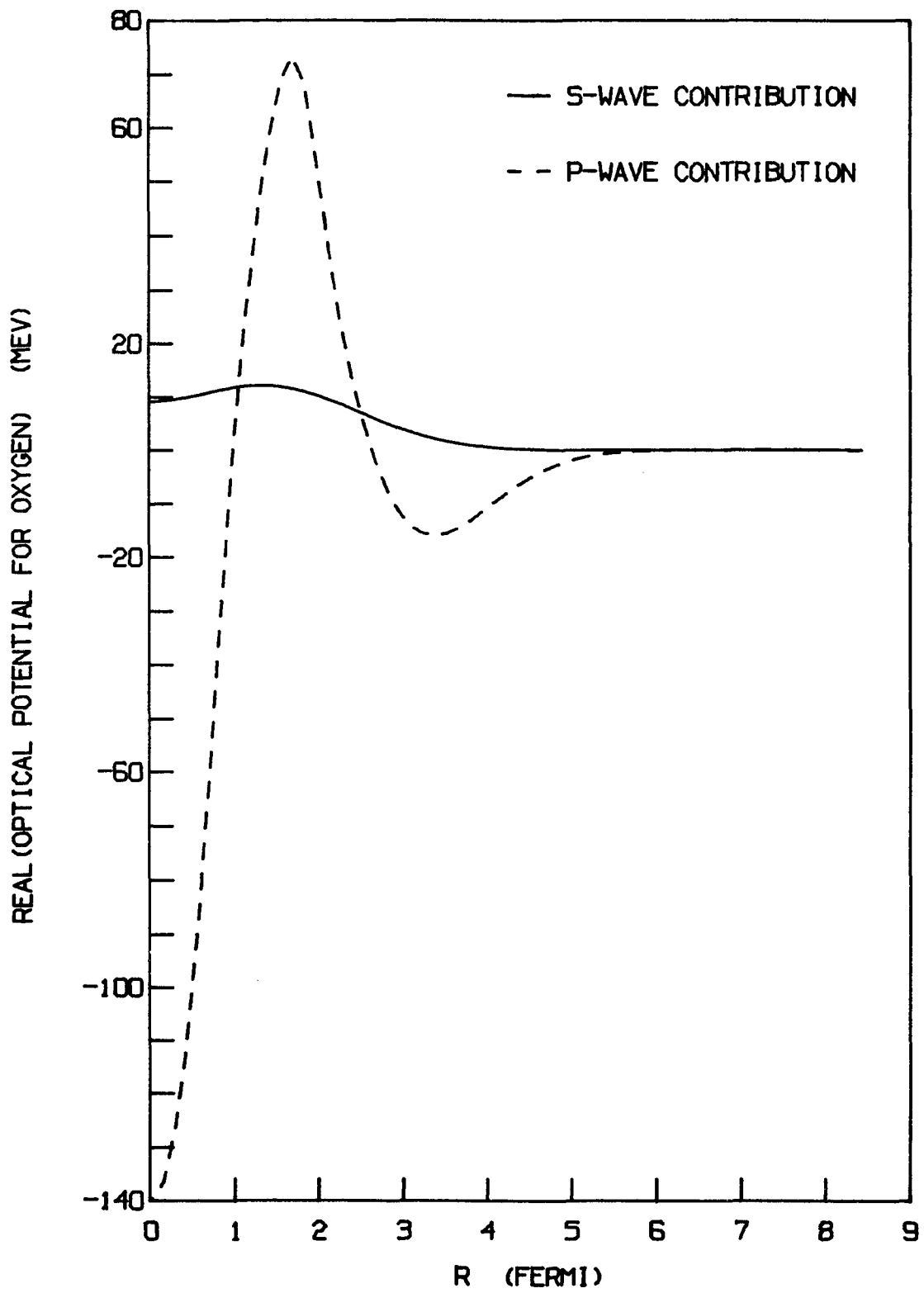


FIGURE 6.

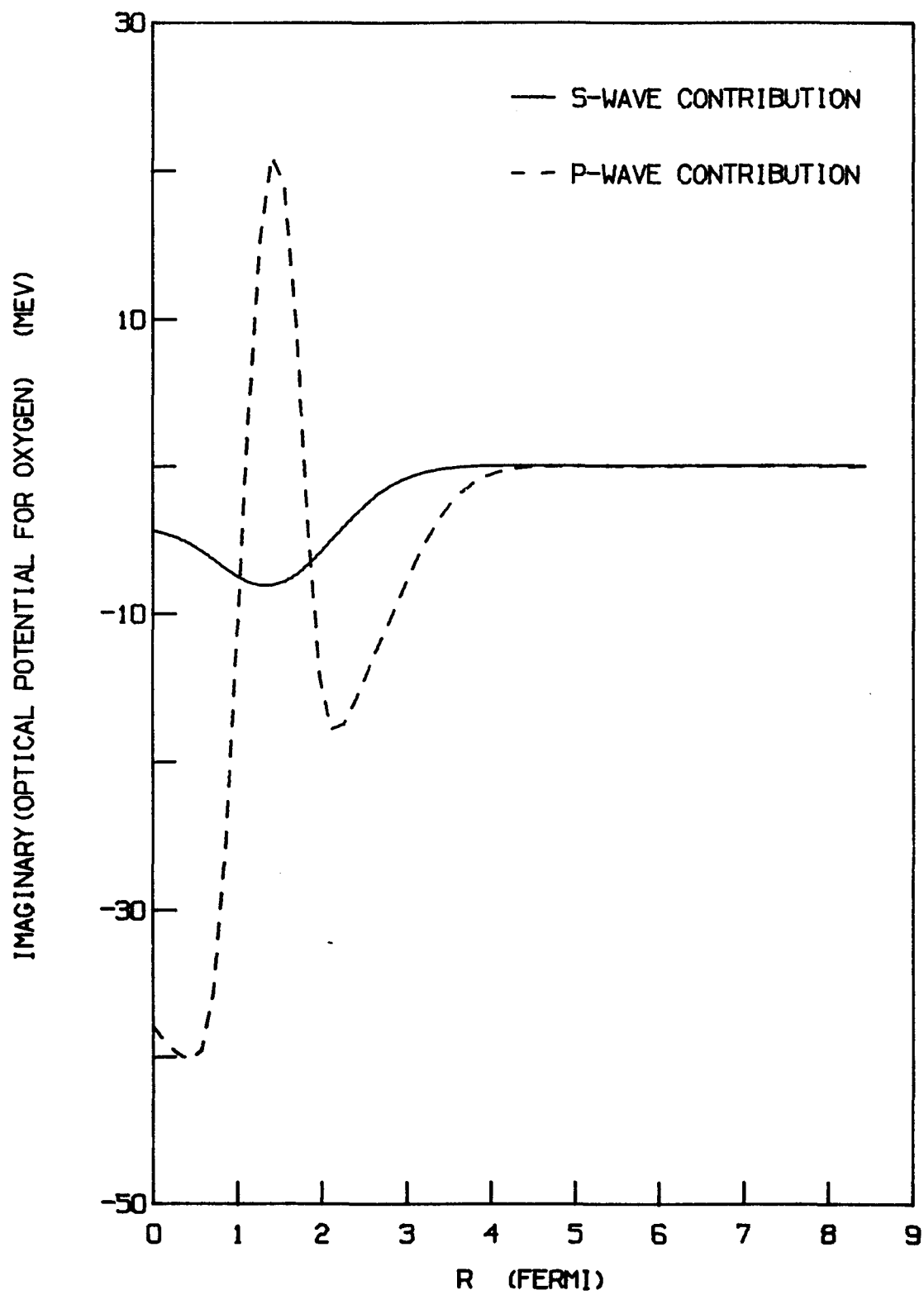


FIGURE 7.

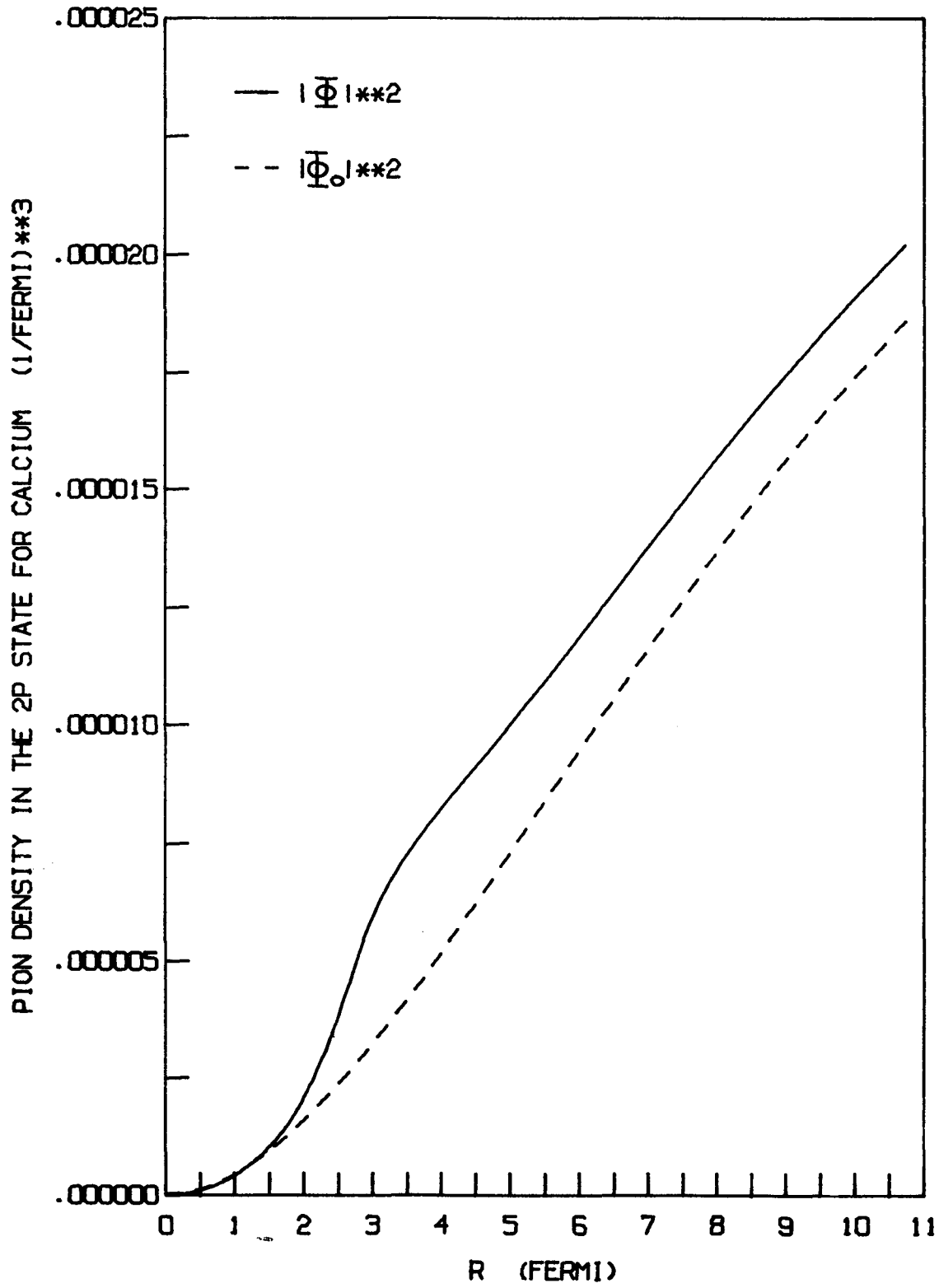


FIGURE 8.

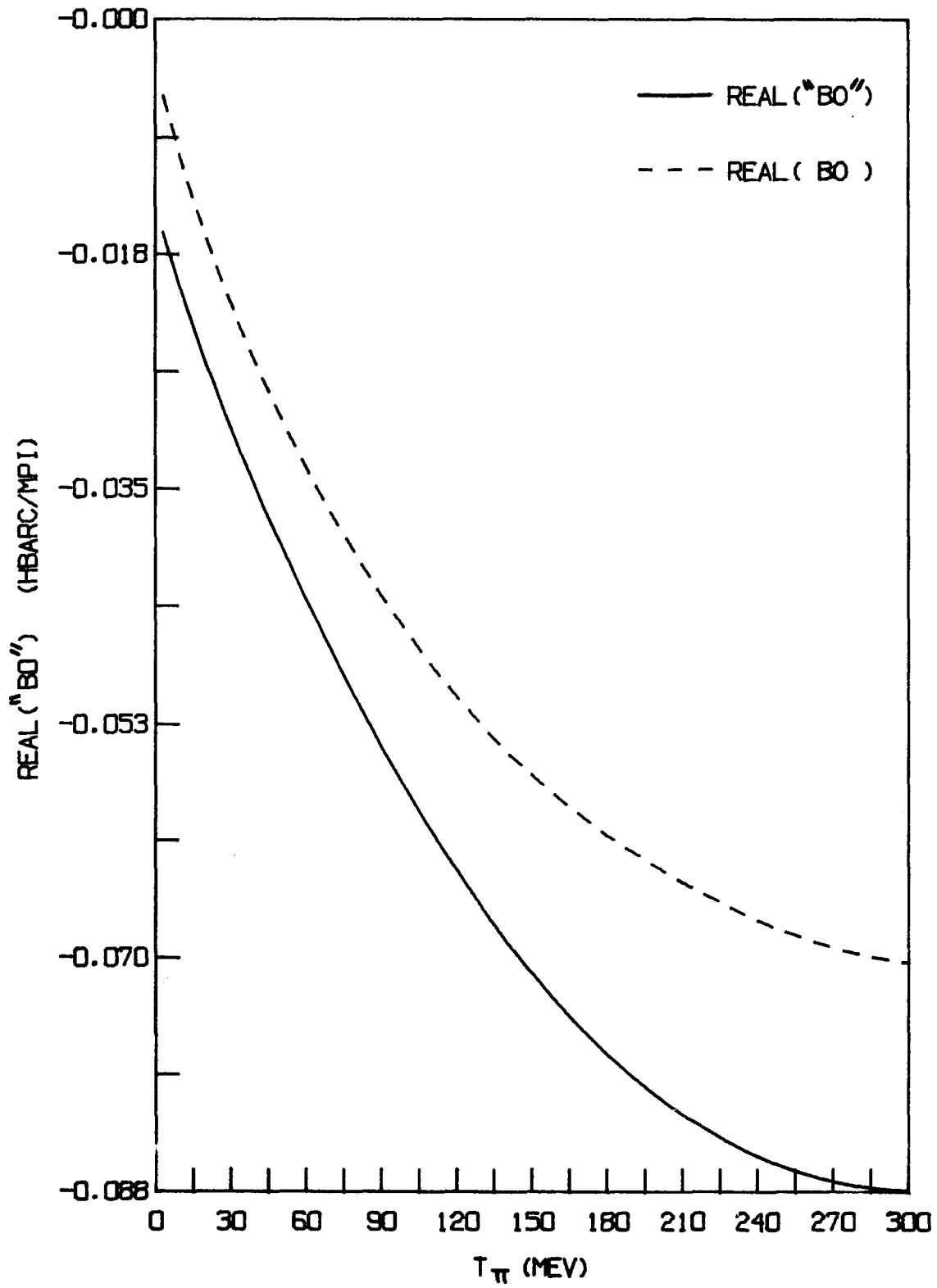


FIGURE 9.

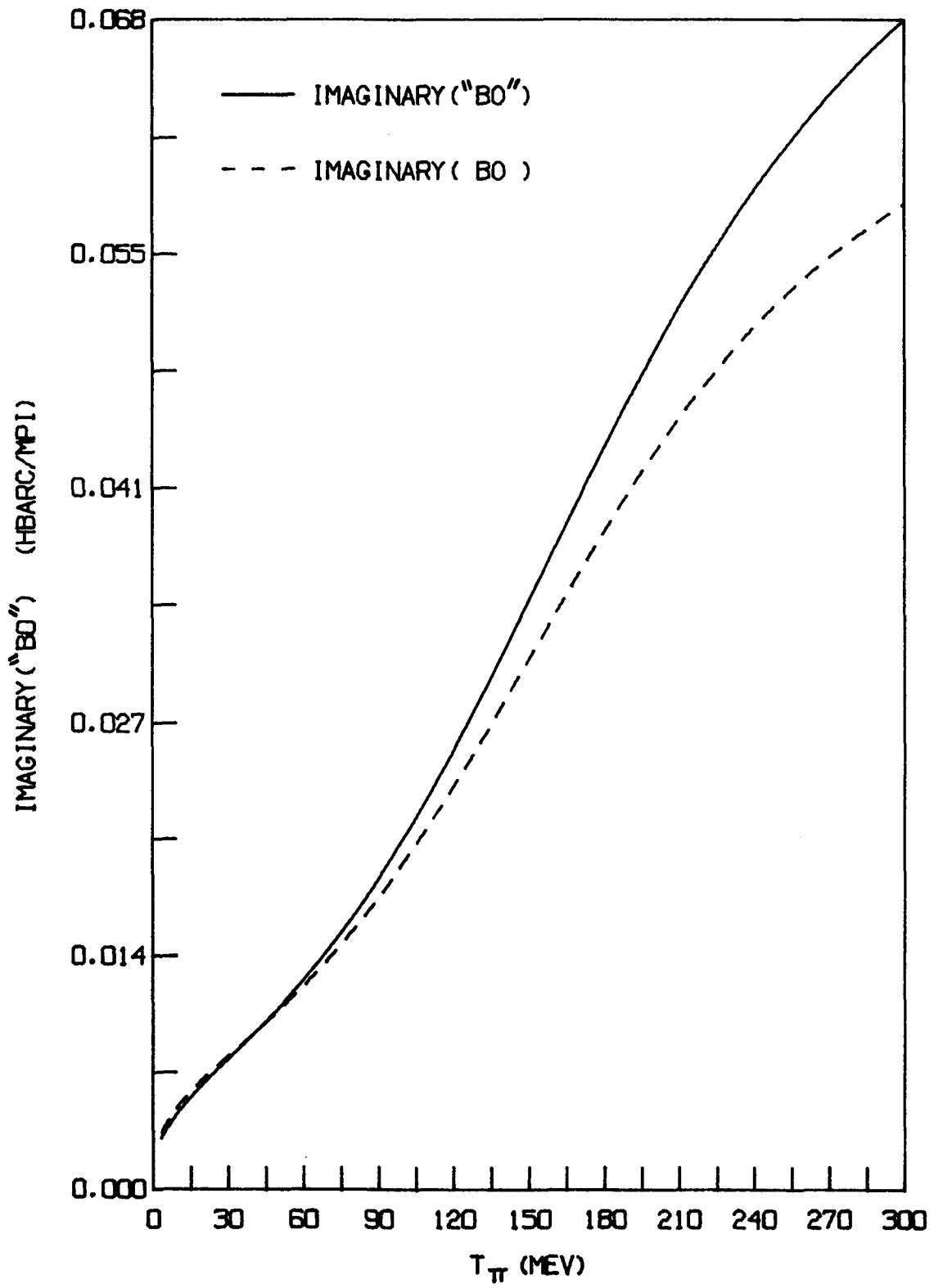


FIGURE 10.

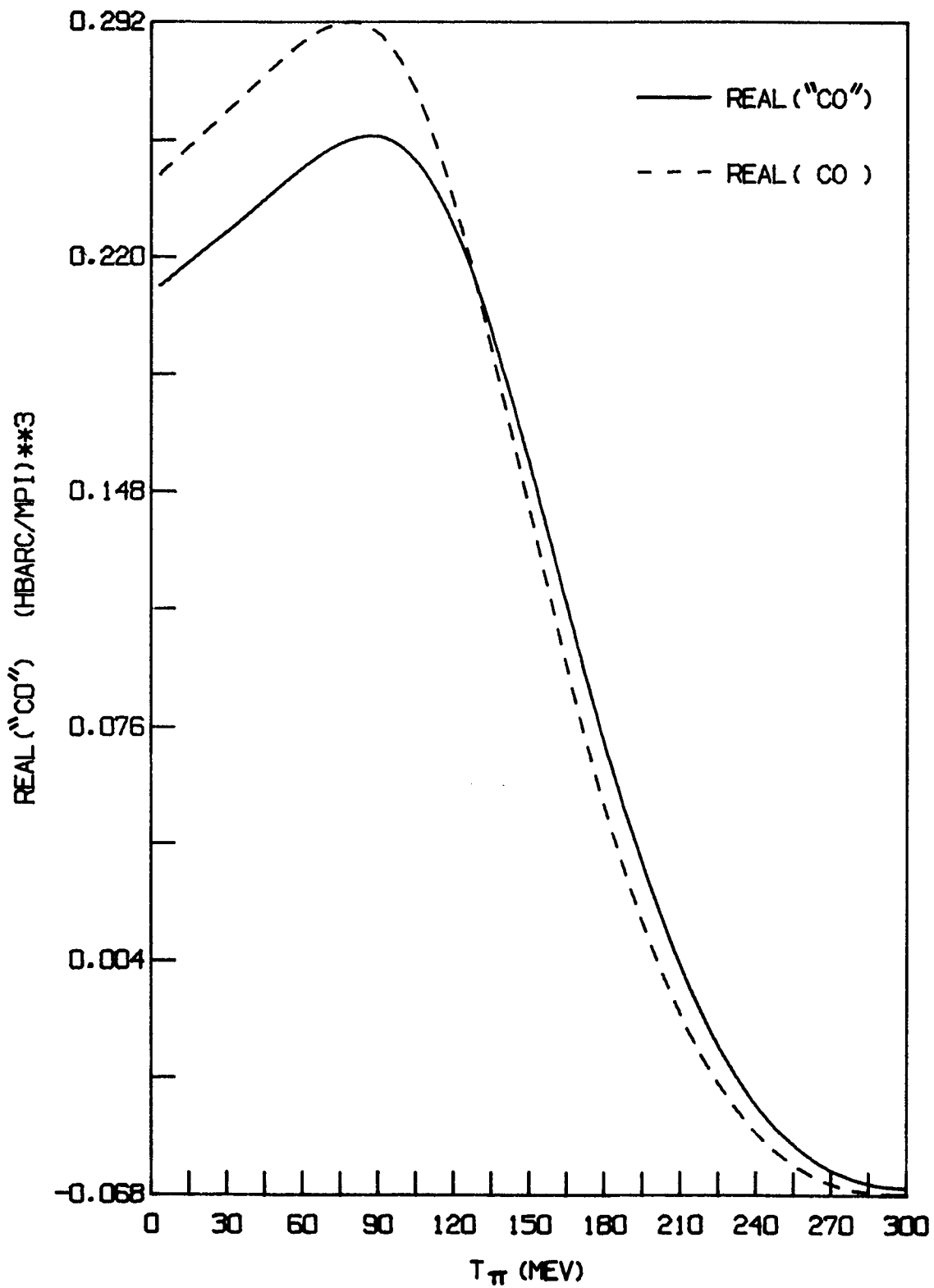


FIGURE 11.

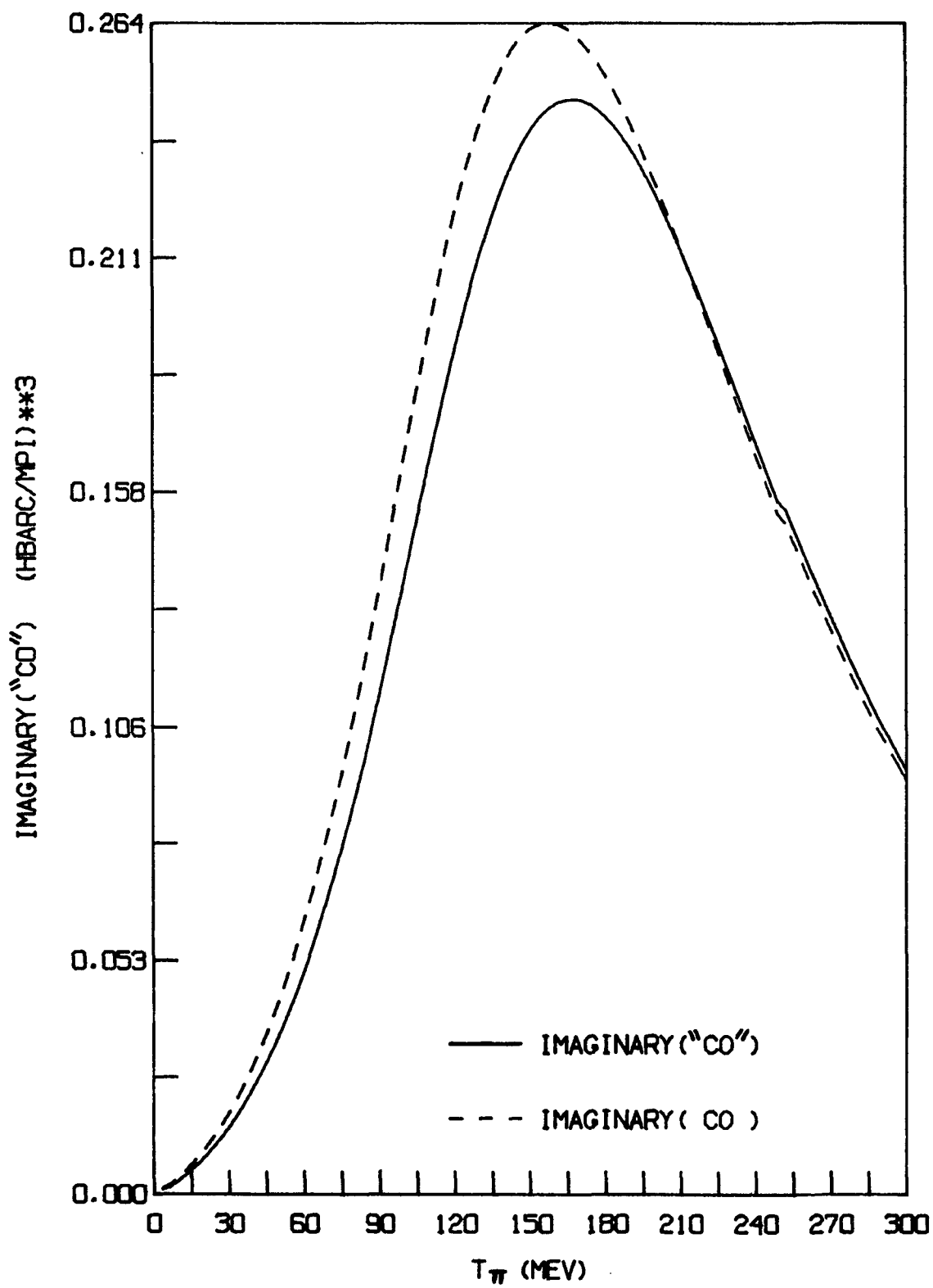


FIGURE 12.

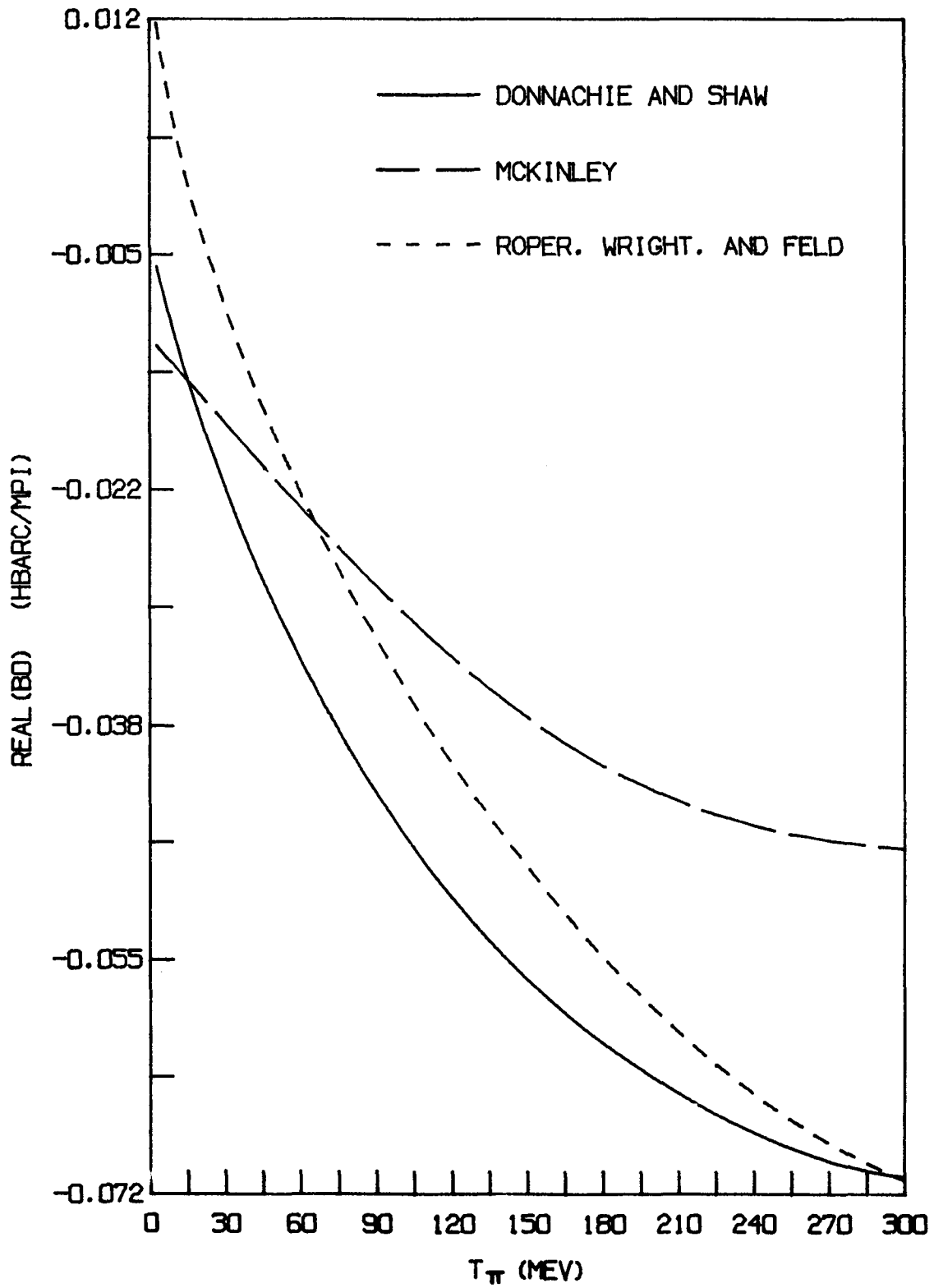


FIGURE 13.

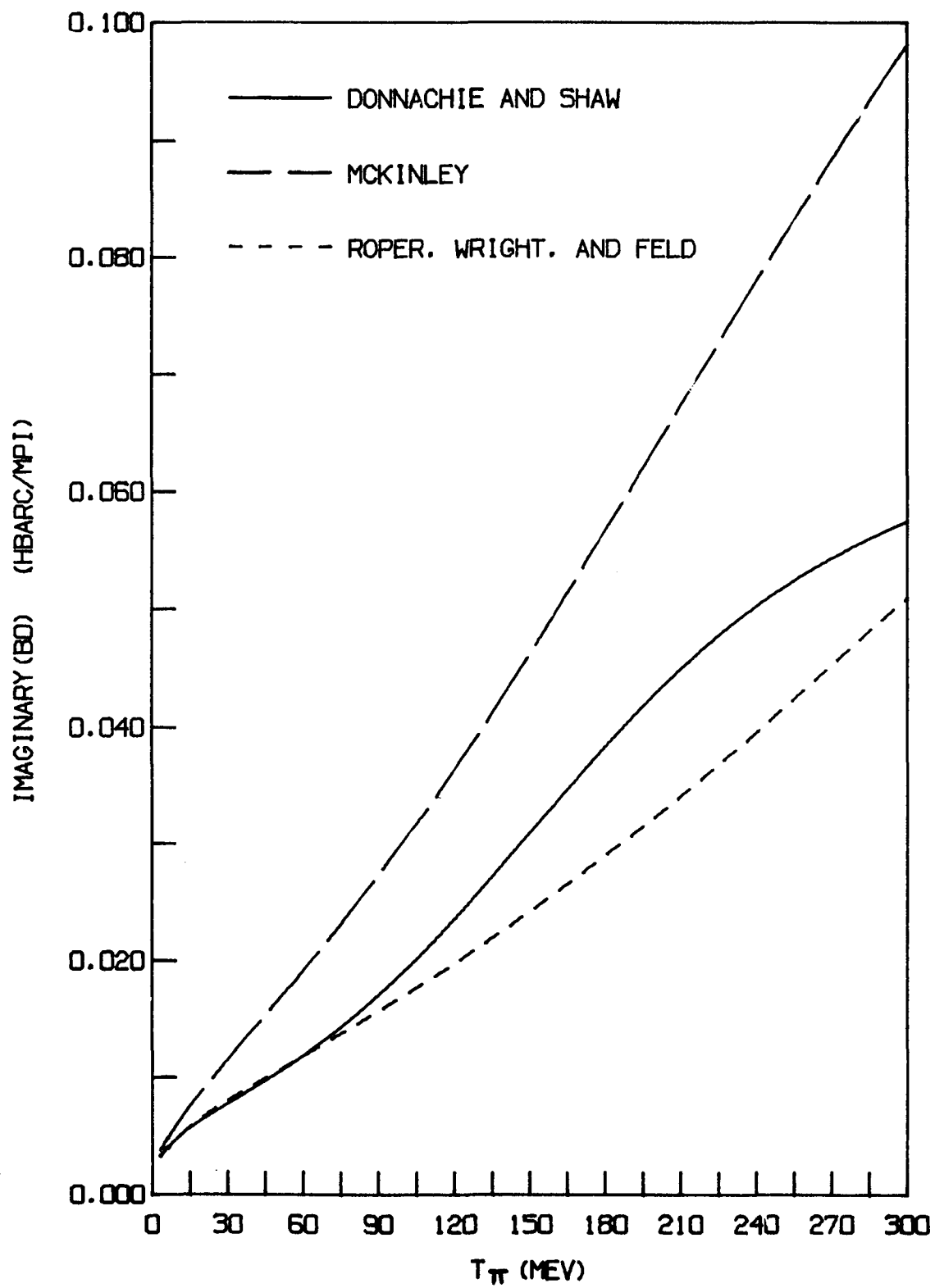


FIGURE 14.

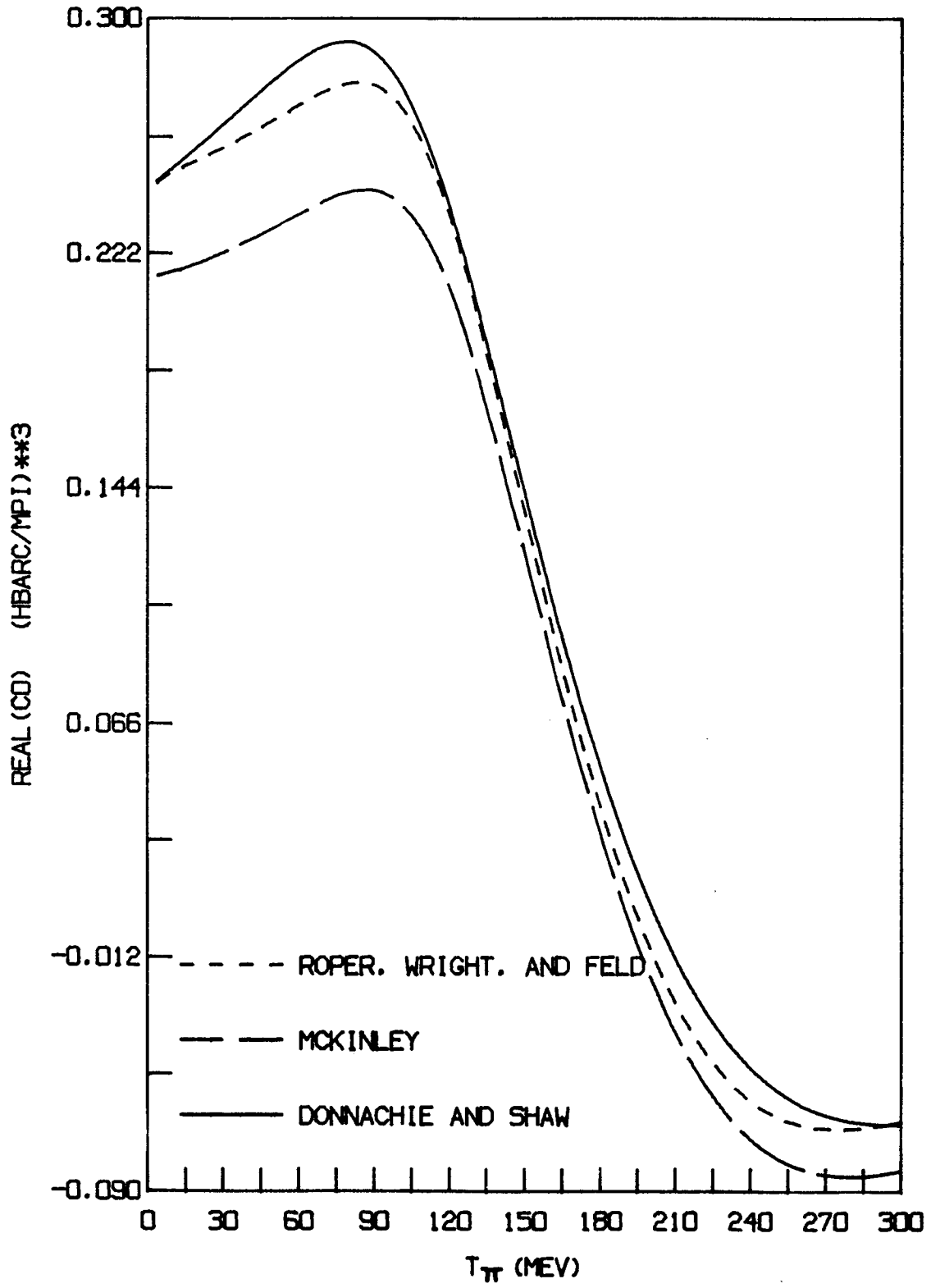


FIGURE 15.

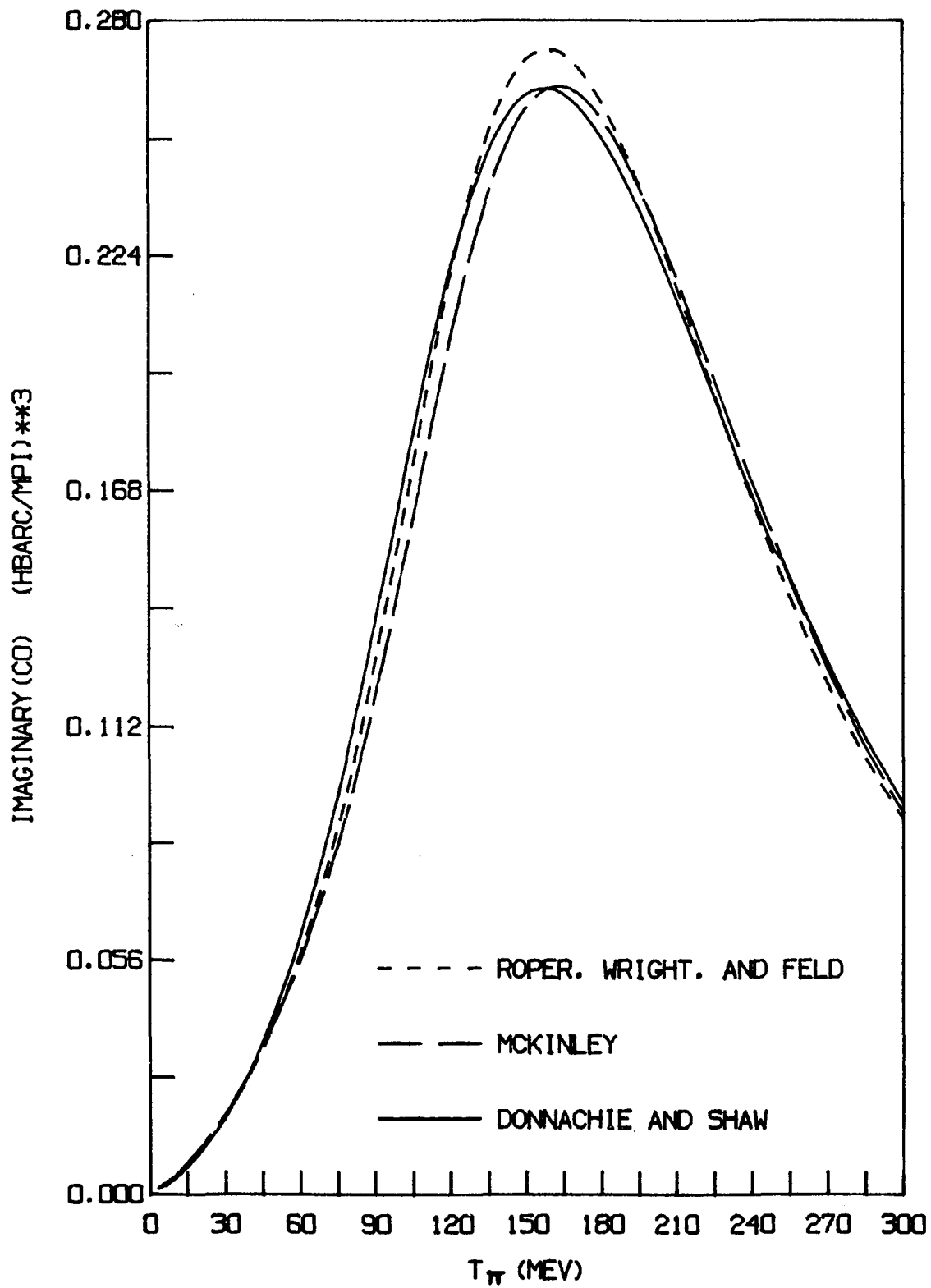


FIGURE 16.

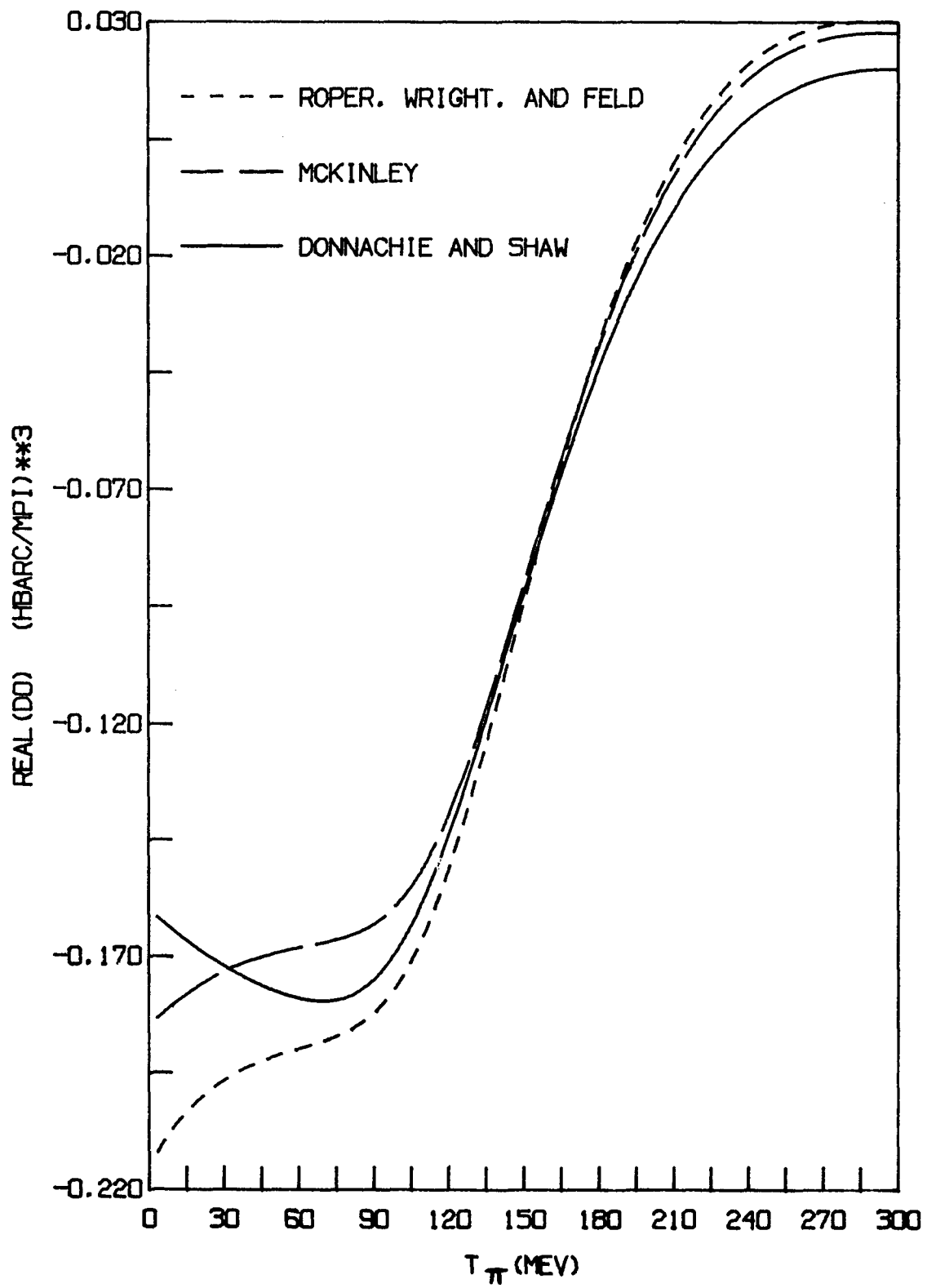


FIGURE 17.

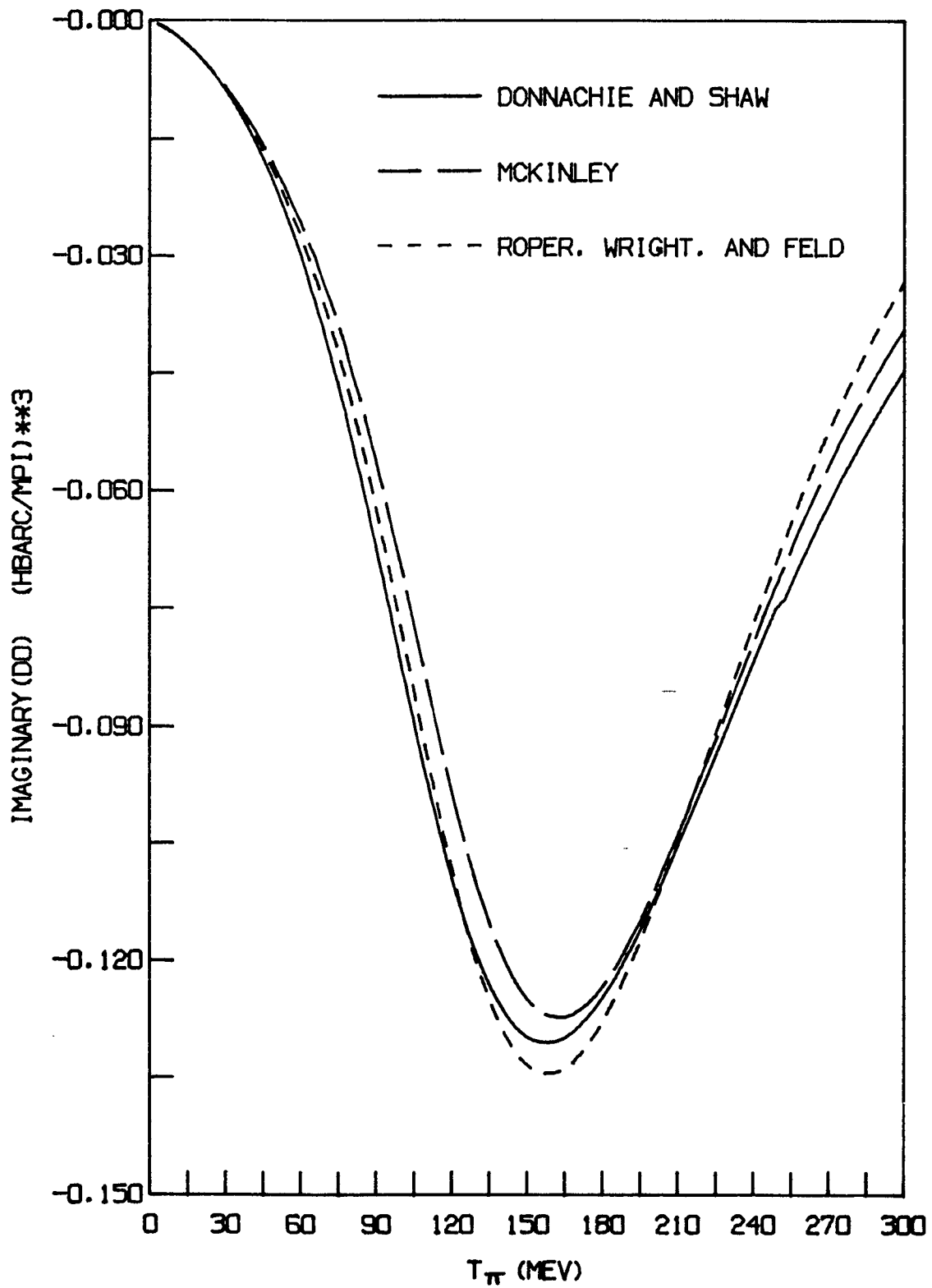


FIGURE 18.

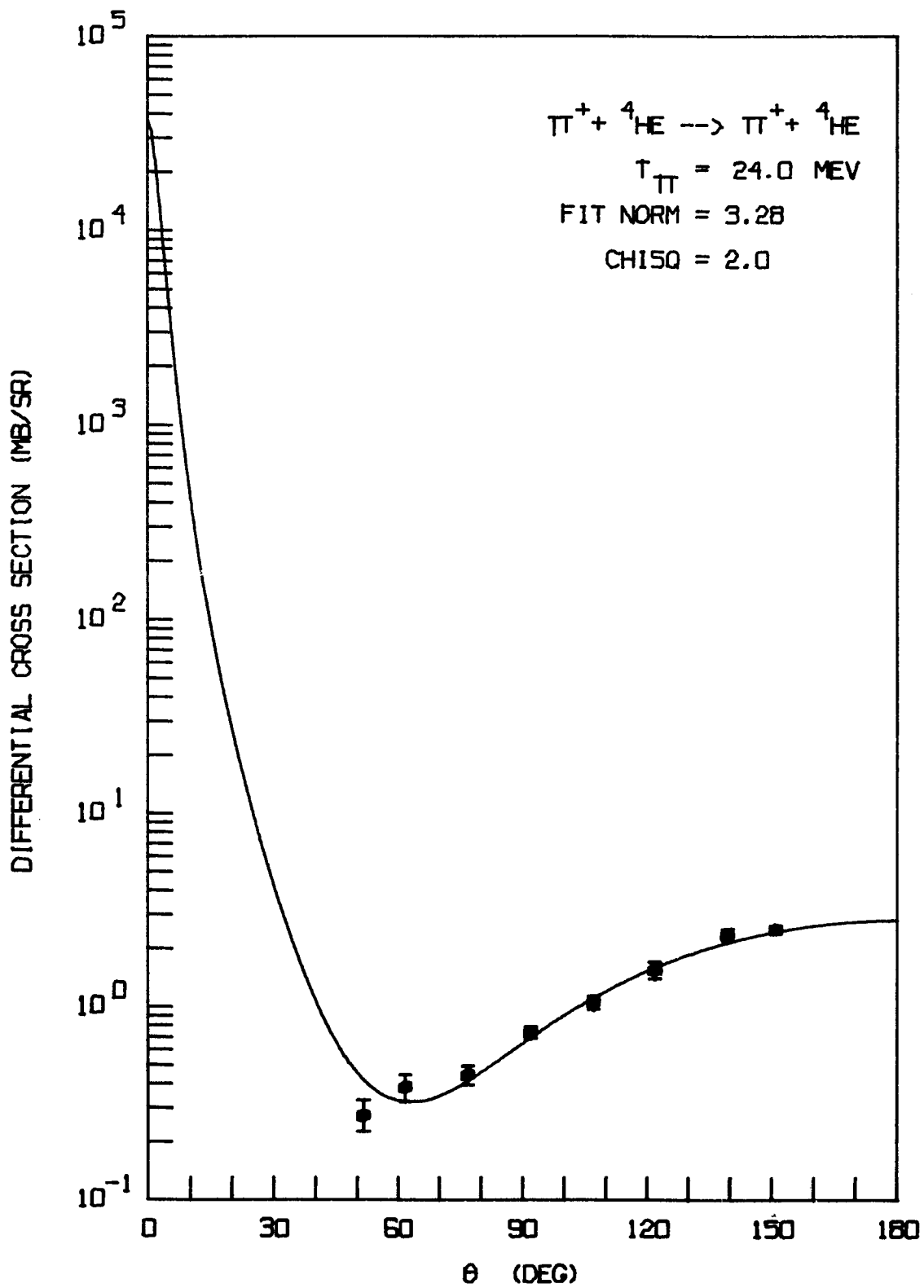


FIGURE 19.

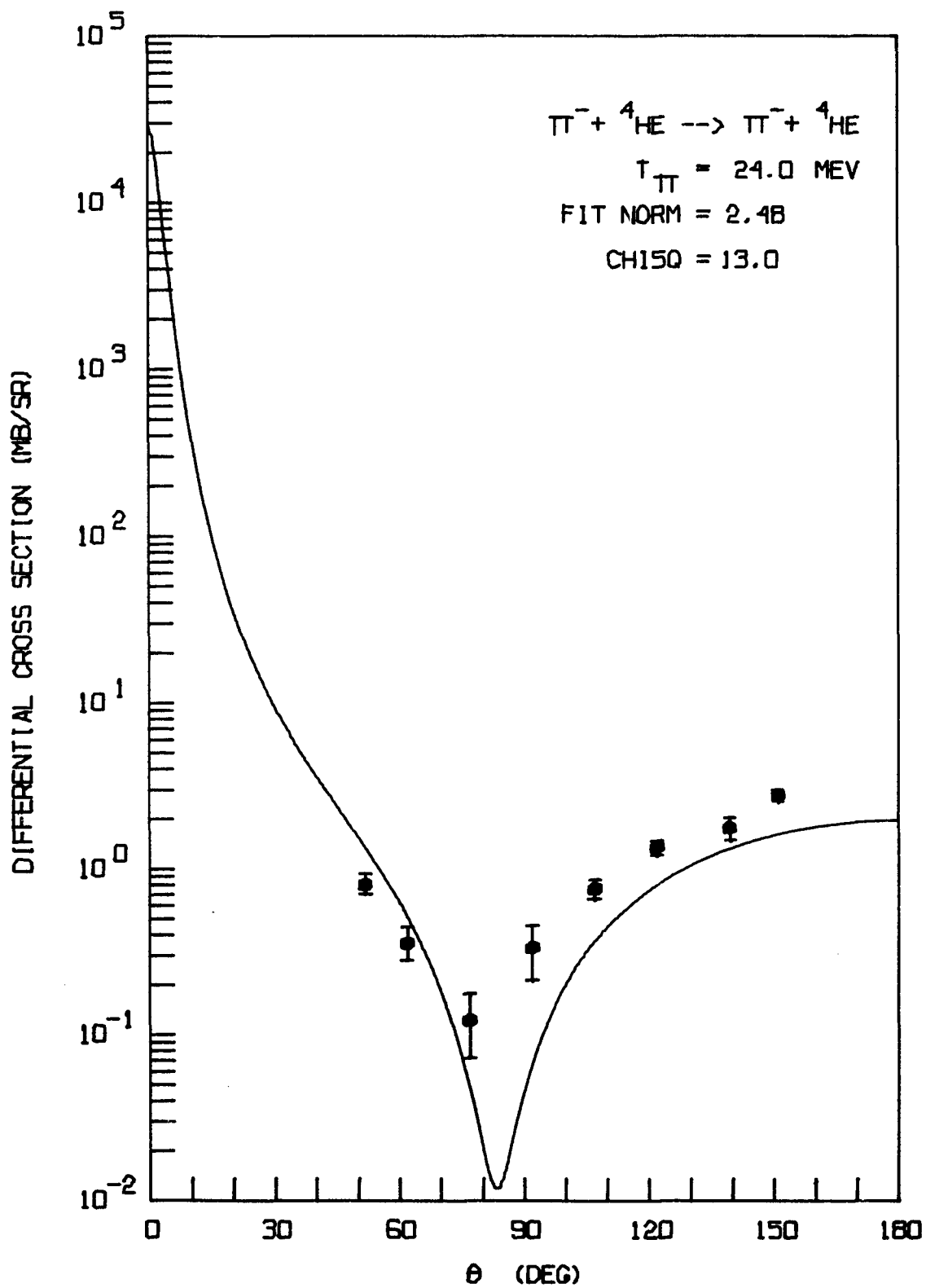


FIGURE 20.

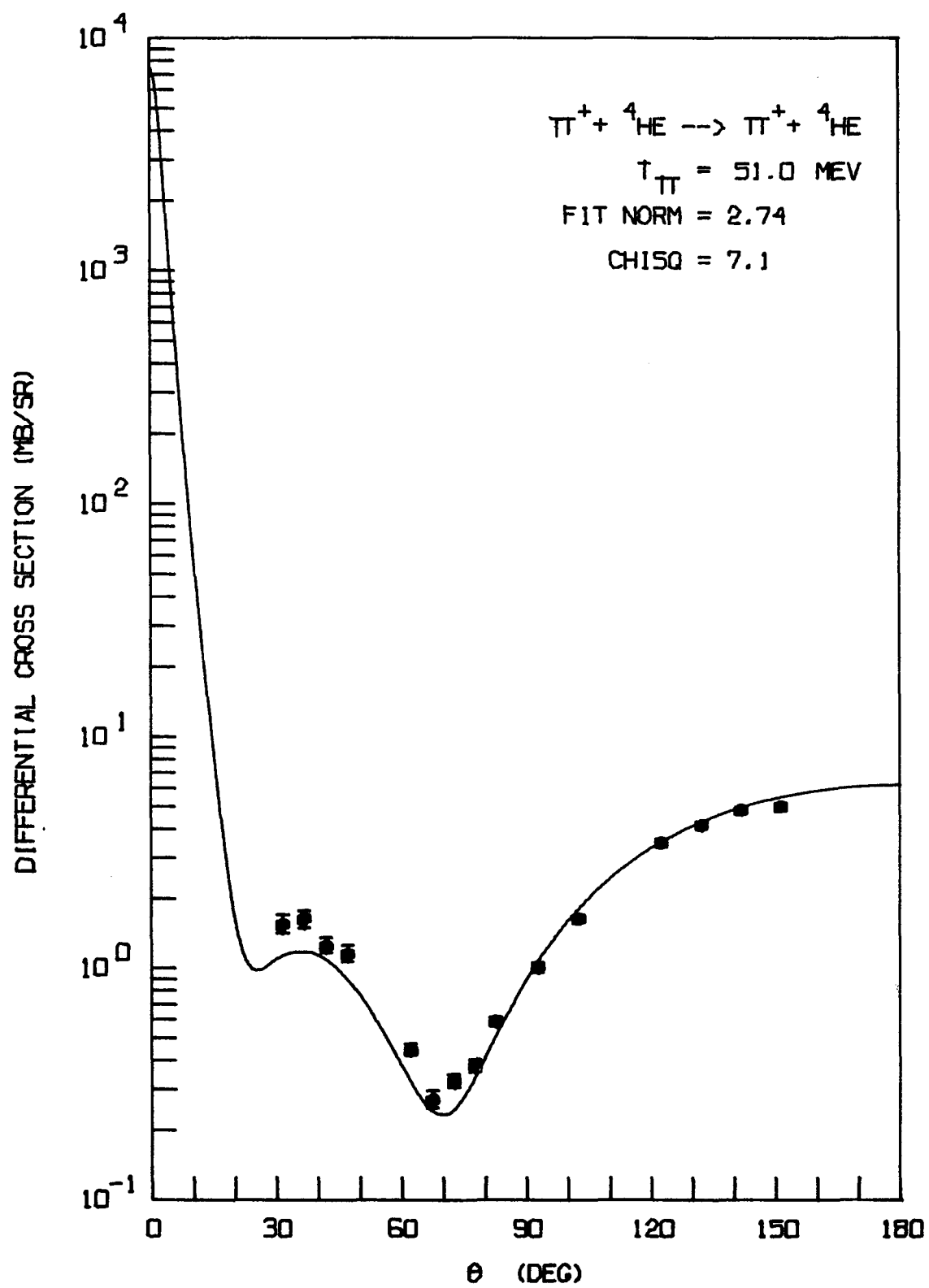


FIGURE 21.

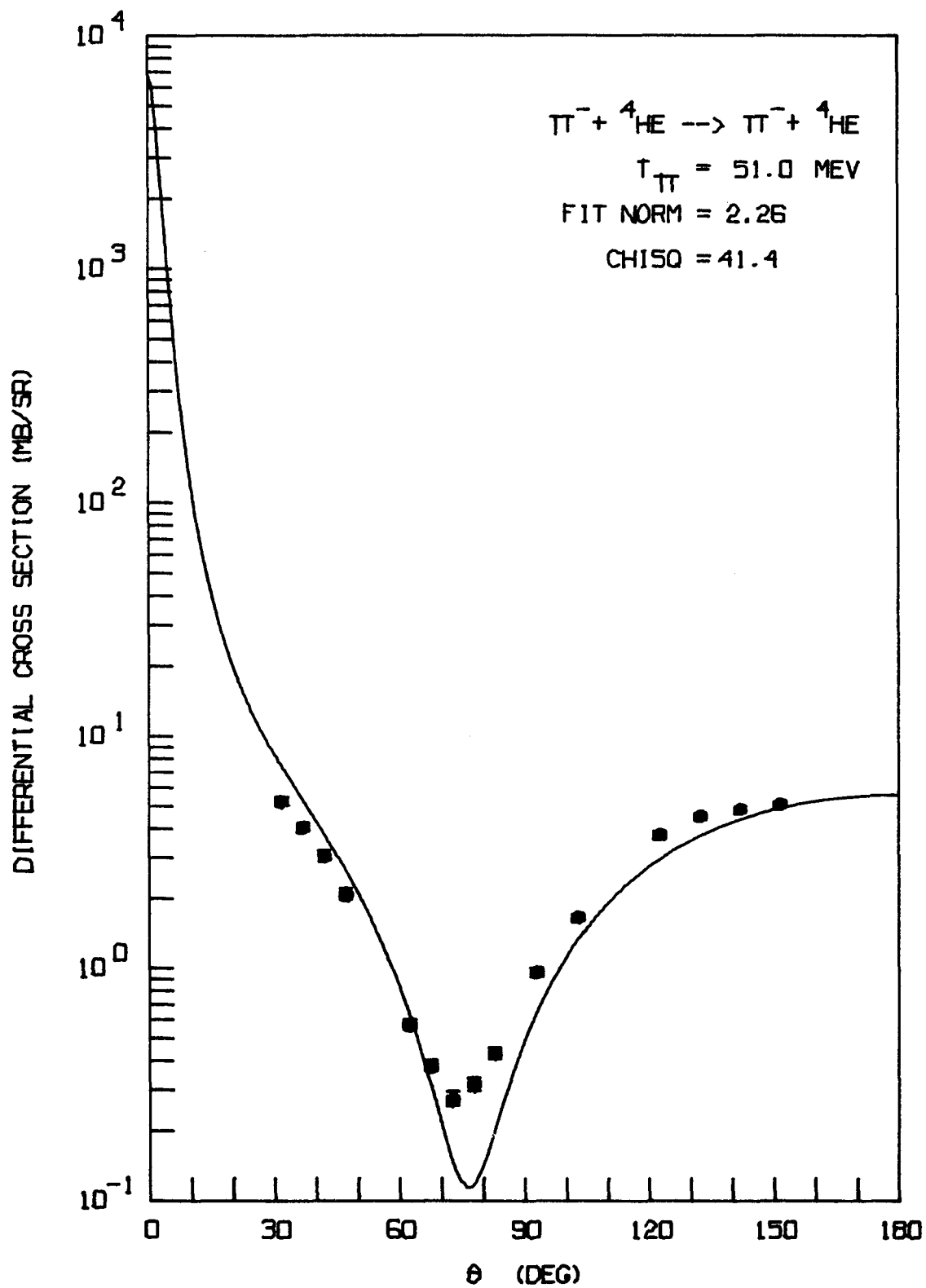


FIGURE 22.

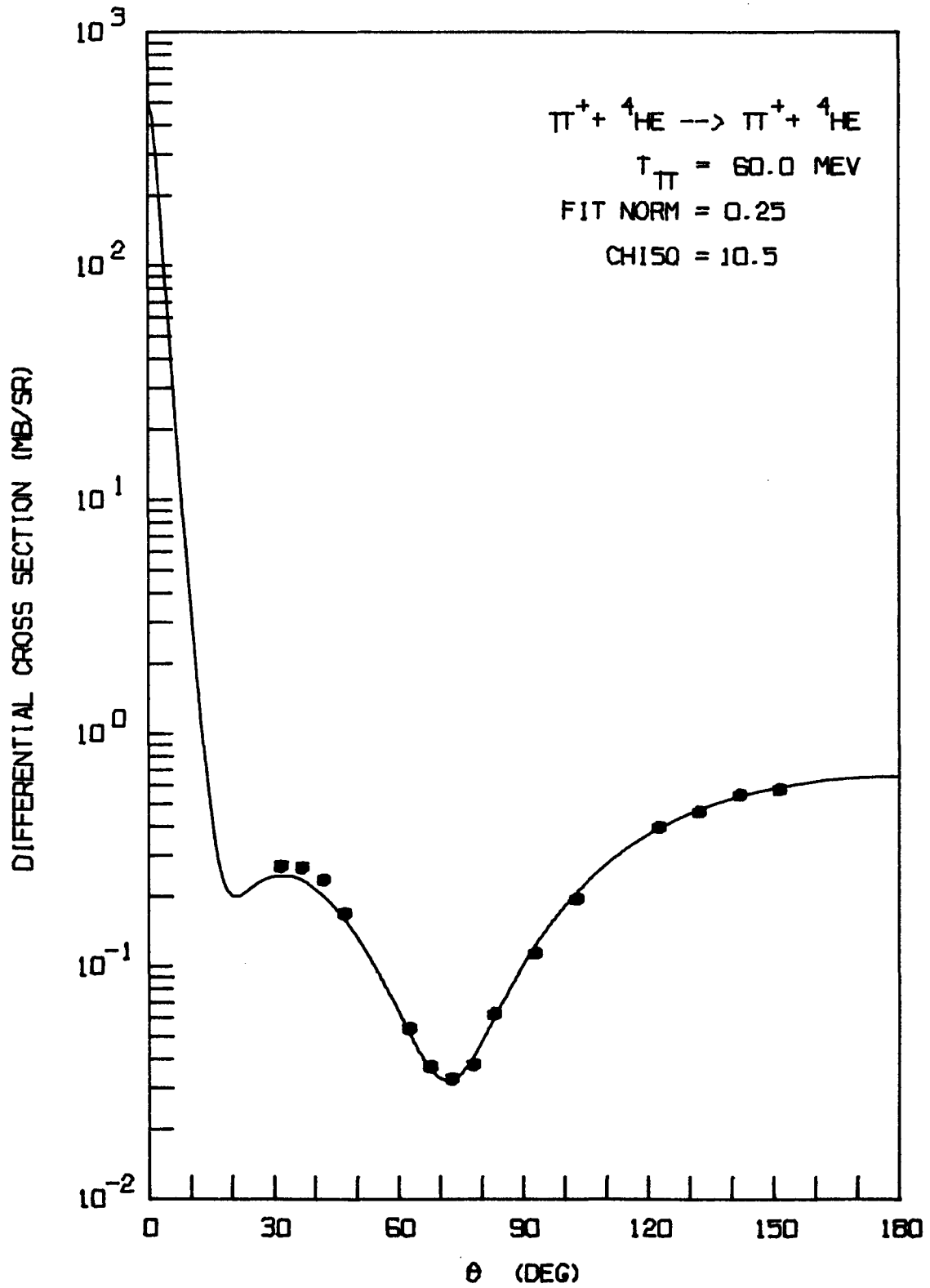


FIGURE 23.

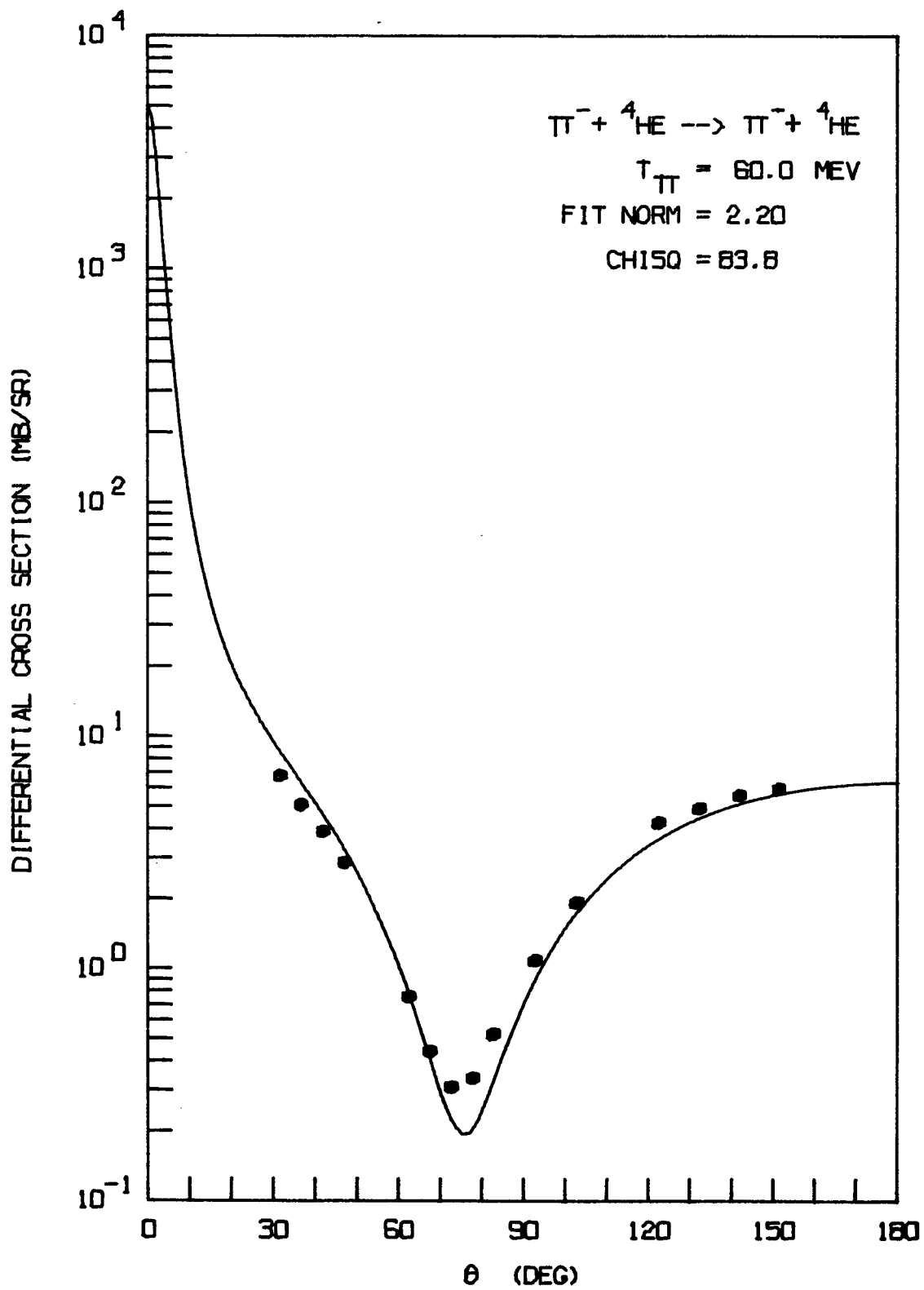


FIGURE 24.

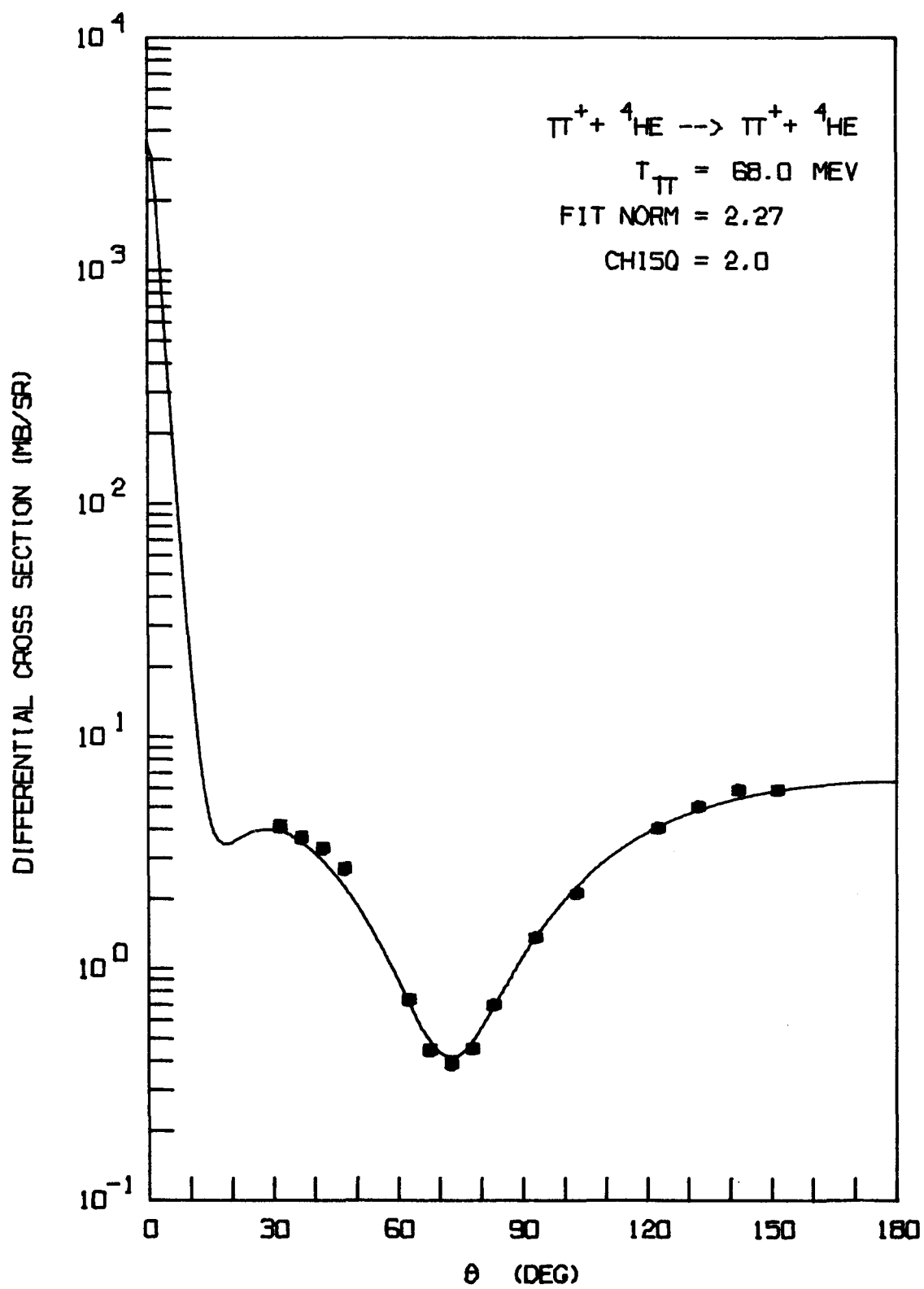


FIGURE 25.

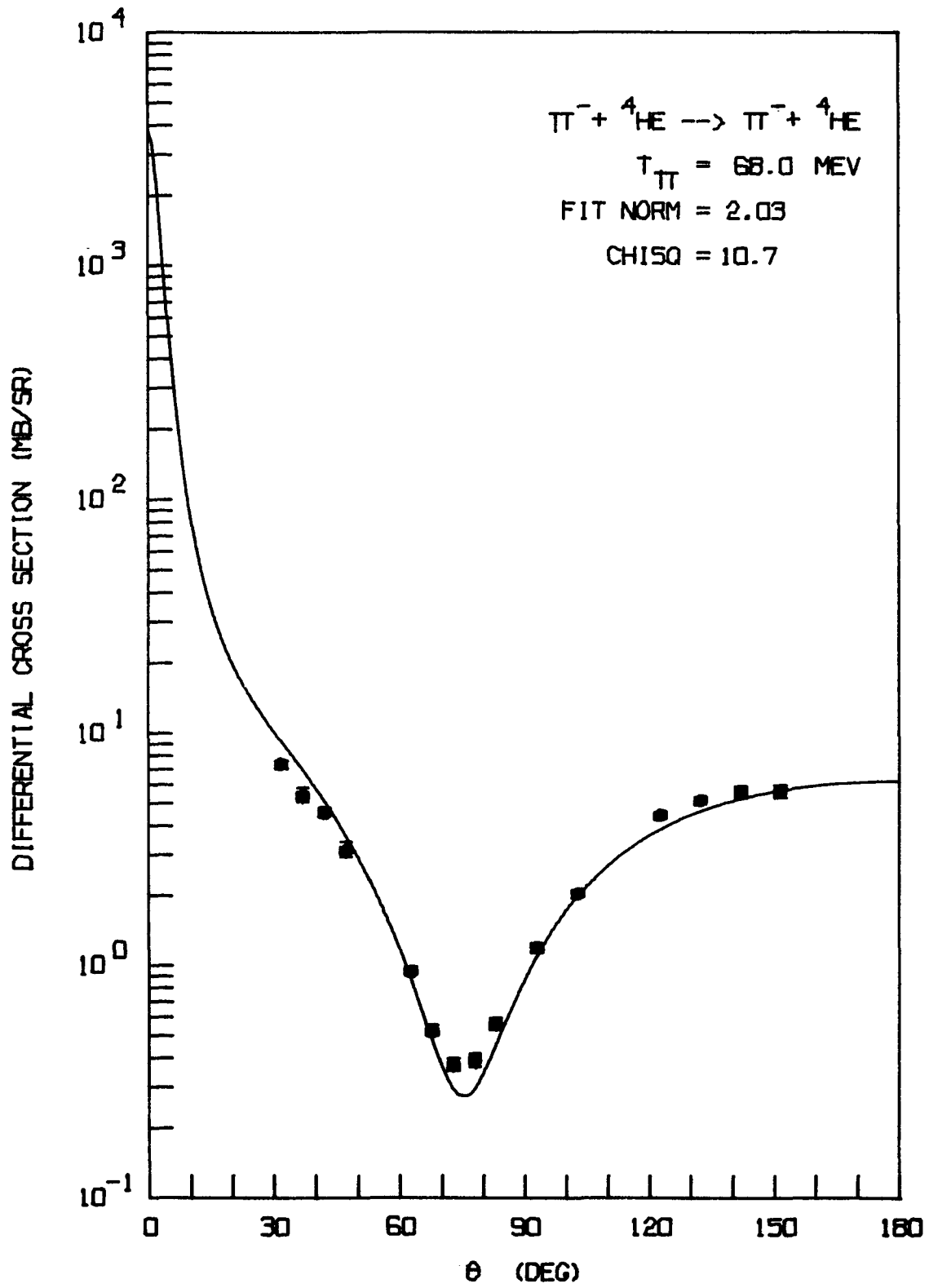


FIGURE 26.

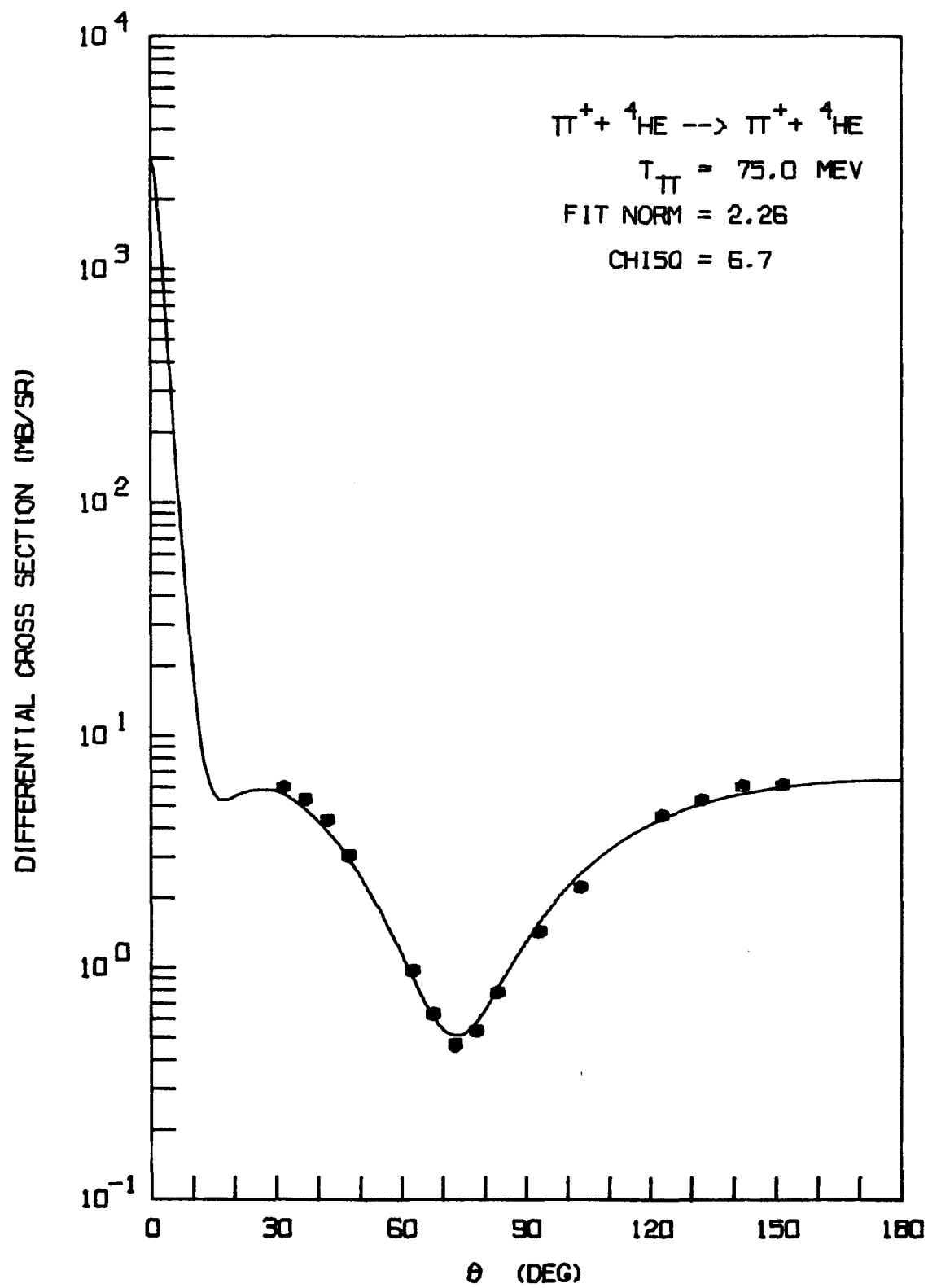


FIGURE 27.

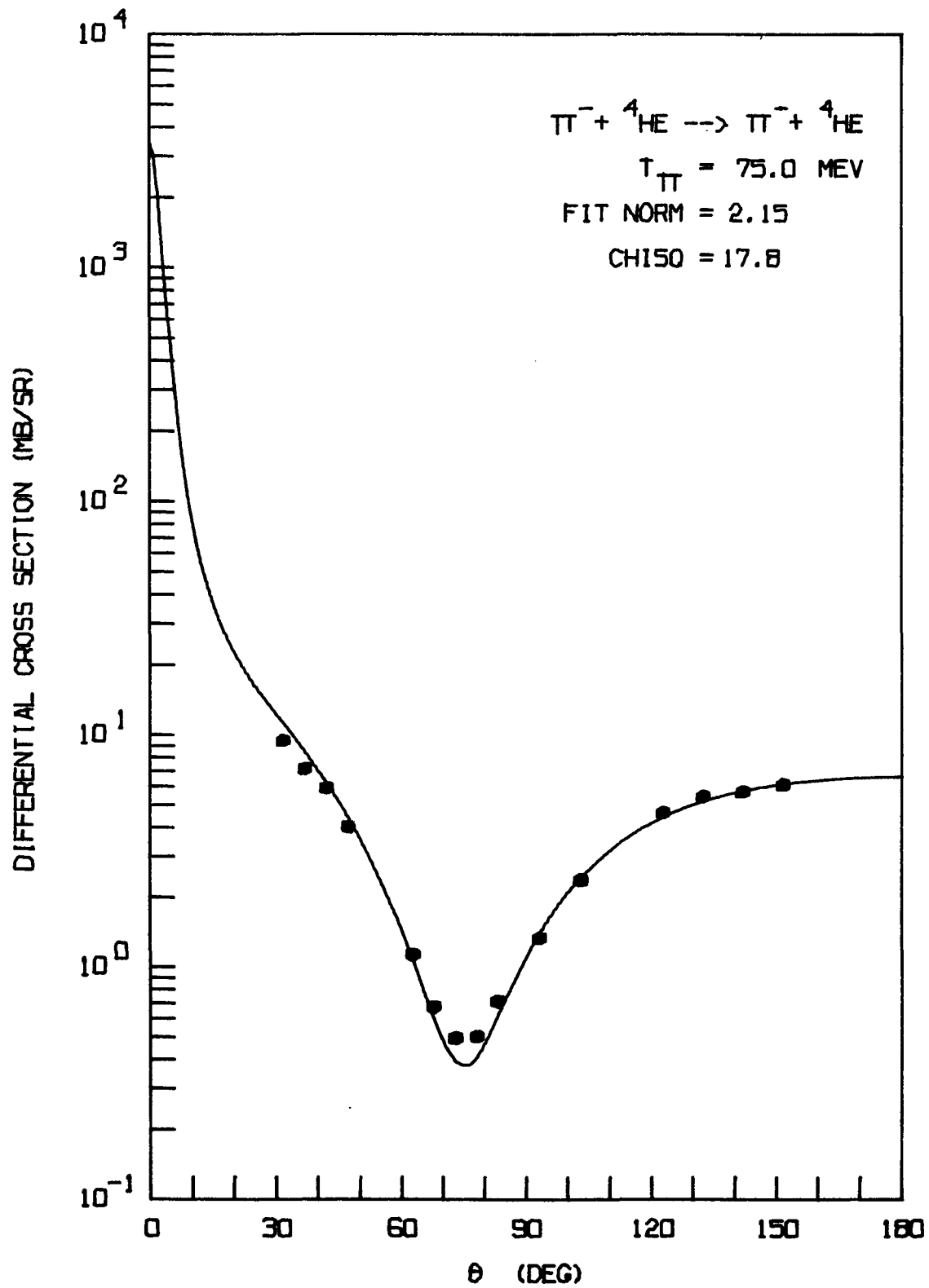


FIGURE 28.

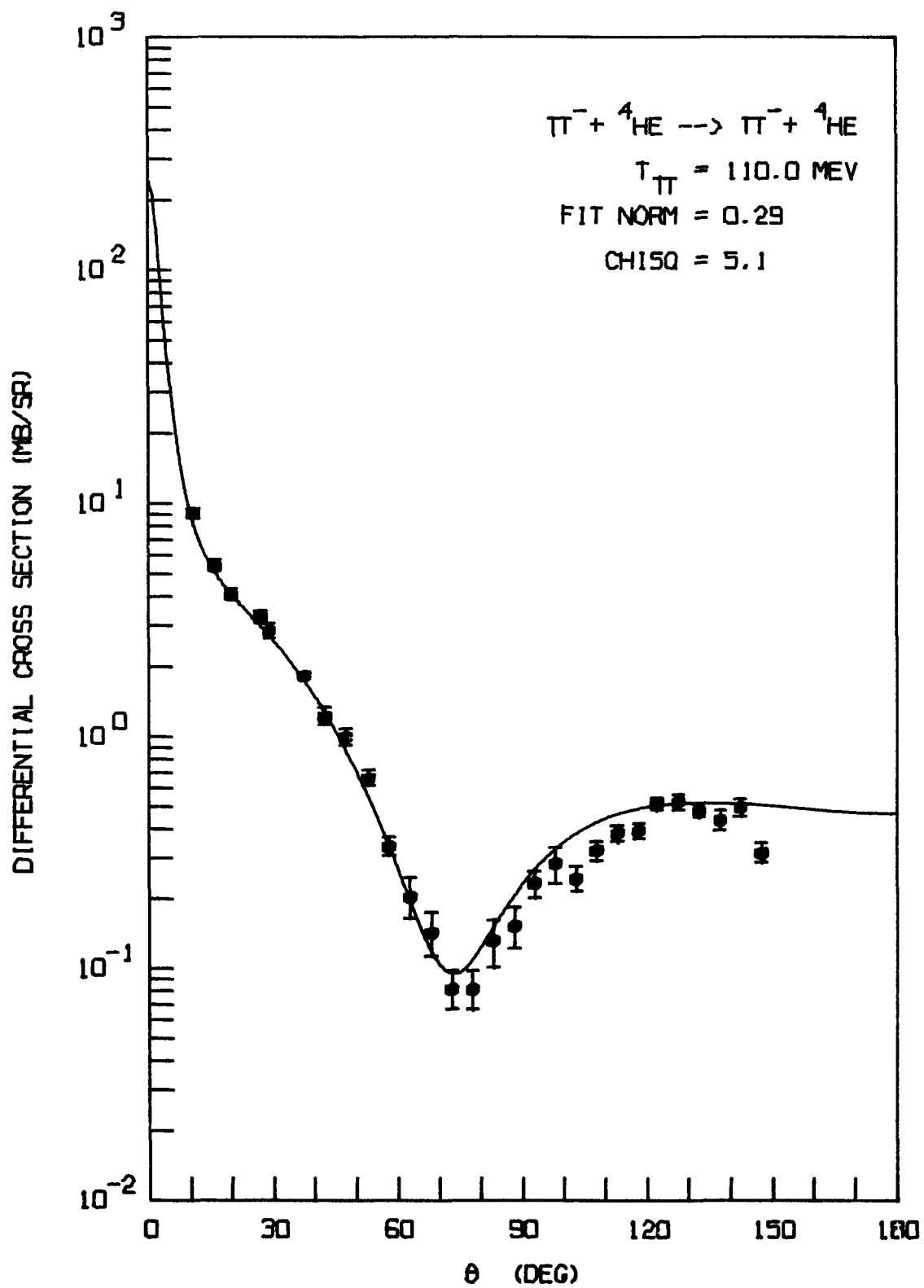


FIGURE 29.

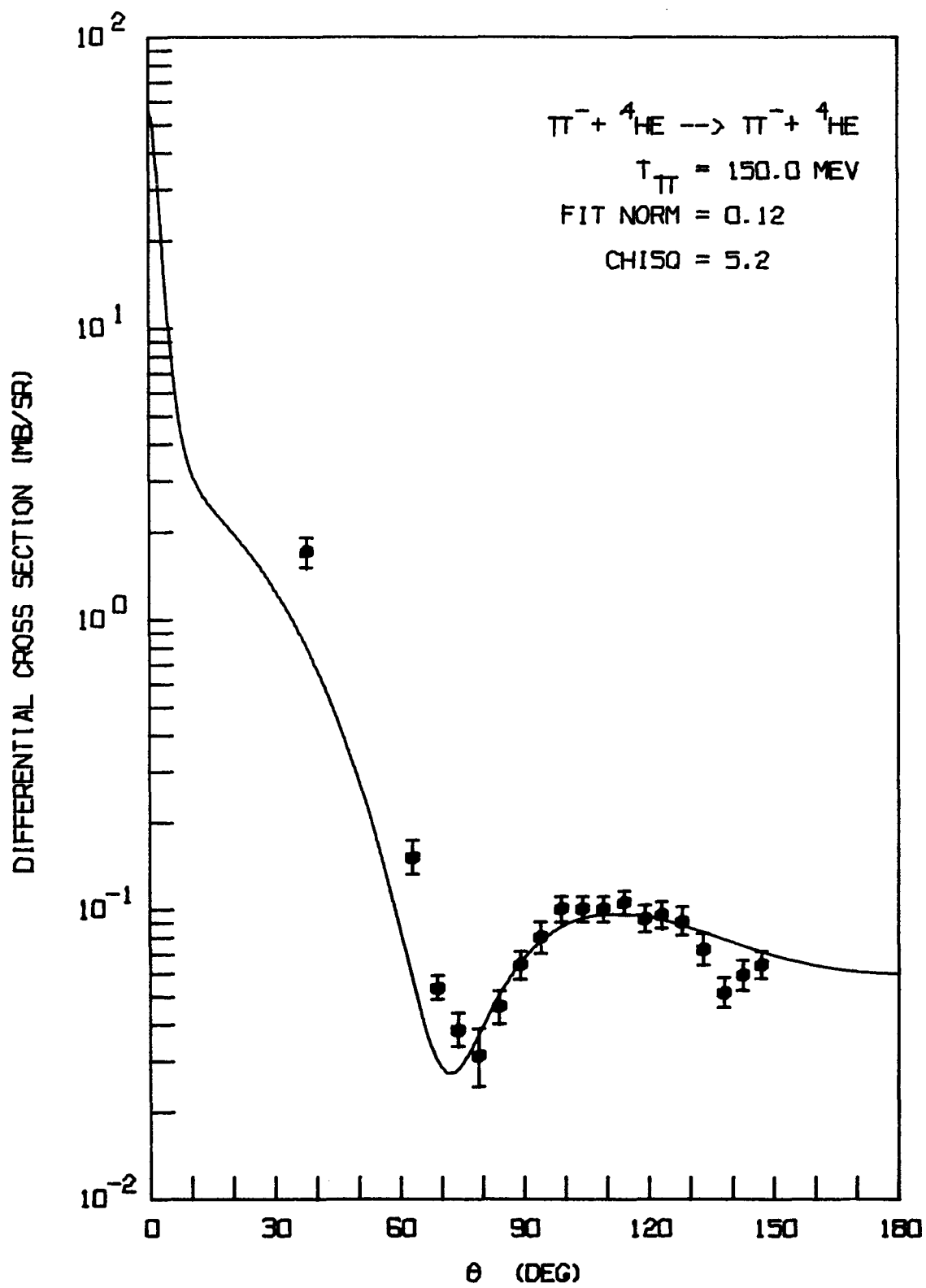


FIGURE 30.

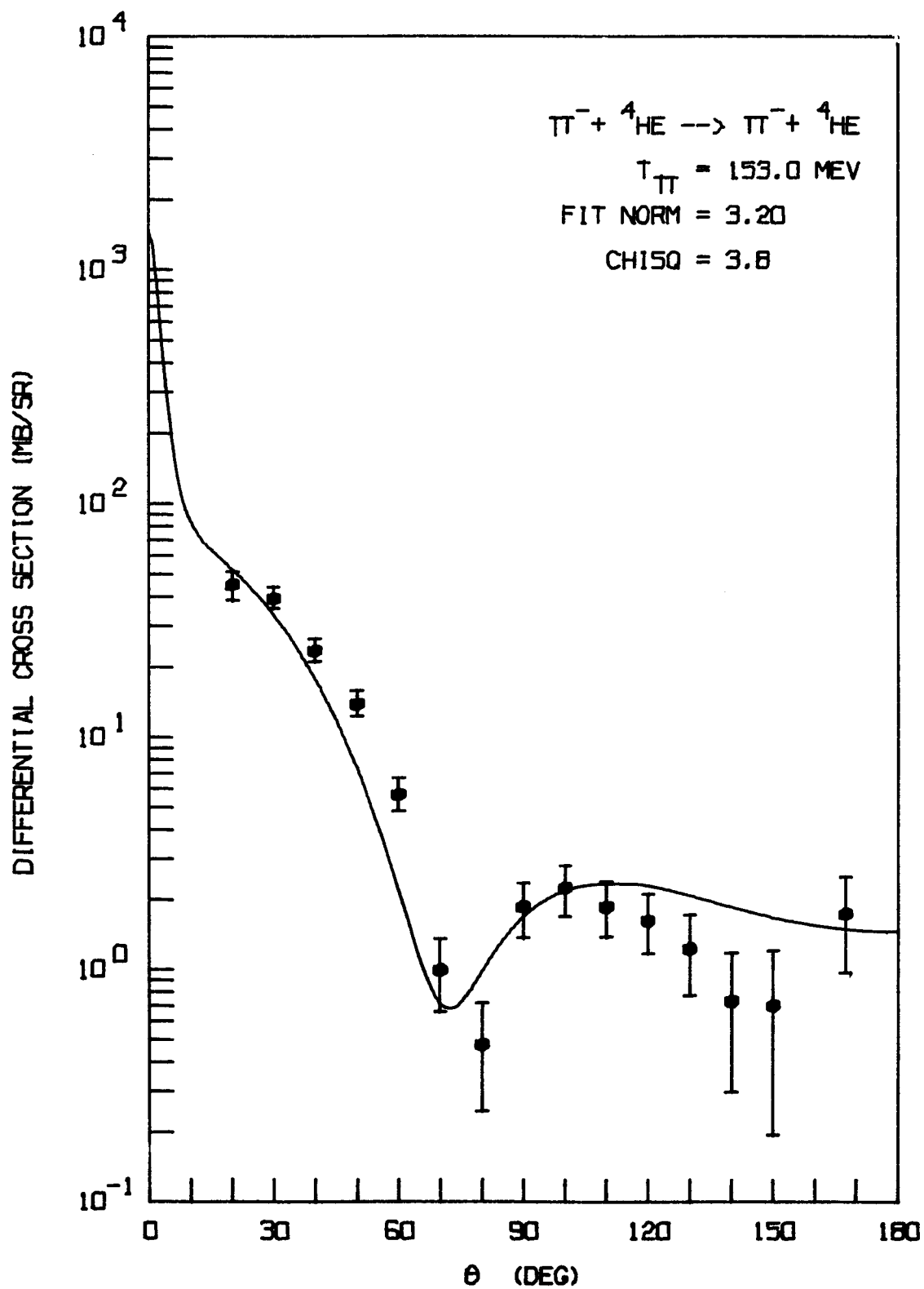


FIGURE 31.

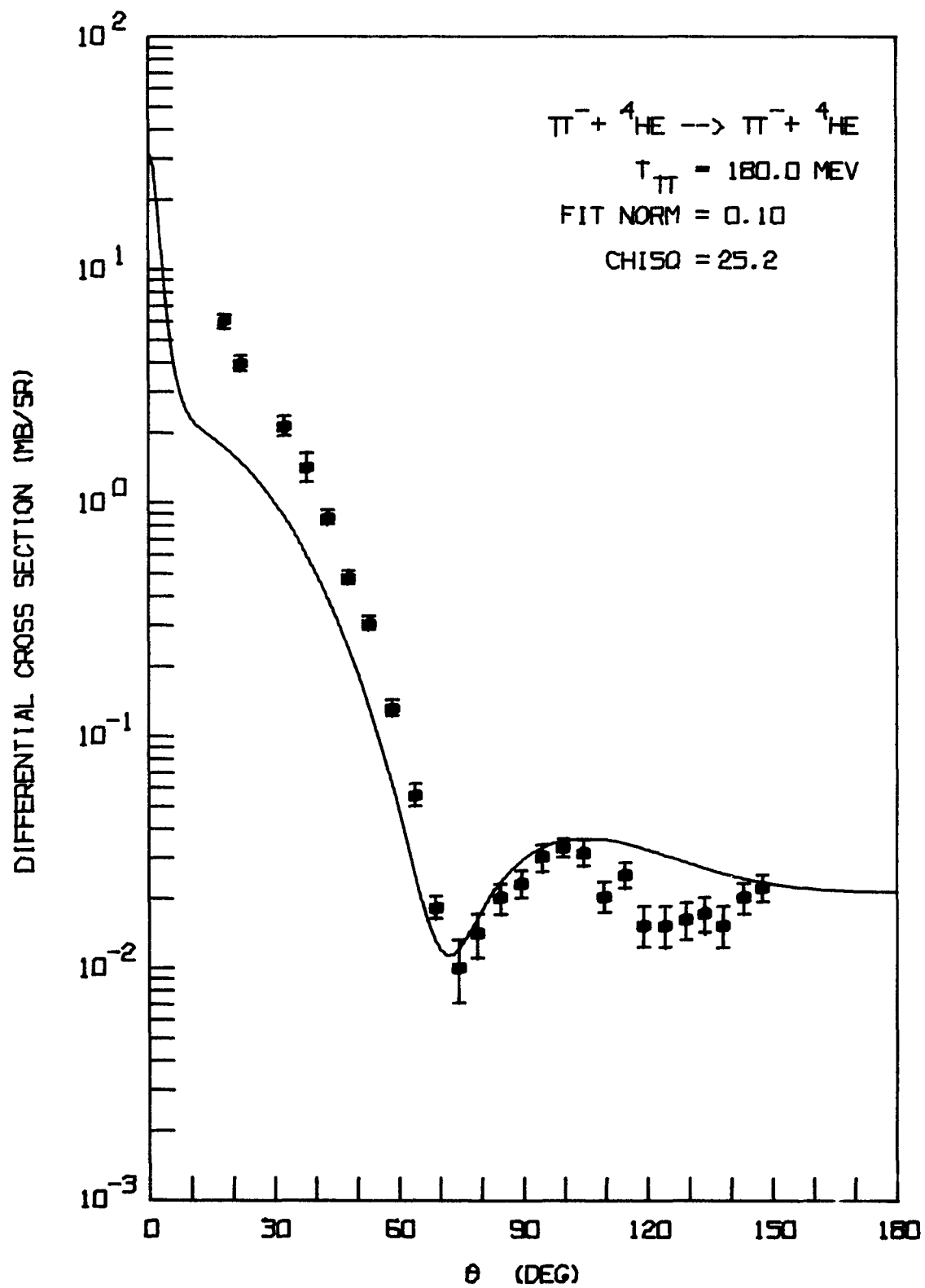


FIGURE 32.

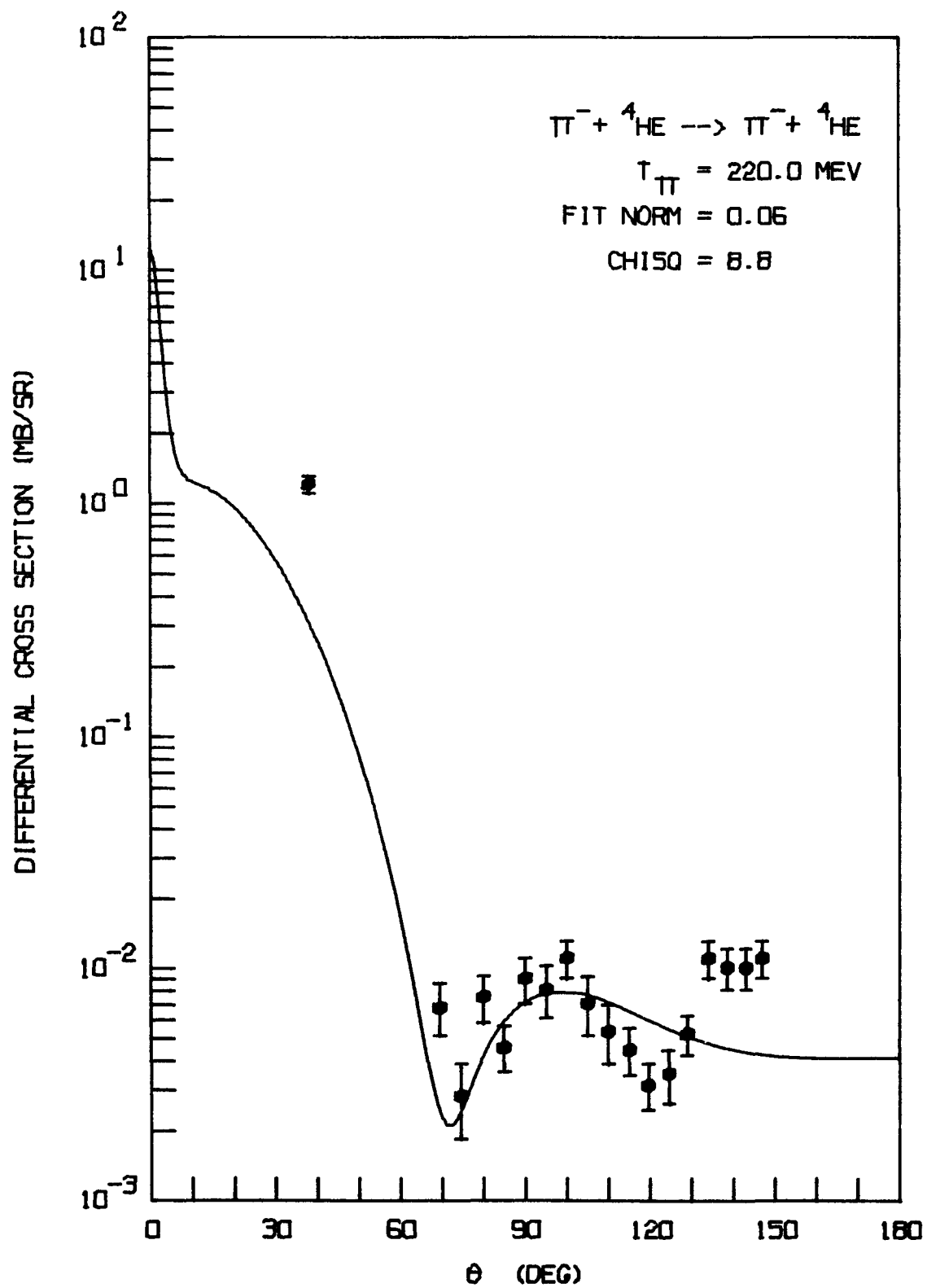


FIGURE 33.

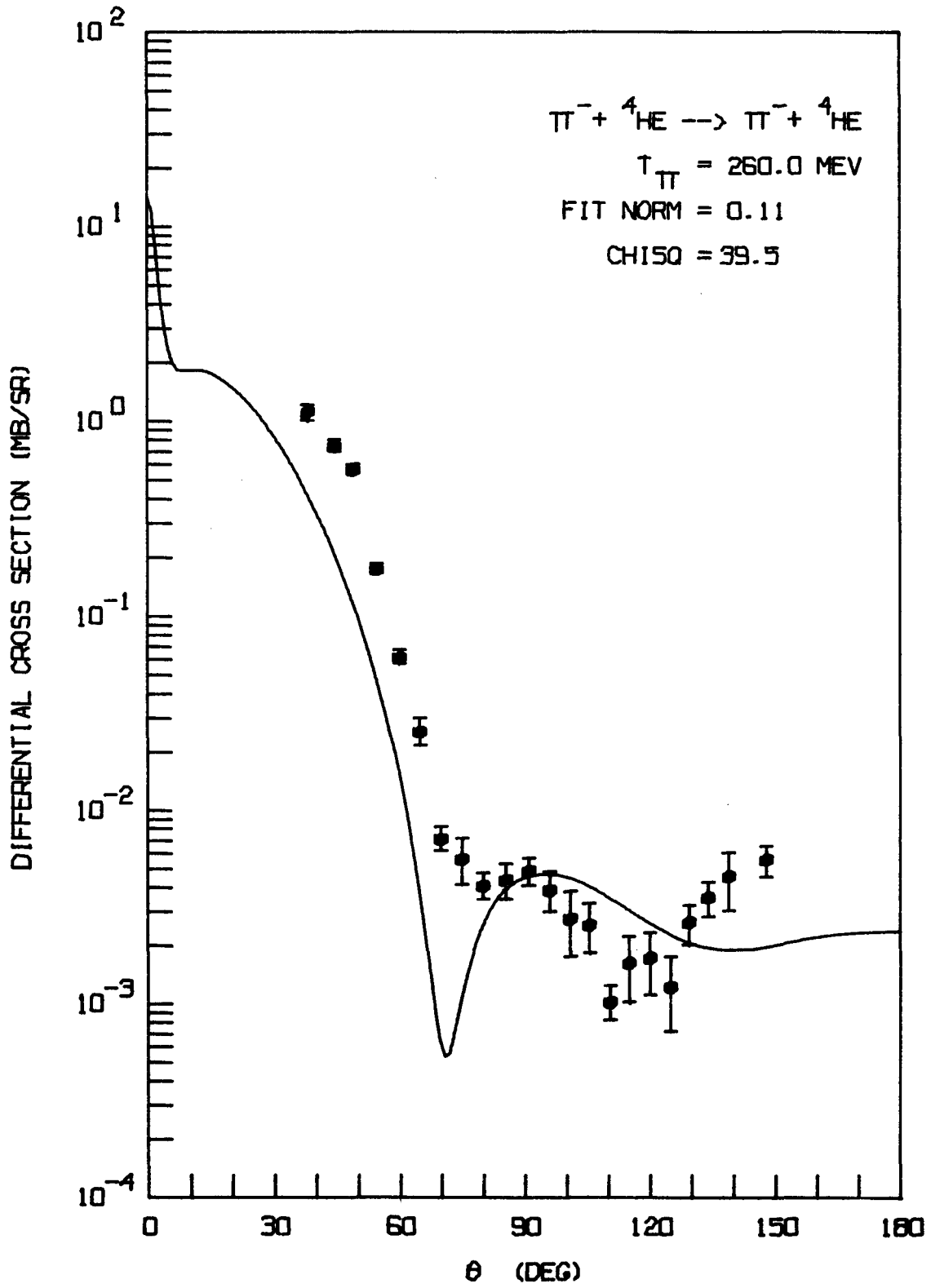


FIGURE 34.

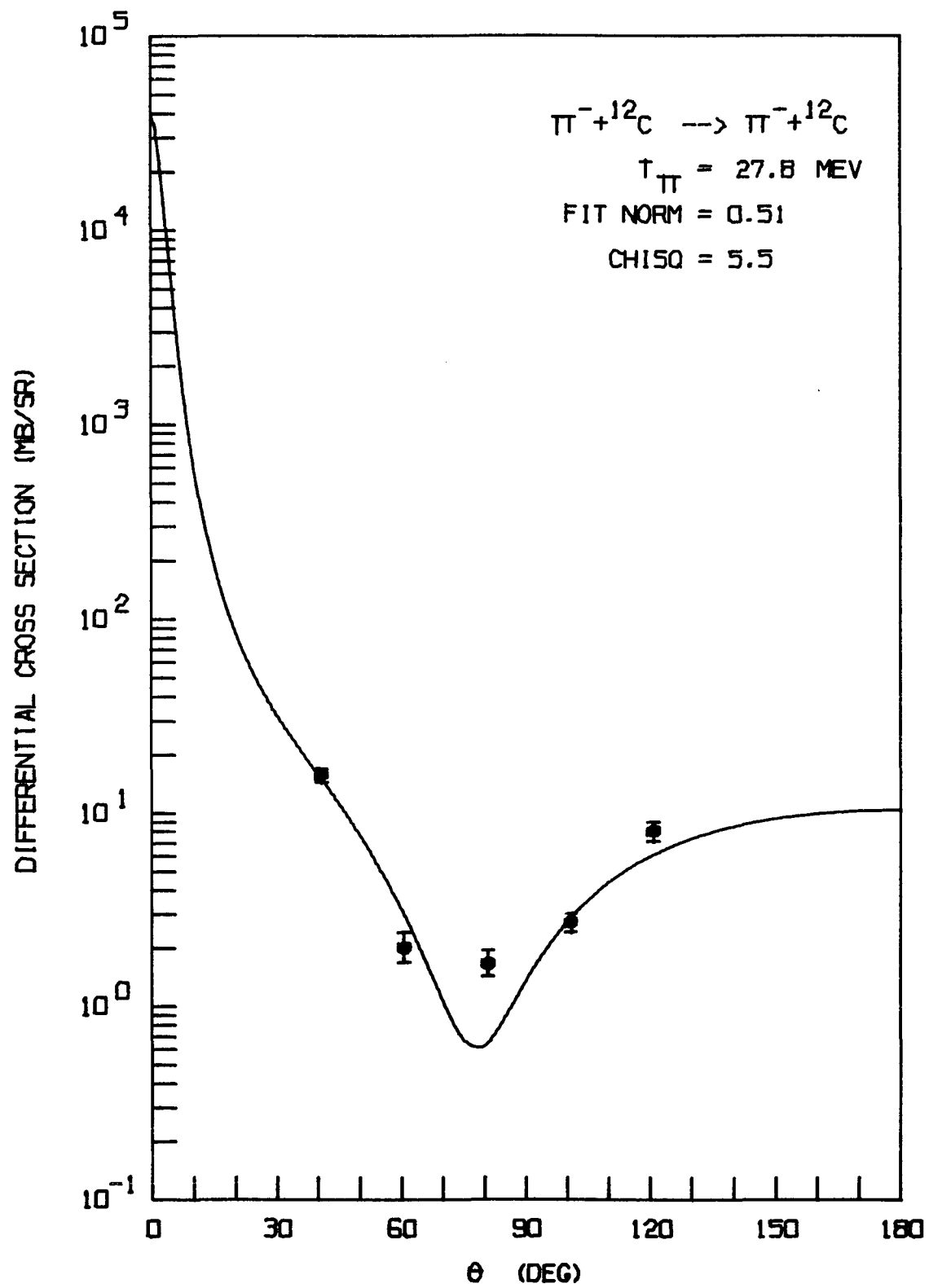


FIGURE 35.

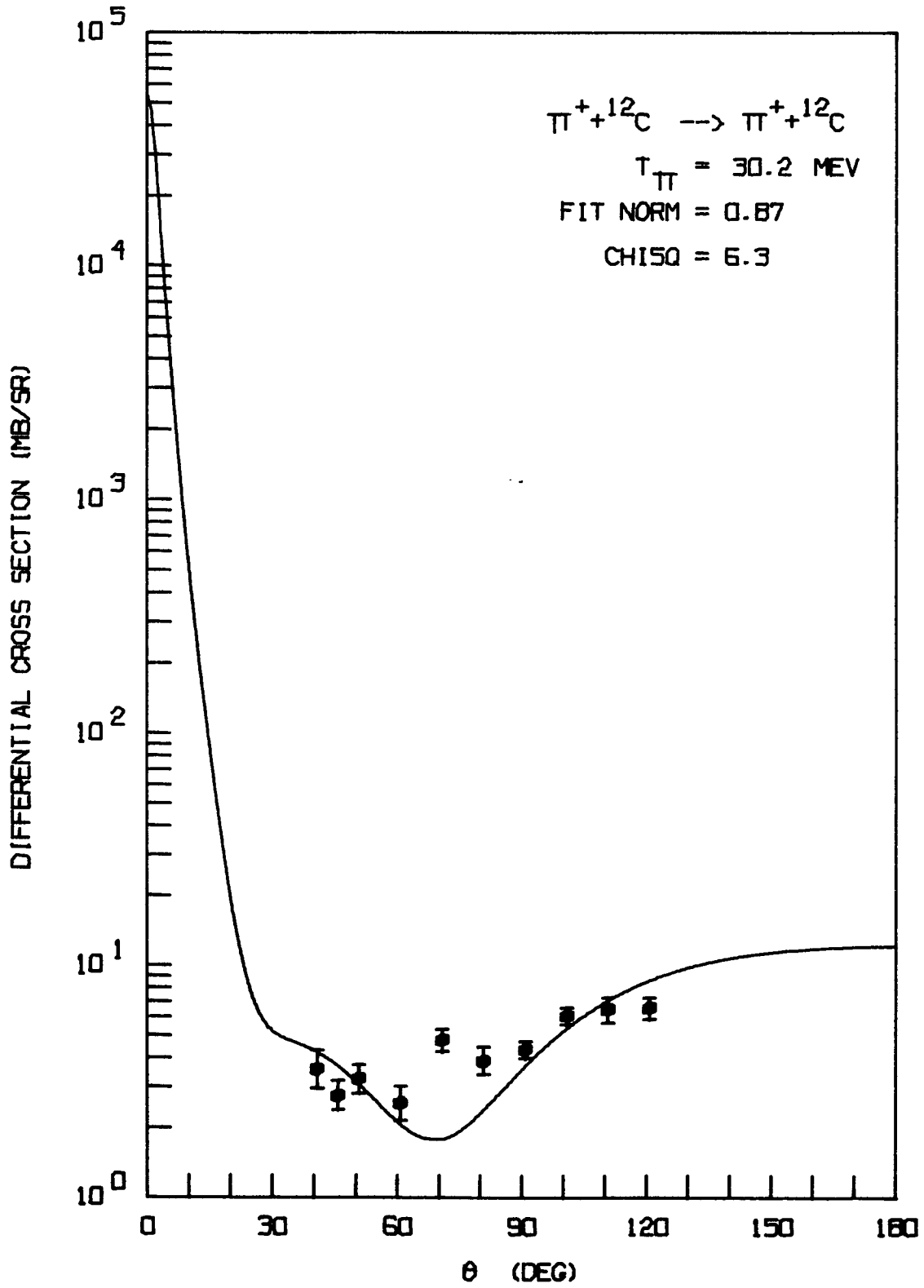


FIGURE 36.

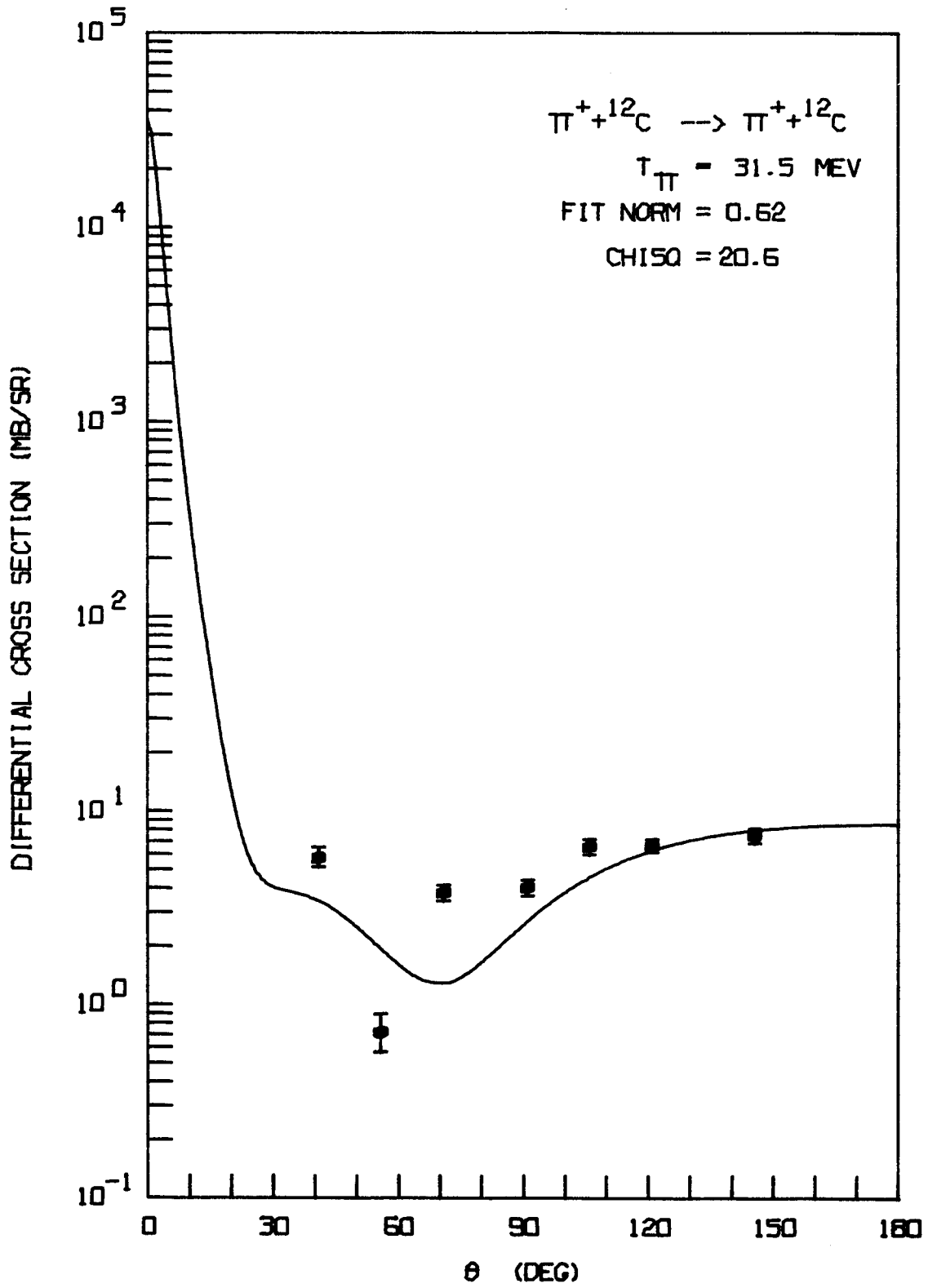


FIGURE 37.

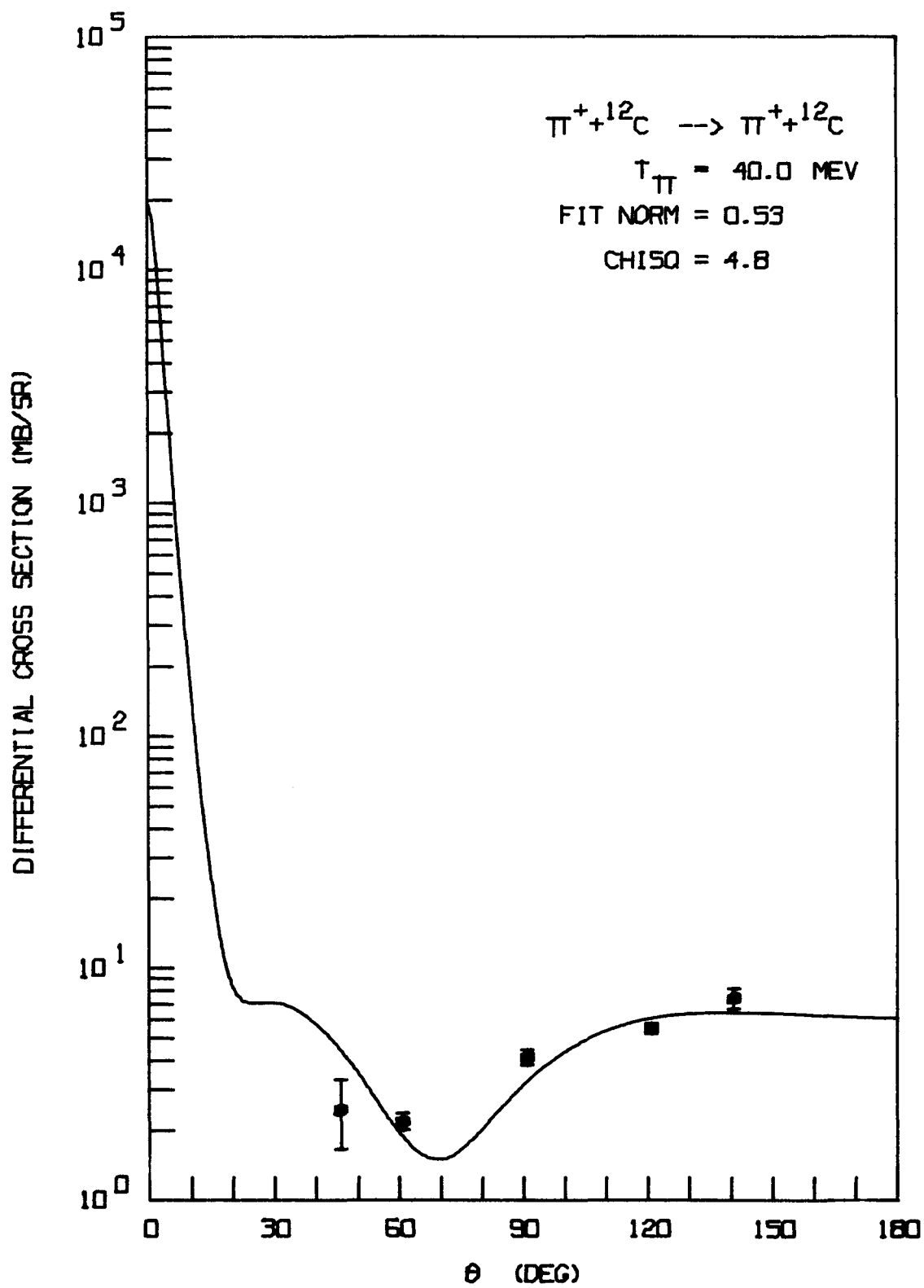


FIGURE 38.

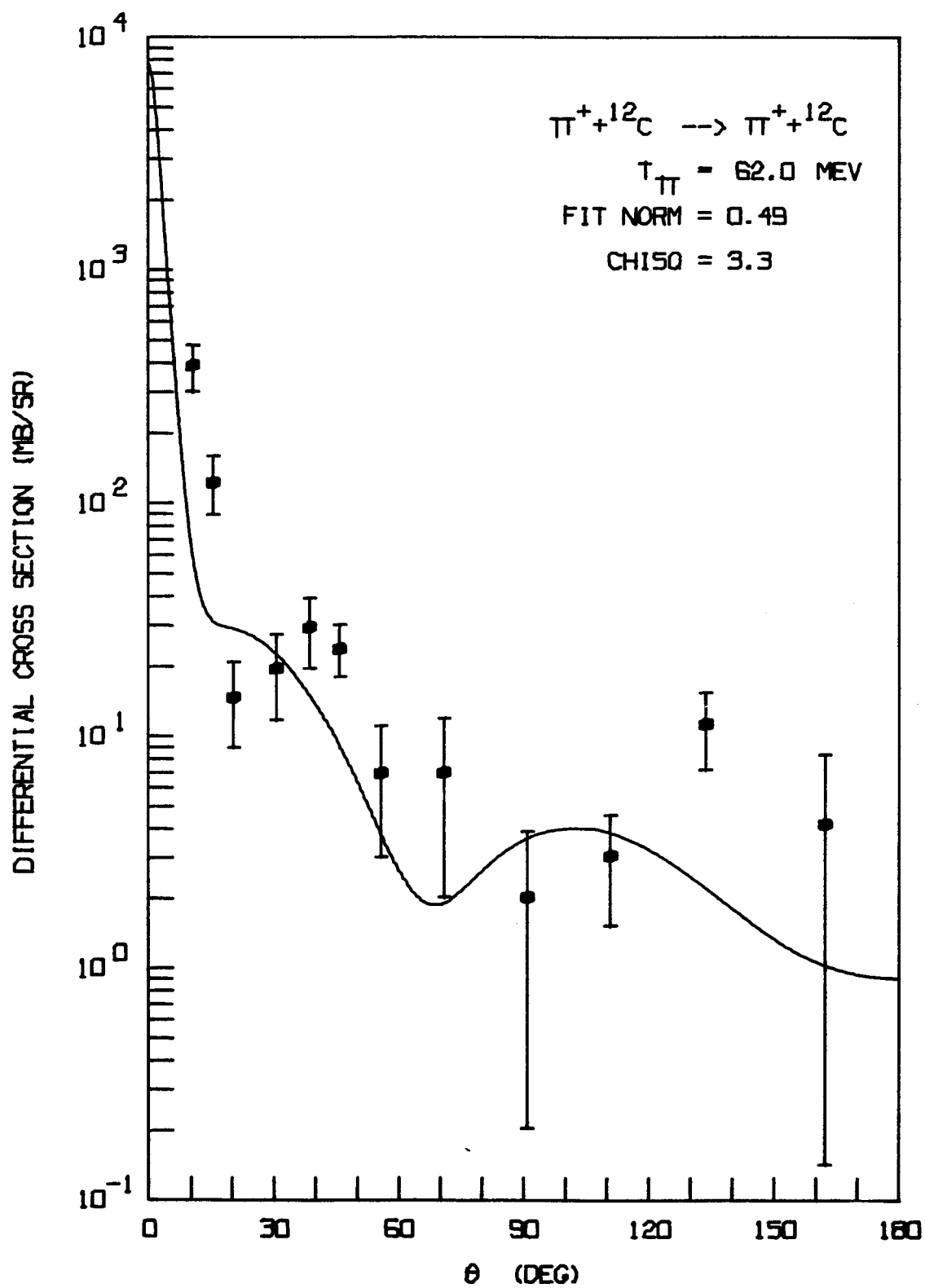


FIGURE 39.

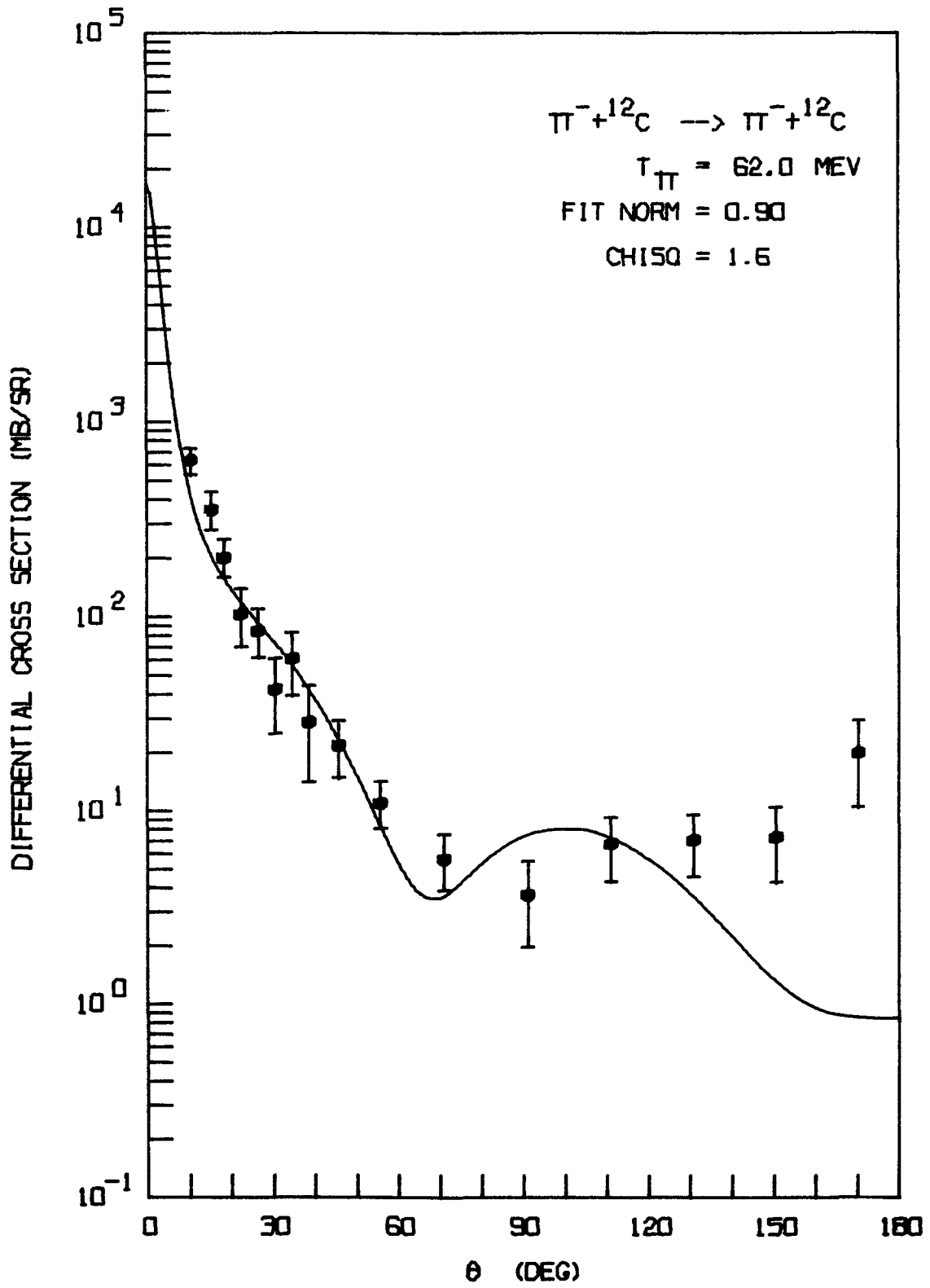


FIGURE 40.

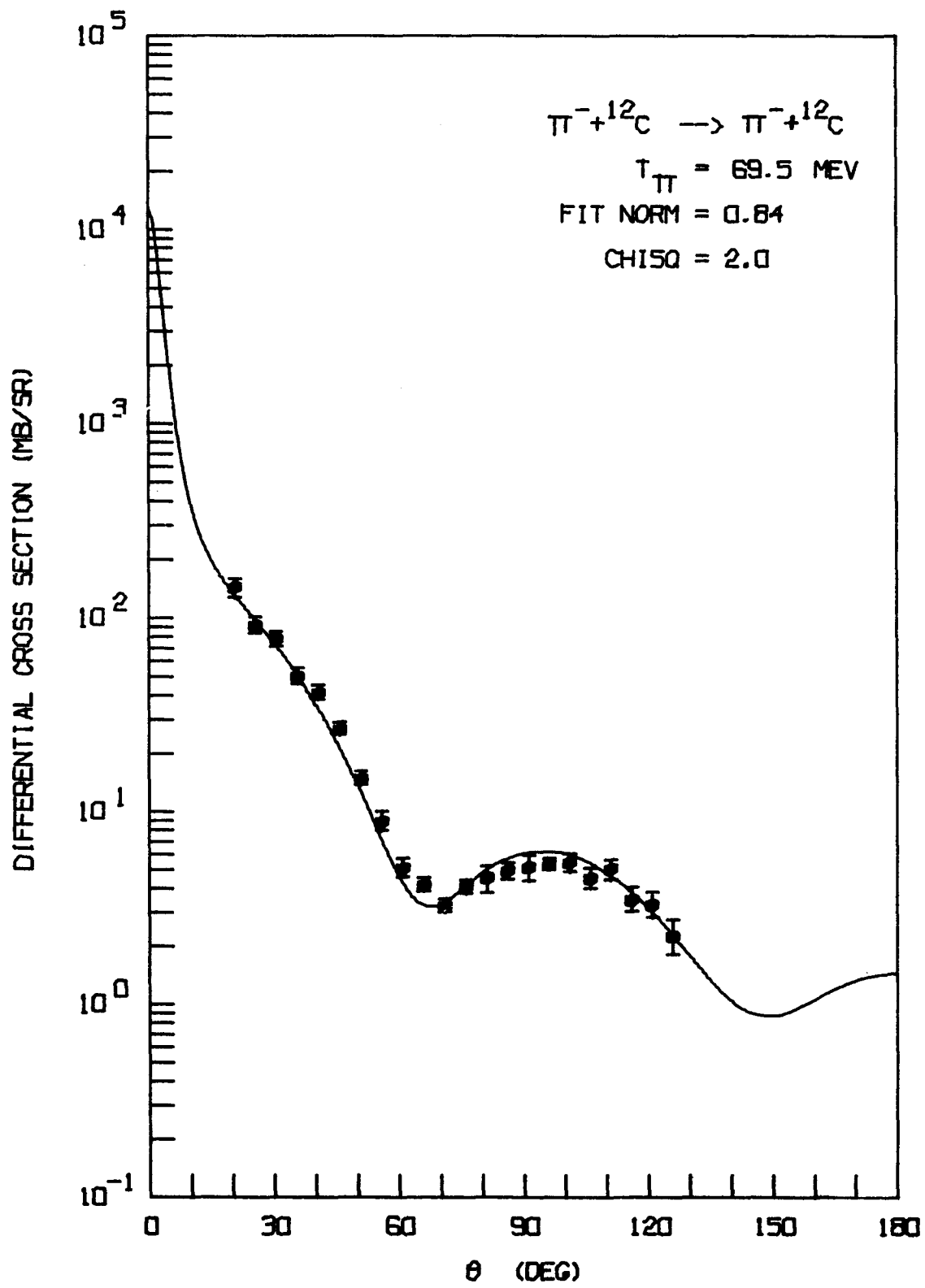


FIGURE 41.

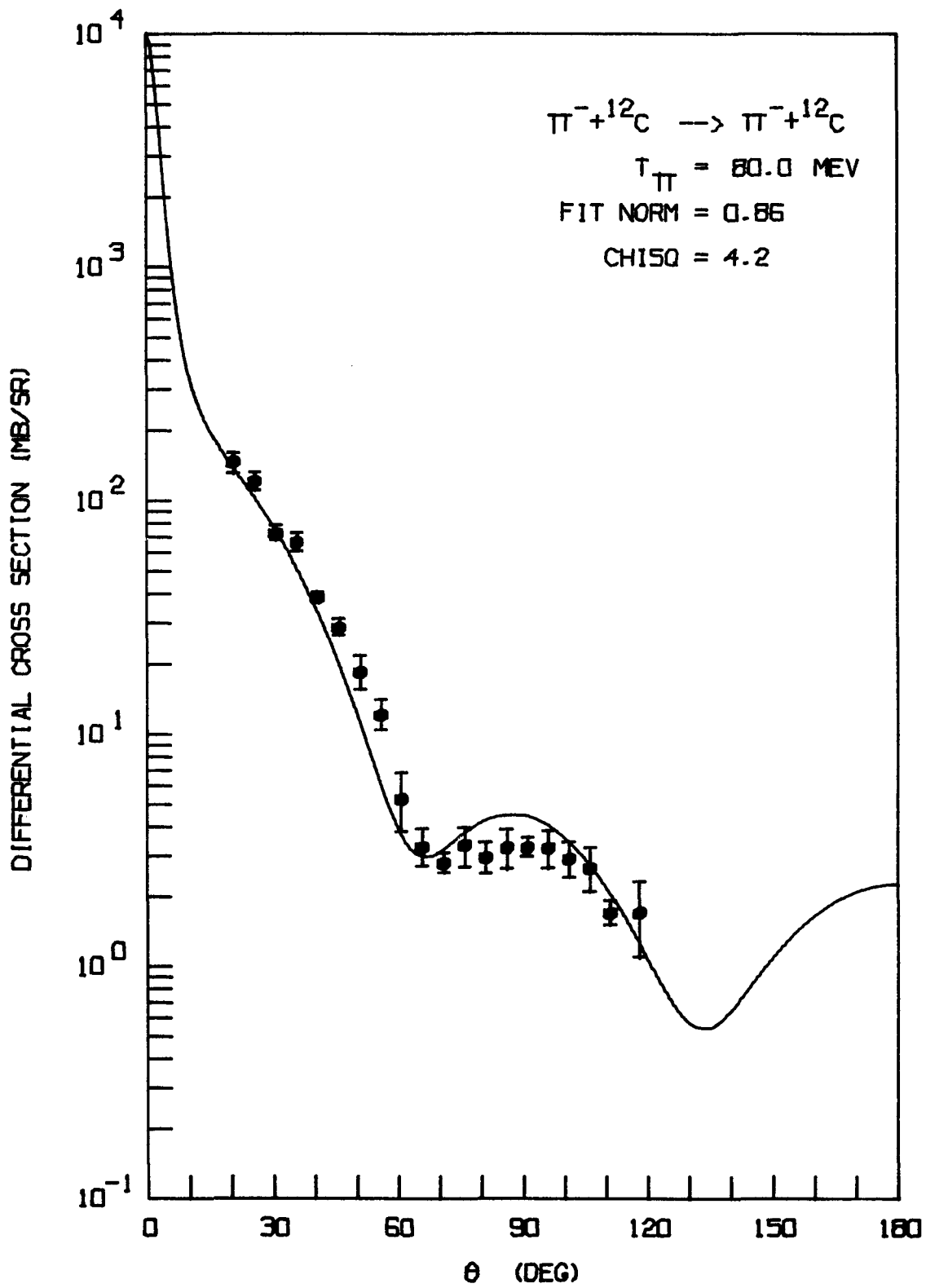


FIGURE 42.

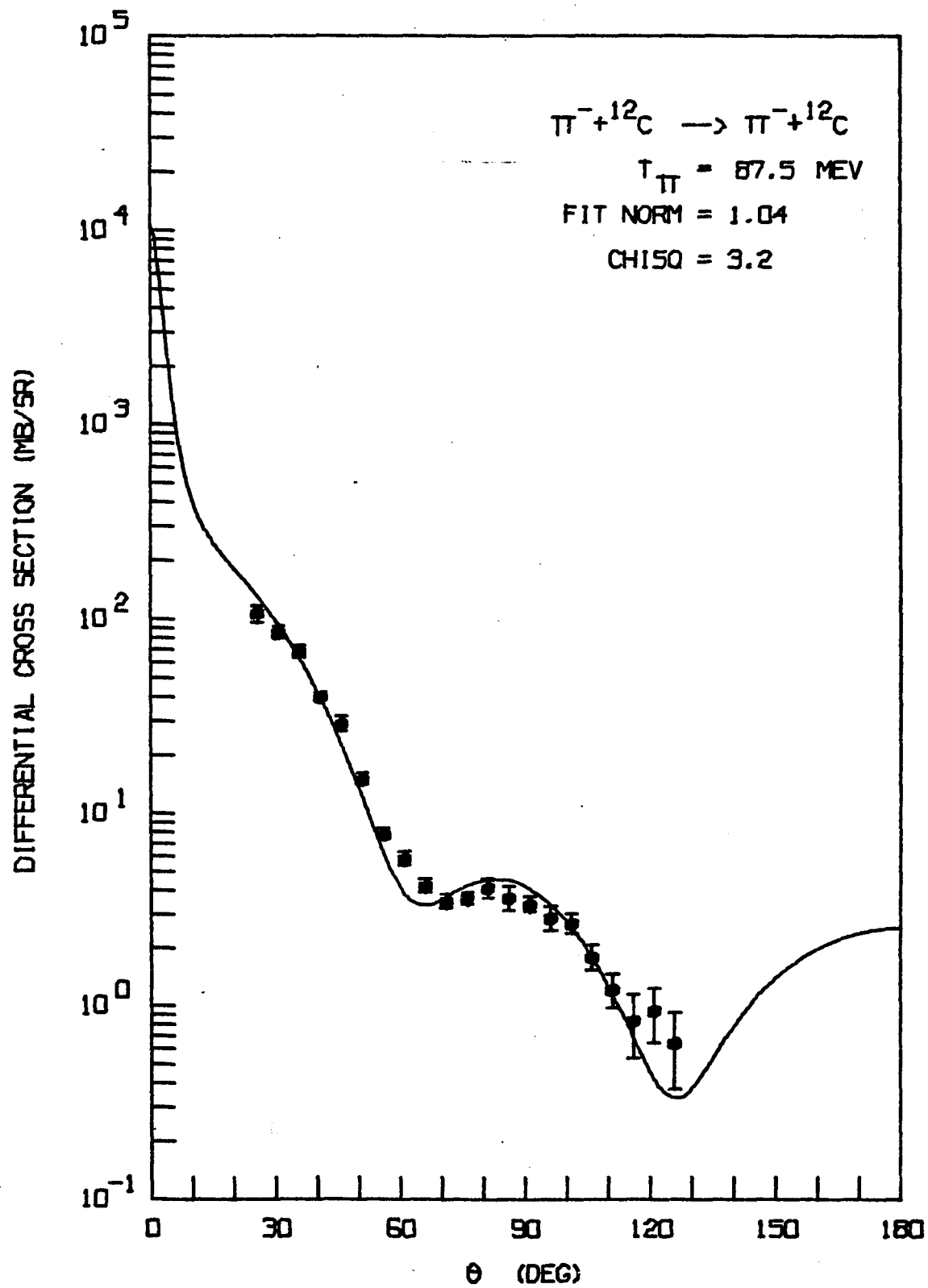


FIGURE 43.

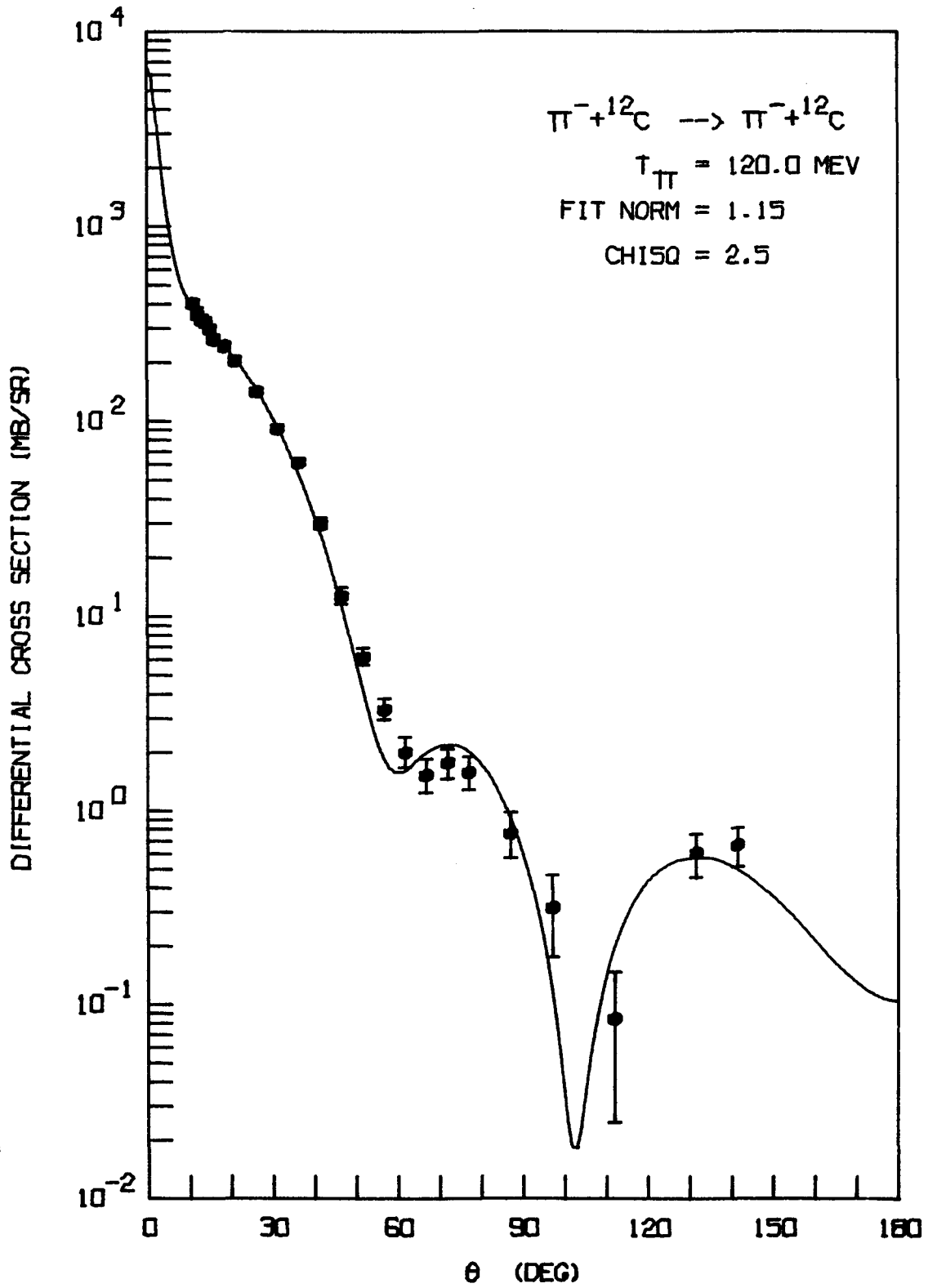


FIGURE 44.

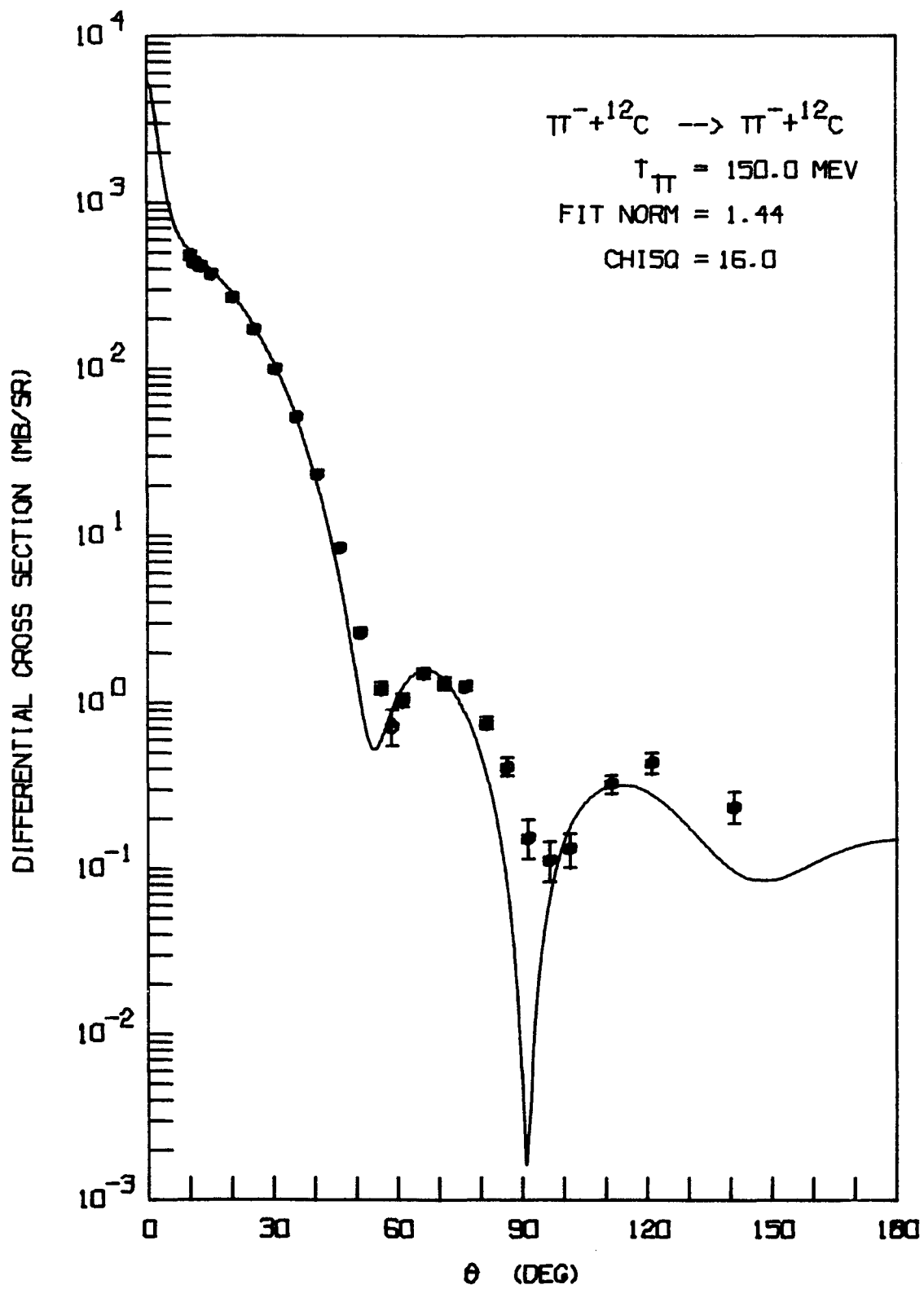


FIGURE 45.

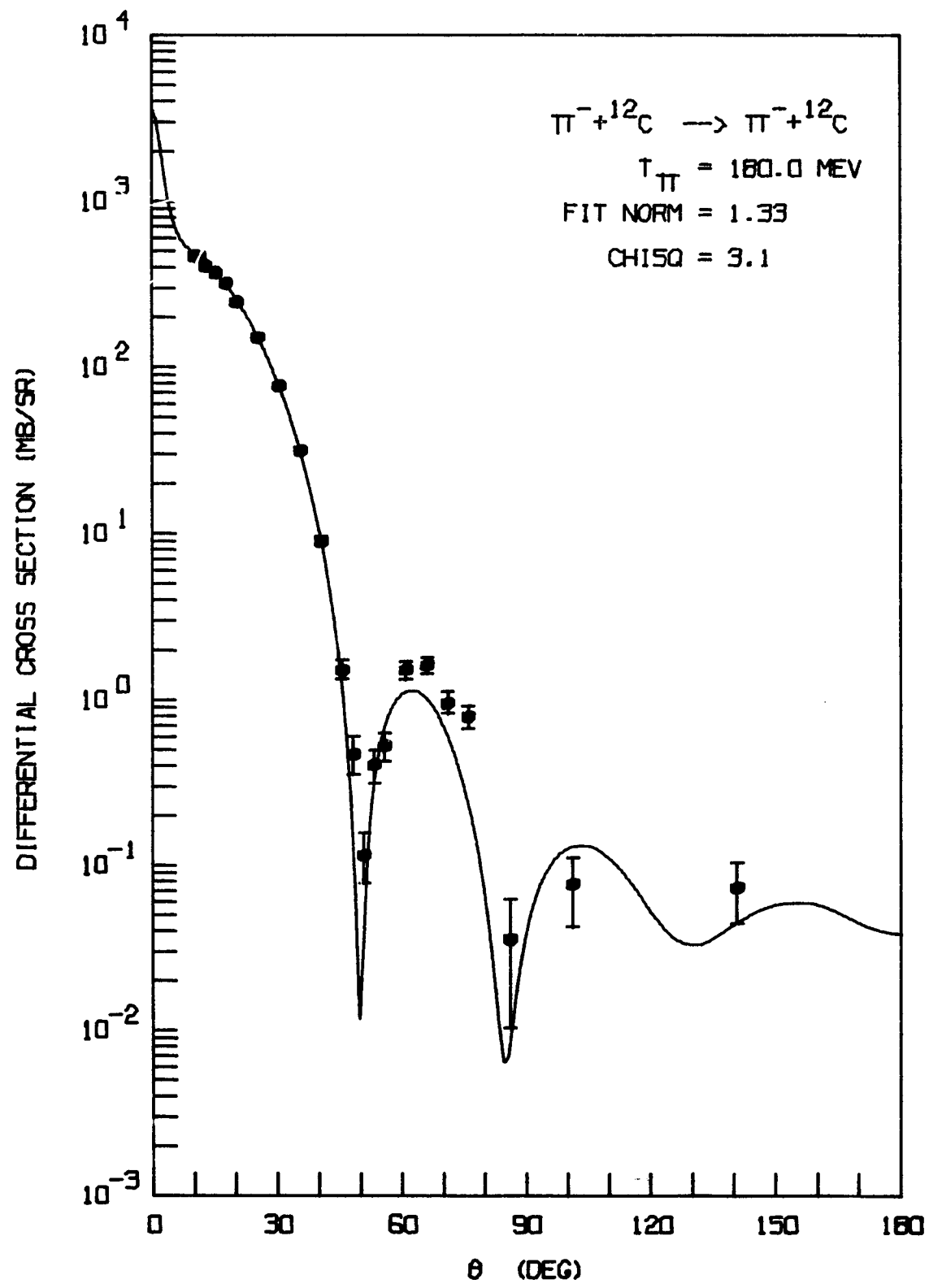


FIGURE 45.

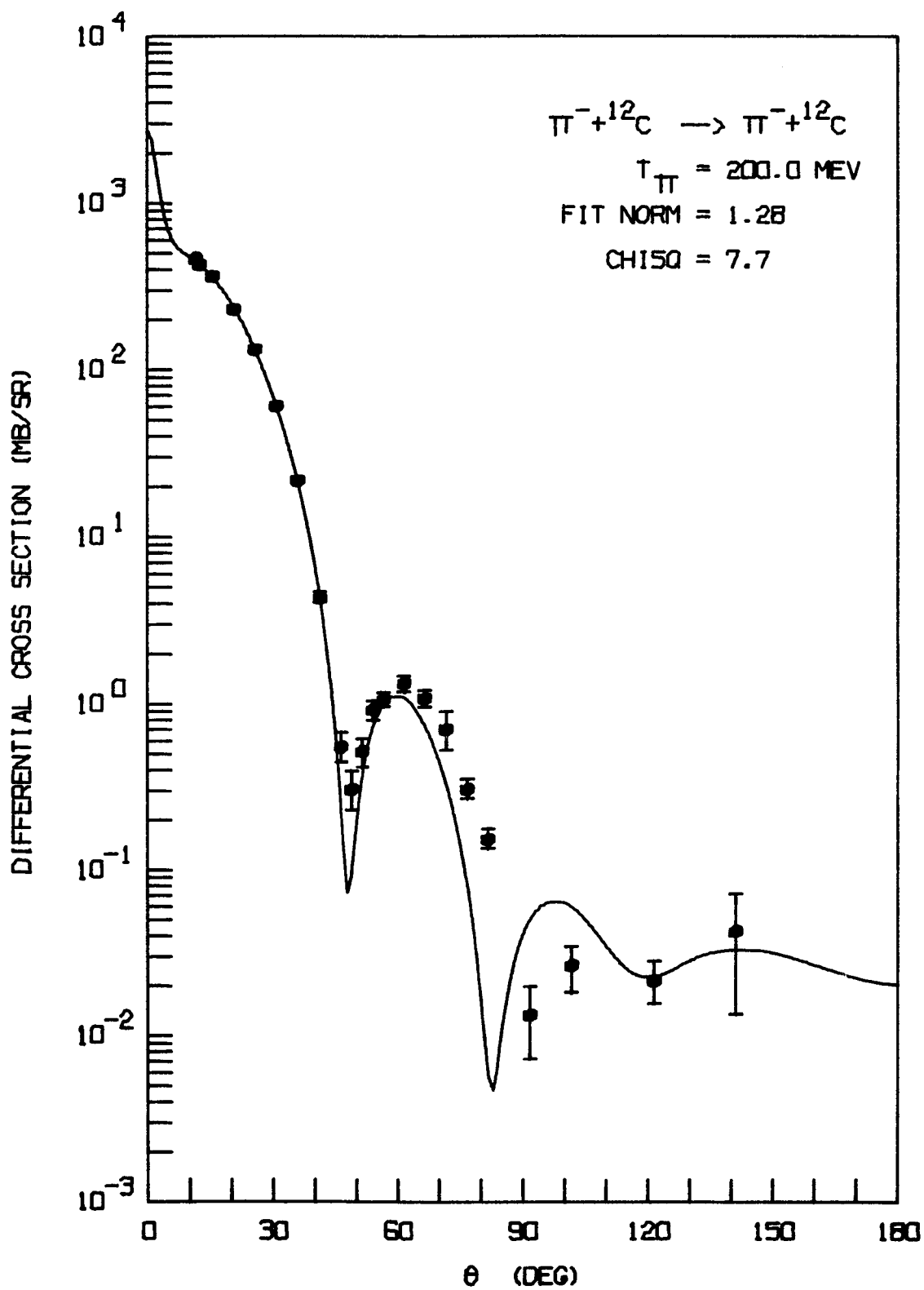


FIGURE 47.

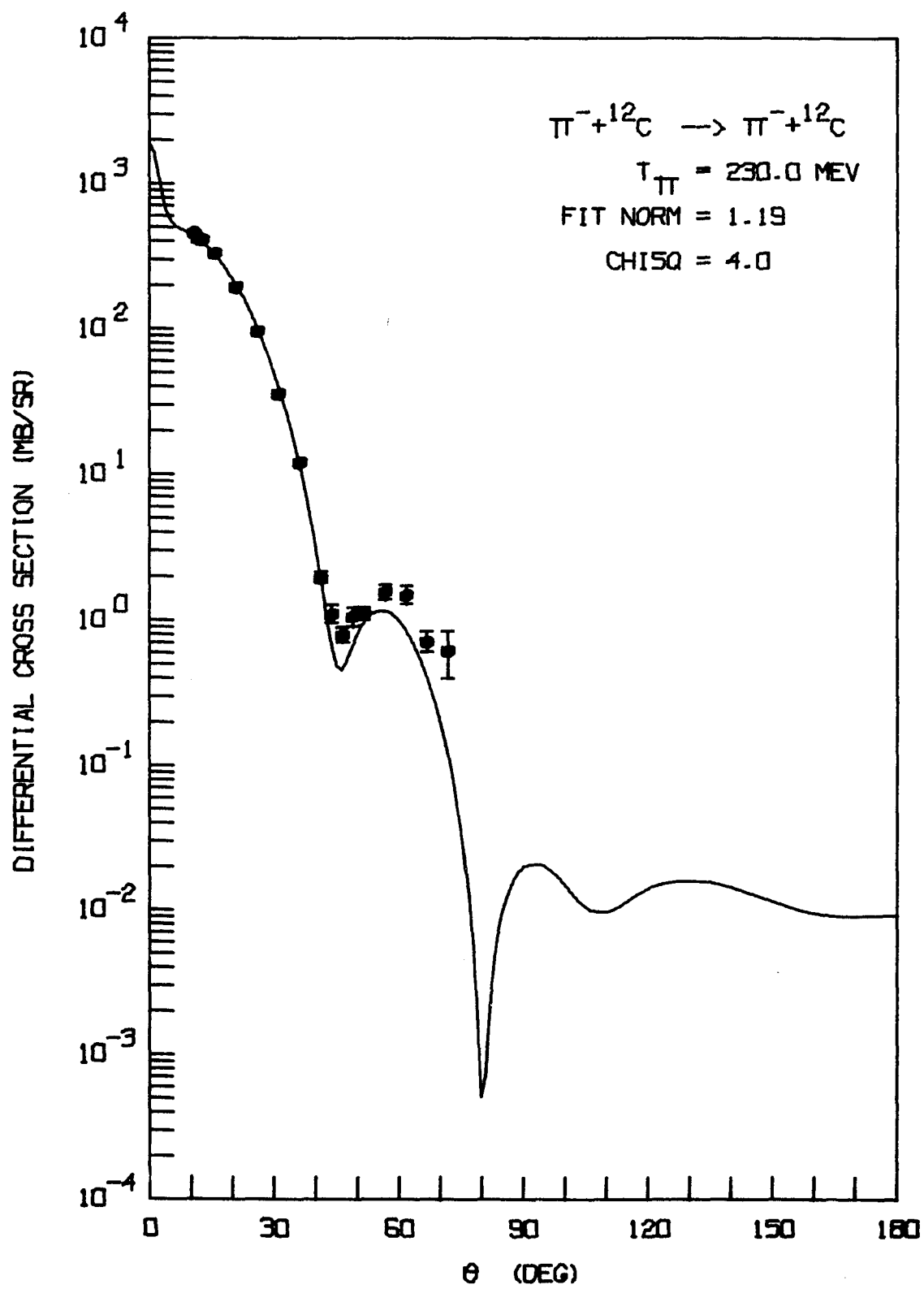


FIGURE 48.

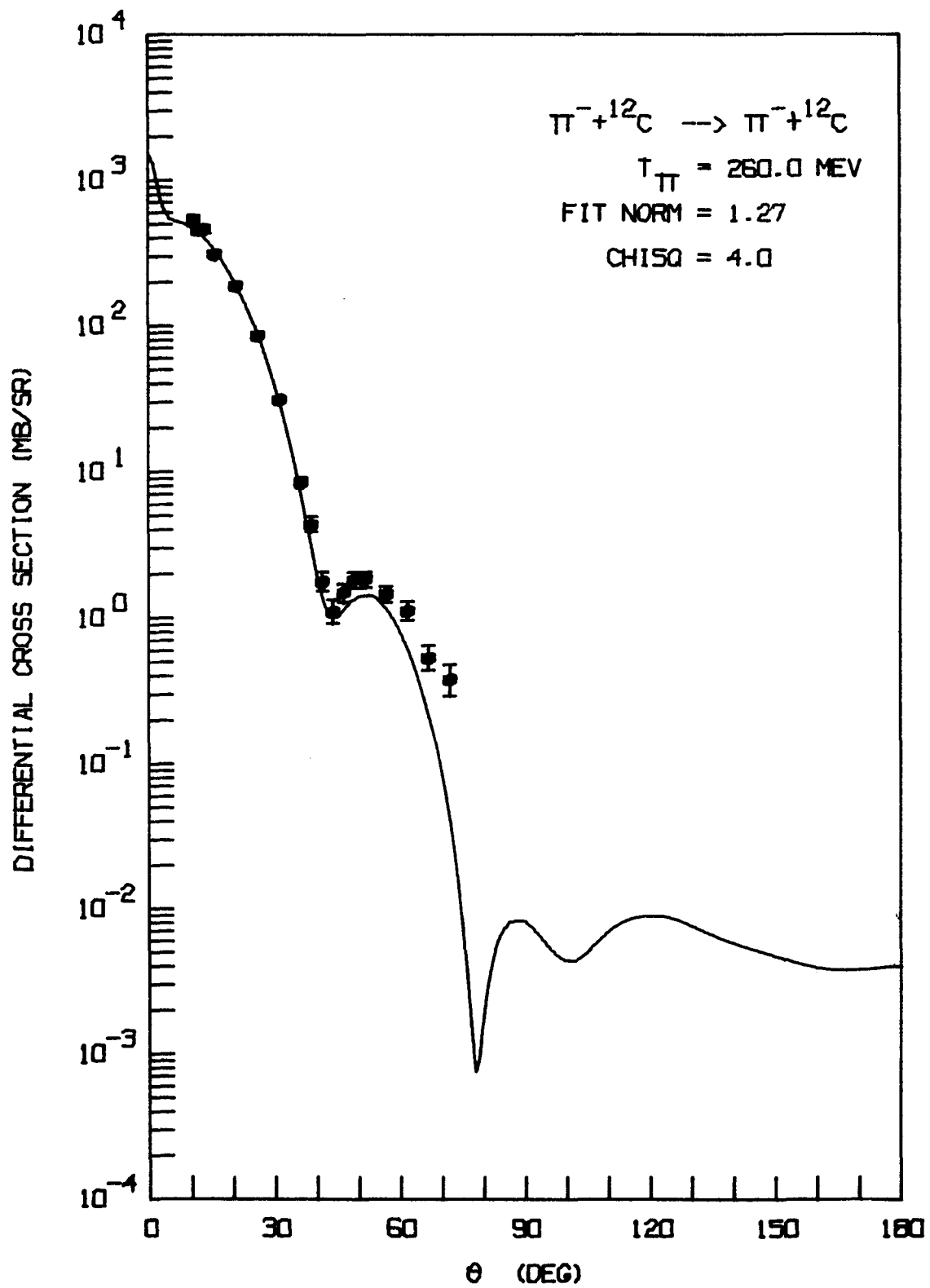


FIGURE 49.

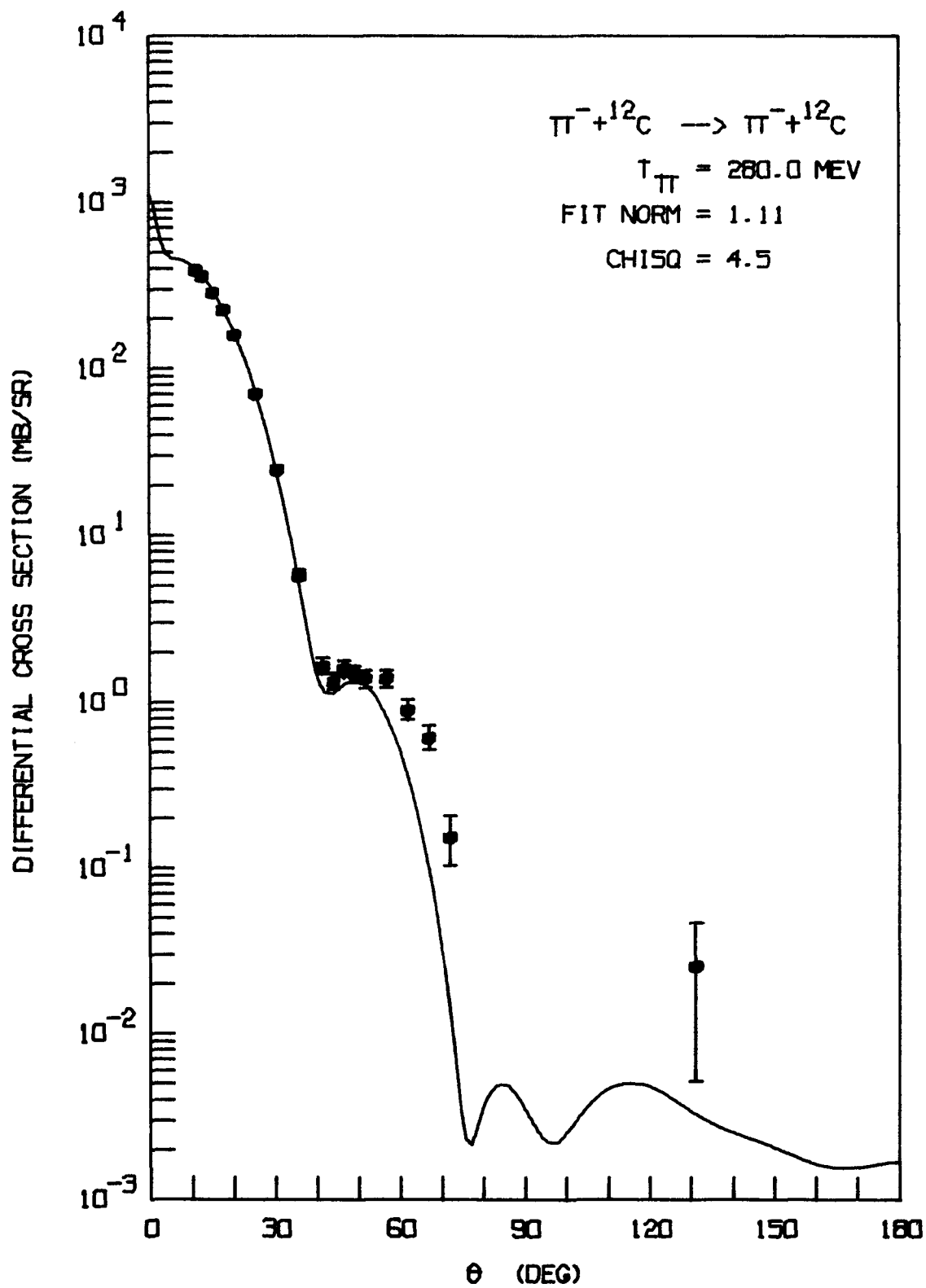


FIGURE 50.

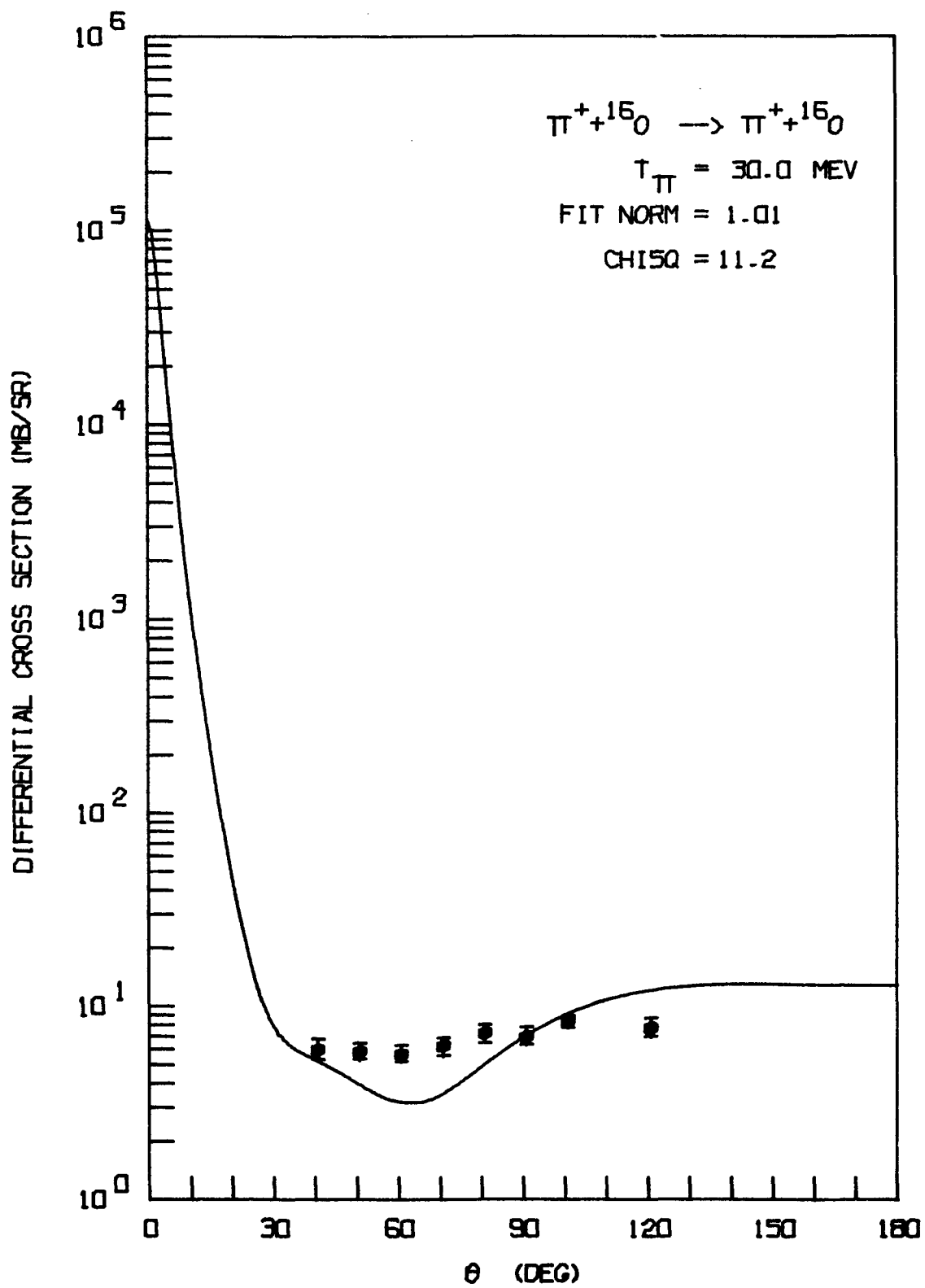


FIGURE 51.

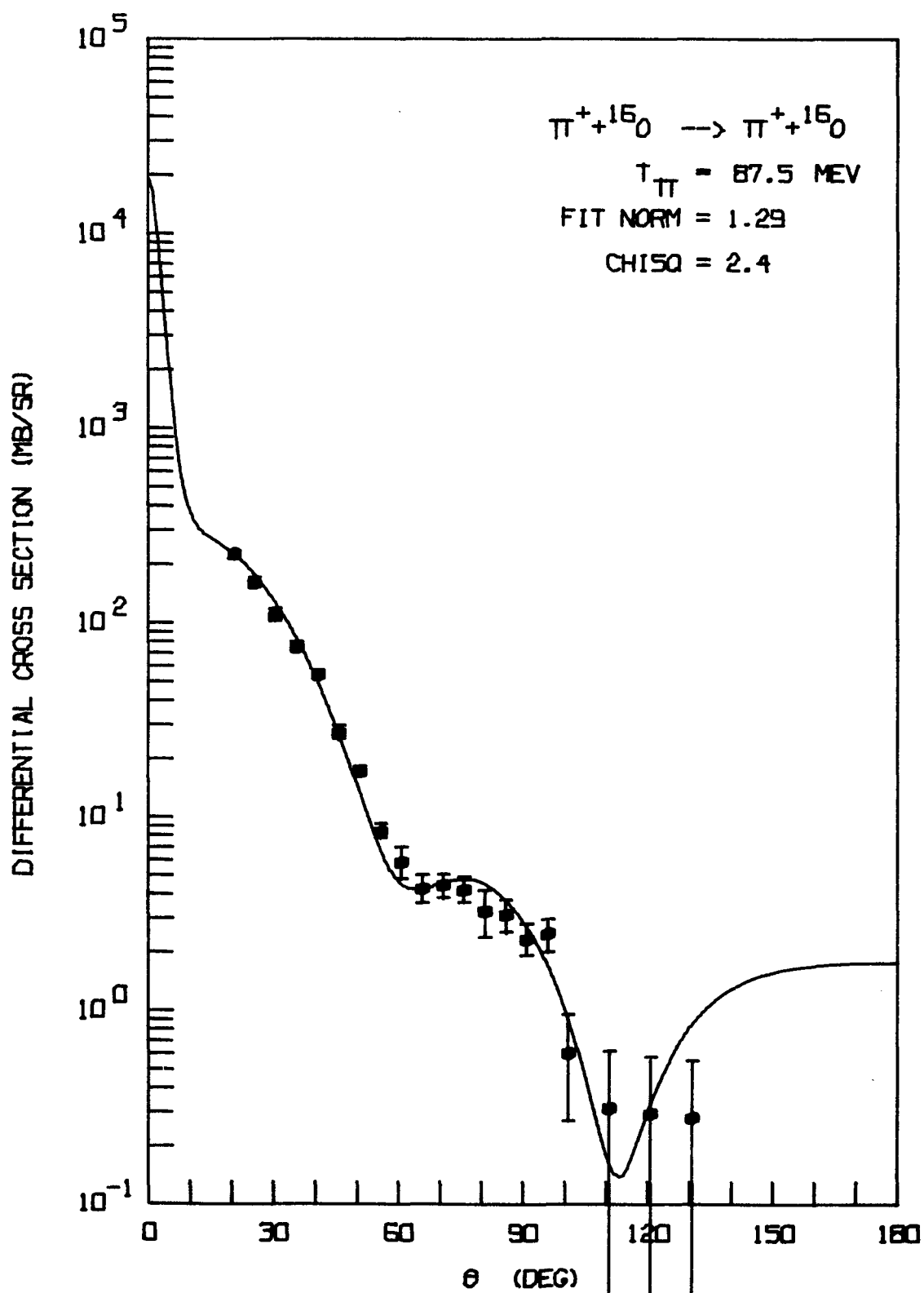


FIGURE 52.

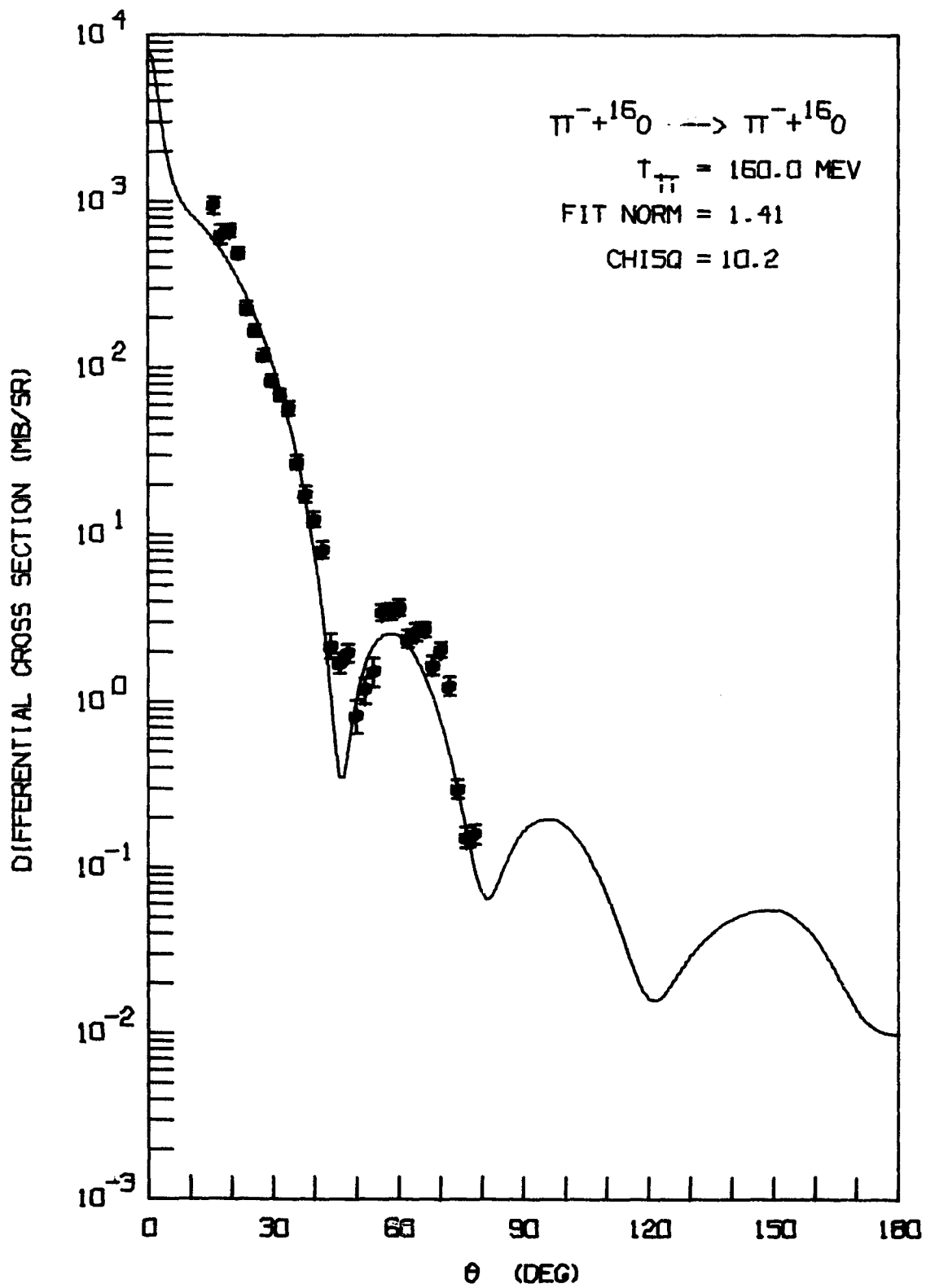


FIGURE 53.

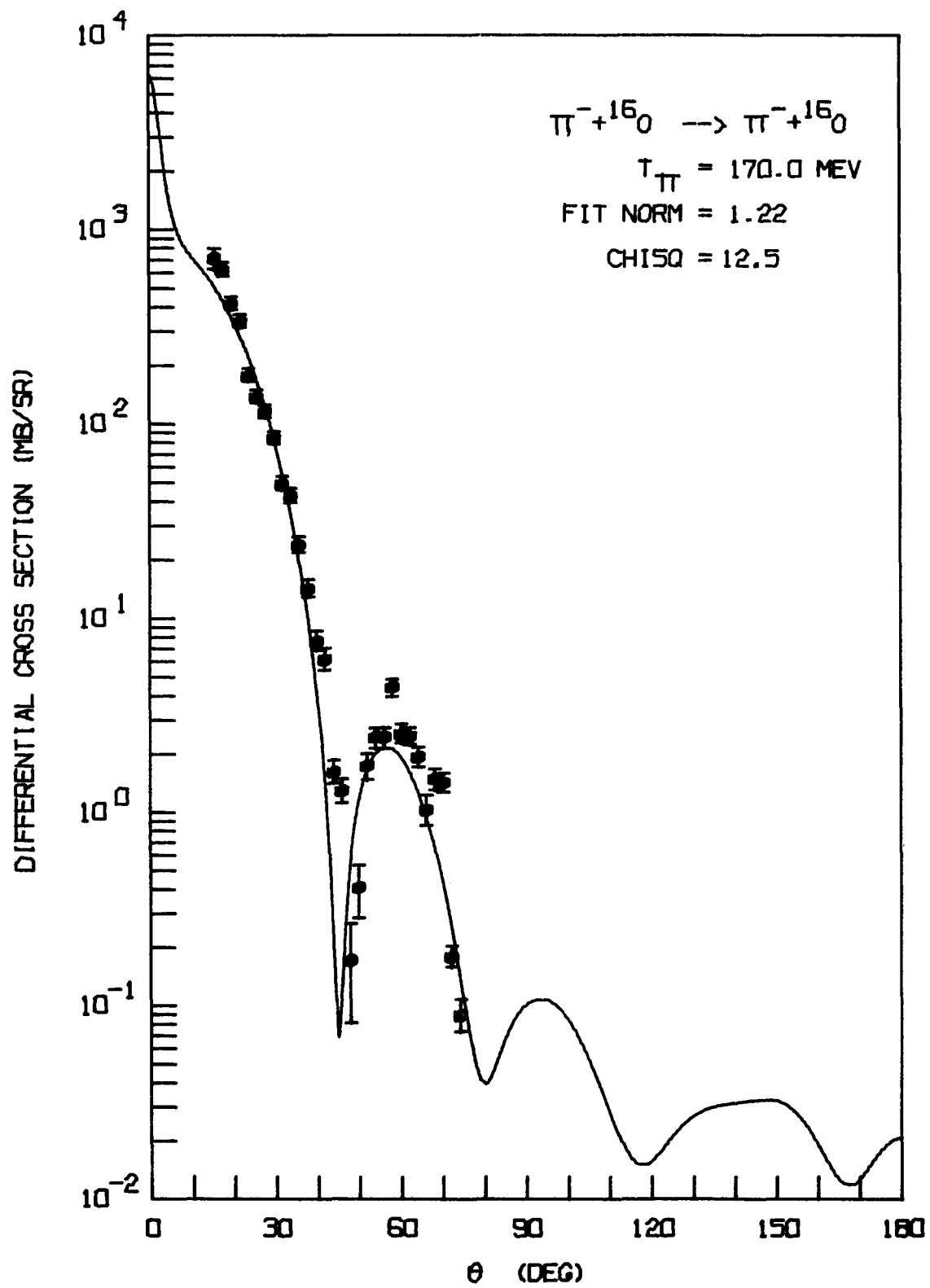


FIGURE 54.

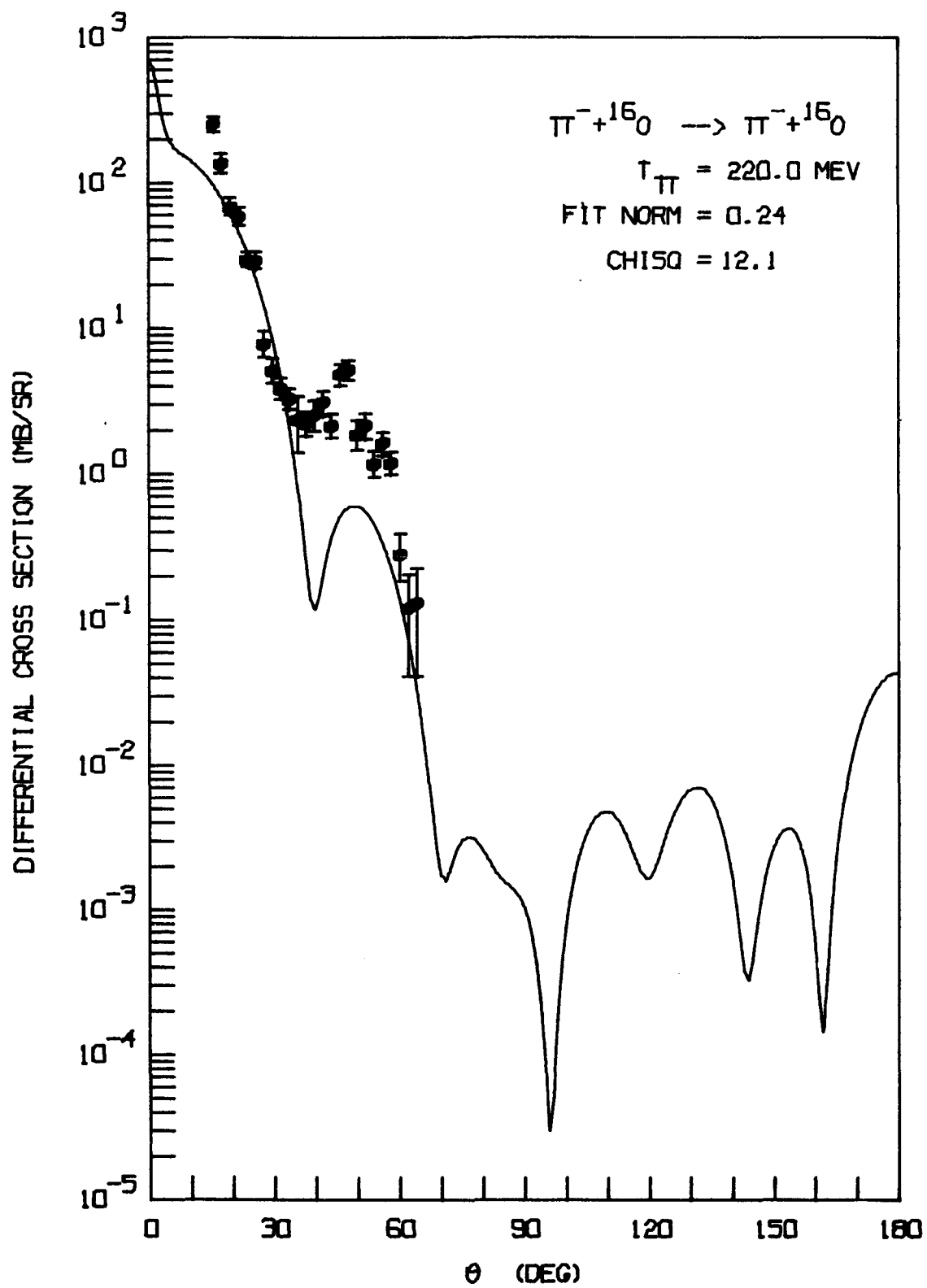


FIGURE 55.

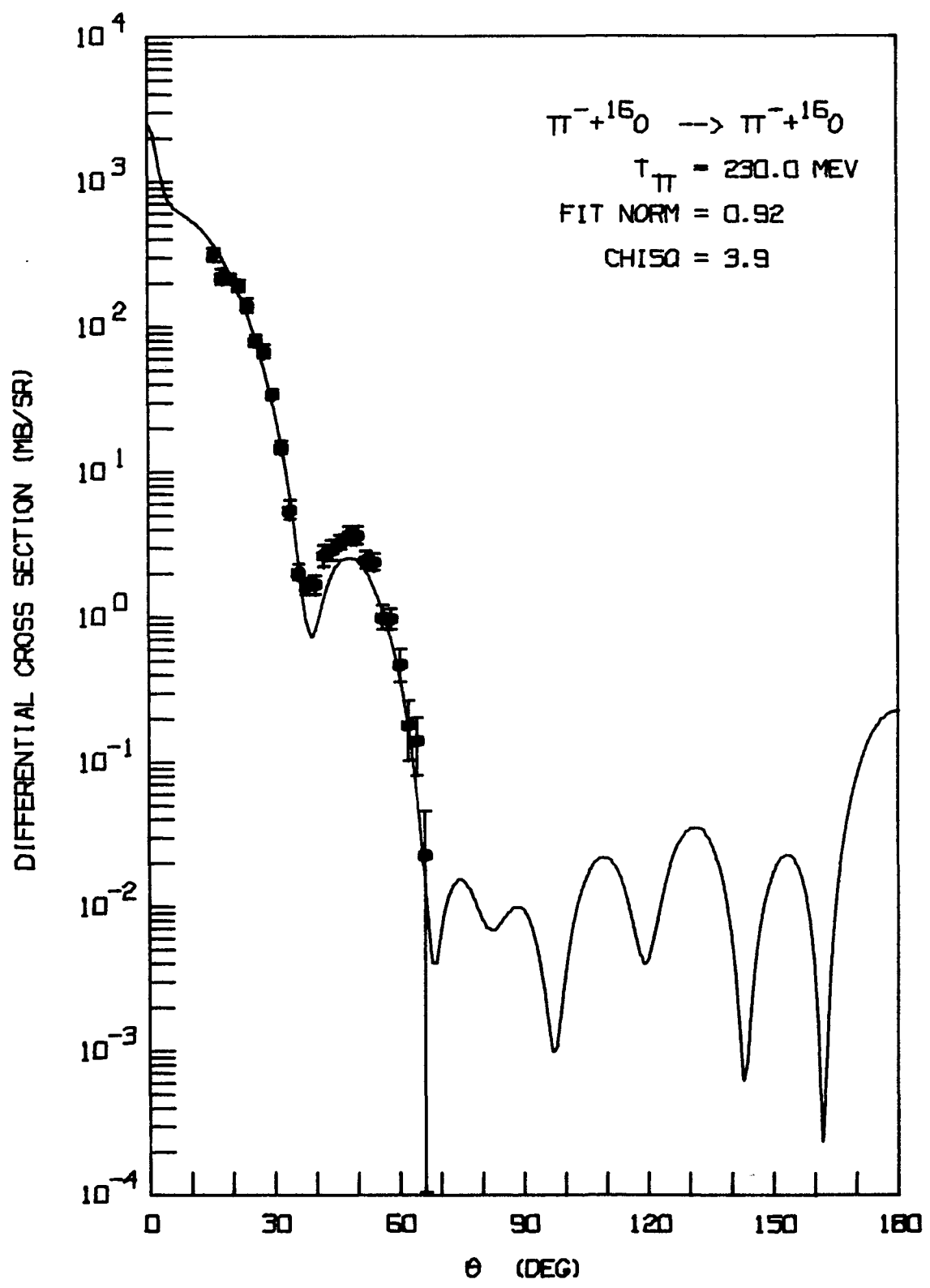


FIGURE 56.

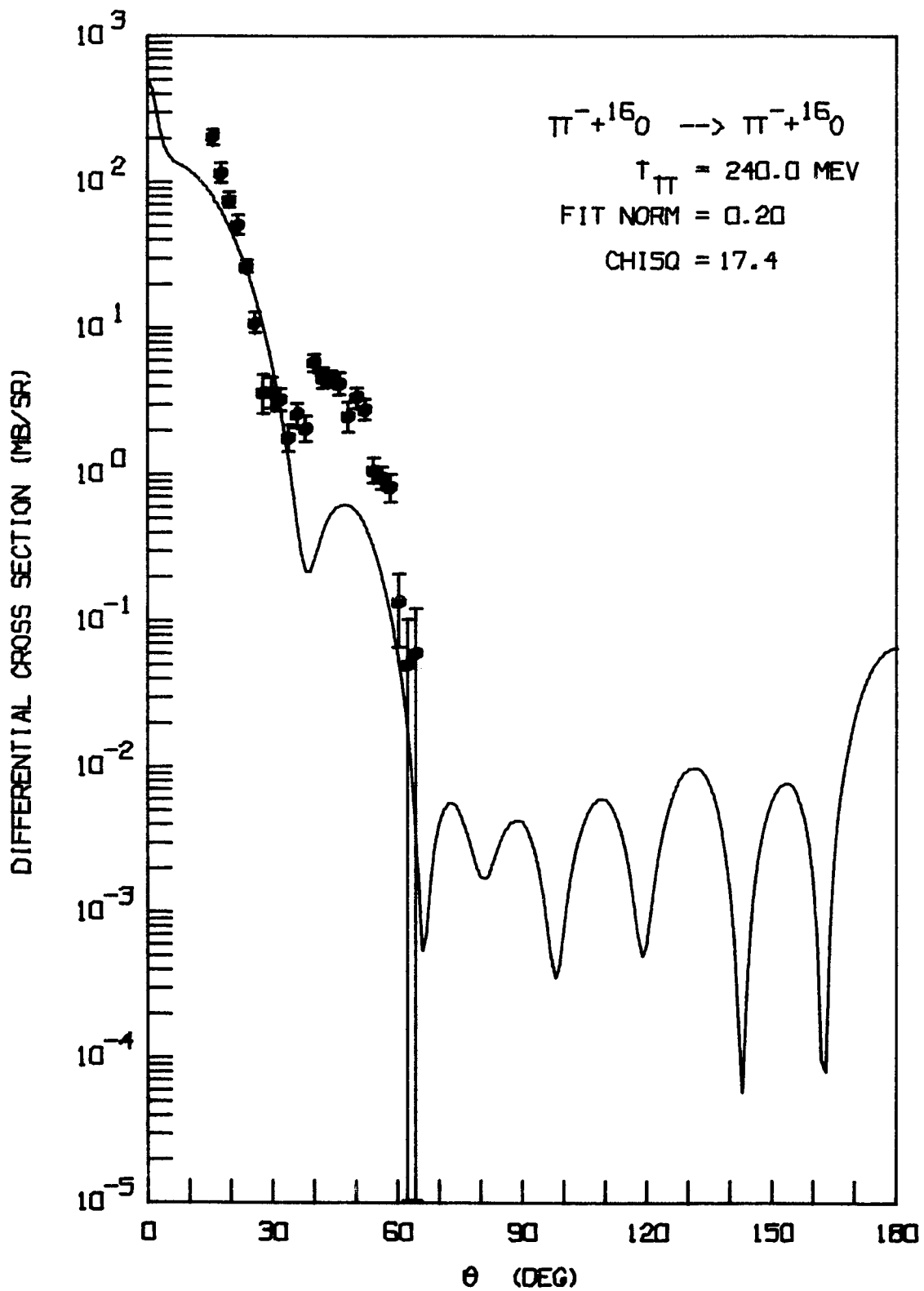


FIGURE 57.

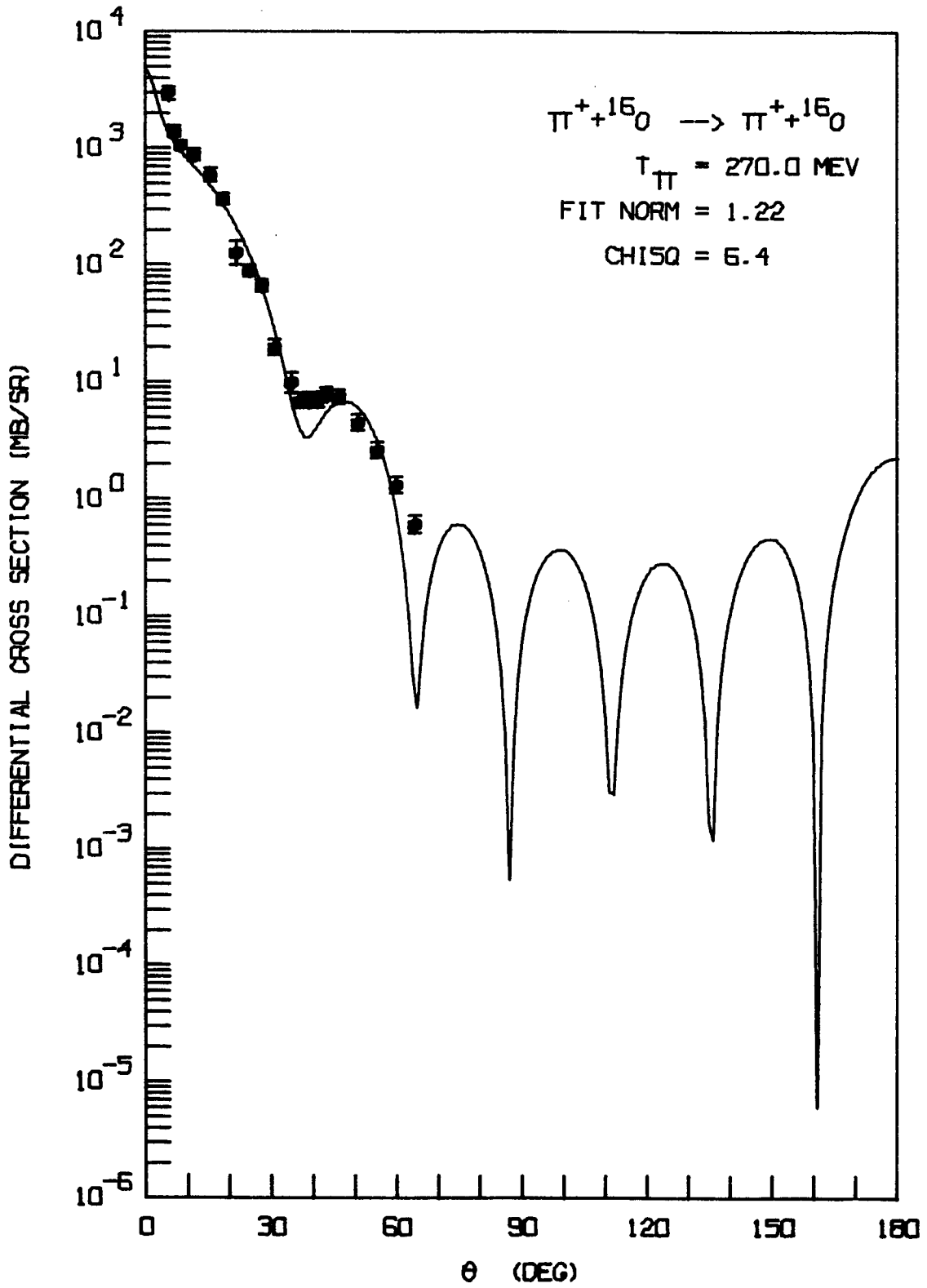


FIGURE 58.

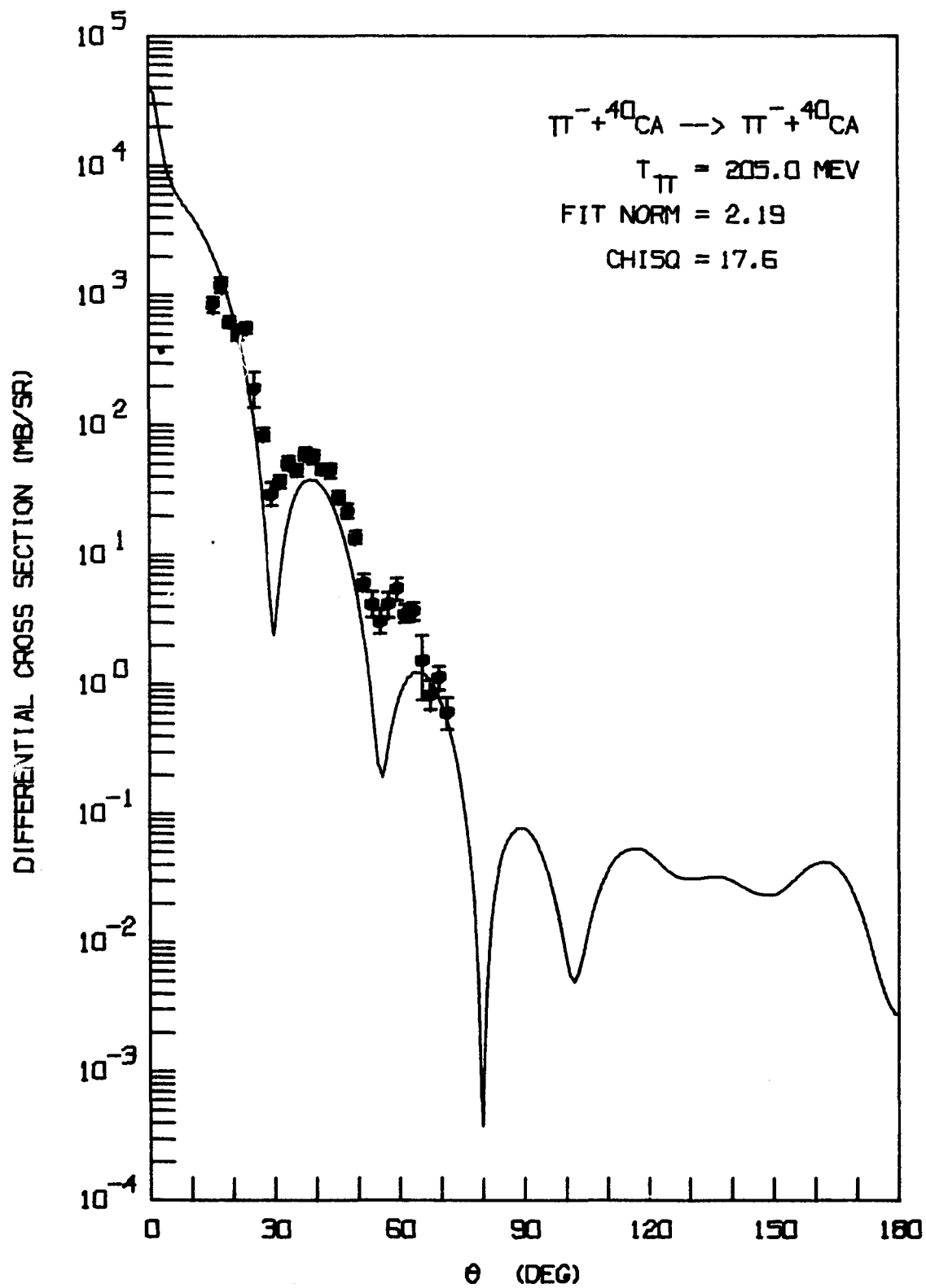


FIGURE 59.

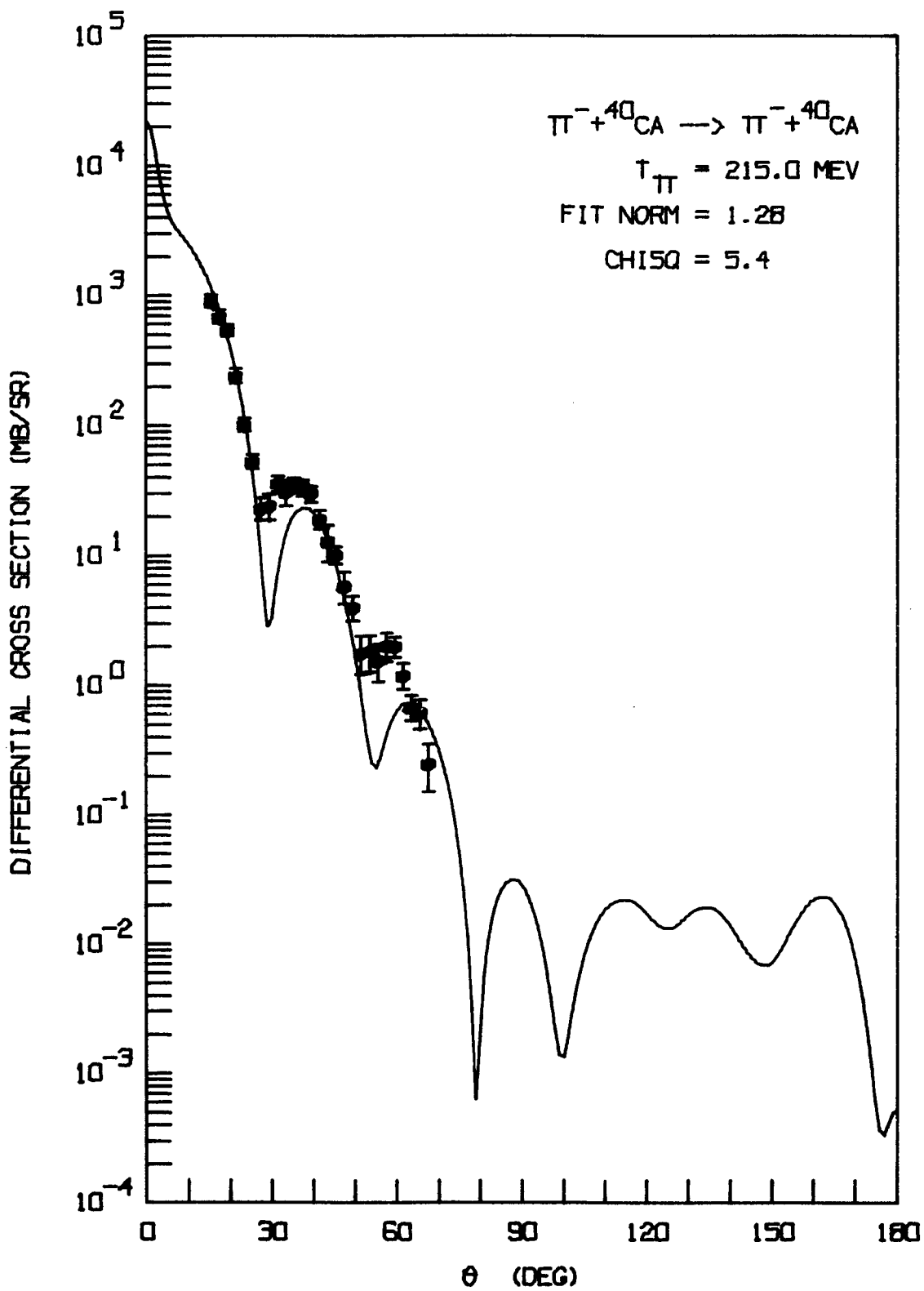


FIGURE 60.

## XI. LIST OF REFERENCES

1. R. J. Wetmore, D. C. Buckle, J. R. Kane, and R. T. Siegel, Phys. Rev. Lett. 19, 1003 (1967).
2. R. J. Harris, W. B. Shuler, M. Eckhause, R. T. Siegel, and R. E. Welsh, Phys. Rev. Lett. 20, 505 (1968).
3. G. H. Miller, M. Eckhause, W. W. Sapp, and R. E. Welsh, Phys. Letters 27B, 663 (1968).
4. M. Eckhause, F. R. Kane, J. R. Kane, P. Martin, G. H. Miller, C. B. Spence, Jr., and R. E. Welsh, Nuc. Phys. B44, 83 (1972).
5. D. A. Jenkins, R. Kunselman, M. K. Simmons, and T. Yamazaki, Phys. Rev. Lett. 17, 1 (1966).
6. D. A. Jenkins and R. Kunselman, Phys. Rev. Lett. 17, 1148 (1966).
7. G. Backenstoss, S. Charalambus, H. Daniel, H. Koch, G. Poelz, H. Schmitt, and L. Tauscher, Phys. Letters 25B, 365 (1967).
8. J. F. Marshall, M. E. Nordberg, Jr., and R. L. Burman, Phys. Rev. C1, 1685 (1970).
9. R. M. Edelstein, W. F. Baker, and J. Rainwater, Phys. Rev. 122, 252 (1961).
10. F. Binon, P. Duteil, J. P. Garron, J. Gorres, L. Hugin, J. P. Peigneux, C. Schmit, M. Spighel, and J. P. Stroot, Nuc. Phys. B17, 168 (1970).
11. M. E. Nordberg, Jr., and K. F. Kinsey, Phys. Letters 20, 692 (1966).
12. K. M. Crowe, A. Fainberg, J. Miller, and A. S. L. Parsons, Phys. Rev. 180, 1349 (1969).
13. Yu. A. Budagov, P. F. Ermolov, E. A. Kushnirenko, and V. I. Moskalev, Zh. Eksperim. i Teor. Fiz. (USSR) 42, 1191 (1961) [Soviet Phys. - JETP (USA) 15, 824 (1962)].
14. R. W. Bercaw, J. S. Vincent, E. T. Boschitz, M. Blecher, K. Gotow, D. K. Anderson, R. Kerns, R. Minehart, K. Ziock, and R. Johnson, Phys. Rev. Lett. 29, 1031 (1972). The numerical values given in the tables were received by private communication from Gotow.
15. Los Alamos Meson Physics Facility at Los Alamos, New Mexico.

16. Schweizerisches Institut für Nuklearforschung in Villigen, Switzerland.
17. The Columbia University Nevis Synchrocyclotron at Irvington-on-Hudson, New York.
18. Tri-University Meson Physics Facility in Vancouver, British Columbia, Canada.
19. M. Ericson and T. E. O. Ericson, *Ann. Phys.* 36, 323 (1966).
20. C. B. Dover, *Ann. Phys.* 79, 441 (1973).
21. M. Krell and T. E. O. Ericson, *Nuc. Phys.* B11, 521 (1969).
22. G. Backenstoss, in invited paper presented at the International Conference in High-Energy Physics and Nuclear Structure at Columbia University in New York from September 8-12, 1969.
23. D. K. Anderson, D. A. Jenkins, and R. J. Powers, *Phys. Rev.* 188, 9 (1969).
24. E. H. Auerbach, D. M. Fleming, and M. M. Sternheim, *Phys. Rev.* 162, 1683 (1967).
25. D. S. Koltun in *Advances in Nuclear Physics Vol. III*, (M. Baranger and E. Vogt editors), (Plenum Press, New York, 1969).
26. M. L. Goldberger and K. M. Watson, *Collision Theory*, (John Wiley and Sons, Inc., New York, 1964).
27. H. Byfield, J. Kessler, and L. M. Lederman, *Phys. Rev.* 86, 17 (1952).
28. K. M. Watson, *Phys. Rev.* 89, 575 (1953).
29. N. C. Francis and K. M. Watson, *Phys. Rev.* 92, 291 (1953).
30. M. Stearns and M. B. Stearns, *Phys. Rev.* 103, 1534 (1956).
31. M. Camac, A. D. McGuire, J. B. Platt, and H. B. Shulte, *Phys. Rev.* 88, 1934 (1952).
32. W. F. Baker, J. Rainwater, and R. E. Williams, *Phys. Rev.* 112, 1763 (1958).
33. W. F. Baker, H. Byfield, and J. Rainwater, *Phys. Rev.* 112, 1773 (1958).
34. L. S. Kisslinger, *Phys. Rev.* 98, 761 (1955).
35. R. M. Edelstein, W. F. Baker, and J. Rainwater, *Phys. Rev.* 122, 252 (1961).
36. E. P. G. Valckx, E. S. Gelsema, and M. Kruiskamp, *Nuovo Cimento* 23, 1005 (1962).

37. A. K. Kerman and R. K. Logan, in "Nuclear Spectroscopy with Direct Reactions Vol. I," Argonne National Lab Report - 6848, p. 236 (1964).
38. D. Chivers, J. J. Domingo, E. M. Rimmer, R. C. Whitcomb, B. W. Allardyce, and N. N. Tanner, Phys. Letters 26B, 573 (1968).
39. M. Krell and S. Barao, Nuc. Phys. B20, 461 (1970).
40. K. A. Brueckner, Phys. Rev. 98, 769 (1955).
41. D. J. Thouless, Proc. Phys. Soc. 69, 280 (1956).
42. S. D. Drell, H. J. Lipkin, and A. de Shalit unpublished paper referred to in reference 14.
43. N. M. Kroll, private communication as reported in reference 9.
44. J. Hamilton, "Pion-Nucleon Interactions," in High Energy Physics, edited by E. H. S. Burhop (Academic Press, New York and London, 1967) Vol. I p. 194.
45. S. L. Adler and R. F. Dashen, Current Algebras (W. A. Benjamin, New York and Amsterdam, 1968).
47. K. A. Brueckner, R. Serber, and K. M. Watson, Phys. Rev. 84, 258 (1951).
48. S. Ozaki, R. Weinstein, G. Glass, E. Loh, E. Neimela, and A. Wattenberg, Phys. Letters 4, 533 (1960).
49. M. E. Nordberg, Jr., K. F. Kinsey, and R. L. Burman, Phys. Rev. 165, 1096 (1968).
50. H. W. Bertini, Phys. Letters 30B, 300 (1969).
51. H. L. Anderson, E. P. Hinks, C. S. Johnson, C. Rey, A. M. Segar, Phys. Rev. 133, B392 (1964).
52. R. Serber, Phys. Rev. 72, 1114 (1947).
53. J. Heidmann and L. Leprince-Ringuet, Comptes Rendue 226, 1716 (1948).
54. S. Tamor, Phys. Rev. 77, 412 (1950).
55. P. Cuer, Comptes Rendue 231, 846 (1950).
56. L. Rosen, Peaceful Uses of Atomic Energy Vol. 4 (United Nations, New York, 1956).
57. K. J. LeCouteur, in Nuclear Reactions Vol. I, edited by P. M. Endt and M. Demur (North-Holland Publishing Company, Amsterdam, 1959) pp. 318-355.
58. V. Weisskopf, Phys. Rev. 52, 295 (1937).

59. K. J. LeCouteur, Proc. Phys. Soc. A63, 259 (1950).
60. K. J. LeCouteur, Proc. Phys. Soc. A65, 718 (1952).
61. P. Ammiraju and L. M. Lederman, Nuovo Cimento 4, 283 (1956).
62. M. Schiff, R. H. Hildebrand, and C. Giese, Phys. Rev. 122, 265 (1961).
63. R. Bizzari, E. Di Capua, U. Dore, G. Gialanella, P. Guidoni, and I. Laakso, Nuovo Cimento 33, 1497 (1964).
64. M. M. Block, T. Kikuchi, D. Koetke, J. Kopelman, C. R. Sun, R. Walker, G. Culligan, V. L. Telegdi, and R. Winston, Phys. Rev. Letters 11, 301 (1963).
65. O. A. Zaimidoroga, M. M. Kulyukin, R. M. Sulyaev, I. V. Falomkin, A. I. Filippov, V. M. Tsupko-Sitnikov, and Yu. A. Scherbakov, Zh. Eksper. Teor. Fiz. (USSR) 51, 1646 (1966) [Soviet Phys. JETP (USA) 24, 1111 (1967)].
66. A. O. Vaisenberg, E. D. Kulganova, and N. V. Rabin, Zh. Eksper. Teor. Fiz. (USSR) 47, 1262 (1964) [Soviet Phys. JETP (USA) 20, 854 (1965)].
67. I. S. Shapiro and V. M. Kolybasov, Zh. Eksper. Teor. Fiz. (USSR) 44, 270 (1963) [Soviet Phys. JETP (USA) 17, 185 (1963)].
68. V. M. Kolybasov, Yaderna Fizika (USSR) 3, 729 (1966) [Soviet J. Nuclear Phys. (USA) 3, 535 (1966)].
69. V. M. Kolybasov, Yaderna Fizika (USSR) 3, 965 (1966) [Soviet J. Nuclear Phys. (USA) 3, 704 (1966)].
70. S. G. Eckstein, Phys. Rev. 129, 413 (1963).
71. Actually Eckstein associated the delta functions with the scattering operator.
72. M. Ericson, Comptes Rendue 258, 1471 (1964).
73. S. Deser, M. L. Goldberger, K. Baumann, and W. Thirring, Phys. Rev. 96, 774 (1954).
74. D. D. Ivanenko and G. E. Pustovalov, Usp. Fiz. Nauk (USSR) 61, 27 (1957) [Soviet Phys. - Usp. (USA) 63, 1043 (1961)].
75. R. Seki and A. H. Cromer, Phys. Rev. 156, 93 (1967).
76. B. Blum, Nuc. Phys. B23, 155 (1970).
77. S. Chapman and T. C. Cowling, Mathematical Theory of Non-Uniform Cases (Cambridge University Press, Teddington, 1939).
78. R. E. Marshak, Revs. Mod. Phys. 19, 185 (1947).

79. O. Halpern and R. K. Luneburg, *Phys. Rev.* 76, 1811 (1949).
80. Marshak, Brooks, and Hurwitz, *Nucleonics* 4, 10, 43 (1949) and 5, 53, 59 (1949).
81. E. Hopf, "Problems in Radiative Equilibrium," Cambridge Tract No. 31 (1934).
82. S. Chandrasekhar, Radiative Transform (Oxford University Press, London, 1950).
83. H. S. Snyder and W. T. Scott, *Phys. Rev.* 76, 220 (1949).
84. U. Fano, *Phys. Rev.* 76, 739 (1949).
85. W. R. Faust, *Phys. Rev.* 77, 227 (1950).
86. B. Rossi and K. Greisen, *Revs. Mod. Phys.* 13, 240 (1941).
87. H. S. Snyder, *Phys. Rev.* 76, 1563 (1949).
88. E. Conwell and V. F. Weisskopf, *Phys. Rev.* 77, 388 (1950).
89. A. H. Wilson, The Theory of Metals (Cambridge University Press, Teddington, 1936).
90. S. DeBenedetti, Nuclear Interactions (John Wiley and Sons, Inc., New York, London, and Sydney, 1964), pp. 163.
91. M. Lax, *Revs. Mod. Phys.* 23, 287 (1951).
92. E. Merzbacher, Quantum Mechanics (John Wiley and Sons, Inc., New York and London, 1961) pp. 221-228.
93. P. P. Ewald, *Ann. Physik* 49, 4 (1916).
94. R. M. Rockmore, *Phys. Rev.* 105, 256 (1957).
95. H. A. Bethe and P. M. Morrison, Elementary Nuclear Theory (John Wiley and Sons, Inc., New York, 1956) p. 63.
96. V. I. Petrukhin and Yu. D. Prokoshkin, *Nuc. Phys.* 54, 414 (1964).
97. W. K. H. Panofsky, R. L. Aamodt, and J. Hadley, *Phys. Rev.* 81, 565 (1951).
98. R. A. Stallwood, R. B. Sutton, T. H. Fields, J. G. Fox, and J. A. Kane, *Phys. Rev.* 109, 1716 (1958).
99. E. H. S. Burhop, in High Energy Physics Vol. III, edited by E. H. S. Burhop (Academic Press, New York and London, 1969).
100. A. Partensky and M. Ericson, *Nuc. Phys.* 81, 382 (1967).

101. A. Donnachie, in Particle Interactions at High Energies edited by T. W. Priest and L. L. J. Vick (Plenum Press, New York, 1967), p. 330.
102. F. Bierman, Phys. Rev. 127, 599 (1962).
103. G. E. Fisher and E. W. Jenkins, Phys. Rev. 116, 749 (1959).
104. J. M. McKinley, Revs. Mod. Phys. 35, 788 (1963).
105. J. Hamilton and W. S. Woolcock, Revs. Mod. Phys. 35, 737 (1963).
106. V. K. Samaranyake and W. S. Woolcock, Phys. Rev. Letters 15, 936 (1965).
107. M. L. Goldberger, H. Miyazawa, and R. Oehme, Phys. Rev. 99, 986 (1955).
108. J. Hamilton, Phys. Letters 20, 687 (1966).
109. R. A. Donald, W. H. Evans, W. Hart, P. Mason, D. E. Plane, and E. J. C. Read, Proc. Phys. Soc. 87, 445 (1966).
110. R. A. Donald, Proc. Phys. Soc. 88, 1047 (1966).
111. S. W. Barnes, B. Rose, G. Giacomelli, J. Ring, K. Miyake, and K. Kinsey, Phys. Rev. 117, 226 (1960).
112. S. W. Barnes, H. Winick, K. Miyake, and K. Kinsey, Phys. Rev. 117, 238 (1960).
113. S. W. Barnes et al., Atomic Energy Commission Report NYO-2170 (unpublished).
114. W. Johnson and M. Camac, Atomic Energy Commission Report NYO-2169 (unpublished).
115. A. E. Woodruff, Phys. Rev. 117, 1113 (1960).
116. Iu. M. Kazarinov and Iu. N. Simonov, Zh. Eksper. Teor. Fiz. 35, 78 (1958).
117. H. L. Anderson, in Rochester Conference in High Energy Nuclear Physics (Interscience Publishers, Inc., New York, 1956), Sec. I, p. 20.
118. J. M. McKinley, Revs. Mod. Phys. 35, 788 (1963).
119. J. M. Blatt and J. D. Jackson, Phys. Rev. 76, 18 (1949).
120. L. D. Roper, R. M. Wright, and B. T. Feld, Phys. Rev. 138, B190 (1965).

121. A. Donnachie and G. Shaw, *Ann. of Phys.* 37, 333 (1966).
122. R. A. Krafcik and L. L. Foldy, *Phys. Rev. Lett.* 24, 545 (1970).
123. C. W. Lucas, Jr. and C. W. Wernitz, *Bull. Am. Phys. Soc.* 10, 1409 (1973).
124. J. J. Sakurai, *Invariance Principles and Elementary Particles* (Princeton University Press, Princeton, 1964).
125. I. S. Gradshteyn and I. M. Ryzhik, *Tables of Integrals, Series, and Products* (Academic Press, New York, 1965).
126. I. Sick and J. S. McCarthy, *Nuc. Phys.* A150, 631 (1970).
127. L. R. B. Elton, *Nuclear Sizes* (Oxford University Press, London, 1961), p. 21.
128. R. Hofstadter, *Ann. Rev. Nucl. Sci.* 7, 231 (1957).
129. H. F. Ehrenberg, R. Hofstadter, U. Meyer-Berkhout, D. G. Ravenhall, and S. E. Sobottka, *Phys. Rev.* 113, 666 (1959).
130. U. Meyer-Berkhout, K. W. Ford, and A. E. S. Green, *Ann. Phys.* 8, 119 (1959).
131. H. Crannell, *Phys. Rev.* 148, 1107 (1966).
132. R. F. Frosh, J. S. McCarthy, R. E. Rand, and M. R. Yearian, *Phys. Rev.* 160, 874 (1967).
133. H. Uberall, *Electron Scattering from Complex Nuclei* (Academic Press, New York and London, 1971), p. 214.
134. M. Croissiaux, R. Hofstadter, A. E. Walker, M. R. Yearian, D. G. Ravenhall, B. C. Clark, and R. Herman, *Phys. Rev.* 137, B865 (1965).
135. B. Fricke, *Z. Physik* 218, 495 (1969).
136. U. S. Dept. of Commerce, National Bureau of Standards Applied Mathematics Series 55, *Handbook of Mathematical Functions with Formulas, Graphs, and Mathematical Tables* (U. S. Government Printing Office, Washington, D. C., 1964).
137. R. C. Barrett, S. J. Brodsky, G. W. Erickson, and M. H. Goldhaber, *Phys. Rev.* 166, 1589 (1968).
138. A. B. Mickelwait and H. C. Corben, *Phys. Rev.* 96, 1145 (1954).
139. C. W. Terrill and C. W. Lucas, Jr., unpublished. This work was an extension of C. W. Terrill's Honors thesis, "A Calculation of the Energy Level Shifts in Pionic Atoms Due to Vacuum Polarization", in which the strong interaction potential was approximated by a

square well potential.

140. This form of the wave equation is not unique. One could have  $V_{st}(r)$  terms squared.
141. L. I. Schiff, Quantum Mechanics (McGraw-Hill Book Company, Inc., New York and London and Toronto, 1955), Second edition, p. 322.
142. N. N. Lebedev, Special Functions and Their Applications (Prentice-Hall, Inc., Englewood Cliffs, New Jersey, 1965), p. 263. (Note that there is a misprint in the second term. The  $(4\alpha - \gamma)$  should be  $(1 + \alpha - \gamma)_k$ ).
143. E. T. Whittaker and E. N. Watson, A Course in Modern Analysis (Cambridge University Press, Cambridge, 1963).
144. R. E. Bellman and R. E. Kalaba, Quasilinearization and Nonlinear Boundary Value Problems (American Elsevier Pub. Co., New York, 1965).
145. E. S. Lee, Quasilinearization and Invariant Imbedding which is volume 41 of Mathematics in Science and Engineering, edited by R. E. Bellman (Academic Press, New York and London, 1968).
146. S. DeBenedetti, Nuclear Interactions (John Wiley and Sons, Inc., New York, 1964), p. 149.
147. S. Berezin, G. Bureson, D. Eartly, A. Roberts, and T. O. White, Nuc. Phys. B16, 389 (1970).
148. H. Koch, G. Poelz, H. Schmitt, L. Tauscher, G. Backenstoss, S. Charalambus, and H. Daniel, Phys. Letters 28B, 279 (1968).
149. H. Koch, M. Krell, C. V. D. Malsburg, G. Poelz, H. Schmitt, L. Tauscher, G. Backenstoss, S. Charalambus, and H. Daniel, Phys. Letters 29B, 140 (1969).
150. W. W. Sapp, Jr., College of William and Mary Report WM 70-21, August 1970.
151. M. E. Nordberg, Jr., and K. F. Kinsey, Phys. Lett. 20, 692 (1966).
152. K. M. Crowe, A. Fainberg, J. Miller, and A. S. L. Parsons, Phys. Rev. 180, 1349 (1969).
153. F. Binon, talk on "Pion-Nucleus Scattering" given at International Seminar on -Meson Nucleus Interactions, Strassbourg, September 20-22, 1971.
154. Yu. A. Budagor, P. F. Ermolov, E. A. Kushnirenko, and V. I. Moskalev, Soviet Physics JETP 15, 824 (1962).
155. P. P. Kane, Phys. Rev. 112, 1337 (1958).

156. J. Perry, Doctoral dissertation submitted to the University of Rochester, 1953 (unpublished).
157. F. Binon, V. Bobyr, P. Duteil, M. Gouanere, L. Hugon, J. P. Pelgneux, J. Renuart, C. Schmitt, M. Spignel, and J. P. Stroot, *Nuc. Phys.* B33, 42 (1971).
158. J. Rohlin, S. Rohlin, B. W. Allardyce, J. J. Domingo, C. H. Ingram, N. W. Tanner, E. Rimmer, and J. P. Girardeau-Montart, *Nuc. Phys.* B37, 461 (1972).
159. R. E. Shafer, *Phys. Rev.* 163, 1451 (1967).
160. A. Astbury, J. P. Deutsch, K. M. Grove, R. E. Shafer, and R. E. Taylor, *Comptes Rendus du Congrès Int. de Phys. Nucl.*, Paris 1964, Vol. 2, p. 225.
161. A. R. Kunselmann, Doctoral dissertation submitted to the University of California, Berkeley, 1969, UCRLR Report 18654.
162. G. Poelz, H. Schmitt, L. Tauscher, G. Backenstoss, S. Charalambus, H. Daniel, and H. Koch, *Phys. Letters* 26B, 331 (1968).
163. D. A. Jenkins, R. J. Powers, and G. H. Miller, *Phys. Rev.* 185, 1508 (1969).
164. H. Schmitt, L. Tauscher, G. Backenstoss, S. Charalambus, H. Daniel, H. Koch, and G. Poelz, *Phys. Letters* 27B, 530 (1968).
165. R. A. Carrigan, W. W. Sapp, W. B. Shuler, R. T. Siegel, and R. E. Welsh, *Phys. Letters* 25B, 193 (1967).
166. R. Mach, *Nucl. Phys.* A205, 56 (1973).
167. L. S. Kisslinger and F. Tabakin, *Phys. Rev.* C9, 188 (1974).
168. B. Goplen, W. R. Gibbs, and E. L. Lomon, *Phys. Rev. Letters* 32, 1012 (1974).
169. J. Hufner, *Nuc. Phys.* B58, 55 (1973).
170. G. Faldt, *Nuovo Cimento Letters* 8, 655 (1973).
171. F. Cannata, C. W. Lucas, Jr., and C. Werntz, to be published.

## VITA

Charles William Lucas, Jr.

Born March 21, 1942, in Washington, D.C. Graduated from Fairfax High School, Fairfax, Virginia, 1960; the College of William and Mary, Williamsburg, Virginia, B.S., 1964; the University of Maryland--College Park, M.S., 1967. The thesis for the master's degree in experimental solid state physics was entitled "The Temperature Dependence of the Saturation Magnetization of Nickel."

In September 1967 the author entered the College of William and Mary as a graduate student in the Department of Physics. Before formally completing the thesis the author took in November 1972 a position as research associate in the physics department of the Catholic University of America, Washington, D.C., where he has been engaged in theoretical studies concerning photo-pion production.